CHEM 370: PHYSICAL CHEMISTRY 1 - THERMODYNAMICS



Jonathan Gutow
University of Wisconsin Oshkosh

LibreTexts™

P-Chem 1

to accommodate biophysical and traditional students

Jonathan Gutow

University of Wisconsin Oshkosh

1: About this resource

This text/resource was developed for use in a first semester physical chemistry course meant to accommodate both students needing a one semester biophysical course and traditional chemistry majors who will go on to take a second semester of physical chemistry. Because of this more topics are covered in less depth than a traditional first semester physical chemistry course. The second semester course must then loop back to fill in the depth. Although very different from the traditional physical chemistry sequence there are some potential advantages:

- The spiral nature of returning to a topic to add depth may help with long term retention of the material.
- This text for the first semester only expects completion of one semester of calculus (including basic integration) and one semester of organic chemistry. The second semester of organic chemistry, an introductory biology course or semester of biochemistry is nice, but not necessary. This allows for scheduling flexibility. Students could potentially take this course sophomore, junior or senior year.
- Enough is covered for a course based on this resource to serve as a prerequisite for an upper-level inorganic course. If students take this first semester physical chemistry course earlier in their career they would have more flexibility in when they schedule their inorganic course.

The sequence of topics follows closely with that of Atkins' and De Paula's *Physical Chemistry for the Life Sciences* and Chang's *Physical Chemistry for the Biosciences*. The thermodynamics discussions are somewhat more detailed. Because this was developed for use in a short semester (14 weeks, without a separate exam period), there are no sections devoted solely to spectroscopy. Those with the luxury of a longer semester are encouraged to include more on spectroscopy.

Topics:

- Thermodynamics (equations of state, 1st law, thermochemistry, 2nd law, Boltzmann distribution and statistics of entropy, Gibbs and Helmholtz energies, phase equilibria, mixtures, colligative properties).
- Chemical equilibria (composition dependence, biological standard state, coupled equilibria, impact of physical conditions, acid-base, buffers).
- Ions and electrochemistry (Debye-Hückel theory, ion transport, redox, half-cell potentials, Nernst equation, thermodynamics from electrochemistry, biological phosphorylation, batteries).
- Reaction kinetics (differential rate laws, integrated rate laws, reaction order, temperature dependence, mechanisms, steady-state and related approximations, relaxation methods, molecular level models, oscillating reactions, numerical modeling, diffusion, ion mobilities, electron transfer reactions).
- Quantum mechanics (fundamental examples overview, tunneling, atomic, molecular valence bond and molecular orbital theory, intro to numerical methods).
- Aggregates and macromolecules (mass spectrometry, X-ray, cryo-EM, intermolecular forces, structure, simulations).

Biophysical courses typically do not have a lab associated with them. This resource was developed for a course that did include a lab with the following topics and experiments: literature searching using CAS SciFinder^{n}; data analysis and symbolic mathematics using open source tools; formal error propagation; thermodynamics of an electrochemical cell; solution calorimetry; ionic strength, activities and pKa; solubility equilibria (gel versus solution); solution kinetics using spectroscopy and pseudo order methods; quantum computations of geometry, UV-Vis spectra and vibrational modes.

When choices had to be made about what examples to include preference was given to biochemical examples and then examples related to the chemistry of current topics: battery technologies, pollution, etc.

> As much as possible this resource was created by adopting, updating or editing existing OER resources, but parts were created by the author *de-nuevo* when necessary.

2: About LibreTexts resources

This text is disseminated via the Open Education Resource (OER) LibreTexts Project (https://LibreTexts.org) and like the thousands of other texts available within this powerful platform, it is freely available for reading, printing, and "consuming."

The LibreTexts mission is to bring together students, faculty, and scholars in a collaborative effort to provide and accessible, and comprehensive platform that empowers our community to develop, curate,

adapt, and adopt openly licensed resources and technologies; through these efforts we can reduce the financial burden born from traditional educational resource costs, ensuring education is more accessible for students and communities worldwide.

Most, but not all, pages in the library have licenses that may allow individuals to make changes, save, and print this book. Carefully consult the applicable license(s) before pursuing such effects. Instructors can adopt existing LibreTexts texts or Remix them to quickly build course-specific resources to meet the needs of their students. Unlike traditional textbooks, LibreTexts' web based origins allow powerful integration of advanced features and new technologies to support learning.



LibreTexts is the adaptable, user-friendly non-profit open education resource platform that educators trust for creating, customizing, and sharing accessible, interactive textbooks, adaptive homework, and ancillary materials. We collaborate with individuals and organizations to champion open education initiatives, support institutional publishing programs, drive curriculum development projects, and more.

The LibreTexts libraries are Powered by NICE CXone Expert and was supported by the Department of Education Open Textbook Pilot Project, the California Education Learning Lab, the UC Davis Office of the Provost, the UC Davis Library, the California State University Affordable Learning Solutions Program, and Merlot. This material is based upon work supported by the National Science Foundation under Grant No. 1246120, 1525057, and 1413739.

Any opinions, findings, and conclusions or recommendations expressed in this material are those of the author(s) and do not necessarily reflect the views of the National Science Foundation nor the US Department of Education.

Have questions or comments? For information about adoptions or adaptions contact info@LibreTexts.org or visit our main website at https://LibreTexts.org.

This text was compiled on 07/30/2025

TABLE OF CONTENTS

Licensing

1: Thermodynamics

- 1.1: Thermodynamic Variables and Equations of State
- 1.2: The First Law of Thermodynamics
- 1.3: Thermochemistry
- 1.4: The Second Law of Thermodynamics
- 1.5: The Boltzmann Distribution and the Statistical Definition of Entropy
- 1.6: The Gibbs and Helmholtz Energy
- 1.7: Phase Equilibria and Mixtures
- 1.8: Colligative Properties
- 1.9: Henry's Law

2: Chemical Equilibria

- 2.1: Chemical Equilibria
- 2.2: Composition Dependence of Free Energy (G)
- 2.3: Equilibrium Calculations (ICE) Review
- 2.4: Fractional Composition at Equilibrium
- 2.5: Coupled Equilibria
- 2.6: Equilibrium Dependence on Conditions
- 2.7: Coupled Equilibria Driving Nonspontaneous Reactions
- 2.8: Brønsted-Lowry Acids and Bases
- 2.9: pH and pOH
- 2.10: Acid-Base Equilibria
- 2.11: Hydrolysis of Salts
- 2.12: Polyprotic Acids
- 2.13: Buffers

3: Ions and Electrochemistry

- 3.1: Mean Ionic Activity Coefficients and the Debye-Hückel Model
- 3.2: Extending Debye-Hückel Theory to Higher Concentrations
- 3.3: Ion Transport
- 3.4: Review of Redox Chemistry
- 3.5: Half Cells and Standard Reduction Potentials
- 3.6: Cell potentials under non-standard conditions (Nernst equation)
- 3.7: Thermodynamics from Electrochemistry
- 3.8: Redox Examples

4: Reaction Kinetics

- 4.1: Reaction Rates and Rate Laws
- 4.2: Measuring Reaction Rates
- 4.3: Determining Rate Laws
- 4.4: Integrated Rate Laws
- 4.5: Examples of Using Graphs to Determine Reaction Order
- 4.6: Temperature Dependence of Rate Constants

5: Kinetic Mechanisms 1

- 5.1: Reaction Mechanisms
- 5.2: Relaxation Methods
- 5.3: Representative Reaction Mechanisms
- 5.4: The Rate Determining Step Approximation
- 5.5: The Equilibrium Approximation
- 5.6: The Steady-State Approximation

6: Molecular Level Models of Kinetics

- 6.1: Kinetics of Reactions in Solution
- 6.2: Kinetic vs. Thermodynamic Control of Reactions
- 6.3: Collision Theory
- 6.4: Transition State Theory
- 6.5: Reactions Involving Ions

7: Kinetic Mechanisms 2

- 7.1: Numerical Modeling of Mechanisms
- 7.2: The Michaelis-Menten Mechanism
- 7.3: The Lindemann Mechanism
- 7.4: Chain Reactions
- 7.5: Catalysis (ozone example)
- 7.6: Oscillating Reactions
- 7.7: Diffusion
- 7.8: Membrane Diffusion
- 7.9: Ion Mobilities
- 7.10: Transport Across Cell Membranes
- 7.11: Kinetics of Electron Transfer Reactions

8: Quantum Chemistry Fundamentals

- 8.1: Failures of Classical Physics
- 8.2: The Schrödinger Wave Equation
- 8.3: Particle in a One-Dimensional Box
- 8.4: Tunneling
- 8.5: Particle in a 2-Dimensional Box
- 8.6: Particle on a Ring
- 8.7: The Schrödinger Wave Equation for the Hydrogen Atom
- 8.8: Many-Electron Atoms and the Periodic Table
- 8.9: Harmonic Oscillator

9: Molecular Quantum Mechanics

- 9.1: The Born-Oppenheimer Approximation Simplifies the Schrödinger Equation for Molecules
- 9.2: Valence Bond Theory
- 9.3: Hybridization of Atomic Orbitals
- 9.4: Molecular Orbital Theory
- 9.5: Diatomic Molecules With More Than s Orbitals
- 9.6: Hückel MO Model of Conjugation
- 9.7: Benzene and Aromaticity
- 9.8: Numerical QM Methods

10: Aggregates and Macromolecules

- 10.1: Mass Spectrometry
- 10.2: X-Ray Crystallography
- 10.3: Cryo-Electron Microscopy
- 10.4: Intermolecular Forces
- 10.5: Structure of Gases, Liquids and Glasses
- 10.6: Macromolecules
- 10.7: Simulations

Index

Glossary

Detailed Licensing

Detailed Licensing

Licensing

*A detailed breakdown of this resource's licensing can be found in **Back Matter/Detailed Licensing**.*

CHAPTER OVERVIEW

1: Thermodynamics

1.1: Thermodynamic Variables and Equations of State
1.2: The First Law of Thermodynamics
1.3: Thermochemistry
1.4: The Second Law of Thermodynamics
1.5: The Boltzmann Distribution and the Statistical Definition of Entropy
1.6: The Gibbs and Helmholtz Energy
1.7: Phase Equilibria and Mixtures
1.8: Colligative Properties
1.9: Henry's Law

This page titled 1: Thermodynamics is shared under a CC BY-NC-SA 4.0 license and was authored, remixed, and/or curated by Jonathan Gutow.

1.1: Thermodynamic Variables and Equations of State

Based on "Thermodynamic Variables and Equations of State" by Serge L. Smirnov and James McCarty, LibreTexts is licensed under CC BY-NC-SA

Classical thermodynamics provides a conceptual framework from which we can understand the behavior of molecular systems at a quantitative level. This chapter introduces some of the concepts relating to properties of a system and its surroundings that we will need to study classical thermodynamics. In this chapter, we will focus on how the macroscopic properties of a system are related to and depend on the properties of the constituent atoms and molecules. As an example we will discuss the ideal-gas equation, its range of validity, and how it can be extended to real gases or fluids of interacting molecules.

Learning Objectives

- Build a precise vocabulary of thermodynamic definitions before applying them to chemical systems.
- Understand state variables and how they are mathematically related in an equation of state.
- Be able to manipulate the ideal gas equation of state.
- Understand how real gases deviate from ideality and how real gases and can be modeled by the virial equation of state, which is an expression for the pressure of a gas as a polynomial in the density.

1.1.1: Basic Definitions

We begin our discussion of thermodynamics with some definitions that will allow us to make general statements about how energy is exchanged and converted into various forms.

A **system** is any part of the universe that is of interest to us. This might be the Sun-Earth-Moon system, a human lung, fruit fly, a single bacteria cell, or a container on a bench top. Some example systems are shown in figure 1.1.1.



Figure 1.1.1: Some systems of varying complexity include the sun-earth-moon system, a human lung, a fruit fly, a single bacteria cell, or a Erlenmeyer flask.

Everything else in the universe that is not part of the system is called the **surroundings.** The system + the surroundings constitutes the **universe.**

We can classify systems into 3 types: open systems, closed systems, or isolated systems. An **open system** is able to exchange both matter and heat with the surroundings. A **closed system** cannot exchange matter with the surroundings but *can* exchange heat with the surroundings. An **isolated system** cannot exchange any heat or any matter with surroundings. These three types of systems are depicted in figure 1.1.2:

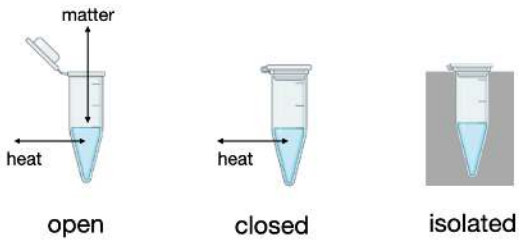


Figure 1.1.2: An open system can exchange both matter and heat with the surroundings. A closed system cannot exchange matter with the surroundings but can exchange heat. An isolated system cannot exchange heat or matter with the surroundings.

The branch of science called **thermodynamics** is interested in the relationships between properties of a system and how properties change as the system changes state. A **property** is any mathematically quantifiable parameter of the system. Some properties could include the pressure, the temperature, the density, the index of refraction, etc ….

We can distinguish between two types of properties: intensive and extensive. **Intensive** properties are *independent* of the quantity (amount of matter) being measured. Some intensive properties include the density, pressure, and temperature. On the other hand,

Extensive properties *depend* on the quantity (amount) being measured. Some extensive properties are the mass, the volume, and the number of moles.

Intensive properties can be constructed as the ratio between two extensive properties. For example the **density** is

$$\text{density} = \frac{\text{mass}}{\text{volume}} \tag{1.1.1}$$

Notice that both **mass** and **volume** are extensive (depend on the amount), but the density (the ratio of the mass over volume) is intensive.

Similarly, the **pressure** is defined as

$$\text{pressure} = \frac{\text{force}}{\text{area}} \tag{1.1.2}$$

The SI units of pressure is the Pascal (Pa) and 1 Pa = 1 N· m^{-2} = 1 kg·m^{-1}· s^{-2} = 1 J· m^{-3}. Table 1.1.1 relates some common units of pressure.

Table 1.1.1: Some common units of pressure

1 Pa = 1 N m^{-2}
1 bar = 100 kPa (10^5 Pa)
1 atm = 101.325 kPa
1 torr (mm Hg) = 1/760 atm

Note: **Energy** by itself (measured in Joules or calories) is an *extensive* property. Often, we report energies as a molar ratio in units of J/mol or cal/mol which is an *intensive* property.

A common way to define an intensive property is to define the **molar** quantity by dividing some extensive variable by the number of moles. For example, the **molar volume** is defined as:

$$\bar{V} = \frac{V}{n} \tag{1.1.3}$$

Here **n** is the number of moles and $\bar{\mathbf{V}}$ is called the molar volume and is an intensive quantity.

Temperature is another important thermodynamic parameter that will be defined in serval ways throughout this text. For now, we will define the **temperature** as the measure of the motion of the atoms within the system. This definition of temperature implies that the "thermodynamic" temperature is measured in Kelvin, because the Kelvin scale is the absolute temperature scale. In the limit that T=0 K (absolute zero), the motion of the atoms approaches zero. We can convert between temperature in Kelvin and Celsius scales using the relation:

$$T(\text{in Kelvins}) = T(\text{in }^\circ C)\frac{1K}{1^\circ C} + 273.15K \tag{1.1.4}$$

Caution

Note: Absolute temperatures (in K) must be used in thermodynamic calculations.

See Practice Problems 1.1.1 and 1.1.2.

1.1.2: Thermodynamic Equations of State

An **equation of state** is a mathematical expression that fully describes the thermodynamic state of the system in terms of a set of physical properties. The most familiar example is the ideal gas law:

$$PV = nRT \tag{1.1.5}$$

or, introducing the molar volume (Equation 1.1.3):

$$P\bar{V} = RT \tag{1.1.6}$$

where $\mathbf{P}$ is the pressure, $\mathbf{V}$ is the volume, $\mathbf{n}$ is the number of moles, $\mathbf{T}$ is the temperature. $\mathbf{R}$ is the gas constant given in table 1.1.2:. Equation 1.1.5 is known as the **ideal gas equation of state**. The ideal gas equation of state (PV=nRT) allows us to see how the properties of an ideal gas are related.

Table 1.1.2: Common units for the ideal gas constant R.

R = 8.314462618 J K^{-1} mol^{-1} = 0.08206 L atm K^{-1} mol^{-1}	L atm = 101.325 J

The ideal gas equation of state will be a useful model for us to work with as we derive thermodynamic relationships because it is intuitive and algebraically easy to manipulate. At this point, it is worthwhile to make some comments concerning the ideal gas equation of state:

1. The ideal gas equation of state can be derived from first principles (kinetic theory of gases).
2. At sufficiently *high* temperature and *low* pressure, all gases fit the ideal gas law.
3. Assumptions made in the ideal gas law:
   - The gas molecules themselves occupy no volume.
   - There are no attractive or repulsive forces between gas molecules.
   - All collisions are perfectly elastic.

See Practice Problems 1.1.3 and 1.1.4.

Because of these assumptions, we expect all **real gases** to deviate from ideal behavior. To quantify this we define the **compressibility factor, Z,** as

$$Z = \frac{P\bar{V}}{RT} \tag{1.1.7}$$

Notice from Equation 1.1.5 that for an ideal gas, $Z = 1$. All real gases will deviate from this ideal behavior. Figure 1.1.3 shows the compressibility factor Z as a function of pressure for N_2 gas at different temperatures. A perfect ideal gas would have $Z = 1$ for all pressures and temperatures. For N_2 gas we see that at sufficiently low pressure $Z \to 1$ and that at higher temperature (purple curve), the gas behalves more like an ideal gas (dotted line).

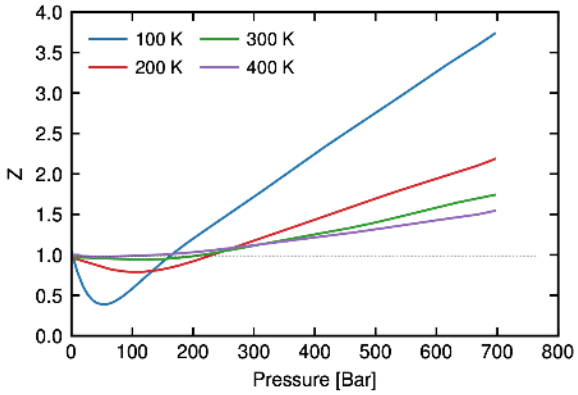


Figure 1.1.3: Compressibility factor of nitrogen gas as a function of pressure for different temperatures. The ideal gas limit is shown by the dotted line at Z=1.

In order to derive an equation of state for a non-ideal gas, we can consider a series expansion of the compressibility factor, $\mathbf{Z}$, in powers of the inverse molar volume, $\mathbf{1/\bar{V}}$:

$$Z = 1 + \frac{B_2}{\bar{V}} + \frac{B_3}{\bar{V}^2} + \frac{B_4}{\bar{V}^3} + \ldots \tag{1.1.8}$$

Equation 1.1.8 is called the **virial equation of state**, and $\mathbf{B_2}$ is called the **second virial coefficient**, $\mathbf{B_3}$ is called the third virial coefficient, etc…. The virial coefficients (B_2, B_3, …) are typically fit to experimental data and are temperature dependent. Notice that for a perfect ideal gas, the second and higher virial coefficients are all zero. The virial equation of state works well to describe any gas, but has the drawback of needing the virial coefficients from fitting to experimental data.

For gases that exhibit small deviations from ideal gas behavior, we can truncate Equation 1.1.8 to include just the second virial coefficient:

$$Z \approx 1 + \frac{B_2}{\bar{V}} \tag{1.1.9}$$

The second viral coefficient, $\mathbf{B_2}$ is related to the interactions between atoms described by a potential energy function $U(r)$, where r is the distance between atom pairs. For a dilute system of non-polar molecules, the relationship between the second virial coefficient and the potential energy is

$$B_2 = N_A \frac{1}{2} \int_0^\infty \left[1 - e^{-U(r)/k_B T}\right] 4\pi r^2 dr \tag{1.1.10}$$

where $\mathbf{N_A}$ is Avogadro's number, $\mathbf{k_B}$ is Boltzmann's constant, and $\mathbf{T}$ is the temperature. In most cases, we cannot analytically solve the integral in Equation 1.1.10. Note that in the absence of interactions, $U(r) = 0$, then from Equation 1.1.10, $B_2 = 0$ and the gas behaves like an ideal gas as we would expect for non-interacting gas molecules.

See Practice Problems 1.1.5 — 1.1.7.

1.1.3: Examples

Example 1.1.1

Classify each of the following systems as either open, closed, or isolated. (a) A red blood cell, (b) a gas in a piston without valves, (c) boiling water in a kettle on the stove, (d) A closed Thermos flask of hot coffee (approximately).

Solution

(a) open; (b) closed; (c) open; (d) isolated

Example 1.1.2

Classify each of the following properties as intensive or extensive: (a) molar mass, (b) pressure, (c) temperature, (d) mass

Solution

(a) intensive; (b) intensive; (c) intensive; (d) extensive

Example 1.1.3

A Bellingham homebrewer collects the amount of gas evolved during the fermentation process. Later, the brewer measures the volume of gas to be 0.64 L at a cold temperature of 12.3 °C and 1 atm. Assuming ideal gas behavior, what was the volume of the gas at the fermentation temperature of 37.0 °C and 1 atm.

Solution

We use the ideal gas equation: PV=nRT to set up a ratio between the low temperature and high temperature system:

$$\frac{V_1}{V_2} = \frac{T_1}{T_2} \tag{1.1.11}$$

$$\frac{0.64\ \text{L}}{V_2} = \frac{285.45\ \text{K}}{310.15\ \text{K}} \tag{1.1.12}$$

$$V_2 = 0.695\ \text{L} \tag{1.1.13}$$

1.1.4: Practice problems

Problem 1.1.1. Classify each of the following systems as either open, closed, or isolated. (a) perfectly insulated water heater, (b) a glass thermometer (c) the universe (d) soup cooking on a stove (e) the earth (f) automobile (g) a sealed reaction flask

Problem 1.1.2. Classify each of the following properties as intensive or extensive: (a) density, (b) force, (c) molar volume, (d) heat.

Problem 1.1.3. Under which of the following sets of conditions would you expect a real gas to be adequately described by the ideal gas model (a) low pressure and low temperature; (b) low pressure and high temperature, (c) high pressure and high temperature, and (d) high pressure and low temperature.

Problem 1.1.4. An ideal gas in a piston is originally at a pressure of 118.0 atm and 85 °C. When the piston expands, its final volume, pressure, and temperature were 3.5 L, 1.0 atm, and 45 °C, respectively. What was the initial volume of the gas?

Problem 1.1.5. At 300 K, the second virial coefficient (B_2) of CO_2 gas is -120.5 cm^3 mol^{-1} , for methane gas, CH_4, the second virial coefficient is -41.9 cm^3 mol^{-1} , and for N_2 gas the second virial coefficient is -4.2 cm^3 mol^{-1} . Rank these gases from most ideal gas to least idea gas at this temperature? Explain your reasoning.

Problem 1.1.6. Calculate the pressure of methane at 398.15 K if the molar volume is 0.2 L mol^{-1}, given that the second virial coefficient (B_2) of methane is -0.0163 L mol^{-1}. Compare your results with that obtained using the ideal gas equation. Is methane more or less compressible than an ideal gas at this temperature? (Assume that all other higher order virial coefficients can be neglected).

Problem 1.1.7. The **Boyle temperature** is the temperature at which the coefficient B_2 is zero. Therefore, a real gas behaves like an ideal gas at this temperature. **(a)** give a physical interpretation of this behavior. **(b)** Calculate the Boyle temperature for a gas whose second virial coefficient has the following form: $B_2 = a - \frac{b}{T}$ with the experimentally determined second virial coefficient measured at the following temperatures:

Second virial coefficient (B_2) (L mol^{-1})	Temperature (K)
-0.0237	292.95
-0.0231	296.15
-0.0228	298.15
-0.0218	303.15
-0.0201	313.15
-0.0185	323.15
-0.0117	373.15
-0.0065	423.15

This page titled 1.1: Thermodynamic Variables and Equations of State is shared under a CC BY-NC-SA 4.0 license and was authored, remixed, and/or curated by Jonathan Gutow.

- **1.1: Thermodynamic Variables and Equations of State** by Serge L. Smirnov and James McCarty is licensed CC BY-NC-SA 4.0.

1.2: The First Law of Thermodynamics

Based on "The First Law of Thermodynamics" by Serge L. Smirnov and James McCarty, LibreTexts is licensed under CC BY-NC-SA .

Systems can undergo a change of state from some initial state to a final state accompanied by a change in the system's energy. In this chapter, we analyze two types of energy: heat and work. This leads to a presentation of the first law of thermodynamics that deals with the conservation of energy, stating that any changes in the total internal energy of the system must be due to exchanges of either heat or work with the surroundings. Emphasis is placed on ideal gases because their equation of state is known. We also introduce an important property of a material, the heat capacity, that allows us to calculate the change in temperature as a function of heat. Finally, the concept of enthalpy is introduced that plays an important role in chemical reactions.

Learning Objectives

- Be able to explain and give some examples of state properties.
- Be able to define heat and work and understand heat and work are types of energy.
- Understand that heat and work are path-dependent (not state properties).
- Understand that energy is conserved: changes in the total internal energy must be due to either heat flow between the system and the surroundings or work being done by the system on the surroundings or the surroundings on the system.
- Be able to calculate the change in energy, enthalpy, work and heat exchange for the compression/expansion of an ideal gas and generalize these observations to other systems.

1.2.1: State properties and the internal Energy (U)

Previously, we introduced the concept of an equation of state that relates **state** properties (also called **state** variables or **state** functions). **State properties** describe the thermodynamic state of the system in terms of quantifiable observables such as temperature, pressure, volume, and number of moles for an ideal gas.

An important feature of state properties is that they are independent of the system's history. In other words, if the system is changed from some *initial* state to a *final* state, the corresponding change in any state function does not depend on the path taken from the *initial* to *final* state or on any intermediate states. An example of a state property is the **total internal energy** of the system, which we will give the symbol **U**. The total internal energy includes the translational, rotational, vibrational, electronic, and nuclear energies of all the particles, as well as the energy due to intermolecular interactions.

Figure 1.2.1 shows a schematic energy diagram of changing the system from some initial state *A* into some final state *B*.

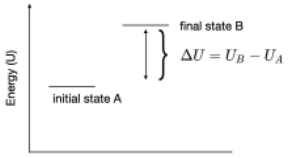


Figure 1.2.1: The change in internal energy (U) in going from some initial state A to some final state B does not depend on the process of going from A to B but only on the difference in energy between A and B.

Notice that the overall change in energy, ΔU does not depend on how the system was change from $A \rightarrow B$. For state variables we write the change in energy

$$\Delta U = U_f - U_i \tag{1.2.1}$$

As an example, consider a piston containing an ideal gas as shown in figure 1.2.2:

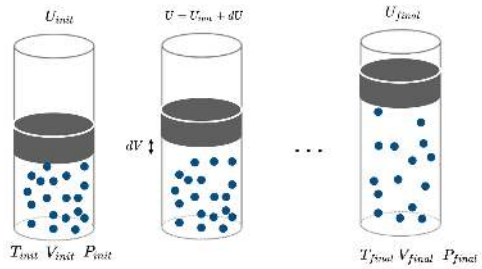


Figure 1.2.2: A gas at an initial temperature, pressure, and volume has an initial energy given by U_{init}. Expanding the piston an infinitesimal amount dV, the infinitesimal change in energy is dU. After expansion of the gas the system is in a new state with a different temperature, volume, pressure. The final energy is U_{final}.

Since the molecules do not interact, the total internal energy depends only on the kinetic energy of all the gas molecules, which is related to the temperature. We now expand the piston through a series of infinitesimal steps such that the temperature of the gas changes as the volume increases. At each infinitesimal step, the infinitesimal change in the internal energy is dU. Summing over all the infinitesimal steps gives the total change in internal energy as

$$\int_{U_i}^{U_f} dU = U_f - U_i = \Delta U \tag{1.2.2}$$

Mathematically, **U** is an *exact differential* (discussed later), meaning that integration from an initial state to a final state is independent of the path. For any state property dz, the differential is exact, and we can write:

$$\int_{z_i}^{z_f} dz = \Delta z \tag{1.2.3}$$

Equation 1.2.3 will serve as a definition of a state property since all state properties are exact differentials because they are independent of the path.

1.2.2: Work

We have seen how the total internal energy is a state property of a system. At this point, we might ask ourselves what would be an example of a quantity that is *not* a state property? One such example would be the work done by the system in going from an initial to a final state. **Work** is the physical activity directed towards the production of accomplishing something. Work can be *performed on* the system by the surroundings, or work can be *done by* the system on the surroundings; however, work is not an intrinsic property of the system itself and is not a state property. The amount of work performed will depend on the path taken to change the state from some initial state to some final state. As an example, we can consider a hiker walking in the Sehome Arboretum. Figure 1.2.3 shows the situation of a hiker starting at some initial position *A* and reaching the final position B by two different paths. Because these paths are different, the hikers will have performed a different amount of work in traveling from point A to point B, depending on the path taken.



Figure 1.2.3: Two hikers in the Sehome Arboretum travel from the same initial point **A** to the same final point **B**, but they travel by different paths. Because the paths differ, the hikers will have performed a different amount of work in traversing from A to B.

In classical mechanics the work is defined as the force times the distance. For an infinitesimal displacement $\mathbf{dx}$ the work is

$$\delta w = F \cdot dx \tag{1.2.4}$$

where F is the applied force.

Note

Note: The quantity δw denotes an infinitesimal increment of work. It should be noted that work is not a state function, meaning that the differential is inexact and Equation 1.2.3 cannot be applied. Instead, we write the total work over a path taken from some initial state to some final state as:

$$w = \int_{path} \delta w \tag{1.2.5}$$

Because the differential δw is *inexact*, the integral over different paths with the same end points will be different.

In thermodynamics we generalize this concept of work to consider different types of work summarized in Table 1.2.1.

Table 1.2.1: Various types of work and their mathematical expressions

Types of work	δw	Generic force, displacement
mechanical work	F · dx	F is the force, dx is the distance
Surface work	γ · dA	γ is the surface tension, dA is the change in area
Electrical work	Q · dφ	Q is the electric charge, dφ is the electric potential change
Gravitational work	mg · dh	mg is the gravitational force, dh is the change in height
Stretching work	τ · dL	τ is the tension, dL is the change in length
Expansion (compression)	P · dV	P is the pressure, dV is the change in volume

We will mainly focus our attention on the expansion (compression) type work of work (sometimes called PV-work) of a gas in a cylinder. Figure 1.2.4 shows the situation of a gas in a cylinder with a piston with some opposing, external pressure, $\mathbf{P_{ex}}$, acting on the gas. We will assume the piston operates without friction and the piston head (sealing disk) is massless.



Figure 1.2.4: A gas in a cylinder with a piston. An external pressure pushing down on the piston acts to oppose the expansion of the gas. The assumption when this system expands or contracts is that the piston is frictionless and massless.

Because the external pressure is pushing against the gas (the direction of the force is pointing down on the piston), we define the work of expansion as:

$$\delta w \equiv -P_{ex} \cdot dV \tag{1.2.6}$$

where $\boldsymbol{\delta w}$ is some infinitesimal amount of work and $\mathbf{dV}$ is an infinitesimal change in the volume due to expansion or compression of the piston. Equation 1.2.6 is the definition of the work of expansion/compression of a gas. Let's look at some examples for how to calculate the work for a gas in a cylinder.

1.2.2.1: Example 1: Expansion of a gas against a constant pressure

As our first example, we consider the expansion of a gas against a constant pressure. The situation is shown in figure 1.2.5. Initially, two masses oppose the piston. Removal of one of the masses, causes the gas in the cylinder to expand against the constant pressure due to the remaining mass from an initial volume $\mathbf{V_i}$ to a final volume $\mathbf{V_f}$.

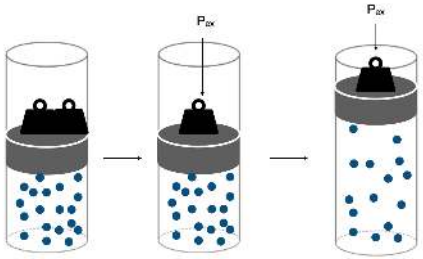


Figure 1.2.5: **Expansion of a gas against a constant pressure.** A gas is held at an initial volume $\mathbf{V_i}$ by two masses on a piston. Upon removal of one of the masses, the gas expands to a new volume $\mathbf{V_f}$ against a constant pressure $\mathbf{P_{ext}}$.

The total work performed by the gas can be calculated by integrating Equation 1.2.6

$$w = -\int_{V_i}^{V_f} P_{ext} \cdot dV \tag{1.2.7}$$

Because the external applied pressure in this case is constant, it can be taken out of the integral to give:

$$\begin{aligned} w &= -P_{ext} \int_{V_i}^{V_f} dV \\ &= -P_{ext}\,\Delta V \end{aligned} \tag{1.2.8}$$

where $\Delta V = (V_f - V_i)$. Notice that in the last line we have used the fact that the volume is a state variable so that $\Delta V = \int dV$.

Key Result: The work performed during the expansion of a gas against a constant external pressure is $w = -P_{ext} \cdot \Delta V$

See Practice Problem 1.2.1.

1.2.2.2: Example 2: Free expansion of a gas against a vacuum

We now consider a slightly different situation when a gas is allowed to freely expand into a vacuum. The situation is illustrated in figure 1.2.6. A gas is compressed to a volume $\mathbf{V_i}$ by a piston that is held in place by a mass, and a vacuum is created by removal of air from the space above the piston. When the mass is removed, the gas will freely expand against the vacuum to fill the cylinder to a final volume of $\mathbf{V_f}$.

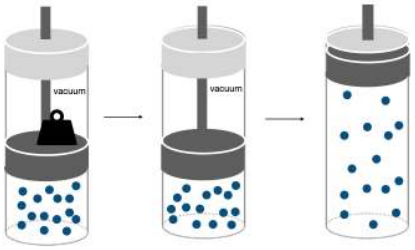


Figure 1.2.6: **Expansion of a gas into a vacuum.** In the cylinder on the left, an applied pressure is used to compress a gas, and a vacuum is created in the space above the piston. When the weight is removed (middle cylinder), the compressed gas will expand from an initial volume $\mathbf{V_i}$ against the vacuum until it occupies the available space (right cylinder) with final volume $\mathbf{V_f}$.

We can again use Equation 1.2.6 to obtain:

$$w = -P_{ext} \cdot \Delta V \tag{1.2.9}$$

However, here we note that the external pressure $P_{ext} = 0$ because the gas is expanding into a vacuum. Thus, the work performed by the expansion is $w = 0$.

> Key Result: There is no work performed in the free expansion of a gas against a vacuum. $w = 0$.

See Practice Problems 1.2.2 and 1.2.3.

1.2.2.3: Work is not a state property

Notice that in the first example the work performed in expanding the gas was $w = -P_{ext} \cdot \Delta V$, but in the second example, expanding the gas to the same final volume against a vacuum resulted in no work being performed. Thus, we see that the amount of work being performed *depends on the path taken* and hence work is not a state property.

Note: In this book we adopt the convention that work being performed **on the system** by the surroundings is positive. This means that work being performed **by the system** on the surroundings will be negative by convention. Work being done on the system by the surrounding is shown on the right of figure 1.2.6 with an arrow showing the direction of work pointing from the surroundings to the system. The left of figure 1.2.6 shows the situation of work being performed by the system with an arrow pointing from the system to the surroundings. For the situation on the left, the work will have a negative sign.

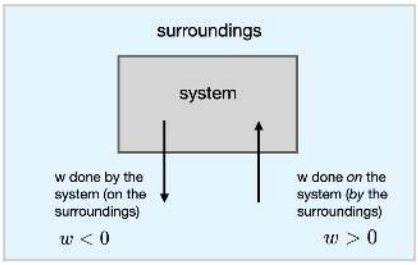


Figure 1.2.6 : Sign convention for work. Work performed by the system on the surrounding is depicted by an arrow pointing from the system to the surroundings and has a negative sign by convention. Work performed on the system (by the surroundings) is depicted by an arrow pointing from the surroundings into the system and is positive by convention.

1.2.3: Heat

Heat is another type of energy that can flow across the system boundary causing the system to change its state. As an example we can consider the situation shown in figure 1.2.7 of two equal volumes of the same liquid: one at 25 °C and one at 75 °C. If the two containers are brought into thermal contact, heat will flow out of the hotter (75 °C) liquid into the cooler (25 °C) liquid until thermal equilibrium is reached and both liquids reach the same final temperature.

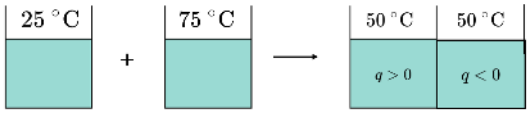


Figure 1.2.7: When two systems at different temperature are brought into thermal contact, heat will flow from the hotter system into the colder system until the two systems are at thermal equilibrium. The illustration is for the special case where the two systems have the same heat total heat capacity, leading to a final temperature half-way between the two initial temperatures.

1.2.3.1: Heat is not a state property

Just like work, heat is not a state property, and the amount of heat flow into or out of the system depends on the path taken from the initial state to the final state. We will use the symbol q to represent heat.

Note: In this book we adopt the same sign convention that we used for work. Heat being **absorbed by the system** from the surroundings will be defined as positive and represented with an arrow pointing from the surroundings to the system to indicate the direction of heat flow. On the other hand, heat **given off by the system** into the surroundings will have a negative sign and will be depicted with an arrow pointing from the system into the surroundings as shown in figure 1.2.8.

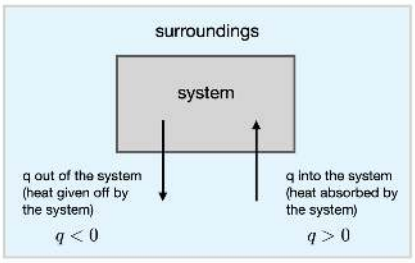


Figure 1.2.8: **Sign convention for heat.** Heat flowing out of the system into the surroundings (exothermic) is depicted by an arrow pointing form the system to the surroundings and has a negative sign by convention. Heat flowing into the system from the surroundings (endothermic) is depicted by an arrow pointing from the surroundings into the system and is positive by convention.

1.2.3.2: The Zeroth Law of Thermodynamics

The concept that heat flows from hot to cold establishes what is known as the **zeroth law of thermodynamics**. The zeroth law states that if system A is in thermal equilibrium with system B, and system B is in thermal equilibrium with system C, then system A must also be in thermal equilibrium with systems C. Figure 1.2.9summarizes the zeroth law of thermodynamics.

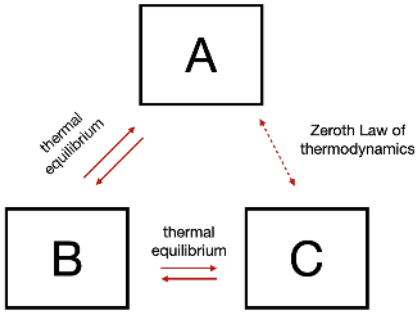


Figure 1.2.9: The Zeroth Law of Thermodynamics establishes that if two systems (A and B) are in thermal equilibrium with each other and another system (C) is brought into thermal equilibrium with one of the systems (B), then C is also in thermal equilibrium with system A.

Although conceptually simple, the zeroth law is important because it formally establishes temperature as a well-defined quantity.

1.2.4: First Law of Thermodynamics

Having defined **heat** and **work** as types of energy, we are now in a position to state the **first law of thermodynamics**. The first law states that the change in energy (ΔU) of a system is equal to the sum of the work done on the system (w) and heat (q) put into the system. Mathematically, we can express the first law as:

$$\Delta U = q + w \tag{1.2.10}$$

We see from Equation 1.2.10that the first law of thermodynamics is a statement about the **conservation of energy**. In order for the energy of the system to change, energy must be transferred to/from the surroundings in the form of either heat or work.

For dealing with infinitesimal changes of energy (dU) the first law can be written in differential form:

$$dU = \delta q + \delta w \tag{1.2.11}$$

1.2.4.1: Reversible vs. Irreversible Processes

Both **Example 1** and **Example 2** above are examples of an *irreversible* process, meaning that the expansion against a constant pressure or against a vacuum occurs spontaneously in one direction, but the reverse process does not occur spontaneously. This directionality of spontaneous change results from the fact that the system is not maintained at equilibrium during the expansion. When the gas is expanding, the pressure inside is not equal to the external applied pressure causing a net force to push the gas molecules into the larger volume.

Imagine the equilibrium situation shown in figure 1.2.10 where the internal pressure of the gas is equal to the external pressure applied by the piston.

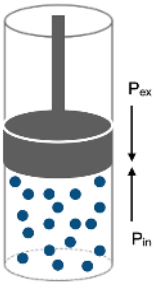


Figure 1.2.10: A gas in a cylinder at equilibrium with the surroundings. At equilibrium the pressure exerted by the gas on the piston ($\mathbf{P_{in}}$) is equal and opposite to the pressure exerted by the surroundings on the piston ($\mathbf{P_{ex}}$).

We could now consider expanding the gas through a series of infinitesimal steps where equilibrium is maintained throughout the expansion by adjusting the external pressure so that it is always equal to the internal pressure of the gas. Note that in this case the external applied pressure will not be constant since it is adjusted to maintain equilibrium at each step. The situation is illustrated in figure 1.2.11. At each infinitesimal step, there is no net force pushing the gas to change volume in any one direction so the process is said to be **reversible**.

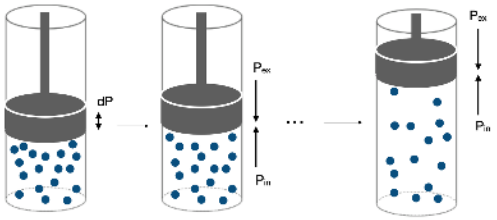


Figure 1.2.11: Reversible expansion of a gas. A gas in a cylinder initially at volume $\mathbf{V_i}$ is slowly expanded to a final volume $\mathbf{V_f}$ such that the internal pressure $\mathbf{P_{in}}$ remains equal and opposite to the external pressure $\mathbf{P_{ex}}$ at each infinitesimal step. During a reversible process, quasi-equilibrium is maintained throughout.

A **reversible process** is a process which is at equilibrium at each infinitesimal step. Because work depends on the path (not a state property), the amount of work performed (and thus also the amount of heat flow) will depend on if the process occurs reversibly or irreversibly. As an example we will consider the *reversible* expansion of a gas.

1.2.4.1.1: Example 3: Isothermal Reversible Expansion of a Gas

Consider the isothermal reversible expansion of a gas. The situation is similar to the situation illustrated in figure 1.2.11. The gas is initially at a volume $\mathbf{V_i}$ and is expanded reversibly to a final volume of $\mathbf{V_f}$ while maintaining a constant temperature. Because the processes is reversible, the external pressure ($\mathbf{P_{ext}}$) is always equal to the internal pressure of the gas ($\mathbf{P_{in}}$) which can both be replaced by the variable $P = P_{in} = P_{ext}$. The work is again calculated by integrating Equation 1.2.6:

$$w = -\int_{V_i}^{V_f} P \cdot dV \tag{1.2.12}$$

Note that in this case, we cannot take the variable $\mathbf{P}$ outside of the integral because the pressure is not constant but depends on the volume during the expansion. In order to proceed, we need to know how the pressure $\mathbf{P}$ depends on the volume $\mathbf{V}$. For an ideal gas, we know the relation from the ideal gas equation of state:

$$P = \frac{nRT}{V} \tag{1.2.13}$$

Substituting this into Equation 1.2.12 gives:

$$w = -\int_{V_i}^{V_f} \frac{nRT}{V} \cdot dV \tag{1.2.14}$$

We can now use the fact that $\mathbf{n}$ (constant number of moles), $\mathbf{R}$, and $\mathbf{T}$ (isothermal = constant temperature) are constants and can be pulled out of the integral so that the integrand only depends on the volume:

$$w = -nRT \int_{V_i}^{V_f} \frac{dV}{V}$$
$$= -nRT \ln\left(\frac{V_f}{V_i}\right) \tag{1.2.15}$$

Note

We have used the integral: $\int \frac{1}{x} dx = \ln x + C$

Key Result: For the *reversible* isothermal expansion of a gas, the work performed is $w = -nRT \ln\left(\frac{V_f}{V_i}\right)$

See Practice Problems 4 and 5

Theorem 1.2.1: Maximum Work Theorem

A comparison of Equation 1.2.15 with the result above from Equation 1.2.8 shows that the amount of work performed is different if the process is performed reversibly than if the process is performed irreversibly. Figure 1.2.12 shows a plot of the Pressure vs. the Volume for the two different expansions. A plot of P vs. V is called a PV-diagram and the work performed is the area under the curve. Notice that the work performed (area under the curve) is *greater* for the reversible expansion than the work performed for the irreversible expansion. It turns out that for any reversible process, the amount of work performed is maximized as compared to the equivalent irreversible processes. This principle is called the **maximum work theorem.**

Key result: The **maximum work theorem** states that for all processes leading from a specified initial state to some specified final state, the work performed is a maximum for a reversible process.

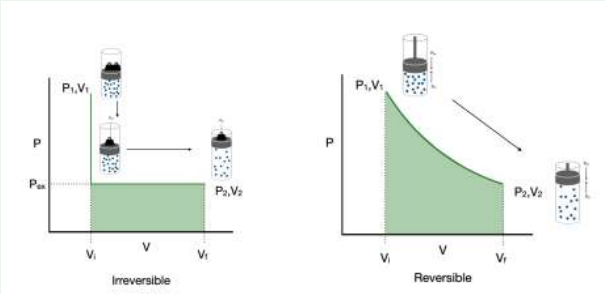


Figure 1.2.12: **Left**: The situation described in Example 1 of the irreversible expansion of a gas against a constant pressure. **Right**: The situation described in Example 3 of the reversible expansion of a gas. The area under the curve between the initial state and final state is the magnitude of the work performed by the piston. Note that that area under the curve is always greater in the reversible process.

1.2.5: The Heat Capacity

A useful property of a system is the **heat capacity**. The **heat capacity** is the amount of energy (heat) required to raise the temperature of a material by some infinitesimal amount dT.

$$\delta q = C \cdot dT \tag{1.2.16}$$

Equation 1.2.16 says that the amount of heat transferred to the systems (δq) is proportional to the change in temperature (dT) and the proportionality factor is the **heat capacity** of the material. How much the temperature rises in a material as it is heated depends on:

- the amount of heat delivered (q)
- the amount of substance present
- the chemical nature and physical state of the material

- the conditions under which the energy is added

Integrating both sides of Equation 1.2.16 from an initial temperature $\mathbf{T_i}$ to a final temperature $\mathbf{T_f}$ gives:

$$q = \int_{T_i}^{T_f} C \cdot dT \tag{1.2.17}$$

In general, the heat capacities $\mathbf{C}$ also depend on the temperature. However, for an ideal gas, the heat capacity is independent of temperature and can be taken out of the integral to give:

$$q = C \int_{T_i}^{T_f} dT$$

$$q = C\Delta T \tag{1.2.18}$$

where $\Delta T = T_f - T_i$ and we have used the fact that temperature is a state property.

For a gas, the heat capacity depends on whether the gas undergoes a change of state at constant volume conditions (isochoric) or at constant pressure conditions (isobaric).

We denote the heat capacity at constant volume as C_v and the heat capacity at constant pressure as C_p. At constant volume we have:

$$\delta q_v = C_v \cdot dT \tag{1.2.19}$$

and at constant pressure we have:

$$\delta q_p = C_p \cdot dT \tag{1.2.20}$$

where the subscript indicates whether we are under conditions of constant volume or pressure. Rearranging Equation 1.2.19 and Equation 1.2.20 we see that the heat capacity is given by:

$$C_v = \left(\frac{\partial q}{\partial T}\right)_V \tag{1.2.21}$$

and at constant pressure we have:

$$C_p = \left(\frac{\partial q}{\partial T}\right)_P \tag{1.2.22}$$

The heat capacities C_p and C_v are the slope of the curve of heat vs. temperature.

1.2.6: Enthalpy

We saw above that work and heat depend on the path taken from an initial state to a final state. Let's consider in more detail the *reversible* expansion/compression of a gas in a cylinder under the conditions of constant pressure (isobaric). From the first law of the thermodynamics we can write the change of energy as:

$$dU = \delta q_p + \delta w$$

$$dU = \delta q_p - P \cdot dV \tag{1.2.23}$$

where the subscript on δq_p indicates we are under conditions of constant pressure (isobaric) and we have used the fact that the reversible work is $\delta w = -P \cdot dV$. Rearranging Equation 1.2.23 for δq_p we have:

$$\delta q_p = dU + PdV$$

$$\delta q_p = d(U + PV) \tag{1.2.24}$$

where the second line is true because the pressure $\mathbf{P}$ is constant. We now introduce a new quantity called the **enthalpy** that gets the symbol $\mathbf{H}$ that is defined as the energy + PV:

$$H = U + PV \tag{1.2.25}$$

Equation 1.2.25 is the definition of the enthalpy. Substituting Equation 1.2.25 into Equation 1.2.24 gives:

$$\delta q_p = dH \tag{1.2.26}$$

or, upon integrating both sides:

$$q_p = \Delta H \tag{1.2.27}$$

From Equation 1.2.26 and Equation 1.2.27, we see that the change in enthalpy of the system is equal to the amount of heat gained by the system under the conditions of constant pressure.

Key result: Enthalpy is defined as: $H = U + PV$

Key result: The change in enthalpy of the system is equal to the heat gained by the system **at constant pressure**: $q_p = \Delta H$

Note

Note: Although heat is not a state property and thus depends on the path, the enthalpy H *is* a state property and so the change of enthalpy ΔH will be *independent* of the path taken.

1.2.7: Heat Capacity Revisited

Constant Pressure

Recall that the heat capacity for a gas depends on if the conditions are isobaric (constant P) or isochoric (constant V). At constant pressure, we copy the expression from Equation 1.2.20 above:

$$\delta q_p = C_p \cdot dT$$

We have also shown that the heat gained at constant pressure is equivalent to the change in enthalpy $\mathbf{dH}$ (Equation 1.2.26). Substituting Equation 1.2.26 into Equation 1.2.20 gives:

$$dH = C_p \cdot dT \tag{1.2.28}$$

or, rearranging in terms of C_p:

$$C_p = \left(\frac{\partial H}{\partial T}\right)_P \tag{1.2.29}$$

Equation 1.2.29 shows that the slope of the enthalpy $\mathbf{H}$ with respect to the temperature $\mathbf{T}$ at constant pressure is the heat capacity $\mathbf{C_p}$.

Constant Volume

At constant volume, we copy the expression from Equation 1.2.19 above:

$$\delta q_v = C_v \cdot dT \tag{1.2.30}$$

From the first law of thermodynamics we have the change in energy $\mathbf{dU}$ is given by: $dU = \delta q_v - PdV$ where the subscript $\delta \mathbf{q_v}$ indicates we are at constant volume conditions. Since the volume is constant, there is *no work being performed* since $\mathbf{dV = 0}$. *At constant volume conditions* we can write:

$$dU = \delta q_v \tag{1.2.31}$$

since all the change in energy at constant volume is due to heat flow (no work). Substituting Equation 1.2.31 into Equation 1.2.30 gives:

$$dU = C_v \cdot dT \tag{1.2.32}$$

or, rearranging in terms of $\mathbf{C_v}$:

$$C_v = \left(\frac{\partial U}{\partial T}\right)_V \tag{1.2.33}$$

Equation 1.2.33 shows that the slope of the energy $\mathbf{U}$ with respect to the temperature $\mathbf{T}$ at constant volume is the heat capacity $\mathbf{C_v}$.

Relation between C_v and C_p for an ideal gas

To relate $\mathbf{C_v}$ and $\mathbf{C_p}$ for an ideal gas, we begin with the definition of the enthalpy: $H = U + PV$. Recall that for an ideal gas, $PV = nRT$. Substituting the ideal gas law into the definition of the enthalpy gives:

$$H = U + nRT \tag{1.2.34}$$

Note that because we have used the ideal gas law, Equation 1.2.34 only applies to an ideal gas. Taking $\mathbf{n}$ and $\mathbf{R}$ to be constants, we can write the differential form of Equation 1.2.34 as:

$$dH = dU + nRdT \tag{1.2.35}$$

Substituting Equation 1.2.32 and Equation 1.2.28 into Equation 1.2.35 and dividing out the dT gives:

$$C_p = C_v + nR \tag{1.2.36}$$

Equation 1.2.36 relates the heat capacity at constant pressure $\mathbf{C_p}$ and the heat capacity at constant volume $\mathbf{C_v}$ for an ideal gas.

> Key result: For an ideal gas the heat capacity at constant pressure C_p and the heat capacity at constant volume C_v are related by $C_p = C_v + nR$

See Practice Problem 1.2.6.

1.2.8: Examples

Example 1.2.1

One mole of an ideal gas in a cylinder is initially held at 12 atm of pressure and 298 K. Calculate the work done by a piston if the gas is expanded against a constant external pressure of 1.0 atm while the temperature is kept constant at 298 K.

Solution

For the expansion of an ideal gas at constant external pressure the work is given by Equation 1.2.8

$w = -P_{ext} \cdot \Delta V$

First, we use PV=nRT to find the initial and final volumes of the gas:

$V_i = \frac{1 \text{ mole} \times 0.08206 \text{ L atm K}^{-1} \text{ mol}^{-1} \times 298 \text{ K}}{12 \text{ atm}}$

$V_i = 2.038 \text{ L}$

Note that the final pressure inside the cylinder is equal to the external pressure of 1.0 atm:

$V_f = \frac{1 \text{ mole} \times 0.08206 \text{ L atm K}^{-1} \text{ mol}^{-1} \times 298 \text{ K}}{1 \text{ atm}}$

$V_f = 24.45 \text{ L}$

This gives the total work as:

$w = -1.0 \text{ atm}(24.45 \text{ L} - 2.038 \text{ L})$

$w = -22.4 \text{ L atm}$

$w = -22.4 \text{ L atm} \times \frac{101.325 \text{ J}}{1 \text{ L atm}} = -2270 \text{ Joules}$

Notice in the final step we convert L atm to Joules, which is the more conventional energy units. Also notice that the sign of the work is *negative* by our convention because the system is doing work on the surroundings (expansion).

Example 1.2.2

During the reversible isothermal compression of 3.0 moles of an ideal gas at T=291 K, the pressure changes from 3.0 atm to 5.0 atm. Calculate the work done.

Solution

We use the fact that for the *reversible* isothermal expansion of a gas, the work performed is $w = -nRT\ln\left(\frac{V_f}{V_i}\right)$ (See Equation 1.2.15).

For an ideal gas at constant number of moles and constant temperature:

$\frac{V_f}{V_i} = \frac{P_i}{P_f}$

So the work (for an isothermal process) can be expressed in terms of the pressure as:

$w = -nRT\ln\left(\frac{P_i}{P_f}\right)$

$w = -3.0 \text{ moles } \times \ 8.314 \text{ J K}^{-1} \text{ mol}^{-1} \ \times 291 \text{ K } \ln\left(\frac{3.0}{5.0}\right)$

$w = 3707.6 \text{ Joules}$

Note that the work is *positive* by our convention since the surroundings is doing work on the system (compression).

Example 1.2.3

The molar heat capacity at constant volume of a monatomic idea gas is 3/2 R. How much heat must be added to raise the temperature of 2.0 moles of an ideal gas by 10 °C?

Solution

We use the fact that the heat at constant volume is given by Equation 1.2.19:

$\delta q_v = C_v \cdot dT$

Integrating both sides gives:

$q_v = C_v \Delta T$

Inserting the definition of the molar heat capacity $\bar{C}_v = C_v/n$ into our expression for the heat gives:

$q_v = n\bar{C}_v \Delta T$

where n is the number of moles. Now we solve for the heat:

$q_v = 2.0 \text{ moles } \times \ \frac{3}{2} \ \times 8.314 \text{ J K}^{-1} \text{ mol}^{-1} \ \times \ 10 \text{ K}$

$q_v = 249.42 \text{ Joules}$

1.2.9: Practice Problems

Problem 1.2.1. Consider an experiment where a gas is compressed isothermally (constant temperature) from an initial pressure of 1.0 atm and a volume of 3.0 L to a final pressure of 4.0 atm and a volume of 1.0 L. The temperature remains constant at 20.0 °C. Calculate the work done if the compression is performed in a single step against a constant external pressure of 4.0 atm. (Report your answer in Joules).

Problem 1.2.2. You are traveling in a space ship whose cabin volume is 10.0 m^3. The air inside the cabin is maintained at 1 atm and 298 K, suitable for human space travel. Suddenly, the cabin springs a leak, allowing 1.8 moles of gas to escape into the vacuum before you are able to repair the damage. Calculate **a)** q, **b)** w, and **c)** ΔU for this process, assuming that the walls of the cabin are perfect insulators (adiabatic).

Problem 1.2.3. Calculate the work done when 50.0 g of iron reacts with hydrochloric acid:

Fe (s) + 2 HCl (aq) → $FeCl_2$ (aq) + H_2 (g)

assuming the reaction takes place in **a)** a **closed** vessel of fixed volume, and **b)** an **open** beaker at 25 °C. (The atomic mass of iron is 55.85 g/mol)

Problem 1.2.4. In *Example 3* of the main text an expression was derived for the reversible isothermal expansion of an ideal gas. Now consider the reversible expansion of a gas under **isobaric** (constant P) conditions. Show that for the reversible isobaric expansion of an ideal gas the work is

$$w = -nR\Delta T \tag{1.2.37}$$

(Hint: start with the definition of the work of expansion as $dw = -P_{ex} \cdot dV$.)

Problem 1.2.5. Derive an expression for ΔH, ΔU, w, and q for the reversible expansion of an ideal gas under the following conditions: **a)** isobaric (Hint: see Problem 4), **b)** isochoric (constant V), **c)** isothermal (Hint: see Example 3), **d)** adiabatic (no heat flow, Hint: q=0).

Problem 1.2.6. The molar heat capacity for **liquid** methanol is $\bar{C}_v = 68.624$ J K^{-1} mol^{-1}. The density of methanol is 0.792 g/mL. How much heat is released when 50 mL of liquid methanol is cooled from 60 °C to 10 °C? If the process is performed in an open container, what is the change in enthalpy ΔH? (Hint: $\bar{C}_v \approx \bar{C}_p$ for a liquid).

This page titled 1.2: The First Law of Thermodynamics is shared under a CC BY-NC-SA 4.0 license and was authored, remixed, and/or curated by Jonathan Gutow.

- **1.2: The First Law of Thermodynamics** by Serge L. Smirnov and James McCarty is licensed CC BY-NC-SA 4.0.

1.3: Thermochemistry

In this chapter we apply the first law of thermodynamics and the concept of enthalpy to chemical reactions. At standard state conditions we can use tabulated heats of formation to calculate the change in enthalpy for any reaction. At temperatures other than standard conditions we use the temperature dependence of the enthalpy to derive an expression for the change in enthalpy of a reaction at any temperature in relation to a reference temperature.

Learning Objectives

- Understand how the first law of thermodynamics describes energy changes in chemical reactions.
- Be able to calculate the change in enthalpy for a reaction using the standard enthalpy of formation.
- Be able to calculate the change in enthalpy for a reaction at non-standard temperature from a reference value and reference temperature.

1.3.1: Thermochemistry: Heat of reaction

Chemical reactions almost always involve heat transfer. In an **exothermic reaction**, heat is given off during the reaction, meaning that heat is transferred from the system to the surroundings. In an **endothermic reaction**, heat is absorbed during the reaction, meaning that heat is transferred from the surroundings into the system. Recall that under the conditions of constant pressure, the amount of heat, $\mathbf{q_p}$, is equal to the change in enthalpy. Most laboratory and biochemical reactions occur under conditions of constant pressure and so we can equate the change in enthalpy of a reaction $\mathbf{\Delta_r H}$ with the **heat of the reaction**. The subscript in $\mathbf{\Delta_r H}$ indicates that we are here concerned with a chemical reaction and the change of enthalpy associated with that reaction.

Since enthalpy is a state function (does not depend on the path) we can write:

$$\Delta_r H = H_{\text{products}} - H_{\text{reactants}} \tag{1.3.1}$$

Equation 1.3.1 says that the change in enthalpy of a reaction is the difference in enthalpies of the products and reactants. Consider the following reaction of the dimerization of nitrogen dioxide to form dinitrogen tetroxide:

$$2\,\mathrm{NO_2(g)} \rightarrow \mathrm{N_2O_4(g)} \tag{Reaction I}$$

For this reaction, 2 moles of NO_2*(g)* react to form 1 mole of N_2O_4*(g)*. The molar change in enthalpy will be:

$$\Delta_r H = H(\mathrm{N_2O_4}) - 2H(\mathrm{NO_2}) \tag{1.3.2}$$

Notice that because we have two moles of reactant NO_2*(g)* for every one mole of product N_2O_4*(g)* we multiply the molar enthalpy of NO_2*(g)* by the stoichiometric coefficient 2. The absolute molar enthalpies of the individual reactants and products are not easily measured. Fortunately, because enthalpy is a state function, the change in enthalpy for the reaction will be the same no matter what path is taken from reactant to product. To calculate $\mathbf{\Delta_r H}$ for the reaction, we break the reaction into two intermediate steps, shown schematically in figure 1.3.1. We first break the reactants into their constituent elements at standard state and then form the products from their constituent elements in the standard state. The reason for breaking the reaction into these intermediate steps is that we can look-up tabulated values for the standard heats of formation for these reactions. We can then sum together the change in enthalpy for the individual steps to obtain the overall change in enthalpy.

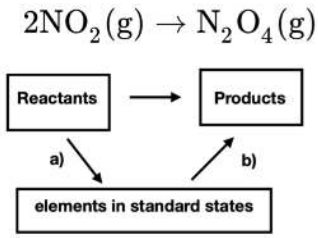


Figure 1.3.1: Schematic description of Hess's law. The total reaction is broken into two elementary steps. In step a) the reactants are broken into their constituent elements, and in step b) the products are formed from the constituent elements.

In our example, we first write the reaction for breaking reactant NO_2*(g)* into its elements at standard state:

$$2\,\mathrm{NO_2(g)} \rightarrow \mathrm{N_2(g)} + 2\,\mathrm{O_2(g)} \tag{Reaction I.a}$$

We can look up the change in molar enthalpy of formation, $\Delta_f \bar{H}^\circ$, for NO_2 *(g)*. Notice that the superscript $^\circ$ indicates standard state conditions. The change in enthalpy of formation, $\Delta_f H^o$ for NO_2*(g)* is for the formation of one mole of NO_2 *(g)* from its constituent elements as shown in this reaction:

$$\tfrac{1}{2}\mathrm{N_2(g)} + \mathrm{O_2(g)} \rightarrow \mathrm{NO_2(g)}$$

Notice that the $\Delta_r H^o$ for *Reaction I.a* above is -2 $\Delta_f H^o$ for NO_2 *(g)*.

Similarly, for the products we write the reaction for the formation of products from their constituent elements:

$$\mathrm{N_2(g)} + 2\,\mathrm{O_2(g)} \rightarrow \mathrm{N_2O_4(g)} \qquad \text{(Reaction I.b)}$$

We can look up in a table the value of $\Delta_f H^o$ for N_2O_4 *(g)*. Notice that the $\Delta_r H^o$ for Reaction I.b is equal to $\Delta_f H^o$ for N_2O_4 (g) as shown in this reaction:

$$\mathrm{N_2(g)} + 2\,\mathrm{O_2(g)} \rightarrow \mathrm{N_2O_4(g)}$$

Summing *Reaction I.a* and *Reaction I.b* gives the overall reaction:

a)	$2\mathrm{NO_2}(g) \rightarrow \cancel{\mathrm{N_2}(g)} + \cancel{2\mathrm{O_2}}$	$-2\Delta_f H(\mathrm{NO_2})$
b)	$\cancel{\mathrm{N_2}(g)} + \cancel{2\mathrm{O_2}}(g) \rightarrow \mathrm{N_2O_4}(g)$	$\Delta_f H(\mathrm{N_2O_4})$
Reaction I	$2\mathrm{NO_2}(g) \rightarrow \mathrm{N_2O_4}(g)$	$\Delta_r H^\circ$

and we can write the $\Delta_r H^o$ for the overall reaction as the sum of the two intermediate steps:

$$\Delta_r H^o = \Delta_f H^o(\mathrm{N_2O_4}) - 2\Delta_f H^o(\mathrm{NO_2}) \tag{1.3.3}$$

In general, we can write the change of enthalpy of a reaction at standard conditions as

$$\Delta_r H^o = \sum \nu \Delta_f H^o(\text{products}) - \sum \nu \Delta_f H^o(\text{reactants}) \tag{1.3.4}$$

where $\Delta_f H^o$ are the standard molar heats of formation, ν are the stoichiometric coefficients, and the sum is over the products minus the sum over the reactants. Equation 1.3.4 is a specific application of **Hess's law** which states that in a chemical reaction $\Delta_r H^o$ does not depend on the intermediate steps.

See Practice Problems 1.3.1 and 1.3.2.

1.3.2: Temperature dependence of heat of reaction

Hess's Law and Equation 1.3.4 allows us to calculate $\mathbf{\Delta_r H^\circ}$ at standard conditions using tabulated data for standard heats of formation. In order to calculate $\Delta_r H$ at non-standard state conditions, we need to know how $\Delta_r H$ varies with temperature. Recall that the slope of the enthalpy vs. temperature at constant pressure gives the heat capacity:

$$C_p = \left(\frac{\partial H}{\partial T}\right)_P \tag{1.3.5}$$

or, rearranging we get:

$$dH = C_p \cdot dT \tag{1.3.6}$$

For considering changes in $\Delta_r H$ with temperature, we replace $\mathbf{H}$ in Equation 1.3.6 with $\mathbf{\Delta_r H}$ to get:

$$d\Delta_r H = \Delta_r C_p \cdot dT \tag{1.3.7}$$

where $\mathbf{\Delta_r C_p}$ is the difference in heat capacities of products and reactants and is given by a Hess's Law-type analog:

$$\Delta_r C_p = \sum \nu C_p^{(\text{products})} - \sum \nu C_p^{(\text{reactants})} \tag{1.3.8}$$

where the sum is over the individual heat capacities of the products minus the reactants weighted by their stoichiometric coefficients. We integrate both sides of Equation 1.3.7 from an initial reference state to a final state:

$$\int_{T^\circ}^{T_2} d\Delta_r H = \int_{T^\circ}^{T_2} \Delta_r C_p \cdot dT$$

$$\Delta_r H_{T_2} - \Delta_r H_{T^\circ} = \int_{T^\circ}^{T_2} \Delta_r C_p \cdot dT$$

$$\Delta_r H_{T_2} = \Delta_r H_{T^\circ} + \int_{T^\circ}^{T_2} \Delta_r C_p \cdot dT \tag{1.3.9}$$

Equation 1.3.9 allows us to compute the $\mathbf{\Delta H}$ of a reaction at any non-standard temperature if we know how $\mathbf{\Delta_r C_p}$ depends on temperature. Usually this is determined experimentally and $\mathbf{\Delta_r C_p}$ is fit to a polynomial function that interpolates the data. However, if the heat capacity is independent of temperature (as it is for an ideal gas), we can take $\mathbf{\Delta_r C_p}$ out of the integral to obtain:

$$\Delta_r H_{T_2} = \Delta_r H_{T^\circ} + \Delta_r C_p \int_{T^\circ}^{T_2} dT$$

$$\Delta_r H_{T_2} = \Delta_r H_{T^\circ} + \Delta_r C_p (T_2 - T^\circ) \tag{1.3.10}$$

Equation 1.3.10 is known as **Kirchhoff's law** and is valid if $\mathbf{\Delta_r C_p}$ is independent of temperature. We can see schematically that Kirchhoff's law results from taking the reaction at T_2 and breaking it into three steps:

1. Heat/cool the reactant from T_2 to T° using $\Delta H = C_p^{reactants} \Delta T$.
2. Find $\Delta_r H$ of the reaction at T° using the tabulated heats of formation and Hess's law.
3. Cool/heat the products from T° back to T_2 using $\Delta H = C_p^{products} \Delta T$

Summing these three steps results in Kirchhoff's law Equation 1.3.10 where $\mathbf{\Delta_r C_p}$ is the difference in heat capacities between the products and reactants. figure $PageIndex2$ shows a schematic of this process.

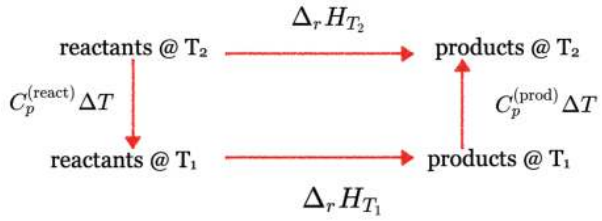


Figure 1.3.2: Schematic depiction of Kirchhoff's law: The $\Delta_r H$ at some non-standard temperature T_2 is calculated in a three-step process where in step 1) the reactants are heated/cooled from T_2 to T_1. In step 2) the reactants are converted into products at a reference temperature for which $\Delta_r H$ is known. In step 3) the products are cooled/heated from the reference temperature T_1 back to the temperature of interest T_2.

Note

In figure 1.3.2 C_p may be temperature dependent. In that case each temperature change step contribution to $\Delta_r H$ is replaced by $\int_{T_i}^{T_f} C_p(T) dT$. This results in a expression that collapses to the integral expression in equation 1.3.9:

$$\Delta_r H_{T_2} = \int_{T_2}^{T_1} C_p^{(reac)} dT + \Delta_r H_{T_1} + \int_{T_1}^{T_2} C_p^{(prod)} dT \implies \Delta_r H_{T_2} = \Delta_r H_{T_1} + \int_{T_1}^{T_1} \Delta_r C_p dT$$

See Practice Problem 1.3.3.

1.3.3: Examples

Example 1.3.1

Methane gas is burned in a Bunsen burner. Use Hess's law to calculate $\Delta_r H^\circ$ of the combustion of methane at 298 K and 1 bar. The standard molar enthalpies of formation at 298 K and 1 bar are:

CH_4 (g)	$\Delta_f \bar{H}^\circ$ = -74.85 kJ/mol

CO_2 (g)	$\Delta_f \bar{H}^\circ$ = -393.5 kJ/mol
H_2O (g)	$\Delta_f \bar{H}^\circ$ = -241.8 kJ/mol

Solution

For the combustion of methane, the balanced chemical reaction is:

$CH_4\,(g) + 2\,O_2\,(g) \rightarrow CO_2(g) + 2\,H_2O\,(g)$

From Equation 1.3.4:

$\Delta_r H^\circ = [\,\Delta_f H^\circ\,(CO_2) + 2\,\Delta_f H^\circ\,(H_2O)\,] - [\Delta_f H^\circ\,(CH_4) + 2\,\Delta_f H^\circ\,(O_2)]$

By convention, we assigne a value of zero to $\Delta_f \bar{H}^\circ$ for elements in their most stable allotropic state, so $\Delta_f \bar{H}^\circ$ (O2) = 0 at 298 K. Using the tabulated values of $\Delta_f H^\circ$:

$$\Delta_r H^\circ = [-393.5\ \text{kJ/mol} + 2(-241.8\ \text{kJ/mol})] - (-74.85\ \text{kJ/mol})$$

$$\Delta_r H^\circ = -802.3\ \text{kJ/mol}$$

Example 1.3.2

Calculate the value of $\Delta_r \bar{H}$ for the dimerization of nitrogen dioxide to form dinitrogen tetroxide at 600 K.

$$2\,NO_2(g) \rightarrow N_2O_4(g) \tag{1.3.11}$$

The standard molar enthalpies of formation and molar heat capacities are:

$NO_2(g)$	$\Delta_f \bar{H}^\circ$ = 33.9 kJ/mol	$\bar{C}_p$ = 37.9 J K^{-1} mol^{-1}
$N_2O_4(g)$	$\Delta_f \bar{H}^\circ$ = 9.7 kJ/mol	$\bar{C}_p$ = 79.1 J K^{-1} mol^{-1}

Solution

First, we use Hess's law to find $\Delta_r \bar{H}^\circ$ of the reaction at standard conditions. From Equation 1.3.3 we have:

$$\Delta_r H^\circ = \Delta_f \bar{H}^\circ(N_2O_4) - 2\Delta_f \bar{H}^\circ(NO_2)$$

$$\Delta_r H^\circ = 9.7\ \text{kJ/mol} - 2(33.9\ \text{kJ/mol}$$

$$\Delta_r H^\circ = -58.1\ \text{kJ/mol}$$

To find $\Delta_r \bar{H}$ at 600 K we use Equation 1.3.10. Assuming the molar heat capacity is independent of temperature we use:

$$\Delta_r \bar{H} = \Delta_r H_{T^\circ} + \Delta_r C_p (T_2 - T^\circ)$$

We find $\Delta_r C_p$ from Equation 1.3.8:

$$\Delta_r \bar{C}_p = \bar{C}_p(N_2O_4) - 2\bar{C}_p(NO_2)$$

$$\Delta_r \bar{C}_p = 79.1\ \text{J K}^{-1}\ \text{mol}^{-1} - 2(37.9\ \text{J K}^{-1}\ \text{mol}^{-1})$$

$$\Delta_r \bar{C}_p = 3.3\text{J K}^{-1}\ \text{mol}^{-1}$$

$$\Delta_r \bar{C}_p = 0.0033\text{kJ K}^{-1}\ \text{mol}^{-1}$$

Finally, we compute $\Delta_r \bar{H}$ at 600 K:

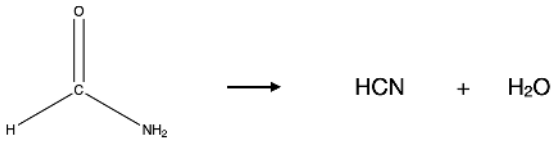
$$\Delta_r \bar{H} = -58.1\ \text{kJ/mol} + 0.0033\text{kJ K}^{-1}\ \text{mol}^{-1}(600 - 298)$$

$$\Delta_r \bar{H} = -57.1\ \text{kJ/mol}$$

Notice that $\Delta_r \bar{H}$ at 600 K is not very different from $\Delta_r H^\circ$ at 298 K. For gas-phase reactions, the change in enthalpy due to the molar heat capacities tends to cancel between the reactants and products.

1.3.4: Practice Problems

Problem 1.3.1. Formamide ($HCONH_2$) is used in the industrial production of hydrogen cyanide. Calculate the change in enthalpy for the dehydration of formamide to form water and hydrogen cyanide.



using the tabulated heat of formation data:

Water (g)	$\Delta_f \bar{H}^\circ$ = -241.8 kJ/mol
Formamide	$\Delta_f \bar{H}^\circ$ = -188.79 kJ/mol
Hydrogen cyanide	$\Delta_f \bar{H}^\circ$ = 129.286 kJ/mol

Problem 1.3.2. Alcohol fermentation is the process in which carbohydrates are broken down into ethanol and carbon dioxide. The overall reaction is

$C_6H_{12}O_6$ (s) → 2 C_2H_5OH (l) + 2 CO_2 (g)

Given that $\Delta_f \bar{H}^\circ$ for C_2H_5OH (l) is -277.0 kJ/mol, $\Delta_f \bar{H}^\circ$ for CO_2 (g) is -393.5 kJ/mol, and $\Delta_f \bar{H}^\circ$ for $C_6H_{12}O_6$ (s) is -1274 kJ/mol, calculate $\Delta_r H^\circ$ for the fermentation reaction shown.

Problem 1.3.3. The thermal denaturation of a globular protein with $T_m = 40$ °C has $\Delta \bar{H} = 300$ kJ/mol for unfolding at the melting temperature (T_m). The difference in the constant-pressure molar heat capacity between the denatured state (unfolded) and the folded state (N) is 9.0 kJ mol^{-1} K^{-1}. Find the molar enthalpy of denaturation at $T = 25$ °C. (Assume the heat capacity does not depend on temperature).

This page titled 1.3: Thermochemistry is shared under a CC BY-NC-SA 4.0 license and was authored, remixed, and/or curated by Jonathan Gutow.

- **1.3: Thermochemistry** by Serge L. Smirnov and James McCarty is licensed CC BY-NC-SA 4.0.

1.4: The Second Law of Thermodynamics

The first law of thermodynamics describes the conservation of energy but does not tell us anything about the direction or spontaneity of a reaction. In this chapter we introduce the concept of entropy as derived by Rudolf Clausius and formulate the second law of thermodynamics. The second law of thermodynamics is of central importance in science and tells us the direction of spontaneous change for any process. We then calculate the change of entropy for a number of example cases.

Learning Objectives

- Be able to provide a thermodynamic definition of entropy as the reversible heat divided by the temperature.
- Be able to articulate the second law of thermodynamics and understand its meaning and significance: the entropy of the universe increases for all spontaneous processes and the entropy of the universe remains unchanged for an equilibrium (reversible) process.
- Be able to calculate the change in entropy for the compression/expansion of an ideal gas.
- Be able to calculate the change in entropy for the various processes: heating/cooling, phase transition, ideal mixing.

1.4.1: Relevance of the first law of thermodynamics

So far we have been concerning ourselves with the interconversion of heat and work as two form of energy. The first law sets a limit on the *magnitude* of energy transfer by stating that energy cannot be created or destroyed, thus any change in energy (ΔU) must be due to work (w) or heat (q) transferred to/from the system with the surroundings.

The mathematical statement of the first law, $\Delta U = q + w$ is a consequence of the fact that energy is neither created or destroyed but flows from one part of the universe (the system) to another (the surroundings) or is converted from one form to another. Although the first law limits the magnitude of energy change, it says nothing about the *directionality* of energy transfer or whether or not a process will be *spontaneous*.

Consider an example sketched in figure 1.4.1. A rubber ball is held some height h above a table. The ball has some potential energy due to gravity. When the ball is released, its potential energy is converted to kinetic energy, and the ball bounces off the table. Each time the ball bounces, it does not reach the same height as the previous bounce because some of the kinetic energy is being dissipated to the molecules in the table. Eventually, the ball comes to rest, and all its kinetic energy has been transferred to the molecules in the table. This increase in kinetic energy results in the temperature of the table rising, and we can say that the kinetic energy of the ball was converted into heat. This process occurs spontaneously once the ball is dropped and is indicated by the forward arrow labeled **a)** in figure 1.4.1.

Let's now consider the reverse process in which the ball at rest on the table absorbs the kinetic energy of the molecules in the table and converts this energy into work by spontaneously levitating against the force of gravity. During this process, the molecules in the table lose some kinetic energy, causing the temperature of the table to decrease. Thus, heat has been converted to work needed to raise the ball to some height h. This process is indicated by the reverse arrow labeled **b)** in figure 1.4.1.

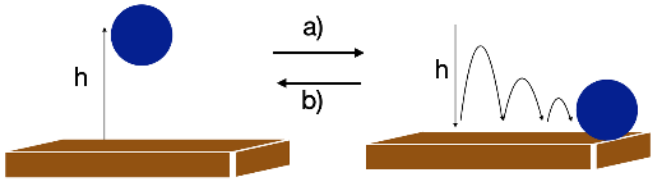


Figure 1.4.1: **a)** A ball suspended at a height h will spontaneous bounce off the table, converting its potential energy into kinetic energy and heat. **b)** In the reverse process, the ball absorbs heat from the table, converts this heat to kinetic energy to elevate a distance h above the table.

In both cases, the total energy is conserved in compliance with the first law of thermodynamics, but the first process occurs spontaneously, while the second process does not occur spontaneously. For the second process to occur, all the molecules in the table would need to spontaneously synchronize their random motion and transfer their kinetic energy to the ball. If there are sufficiently many molecules in the table, the probability for these molecules to synchronize their random motion is extremely unlikely. The second law of thermodynamics will set a limit on the *direction* of energy transfer, such that case 1 (potential energy → kinetic energy → heat) is spontaneous, but that the reverse process, case 2 (heat → kinetic energy → potential energy), will not happen.

1.4.2: Thermodynamic Definition of Entropy

In this chapter we consider the **thermodynamic definition of entropy** as formulated by Rudolf Clausius (1822-1888). Let's consider again the *reversible* heat transfer of a system going from some initial state (P_1, T_1, V_1) to some final state (P_2, T_2, V_2). From the first law of thermodynamics we have $dU = \delta w + \delta q_{rev}$ where the subscript on δq_{rev} indicates that the heat transfer we are considering is for a reversible process. Recall that both work and heat are not state properties and thus depend on the path taken. For reversible work we know that $\delta w = -P \cdot dV$. Also, we know that $dU = C_v \cdot dT$. Inserting these into the equation for the first law and solving for the unknown δq_{rev}, we have:

$$\delta q_{rev} = C_v \cdot dT + P \cdot dV \tag{1.4.1}$$

Equation 1.4.1 is an expression for the reversible heat. Integrating both sides of Equation 1.4.1 from an initial state i to a final state f:

$$q_{rev} = C_v \Delta T + \int_i^f P \cdot dV \tag{1.4.2}$$

We see that the reversible heat depends on the path due to the work term $P \cdot dV$. This is not surprising because the heat is not a state property.

Following Clausius, let's now consider a slightly different quality $\frac{\delta q_{rev}}{T}$. From Equation 1.4.1, dividing both side by T, we have:

$$\frac{\delta q_{rev}}{T} = C_v \cdot \frac{dT}{T} + \frac{P}{T} \cdot dV \tag{1.4.3}$$

Using the fact that $\frac{P}{T} = \frac{nR}{V}$ for an ideal gas, we can integrate both sides of Equation 1.4.3 *independently of the path!*

$$\begin{aligned} \int_i^f \frac{\delta q_{rev}}{T} &= C_v \int_i^f \frac{dT}{T} + nR \int_i^f \frac{dV}{V} \\ &= C_v \ln\left(\frac{T_f}{T_i}\right) + nR \ln\left(\frac{V_f}{V_i}\right) \end{aligned} \tag{1.4.4}$$

Therefore, we conclude that the quantity $\frac{\delta q_{rev}}{T}$ is a state property! We define this new state property $\mathbf{S}$, so that:

$$dS = \frac{\delta q_{rev}}{T} \tag{1.4.5}$$

and, integrating both sides from an initial state i to a final state f:

$$\int_i^f dS = \int_i^f \frac{\delta q_{rev}}{T} = \Delta S \tag{1.4.6}$$

where $\Delta S = S_f - S_i$. The state property $\mathbf{S}$ is called the **entropy**.

> Key Result: The infinitesimal change in entropy is defined as $dS = \frac{\delta q_{rev}}{T}$. Notice the entropy is defined in terms of the *reversible* heat.

From equation 1.4.4 and equation 1.4.6 we have that for the expansion of an ideal gas, the change in entropy is:

$$\Delta S = C_v \ln\left(\frac{T_2}{T_1}\right) + nR \ln\left(\frac{V_2}{V_1}\right) \tag{1.4.7}$$

Notice that Equation 1.4.7 is valid for any expansion/compression of an ideal gas regardless of whether the process was carried our reversibly or irreversibly because entropy is a state property.

> Key Result: The change in entropy for the reversible or irreversible expansion/compression of an ideal gas is: $\Delta S = C_v \ln\left(\frac{T_2}{T_1}\right) + nR \ln\left(\frac{V_2}{V_1}\right)$

Note

Note: Clausius was able to find a new state property by dividing the reversible heat $\delta \mathbf{q_{rev}}$ (not a state property) by the temperature. The temperature in this case is called an *integrating factor* that makes the integral $\int \frac{\delta q_{rev}}{T}$ exact.

1.4.3: Entropy for an irreversible vs. reversible process

So far, we have defined $\mathbf{dS}$ from Equation 1.4.5 in terms of the *reversible* heat $\delta \mathbf{q_{rev}}$. Note that the subscript *rev* indicates the process is reversible. While the entropy is a state property (independent of the path), the heat is not and will depend on the path. Therefore, the equivalence in Equation 1.4.5 is valid only for a reversible path. Even though the entropy is the same, the magnitude of the heat transfer is greater for the *reversible* process, so we have:

$$\delta q_{rev} > \delta q_{irrev} \tag{1.4.8}$$

Dividing both sides of Equation 1.4.8 by $\mathbf{T}$ and inserting the definition of entropy from equation 1.4.5 gives:

$$dS > \frac{\delta q_{irrev}}{T} \tag{1.4.9}$$

While the entropy change would be the same for an irreversible or reversible process, $\Delta S = \Delta S_{rev} = \Delta S_{irrev}$, the heat flow is not the same, so for any irreversible process $\Delta S > q_{irrev}/T$.

Key Result: For any process the change in entropy is $dS \geq \frac{\delta q}{T}$. The equality holds only for a *reversible* process, whereas the inequality holds if the process is *irreversible*.

1.4.4: Entropy of the Surroundings

So far we have only focused on the entropy of the system. In this section we will consider the change in entropy of the *surroundings*. First, we notice that any heat gained (or lost) by the system must have come from (or go to) the surroundings:

$$\delta q_{sys} = - \delta q_{surr} \tag{1.4.10}$$

We consider the surroundings as an infinitely large reservoir. *Any* amount of heat transferred to the surroundings (δq_{surr}) will only lead to an infinitesimally small change in the reservoir, given that the reservoir is sufficiently large. Infinitesimally small changes are characteristic of a *reversible* process, so any heat transfer from the perspective of the surroundings can be treated as reversible, since it will have the same effect on the surroundings as a reversible process. Thus, from equation 1.4.5, we can always write for the surroundings:

$$dS_{surr} = \frac{\delta q_{surr}}{T} \tag{1.4.11}$$

or

$$\Delta S_{surr} = \frac{q_{surr}}{T} \tag{1.4.12}$$

1.4.5: The Second Law of Thermodynamics

The Second Law of Thermodynamics deals with the change in entropy of the universe. The change of entropy of the universe is:

$$\Delta S_{universe} = \Delta S_{sys} + \Delta S_{surr} \tag{1.4.13}$$

Substituting Equation 1.4.12 into Equation 1.4.13 gives:

$$\Delta S_{universe} = \Delta S_{sys} + \frac{q_{surr}}{T} \tag{1.4.14}$$

For a reversible process we can substitute the equality of Equation 1.4.5 to give:

$$\Delta S_{universe} = \frac{q_{rev}}{T} + \frac{q_{surr}}{T}$$

$$\Delta S_{universe} = 0 \tag{1.4.15}$$

where the last line follows from the fact that the heat gained by the surroundings is equal and opposite to the heat lost by the system ($q_{sys} = -q_{surr}$). We see that for a *reversible process* the change of entropy of the universe is zero.

Now, if the processes is *irreversible* we have to use the inequality of Equation 1.4.9. Substituting this into equation 1.4.14 gives for an *irreversible processes:*

$$\Delta S_{universe} > \frac{q_{rev}}{T} + \frac{q_{surr}}{T}$$

$$\Delta S_{universe} > 0 \tag{1.4.16}$$

where again the last line follows from the fact that the heat gained by the surroundings is equal and opposite to the heat lost by the system ($q_{sys} = -q_{surr}$). Thus, for an *irreversible* process, the change in entropy of the universe must be greater than zero.

This result is known as the **Second Law of Thermodynamics** which can be expressed in mathematical form as:

$$\Delta S_{universe} \geq 0 \tag{1.4.17}$$

Where the equality holds if the process is reversible, and the inequality applies if the process is irreversible.

> Key Result: The entropy of an *isolated* system always increases in an irreversible process and remains unchanged in a reversible process. It can never decrease. This statement is known as the **second law of thermodynamics** and is expressed mathematically as: $\Delta S_{universe} \geq 0$

See Practice Problem 1.4.1

1.4.6: Some applications of calculating the entropy

Having defined the second law of thermodynamics, we will now consider some specific examples of calculating ΔS.

1.4.6.1: Example 1: Cyclic process

A cyclic process is any series of steps that returns the system to its original state. Because entropy is a state property:

$$\Delta S = \sum_i \Delta S_i = 0 \tag{1.4.18}$$

where ΔS_i is the entropy change for the ith step and the change in entropy for the cycle is zero because S is a state property.

1.4.6.2: Example 2: Reversible adiabatic process

An **adiabatic process** is a process in which no heat is exchanged between the system and surroundings. For a reversible adiabatic processes, $\delta q_{rev} = 0$ since no heat is exchanged. Integrating Equation 1.4.5 gives:

$$\Delta S = \int \frac{\delta q_{rev}}{T}$$

$$\Delta S = 0 \tag{1.4.19}$$

where the second line follows for an adiabatic process ($\delta q_{rev} = 0$).

1.4.6.3: Example 3: Reversible phase change at constant T and P

At the phase transition temperature, both the forward and reverse reactions are in equilibrium. Therefore, at precisely the phase transition temperature, the phase transition is reversible. For example, the freezing of liquid water is reversible (at equilibrium) at the phase transition temperature of 0 °C.

$$H_2O\ (l) \leftrightarrow H_2O\ (s)\ T = 0\ °C$$

From Equation 1.4.5 at constant **T** we can write:

$$\Delta S = \frac{q_{rev}}{T} \tag{1.4.20}$$

Recalling, that under constant pressure conditions, $q_p = \Delta H$, we can write, for a reversible phase transition:

$$\Delta S = \frac{\Delta H}{T} \tag{1.4.21}$$

where ΔH is the change in enthalpy of the associated phase transition.

1.4.6.4: Example 4: Constant pressure (reversible) heating (no phase change)

Consider heating a substance from some initial temperature $\mathbf{T_i}$ to some final temperature $\mathbf{T_f}$ reversibly. We assume that there are no phase transitions between $\mathbf{T_i}$ and $\mathbf{T_f}$. At constant pressure, we begin with the definition of the heat capacity:

$$\delta q = C_p \cdot dT \tag{1.4.22}$$

Substituting Equation 1.4.22 into the definition of the entropy, Equation 1.4.5 gives:

$$\begin{aligned} \Delta S &= \int_{T_i}^{T_f} C_p \frac{dT}{T} \\ \Delta S &= C_p \int_{T_i}^{T_f} \frac{dT}{T} \\ \Delta S &= C_p \ln\left(\frac{T_f}{T_i}\right) \end{aligned} \tag{1.4.23}$$

where we have assumed the heat capacity $\mathbf{C_p}$ is independent of temperature.

See Practice Problem 1.4.2

1.4.6.5: Example 5: Ideal mixing of two inert gases at constant T and P

In this example, we consider the mixing of two ideal gases. Consider the situation shown in figure 1.4.2. Two gases of different chemical identities A and B are contained in two flasks of volume V_A and V_B. Let n_A be the number of moles of gas A, and n_B be the number of moles of gas B. When the stopcock separating the two flasks is open, the gases will spontaneously mix so that both gases fill the final volume of $V = V_A + V_B$. Similarly, the total number of moles of the combined system is $n = n_A + n_B$.

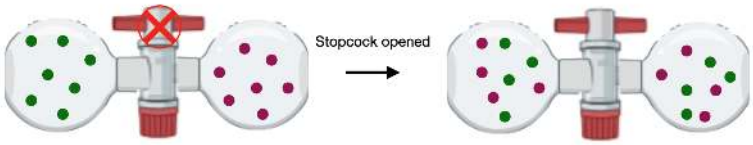


Figure 1.4.2. Ideal mixing of two inert gases. When the stopcock is opened, gas A initially contained in a volume V_A with n_A number of moles spontaneously mixes with n_B moles of gas B initially contained in volume V_B. The final volume is $V=V_A + V_B$ and the total number of moles of gas is $n = n_A + n_B$.

The overall change in entropy for the mixing of two gases is the sum of the change in entropy for each gas:

$$\Delta S = \Delta S_A + \Delta S_B \tag{1.4.24}$$

At constant $\mathbf{T}$, the entropy change for gas A is given by the second term in Equation 1.4.7:

$$\Delta S_A = n_A R \ln\left(\frac{V}{V_A}\right) \tag{1.4.25}$$

and similarly for gas B:

$$\Delta S_B = n_B R \ln\left(\frac{V}{V_B}\right) \tag{1.4.26}$$

Substituting Equation 1.4.25 and Equation 1.4.26 into equation 1.4.24 gives:

$$\Delta S = n_A R \ln\left(\frac{V}{V_A}\right) + n_B R \ln\left(\frac{V}{V_B}\right) \tag{1.4.27}$$

Using the fact that the total volume is $V = nRT/P$ for an ideal gas, Equation 1.4.27 becomes:

$$\Delta S = -n_A R \ln\left(\frac{n_A}{n}\right) - n_B R \ln\left(\frac{n_B}{n}\right)$$

$$\Delta S = -n_A R \ln(x_A) - n_B R \ln(x_B) \tag{1.4.28}$$

where x_A is the mole fraction of gas A defined as $x_A = n_A/n$ and x_B is the mole fraction of gas B. Notice that because the mole fraction is less than one, ΔS for mixing of two ideal gases is be greater than zero.

See Practice Problem 1.4.3

1.4.7: Examples

Example 1.4.1

What is the change in entropy when one mole of liquid water is heated from its freezing point to its boiling point in an open container. The molar heat capacity of liquid water is 75.38 J mol^{-1} K^{-1}.

Solution

Since the water is being heated at constant pressure, we use Equation 1.4.23:

$$\Delta S = C_p \ln\left(\frac{T_f}{T_i}\right)$$

or, after introducing the definition of the molar heat capacity:

$$\Delta S = n\bar{C}_p \ln\left(\frac{T_f}{T_i}\right)$$

Substituting in the values of the initial and final temperatures gives:

$$\Delta S = 1 \text{ mole} \times 75.38 \text{ J mol}^{-1} \text{ K}^{-1} \ln\left(\frac{373.15 \text{ K}}{273.15 \text{ K}}\right)$$

$$\Delta S = 23.52 \text{ J K}^{-1}$$

Notice that the entropy increases upon heating.

Example 1.4.2

Show that for a *reversible* adiabatic expansion of an ideal gas $\Delta S = 0$, but for an *irreversible* adiabatic expansion of an (isolated) ideal gas $\Delta S > 0$

Solution

For a *reversible* process, (see Example 2), we have from the definition of the entropy:

$$\Delta S = \int \frac{\delta q_{rev}}{T}$$

Since the process is adiabatic, there is no heat exchange with the surroundings, meaning that $q_{rev} = 0$ and

$$\Delta S = 0$$

For an *irreversible* process, we have from Equation 1.4.9:

$$\Delta S > \int \frac{\delta q_{irrev}}{T}$$

Again, the process is adiabatic so there is no heat exchange with the surroundings, meaning that $q_{irrev} = 0$, giving:

$$\Delta S > 0$$

Note that this result applies only to an isolated system. It is possible to reduce the entropy of the system with the aid of the external surroundings. The entropy change of both system + surroundings taken together, however, cannot decrease.

1.4.8: Practice Problems

Problem 1.4.1. One mole of an ideal gas is isothermally expanded from 5.0 L to 10 L at 300 K. Compare the entropy changes for the system, surroundings, and the universe if the process is carried out **a)** reversibly, and **b)** irreversibly against a constant external pressure of 2.0 atm.

Problem 1.4.2. The molar enthalpy of vaporization of water is $\Delta H_{vap} = 40.6$ kJ/mol at the boiling temperature of 100 °C. **a)** What is the value of ΔS when one mole of liquid water is converted to a gas at 100 °C. **b)** What is ΔS for the conversion of one mole of liquid water to a gas at a temperature of 120 °C. The molar heat capacity of liquid water is 75.38 J mol^{-1} K^{-1} and the molar heat capacity of water vapor is 36.57 J mol^{-1} K^{-1}.
Hint consider ΔS of heating/cooling from *Example 4* in addition to ΔS for a phase transition in *Example 3*.

Problem 1.4.3. Suppose you have a compartment that contains 1 mole of NO and a second compartment that contains 0.3 moles of O_2. Calculate the change in entropy ΔS of mixing the two gasses together. Assume the gasses do not react and are ideal gasses.

This page titled 1.4: The Second Law of Thermodynamics is shared under a CC BY-NC-SA 4.0 license and was authored, remixed, and/or curated by Jonathan Gutow.

- **1.4: The Second Law of Thermodynamics** by Serge L. Smirnov and James McCarty is licensed CC BY-NC-SA 4.0.

1.5: The Boltzmann Distribution and the Statistical Definition of Entropy

In this chapter we introduce the statistical definition of entropy as formulated by Boltzmann. This allows us to consider entropy from the perspective of the probabilities of different configurations of the constituent interacting particles in an ensemble. This conception of entropy led to the development of modern statistical thermodynamics. For systems that can exchange thermal energy with the surroundings, the equilibrium probability distribution will be the Boltzmann distribution. Knowing this equilibrium probability distribution allows us to calculate various thermodynamics observables.

Learning Objectives

- Understand the statistical definition of entropy and be able to use the number of available microstates of the system to calculate the entropy.
- Understand how all thermodynamic properties ultimately can be traced back to the number of occupied microstates and their probability.
- Be able to use the Boltzmann distribution to calculate the ratio of occupied energy states at a given temperature and the probability of a particle being in any particular energy level.

1.5.1: Microstates and Boltzmann Entropy

In our discussion of thermodynamics, thus far we have neglected the molecular nature of reality: that molecular systems are composed of many interacting atoms and molecules. In this chapter we will explore how the large number of particles in a system gives rise to thermodynamic observables. We have seen that the thermodynamic state of the system can be designated by a set of state properties (P, V, n, T, U, H, S). The macroscopic state of the system is called a **macrostate.** In contrast, a **microstate** is a specific configuration of all the constituent parts that make up the system.

As an illustrative example of a microstate is to consider the number of ways any given state may be constructed. Consider the question of how many unique ways there are to arrange four particles as shown in figure 1.5.1 into two bins.

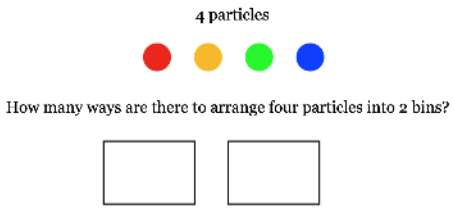


Figure 1.5.1 Consider the number of possible ways to arrange four particles into two bins. The are a total of 16 unique configurations as shown in figure 1.5.1.

It turns out that there are 16 different ways we could arrange four particles into two bins as shown in figure 1.5.2.

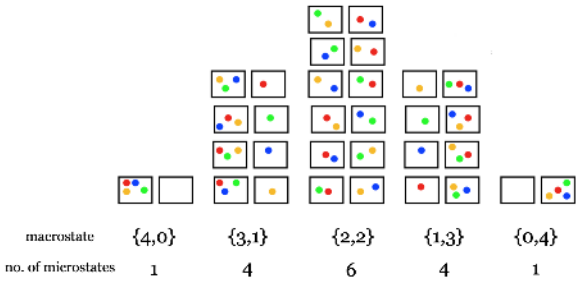


Figure 1.5.2 The total number of ways to arrange four particles into two bins. There are five possible macrostates defined by the number of particles in each bin ({4,0}, {3,1}, {2,2}, {1,3},{0,4}). Whereas the macrostate {4,0} can only be achieved in one way, the macrostate {2,2} can be achieved in six different ways.

If we define each unique arrangement of the four particles as a microstate, then there are 16 possible microstates. The overall number of particles in each bin defines the macrostate, so from figure 1.5.2 we see that there are five macrostates, and that the number of microstates making up the different macrostates is not equal. The macrostate that corresponds to a configuration with two particles in each bin ({2,2}) has the highest number of microstates (6), while the macrostates that correspond to configurations with all the particles in one of the bins ({4,0} and {0,4}) have the fewest number of microstates (1).

In general, we can calculate the number of microstates in a given distribution according to the formula:

$$W = \frac{N!}{n_1!n_2!,\ldots} \tag{1.5.1}$$

where W is the number of ways of distributing N total particles into bins, and n_1, n_2, … is the number of particles in each bin.

Example 1.5.1

Example 1: Use Equation 1.5.1 to calculate the number of ways to arrange four particles into two bins such that there are two particles in each bin ({2,2}).

Solution

We have four total particles, so $N = 4$. To calculate the number of ways to arrange four particles into a configuration with $n_1 = 2$ and $n_2 = 2$ we have:

$$W = \frac{4!}{2!2!}$$
$$W = \frac{4 \times 3 \times 2 \times 1}{2 \times 1 \times 2 \times 1}$$
$$W = 6 \tag{1.5.2}$$

We calculate that there are six different microstates corresponding to the macrostate with two particles in each bin ({2,2}), which agrees with the drawing in figure $|PageIndex2$.

See Practice Problems 1.5.1 and 1.5.2.

The **Boltzmann definition of entropy** relates the entropy as the natural logarithm of the number of microstates, **W**:

$$S = k_B \ln W \tag{1.5.3}$$

where $\mathbf{k_B}$ is a constant of proportionality known as Boltzmann's constant:

$$k_B = 1.380658 \times 10^{-23}\ \text{J K}^{-1} \tag{1.5.4}$$

Since W is unitless, the units on $\mathbf{k_B}$ give entropy the correct thermodynamic units, and the value of Boltzmann's constant ensures that the statistical definition of entropy from Equation 1.5.3 is in agreement with the thermodynamic definition of entropy.

1.5.2: The Boltzmann Distribution

Equation 1.5.3 allows us to compute the entropy **S** for any given configuration of particles. Looking again at figure 1.5.2, we see that the configuration with two particles in each bin ({2,2}) has more accessible microstates (W=6) than a configuration with all four particles in one bin ({4,0} with W=1). Therefore, the macrostate with configuration {2,2} has a greater entropy than the macrostate with configuration {4,0}.

As a second example consider a system of four particles with two discrete energy levels as shown in figure 1.5.3.



Figure 1.5.3: Two level system. Consider a system of four particles each with two accessible energy levels: a ground state energy with energy E_0 and a single excited state with energy E_1. If all particles are in the ground state, the total energy is $E = 4E_0$ as shown on the left. There is only one way to have all the particles in the ground state so W=1. If one of the particles is in the excited state, the total energy is $E = 3E_0 + E_1$ and W=4 since there are four possible ways to have a configuration with one particle in the excited state.

The particles can either be at the ground state energy E_0 or the excited state energy E_1. For example, the left side of figure 1.5.3 shows the microstate with all four particles in the ground state. In this state, the total energy is $E = 4E_0$, and there is only one possible microstate (W=1). The configuration on the left corresponds to the macrostate with the lowest entropy. The right side of figure 1.5.3 shows three particles in the ground state and one particle in the excited state. In the configuration on the right, the total

energy is $E = 3E_0 + E_1$ and there are four possible microstates since any one our of the four particles could be in the excited state (W=4). The entropy of each of these configurations can be calculated from Equation 1.5.3 using equation 1.5.1.

We now ask ourselves, is there a dominant configuration of particles? The dominant configuration will be the configuration that maximizes **W**, or equivalently the configuration that maximizes the entropy **S**. Since W is a function of all the n_i, the dominant configuration (that maximizes S) will be given by:

$$\left(\frac{\partial \ln W}{\partial n_i}\right) = 0 \tag{1.5.5}$$

where $\mathbf{n_i}$ is the number of particles in energy level i.

In solving for the maximum entropy condition of Equation 1.5.5, we must also enforce the constraint that the total energy of the system is:

$$E_{total} = \sum_i n_i E_i \tag{1.5.6}$$

and that the total number of particles **N** is:

$$N = \sum_i n_i \tag{1.5.7}$$

Maximizing a function subject to constraints can be done using a mathematical technique called *Lagrange's method of undetermined multipliers*. The result is that at a given temperature **T**, the fraction of particles with energy E_i is given by:

$$\frac{n_i}{N} = \frac{e^{-E_i/k_BT}}{q}. \tag{1.5.8}$$

Equation 1.5.8 is known as the **Boltzmann distribution** and gives the probability of a particle occupying a given energy level $\mathbf{E_i}$ at temperature **T**. The term in the denominator **q** is called the **partition function** and is given by:

$$q = \sum_i e^{-E_i/k_BT} = e^{-E_0/k_BT} + e^{-E_1/k_BT} + \ldots \tag{1.5.9}$$

The ratio of the number of particles (populations) between any two energy levels $\mathbf{n_1}$ and $\mathbf{n_2}$ is given by:

$$\frac{n_2}{n_1} = e^{-\Delta E/k_BT} \tag{1.5.10}$$

where $\mathbf{\Delta E}$ is the difference in energy between the two energy levels $\Delta E = E_2 - E_1$

Key Result: The Boltzmann distribution gives the distribution of particles that corresponds to the most probable populations and is given by the formula:

$$\frac{n_i}{N} = \frac{e^{-E_i/k_BT}}{\sum_i e^{-E_i/k_BT}}.$$

The ratio of the number of particles between any two energy levels is

$$\frac{n_2}{n_1} = e^{-\Delta E/k_BT}.$$

See Practice Problem 1.5.3.

1.5.3: Degenerate Energy Levels

Equation 1.5.8 and Equation 1.5.10 were derived without considering the case of **degeneracy**. In practice, there may be two or more distinct states with the same energy. Two distinct states with the same energy are called **degenerate** energy levels. We specify the degeneracy of a particular energy level i with the symbol $\mathbf{g_i}$. Figure 1.5.4 shows a situation where the ground state is not degenerate ($\mathbf{g_0 = 1}$), and the excited state has a degeneracy of $\mathbf{g_1 = 2}$ because there are two possible states with the same energy E_1.

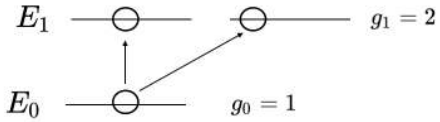


Figure 1.5.4: Degenerate energy levels. In this example there is only one ground state level with energy E_0, but there are two possible excited state energy levels with the same energy E_1. A particle in the ground state can be excited into either of the two excited states. Because these two states have the same energy they are called **degenerate** energy levels. In this example, the excited state E_1 has a degeneracy $g_1 = 2$ while the ground state has a degeneracy $g_0 = 1$.

For the case where there are degenerate energy levels, we generalize the probabilities given by Equation 1.5.8 and equation I.5. 1.5.10. The general Boltzmann distribution will be:

$$\frac{n_i}{N} = \frac{g_i e^{-E_i/k_B T}}{q}. \tag{1.5.11}$$

with g_i the degeneracy of state i and the partition function:

$$q = \sum_i g_i e^{-E_i/k_B T} = g_0 e^{-E_0/k_B T} + g_1 e^{-E_1/k_B T} + \ldots \tag{1.5.12}$$

The ratio of the number of particles (populations) between any two energy levels $\mathbf{n_1}$ and $\mathbf{n_2}$ is given by:

$$\frac{n_2}{n_1} = \frac{g_2}{g_1} e^{-\Delta E/k_B T} \tag{1.5.13}$$

1.5.4: Examples

Example 1.5.2

Calculate the number of microstates for 8 particles to be arranged into 4 bins such that the configuration of particles is {6,0,0,2}

Solution

The number of microstates is given by Equation 1.5.1:

$W = \frac{N!}{n_1! n_2!, \ldots}$

$W = \frac{8!}{6!0!0!2!}$

$W = 28$

Example 1.5.2

a) Write an expression for the partition function for the two-level system shown in Figure I.5.D with energy in the ground state E_0 and degeneracy $g_0 = 1$ and energy in the excited state E_1 and degeneracy $g_1 = 2$. **b)** Let the energy of the ground state be $E_0 = 0$ and the energy in the excited state be $E_1 = 2.41$ kJ mol^{-1}. Evaluate the value of the partition function at T=298 K. **c)** What is the probability to find the system in the ground state at T=298 K?

Solution

a) Using Equation 1.5.12, for a two-level system we have:

$q = g_0 e^{-E_0/k_B T} + g_1 e^{-E_1/k_B T}$

and substituting the values of the degeneracy gives:

$q = e^{-E_0/k_B T} + 2e^{-E_1/k_B T}$

b) When energies are given in molar units (kJ mol^{-1}), it is useful to use the gas constant $R = 8.314$ J mol^{-1} K^{-1} $= N_A k_B$. The the partition function becomes:

$q = 1 + 2e^{-2410/(8.314 \cdot 298)}$

$q = 1.756$

c) The probability for the system to be in the ground state is given by Equation 1.5.11:

$p_0 = \frac{g_0 e^{-E_0/k_B T}}{q}$

$p_0 = \frac{1}{q}$

Inserting the value of q from part b):

$p_0 = 0.569$

1.5.5: Practice Problems

Problem 1.5.1. Calculate the total number of ways to arrange 16 particles into four bins such that there are four particles in each bin ({4,4,4,4}). What can you say about the entropy of this macrostate as compared to any other macrostate? Explain your answer.

Problem 1.5.1. Suppose we have 8 particles that are arranged into 4 bins. Calculate the number of microstates (W) for each of the following distributions of particles: **a)** {5,1,1,1}, **b)** {4,2,2,0}, **c)** {2,6,0,0}

Problem 1.5.1. Suppose a protein can exist in two conformations that have an energy difference of 2.0 kJ/mol. What is the estimated ratio of the two conformations at 300 K?

This page titled 1.5: The Boltzmann Distribution and the Statistical Definition of Entropy is shared under a CC BY-NC-SA 4.0 license and was authored, remixed, and/or curated by Jonathan Gutow.

- **1.5: The Boltzmann Distribution and the Statistical Definition of Entropy** by Serge L. Smirnov and James McCarty is licensed CC BY-NC-SA 4.0.

1.6: The Gibbs and Helmholtz Energy

Based on "The Gibbs and Helmholtz Energy" by Serge L. Smirnov and James McCarty, LibreTexts is licensed under CC BY-NC-SA .

In this chapter we introduce two additional state properties: the Gibbs energy and the Helmholtz energy. These additional variables are useful for allowing us to determine the direction of spontaneous change without having to directly calculate the change in entropy of the universe from the second law. The Gibbs energy has particular importance in chemistry.

Learning Objectives

- Know the thermodynamic definitions of the Gibbs energy and Helmholtz energy and why these two properties are important.
- Understand that the change in Gibbs energy has both an enthalpic and entropic contribution.
- Know that at constant pressure and temperature the Gibbs energy decreases for a spontaneous process, and at constant volume and temperature the Helmholtz energy decreases for a spontaneous process.
- Be able to identify the fundamental differentials for dU, dH, dG, and dA and how these can be used to arrive at thermodynamic relationships.

1.6.1: The Gibbs and Helmholtz energy

The first law of thermodynamics accounts for the conservation of energy and the second law of thermodynamics determines the spontaneity. Together, these laws should allow us to deal with the thermodynamics of any system, but their direct application is not always convenient. In addition to our current set of state properties it is useful to define two additional state properties: the **Gibbs energy** and the **Helmholtz energy**.

Recall that we have already define the **total internal energy** U and the **enthalpy** H=U+PV. Similarly, we now define the **Gibbs energy:**

$$G = H - TS \tag{1.6.1}$$

The Gibbs energy (G) is the enthalpy minus the product of the temperature and the entropy.

We also define the **Helmholtz energy:**

$$A = U - TS \tag{1.6.2}$$

The Helmholtz energy (A) is the total internal energy minus the product of the temperature and the entropy.

If we are interested in infinitesimal changes in the Gibbs or Helmholtz energies we can consider the differential form of equations 1.6.1 and 1.6.2

$$dG = dH - TdS - SdT \tag{1.6.3}$$

$$dA = dU - Tds - SdT \tag{1.6.4}$$

Note

Note: In the differential form of Equation 2 we have made use of the product rule for derivatives: d(AB)=BdA+AdB

1.6.2: The Significance of the Gibbs and Helmholtz energy

In order to understand why the Gibbs and Helmholtz energies are important, we need to recall the second law of thermodynamics which states

$$dS_{sys} + dS_{surr} \geq 0 \tag{1.6.5}$$

Recalling that for the surroundings:

$$dS_{surr} = \frac{\partial q_{surr}}{T} = -\frac{\partial q_{sys}}{T} \tag{1.6.6}$$

We can substitute equation 1.6.6 into Equation 1.6.5 to obtain an alternative expression for the second law in terms of only the system variables:

$$dS_{sys} - \frac{\delta q_{sys}}{T} \geq 0 \implies TdS_{sys} - \delta q_{sys} \geq 0 \tag{1.6.7}$$

Equation 1.6.7 follows from the second law of thermodynamics. We will now consider two particular cases. Since all the quantities refer to the system we will drop the subscript "sys" in the remaining discussion.

1.6.3: Case 1: Constant T and P Conditions

At constant P, the heat transfer is equivalent to the enthalpy:

$$\delta q_p = dH \tag{1.6.8}$$

Substitution of equation 1.6.8 into equation 1.6.7 gives:

$$TdS - dH \geq 0 \tag{1.6.9}$$

Solving the differential form of the Gibbs energy (equation 1.6.3) for dH and then substituting into equation 1.6.9 gives:

$$\cancel{TdS} - dG - \cancel{TdS} - SdT \geq 0 \implies dG + SdT \leq 0 \tag{1.6.10}$$

At constant T, the second term SdT=0 because T is not changing, giving the final result:

$$dG \leq 0 \tag{1.6.11}$$

or upon integrating both sides from an initial to final state:

$$\Delta G \leq 0 \tag{1.6.12}$$

The equality holds for a reversible (equilibrium) process, and the inequality holds for any spontaneous process at constant T and P.

> Key Result: At constant T and P conditions $\Delta G < 0$ for a spontaneous process and ΔG=0 for a reversible process.

Since we are at constant T, the differential form of dG from equation 1.6.3 simplifies to:

$$dG = dH - TdS \tag{1.6.13}$$

Integrating both sides at constant T and P from an initial state to a final state gives:

$$\Delta G = \Delta H - T\Delta S \tag{1.6.14}$$

from which we see that the Gibbs energy has an enthalpic term and an entropic term.

> Key Result: $\Delta G = \Delta H - T\Delta S$. This expression is valid at constant T and P.

1.6.4: Case 2: Constant T and V Conditions

For the case of constant volume, the heat transfer is equivalent to the total internal energy:

$$\delta q_v = dU \tag{1.6.15}$$

Substitution of Equation 1.6.15 into equation 1.6.7 gives:

$$TdS - dU \geq 0 \tag{1.6.16}$$

Solving the differential form of the Helmholtz energy (equation 1.6.4) for dU and substituting into Equation 1.6.16 gives:

$$\cancel{TdS} - dA - \cancel{TdS} - SdT \geq 0 \implies dA + SdT \leq 0 \tag{1.6.17}$$

Again at constant T, the second term SdT=0 because T is not changing, giving the final result:

$$dA \leq 0 \tag{1.6.18}$$

or upon integrating both sides from an initial to final state:

$$\Delta A \leq 0 \tag{1.6.19}$$

The equality holds for a reversible (equilibrium) process, and the inequality holds for any spontaneous process at constant T and V.

> Key Result: At constant T and V conditions $\Delta A < 0$ for a spontaneous process and ΔA=0 for a reversible process.

Since we are at constant T, the differential form of dA from equation 1.6.4 simplifies to:

$$dA = dU - TdS \tag{1.6.20}$$

Integrating both sides at constant T and V from an initial state to a final state gives:

$$\Delta A = \Delta U - T\Delta S \tag{1.6.21}$$

> Key Result: $\Delta A = \Delta U - T\Delta S$. This expression is valid at constant T and V.

1.6.5: Four Fundamental differentials of thermodynamics

The first law of thermodynamics in differential form is:

$$dU = \delta q + \delta w \tag{1.6.22}$$

For a reversible process we have defined the entropy as $dS = \delta q_{rev}/T$ and the reversible work as $\delta w = -P \cdot dV$. Substituting these identities into equation 1.6.22 gives the following differential form of the first law:

$$dU = TdS - PdV \tag{1.6.23}$$

Note that Equation 1.6.23 is valid for a reversible process in which the only work is due to compression/expansion.

The enthalpy is defined as:

$$H = U + PV \tag{1.6.24}$$

From Equation 1.6.24 we can write a differential form of the enthalpy as:

$$dH = dU + PdV + VdP \tag{1.6.25}$$

where we have again used the product rule from calculus on the PV term. Substituting equation 1.6.23 into equation 1.6.25 for the dU term gives another differential relation for dH:

$$dH = TdS - \cancel{PdV} + \cancel{PdV} + VdP = TdS + VdP \tag{1.6.26}$$

Similarly, substitution of equation 1.6.23 into the dU term in the differential form for dA in equation 1.6.4 gives another differential for dA:

$$dA = \cancel{TdS} - PdV - \cancel{TdS} - SdT = -PdV - SdT \tag{1.6.27}$$

Finally, substitution of equation 1.6.26 into the dH term differential form for dG in equation 1.6.3 gives another differential for dG:

dGdGamp;=amp;=amp;TdS+VdP−TdS−SdTamp;VdP−SdT(24)

$$dG = \cancel{TdS} + VdP - \cancel{TdS} - SdT = VdP - SdT \tag{1.6.28}$$

These results are summarized in table 1.6.1.

Table 1.6.1: the four fundamental differential relations for dU, dH, dG, and dA.

Differential Relation	Equation
dU=TdS−PdV	1.6.23
dH = TdS – VdP	1.6.26
dA=−PdV−SdT	1.6.27

Differential Relation	Equation
dG=VdP−SdT	1.6.28

1.6.6: Pressure dependence of ΔG

The fundamental differentials from table 1.6.1 are useful for deriving various thermodynamic relationships. As an example, we can use equation 1.6.28 to derive the pressure dependence of ΔG. Starting from equation 1.6.28, at **constant T** the second term SdT=0, giving:

$$dG = VdP \tag{1.6.29}$$

or

$$\left(\frac{\partial G}{\partial P}\right)_T = V \tag{1.6.30}$$

Integrating both sides of equation 1.6.29 from an initial pressure P_i to a final pressure P_f gives:

$$\Delta G = \int_{P_i}^{P_f} V dP \tag{1.6.31}$$

Solids and liquids are nearly incompressible, so the volume does not change significantly with changes in the pressure. Therefore, for **solids and liquids** the volume can be treated as constant in equation 1.6.31, and upon integration gives:

$$\Delta G = V\Delta P \tag{1.6.32}$$

Note that equation 1.6.32 is valid for solids and liquids. For an ideal gas we can substitute V=nRT/P for the volume in equation 1.6.31:

$$\Delta G = \int_{P_i}^{P_f} \frac{nRT}{P} dP$$

$$\Delta G = nRT \int_{P_i}^{P_f} \frac{dP}{P}$$

$$\Delta G = nRT \ln\left(\frac{P_f}{P_i}\right) \tag{1.6.33}$$

If we set the initial pressure to 1 bar (standard pressure), and replace the initial Gibbs energy G_i with the symbol for G at the standard state G^o, then equation 1.6.33 becomes:

$$G = G^\circ + nRT \ln\left(\frac{P}{1\text{ bar}}\right) \tag{1.6.34}$$

See Practice Problem 1.6.2.

1.6.7: Examples

Example 1.6.1

Show that at constant pressure, the entropy is given by:

$S = -\left(\frac{\partial G}{\partial T}\right)_P$

Solution

Starting with equation 1.6.28:

dG=VdP−SdT

At constant pressure (dP=0), we have:

dG=−SdT

or, solving for S:

$S = -\left(\frac{\partial G}{\partial T}\right)_P$

1.6.8: Practice Problems

Problem 1.6.1: Starting with equation 1.6.23, show that temperature has the thermodynamic definitions $T = \left(\frac{\partial U}{\partial S}\right)_V$.

Problem 1.6.2: Assume we have 2.00 moles of ideal gas at 20.0 mbar and 37.0 ^oC and compress it to 100. mbar while keeping the temperature constant. What is the change in the free energy of this sample?

This page titled 1.6: The Gibbs and Helmholtz Energy is shared under a CC BY-NC-SA 4.0 license and was authored, remixed, and/or curated by Jonathan Gutow.

- **1.6: The Gibbs and Helmholtz Energy** by Serge L. Smirnov and James McCarty is licensed CC BY-NC-SA 4.0.

1.7: Phase Equilibria and Mixtures

Based on "Equilibria in Biochemical Systems" by Serge L. Smirnov and James McCarty, LibreTexts is licensed under CC BY-NC-SA .

In this chapter we extend the concept of the Gibbs energy to phase transitions and mixtures. In the case of mixtures, the number of moles of the different components can change as a result of a chemical reaction or a phase transition. The partial molar Gibbs energy or chemical potential can be used to determine the spontaneity a process. We first derive an expression for the chemical potential. Then we will consider the impacts of pressure and temperature and use that to understand phase transitions, vapor pressure of volatile liquids, and ideal solutions. We then introduce the concept of the activity to write a general expression for the chemical potential.

Learning Objectives

- Know the definition of the chemical potential as the partial molar Gibbs energy, and be able to analyze the spontaneity of a phase transition based on the change in chemical potential.
- Be able to use the chemical potential to calculate the change in Gibbs energy for a process involving changing number of moles.
- Understand how to model the shapes of the phase boundaries in a pressure versus temperature phase diagram.
- Understand the definition of the activity and how it can be used to describe both ideal and real solutions.

1.7.1: Gibbs energy and phase equilibria

For a phase transition in equilibrium at the phase transition temperature, such as the freezing of liquid water at 0 °C, the process is reversible. At equilibrium, the change in the *molar* Gibbs energy $\Delta G_{molar} = 0$, meaning that if two phases are at equilibrium,

$$G_{molar}(solid) = G_{molar}(liquid) \tag{1.7.1}$$

Notice here that the molar Gibbs energy is the same for the two phases. The molar Gibbs energy is an *intensive* variable (Gibbs energy per mole). We must use the molar Gibbs energy because the phase equilibrium is independent of the amount of substance. For example, we could have a small ice cube in equilibrium with a large volume of water at 0 °C.

If we have multiple species in our system, the intensive variable of interest is the **partial molar Gibbs energy** that is defined for the ith component of the system as:

$$G_{molar,i} = \left(\frac{\partial G}{\partial n_i}\right)_{T,P,n_j} \tag{1.7.2}$$

where n_i is the number of moles of the ith component, and n_j is the number of moles of all the other components in the system. The total Gibbs energy is a function of the number of moles of each species:

$$G = \sum_i n_i G_{molar,i} \tag{1.7.3}$$

The partial molar Gibbs, $G_{molar,i}$ also shows how infinitesimal changes in the Gibbs energy, dG, depend on infinitesimal changes in the number of moles of a component (n_1, n_2, …):

$$dG = G_{molar,1} dn_1 + G_{molar,2} dn_2 + \ldots \tag{1.7.4}$$

1.7.2: The chemical potential

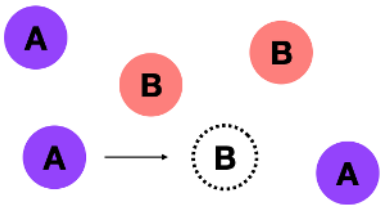
Because the partial molar Gibbs is used so often when considering equilibria, we give this quantity a special name called the **chemical potential** which gets the Greek symbol μ, and we write the chemical potential of the ith component as:

$$\mu_i = G_{molar,i} = \left(\frac{\partial G}{\partial n_i}\right)_{T,P,n_j} \tag{1.7.5}$$

Substituting into Equation 1.7.4 gives:

$$dG = \mu_1 dn_1 + \mu_2 dn_2 + \ldots = \sum_i \mu_i dn_i \tag{1.7.6}$$

Consider the spontaneous transfer of some moles of a molecule from state A to state B as shown in figure 1.7.1 .



$$dn_B = -dn_A$$

Figure 1.7.1 The conversion of a molecule from state A into state B. The number of moles converted from state A into state B is given by dn_B, and is equal and opposite to dn_A.

The change in the number of moles in state A, dn_A will be equal and opposite to the change in the number of moles in state B, dn_B, so we can write the total change in Gibbs energy from equation 1.7.6 as

$$dG = \mu_A dn_A + \mu_B dn_B = (\mu_B - \mu_A) dn_B \tag{1.7.7}$$

We now ask ourselves, when will the transition from state A into state B become spontaneous? For a spontaneous process dG < 0. Thus, the transition of dn_B moles from state A to state B, will be *spontaneous* if

$$(\mu_B - \mu_A) dn_B < 0 \implies \mu_B < \mu_A \tag{1.7.8}$$

We see that matter flows in the direction of lower chemical potential.

Key Result: Matter flows spontaneously from high chemical potential to low chemical potential. The flow of matter will continue until the chemical potentials are equal, which is the equilibrium condition.

1.7.3: How does changes in conditions change G and thus μ?

In order to determine how the equilibria between phases change as conditions change we need to understand the dependence of G (and thus μ) on state variables such as T and P.

1.7.3.1: Changes in pressure

Recall that:

$$\left(\frac{\partial G}{\partial P}\right)_T = V \tag{1.7.9}$$

or for μ:

$$\left(\frac{\partial \mu}{\partial P}\right)_T = V_{molar} \tag{1.7.10}$$

For an ideal gas V_{molar} depends on P :

$$\left(\frac{\partial \mu}{\partial P}\right)_T = \frac{RT}{P} \tag{1.7.11}$$

For incompressible liquids and solids V_{molar} is a constant.

1.7.3.2: Changes in temperature

Recall that the fundamental differential relation for free energy is:

$$dG = V dP - S dT \implies d\mu = V_{molar} dP - S_{molar} dT \tag{1.7.12}$$

If pressure is constant dP = 0 and and equation 1.7.12 becomes:

$$d\mu = -S_{molar} dT \implies \left(\frac{\partial \mu}{\partial T}\right)_P = -S_{molar} \tag{1.7.13}$$

1.7.4: Single species phase equilibria

The simplest use of these relations is to understand the shape of the curves in a pressure versus temperature phase diagram for a pure substance. If we have two phases A and B equilibrium is when $\mu_A = \mu_B$. We need to understand how the combinations of P and T where

this is true change.

1.7.4.1: Impact of changes in P

First, we **consider how P impacts the values of μ at constant T**. Since matter takes up space $V_{molar} > 0$ (equations 1.7.10 and 1.7.11), μ increases with pressure (P). The slope of the increase is the constant V_{molar} for solids and liquids, while for gases the slope is steepest at lower pressures. Without knowing actual values of μ we can sketch a μ versus P diagram showing when the chemical potential of pairs of phases are equal. At high pressure the most stable phase will be the one with the lowest V_{molar} (highest density, usually the solid phase) because as pressure increases that one will increase the least. In figure 1.7.2 this is indicated by the right most point on the line for μ_s. Likewise the liquid phase will have a slightly higher μ_l indicated by the right most point on the line for μ_l in figure 1.7.2. The gas phase has the highest μ_g at high pressure, with a μ that drops off more steeply as the pressure drops.

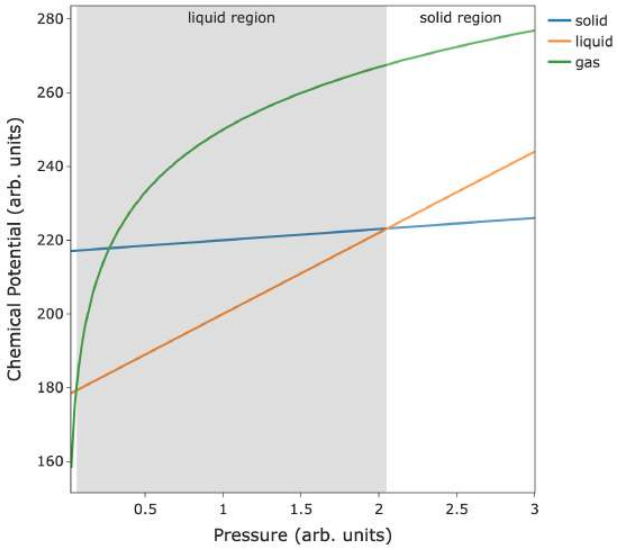


Figure 1.7.2: Variation of μ for solids, liquids and gases versus pressure. Each phase is stable in the region where μ of that phase is lowest. In this example only a little sliver near P = 0 favors the gas phase.

As seen in figure 1.7.2, this leads to the lowest pressure equilibrium occurring where the gas and liquid lines cross. The next equilibrium occurs at a slightly higher pressure where the gas and solid lines cross. The final equilibrium occurs at the highest pressure between the liquid and solid. As noted matter flows towards the lowest μ. Thus figure 1.7.2 can be divided into three pressure regions demarcated by the pressures of the equlibriums: 1) the lowest pressure region is where the gas phase is thermodynamically favored; 2) the middle pressure region where the liquid phase is favored; and 3) the high pressure region where the solid phase is favored. Thus, if we started with a sample in the gas phase and increased the pressure it would undergo a phase transition to the liquid phase at the left edge of the liquid region. The chemical potential μ would then follow the liquid line until reaching the right edge of the liquid region. The material then undergoes a phase transition to the solid phase and follows the solid μ line as the pressure increases more.

1.7.4.2: Impact of changes in T

Second, we **consider how T impacts the values of μ at constant P**. Since entropy is always greater than zero the slope of μ (equation 1.7.13) is negative for all phases. As before, we can draw a qualitative diagram showing the relations of the chemical potentials as the temperature is varied. At any temperature $S_{molar}(g) > S_{molar}(l) > S_{molar}(s)$. Thus at low temperatures the most stable phase will be the the solid; the next most stable the liquid and the least stable the gas. This relationship is indicated by the initial (leftmost) values of the μ for each phase in figure 1.7.3. Although entropy increases with temperature, so that the slopes of the curves should get more steeply negative, in this diagram we assume the temperature range is small enough that S_{molar} is nearly constant leading to linear behavior over the temperature range plotted. Once again this leads to three places where two of the phases are in equilibrium and three regions of phase stability: 1) solid stable at low temperature; 2) liquid stable in an intermediate range and 3) gas stable at the highest temperatures (see figure 1.7.3).

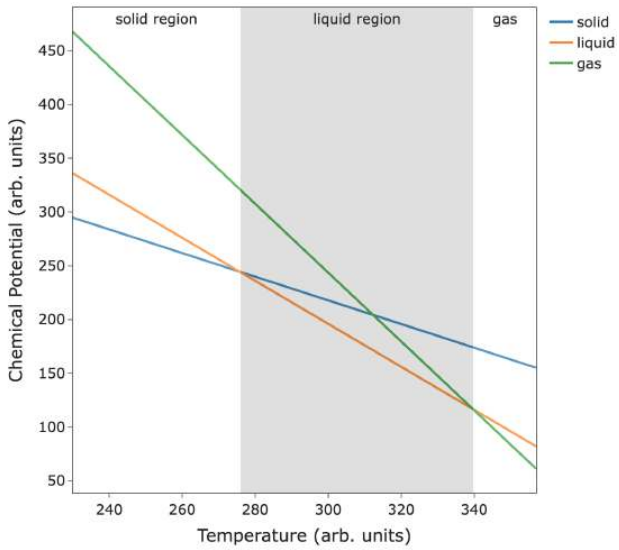


Figure 1.7.3: Variation of μ for solids, liquids and gases versus temperature. Each phase is stable in the region where μ of that phase is lowest. We hava assumed that the temperature range of this figure is small enough that the entropies of each phase is nearly constant, leading to a nearly constant slope.

1.7.4.3: Pressure versus temperature phase diagrams

Typical phase diagrams for pure substances display curves in P-T space, where the curves indicate the boundaries between the phases. Alternatively, you can think of the curves as representing the combinations of P and T where the neighboring phases A and B are in equilibrium ($\mu_A = \mu_B$). To describe the shapes of these curves we require expressions for $\frac{dP}{dT}$ along these boundaries. First we will derive the generic relation and then examine the implications for the shape of each boundary.

Beginning with equation 1.7.12 in its chemical potential form we note that chemical potentials of the two species must stay equal to stay on the boundary. This means the the changes in the two chemical potentials must be equal:

$$d\mu_A = V_{molar,A}dP - S_{molar,A}dT = d\mu_B = V_{molar,B}dP - S_{molar,B}dT \implies V_{molar,A}dP - S_{molar,A}dT = V_{molar,B}dP - S_{molar,B}dT \quad (1.7.14)$$

Rearranging the last expression to get the molar volumes on one side and the molar entropies on the other leads to:

$$S_{molar,B}dT - S_{molar,A}dT = V_{molar,B}dP - V_{molar,A}dP \implies (S_{molar,B} - S_{molar,A})dT = (V_{molar,B} - V_{molar,A})dP \quad (1.7.15)$$

Notice that in equation 1.7.15 the collected differences are just the changes in the molar entropy and volume on shifting phases. So this can be rewritten as:

$$\Delta S_{molar}dT = \Delta V_{molar}dP \quad (1.7.16)$$

Dividing both sides by ΔV_{molar} and dT yields an expression for the change in P for a change in T:

$$\frac{dP}{dT} = \frac{\Delta S_{molar}}{\Delta V_{molar}} = \frac{\Delta S_{trs}}{\Delta V_{trs}} \quad (1.7.17)$$

where in the final version the subscript 'trs' stands for transition ('vap' for vaporization, 'fus' for melting, 'sub' for sublimation). This is the fundamental form of the Clapeyron equation. A very useful alternative form of this equation makes use of the fact that when P and T are constant (at a particular equilibrium point on the boundary) $\Delta S_{trs} = \frac{\Delta H_{trs}}{T_{trs}}$. Substituting this into equation 1.7.17 yields:

$$\frac{dP}{dT} = \frac{\Delta H_{trs}}{T_{trs}\Delta V_{trs}} \quad (1.7.18)$$

With this expression we can estimate the slope at any point along a phase boundary given enthalpy, temperature and molar volume change or a way to estimate them.

Carbon dioxide exhibits a phase diagram (figure 1.7.4) that is typical of substances that exist as solids, liquids and gases between a 0 and a few hundred atmospheres of pressure and between temperatures that are easily achieved in the lab. Thus it is a good example to keep in mind as we look at the slopes of the phase boundaries.

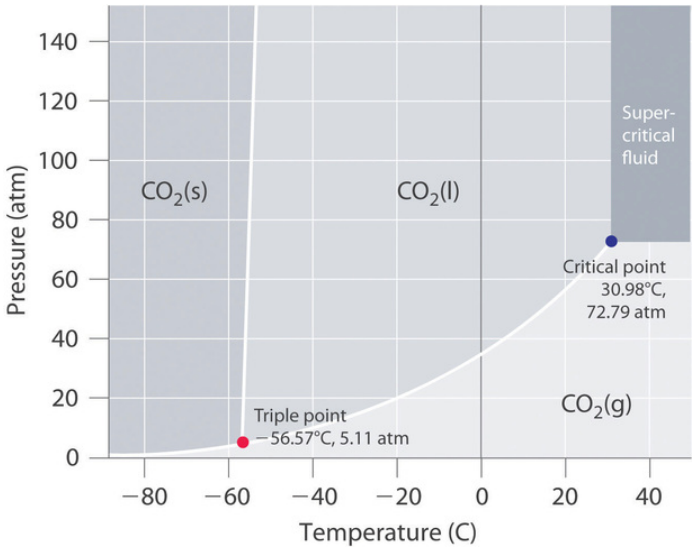


Figure 1.7.4 Phase diagram of CO_2. This is an example of a typical phase diagram.

1.7.4.4: Solid — liquid phase boundary

In most cases V_{molar}(solid) < V_{molar}(liquid) so $\Delta V_{trs} > 0$. Also $\Delta H_{trs} > 0$. Since temperature is also positive, equation 1.7.18 implies that the solid - liquid coexistence boundary will have a positive slope. As the enthalpy and volume change are nearly constant with pressure and temperature the slope will slowly decrease as the temperature increases. In the part of the CO_2 phase diagram shown in figure 1.7.4 this phase boundary appears to grow linearly. This is because the ratio $\frac{\Delta H}{\Delta V}$ is so large that the temperature changes little in the pressure range considered. We can rearrange 1.7.18 and integrate to get an expression for the change in P for a given change in T assuming $\frac{\Delta H}{\Delta V}$ is constant:

$$\frac{dP}{dT} = \frac{\Delta H}{T\Delta V} \implies dP = \frac{\Delta H}{T\Delta V} dT \tag{1.7.19}$$

so, assuming constant enthalpy and volume changes:

$$\int_{P_1}^{P_2} dP = \int_{T_1}^{T_2} \frac{\Delta H}{T\Delta V} dT \implies \Delta P = \frac{\Delta H}{\Delta V} \int_{T_1}^{T_2} \frac{dT}{T} \tag{1.7.20}$$

which integrates to:

$$\Delta P = \frac{\Delta H}{\Delta V} ln\left(\frac{T_2}{T_1}\right) \tag{1.7.21}$$

So given a starting point on the curve we can estimate nearby P and T combinations on the curve.

Note

Note that water has a solid - liquid phase boundary with a negative slope because V_{molar}(ice) > V_{molar}(water); thus $\Delta V < 0$ (see figure 1.7.5).

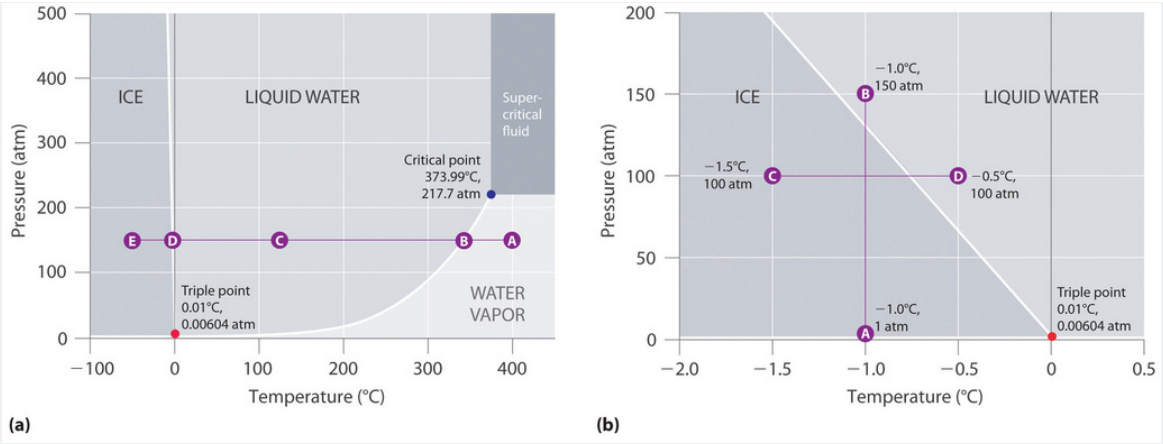


Figure 1.7.5: Two Versions of the Phase Diagram of Water. (a) In this graph with linear temperature and pressure axes, the boundary between ice and liquid water is almost vertical. (b) This graph with an expanded scale illustrates the decrease in melting point with increasing pressure.

1.7.4.5: Liquid — gas and solid — gas phase boundaries

In this case V_{molar}(g) is much greater than V_{molar}(l) or V_{molar}(s). For example near room temperature the molar volume of liquid water is about 18 mL, while the molar volume of gaseous water is about 800 L. So V_{molar}(g) is around 40000 times larger than that of the liquid or solid. Thus, to within about 1 part in 10^5:

$$\Delta V_{trs} = V_{molar}(g) - V_{molar}(\text{s or l}) \approx V_{molar}(g) \tag{1.7.22}$$

Substituting this into the Clapeyron equation 1.7.18 and assuming the gas behaves ideally, $V_{molar} = \frac{RT}{P}$, yields:

$$\frac{dP}{dT} = \frac{\Delta H_{trs}}{T_{trs} V_{molar}(g)} = \frac{P \Delta H_{trs}}{RT^2} \tag{1.7.23}$$

Collecting all the Ps on one side and Ts on the other allows us to integrate one side versus P and the other versus T. First consider the indefinite integral:

$$\int \frac{dP}{P} = \int \frac{\Delta H_{trs}}{RT^2} dT \implies lnP = \frac{-\Delta H}{RT} + C \tag{1.7.24}$$

where we have collected the constants of integration from both sides into C. Exponentiating both sides and calling e^C C' gives us an expression for the temperature dependence of P along the phase boundary:

$$P = C' exp\left(\frac{-\Delta H}{RT}\right) = C' e^{\frac{-\Delta H}{RT}} \tag{1.7.25}$$

So, we expect to see exponentially increasing curves as T increases ($\frac{-\Delta H}{RT} \to 0$). These terminate at the triple and critical points, so do not blow up. We can also do the definite integrals of equation 1.7.23, which yields the most commonly used form of the Clausius-Clapeyron equation:

$$ln\left(\frac{P_2}{P_1}\right) = \frac{-\Delta H}{R}\left(\frac{1}{T_2} - \frac{1}{T_1}\right) \tag{1.7.26}$$

Vapor pressure of a pure substance

Equations 1.7.25 and 1.7.26 also show how the vapor pressure of a pure substance varies with temperature.

NOTE: keep in mind that the assumption that ΔH_{vap} is constant means that the equation is only valid over relatively small temperature changes. For larger changes the the variation must be taken into account, usually by measuring the values experimentally.

1.7.5: Mixtures

For a multi-component system of ideal gases, chemical potential for each component is related to the partial pressure P_i of each species compared to the standard potential at 1 bar. Rearranging and integrating equation 1.7.11 we get:

$$\int_{P^o}^{P_i} d\mu = \int_{P^o}^{P_i} \frac{RT}{P} dP \implies \Delta\mu = RTln\left(\frac{P_i}{P^o}\right) \tag{1.7.27}$$

Adding this to the standard chemical potential of the species μ_i^o yields:

$$\mu_i = \mu_i^o + RTln\left(\frac{P_i}{P^o}\right) \tag{1.7.28}$$

Key Result: For a mixture of ideal gases, the chemical potential of the i[th] species is $\mu_i = \mu^o + RTln\left(\frac{P_i}{P^o}\right)$ where P_i is the partial pressure of the gas and μ_i^o is the standard chemical potential of component i when its partial pressure is 1 bar.

1.7.6: Thermodynamics of mixing volatile liquids

Figure 1.7.6 shows a pure liquid at equilibrium with its vapor in a closed container.

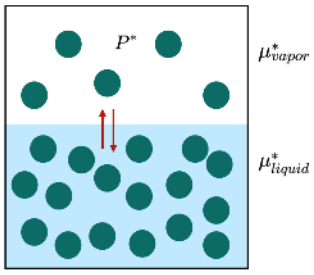


Figure 1.7.6

Since the system is at equilibrium the chemical potentials are equal:

$$\mu^*_{vapor} = \mu^*_{liquid} \tag{1.7.29}$$

where the asterisk (*) indicates a pure substance. From equation 1.7.28 for the gas phase we can write:

$$\mu^*_{vapor} = \mu^*_{liquid} = \mu^o_{vapor} + RTln\left(\frac{P^*}{P^o}\right) \tag{1.7.30}$$

where P* is the vapor pressure and μ^o_{vapor} is the chemical potential at P^o = 1 bar.

Now consider a mixture of volatile liquids as shown in figure 1.7.7

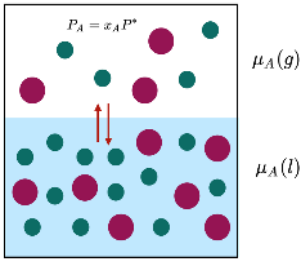


Figure 1.7.7

Since both components are in equilibrium with their vapors, the chemical potential for each component is still equal in the two phases. For example, for component A, we have:

$$\mu_A(l) = \mu_A(g) = \mu_A^o(g) + RTln\left(\frac{P_A}{P^o}\right) \tag{1.7.31}$$

where P_A is the partial pressure of vapor A. Because, $\mu^o_{vapor} = \mu^o_A(g)$, we subtract equation 1.7.30 from equation 1.7.31 to obtain:

$$\mu_A(l) - \mu_A^*(l) = RT\ln\left(\frac{P_A}{P^o}\right) - RT\ln\left(\frac{P^*}{P^o}\right) \implies \mu_A(l) = \mu_A^*(l) + RT\ln\left(\frac{P_A}{P_A^*}\right) \tag{1.7.32}$$

Thus, from equation 1.7.32, the chemical potential of a liquid in a mixture, $\mu_A(l)$, is given in terms of the chemical potential of the pure liquid ($\mu_A^*(l)$) and the ratio of the vapor pressure in the pure state over the vapor pressure in the mixture.

The relationship between the two vapor pressures in equation is given by **Raoult's law** which states that the vapor pressure of a substance in a mixture is the product of its vapor pressure as a pure liquid and its mole fraction:

$$P_A = x_A P_A^* \tag{1.7.33}$$

where x_A is the mole fraction of component A in the mixture. Inserting equation 1.7.33 into equation 1.7.32 gives the final expression for the chemical potential of a liquid in an **ideal** mixture:

$$\mu_A(l) = \mu_A^*(l) + RTln(x_A) \tag{1.7.34}$$

Raoult's law is based on a lifetime of work measuring vapor pressures (partial pressures) of liquid vapor above solutions by F. Raoult in the 1800s. It is only valid for solutions that behave ideally or are very dilute ($x_A \approx 1$).

Very dilute conditions are met when the volatile liquid of interest is in large excess (often the case for the solvent in a solution). The closer the mole fraction of the solvent is to 1, the more ideally it behaves. There are some cases where the two species being mixed are similar enough that ideal behavior is seen for all mole fractions. An example where ideal behavior is seen at all concentrations is when mixing benzene and methylbenzene.

Physical interpretation of Raoult's law: For an ideal mixture of two substances the fraction of each substance at the surface will be their mole fractions. This means that the chance a molecule of a substance can escape the surface will be reduced from the pure case by a factor of its mole fraction.

Thermodynamic interpretation of Raoult's law: A mixture has a higher entropy than a pure substance. This reduces the propensity of liquid molecules escaping into the gas phase to increase their entropy.

See Practice Problems 1.7.4 and 1.7.5.

1.7.7: Thermodynamics of ideal solutions

For the case of a solute dissolved in a solvent (liquid), the chemical potential of the solvent is the same as for a mixture of volatile liquids:

$$\mu_{solvent}(l) = \mu^*_{solvent}(l) + RT \ln x_{solvent} \tag{1.7.35}$$

For the case of the solute, it is often more convenient to express the chemical potential in terms of the *molality* m defined as

$$\text{molality} = \frac{\text{moles of solute}}{\text{mass of solvent in kg}}$$

For the solute, the chemical potential is:

$$\mu_{solute}(l) = \mu^\circ_{solute}(l) + RT \ln\left(\frac{m_{solute}}{m^\circ}\right) \tag{1.7.36}$$

Note here the careful choice of the reference state for the solute. The references state is defined as a state of unit molality where $m^o = 1$ mol kg^{-1}.

1.7.8: Thermodynamics of real solutions

Under realistic conditions such as inside a cell or in a body of surface water (oceans and most lakes and streams) the conditions are far from that of an ideal solution. To account for more realistic conditions while maintaining the mathematical formulations as close to what we have derived as possible we write the chemical potential of a species as:

$$\mu_i = \mu_i^\circ + RT \ln a_i \tag{1.7.37}$$

where a_i is called the **activity** and μ°_i is a reference state. For real solutions, the activity is given as

$$a_i = \gamma_i(m_i/m^\circ) \tag{1.7.38}$$

where γ_i is called the **activity coefficient** that is a measure of the deviation from ideality. For an ideal solution, $\gamma=1$ and $a_i = \frac{m_i}{m^o}$. Table 1.7.1 summarizes the expression of the activity and standard state for various substances. Note that for a pure sold and a pure liquid the activity is one.

Table 1.7.1 Activity and standard state for various substances.

Substance	Standard State (μ^o)	activity (a)
solid	pure solid, 1 bar	1

Substance	Standard State (μ^o)	activity (a)
liquid	pure liquid, 1 bar	1
gas	pure gas, 1 bar	P^*/(1 bar)
solvent	pure solvent	mole fraction x_i
ideal solute	molality of 1 mol kg^{-1}	$\frac{m_i}{m^o}$
real solution	molality of 1 mol kg^{-1}	$\gamma_i(m_i/m^\circ)$

1.7.9: Practice Problems

Problem 1.7.1. At high pressure, graphite (density ρ=2.25 g/cm^3) can be spontaneously converted into diamond (density ρ=3.51 g/cm^3) through a solid-to-solid phase transition:

C (graphite) → C (diamond)

At 1 atm of pressure the standard molar Gibbs energy of this reaction is ΔG^o=2.84 kJ/mol. At what pressure does the reaction become spontaneous (i.e. at what pressure does ΔG_{molar}=0)?

Problem 1.7.2. Consider the *reversible* freezing of liquid water into ice at a constant temperature of 0 °C and constant pressure of 1 atm.

H_2O (l) ↔ H_2O (g) 0 °C

Show that ΔG for this process is 0. (Hint: use the relation $\Delta G = \Delta H - T\Delta S$).

Problem 1.7.3. Which of the following has a higher chemical potential? (If neither, answer “same”)

(a) H_2O (l) or H_2O (s) at water’s normal melting point (0 ºC).

(b) H_2O (l) or H_2O (s) at -5 ºC and 1 bar.

Problem 1.7.4. Which would have the higher chemical potential? Benzene at 25 ºC and 1 bar or benzene in a 0.1 M toluene solution at 25 ºC and 1 bar.

Problem 1.7.5. Calculate the chemical potential of ethanol in solution relative to that of pure ethanol when its mole fraction is 0.40 at its boiling point (78.3 ºC.)

This page titled 1.7: Phase Equilibria and Mixtures is shared under a CC BY-NC-SA 4.0 license and was authored, remixed, and/or curated by Jonathan Gutow.

- **1.7: Equilibria in Biochemical Systems** by Serge L. Smirnov and James McCarty is licensed CC BY-NC-SA 4.0.
- **1.6: The Gibbs and Helmholtz Energy** by Serge L. Smirnov and James McCarty is licensed CC BY-NC-SA 4.0.

1.8: Colligative Properties

Colligative properties are important properties of **solutions** as they describe how the properties of the **solvent** will change as **solute** (or solutes) is (are) added. Before discussing these important properties, let us first review some definitions.

- **Solution** – a homogeneous mixture.
- **Solvent** – The component of a solution with the largest mole fraction
- **Solute** – Any component of a solution that is not the solvent.

Solutions can exist in solid (alloys of metals are an example of solid-phase solutions), liquid, or gaseous forms. For the most part, this discussion will focus on liquid-phase solutions.

1.8.1: Freezing Point Depression

Empirically it is found that the change in freezing point is proportional to the molality of the solute:

$$\Delta T_f = K_f m_B \tag{1.8.1}$$

where ΔT gives the magnitude of the reduction of freezing point for the solution, K_f is is the **cryoscopic constant** for the solvent and m_B is the molality of the solute.

Caution

m_B is the **molality of particles dissolved** not molality of empirical formula units. If the solute is NaCl than $m_B \approx 2$(molality of NaCl). This is often indicated by including the van 't Hoff factor (usually represented by i): $\Delta T_f = K_f i m_B$. Because many salts do not dissociate completely except at very low concentrations the van 't Hoff factor is an additional empirically determined quantity.

In equation 1.8.1 K_f is a negative value. However, many tabulations record K_f as a positive value. You must remember that ΔT for freezing point depression is < 0 and change the sign of tabulated K_f values accordingly.

Notice that this result is independent of the identity of the solute.

The solute particles do not dissolve in the solid. This means that adding solute to the liquid phase increases its entropy relative to the solid phase, favoring the liquid phase. Thus, the temperature must drop to a lower value to favor the solid phase. It is important to keep in mind that for a real solution, freezing of the solvent changes the composition of the solution by decreasing the mole fraction of the solvent and increasing that of the solute. As such, the magnitude of ΔT will change as the freezing process continually removes solvent from the liquid phase of the solution.

Demonstration of why the dependence on concentration is expected to be nearly linear.

In general a liquid will freeze when

$$\mu_s \leq \mu_l$$

The key is that the solute remains in the liquid solvent. As such, the freezing point of the solvent in a solution will be affected by anything that changes the chemical potential of the solvent, while the chemical potential of the solid will only be impacted by the temperature change. In a mixture, the chemical potential of component A can be calculated by

$$\mu_A = \mu_A^o + RT \ln x_A \tag{1.8.2}$$

And because x_A is always less than (or equal to) 1, the chemical potential is always reduced by the addition of another component.

We also know how temperature impacts chemical potential, which will effect both phases:

$$\left(\frac{\partial \mu}{\partial T}\right)_P = -S_{molar} \implies \Delta\mu = -S_{molar}\Delta T \tag{1.8.3}$$

The condition under which the solvent will freeze is

$$\mu_s = \mu_l$$

If we start at the standard freezing point of the pure solvent we can call the chemical potential μ^{fp}. For the solid phase when we reach the new equilibrium this is only impacted by the temperature change, while the solvent chemical potential is changed by both

dissolving the solute and the temperature change. Thus, at the new equilibrium we have new chemical potentials for the two phases:

$$\mu_s(T_2) = \mu^{fp} - S_{molar}(s)\Delta T \tag{1.8.4}$$

$$\mu_l(T_2) = \mu^{fp} - S_{molar}(l)\Delta T + RT_2 ln(x_A) \tag{1.8.5}$$

Setting these equal to each other:

$$\cancel{\mu^{fp}} - S_{molar}(s)\Delta T = \cancel{\mu^{fp}} - S_{molar}(l)\Delta T + RT_2 ln(x_A) \implies -S_{molar}(s)\Delta T = -S_{molar}(l)\Delta T + RT_2 ln(x_A) \tag{1.8.6}$$

Collecting the entropy terms on one side and recognizing that $x_A = 1 - x_B$ yields:

$$S_{molar}(l)\Delta T - S_{molar}(s)\Delta T = RT_2 ln(x_A) \implies \Delta S_{fus}\Delta T = RT_2 ln(1 - x_B) \tag{1.8.7}$$

For small x_B, $ln(1 - x_B) \approx -x_B$:

$$\Delta S_{fus}\Delta T = -RT_2 x_B \tag{1.8.8}$$

which can be rearranged to:

$$\Delta T = -\frac{RT_2}{\Delta S_{fus}} x_B \tag{1.8.9}$$

Since we have assumed a relatively small x_B the temperature change will be small meaning ΔS will be nearly constant. Thus, everything in the fraction on the right-hand-side of equation 1.8.9 can be identified as the constant K_f. As molality is proportional to mole fraction this justifies the form of the freezing point depression equation.

1.8.2: Boiling Point Elevation

Boiling point elevation is similar to freezing point depression. In short, the introduction of a solute into a liquid solvent lowers the chemical potential of the solvent, causing it to favor the liquid phase over the vapor phase. As such, the temperature must be increased to increase the chemical potential of the solvent in the liquid solution until it is equal to that of the vapor-phase solvent. The increase in the boiling point can be expressed as

$$\Delta T = K_b m_B$$

K_b is called the **ebullioscopic constant** and, like the cryoscopic constant, is a property of the solvent that is independent of the solute or solutes.

Caution

As with freezing point depression m_B is the molality of dissolved particles.

Some values of K_f and K_b are shown in the table below.

Substance	K_f (°C kg mol-1)	T_f^o (°C)	K_b (°C kg mol-1)	T_b^o (°C)
Water	1.86	0.0	0.51	100.0
Benzene	5.12	5.5	2.53	80.1
Ethanol	1.99	-114.6	1.22	78.4
CCl_4	29.8	-22.3	5.02	76.8

Example 1.8.1:

The boiling point of a solution of 3.00 g of an unknown compound in 25.0 g of CCl_4 raises the boiling point to 81.5 °C. What is the molar mass of the compound?

Solution

The approach here is to find the number of moles of solute in the solution. First, find the concentration of the solution:

$$(85.5\ ^\circ C - 76.8\ ^\circ C) = (5.02\ ^\circ C\ Kg/mol)\, m$$

$$m = 0.936\, mol/kg$$

Using the number of kg of solvent, one finds the number for moles of solute:

$$\left(0.936\, mol/\ \cancel{kg}\right)(0.02\ \ \cancel{kg}) = 0.0234\, mol$$

The ratio of mass to moles yields the final answer:

$$\frac{3.00\, g}{0.0234} = 128 g/mol$$

1.8.3: Vapor Pressure Lowering

For volatile solutes we have noted that Raoult's Law $P_A = x_A P_A^*$ is usually only valid at low solute concentrations. The derivation below shows that for non-volatile solutes Raoult's law can be expected to work over a much larger mole fraction range.

For much the same reason as the lowering of freezing points and the elevation of boiling points for solvents into which a solute has been introduced, the vapor pressure of a volatile solvent will be decreased due to the introduction of a solute. The magnitude of this decrease can be quantified by examining the effect the solute has on the chemical potential of the solvent.

In order to establish equilibrium between the solvent in the solution and the solvent in the vapor phase above the solution, the chemical potentials of the two phases must be equal.

$$\mu_{vapor} = \mu_{solvent}$$

If the solute is not volatile, the vapor will be pure, so (assuming ideal behavior)

$$\mu_{vap}^o + RT \ln \frac{P'}{P^o} = \mu_A^o + RT \ln x_A \tag{1.8.10}$$

Where P' is the vapor pressure of the solvent over the solution. Similarly, for the pure solvent in equilibrium with its vapor

$$\mu_A^o = \mu_{vap}^o + RT \ln \frac{P_A^*}{P^o} \tag{1.8.11}$$

where P^o is the standard pressure of 1 atm, and P_A^* is the vapor pressure of the pure solvent. Substituting Equation 1.8.11 into Equation 1.8.10 yields

$$\cancel{\mu_{vap}^o} + RT \ln \frac{P'}{P^o} = \left(\cancel{\mu_{vap}^o} + RT \ln \frac{P_A^*}{P^o} \right) + RT \ln x_A$$

The terms for μ_{vap}^o cancel, leaving

$$RT \ln \frac{P'}{P^o} = RT \ln \frac{P_A^*}{P^o} + RT \ln x_A$$

Subtracting $RT \ln(P_A^*/P^o)$ from both side produces

$$RT \ln \frac{P'}{P^o} - RT \ln \frac{P_A^*}{P^o} = RT \ln x_A$$

which rearranges to

$$RT \ln \frac{P'}{P_A^*} = RT \ln x_A$$

Dividing both sides by RT and then exponentiating yields

$$\frac{P'}{P_A^*} = x_A$$

or

$$P' = x_A P_A^* \tag{1.8.12}$$

This last result is Raoult's Law. A more formal derivation would use the fugacities of the vapor phases, but would look essentially the same. Also, as in the case of freezing point depression and boiling point elevations, this derivation did not rely on the nature of the solute!

However, unlike freezing point depression and boiling point elevation, this derivation did not rely on the solute being dilute, so the result should apply the entire range of concentrations of the solution.

Example 1.8.2:

Consider a mixture of two volatile liquids A and B. The vapor pressure of pure A is 150 Torr at some temperature, and that of pure B is 300 Torr at the same temperature. What is the total vapor pressure above a mixture of these compounds with the mole fraction of B of 0.600. What is the mole fraction of B in the vapor that is in equilibrium with the liquid mixture?

Solution

Using Raoult's Law (Equation 1.8.12)

$$P_A = (0.400)(150\,Toor) = 60.0\,Torr$$

$$P_B = (0.600)(300\,Toor) = 180.0\,Torr$$

$$P_{tot} = P_A + P_B = 240\,Torr$$

To get the mole fractions in the gas phase, one can use Dalton's Law of partial pressures.

$$x_A = \frac{P_A}{P_{tot}} = \frac{60.0\,Torr}{240\,Torr} = 0.250$$

$$x_B = \frac{P_B}{P_{tot}} = \frac{180.0\,Torr}{240\,Torr} = 0.750$$

And, of course, it is also useful to note that the sum of the mole fractions is 1 (as it must be!)

$$x_A + x_B = 1$$

1.8.4: Osmotic Pressure and Osmotic Virial Coefficients

In dealing with solutions (either solutions of small molecule solutes or macromolecules in solution), an important colligative property is the **osmotic pressure**. The osmotic pressure is given by the symbol Π and is different from the pressure of a gas (P) because it does not arise from collisions of molecules against the wall of a container. The osmotic pressure is a *hydrostatic* pressure that arises when solvent molecules pass through a semipermeable membrane to the more concentrated side of the membrane as shown in figure 1.8.1. The flow of solvent across the semipermeable membrane is called **osmosis**. Consider the osmotic pressure (Π) that develops on the more concentrated side of the membrane due to solvent molecules moving from the dilute to the concentrated side of the membrane. This situation illustrated in figure 1.8.1.

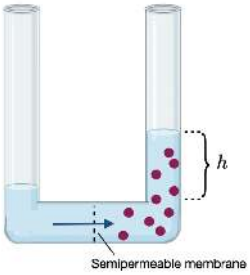


Figure 1.8.1: Definition of osmotic pressure. The difference in concentration across the membrane causes a chemical potential. Solvent flows from the dilute to the concentrated side in an attempt to equalize the chemical potential. As water flows from the dilute to concentrated side, the water level will rise on the concentrated side. At equilibrium, the pressure differential is equal to the osmotic pressure.

As the pressure builds up on the high concentration side, the solvent level will rise by a height, h. The hydrostatic pressure is the difference between the pressure on the two sides of the semipermeable membrane and is given as

$$\Pi = \rho g h \tag{1.8.13}$$

where ρ is the solvent density, and g is the acceleration due to gravity. For an **ideal solution**, the osmotic pressure, Π, resembles the form of the ideal gas law:

$$\Pi V = nRT \tag{1.8.14}$$

Using the fact that n/V is the **concentration** (i.e. number of moles per unit volume of solution), we can rewrite Equation 1.8.14 in terms of the **molarity** (M):

$$\Pi = MRT \tag{1.8.15}$$

If we define the **mass concentration** (C) of the solute, then we can rewrite 1.8.15 as:

$$\Pi = \frac{CRT}{M_w} \implies \frac{\Pi}{RTC} = \frac{1}{M_w} \tag{1.8.16}$$

where M_w is the molar mass of the solute molecule, and C is the mass concentration of the solute ($C = nM_w/V$). In this case we can extract the molar mass as:

$$M_w = \frac{RTC}{\Pi}$$

from any single measurement of the osmotic pressure.

Equation 1.8.16 assumes we are dealing with an ideal solution in which the solute particles are non-interacting. If this is not the case than a plot of Π versus C will not be linear as implied by equation 1.8.16. Instead, if we want to consider a *non-ideal* solution of weakly interacting molecules, we can expand Equation 1.8.16 in powers of C to obtain a virial equation of state for the osmotic pressure of a real solution:

$$\frac{\Pi}{RTC} = \frac{1}{M_w}\left[1 + B_2'C + B_3'C^2 + B_4'C^3 + \ldots\right] \tag{1.8.17}$$

where $B_2', B_3', B_4' \ldots$ are the second, third, and fourth osmotic virial coefficients.

In the dilute limit ($C << 1$), we can truncate the expansion at the second virial coeffient:

$$\frac{\Pi}{RTC} = \frac{1}{M_w}\left[1 + B_2'C\right] \tag{1.8.18}$$

The second virial coefficient B' is related to the interactions between particles. The second virial coefficent may be positive or negative depending on the nature of the particle-particle interactions. A negative coefficient corresponds to net attractive interactions, and a positive coefficient correspond to repulsive interactions.

Example 1.8.1

Equation 1.8.18 is sometimes used to **estimate the molar mass** of macromolecules. Consider the following data for a hypothetical macromolecule that cannot pass through the membrane. Experimentally you measure the mass concentration of the macromolecule, the solution density and the height the solution rises to counteract the osmotic pressure between the side with no macromolecules and the side containing macromolecules.

Table 1.8.2: mass concentration, solution density and height from osmotic pressure for unknown macromolecule at 298.0 K.

C (mg/mL)	ρ (g/mL)	h (cm)
0.531	1.005	1.10
1.678	1.017	5.38
2.444	1.024	9.65
3.204	1.032	14.97
4.113	1.041	22.72

Solution

The linearized form of equation 1.8.18 suggests that the intercept of a plot of $\frac{\Pi}{RTC}$ is the inverse of the molecular weight. Alternatively, with modern fitting software we could fit Π versus C which would follow the form:

$$\Pi = \frac{RT}{M_w}C + \frac{RTB_2}{M_w}C^2 = aC + bC^2$$

Thus, M_w = RT/a. This gives the same value as calculating $\frac{\Pi}{RTC}$ making the plot followed by taking the inverse of the intercept. The more traditional method is illustrated immediately below:

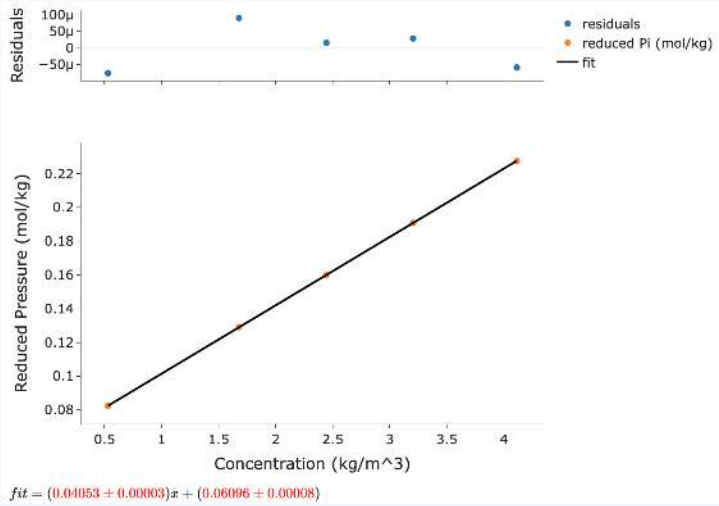
1) Calculate values for Π using $\Pi = \rho g h$, equation 1.8.13. It is best to decide on units. For this example everything is converted to SI. So C is converted to kg/m^3 by multiplication by (kg/10^6 mg)(10^{6}mL/m^3) = 1(kg/m^3)/(mg/mL) and cm are converted to meters.

2) Calculated the reduced osmotic pressure $\frac{\Pi}{RTC}$.

Results of 1 and 2 are shown in the table below:

C (mg/mL)	Π (Pa)	$\frac{\Pi}{RTC}$ (mol/kg)
0.531	108	0.0824
1.678	537	0.129
2.444	969	0.160
3.204	1515	0.1908
4.113	2319	0.2276

3) Plot and fit.



4) Calculate M_w as the inverse of the intercept.

$$M_w = \frac{1}{0.06096\ mol/kg} = 16.40\ kg/mol$$

A plot of Π versus concentration shows a definite positive curvature. So, this analysis is necessary to account for non-ideality.

Osmotic pressure plays an important role in biology. For example, trees use osmotic pressure to transport water from the roots to the upper branches. The effect of osmotic pressure on the cell is illustrated in figure 1.8.2. When red blood cells are placed in a salt solution having a lower concentration than the intracellular fluid, the solution is **hypotonic**, and the cell will gain water through osmosis in an attempt to equalize the osmotic pressure. This situation is illustrated in figure 1.8.2 (a). The cells will swell and potentially burst. When red blood cells are placed in a salt solution with the same osmotic pressure as the intracellular fluid, the solution is **isotonic** with respect to the cytoplasm. This situation is illustrated in See figure 1.8.2 (b). Finally, when red blood cells are placed in a solution with a higher salt concentration than the intracellular fluid, the solution is **hypertonic** and water inside the cell flows outside the cell in an attempt to equalize the osmotic pressure, causing the cell to shrink. This is the situation illustrated in figure 1.8.2 (c).

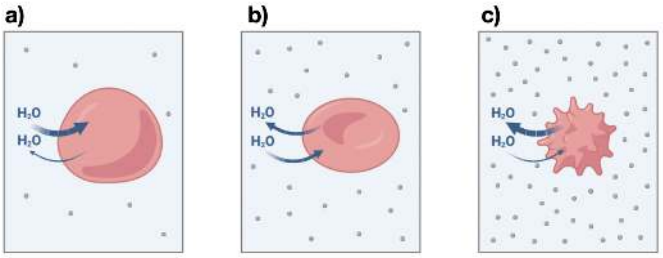
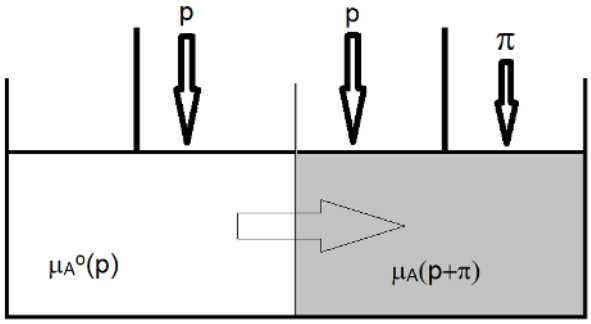


Figure 1.8.2: a) When red blood cells are placed in a hypotonic solution whose osmotic pressure is less than that of the intracellular fluid, water flows into the cells and the cell swells and eventually bursts. b) When red blood cells are placed in an isotonic salt solution having the same osmotic pressure as the intracellular fluid, the rate of flow of water into and out of the cells is the same and the cell does not change shape. c) When red blood cells are placed in a hypertonic solution, the osmotic pressure is greater outside than that of the intracellular fluid, and water flows out of the cells. The cells shrink.

1.8.5: Derivation of osmotic pressure equation form

Osmosis is a process by which solvent can pass through a semi-permeable membrane (a membrane through which solvent can pass, but not solute) from an area of low solute concentration to a region of high solute concentration. The **osmotic pressure** is the pressure that when exerted on the region of high solute concentration will halt the process of osmosis.



The nature of osmosis and the magnitude of the osmotic pressure can be understood by examining the chemical potential of a pure solvent and that of the solvent in a solution. The chemical potential of the solvent in the solution (before any extra pressure is applied) is given by

$$\mu_A = \mu_A^o + RT \ln x_A$$

And since $x_A < 1$, the chemical potential is of the solvent in a solution is always lower than that of the pure solvent. So, to prevent osmosis from occurring, something needs to be done to raise the chemical potential of the solvent in the solution. This can be accomplished by applying pressure to the solution. Specifically, the process of osmosis will stop when the chemical potential solvent in the solution is increased to the point of being equal to that of the pure solvent. The criterion, therefore, for osmosis to cease is

$$\mu_A^o(p) = \mu_A(x_b, +\Pi)$$

To solve the problem to determine the magnitude of p, the pressure dependence of the chemical potential is needed in addition to understanding the effect the solute has on lowering the chemical potential of the solvent in the solution. The magnitude, therefore, of the increase in chemical potential due to the application of excess pressure p must be equal to the magnitude of the reduction of chemical potential by the reduced mole fraction of the solvent in the solution. We already know that the chemical potential of the solvent in the solution is reduced by an amount given by

$$\mu_A^o - \mu_A = RT \ln x_A$$

And the increase in chemical potential due to the application of excess pressure is given by

$$\mu(p+\Pi) = \mu(p) + \int_p^{\Pi} \left(\frac{\partial \mu}{\partial p}\right)_T dp$$

The integrals on the right can be evaluated by recognizing

$$\left(\frac{\partial \mu}{\partial p}\right)_T = V$$

where V is the molar volume of the substance. Combining these expressions results in

$$-RT \ln x_A = \int_p^{p+\Pi} V \, dp$$

If the molar volume of the solvent is independent of pressure (has a very small value of κ_T, constant temperature compressibility – which is the case for most liquids) the term on the right becomes.

$$\int_p^{\Pi} V \, dP = Vp|_p^{p+\Pi} = V\Pi$$

Also, for values of x_A very close to 1

$$\ln x_A \approx -(1 - x_A) = -x_B$$

So, for dilute solutions

$$x_B RT = V\Pi$$

Or after rearrangement

$$\Pi = \frac{x_B RT}{V}$$

again, where V is the molar volume of the solvent. And finally, since x_B/V is the concentration of the solute B for cases where $n_B \ll n_A$. This allows one to write a simplified version of the expression which can be used in the case of very dilute solutions

$$\Pi = [B]RT$$

When a pressure exceeding the osmotic pressure Π is applied to the solution, the chemical potential of the solvent in the solution can be made to exceed that of the pure solvent on the other side of the membrane, causing reverse osmosis to occur. This is a very effective method, for example, for recovering pure water from a mixture such as a salt/water solution.

Colligative properties are properties that depend on the *number* of particles rather than their total mass. This implies that these properties can be used to measure molar mass. Colligative properties include:

- melting point depression
- boiling point elevation
- osmotic pressure

1.8.6: Problems

Problem 1.8.1. The osmotic pressure of a protein in solution at 298 K (under crystallization conditions) was measured at the following concentrations:

Concentration (g L^{-1})	osmotic pressure (10^{-2} kPa)
0.50	1.85
1.00	3.68
1.50	5.48
2.00	7.25
2.50	9.00

Assuming that the osmotic virial equation of state can be truncated after the second virial coefficient,

a) What is the molar mass of the protein?

b) What is the value of the second osmotic virial coefficient in units of L/g?

c) Based on the sign of the second virial coefficient, what might you speculate about the average contribution of intermolecular interactions under crystallization conditions? (For reference see: A. George and W.W. Wilson, "Predicting Protein Crystallization from Dilute Solution Property," *Acta Cryst.* (1994). D50, 361-365).

This page titled 1.8: Colligative Properties is shared under a CC BY-NC-SA 4.0 license and was authored, remixed, and/or curated by Jonathan Gutow.

- **7.6: Colligative Properties** by Patrick Fleming is licensed CC BY-NC-SA 4.0.
- **1.1: Thermodynamic Variables and Equations of State** by Serge L. Smirnov and James McCarty is licensed CC BY-NC-SA 4.0.
- **25.3: Colligative Properties Depend only on Number Density** is licensed CC BY-NC-SA 4.0.

1.9: Henry's Law

Henry's law is one of the gas laws formulated by William Henry in 1803 and states: "At a constant temperature, the amount of a given gas that dissolves in a given type and volume of liquid is directly proportional to the partial pressure of that gas in equilibrium with that liquid." An equivalent way of stating the law is that the solubility of a gas in a liquid is directly proportional to the partial pressure of the gas above the liquid:

$$C = kP_{gas} \tag{1.9.1}$$

where

- C is the solubility of a gas at a fixed temperature in a particular solvent (in units of M or mL gas/L)
- k is Henry's law constant (often in units of M/atm)
- P_{gas} is the partial pressure of the gas (often in units of atm)

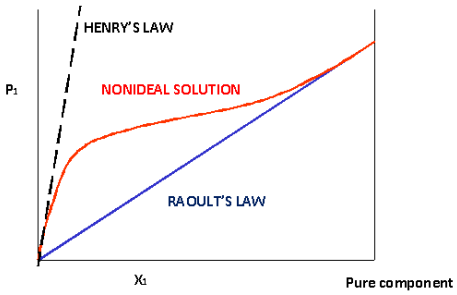


Figure 1.9.1: Positive non-ideal behavior of the vapor pressure of a solution follows Henry's Law at low concentrations and Raoult's Law at high concentrations (pure).

Key differences between Raoult's Law and Henry's Law

Raoult's and Henry's laws are limiting laws, generally applicable when the solute concentration goes to zero. In this limit the vapor pressure of any component in the solution depends linearly on its mole fraction, implying the absence of solute-solute interactions.

Raoult's law describes the dependence of the vapor pressure of a solvent as a function of its mole fraction χ_1:

$$\lim_{\chi_1 \to 1} \left(\frac{p}{\chi_1} \right) = p^*$$

where p^* is the vapor pressure of the pure solvent.

Henry's law describes the dependence of the vapor pressure of a solute as a function of its concentration. In terms of mole fraction χ_2:

$$\lim_{\chi_2 \to 0} \left(\frac{p}{\chi_2} \right) = K$$

For a binary mixture of pure substances it can be shown that the laws are complementary: if one law holds for one component then the other law holds for the other component. It can also be shown that the laws imply that the solution satisfies other criteria for ideality, including zero enthalpy and volume of mixing.

Example 1.9.1

What is Henry's constant for neon dissolved in water given: $C_{Ne} = 23.5\, mL/L$ solution and STP (22,414 mL/mole gas) and pressure (1 atm)?

Solution

Now we can rearrange our equation from above to solve for the constant:

$$C = kP_{Ne}$$

To use C we must convert 23.5 mL/L solution to Molarity. Since Ne is a gas, we can use our standard molar volume. Thus giving us:

$$\frac{23.5\ \text{mL/L soln}}{1\ \text{mole Ne}/22{,}414\ \text{mL}} = 0.00105\ M. \tag{1.9.2}$$

Now we have solved for the solubility of Ne in the solution. C= 0.00105M and we know the pressure at STP is 1 atm, so we can now use our rearranged equation:

$$k = \frac{C}{P_{Ne}}$$

Where C= 0.00105M, P_{Ne} = 1 atm, thus giving us k=0.00105 M/atm

Example 1.9.2

Compute the molar solubility in water that is saturated with air.

Solution

This time, we need to use constant (k) that we just calculated and our P_{Ne} in air.

$$\begin{aligned} C &= kP_{gas} \\ &= (0.00105\ M/atm)(0.0341\ atm) \\ &= 3.58 \times 10^{-5}\ M \end{aligned}$$

Applicability of Henry's Law

- Henry's law only works if the molecules are at equilibrium.
- Henry's law does not work for gases at high pressures (e.g., $N_{2\ (g)}$ at high pressure becomes very soluble and harmful when in the blood supply).
- Henry's law does not work if there is a chemical reaction between the solute and solvent (e.g., $HCl_{(g)}$ reacts with water by a dissociation reaction to generate H_3O^+ and Cl^- ions).

1.9.1: References

1. Zumdahl, Steven and Susan. Chemistry. Fifth Edition. Boston, MA: Houghton Mifflin Company, 2000.
2. Petrucci, Ralph, and William Harwood. F. Geoffrey Herring. Jeffry Madura. General Chemistry: Principles and Modern Applications. 9th ed. Upper Saddle River, NJ: Pearson, 2007.

This page titled 1.9: Henry's Law is shared under a CC BY-NC-SA 4.0 license and was authored, remixed, and/or curated by Sannah Khan.

- **Henry's Law** by Sannah Khan is licensed CC BY-NC-SA 4.0.

CHAPTER OVERVIEW

2: Chemical Equilibria

An understanding of chemical equilibria will allow you to understand how the chemical composition of a sample, in which the components can undergo chemical reactions, will stabilize over time or upon the input of energy or additional matter will change. This section discusses the thermodynamics of chemical equilibria, estimating equilibrium compositions, and accounting for changing conditions. The examples will focus primarily on acid-base equilibria as they are so important to the composition of water on this planet and the biology of living organisms.

2.1: Chemical Equilibria
2.2: Composition Dependence of Free Energy (G)
2.3: Equilibrium Calculations (ICE) Review
2.4: Fractional Composition at Equilibrium
2.5: Coupled Equilibria
2.6: Equilibrium Dependence on Conditions
2.7: Coupled Equilibria Driving Nonspontaneous Reactions
2.8: Brønsted-Lowry Acids and Bases
2.9: pH and pOH
2.10: Acid-Base Equilibria
2.11: Hydrolysis of Salts
2.12: Polyprotic Acids
2.13: Buffers

This page titled 2: Chemical Equilibria is shared under a CC BY-NC-SA 4.0 license and was authored, remixed, and/or curated by Jonathan Gutow.

2.1: Chemical Equilibria

2.1.1: Introduction

A chemical system is at equilibrium when the macroscopic fractional amounts of each chemical species in the system is not changing. When we say that a chemical reaction has "stopped" what we actually mean is that it has reached equilibrium. The equilibrium for some reactions lies strongly towards products. Some examples are the combustion of methane to producing water and carbon dioxide ($CH_4 + 2\,O_2 \longrightarrow CO_2 + 2\,H_2O$) or the conversion of diamond to graphite (this goes so slowly under standard conditions that it would take a very long time to reach equilibrium). In other cases, such as the dissociation of a weak acid ($CH_3(CO)OH(aq) \rightleftharpoons CH_3COO^-(aq) + H^+(aq)$), the equilibrium lies strongly towards the reactants and only a small fraction of the molecules are dissociated into ions.

2.1.2: Chemical equilibria are dynamic

Throughout our discussions of chemical equilibria it is important to keep in mind that these equilibria are dynamic in the sense that the forward and reverse of all the chemical reactions possible in the sample are always occurring. The equilibrium is maintained by the balance of the rates of interconversion between species. As a simple example consider the reaction $A \rightleftharpoons B$. If the probability of an A converting to a B is twice that of B converting to an A the composition will stop changing when the number of B are twice the number of A, because at that point the rate of production of A from B and B from A are equal. A cartoon of a dynamic equilibrium between two species is shown in figure 2.1.1.

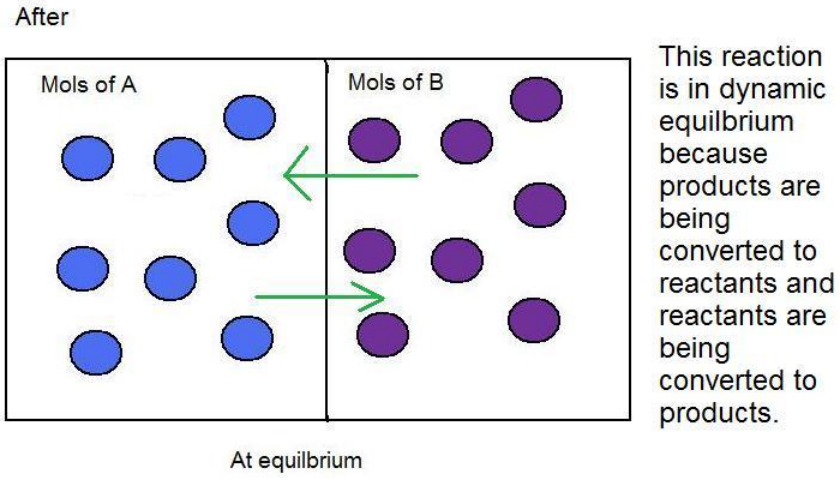


Figure 2.1.1: A cartoon of the dynamic equilibrium of two species, where the probability of converting from one species to the other is equal. Notice that the number of species of each type is the same at equilibrium.

2.1.3: Thermodynamic description

For reactions occurring under typical bench top constant pressure conditions equilibrium is described by free energy, G. As with phase equilibria we will consider how G changes as the composition of the system changes. When the G of the system has reached a minimum the system is at equilibrium. In terms of composition this means that any change would increase the free energy (G) of the system.

This page titled 2.1: Chemical Equilibria is shared under a CC BY-NC-SA 4.0 license and was authored, remixed, and/or curated by Jonathan Gutow.

2.2: Composition Dependence of Free Energy (G)

2.2.1: Change in G (dG) with composition

At a particular composition the free energy of a sample can be defined as:

$$G = \sum_i n_i . \mu_i \tag{2.2.1}$$

where n_i = the moles of species i and μ_i = the chemical potential of species i at the particular conditions and composition of the sample. Considering a sample of two species B and C this would be written as:

$$G = n_B \mu_B + n_C \mu_C \tag{2.2.2}$$

If the composition changes then applying the product rule for derivative to equation 2.2.2:

$$dG = n_B d\mu_B + \mu_B dn_B + n_C d\mu_C + \mu_C dn_C \tag{2.2.3}$$

Assuming the chemical potential changes little with composition, ($d\mu_i \approx 0$, or activities are close to 1) equation 2.2.3 simplifies to:

$$dG = \mu_B dn_B + \mu_C dn_C \tag{2.2.4}$$

2.2.2: dG during a reaction and $\Delta_r G$ going to equilibrium

Consider the case where the species can interconvert in a chemical reaction: $\mathrm{bB} \rightleftharpoons \mathrm{cC}$. We can then use the stoichiometry of the reaction to rewrite the infinitesimal changes in the moles of each species in terms of a single quantity, which we can think of as the reaction progress coordinate $d\zeta$. In this case $dn_C = cd\zeta$ and $dn_B = -bd\zeta$. Substituting these into equation 2.2.4 yields:

$$dG = -\mu_B b d\zeta + \mu_C c d\zeta = (c\mu_C - b\mu_B) d\zeta \tag{2.2.5}$$

Because chemical potential is composition dependent there is some point in the progress of the reaction where the difference $c\mu_C - b\mu_B = 0$. This is when dynamic equilibrium is reached and we say the reaction has "stopped."

If we consider the free energy of reaction as written it is just $\Delta_r G = c\mu_C - b\mu_B$. Substituting in the full composition dependence of the chemical potentials $\mu = \mu^o + RTln(a)$ gives us:

$$\Delta_r G = c\left(\mu_C^o + RTln(a_C)\right) - b\left(\mu_B^o + RTln(a_B)\right) = c\mu_C^o - b\mu_B^o + RTln\left(\frac{a_C^c}{a_B^b}\right) \tag{2.2.6}$$

Since $\Delta_r G^o = c\mu_C^o - b\mu_B^o$ we can simplify this further:

$$\Delta_r G = \Delta_r G^o + RTln\left(\frac{a_C^c}{a_B^b}\right) \tag{2.2.7}$$

When not at equilibrium this is often written with a Q for the fraction within the logarithm, where Q stands for **reaction quotient**:

$$\Delta_r G = \Delta_r G^o + RTlnQ \tag{2.2.8}$$

At equilibrium $\Delta_r G = 0$ and we can rearrange to:

$$\Delta_r G^o = -RTln\left(\frac{a_C^c}{a_B^b}\right) = -RTlnK_{eq} \tag{2.2.9}$$

> Note that because we are using activities Q and K_{eq} do not have any units. **When we use concentration units to approximate activities we reference them to the standard concentration as in [B]/(1 M) or in the case of molality we divide by 1 molal.** This maintains the lack of units in the fraction.

Using the Π notation for multiplication of many factors, we can write the general form of Q:

$$Q = \frac{\prod_{k=prod} a_k^{n_k}}{\prod_{j=reac} a_j^{n_j}} \tag{2.2.10}$$

where the n_k and n_j refer to stoichiometric coefficients.

2.2.3: Interconverting standard Gibbs reaction energy and K_{eq}

Equation 2.2.9 implies that there is a close relationship between the standard Gibbs reaction energy and the equilibrium constant. Repeating the equation in shortened form we have:

$$\Delta_r G^o = -RTlnK_{eq} \tag{2.2.11}$$

Thus, with a measured K_{eq} at T = 298 K, the $\Delta_r G^o$ can be calculated from this equation. We can also rearrange this to get K_{eq} at T = 298 K from $\Delta_r G^o$:

$$K_{eq} = exp\left(\frac{-\Delta_r G^o}{RT}\right) \tag{2.2.12}$$

2.2.4: Reaction Quotient and Equilibrium Constant Ratio Determines Reaction Direction

The Gibbs free energy function was constructed to be able to predict which changes could occur spontaneously. If we start with a set of initial concentrations we can write them in a reaction quotient

$$\Delta_r G = \Delta_r G^o + RT \ln Q$$

if we subtract the equilibrium version of this expression:

$$0 = \Delta_r G^o + RT \ln K$$

we get

$$\Delta_r G = RT \ln\left(\frac{Q}{K}\right)$$

That gives us the sign of $\Delta_r G$. If this is negative the reaction will spontaneously proceed from left to right as written, if positive it will run in reverse. In both case the value of Q will change until $Q = K$ and equilibrium has been reached.

The main difference between K and Q is that K describes a reaction that is at equilibrium, whereas Q describes a reaction that is not at equilibrium. To determine Q, the concentrations of the reactants and products must be known. For a given general chemical equation:

$$aA + bB \rightleftharpoons cC + dD \tag{2.2.13}$$

the Q equation is written by multiplying the activities for the species of the products and dividing by the activities of the reactants. If any component in the reaction has a coefficient, indicated above with lower case letters, the concentration is raised to the power of the coefficient. Q for the above equation is therefore:

$$Q = \frac{[C]^c[D]^d}{[A]^a[B]^b} \tag{2.2.14}$$

Note

A comparison of Q with K indicates which way the reaction shifts and which side of the reaction is favored:

- If $Q > K$, then the reaction favors the reactants. This means that in the Q equation, the ratio of the numerator (the concentration or pressure of the products) to the denominator (the concentration or pressure of the reactants) is larger than that for K, indicating that more products are present than there would be at equilibrium. Because reactions always tend toward equilibrium (Le Châtelier's Principle), the reaction produces more reactants from the excess products, therefore causing the system to shift to the **LEFT.** This allows the system to reach equilibrium.
- If $Q < K$, then the reaction favors the products. The ratio of products to reactants is less than that for the system at equilibrium—the concentration or the pressure of the reactants is greater than the concentration or pressure of the products. Because the reaction tends toward reach equilibrium, the system shifts to the **RIGHT** to make more products.

- If $Q = K$, then the reaction is already at equilibrium. There is no tendency to form more reactants or more products at this point. No side is favored and no shift occurs.

This page titled 2.2: Composition Dependence of Free Energy (G) is shared under a CC BY-NC-SA 4.0 license and was authored, remixed, and/or curated by Jonathan Gutow.

- **26.5: Reaction Quotient and Equilibrium Constant Ratio Determines Reaction Direction** is licensed CC BY 4.0.

2.3: Equilibrium Calculations (ICE) Review

Learning Objectives

By the end of this section, you will be able to:

- Identify the changes in concentration or pressure that occur for chemical species in equilibrium systems
- Calculate equilibrium concentrations or pressures and equilibrium constants, using various algebraic approaches

Having covered the essential concepts of chemical equilibria in the preceding sections of this chapter, this final section will demonstrate the more practical aspect of using these concepts and appropriate mathematical strategies to perform various equilibrium calculations. These types of computations are essential to many areas of science and technology—for example, in the formulation and dosing of pharmaceutical products. After a drug is ingested or injected, it is typically involved in several chemical equilibria that affect its ultimate concentration in the body system of interest. Knowledge of the quantitative aspects of these equilibria is required to compute a dosage amount that will solicit the desired therapeutic effect.

Many of the useful equilibrium calculations that will be demonstrated here require terms representing changes in reactant and product concentrations. These terms are derived from the stoichiometry of the reaction, as illustrated by decomposition of ammonia:

$$2\,\mathrm{NH_3(g)} \rightleftharpoons \mathrm{N_2(g)} + 3\,\mathrm{H_2(g)}$$

As shown earlier in this chapter, this equilibrium may be established within a sealed container that initially contains either NH_3 only, or a mixture of any two of the three chemical species involved in the equilibrium. Regardless of its initial composition, a reaction mixture will show the same relationships between changes in the concentrations of the three species involved, as dictated by the reaction stoichiometry (see also the related content on expressing reaction rates in the chapter on kinetics). For example, if the nitrogen concentration increases by an amount *x*:

$$\Delta\left[N_2\right] = +x$$

the corresponding changes in the other species concentrations are

$$\Delta\left[\mathrm{H_2}\right] = \Delta\left[\mathrm{N_2}\right]\left(\frac{3\ \mathrm{mol\ H_2}}{1\ \mathrm{mol\ N_2}}\right) = +3x$$

$$\Delta\left[\mathrm{NH_3}\right] = -\Delta\left[\mathrm{N_2}\right]\left(\frac{2\ \mathrm{mol\ NH_3}}{1\ \mathrm{mol\ N_2}}\right) = -2x$$

where the negative sign indicates a decrease in concentration.

Example 2.3.1: Determining Relative Changes in Concentration

Derive the missing terms representing concentration changes for each of the following reactions.

a. $$\underset{x}{\mathrm{C_2H_2(g)}} + 2\,\underset{?}{\mathrm{Br_2(g)}} \rightleftharpoons \underset{?}{\mathrm{C_2H_2Br_4(g)}}$$

b. $$\underset{?}{\mathrm{I_2(aq)}} + \underset{?}{\mathrm{I^-(aq)}} \rightleftharpoons \underset{x}{\mathrm{I_3^-(aq)}}$$

c. $$\underset{x}{\mathrm{C_3H_8(g)}} + 5\,\underset{?}{\mathrm{O_2(g)}} \rightleftharpoons 3\,\underset{?}{\mathrm{CO_2(g)}} + 4\,\underset{?}{\mathrm{H_2O(g)}}$$

Solution

a. $$\underset{x}{\mathrm{C_2H_2(g)}} + 2\,\underset{2x}{\mathrm{Br_2(g)}} \rightleftharpoons \underset{-x}{\mathrm{C_2H_2Br_4(g)}}$$

b. $$\underset{-x}{\mathrm{I_2(aq)}} + \underset{-x}{\mathrm{I^-(aq)}} \rightleftharpoons \underset{x}{\mathrm{I_3^-(aq)}}$$

c. $$\underset{x}{\mathrm{C_3H_8(g)}} + 5\,\underset{5x}{\mathrm{O_2(g)}} \rightleftharpoons 3\,\underset{-3x}{\mathrm{CO_2(g)}} + 4\,\underset{-4x}{\mathrm{H_2O(g)}}$$

Exercise 2.3.1

Complete the changes in concentrations for each of the following reactions:

a. $\underset{?}{2\,SO_2}(g) + \underset{x}{O_2}(g) \rightleftharpoons \underset{?}{2\,SO_3}(g)$

b. $\underset{?}{C_4H_8}(g) \rightleftharpoons \underset{-2x}{2\,C_2H_4}(g)$

c. $\underset{?}{4\,NH_3}(g) + \underset{x}{7\,O_2}(g) \rightleftharpoons \underset{?}{4\,NO_2}(g) + \underset{?}{6\,H_2O}(g)$

Answer

(a) 2*x*, *x*, −2*x;* (b) *x*, −2*x;* (c) 4*x*, 7*x*, −4*x*, −6*x* or −4*x*, −7*x*, 4*x*, 6*x*

2.3.1: Calculation of an Equilibrium Constant

The equilibrium constant for a reaction is calculated from the equilibrium concentrations (or pressures) of its reactants and products. If these concentrations are known, the calculation simply involves their substitution into the K expression, as was illustrated by Example 2.3.1. A slightly more challenging example is provided next, in which the reaction stoichiometry is used to derive equilibrium concentrations from the information provided. The basic strategy of this computation is helpful for many types of equilibrium computations and relies on the use of terms for the reactant and product concentrations *initially* present, for how they *change* as the reaction proceeds, and for what they are when the system reaches *equilibrium*. The acronym ICE is commonly used to refer to this mathematical approach, and the concentrations terms are usually gathered in a tabular format called an ICE table.

Example 2.3.2: Calculation of an Equilibrium Constant

Iodine molecules react reversibly with iodide ions to produce triiodide ions.

$$I_2(aq) + I^-(aq) \rightleftharpoons I_3^-(aq)$$

If a solution with the concentrations of I_2 and I^- both equal to 1.000×10^{-3} M before reaction gives an equilibrium concentration of I_2 of 6.61×10^{-4} M, what is the equilibrium constant for the reaction?

Solution

To calculate the equilibrium constants, equilibrium concentrations are needed for all the reactants and products:

$$K_C = \frac{[I_3^-]}{[I_2]\,[I^-]}$$

Provided are the initial concentrations of the reactants and the equilibrium concentration of the product. Use this information to derive terms for the equilibrium concentrations of the reactants, presenting all the information in an ICE table.

	I_2 + I^- ⇌ I_3^-		
Initial concentration (*M*)	1.000×10^{-3}	1.000×10^{-3}	0
Change (*M*)	$-x$	$-x$	$+x$
Equilibrium concentration (*M*)	$1.000 \times 10^{-3} - x$	$1.000 \times 10^{-3} - x$	x

At equilibrium the concentration of I_2 is 6.61×10^{-4} M so that

$$\begin{aligned} 1.000 \times 10^{-3} - x &= 6.61 \times 10^{-4} \\ x &= 1.000 \times 10^{-3} - 6.61 \times 10^{-4} \\ &= 3.39 \times 10^{-4} M \end{aligned}$$

The ICE table may now be updated with numerical values for all its concentrations:

	I_2 + I^- ⇌ I_3^-		
Initial concentration (*M*)	1.000×10^{-3}	1.000×10^{-3}	0
Change (*M*)	-3.39×10^{-4}	-3.39×10^{-4}	$+3.39 \times 10^{-4}$
Equilibrium concentration (*M*)	6.61×10^{-4}	6.61×10^{-4}	3.39×10^{-4}

Finally, substitute the equilibrium concentrations into the *K* expression and solve:

$$\begin{aligned} K_c &= \frac{\left[I_3^-\right]}{\left[I_2\right]\left[I^-\right]} \\ &= \frac{3.39 \times 10^{-4} M}{\left(6.61 \times 10^{-4} M\right)\left(6.61 \times 10^{-4} M\right)} = 776 \end{aligned}$$

? Exercise 2.3.2

Ethanol and acetic acid react and form water and ethyl acetate, the solvent responsible for the odor of some nail polish removers.

$$C_2H_5OH + CH_3CO_2H \rightleftharpoons CH_3CO_2C_2H_5 + H_2O$$

When 1 mol each of C_2H_5OH and CH_3CO_2H are allowed to react in 1 L of the solvent dioxane, equilibrium is established when $\frac{1}{3}$ mol of each of the reactants remains. Calculate the equilibrium constant for the reaction. (Note: Water is a solute in this reaction.)

Answer

$K_c = 4$

2.3.2: Calculation of a Missing Equilibrium Concentration

When the equilibrium constant and all but one equilibrium concentration are provided, the other equilibrium concentration(s) may be calculated. A computation of this sort is illustrated in the next example exercise.

✓ Example 2.3.3: Calculation of a Missing Equilibrium Concentration

Nitrogen oxides are air pollutants produced by the reaction of nitrogen and oxygen at high temperatures. At 2000 °C, the value of the K_c for the reaction,

$$N_2(g) + O_2(g) \rightleftharpoons 2\,NO(g)$$

is 4.1×10^{-4}. Calculate the equilibrium concentration of NO(*g*) in air at 1 atm pressure and 2000 °C. The equilibrium concentrations of N_2 and O_2 at this pressure and temperature are 0.036 M and 0.0089 M, respectively.

Solution

Substitute the provided quantities into the equilibrium constant expression and solve for [NO]:

$$K_c = \frac{[NO]^2}{[N_2]\,[O_2]}$$

$$[NO]^2 = K_c\,[N_2]\,[O_2]$$

$$[NO] = \sqrt{K_c\,[N_2]\,[O_2]}$$

$$= \sqrt{\left(4.1 \times 10^{-4}\right)(0.036)(0.0089)}$$

$$= \sqrt{1.31 \times 10^{-7}}$$

$$= 3.6 \times 10^{-4}$$

Thus [NO] is 3.6×10^{-4} mol/L at equilibrium under these conditions.

To confirm this result, it may be used along with the provided equilibrium concentrations to calculate a value for *K*:

$$K_c = \frac{[NO]^2}{[N_2]\,[O_2]}$$

$$= \frac{\left(3.6 \times 10^{-4}\right)^2}{(0.036)(0.0089)}$$

$$= 4.0 \times 10^{-4}$$

This result is consistent with the provided value for *K* within nominal uncertainty, differing by just 1 in the least significant digit's place.

? Exercise 2.3.3

The equilibrium constant K_c for the reaction of nitrogen and hydrogen to produce ammonia at a certain temperature is 6.00×10^{-2}. Calculate the equilibrium concentration of ammonia if the equilibrium concentrations of nitrogen and hydrogen are 4.26 *M* and 2.09 *M*, respectively.

Answer

1.53 mol/L

2.3.3: Calculation of Equilibrium Concentrations from Initial Concentrations

Perhaps the most challenging type of equilibrium calculation can be one in which equilibrium concentrations are derived from initial concentrations and an equilibrium constant. For these calculations, a four-step approach is typically useful:

1. Identify the direction in which the reaction will proceed to reach equilibrium.
2. Develop an ICE table.
3. Calculate the concentration changes and, subsequently, the equilibrium concentrations.
4. Confirm the calculated equilibrium concentrations.

The last two example exercises of this chapter demonstrate the application of this strategy.

✔ Example 2.3.4: Calculation of Equilibrium Concentrations

Under certain conditions, the equilibrium constant K_c for the decomposition of $PCl_5(g)$ into $PCl_3(g)$ and $Cl_2(g)$ is 0.0211. What are the equilibrium concentrations of PCl_5, PCl_3, and Cl_2 in a mixture that initially contained only PCl_5 at a concentration of 1.00 *M*?

Solution

Use the stepwise process described earlier.

Step 1.

Determine the direction the reaction proceeds.

The balanced equation for the decomposition of PCl_5 is

$$PCl_5(g) \rightleftharpoons PCl_3(g) + Cl_2(g)$$

Because only the reactant is present initially $Q_c = 0$ and the reaction will proceed to the right.

Step 2:

Develop an ICE table.

	$PCl_5 \rightleftharpoons$	PCl_3 +	Cl_2
Initial concentration (*M*)	1.00	0	0
Change (*M*)	$-x$	$+x$	$+x$
Equilibrium concentration (*M*)	$1.00 - x$	x	x

Step 3.

Solve for the change and the equilibrium concentrations.

Substituting the equilibrium concentrations into the equilibrium constant equation gives

$$\begin{aligned} K_c &= \frac{\left[PCl_3\right]\left[Cl_2\right]}{\left[PCl_5\right]} = 0.0211 \\ &= \frac{(x)(x)}{(1.00 - x)} \\ 0.0211 &= \frac{(x)(x)}{(1.00 - x)} \\ 0.0211(1.00 - x)7 &= x^2 \\ x^2 + 0.0211x - 0.0211 &= 0 \end{aligned}$$

Appendix B shows an equation of the form $ax^2 + bx + c = 0$ can be rearranged to solve for x:

$$x = \frac{-b \pm \sqrt{b^2 - 4ac}}{2a}$$

In this case, $a = 1$, $b = 0.0211$, and $c = -0.0211$. Substituting the appropriate values for a, b, and c yields:

$$\begin{aligned} x &= \frac{-0.0211 \pm \sqrt{(0.0211)^2 - 4(1)(-0.0211)}}{2(1)} \\ &= \frac{-0.0211 \pm \sqrt{\left(4.45 \times 10^{-4}\right) + \left(8.44 \times 10^{-2}\right)}}{2} \\ &= \frac{-0.0211 \pm 0.291}{2} \end{aligned}$$

The two roots of the quadratic are, therefore,

$$x = \frac{-0.0211 + 0.291}{2} = 0.135$$

and

$$x = \frac{-0.0211 - 0.291}{2} = -0.156$$

For this scenario, only the positive root is physically meaningful (concentrations are either zero or positive), and so x = 0.135 M.

The equilibrium concentrations are

$$[PCl_5] = 1.00 - 0.135 = 0.87\ \text{M}$$
$$[PCl_3] = x = 0.135\ \text{M} =$$
$$[Cl_2] = x = 0.135\ \text{M}$$

Step 4.

Confirm the calculated equilibrium concentrations.

Substitution into the expression for K_c (to check the calculation) gives

$$K_c = \frac{[PCl_3]\,[Cl_2]}{[PCl_5]} = \frac{(0.135)(0.135)}{0.87} = 0.021$$

The equilibrium constant calculated from the equilibrium concentrations is equal to the value of K_c given in the problem (when rounded to the proper number of significant figures).

Exercise 2.3.4A

Acetic acid, CH_3CO_2H, reacts with ethanol, C_2H_5OH, to form water and ethyl acetate, $CH_3CO_2C_2H_5$.

$$CH_3CO_2H + C_2H_5OH \rightleftharpoons CH_3CO_2C_2H_5 + H_2O$$

The equilibrium constant for this reaction with dioxane as a solvent is 4.0. What are the equilibrium concentrations for a mixture that is initially 0.15 M in CH_3CO_2H, 0.15 M in C_2H_5OH, 0.40 M in $CH_3CO_2C_2H_5$, and 0.40 M in H_2O?

Answer

$[CH_3CO_2H]$ = 0.18 M, $[C_2H_5OH]$ = 0.18 M, $[CH_3CO_2C_2H_5]$ = 0.37 M, $[H_2O]$ = 0.37 M

Exercise 2.3.4B

A 1.00-L flask is filled with 1.00 mole of H_2 and 2.00 moles of I_2. The value of the equilibrium constant for the reaction of hydrogen and iodine reacting to form hydrogen iodide is 50.5 under the given conditions. What are the equilibrium concentrations of H_2, I_2, and HI in moles/L?

$$H_2(g) + I_2(g) \rightleftharpoons 2\,HI(g)$$

Answer

$[H_2]$ = 0.06 M, $[I_2]$ = 1.06 M, $[HI]$ = 1.88 M

Example 2.3.5: Calculation of Equilibrium Concentrations Using an Algebra-Simplifying Assumption

What are the concentrations at equilibrium of a 0.15 M solution of HCN?

$$HCN(aq) \rightleftharpoons H^+(aq) + CN^-(aq) \qquad K_c = 4.9 \times 10^{-10}$$

Solution

Using "x" to represent the concentration of each product at equilibrium gives this ICE table.

	$HCN(aq) \rightleftharpoons$	$H^+(aq)$ +	$CN^-(aq)$
Initial concentration (*M*)	0.15	0	0
Change (*M*)	$-x$	$+x$	$+x$
Equilibrium concentration (*M*)	$0.15 - x$	x	x

Substitute the equilibrium concentration terms into the K_c expression

$$K_c = \frac{(x)(x)}{0.15 - x}$$

rearrange to the quadratic form and solve for *x*

$$x^2 + 4.9 \times 10^{-10} - 7.35 \times 10^{-11} = 0$$

$$x = 8.56 \times 10^{-6} M (3 \text{ sig. figs. }) = 8.6 \times 10^{-6} M (2 \text{ sig. figs. })$$

Thus $[H^+] = [CN^-] = x = 8.6 \times 10^{-6}$ M and $[HCN] = 0.15 - x = 0.15$ M.

Note in this case that the change in concentration is significantly less than the initial concentration (a consequence of the small *K*), and so the initial concentration experiences a negligible change:

$$\text{if } x \ll 0.15M, \text{ then } (0.15 - x) \approx 0.15$$

This approximation allows for a more expedient mathematical approach to the calculation that avoids the need to solve for the roots of a quadratic equation:

$$K_c = \frac{(x)(x)}{0.15 - x} \approx \frac{x^2}{0.15}$$

$$4.9 \times 10^{-10} = \frac{x^2}{0.15}$$

$$x^2 = (0.15)\left(4.9 \times 10^{-10}\right)$$

$$= 7.4 \times 10^{-11}$$

$$x = \sqrt{7.4 \times 10^{-11}}$$

$$= 8.6 \times 10^{-6} \text{ M}$$

The value of x calculated is, indeed, much less than the initial concentration

$$8.6 \times 10^{-6} \ll 0.15$$

and so the approximation was justified. If this simplified approach were to yield a value for *x* that did *not* justify the approximation, the calculation would need to be repeated without making the approximation.

Exercise 2.3.5

What are the equilibrium concentrations in a 0.25 *M* NH_3 solution?

$$NH_3(aq) + H_2O(l) \rightleftharpoons NH_4^+(aq) + OH^-(aq) \quad K_c = 1.8 \times 10^{-5}$$

Answer

$[OH^-] = [NH_4^+] = 0.0021$ M

$[NH_3] = 0.25$ M

This page titled 2.3: Equilibrium Calculations (ICE) Review is shared under a CC BY-NC-SA 4.0 license and was authored, remixed, and/or curated by Jonathan Gutow.

- **13.4: Equilibrium Calculations** by OpenStax is licensed CC BY 4.0. Original source: https://openstax.org/details/books/chemistry-2e.

2.4: Fractional Composition at Equilibrium

2.4.1: Simple Example

Consider the simple equilibrium $\mathrm{A} \rightleftharpoons \mathrm{B}$. In this case the reaction quotiend Q assuming we can use concentrations in place of activities is:

$$Q = \frac{[B]}{[A]} \tag{2.4.1}$$

If the equilibrium constant for this reaction has the value K we have at equilibrium:

$$K = \frac{[B]_e}{[A]_e} \tag{2.4.2}$$

If we imagine starting with 100% A and allow it to equilibrate, we can talk about the fraction A remaining or the fraction A converted once equilibrium is reached. Equation 2.4.2 can be solved for $[A]_e$:

$$[A]_e = \frac{[B]_e}{K} \tag{2.4.3}$$

The fraction that converts is just

$$f_B = \frac{[B]_e}{[A]_o} \tag{2.4.4}$$

where $[A]_o$ is how much we would have if the reaction did not proceed at all. Since the stoichiometry is 1:1 A:B any B produced uses an A. This means that $[A]_o = [A]_e + [B]_e$. Substituting this into equation 2.4.4:

$$f_B = \frac{[B]_e}{[A]_e + [B]_e} \tag{2.4.5}$$

Substituting in equation 2.4.3 into 2.4.5 yields:

$$f_B = \frac{\cancel{[B]_e}}{\frac{\cancel{[B]_e}}{K} + \cancel{[B]_e}} = \frac{1}{\frac{1}{K} + 1} = \frac{K}{1+K} \tag{2.4.6}$$

2.4.2: More complex example

We will find this concept particularly useful in situations where multiple species are involved, but we know one of the equilibrium values (e.g. $[H^+]$ because the system is buffered or the partial pressure of CO_2 because it is coming from the air around the sample). As a generic example consider $\mathrm{A} \rightleftharpoons \mathrm{B} + \mathrm{C}$ a dissociation that could be an acid dissociation, the dissociation of a complex such as paired DNA or an enzyme substrate complex. In this case:

$$K = \frac{[B]_e[C]_e}{[A]_e} \tag{2.4.7}$$

Assume $[C]_e$ is fixed by some external process. Collecting the constants on one side of equation 2.4.7 yields:

$$\frac{K}{[C]_e} = \frac{[B]_e}{[A]_e} \tag{2.4.8}$$

The fraction of the original species A dissociated is just the fraction that is B:

$$f_B = \frac{[B]_e}{[A]_e + [B]_e} \tag{2.4.9}$$

Dividing both the top and bottom of the fraction in equation 2.4.9 by $[A]_e$:

$$f_B = \frac{\frac{[B]_e}{[A]_e}}{1 + \frac{[B]_e}{[A]_e}} \tag{2.4.10}$$

Using equation 2.4.8 we can replace the ratios $\frac{[B]_e}{[A]_e}$ in equation 2.4.10 with $\frac{K}{[C]_e}$:

$$f_B = \frac{\frac{K}{[C]_e}}{1 + \frac{K}{[C]_e}} = \frac{K}{[C]_e + K} \tag{2.4.11}$$

So as we increase the concentration [C] we decrease the amount of reactant A that dissociates.

This page titled 2.4: Fractional Composition at Equilibrium is shared under a CC BY-NC-SA 4.0 license and was authored, remixed, and/or curated by Jonathan Gutow.

2.5: Coupled Equilibria

The equilibrium systems discussed so far have all been relatively simple, involving just single reversible reactions. Many systems, however, involve two or more *coupled* equilibrium reactions, those which have in common one or more reactant or product species. Since the law of mass action allows for a straightforward derivation of equilibrium constant expressions from balanced chemical equations, the K value for a system involving coupled equilibria can be related to the K values of the individual reactions. Three basic manipulations are involved in this approach, as described below.

1. Changing the direction of a chemical equation essentially swaps the identities of "reactants" and "products," and so the equilibrium constant for the reversed equation is simply the reciprocal of that for the forward equation.

$$A \rightleftharpoons B \quad K_c = \frac{[B]}{[A]}$$

$$B \rightleftharpoons A \quad K_{c'} = \frac{[A]}{[B]}$$

$$K_{c'} = \frac{1}{K_c}$$

2. Changing the stoichiometric coefficients in an equation by some factor *x* results in an exponential change in the equilibrium constant by that same factor:

$$A \rightleftharpoons B \qquad K_c = \frac{[B]}{[A]}$$

$$xA \rightleftharpoons xB \quad K_c = \frac{[B]^x}{[A]^x}$$

$$K_{c'} = {K_c}^x$$

3. Adding two or more equilibrium equations together yields an overall equation whose equilibrium constant is the mathematical product of the individual reaction's K values:

$$A \rightleftharpoons B \quad K_{c1} = \frac{[B]}{[A]}$$

$$B \rightleftharpoons C \quad K_{c2} = \frac{[C]}{[B]}$$

The net reaction for these coupled equilibria is obtained by summing the two equilibrium equations and canceling any redundancies:

$$A + B \rightleftharpoons B + C$$

$$A + B \rightleftharpoons B + C$$

$$A \rightleftharpoons C$$

$$K_{c'} = \frac{[C]}{[A]}$$

Comparing the equilibrium constant for the net reaction to those for the two coupled equilibrium reactions reveals the following relationship:

$$K_{c1}K_{c2} = \frac{[B]}{[A]} \times \frac{[C]}{[B]} = \frac{\cancel{[B]}[C]}{[A]\,\cancel{[B]}} = \frac{[C]}{[A]} = K_{c'}$$

$$K_{c'} = K_{c1}K_{c2}$$

Example $2.5.5$ demonstrates the use of this strategy in describing coupled equilibrium processes.

Example 2.5.5: Equilibrium Constants for Coupled Reactions

A mixture containing nitrogen, hydrogen, and iodine established the following equilibrium at 400 °C:

$$2\,\mathrm{NH_3(g)} + 3\,\mathrm{I_2(g)} \rightleftharpoons \mathrm{N_2(g)} + 6\,\mathrm{HI(g)}$$

Use the information below to calculate Kc for this reaction.

$$\mathrm{N_2(g)} + 3\,\mathrm{H_2(g)} \rightleftharpoons 2\,\mathrm{NH_3(g)}\ K_{c1} = 0.50 \text{ at } 400^\circ C$$

$$\mathrm{H_2(g)} + \mathrm{I_2(g)} \rightleftharpoons 2\,\mathrm{HI(g)}\ K_{c2} = 50 \text{ at } 400^\circ C$$

Solution

The equilibrium equation of interest and its K value may be derived from the equations for the two coupled reactions as follows.

Reverse the first coupled reaction equation:

$$2NH_3(g) \rightleftharpoons N_2(g) + 3H_2(g) \quad K_{c1}{}' = \frac{1}{K_{c1}} = \frac{1}{0.50} = 2.0$$

Multiply the second coupled reaction by 3:

$$3H_2(g) + 3I_2(g) \rightleftharpoons 6HI(g) \quad K_{c2}{}' = K_{c2}^3 = 50^3 = 1.2 \times 10^5$$

Finally, add the two revised equations:

$$2\,\mathrm{NH_3(g)} + 3\,\mathrm{H_2(g)} + 3\,\mathrm{I_2(g)} \rightleftharpoons \mathrm{N_2(g)} + 3\,\mathrm{H_2(g)} + 6\,\mathrm{HI(g)}$$

$$2\,\mathrm{NH_3(g)} + 3\,\mathrm{I_2(g)} \rightleftharpoons \mathrm{N_2(g)} + 6\,\mathrm{HI(g)}$$

$$K_c = K_{c1}' K_{c2}^3 = (2.0)\left(1.2 \times 10^5\right) = 2.5 \times 10^5$$

Exercise 2.5.5

Use the provided information to calculate Kc for the following reaction at 550 °C:

$$\mathrm{H_2(g)} + \mathrm{CO_2(g)} \rightleftharpoons \mathrm{CO(g)} + \mathrm{H_2O(g)} \qquad K_c = ?$$

$$\mathrm{CoO(s)} + \mathrm{CO(g)} \rightleftharpoons \mathrm{Co(s)} + \mathrm{CO_2(g)} \qquad K_{c1} = 490$$

$$\mathrm{CoO(s)} + \mathrm{H_2(g)} \rightleftharpoons \mathrm{Co(s)} + \mathrm{H_2O(g)} \qquad K_{c1} = 67$$

Answer

K_c = 0.14

This page titled 2.5: Coupled Equilibria is shared under a CC BY-NC-SA 4.0 license and was authored, remixed, and/or curated by Jonathan Gutow via source content that was edited to the style and standards of the LibreTexts platform.

- **13.2: Equilibrium Constants** by OpenStax is licensed CC BY 4.0. Original source: https://openstax.org/details/books/chemistry-2e.

2.6: Equilibrium Dependence on Conditions

Learning Objectives

By the end of this section, you will be able to:

- Describe the ways in which an equilibrium system can be stressed
- Predict the response of a stressed equilibrium using Le Chatelier's principle

A system at equilibrium is in a state of dynamic balance, with forward and reverse reactions taking place at equal rates. If an equilibrium system is subjected to a change in conditions that affects these reaction rates differently (a *stress*), then the rates are no longer equal and the system is not at equilibrium. The system will subsequently experience a net reaction in the direction of greater rate (a *shift*) that will re-establish the equilibrium. This phenomenon is summarized by **Le Chatelier's principle**

Definition: Le Chatelier's Principle

if an equilibrium system is stressed, the system will experience a shift in response to the stress that re-establishes equilibrium.

Reaction rates are affected primarily by concentrations, as described by the reaction's rate law, and temperature, as described by the Arrhenius equation. Consequently, changes in concentration and temperature are the two stresses that can shift an equilibrium.

2.6.1: Effect of a Change in Concentration

If an equilibrium system is subjected to a change in the concentration of a reactant or product species, the rate of either the forward or the reverse reaction will change. As an example, consider the equilibrium reaction

$$\mathrm{H_2(g) + I_2(g) \rightleftharpoons 2\,HI(g)} \quad K_c = 50.0 \text{ at } 400^\circ C$$

The rate laws for the forward and reverse reactions are

$$\begin{aligned} &\text{forward} \quad \mathrm{H_2(g) + I_2(g) \rightarrow 2\,HI(g)} && \text{rate}_f = k_f[\mathrm{H_2}]^m[\mathrm{I_2}]^n \\ &\text{reverse} \quad \mathrm{2\,HI(g) \rightarrow H_2(g) + I_2(g)} && \text{rate}_r = k_r[\mathrm{HI}]^x \end{aligned}$$

When this system is at equilibrium, the forward and reverse reaction rates are equal.

$$\text{rate}_f = \text{rate}_r$$

If the system is stressed by adding reactant, either $\mathrm{H_2}$ or $\mathrm{I_2}$, the resulting increase in concentration causes the rate of the forward reaction to increase, exceeding that of the reverse reaction:

$$\text{rate}_f > \text{rate}_r$$

The system will experience a temporary net reaction in the forward direction to re-establish equilibrium (the equilibrium will shift right). This same shift will result if some product HI is removed from the system, which decreases the rate of the reverse reaction, again resulting in the same imbalance in rates.

The same logic can be used to explain the left shift that results from either removing reactant or adding product to an equilibrium system. These stresses both result in an increased rate for the reverse reaction

$$\text{rate}_f < \text{rate}_r$$

and a temporary net reaction in the reverse direction to re-establish equilibrium.

As an alternative to this kinetic interpretation, the effect of changes in concentration on equilibria can be rationalized in terms of reaction quotients. When the system is at equilibrium,

$$Q_c = \frac{[\mathrm{HI}]^2}{[\mathrm{H_2}]\,[\mathrm{I_2}]} = K_c$$

If reactant is added (increasing the denominator of the reaction quotient) or product is removed (decreasing the numerator), then $Q_c < K_c$ and the equilibrium will shift right. Note that the three different ways of inducing this stress result in three different changes in the composition of the equilibrium mixture. If H_2 is added, the right shift will consume I_2 and produce HI as equilibrium is re-established, yielding a mixture with a greater concentrations of H_2 and HI and a lesser concentration of I_2 than was present before. If I_2 is added, the new equilibrium mixture will have greater concentrations of I_2 and HI and a lesser concentration of H_2. Finally, if HI is removed, the concentrations of all three species will be lower when equilibrium is reestablished. Despite these differences in composition, *the value of the equilibrium constant will be the same after the stress as it was before* (per the law of mass action). The same logic may be applied for stresses involving removing reactants or adding product, in which case $Q_c > K_c$ and the equilibrium will shift left. For gas-phase equilibria such as this one, some additional perspectives on changing the concentrations of reactants and products are worthy of mention. The partial pressure P of an ideal gas is proportional to its molar concentration M,

$$M = \frac{n}{V} = \frac{P}{RT}$$

and so changes in the partial pressures of any reactant or product are essentially changes in concentrations and thus yield the same effects on equilibria. Aside from adding or removing reactant or product, the pressures (concentrations) of species in a gas-phase equilibrium can also be changed by *changing the volume occupied by the system*. Since all species of a gas-phase equilibrium occupy the same volume, a given change in volume will cause the same change in concentration for both reactants and products. In order to discern what shift, if any, this type of stress will induce the stoichiometry of the reaction must be considered.

At equilibrium, the reaction

$$\mathrm{H_2(g) + I_2(g) \rightleftharpoons 2\,HI(g)}$$

is described by the reaction quotient

$$Q_P = \frac{(P_{\mathrm{HI}})^2}{P_{\mathrm{H_2}} P_{\mathrm{I_2}}} = K_p$$

If the volume occupied by an equilibrium mixture of these species is decreased by a factor of 3, the partial pressures of all three species will be increased by a factor of 3:

$$\begin{aligned} Q_p{}' &= \frac{(3P_{HI})^2}{3P_{H_2}3P_{I_2}} = \frac{9P_{H^2}}{9P_{H_2}P_{I_2}} = \frac{P_{HI^2}}{P_{H_2}P_{I_2}} \\ &= Q_P = K_P \end{aligned}$$

And so, changing the volume of this gas-phase equilibrium mixture does not result in a shift of the equilibrium.

A similar treatment of a different system,

$$\mathrm{2\,NO_2(g) \rightleftharpoons 2\,NO(g) + O_2(g)}$$

however, yields a different result:

$$\begin{aligned} Q_P &= \frac{(P_{NO})^2}{(P_{O_2})}(P_{NO_2})^2 \\ Q'_P &= \frac{(3P_{\mathrm{NO}})^2(3P_{\mathrm{O_2}})}{3(P_{\mathrm{NO_2}})^2} = \frac{9(P_{\mathrm{NO}})^2(3P_{\mathrm{O_2}})}{9(P_{\mathrm{NO_2}})^2} = \frac{27(P_{\mathrm{NO}})^2 P_{\mathrm{O_2}}}{9(P_{\mathrm{NO_2}})^2} \\ &= 3Q_P > K_P \end{aligned}$$

In this case, the change in volume results in a reaction quotient greater than the equilibrium constant, and so the equilibrium will shift left.

These results illustrate the relationship between the stoichiometry of a gas-phase equilibrium and the effect of a volume-induced pressure (concentration) change. If the total molar amounts of reactants and products are equal, as in the first example, a change in volume does not shift the equilibrium. If the molar amounts of reactants and products are different, a change in volume will shift the equilibrium in a direction that better "accommodates" the volume change. In the second example, two moles of reactant (NO_2) yield three moles of product ($2NO + O_2$), and so decreasing the system volume causes the equilibrium to shift left since the reverse

reaction produces less gas (2 mol) than the forward reaction (3 mol). Conversely, increasing the volume of this equilibrium system would result in a shift towards products.

Link to Learning

Check out this link to see a dramatic visual demonstration of how equilibrium changes with pressure changes.

Chemistry in Everyday Life: Equilibrium and Soft Drinks

The connection between chemistry and carbonated soft drinks goes back to 1767, when Joseph Priestley (1733–1804) developed a method of infusing water with carbon dioxide to make carbonated water. Priestley's approach involved production of carbon dioxide by reacting oil of vitriol (sulfuric acid) with chalk (calcium carbonate).

The carbon dioxide was then dissolved in water, reacting to produce hydrogen carbonate, a weak acid that subsequently ionized to yield bicarbonate and hydrogen ions:

$$\text{dissolution} \qquad \mathrm{CO_2(g) \rightleftharpoons CO_2(aq)}$$

$$\text{hydrolysis} \qquad \mathrm{CO_2(aq) + H_2O(l) \rightleftharpoons H_2CO_3(aq)}$$

$$\text{ionization} \qquad \mathrm{H_2CO_3(aq) \rightleftharpoons HCO_3^-(aq) + H^+(aq)}$$

These same equilibrium reactions are the basis of today's soft-drink carbonation process. Beverages are exposed to a high pressure of gaseous carbon dioxide during the process to shift the first equilibrium above to

the right, resulting in desirably high concentrations of dissolved carbon dioxide and, per similar shifts in the other two equilibria, its hydrolysis and ionization products. A bottle or can is then nearly filled with the carbonated beverage, leaving a relatively small volume of air in the container above the beverage surface (the *headspace*) before it is sealed. The pressure of carbon dioxide in the container headspace is very low immediately after sealing, but it rises as the dissolution equilibrium is re-established by shifting to the left. Since the volume of the beverage is significantly greater than the volume of the headspace, only a relatively small amount of dissolved carbon dioxide is lost to the headspace.

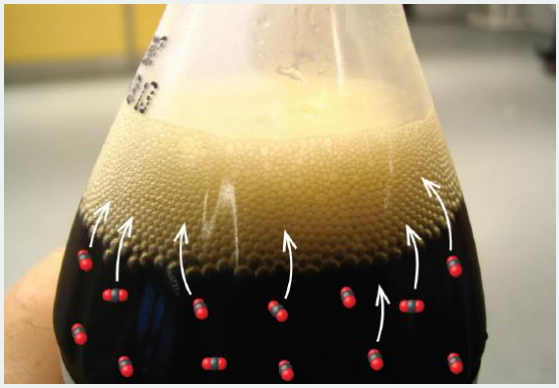


Figure 2.6.1: Opening a soft-drink bottle lowers the CO_2 pressure above the beverage, shifting the dissolution equilibrium and releasing dissolved CO_2 from the beverage. (credit: modification of work by "D Coetzee"/Flickr)

When a carbonated beverage container is opened, a hissing sound is heard as pressurized CO_2 escapes from the headspace. This causes the dissolution equilibrium to shift left, resulting in a decrease in the concentration of dissolved CO_2 and subsequent left-shifts of the hydrolysis and ionization equilibria. Fortunately for the consumer, the dissolution equilibrium is usually re-established slowly, and so the beverage may be enjoyed while its dissolved carbon dioxide concentration remains palatably high. Once the equilibria are re-established, the $CO_2(aq)$ concentration will be significantly lowered, and the beverage acquires a characteristic taste referred to as "flat."

2.6.2: Effect of a Change in Temperature

Unlike changes in composition and pressure changes in temperature change the equilibrium position because the equilibrium constant changes. The underlying reason is because the forward and reverse reaction rates change by different amounts as the temperature changes. We will address this in thermodynamic terms rather than through kinetics.

The relation between $\Delta_r G^o$ and K_{eq} is our starting point:

$$\Delta_r G^o = -RTlnK_{eq} \tag{2.6.1}$$

Which implies:

$$lnK_{eq} = \frac{-\Delta_r G^o}{RT} \tag{2.6.2}$$

Using $\Delta_r G^o = \Delta_r H^o - T\Delta_r S^o$ to replace $\Delta_r G^o$ in equation 2.6.2:

$$lnK_{eq} = \frac{-(\Delta_r H^o - T\Delta_r S^o)}{RT} = \frac{-\Delta_r H^o}{RT} + \frac{\Delta_r S^o}{R} \tag{2.6.3}$$

Consider substituting in two different temperatures into equation 2.6.3 and subtracting the two equations:

$$lnK_{eq,2} - lnK_{eq,1} = \frac{-\Delta_r H^o}{RT_2} + \cancel{\frac{\Delta_r S^o}{R}} - \frac{-\Delta_r H^o}{RT_1} - \cancel{\frac{\Delta_r S^o}{R}} = \frac{\Delta_r H^o}{R}\left(\frac{1}{T_1} - \frac{1}{T_2}\right) \tag{2.6.4}$$

This is equation is often referred to as the van't Hoff equation. However, there are a number of equations associated with this person's name. Notice for an endothermic reaction $\Delta_r H^o > 0$ an increase in temperature ($T_2 > T_1$) would make the equilibrium constant increase as both factors in the equation are positive. For an exothermic process the reaction shifts the other direction.

You can reach the same conclusion by treating the enthalpy change as either a reactant (endothermic) or a product exothermic and applying Le Chatelier's Principle. For example, the decomposition of dinitrogen tetroxide is an endothermic process:

$$\mathrm{N_2O_4(g) \rightleftharpoons 2\,NO_2(g)} \quad \Delta H = +57.20\ \mathrm{kJ}$$

For purposes of applying Le Chatelier's principle, heat (q) may be viewed as a reactant:

$$\mathrm{heat + N_2O_4(g) \rightleftharpoons 2\,NO_2(g)}$$

Raising the temperature of the system is akin to increasing the amount of a reactant, and so the equilibrium will shift to the right. Lowering the system temperature will likewise cause the equilibrium to shift left. For exothermic processes, heat is viewed as a product of the reaction and so the opposite temperature dependence is observed.

2.6.3: Effect of a Catalyst

A *catalyst* is a substance that enables a reaction to proceed via a different mechanism with an accelerated rate. The catalyzed reaction mechanism involves a lower energy transition state than the uncatalyzed reaction, resulting in a lower activation energy, E_a, and a correspondingly greater rate constant.

To discern the effect of catalysis on an equilibrium system, consider the reaction diagram for a simple one-step (elementary) reaction shown in Figure 2.6.2. The lowered transition state energy of the catalyzed reaction results in lowered activation energies for both the forward and the reverse reactions. Consequently, both forward and reverse reactions are accelerated, and equilibrium is achieved more quickly *but without a change in the equilibrium constant*.

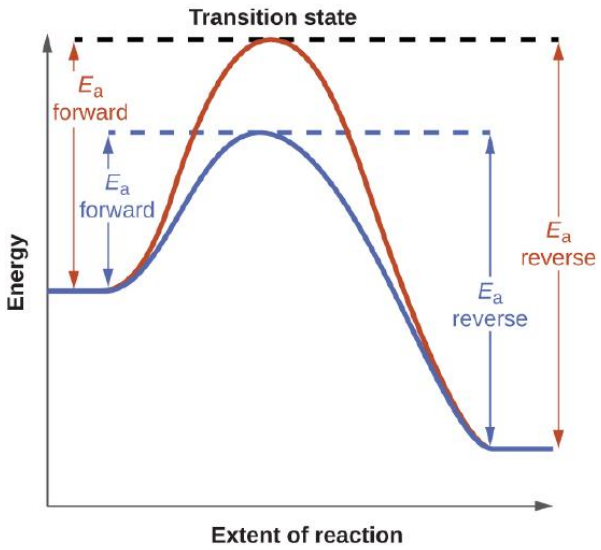


Figure 2.6.2 : Reaction diagrams for an elementary process in the absence (red) and presence (blue) of a catalyst. The presence of catalyst lowers the activation energies of both the forward and reverse reactions but does not affect the value of the equilibrium constant.

Industrial use of equilibria and catalysts

An interesting case study highlighting these equilibrium concepts is the industrial production of ammonia, NH_3. This substance is among the “top 10” industrial chemicals with regard to production, with roughly two billion pounds produced annually in the US. Ammonia is used as a chemical feedstock to synthesize a wide range of commercially useful compounds, including fertilizers, plastics, dyes, and explosives.

Most industrial production of ammonia uses the Haber-Bosch process based on the following equilibrium reaction:

$$\mathrm{N_2(g) + 3\,H_2(g) \rightleftharpoons 2\,NH_3(g)} \quad \Delta H = -92.2\ \mathrm{kJ}$$

The traits of this reaction present challenges to its use in an efficient industrial process. The equilibrium constant is relatively small (Kp on the order of 10^{-5} at 25 °C), meaning very little ammonia is present in an equilibrium mixture. Also, the rate of this reaction is relatively slow at low temperatures. To raise the yield of ammonia, the industrial process is designed to operate under conditions favoring product formation:

- High pressures (concentrations) of reactants are used, ~150−250 atm, to shift the equilibrium right, favoring product formation.
- Ammonia is continually removed (collected) from the equilibrium mixture during the process, lowering its concentration and also shifting the equilibrium right.
- Although low temperatures favor product formation for this exothermic process, the reaction rate at low temperatures is inefficiently slow. A catalyst is used to accelerate the reaction to reasonable rates at relatively moderate temperatures (400−500 °C).

A diagram illustrating a typical industrial setup for production of ammonia via the Haber-Bosch process is shown in Figure 2.6.3.

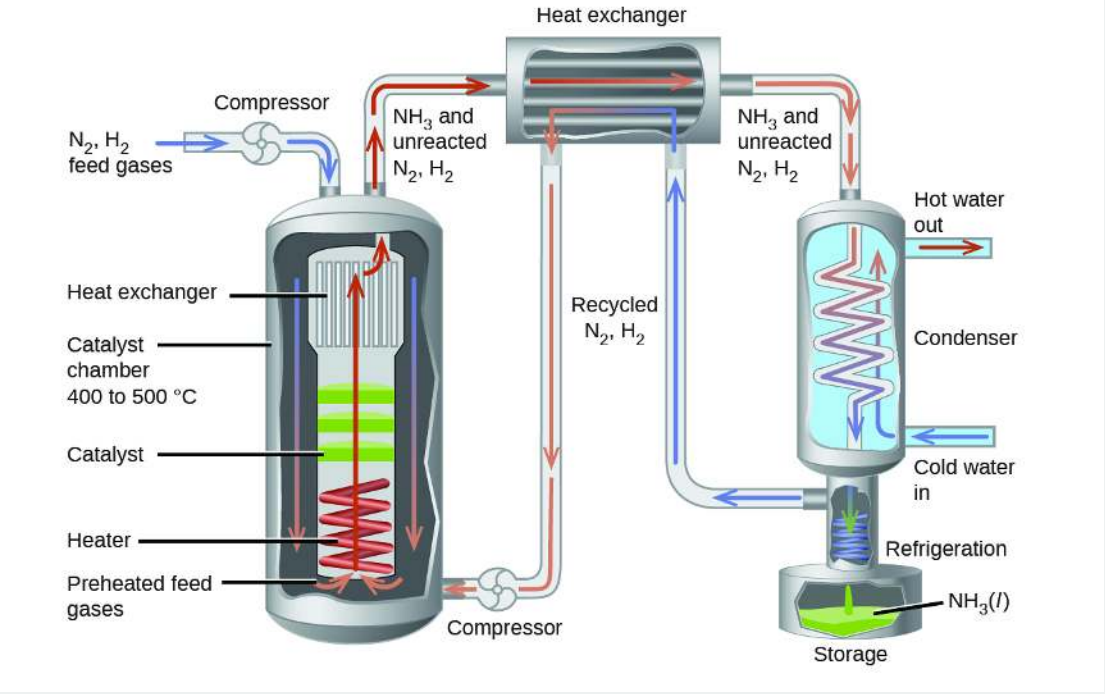


Figure 2.6.3: The figure shows a typical industrial setup for the commercial production of ammonia by the Haber-Bosch process. The process operates under conditions that stress the chemical equilibrium to favor product formation.

This page titled 2.6: Equilibrium Dependence on Conditions is shared under a CC BY-NC-SA 4.0 license and was authored, remixed, and/or curated by Jonathan Gutow via source content that was edited to the style and standards of the LibreTexts platform.

- **13.3: Shifting Equilibria - Le Chatelier's Principle** by OpenStax is licensed CC BY 4.0. Original source: https://openstax.org/details/books/chemistry-2e.

2.7: Coupled Equilibria Driving Nonspontaneous Reactions

2.7.1: Introduction

In many cases reactions that are necessary to our industrial society and the process of living have equilibria that do not favor the desired products. The desired products can often be produced by coupling the nonspontaneous desired reaction to another reaction that is spontaneous and drive the nonspontaneous reaction to the desired products. In outline the idea is to combine the nonspontaneous reaction with a spontaneous one that has overlapping reagents. Consider two hypothetical simple reactions:

$$\mathrm{A} \rightleftharpoons \mathrm{B} + \mathrm{C} \quad \Delta_r G^o = +2kJ \tag{2.7.1}$$

$$\mathrm{C} \rightleftharpoons \mathrm{D} \quad \Delta_r G^o = -3kJ \tag{2.7.2}$$

Adding these two reactions together yields an overall reaction of:

$$\mathrm{A} \rightleftharpoons \mathrm{B} + \mathrm{D} \quad \Delta_r G^o = -1kJ \tag{2.7.3}$$

Reaction 2.7.3 is spontaneous because the overall free energy change is negative, making the production of B favorable if the reaction rate is high enough.

2.7.2: Industrial Example (Smelting of Iron Ore)

Iron is produced from iron ore by driving the nonspontaneous reduction of iron ore to metallic iron by coupling the reaction with the spontaneous oxidation of carbon to CO_2. The actual process involves many reactions but they can be summarized with the following two reactions (one nonspontaneous and one spontaneous):

$$2\,\mathrm{Fe_2O_3(s)} \rightleftharpoons 4\,\mathrm{Fe(s)} + 2\,\mathrm{O_2(g)} \quad \Delta_r G^o = +1484kJ \tag{2.7.4}$$

$$\mathrm{C(s)} + \mathrm{O_2(g)} \rightleftharpoons \mathrm{CO_2(g)} \quad \Delta_r G^o = -394.36kJ \tag{2.7.5}$$

If we add reaction 2.7.4 to four of reaction 2.7.5 we get an overall reaction with $\Delta_r G$ = -93 kJ, which is spontaneous:

$$2\,\mathrm{Fe_2O_3(s)} + 4\,\mathrm{C(s)} + \mathrm{O_2(g)} \rightleftharpoons 4\,\mathrm{Fe(s)} + 4\,\mathrm{CO_2(g)} \quad \Delta_r G^o = -93kJ \tag{2.7.6}$$

A few more details of the smelting process can be found in many general chemistry texts (one example).

2.7.3: Biochemical Example (Nonspontaneous Steps in Glycolysis)

Under "biological standard conditions" of pH =7 and 37 ˚C the reaction of adenosine triphosphate (ATP) to produce adenosine diphosphate (ADP) and hydrogen phosphate illustrated below is spontaneous with a $\Delta_r G$ = -31 kJ/mol ATP. This free energy change means that the equilibrium constant for the overall reaction under these conditions is about 5 X 10^3. So products are strongly favored.

$$\mathrm{ATP^{4-}(aq)} + \mathrm{H_2O(l)} \rightleftharpoons \mathrm{ADP^{3-}(aq)} + \mathrm{HPO_4^{2-}(aq)} + \mathrm{H_3O^+(aq)} \tag{2.7.7}$$

This reaction is coupled with two reactions in the glycolysis process that have positive $\Delta_r G$ in the direction necessary for glycolysis to proceed.

Glycolysis is the catabolic process in which glucose is converted into pyruvate via ten enzymatic steps. There are three regulatory steps, each of which is highly regulated.

There are two phases of Glycolysis:

1. the "priming phase" because it requires an input of energy in the form of 2 ATPs per glucose molecule and
2. the "pay off phase" because energy is released in the form of 4 ATPs, 2 per glyceraldehyde molecule.

The end result of Glycolysis is two new pyruvate molecules which can then be fed into the Citric Acid cycle (also known as the Kreb's Cycle) if oxygen is present, or can be reduced to lactate or ethanol in the absence of of oxygen using a process known as Fermentation. Glycolysis occurs within almost all living cells and is the primary source of Acetyl-CoA, which is the molecule responsible for the majority of energy output under aerobic conditions. The structures of Glycolysis intermediates can be found in the following diagram:

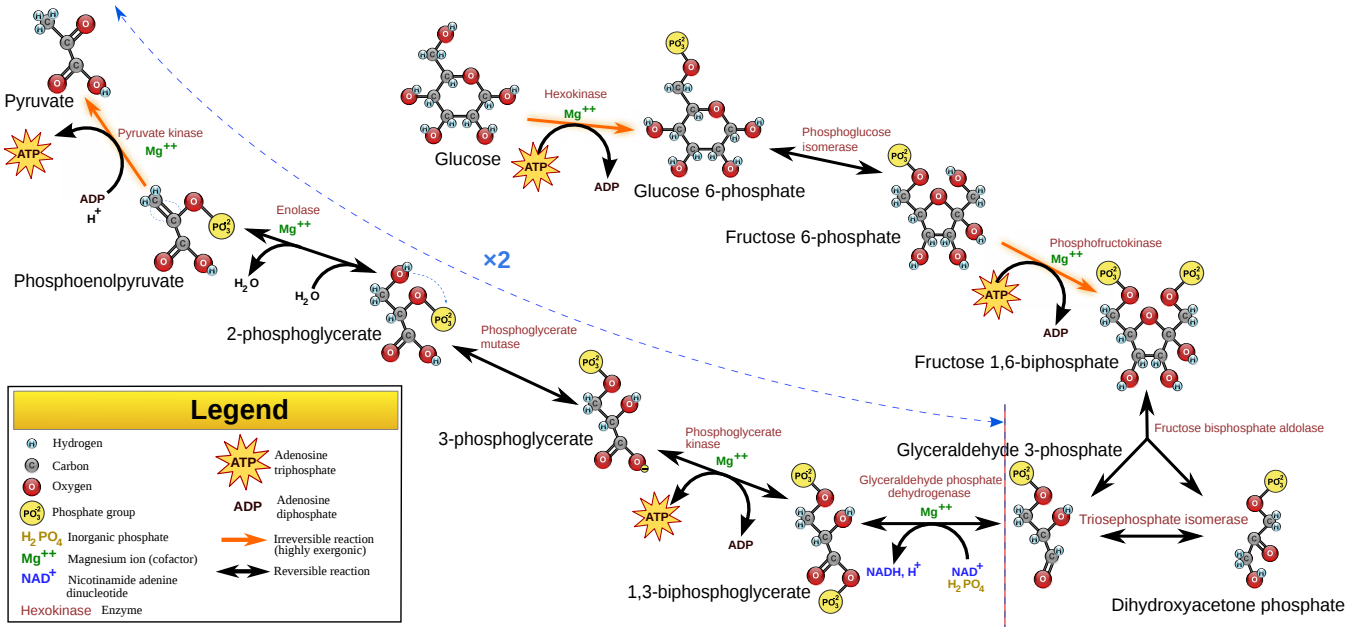


Figure 1: Glycolysis pathway. from Wikipedia (CCBY-SA 3.0; YassineMrabet).

2.7.3.1: Phase 1: The "Priming Step"

The first phase of Glycolysis requires an input of energy in the form of ATP (adenosine triphosphate).

1. alpha-D-Glucose is phosphorolated at the 6 carbon by ATP via the enzyme Hexokinase (Class: Transferase) to yield alpha-D-Glucose-6-phosphate (G-6-P). This is a regulatory step which is negatively regulated by the presence of glucose-6-phosphate.
2. alpha-D-Glucose-6-phosphate is then converted into D-Fructose-6-phosphate (F-6-P) by Phosphoglucoisomerase (Class: Isomerase)
3. D-Fructose-6-phosphate is once again phosphorolated this time at the 1 carbon position by ATP via the enzyme Phosphofructokinase (Class: Transferase) to yield D-Fructose-1,6-bisphosphate (FBP). This is the committed step of glycolysis because of its large ΔG value.
4. D-Fructose-1,6-bisphosphate is then cleaved into two, three carbon molecules; Dihydroxyacetone phosphate (DHAP) and D-Glyceraldehyde-3-phosphate (G-3-P) by the enzyme Fructose bisphosphate aldolase (Class: Lyase)
5. Because the next portion of Glycolysis requires the molecule D-Glyceraldehyde-3-phosphate to continue Dihydroxyacetone phosphate is converted into D-Glyceraldehyde-3-phosphate by the enzyme Triose phosphate isomerase (Class: Isomerase)

2.7.3.2: Phase 2: The "Pay Off Step"

The second phase of Glycolysis where 4 molecules of ATP are produced per molecule of glucose. Enzymes appear in red:

1. D-Glyceraldehyde-3-phosphate is phosphorolated at the 1 carbon by the enzyme Glyceraldehyde-3-phosphate dehodrogenase to yield the high energy molecule 1,3-Bisphosphoglycerate (BPG)
2. ADP is then phosphorolated at the expense of 1,3-Bisphosphoglycerate by the enzyme Phosphoglycerate kinase (Class: Transferase) to yield ATP and 3-Phosphoglycerate (3-PG)
3. 3-Phosphoglycerate is then converted into 2-Phosphoglycerate by Phosphoglycerate mutase in preparation to yield another high energy molecule
4. 2-Phosphoglycerate is then converted to phosphoenolpyruvate (PEP) by Enolase. H_2O, potassium, and magnesium are all released as a result.
5. ADP is once again phosphorolated, this time at the expense of PEP by the enzyme pyruvate kinase to yield another molecule of ATP and and pyruvate. This step is regulated by the energy in the cell. The higher the energy of the cell the more inhibited pyruvate kinase becomes. Indicators of high energy levels within the cell are high concentrations of ATP, Acetyl-CoA, Alanine, and cAMP.

Because Glucose is split to yield two molecules of D-Glyceraldehyde-3-phosphate, each step in the "Pay Off" phase occurs twice per molecule of glucose.

2.7.3.3: References

1. Garrett, H., Reginald and Charles Grisham. Biochemistry. Boston: Twayne Publishers, 2008.
2. Raven, Peter. Biology. Boston: Twayne Publishers, 2005.

2.7.4: Problems

1. What is the net yield of Glycolysis as far as ATP?
2. Name the enzymes that are key regulatory sites in Glycolysis.
3. Why are the enzymes in the previous question targets for regulation?
4. Why is the priming phase necessary?

This page titled 2.7: Coupled Equilibria Driving Nonspontaneous Reactions is shared under a CC BY-NC-SA 4.0 license and was authored, remixed, and/or curated by Darik Benson.

- **Glycolysis** by Darik Benson is licensed CC BY-NC-SA 4.0.

2.8: Brønsted-Lowry Acids and Bases

Learning Objectives

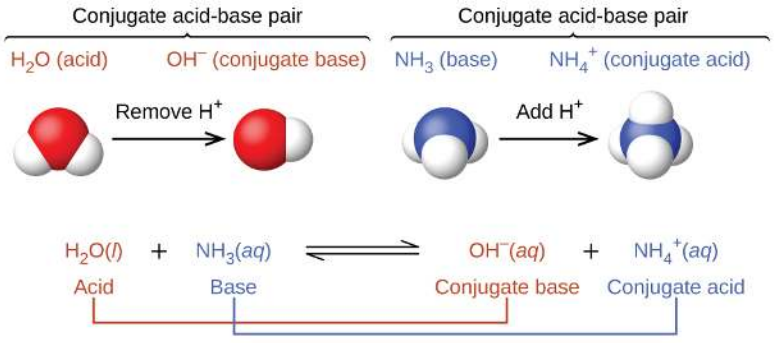
By the end of this section, you will be able to:

- Identify acids, bases, and conjugate acid-base pairs according to the Brønsted-Lowry definition
- Write equations for acid and base ionization reactions
- Use the ion-product constant for water to calculate hydronium and hydroxide ion concentrations
- Describe the acid-base behavior of amphiprotic substances

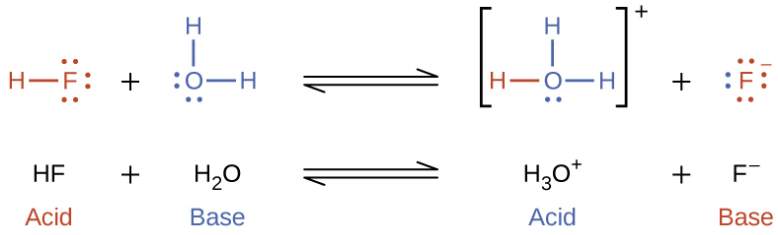
The acid-base reaction class has been studied for quite some time. In 1680, Robert Boyle reported traits of acid solutions that included their ability to dissolve many substances, to change the colors of certain natural dyes, and to lose these traits after coming in contact with alkali (base) solutions. In the eighteenth century, it was recognized that acids have a sour taste, react with limestone to liberate a gaseous substance (now known to be CO_2), and interact with alkalis to form neutral substances. In 1815, Humphry Davy contributed greatly to the development of the modern acid-base concept by demonstrating that hydrogen is the essential constituent of acids. Around that same time, Joseph Louis Gay-Lussac concluded that acids are substances that can neutralize bases and that these two classes of substances can be defined only in terms of each other. The significance of hydrogen was reemphasized in 1884 when Svante Arrhenius defined an acid as a compound that dissolves in water to yield hydrogen cations (now recognized to be hydronium ions) and a base as a compound that dissolves in water to yield hydroxide anions.

Johannes Brønsted and Thomas Lowry proposed a more general description in 1923 in which acids and bases were defined in terms of the transfer of hydrogen ions, H^+. (Note that these hydrogen ions are often referred to simply as *protons*, since that subatomic particle is the only component of cations derived from the most abundant hydrogen isotope, ^1H.) A compound that donates a proton to another compound is called a Brønsted-Lowry acid, and a compound that accepts a proton is called a Brønsted-Lowry base. An acid-base reaction is, thus, the transfer of a proton from a donor (acid) to an acceptor (base).

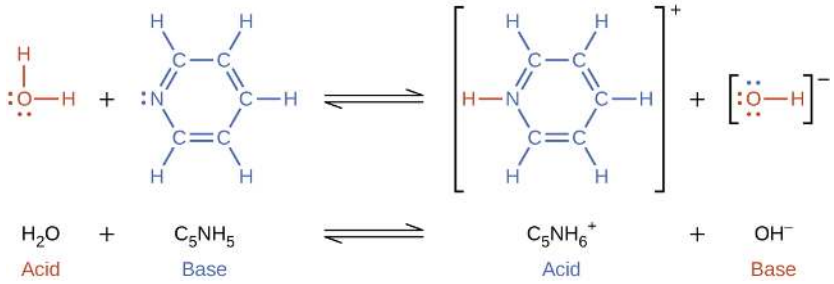
The concept of *conjugate pairs* is useful in describing Brønsted-Lowry acid-base reactions (and other reversible reactions, as well). When an acid donates H^+, the species that remains is called the **conjugate base** of the acid because it reacts as a proton acceptor in the reverse reaction. Likewise, when a base accepts H^+, it is converted to its **conjugate acid**. The reaction between water and ammonia illustrates this idea. In the forward direction, water acts as an acid by donating a proton to ammonia and subsequently becoming a hydroxide ion, OH^-, the conjugate base of water. The ammonia acts as a base in accepting this proton, becoming an ammonium ion, NH_4^+, the conjugate acid of ammonia. In the reverse direction, a hydroxide ion acts as a base in accepting a proton from ammonium ion, which acts as an acid.



The reaction between a Brønsted-Lowry acid and water is called acid ionization. For example, when hydrogen fluoride dissolves in water and ionizes, protons are transferred from hydrogen fluoride molecules to water molecules, yielding hydronium ions and fluoride ions:



Base ionization of a species occurs when it accepts protons from water molecules. In the example below, pyridine molecules, C_5NH_5, undergo base ionization when dissolved in water, yielding hydroxide and pyridinium ions:



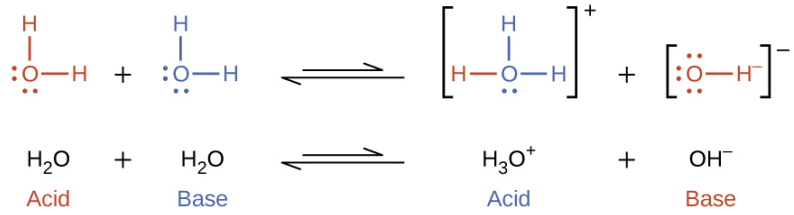
The preceding ionization reactions suggest that water may function as both a base (as in its reaction with hydrogen fluoride) and an acid (as in its reaction with ammonia). Species capable of either donating or accepting protons are called amphiprotic, or more generally, amphoteric, a term that may be used for acids and bases per definitions other than the Brønsted-Lowry one. The equations below show the two possible acid-base reactions for two amphiprotic species, bicarbonate ion and water:

$$\mathrm{HCO_3^-(aq) + H_2O(l) \rightleftharpoons CO_3^{2-}(aq) + H_3O^+(aq)}$$

$$\mathrm{HCO_3^-(aq) + H_2O(l) \rightleftharpoons H_2CO_3(aq) + OH^-(aq)}$$

The first equation represents the reaction of bicarbonate as an acid with water as a base, whereas the second represents reaction of bicarbonate as a base with water as an acid. When bicarbonate is added to water, both these equilibria are established simultaneously and the composition of the resulting solution may be determined through appropriate equilibrium calculations, as described later in this chapter.

In the liquid state, molecules of an amphiprotic substance can react with one another as illustrated for water in the equations below:



The process in which like molecules react to yield ions is called autoionization. Liquid water undergoes autoionization to a very slight extent; at 25 °C, approximately two out of every billion water molecules are ionized. The extent of the water autoionization process is reflected in the value of its equilibrium constant, the ion-product constant for water, K_w:

$$\mathrm{2\,H_2O(l) \rightleftharpoons H_3O^+(aq) + OH^-(aq)} \tag{2.8.1}$$

with

$$K_w = [\mathrm{H_3O^+}][\mathrm{OH^-}] \tag{2.8.2}$$

The slight ionization of pure water is reflected in the small value of the equilibrium constant; at 25 °C, K_w has a value of 1.0×10^{-14}. The process is endothermic, and so the extent of ionization and the resulting concentrations of hydronium ion and hydroxide ion increase with temperature. For example, at 100 °C, the value for K_w is about 5.6×10^{-13}, roughly 50 times larger than the value at 25 °C.

Example 2.8.1: Ion Concentrations in Pure Water

What are the hydronium ion concentration and the hydroxide ion concentration in pure water at 25 °C?

Solution

The autoionization of water yields the same number of hydronium and hydroxide ions. Therefore, in pure water, [H_3O^+] = [OH^-] = *x*. At 25 °C:

$$K_w = \left[H_3O^+\right]\left[OH^-\right] = (x)(x) = x^2 = 1.0 \times 10^{-14}$$

So:

$$x = \left[H_3O^+\right] = \left[OH^-\right] = \sqrt{1.0 \times 10^{-14}} = 1.0 \times 10^{-7} M$$

The hydronium ion concentration and the hydroxide ion concentration are the same, $1.0 \times 10^{-7}\ M$.

Exercise 2.8.1

The ion product of water at 80 °C is 2.4 \times 10^{−13}. What are the concentrations of hydronium and hydroxide ions in pure water at 80 °C?

Answer

$$[\mathrm{H_3O^+}] = [\mathrm{OH^-}] = 4.9 \times 10^{-7}\ M$$

Example 2.8.2: The Inverse Relation between [H_3O^+] and [OH^-]

A solution of an acid in water has a hydronium ion concentration of $2.0 \times 10^{-6}\,M$. What is the concentration of hydroxide ion at 25 °C?

Solution

Use the value of the ion-product constant for water at 25 °C (Equations 2.8.1 and 2.8.2) to calculate the missing equilibrium concentration.

$$2\,\mathrm{H_2O(l)} \rightleftharpoons \mathrm{H_3O^+(aq) + OH^-(aq)}$$

with $K_w = [\mathrm{H_3O^+}][\mathrm{OH^-}]$.

Rearrangement of the K_w expression shows that [OH^-] is inversely proportional to [H_3O^+]:

$$K_w = \left[\mathrm{H_3O^+}\right]\left[\mathrm{OH^-}\right] = \left(2.0 \times 10^{-6}\right)\left(5.0 \times 10^{-9}\right) = 1.0 \times 10^{-14}$$

Compared with pure water, a solution of acid exhibits a higher concentration of hydronium ions (due to ionization of the acid) and a proportionally lower concentration of hydroxide ions. This may be explained via Le Chatelier's principle as a left shift in the water autoionization equilibrium resulting from the stress of increased hydronium ion concentration.

Substituting the ion concentrations into the K_w expression confirms this calculation, resulting in the expected value:

$$K_w = [\mathrm{H_3O^+}][\mathrm{OH^-}] = (2.0 \times 10^{-6})(5.0 \times 10^{-9}) = 1.0 \times 10^{-14}$$

Exercise 2.8.2

What is the hydronium ion concentration in an aqueous solution with a hydroxide ion concentration of 0.001 *M* at 25 °C?

Answer

$$[H_3O^+] = 1 \times 10^{-11}\ M$$

Example 2.8.3: Representing the Acid-Base Behavior of an Amphoteric Substance

Write separate equations representing the reaction of HSO_3^-

a. as an acid with OH^-
b. as a base with HI

Solution

a. $HSO_3^-(aq) + OH^-(aq) \rightleftharpoons SO_3^{2-}(aq) + H_2O(l)$
b. $HSO_3^-(aq) + HI(aq) \rightleftharpoons H_2SO_3(aq) + I^-(aq)$

Exercise 2.8.3

Write separate equations representing the reaction of $H_2PO_4^-$

a. as a base with HBr
b. as an acid with OH^-

Answer

a. $H_2PO_4^-(aq) + HBr(aq) \rightleftharpoons H_3PO_4(aq) + Br^-(aq)$
b. $H_2PO_4^-(aq) + OH^-(aq) \rightleftharpoons HPO_4^{2-}(aq) + H_2O(l)$

This page titled 2.8: Brønsted-Lowry Acids and Bases is shared under a CC BY-NC-SA 4.0 license and was authored, remixed, and/or curated by Jonathan Gutow.

- **14.1: Brønsted-Lowry Acids and Bases** by OpenStax is licensed CC BY 4.0. Original source: https://openstax.org/details/books/chemistry-2e.

2.9: pH and pOH

Learning Objectives

By the end of this section, you will be able to:

- Explain the characterization of aqueous solutions as acidic, basic, or neutral
- Express hydronium and hydroxide ion concentrations on the pH and pOH scales
- Perform calculations relating pH and pOH

Hydronium and hydroxide ions are present both in pure water and in all aqueous solutions, and their concentrations are inversely proportional as determined by the ion product of water (K_w). The concentrations of these ions in a solution are often critical determinants of the solution's properties and the chemical behaviors of its other solutes, and specific vocabulary has been developed to describe these concentrations in relative terms. A solution is neutral if it contains equal concentrations of hydronium and hydroxide ions; acidic if it contains a greater concentration of hydronium ions than hydroxide ions; and basic if it contains a lesser concentration of hydronium ions than hydroxide ions.

A common means of expressing quantities that may span many orders of magnitude is to use a logarithmic scale. One such scale that is very popular for chemical concentrations and equilibrium constants is based on the p-function, defined as shown where "X" is the quantity of interest and "log" is the base-10 logarithm:

$$pX = -\log X$$

The pH of a solution is therefore defined as shown here, where [H_3O^+] is the molar concentration of hydronium ion in the solution:

$$pH = -\log\left[H_3O^+\right]$$

Rearranging this equation to isolate the hydronium ion molarity yields the equivalent expression:

$$\left[H_3O^+\right] = 10^{-pH}$$

Likewise, the hydroxide ion molarity may be expressed as a p-function, or pOH:

$$pOH = -\log\left[OH^-\right]$$

or

$$\left[OH^-\right] = 10^{-pOH}$$

Finally, the relation between these two ion concentration expressed as p-functions is easily derived from the K_w expression:

$$\begin{aligned} K_w &= \left[\mathrm{H_3O^+}\right]\left[\mathrm{OH^-}\right] \\ -\log K_w &= -\log\left(\left[\mathrm{H_3O^+}\right]\left[\mathrm{OH^-}\right]\right) \\ &= -\log\left[\mathrm{H_3O^+}\right] + -\log\left[\mathrm{OH^-}\right] \\ pK_w &= pH + pOH \end{aligned} \tag{2.9.1}$$

At 25 °C, the value of K_w is 1.0×10^{-14}, and so:

$$14.00 = pH + pOH$$

As was demonstrated previously, the hydronium ion molarity in pure water (or any neutral solution) is 1.0×10^{-7} M at 25 °C. The pH and pOH of a neutral solution at this temperature are therefore:

$$pH = -\log\left[H_3O^+\right] = -\log\left(1.0 \times 10^{-7}\right) = 7.00$$

$$pOH = -\log\left[OH^-\right] = -\log\left(1.0 \times 10^{-7}\right) = 7.00$$

And so, *at this temperature*, acidic solutions are those with hydronium ion molarities greater than 1.0×10^{-7} M and hydroxide ion molarities less than 1.0×10^{-7} M (corresponding to pH values less than 7.00 and pOH values greater than 7.00). Basic solutions

are those with hydronium ion molarities less than 1.0×10^{-7} M and hydroxide ion molarities greater than 1.0×10^{-7} M (corresponding to pH values greater than 7.00 and pOH values less than 7.00).

Since the autoionization constant K_w is temperature dependent, these correlations between pH values and the acidic/neutral/basic adjectives will be different at temperatures other than 25 °C. For example, Exercise 2.9.1 showed the hydronium molarity of pure water at 80 °C is 4.9×10^{-7} M, which corresponds to pH and pOH values of:

$$pH = -\log\left[H_3O^+\right] = -\log\left(4.9 \times 10^{-7}\right) = 6.31$$

$$pOH = -\log\left[OH^-\right] = -\log\left(4.9 \times 10^{-7}\right) = 6.31$$

At this temperature, then, neutral solutions exhibit pH = pOH = 6.31, acidic solutions exhibit pH less than 6.31 and pOH greater than 6.31, whereas basic solutions exhibit pH greater than 6.31 and pOH less than 6.31. This distinction can be important when studying certain processes that occur at other temperatures, such as enzyme reactions in warm-blooded organisms at a temperature around 36–40 °C. Unless otherwise noted, references to pH values are presumed to be those at 25 °C (Table 2.9.1).

Table 2.9.1: Summary of Relations for Acidic, Basic and Neutral Solutions

Classification	Relative Ion Concentrations	pH at 25 °C
acidic	$[H_3O^+] > [OH^-]$	pH < 7
neutral	$[H_3O^+] = [OH^-]$	pH = 7
basic	$[H_3O^+] < [OH^-]$	pH > 7

Figure 2.9.1: shows the relationships between $[H_3O^+]$, $[OH^-]$, pH, and pOH for solutions classified as acidic, basic, and neutral.

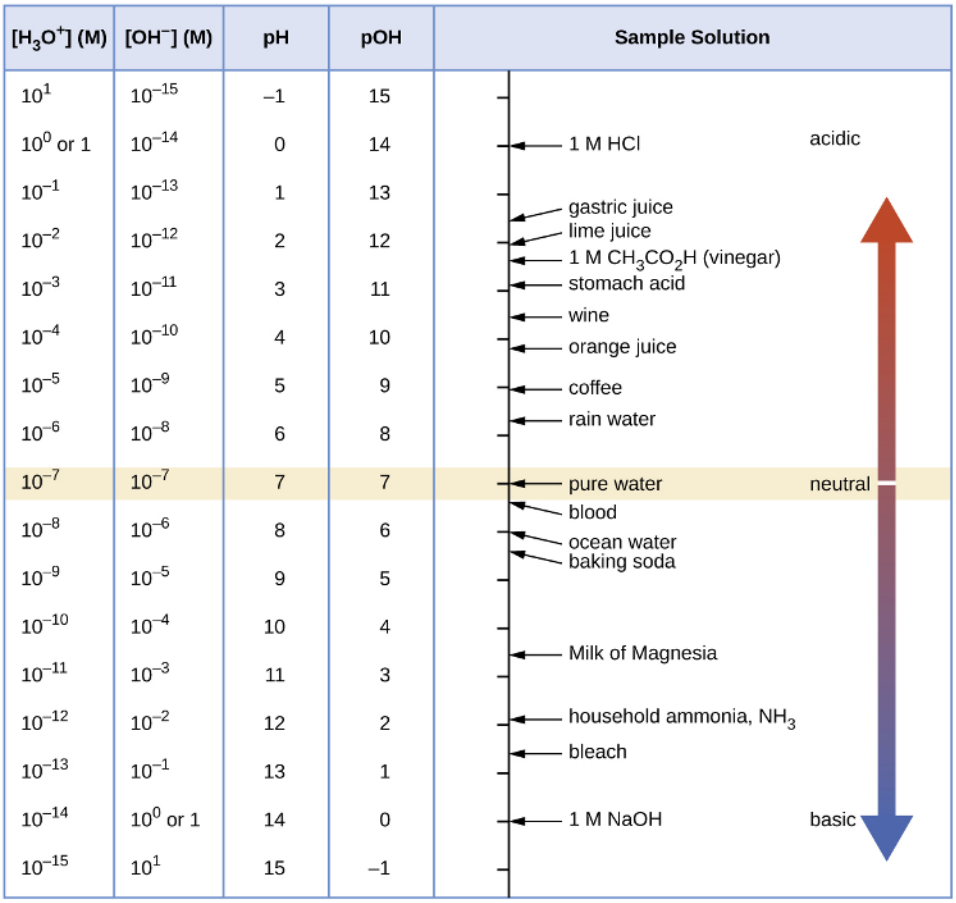


Figure 2.9.1: The pH and pOH scales represent concentrations of H_3O^+ and OH^-, respectively. The pH and pOH values of some common substances at 25 °C are shown in this chart.

Example 2.9.1: Calculation of pH from [H_3O^+]

What is the pH of stomach acid, a solution of HCl with a hydronium ion concentration of $1.2 \times 10^{-3}\ M$?

Solution

$$\begin{aligned} pH &= -\log\left[\mathrm{H_3O^+}\right] \\ &= -\log\left(1.2 \times 10^{-3}\right) \\ &= -(-2.92) = 2.92 \end{aligned}$$

(The use of logarithms is explained in Appendix B. When taking the log of a value, keep as many decimal places in the result as there are significant figures in the value.)

Exercise 2.9.1

Water exposed to air contains carbonic acid, $\mathrm{H_2CO_3}$, due to the reaction between carbon dioxide and water:

$$\mathrm{CO_2(aq) + H_2O(l) \rightleftharpoons H_2CO_3(aq)}$$

Air-saturated water has a hydronium ion concentration caused by the dissolved $\mathrm{CO_2}$ of 2.0×10^{-6} M, about 20-times larger than that of pure water. Calculate the pH of the solution at 25 °C.

Answer

5.70

Example 2.9.2: Calculation of Hydronium Ion Concentration from pH

Calculate the hydronium ion concentration of blood, the pH of which is 7.3.

Solution

$$\begin{aligned} pH = -\log\left[H_3O^+\right] &= 7.3 \\ \log\left[H_3O^+\right] &= -7.3 \\ \left[H_3O^+\right] &= 10^{-7.3} \end{aligned}$$

or

$$\begin{aligned} [\mathrm{H_3O^+}] &= \text{antilog of } -7.3 \\ &= 5 \times 10^{-8} M \end{aligned}$$

(On a calculator take the antilog, or the "inverse" log, of −7.3, or calculate $10^{-7.3}$.)

Exercise 2.9.2

Calculate the hydronium ion concentration of a solution with a pH of −1.07.

Answer

12 *M*

How Sciences Interconnect: Environmental Science

Normal rainwater has a pH between 5 and 6 due to the presence of dissolved $\mathrm{CO_2}$ which forms carbonic acid:

$$\mathrm{H_2O(l) + CO_2(g) \longrightarrow H_2CO_3(aq)}$$

$$\mathrm{H_2CO_3(aq) \rightleftharpoons H^+(aq) + HCO_3^-(aq)}$$

Acid rain is rainwater that has a pH of less than 5, due to a variety of nonmetal oxides, including CO_2, SO_2, SO_3, NO, and NO_2 being dissolved in the water and reacting with it to form not only carbonic acid, but sulfuric acid and nitric acid. The formation and subsequent ionization of sulfuric acid are shown here:

$$H_2O(l) + SO_3(g) \longrightarrow H_2SO_4(aq)$$
$$H_2SO_4(aq) \longrightarrow H^+(aq) + HSO_4^-(aq)$$

Carbon dioxide is naturally present in the atmosphere because most organisms produce it as a waste product of metabolism. Carbon dioxide is also formed when fires release carbon stored in vegetation or fossil fuels. Sulfur trioxide in the atmosphere is naturally produced by volcanic activity, but it also originates from burning fossil fuels, which have traces of sulfur, and from the process of "roasting" ores of metal sulfides in metal-refining processes. Oxides of nitrogen are formed in internal combustion engines where the high temperatures make it possible for the nitrogen and oxygen in air to chemically combine.

Acid rain is a particular problem in industrial areas where the products of combustion and smelting are released into the air without being stripped of sulfur and nitrogen oxides. In North America and Europe until the 1980s, it was responsible for the destruction of forests and freshwater lakes, when the acidity of the rain actually killed trees, damaged soil, and made lakes uninhabitable for all but the most acid-tolerant species. Acid rain also corrodes statuary and building facades that are made of marble and limestone (Figure 2.9.2). Regulations limiting the amount of sulfur and nitrogen oxides that can be released into the atmosphere by industry and automobiles have reduced the severity of acid damage to both natural and manmade environments in North America and Europe. It is now a growing problem in industrial areas of China and India.

For further information on acid rain, visit this website hosted by the US Environmental Protection Agency.



(a)



(b)

Figure 2.9.2: (a) Acid rain makes trees more susceptible to drought and insect infestation, and depletes nutrients in the soil. (b) It also is corrodes statues that are carved from marble or limestone. (credit a: modification of work by Chris M Morris; credit b: modification of work by "Eden, Janine and Jim"/Flickr)

✔ Example ✔ 2.9.3: Calculation of pOH

What are the pOH and the \(\text{pH} of a 0.0125-*M* solution of potassium hydroxide, KOH?

Solution

Potassium hydroxide is a highly soluble ionic compound and completely dissociates when dissolved in dilute solution, yielding $[OH^-]$ = 0.0125 *M*:

$$\text{pOH} = -\log\left[OH^-\right] = -\log 0.0125$$
$$= -(-1.903) = 1.903$$

The pH can be found from the pOH:

$$\begin{aligned} \text{pH} + \text{pOH} &= 14.00 \\ pH &= 14.00 - pOH \\ &= 14.00 - 1.903 = 12.10 \end{aligned}$$

? Exercise 2.9.3

The hydronium ion concentration of vinegar is approximately 4×10^{-3} M. What are the corresponding values of pOH and pH?

Answer

pOH = 11.6, pH = 2.4

This page titled 2.9: pH and pOH is shared under a CC BY-NC-SA 4.0 license and was authored, remixed, and/or curated by Jonathan Gutow.

- **14.2: pH and pOH** by OpenStax is licensed CC BY 4.0. Original source: https://openstax.org/details/books/chemistry-2e.

2.10: Acid-Base Equilibria

Learning Objectives

By the end of this section, you will be able to:

- Assess the relative strengths of acids and bases according to their ionization constants
- Rationalize trends in acid–base strength in relation to molecular structure
- Carry out equilibrium calculations for weak acid–base systems

2.10.1: Acid and Base Ionization Constants

The relative strength of an acid or base is the extent to which it ionizes when dissolved in water. If the ionization reaction is essentially complete, the acid or base is termed *strong*; if relatively little ionization occurs, the acid or base is weak. As will be evident throughout the remainder of this chapter, there are many more weak acids and bases than strong ones. The most common strong acids and bases are listed in Figure 2.10.1.

6 Strong Acids		6 Strong Bases	
$HClO_4$	perchloric acid	LiOH	lithium hydroxide
HCl	hydrochloric acid	NaOH	sodium hydroxide
HBr	hydrobromic acid	KOH	potassium hydroxide
HI	hydroiodic acid	$Ca(OH)_2$	calcium hydroxide
HNO_3	nitric acid	$Sr(OH)_2$	strontium hydroxide
H_2SO_4	sulfuric acid	$Ba(OH)_2$	barium hydroxide

Figure 2.10.1: Some of the common strong acids and bases are listed here.

The relative strengths of acids may be quantified by measuring their equilibrium constants in aqueous solutions. In solutions of the same concentration, stronger acids ionize to a greater extent, and so yield higher concentrations of hydronium ions than do weaker acids. The equilibrium constant for an acid is called the acid-ionization constant, K_a. For the reaction of an acid HA:

$$\mathrm{HA(aq) + H_2O(l) \rightleftharpoons H_3O^+(aq) + A^-(aq)}$$

the acid ionization constant is written

$$K_a = \frac{[\mathrm{H_3O^+}][\mathrm{A^-}]}{[\mathrm{HA}]}$$

where the concentrations are those at equilibrium. Although water is a reactant in the reaction, it is the solvent as well, so we do not include $[\mathrm{H_2O}]$ in the equation.

Note

Equilibrium constant expressions are actually ratios of activities, and the value of *K* is determined at the limit of infinite dilution of the solutes. In these very dilute solutions, the activity of the solvent has a value of unity (1) and the activity of each solute can be approximated by its molar concentration.

The larger the K_a of an acid, the larger the concentration of $\mathrm{H_3O^+}$ and $\mathrm{A^-}$ relative to the concentration of the nonionized acid, HA, in an equilibrium mixture, and the stronger the acid. An acid is classified as “strong” when it undergoes complete ionization, in which case the concentration of HA is zero and the acid ionization constant is immeasurably large ($K_a \approx \infty$). Acids that are partially ionized are called “weak,” and their acid ionization constants may be experimentally measured. A table of ionization constants for weak acids is provided in the resources.

To illustrate this idea, three acid ionization equations and K_a values are shown below. The ionization constants increase from first to last of the listed equations, indicating the relative acid strength increases in the order:

$$\mathrm{CH_3CO_2H} < \mathrm{HNO_2} < \mathrm{HSO_4^-}$$

as demonstrated with the equations below:

$$\mathrm{CH_3CO_2H(aq) + H_2O(l) \rightleftharpoons H_3O^+(aq) + CH_3CO_2^-(aq)} \qquad K_a = 1.8 \times 10^{-5}$$

$$\mathrm{HNO_2(aq) + H_2O(l) \rightleftharpoons H_3O^+(aq) + NO_2^-(aq)} \qquad K_a = 4.6 \times 10^{-4}$$

$$\mathrm{HSO_4^-(aq) + H_2O(aq) \rightleftharpoons H_3O^+(aq) + SO_4^{2-}(aq)} \qquad K_a = 1.2 \times 10^{-2}$$

Another measure of the strength of an acid is its percent ionization. The percent ionization of a weak acid is defined in terms of the composition of an equilibrium mixture:

$$\%\ \text{ionization} = \frac{\left[\mathrm{H_3O^+}\right]_{eq}}{[\mathrm{HA}]_0} \times 100\%$$

where the numerator is equivalent to the concentration of the acid's conjugate base (per stoichiometry, $[A^-] = [H_3O^+]$). Unlike the K_a value, the percent ionization of a weak acid varies with the initial concentration of acid, typically decreasing as concentration increases. Equilibrium calculations of the sort described later in this chapter can be used to confirm this behavior.

Example 2.10.1: Calculation of Percent Ionization from pH

Calculate the percent ionization of a 0.125-*M* solution of nitrous acid (a weak acid), with a pH of 2.09.

Solution

The percent ionization for an acid is:

$$\frac{\left[\mathrm{H_3O^+}\right]_{eq}}{\left[\mathrm{HNO_2}\right]_0} \times 100$$

Converting the provided pH to hydronium ion molarity yields

$$\left[\mathrm{H_3O^+}\right] = 10^{-2.09} = 0.0081M$$

Substituting this value and the provided initial acid concentration into the percent ionization equation gives

$$\frac{8.1 \times 10^{-3}}{0.125} \times 100 = 6.5\%$$

(Recall the provided pH value of 2.09 is logarithmic, and so it contains just two significant digits, limiting the certainty of the computed percent ionization.)

Exercise 2.10.1

Calculate the percent ionization of a 0.10-*M* solution of acetic acid with a pH of 2.89.

Answer

1.3% ionized

Link to Learning

View the simulation of strong and weak acids and bases at the molecular level.

Just as for acids, the relative strength of a base is reflected in the magnitude of its base-ionization constant (K_b) in aqueous solutions. In solutions of the same concentration, stronger bases ionize to a greater extent, and so yield higher hydroxide ion concentrations than do weaker bases. A stronger base has a larger ionization constant than does a weaker base. For the reaction of a base, B:

$$\mathrm{B(aq) + H_2O(l) \rightleftharpoons HB^+(aq) + OH^-(aq)},$$

the ionization constant is written as

$$K_b = \frac{\left[\mathrm{HB^+}\right]\left[\mathrm{OH^-}\right]}{\left[\mathrm{B}\right]}$$

Inspection of the data for three weak bases presented below shows the base strength increases in the order: $\mathrm{NO_2^-} < \mathrm{CH_2CO_2^-} < \mathrm{NH_3}$

$$\mathrm{NO_2^-(aq) + H_2O(l) \rightleftharpoons HNO_2(aq) + OH^-(aq)} \qquad K_b = 2.17 \times 10^{-11}$$

$$\mathrm{CH_3CO_2^-(aq) + H_2O(l) \rightleftharpoons CH_3CO_2H(aq) + OH^-(aq)} \qquad K_b = 5.6 \times 10^{-10}$$

$$\mathrm{NH_3(aq) + H_2O(l) \rightleftharpoons NH_4^+(aq) + OH^-(aq)} \qquad K_b = 1.8 \times 10^{-5}$$

A table of ionization constants for weak bases appears in the resources. As for acids, the relative strength of a base is also reflected in its percent ionization, computed as

$$\%\ \text{ionization} = \left(\frac{[\mathrm{OH^-}]_{eq}}{[\mathrm{B}]_0}\right) \times 100\%$$

but will vary depending on the base ionization constant and the initial concentration of the solution.

2.10.2: Relative Strengths of Conjugate Acid-Base Pairs

Brønsted-Lowry acid-base chemistry is the transfer of protons; thus, logic suggests a relation between the relative strengths of conjugate acid-base pairs. The strength of an acid or base is quantified in its ionization constant, K_a or K_b, which represents the extent of the acid or base ionization reaction. For the conjugate acid-base pair $\mathrm{HA/A^-}$, ionization equilibrium equations and ionization constant expressions are

$$\mathrm{HA(aq) + H_2O(l) \rightleftharpoons H_3O^+(aq) + A^-(aq)}$$

with

$$K_a = \frac{[\mathrm{H_3O^+}][\mathrm{A^-}]}{[\mathrm{HA}]}$$

and

$$\mathrm{A^-(aq) + H_2O(l) \rightleftharpoons OH^-(aq) + HA(aq)}$$

with

$$K_b = \frac{[\mathrm{HA}][\mathrm{OH-}]}{[\mathrm{A-}]}$$

Adding these two chemical equations yields the equation for the autoionization for water:

$$\mathrm{\cancel{HA(aq)} + H_2O(l) + \cancel{A^-(aq)} + H_2O(l) \rightleftharpoons H_3O^+(aq) + \cancel{A^-(aq)} + OH^-(aq) + \cancel{HA(aq)}}$$

$$\mathrm{2\,H_2O(l) \rightleftharpoons H_3O^+(aq) + OH^-(aq)}$$

As discussed in another chapter on equilibrium, the equilibrium constant for a summed reaction is equal to the mathematical product of the equilibrium constants for the added reactions, and so

$$K_a \times K_b = \frac{[\mathrm{H_3O^+}][\mathrm{A^-}]}{[\mathrm{HA}]} \times \frac{[\mathrm{HA}][\mathrm{OH^-}]}{[\mathrm{A^-}]} = [\mathrm{H_3O^+}][\mathrm{OH^-}] = K_w$$

This equation states the relation between ionization constants for any conjugate acid-base pair, namely, their mathematical product is equal to the ion product of water, K_w. By rearranging this equation, a reciprocal relation between the strengths of a conjugate acid-base pair becomes evident:

$$K_a = \frac{K_w}{K_b}$$

or

$$K_b = \frac{K_w}{K_a}$$

The inverse proportional relation between K_a and K_b means the stronger the acid or base, the weaker its **conjugate partner**. A strong acid exhibits an immeasurably large K_a, and so its conjugate base will exhibit a K_b that is essentially zero:

- strong acid: $K_a \approx \infty$
- conjugate base: $K_b = K_w/K_a = K_w/\infty \approx 0$

A similar approach can be used to support the observation that conjugate acids of strong bases ($K_b \approx \infty$) are of negligible strength ($K_a \approx 0$).

Another way of writing this relationship between K_a , K_b and K_w is using logs: -log(K_a) -log(K_b) = -log(K_w) = pK_a + pK_b = pK_w.

Example 2.10.2: Calculating Ionization Constants for Conjugate Acid-Base Pairs

Use the K_b for the nitrite ion, $\mathrm{NO_2^-}$, to calculate the K_a for its conjugate acid.

Solution

K_b for $\mathrm{NO_2^-}$ is given in this section as 2.17×10^{-11}. The conjugate acid of $\mathrm{NO_2^-}$ is $\mathrm{HNO_2}$; K_a for $\mathrm{HNO_2}$ can be calculated using the relationship:

$$K_a \times K_b = 1.0 \times 10^{-14} = K_w$$

Solving for K_a yields

$$K_a = \frac{K_w}{K_b} = \frac{1.0 \times 10^{-14}}{2.17 \times 10^{-11}} = 4.6 \times 10^{-4}$$

This answer can be verified by looking up the Ka for $\mathrm{HNO_2}$.

Exercise 2.10.2

Determine the relative acid strengths of $\mathrm{NH4^+}$ and HCN by comparing their ionization constants. The ionization constant of HCN is given in Appendix H as 4.9×10^{-10}. The ionization constant of $\mathrm{NH4^+}$ is not listed, but the ionization constant of its conjugate base, $\mathrm{NH_3}$, is listed as 1.8×10^{-5}.

Answer

$\mathrm{NH_4^+}$ is the slightly stronger acid (K_a for $\mathrm{NH_4^+}$ is 5.6×10^{-10}).

2.10.3: Acid-Base Equilibrium Calculations

The chapter on chemical equilibria introduced several types of equilibrium calculations and the various mathematical strategies that are helpful in performing them. These strategies are generally useful for equilibrium systems regardless of chemical reaction class, and so they may be effectively applied to acid-base equilibrium problems. This section presents several example exercises involving equilibrium calculations for acid-base systems.

Example 2.10.3: Determination of K_a from Equilibrium Concentrations

Acetic acid is the principal ingredient in vinegar (Figure 2.10.4) that provides its sour taste. At equilibrium, a solution contains $[\mathrm{CH_3CO_2H}] = 0.0787\ M$: and $[\mathrm{H_3O^+}] = [\mathrm{CH_3CO_2^-}] = 0.00118\ M$. What is the value of K_a for acetic acid?



Figure 2.10.4: Vinegar contains acetic acid, a weak acid. (credit: modification of work by "HomeSpot HQ"/Flickr)

Solution

The relevant equilibrium equation and its equilibrium constant expression are shown below. Substitution of the provided equilibrium concentrations permits a straightforward calculation of the Ka for acetic acid.

$$\mathrm{CH_3CO_2H(aq) + H_2O(l) \rightleftharpoons H_3O^+(aq) + CH_3CO_2^-(aq)}$$

$$K_a = \frac{\left[\mathrm{H_3O^+}\right]\left[\mathrm{CH_3CO_2^-}\right]}{\left[\mathrm{CH_3CO_2H}\right]} = \frac{(0.00118)(0.00118)}{0.0787} = 1.77 \times 10^{-5}$$

Exercise 2.10.3

The $\mathrm{HSO_4^-}$ ion, weak acid used in some household cleansers:

$$\mathrm{HSO_4^-(aq) + H_2O(l) \rightleftharpoons H_3O^+(aq) + SO_4^{2-}(aq)}$$

What is the acid ionization constant for this weak acid if an equilibrium mixture has the following composition: $[\mathrm{H_3O^+}] = 0.027\ M$; $[\mathrm{HSO_4^-}] = 0.29\ M$; $[\mathrm{HSO_4^-}] = 0.29\ M$; and $[\mathrm{SO_4^{2-}}] = 0.13\ M$?

Answer

K_a for $\mathrm{HSO_4^-} = 1.2 \times 10^{-2}$

Example 2.10.4: Determination of K_b from Equilibrium Concentrations

Caffeine, $\mathrm{C_8H_{10}N_4O_2}$ is a weak base. What is the value of K_b for caffeine if a solution at equilibrium has $[\mathrm{C_8H_{10}N_4O_2}] = 0.050\ \mathrm{M}$, $[\mathrm{C_8H_{10}N_4O_2H^+}] = 5.0 \times 10^{-3}\ \mathrm{M}$, and $[\mathrm{OH^-}] = 2.5 \times 10^{-3}\ \mathrm{M}$?

Solution

The relevant equilibrium equation and its equilibrium constant expression are shown below. Substitution of the provided equilibrium concentrations permits a straightforward calculation of the K_b for caffeine.

$$\mathrm{C_8H_{10}N_4O_2(aq) + H_2O(l) \rightleftharpoons C_8H_{10}N_4O_2H^+(aq) + OH^-(aq)}$$

$$K_b = [C_8H_{10}N_4O_2H^+][OH^-][C_8H_{10}N_4O_2]$$
$$= (5.0 \times 10^{-3})(2.5 \times 10^{-3})(0.050)$$
$$= 2.5 \times 10^{-4}$$

Exercise 2.10.4

What is the equilibrium constant for the ionization of the HPO_4^{2-} ion, a weak base

$$HPO_4^{2-}(aq) + H_2O(l) \rightleftharpoons H_2PO_4^-(aq) + OH^-(aq)$$

if the composition of an equilibrium mixture is as follows: $[OH^-] = 1.3 \times 10^{-6}\,M$; $H_2PO_4^-] = 0.042\,M$; and $[HPO_4^{2-}] = 0.341\,M$?

Answer

K_b for HPO_4^{2-} is 1.6×10^{-7}

Example 2.10.5: Determination of K_a or K_b from pH

The pH of a 0.0516-M solution of nitrous acid, HNO_2, is 2.34. What is its K_a?

$$HNO_2(aq) + H_2O(l) \rightleftharpoons H_3O^+(aq) + NO_2^-(aq)$$

Solution

The nitrous acid concentration provided is a *formal* concentration, one that does not account for any chemical equilibria that may be established in solution. Such concentrations are treated as "initial" values for equilibrium calculations using the ICE table approach. Notice the initial value of hydronium ion is listed as *approximately* zero because a small concentration of H_3O^+ is present ($1 \times \times 10^{-7}$ M) due to the autoprotolysis of water. In many cases, such as all the ones presented in this chapter, this concentration is much less than that generated by ionization of the acid (or base) in question and may be neglected.

The pH provided is a logarithmic measure of the hydronium ion concentration resulting from the acid ionization of the nitrous acid, and so it represents an "equilibrium" value for the ICE table:

$$\left[H_3O^+\right] = 10^{-2.34} = 0.0046\ \text{M}$$

The ICE table for this system is then

	HNO_2	+ H_2O ⇌	H_3O^+	+ NO_2^-
Initial concentration (*M*)	0.0516		~0	0
Change (*M*)	–0.0046		+0.0046	+0.0046
Equilibrium concentration (*M*)	0.0470		0.0046	0.0046

Finally, calculate the value of the equilibrium constant using the data in the table:

$$K_a = \frac{\left[H_3O^+\right]\left[NO_2^-\right]}{[HNO_2]} = \frac{(0.0046)(0.0046)}{(0.0470)} = 4.6 \times 10^{-4}$$

Exercise 2.10.5

The pH of a solution of household ammonia, a 0.950-M solution of NH_3, is 11.612. What is K_b for NH_3.

Answer

$K_b = 1.8 \times 10^{-5}$

Example 2.10.6: Calculating Equilibrium Concentrations in a Weak Acid Solution

Formic acid, HCO_2H, is one irritant that causes the body's reaction to some ant bites and stings (Figure 2.10.5).



Figure 2.10.5: The pain of some ant bites and stings is caused by formic acid. (credit: John Tann)

What is the concentration of hydronium ion and the pH of a 0.534-*M* solution of formic acid?

$$HCO_2H(aq) + H_2O(l) \rightleftharpoons H_3O^+(aq) + HCO_2^-(aq) \quad K_a = 1.8 \times 10^{-4}$$

Solution

The ICE table for this system is

	HCO_2H	+	H_2O	$\rightleftharpoons$	H_3O^+	+	HCO_2^-
Initial concentration (*M*)	0.534				~0		0
Change (*M*)					$+x$		$+x$
Equilibrium concentration (*M*)	$0.534 - x$				x		x

Substituting the equilibrium concentration terms into the K_a expression gives

$$K_a = 1.8 \times 10^{-4} = \frac{[H_3O^+][HCO_2^-]}{[HCO_2H]}$$

$$= \frac{(x)(x)}{0.534 - x} = 1.8 \times 10^{-4}$$

The relatively large initial concentration and small equilibrium constant permits the simplifying assumption that x will be much lesser than 0.534, and so the equation becomes

$$K_a = 1.8 \times 10^{-4} = \frac{x^2}{0.534}$$

Solving the equation for x yields

$$x^2 = 0.534 \times \left(1.8 \times 10^{-4}\right) = 9.6 \times 10^{-5}$$

$$x = \sqrt{9.6 \times 10^{-5}}$$

$$= 9.8 \times 10^{-3} M$$

To check the assumption that x is small compared to 0.534, its relative magnitude can be estimated:

$$\frac{x}{0.534} = \frac{9.8 \times 10^{-3}}{0.534} = 1.8 \times 10^{-2} (1.8\% \text{ of } 0.534)$$

Because x is less than 5% of the initial concentration, the assumption is valid.

As defined in the ICE table, *x* is equal to the equilibrium concentration of hydronium ion:

$$x = \left[H_3O^+\right] = 0.0098\ \text{M}$$

Finally, the pH is calculated to be

$$\text{pH} = -\log\left[H_3O^+\right] = -\log(0.0098) = 2.01$$

? Exercise 2.10.6

Only a small fraction of a weak acid ionizes in aqueous solution. What is the percent ionization of a 0.100-*M* solution of acetic acid, CH_3CO_2H?

$$CH_3CO_2H(aq) + H_2O(l) \rightleftharpoons H_3O^+(aq) + CH_3CO_2^-(aq) \quad K_a = 1.8 \times 10^{-5}$$

Answer

percent ionization = 1.3%

✓ Example 2.10.7: Calculating Equilibrium Concentrations in a Weak Base Solution

Find the concentration of hydroxide ion, the pOH, and the pH of a 0.25-*M* solution of trimethylamine, a weak base:

$$(CH_3)_3N(aq) + H_2O(l) \rightleftharpoons (CH_3)_3NH^+(aq) + OH^-(aq) \quad K_b = 6.3 \times 10^{-5}$$

Solution

The ICE table for this system is

	$(CH_3)_3N$ + H_2O ⇌		$(CH_3)_3NH^+$ +	OH^-
Initial concentration (*M*)	0.25		0	~0
Change (*M*)	−*x*		*x*	*x*
Equilibrium concentration (*M*)	0.25 + (−*x*)		0 + *x*	~0 + *x*

Substituting the equilibrium concentration terms into the K_b expression gives

$$K_b = \frac{\left[(CH_3)_3NH^+\right]\left[OH^-\right]}{\left[(CH_3)_3N\right]} = \frac{(x)(x)}{0.25 - x} = 6.3 \times 10^{-5}$$

Assuming $x \ll 0.25$ and solving for x yields

$$x = 4.0 \times 10^{-3}\ \text{M}$$

This value is less than 5% of the initial concentration (0.25), so the assumption is justified. As defined in the ICE table, x is equal to the equilibrium concentration of hydroxide ion:

$$\begin{aligned}\left[OH^-\right] &\sim 0 + x \\ &= x = 4.0 \times 10^{-3} M\end{aligned}$$

The pOH is calculated to be

$$\text{pOH} = -\log\left(4.0 \times 10^{-3}\right) = 2.40$$

Using the relation introduced in the previous section of this chapter:

$$\text{pH} + \text{pOH} = pK_w = 14.00$$

permits the computation of pH:

$$\text{pH} = 14.00 - \text{pOH} = 14.00 - 2.40 = 11.60$$

Exercise 2.10.7

Calculate the hydroxide ion concentration and the percent ionization of a 0.0325-*M* solution of ammonia, a weak base with a K_b of 1.76×10^{-5}.

Answer

7.56×10^{-4} M, 2.33%

In some cases, the strength of the weak acid or base and its formal (initial) concentration result in an appreciable ionization. Though the ICE strategy remains effective for these systems, the algebra is a bit more involved because the simplifying assumption that *x* is negligible cannot be made. Calculations of this sort are demonstrated in Example 2.10.8below.

Example 2.10.8: Calculating Equilibrium Concentrations without Simplifying Assumptions

Sodium bisulfate, NaHSO4, is used in some household cleansers as a source of the HSO_4^- ion, a weak acid. What is the pH of a 0.50-M solution of HSO_4^-?

$$HSO_4^-(aq) + H_2O(l) \rightleftharpoons H_3O^+(aq) + SO_4^{2-}(aq) \quad K_a = 1.2 \times 10^{-2}$$

Solution

The ICE table for this system is

	HSO_4^-	+ H_2O ⇌	H_3O^+	+ SO_4^{2-}
Initial concentration (*M*)	0.50		~0	0
Change (*M*)	−*x*		+*x*	+*x*
Equilibrium concentration (*M*)	0.50 − *x*		*x*	*x*

Substituting the equilibrium concentration terms into the K_a expression gives

$$K_a = 1.2 \times 10^{-2} = \frac{\left[H_3O^+\right]\left[SO_4^{2-}\right]}{\left[HSO_4^-\right]} = \frac{(x)(x)}{0.50 - x}$$

If the assumption that $x \ll 0.5$ is made, simplifying and solving the above equation yields

$$x = 0.077 \text{ M}$$

This value of x is clearly not significantly less than 0.50 *M*; rather, it is approximately 15% of the initial concentration: When we check the assumption, we calculate:

$$\frac{x}{\left[HSO_4^-\right]_i}$$

$$\frac{x}{0.50} = \frac{7.7 \times 10^{-2}}{0.50} = 0.15(15\%)$$

Because the simplifying assumption is not valid for this system, the equilibrium constant expression is solved as follows:

$$K_a = 1.2 \times 10^{-2} = \frac{(x)(x)}{0.50 - x}$$

Rearranging this equation yields

$$6.0 \times 10^{-3} - 1.2 \times 10^{-2} x = x^2$$

Writing the equation in quadratic form gives

$$x^2 + 1.2 \times 10^{-2} x - 6.0 \times 10^{-3} = 0$$

Solving for the two roots of this quadratic equation results in a negative value that may be discarded as physically irrelevant and a positive value equal to *x*. As defined in the ICE table, x is equal to the hydronium concentration.

$$x = \left[H3O^+\right] = 0.072 \text{ M}$$

$$\text{pH} = -\log\left[\text{H}_3\text{O}^+\right] = -\log(0.072) = 1.14$$

? Exercise 2.10.8

Calculate the pH in a 0.010-*M* solution of caffeine, a weak base:

$$\text{C}_8\text{H10}\,\text{N}_4\text{O}_2(\text{aq}) + \text{H}_2\text{O}(\text{l}) \rightleftharpoons \text{C}_8\text{H10}\,\text{N}_4\text{O}_2\text{H}^+(\text{aq}) + \text{OH}^-(\text{aq}) \quad K_b = 2.5 \times 10^{-4}$$

Answer

pH = 11.16

This page titled 2.10: Acid-Base Equilibria is shared under a CC BY-NC-SA 4.0 license and was authored, remixed, and/or curated by Jonathan Gutow.

- **14.3: Relative Strengths of Acids and Bases** by OpenStax is licensed CC BY 4.0. Original source: https://openstax.org/details/books/chemistry-2e.

2.11: Hydrolysis of Salts

Learning Objectives

By the end of this section, you will be able to:

- Predict whether a salt solution will be acidic, basic, or neutral
- Calculate the concentrations of the various species in a salt solution
- Describe the acid ionization of hydrated metal ions

2.11.1: Salts with Acidic Ions

Salts are ionic compounds composed of cations and anions, either of which may be capable of undergoing an acid or base ionization reaction with water. Aqueous salt solutions, therefore, may be acidic, basic, or neutral, depending on the relative acid-base strengths of the salt's constituent ions. For example, dissolving ammonium chloride in water results in its dissociation, as described by the equation

$$\mathrm{NH_4Cl(s) \rightleftharpoons NH_4^+(aq) + Cl^-(aq)}$$

The ammonium ion is the conjugate acid of the base ammonia, NH_3; its acid ionization (or acid hydrolysis) reaction is represented by

$$\mathrm{NH_4^+(aq) + H_2O(l) \rightleftharpoons H_3O^+(aq) + NH_3(aq)} \quad K_a = K_w/K_b$$

Since ammonia is a weak base, K_b is measurable and $K_a > 0$ (ammonium ion is a weak acid).

The chloride ion is the conjugate base of hydrochloric acid, and so its base ionization (or *base hydrolysis*) reaction is represented by

$$\mathrm{Cl^-(aq) + H_2O(l) \rightleftharpoons HCl(aq) + OH^-(aq)} \quad K_b = K_w/K_a$$

Since HCl is a strong acid, K_a is immeasurably large and $K_b \approx 0$ (chloride ions don't undergo appreciable hydrolysis).

Thus, dissolving ammonium chloride in water yields a solution of weak acid cations (NH_4^+) and inert anions (Cl^-), resulting in an acidic solution.

Example 2.11.1: Calculating the pH of an Acidic Salt Solution

Aniline is an amine that is used to manufacture dyes. It is isolated as anilinium chloride, a salt prepared by the reaction of the weak base aniline and hydrochloric acid. What is the pH of a 0.233 *M* solution of anilinium chloride

$$\mathrm{C_6H_5NH_3^+(aq) + H_2O(l) \rightleftharpoons H_3O^+(aq) + C_6H_5NH_2(aq)}$$

Solution

The K_a for anilinium ion is derived from the K_b for its conjugate base, aniline (see Appendix H):

$$K_a = \frac{K_w}{K_b} = \frac{1.0 \times 10^{-14}}{4.3 \times 10^{-10}} = 2.3 \times 10^{-5}$$

Using the provided information, an ICE table for this system is prepared:

	$C_6H_5NH_3^+$	+ H_2O ⇌	$C_6H_5NH_2$	+ H_3O^+
Initial concentration (*M*)	0.233		0	~0
Change (*M*)	$-x$		$+x$	$+x$
Equilibrium concentration (*M*)	$0.233 - x$		x	x

Substituting these equilibrium concentration terms into the K_a expression gives

$$K_a = \frac{\left[\mathrm{C_6H_5NH_2}\right]\left[\mathrm{H_3O^+}\right]}{\left[\mathrm{C_6H_5NH_3^+}\right]}$$

$$2.3 \times 10^{-5} = \frac{(x)(x)}{0.233 - x}$$

Assuming $x \ll 0.233$, the equation is simplified and solved for x:

$$2.3 \times 10^{-5} = \frac{x^2}{0.233}$$

$$x = 0.0023\ \mathrm{M}$$

The ICE table defines x as the hydronium ion molarity, and so the pH is computed as

$$\mathrm{pH} = -\log\left[\mathrm{H_3O^+}\right] = -\log(0.0023) = 2.64$$

? Exercise 2.11.1

What is the hydronium ion concentration in a 0.100-*M* solution of ammonium nitrate, $\mathrm{NH_4NO_3}$, a salt composed of the ions NH_4^+ and NO_3^- and.

Which is the stronger acid $\mathrm{C_6H_5NH_3^+}$ or $\mathrm{NH_4^+}$?

Answer

$[\mathrm{H_3O^+}] = 7.5 \times 10^{-6}\ \mathrm{M}$; is the stronger acid.

2.11.2: Salts with Basic Ions

As another example, consider dissolving sodium acetate in water:

$$\mathrm{NaCH_3CO_2(s) \rightleftharpoons Na^+(aq) + CH_3CO_2^-(aq)}$$

The sodium ion does not undergo appreciable acid or base ionization and has no effect on the solution pH. This may seem obvious from the ion's formula, which indicates no hydrogen or oxygen atoms, but some dissolved metal ions function as weak acids, as addressed later in this section.

The acetate ion, $\mathrm{CH_3CO_2^-(aq)}$, is the conjugate base of acetic acid, $\mathrm{CH_3CO_2H}$, and so its base ionization (or *base hydrolysis*) reaction is represented by

$$\mathrm{CH_3CO_2^-(aq) + H_2O(l) \rightleftharpoons CH_3CO_2H(aq) + OH{-}(aq)} \quad K_b = K_w/K_a$$

Because acetic acid is a weak acid, its K_a is measurable and $K_b > 0$ (acetate ion is a weak base).

Dissolving sodium acetate in water yields a solution of inert cations (Na^+) and weak base anions ($\mathrm{CH_3CO_2^-}$), resulting in a basic solution.

✓ Example 2.11.2: Equilibrium in a Solution of a Salt of a Weak Acid and a Strong Base

Determine the acetic acid concentration in a solution with and $[\mathrm{OH^-}] = 0.050\ \mathrm{M}$ and $[\mathrm{OH^-}] = 2.5 \times 10^{-6} M$ at equilibrium. The reaction is:

$$\mathrm{CH_3CO_2^-(aq) + H_2O(l) \rightleftharpoons CH_3CO_2H(aq) + OH^-(aq)}$$

Solution

The provided equilibrium concentrations and a value for the equilibrium constant will permit calculation of the missing equilibrium concentration. The process in question is the base ionization of acetate ion, for which

$$\mathrm{CH_3CO_2^-(aq) + H_2O(l) \rightleftharpoons CH_3CO_2H(aq) + OH^-(aq)}$$

Substituting the available values into the K_b expression gives

$$K_b = \frac{[CH_3CO_2H]\left[\mathrm{OH^-}\right]}{\left[\mathrm{CH_3CO_2^-}\right]} = 5.6 \times 10^{-10}$$

$$= \frac{\left[\mathrm{CH_3CO_2H}\right]\left(2.5 \times 10^{-6}\right)}{(0.050)} = 5.6 \times 10^{-10}$$

Solving the above equation for the acetic acid molarity yields $\left[\mathrm{CH_3CO_2H}\right] = 1.1 \times 10^{-5}\ \mathrm{M}$.

? Exercise 2.11.2

What is the pH of a 0.083-*M* solution of NaCN?

Answer

11.11

2.11.3: Salts with Acidic and Basic Ions

Some salts are composed of both acidic and basic ions, and so the pH of their solutions will depend on the relative strengths of these two species. Likewise, some salts contain a single ion that is amphiprotic, and so the relative strengths of this ion's acid and base character will determine its effect on solution pH. For both types of salts, a comparison of the K_a and K_b values allows prediction of the solution's acid-base status, as illustrated in the following example exercise.

✓ Example 2.11.3: Determining the Acidic or Basic Nature of Salts

Determine whether aqueous solutions of the following salts are acidic, basic, or neutral:

a. KBr
b. $NaHCO_3$
c. Na_2HPO_4
d. NH_4F

Solution

Consider each of the ions separately in terms of its effect on the pH of the solution, as shown here:

(a) The K^+ cation is inert and will not affect pH. The bromide ion is the conjugate base of a strong acid, and so it is of negligible base strength (no appreciable base ionization). The solution is neutral.

(b) The Na^+ cation is inert and will not affect the pH of the solution; while the HCO_3^- anion is amphiprotic. The K_a of HCO_3^- is 4.7×10^{-11}, and its K_b is:

$$\frac{1.0 \times 10^{-14}}{4.3 \times 10^{-7}} = 2.3 \times 10^{-8}$$

Since $K_b \gg K_a$, the solution is basic.

(c) The Na^+ cation is inert and will not affect the pH of the solution, while the HPO_4^{2-} anion is amphiprotic. The K_a of HPO_4^{2-} is 4.2×10^{-13}, and its K_b is:

$$\frac{1.0 \times 10^{-14}}{6.2 \times 10^{-8}} = 1.6 \times 10^{-7}$$

Because $K_b \gg K_a$, the solution is basic.

(d) The NH_4^+ ion is acidic (see above discussion) and the F^- ion is basic (conjugate base of the weak acid HF). Comparing the two ionization constants: K_a of NH_4^+ is 5.6 × 10−10 and the K_b of F^- is 1.6×10^{-11}, so the solution is acidic, since $K_a > K_b$.

Exercise 2.11.3

Determine whether aqueous solutions of the following salts are acidic, basic, or neutral:

a. K_2CO_3
b. $CaCl_2$
c. KH_2PO_4
d. $(NH_4)_2CO_3$

Answer

(a) basic; (b) neutral; (c) acidic; (d) basic

This page titled 2.11: Hydrolysis of Salts is shared under a CC BY-NC-SA 4.0 license and was authored, remixed, and/or curated by Jonathan Gutow.

- **14.4: Hydrolysis of Salt Solutions** by OpenStax is licensed CC BY 4.0. Original source: https://openstax.org/details/books/chemistry-2e.

2.12: Polyprotic Acids

2.12.1: Diprotic Acids

Diprotic acids contain two ionizable hydrogen atoms per molecule; ionization of such acids occurs in two steps. The first ionization always takes place to a greater extent than the second ionization. For example, sulfuric acid, a strong acid, ionizes as follows:

$$\mathrm{H_2SO_4(aq) + H_2O(l) \rightleftharpoons H_3O^+(aq) + HSO_4^-(aq)} \qquad \text{(First ionization)}$$

with $K_{a1} > 10^2$.

$$\mathrm{HSO_4^-(aq) + H_2O(l) \rightleftharpoons H_3O^+(aq) + SO_4^{2-}(aq)} \qquad \text{(Second ionization)}$$

with $K_{a2} = 1.2 \times 10^{-2}$.

This stepwise ionization process occurs for all polyprotic acids. Carbonic acid, $\mathrm{H_2CO_3}$, is an example of a weak diprotic acid. The first ionization of carbonic acid yields hydronium ions and bicarbonate ions in small amounts.

$$\mathrm{H_2CO_3(aq) + H_2O(l) \rightleftharpoons H_3O^+(aq) + HCO_3^-(aq)} \qquad \text{(First ionization)}$$

with

$$K_{H_2CO_3} = \frac{\left[\mathrm{H_3O^+}\right]\left[\mathrm{HCO_3^-}\right]}{\left[\mathrm{H_2CO_3}\right]} = 4.3 \times 10^{-7}$$

The bicarbonate ion can also act as an acid. It ionizes and forms hydronium ions and carbonate ions in even smaller quantities.

$$\mathrm{HCO_3^-(aq) + H_2O(l) \rightleftharpoons H_3O^+(aq) + CO_3^{2-}(aq)} \qquad \text{(Second ionization)}$$

with

$$K_{\mathrm{HCO_3^-}} = \frac{\left[\mathrm{H_3O^+}\right]\left[\mathrm{CO_3^{2-}}\right]}{\left[\mathrm{HCO_3^-}\right]} = 4.7 \times 10^{-11}$$

$K_{\mathrm{H_2CO_3}}$ is larger than $K_{\mathrm{HCO_3^-}}$ by a factor of 10^4, so $\mathrm{H_2CO_3}$ is the dominant producer of hydronium ion in the solution. This means that little of the formed by the ionization of $\mathrm{H_2CO_3}$ ionizes to give hydronium ions (and carbonate ions), and the concentrations of $\mathrm{H_3O^+}$ and are practically equal in a pure aqueous solution of $\mathrm{H_2CO_3}$.

If the first ionization constant of a weak diprotic acid is larger than the second by a factor of at least 20, it is appropriate to treat the first ionization separately and calculate concentrations resulting from it before calculating concentrations of species resulting from subsequent ionization. This approach is demonstrated in the following example and exercise.

Example 2.12.1: Ionization of a Diprotic Acid

"Carbonated water" contains a palatable amount of dissolved carbon dioxide. The solution is acidic because $\mathrm{CO_2}$ reacts with water to form carbonic acid, $\mathrm{H_2CO_3}$. What are and in a saturated solution of $\mathrm{CO_2}$ with an initial $[\mathrm{H_2CO_3}]=0 \cdot 033$ M?

$$\mathrm{H_2CO_3(aq) + H_2O(l) \rightleftharpoons H_3O^+(aq) + HCO_3^-(aq)} \quad K_{a1} = 4.3 \times 10^{-7}$$

$$\mathrm{HCO_3^-(aq) + H_2O(l) \rightleftharpoons H_3O^+(aq) + CO_3^{2-}(aq)} \quad K_{a2} = 4.7 \times 10^{-11}$$

Solution

As indicated by the ionization constants, $\mathrm{H_2CO_3}$ is a much stronger acid than so the stepwise ionization reactions may be treated separately.

The first ionization reaction is

$$\mathrm{H_2CO_3(aq) + H_2O(l) \rightleftharpoons H_3O^+(aq) + HCO_3^-(aq)} \quad K_{a1} = 4.3 \times 10^{-7}$$

Using provided information, an ICE table for this first step is prepared:

	H_2CO_3	+	H_2O	$\rightleftharpoons$	H_3O^+	+	HCO_3^-
Initial concentration (*M*)	0.033				~0		0
Change (*M*)	$-x$				$+x$		$+x$
Equilibrium concentration (*M*)	$0.033 - x$				x		x

Substituting the equilibrium concentrations into the equilibrium equation gives

$$K_{H_2CO_3} = \frac{[H3O^+]\left[HCO_3^-\right]}{[H_2CO_3]} = \frac{(x)(x)}{0.033 - x} = 4.3 \times 10^{-7}$$

Assuming $x \ll 0.033$ and solving the simplified equation yields

$$x = 1.2 \times 10^{-4}$$

The ICE table defined *x* as equal to the bicarbonate ion molarity and the hydronium ion molarity:

$$[H_2CO_3] = 0.033M$$

$$\left[H3O^+\right] = \left[HCO_3^-\right] = 1.2 \times 10^{-4}M$$

Using the bicarbonate ion concentration computed above, the second ionization is subjected to a similar equilibrium calculation:

$$\mathrm{HCO_3^-(aq) + H_2O(l) \rightleftharpoons H_3O^+(aq) + CO_3^{2-}(aq)}$$

$$K_{HCO_{3^-}} = \frac{[H3O^+]\left[CO_3^{2-}\right]}{\left[HCO_3^-\right]} = \frac{\left(1.2 \times 10^{-4}\right)\left[CO_3^{2-}\right]}{1.2 \times 10^{-4}}$$

$$\left[CO_3^{2-}\right] = \frac{\left(4.7 \times 10^{-11}\right)\left(1.2 \times 10^{-4}\right)}{1.2 \times 10^{-4}} = 4.7 \times 10^{-11}M$$

To summarize: at equilibrium $[\mathrm{H_2CO_3}] = 0.033M$; $[\mathrm{H_3O^+}] = 1.2 \times 10^{-4}$; $[\mathrm{HCO_3^-}] = 1.2 \times 10^{-4}\ M$; $[\mathrm{CO_{32}^-}] = 4.7 \times 10^{-11}\ M$.

? Exercise 2.12.1

The concentration of $\mathrm{H_2S}$ in a saturated aqueous solution at room temperature is approximately 0.1 M. Calculate, $\mathrm{H_3O^+}$, $[\mathrm{HS^-}]$, and $[\mathrm{S^{2-}}]$ in the solution:

$$\mathrm{H_2S(aq) + H_2O(l) \rightleftharpoons H_3O^+(aq) + HS^-(aq)} \quad K_{a1} = 8.9 \times 10^{-8}$$

$$\mathrm{HS^-(aq) + H_2O(l) \rightleftharpoons H_3O^+(aq) + S^{2-}(aq)} \quad K_{a2} = 1.0 \times 10^{-19}$$

Answer

$[\mathrm{H_2S}] = 0.1\ M$

$[\mathrm{H_3O^+}] = [\mathrm{HS^-}] = 0.000094\ M$

$[\mathrm{S^{2-}}] = 1 \times 10^{-19}\ M$

2.12.2: Triprotic Acids

A **triprotic acid** is an acid that has three ionizable H atoms. Phosphoric acid is one example:

$$\mathrm{H_3PO_4(aq) + H_2O(l) \rightleftharpoons H_3O^+(aq) + H_2PO_4^-(aq)} \quad K_{a1} = 7.5 \times 10^{-3} \qquad \text{(First ionization)}$$

$$\mathrm{H_2PO_4^-(aq) + H_2O(l) \rightleftharpoons H_3O^+(aq) + HPO_4^{2-}(aq)} \quad K_{a2} = 6.2 \times 10^{-8} \qquad \text{(Second ionization)}$$

$$\mathrm{HPO_4^{2-}(aq) + H_2O(l) \rightleftharpoons H_3O^+(aq) + PO_4^{3-}(aq)} \quad K_{a3} = 4.2 \times 10^{-13} \qquad \text{(Third ionization)}$$

As for the diprotic acid examples, each successive ionization reaction is less extensive than the former, reflected in decreasing values for the stepwise acid ionization constants. This is a general characteristic of polyprotic acids and successive ionization constants often differ by a factor of about 10^5 to 10^6.

This set of three dissociation reactions may appear to make calculations of equilibrium concentrations in a solution of $\mathrm{H_3PO_4}$ complicated. However, because the successive ionization constants differ by a factor of 10^5 to 10^6, large differences exist in the small changes in concentration accompanying the ionization reactions. This allows the use of math-simplifying assumptions and processes, as demonstrated in the examples above.

Polyprotic bases are capable of accepting more than one hydrogen ion. The carbonate ion is an example of a **diprotic base**, because it can accept two protons, as shown below. Similar to the case for polyprotic acids, note the ionization constants decrease with ionization step. Likewise, equilibrium calculations involving polyprotic bases follow the same approaches as those for polyprotic acids.

$$\mathrm{H_2O(l) + CO_3^{2-}(aq) \rightleftharpoons HCO_3^-(aq) + OH^-(aq)} \quad K_{b1} = 2.1 \times 10^{-4}$$

$$\mathrm{H_2O(l) + HCO_3^-(aq) \rightleftharpoons H_2CO_3(aq) + OH^-(aq)} \quad K_{b2} = 2.3 \times 10^{-8}$$

2.12.3: Dependence of Degree of Protonation on pH for Polyprotic acids

Many natural bodies of water and living organisms contain high concentrations of salts that maintain (buffer) the proton concentration (pH) at particular values. This means that the protonation state of low concentration polyprotic acids is determined by the pH and not concentration of the particular acid. An important example of this is the amino acids that our bodies use to build proteins. They are all either diprotic or triprotic acids. We will consider arginine (Arg) which is triprotic. The four forms are Abbreviated $\mathrm{H_3Arg^{2+}}$, $\mathrm{H_2Arg^+}$, HArg and $\mathrm{Arg^-}$. The equilibria are:

$$\mathrm{H_3Arg^{2+}(aq) \rightleftharpoons H_2Arg^+(aq) + H^+(aq)} \quad pK_{a1} = 2.03 \tag{2.12.1}$$

$$\mathrm{H_2Arg^+(aq) \rightleftharpoons HArg(aq) + H^+(aq)} \quad pK_{a2} = 9.00 \tag{2.12.2}$$

$$\mathrm{HArg(aq) \rightleftharpoons Arg^-(aq) + H^+(aq)} \quad pK_{a3} = 12.10 \tag{2.12.3}$$

We can solve the equilibrium constant expressions for each equilibrium for the concentration of the deprotonated species as follows:

$$K_{a1} = \frac{[H^+][H_2Arg^+]}{[H_3Arg^{2+}]} \implies [H_2Arg^+] = K_{a1}\frac{[H_3Arg^{2+}]}{[H^+]} \tag{2.12.4}$$

$$K_{a2} = \frac{[H^+][HArg]}{[H_2Arg^+]} \implies [HArg] = K_{a2}\frac{[H_2Arg^+]}{[H^+]} = K_{a1}K_{a2}\frac{[H_3Arg^{2+}]}{[H^+]^2} \tag{2.12.5}$$

$$K_{a3} = \frac{[H^+][Arg^-]}{[HArg]} \implies [Arg^-] = K_{a3}\frac{[HArg]}{[H^+]} = K_{a1}K_{a2}K_{a3}\frac{[H_3Arg^{2+}]}{[H^+]^3} \tag{2.12.6}$$

Where the last expression in each of 2.12.4, 2.12.5 and 2.12.6 results from substituting the final expression from the previous equation in for the numerator. To calculate the fraction in each protonation state we need the total of all the arginine species:

$$Arg_{tot} = [H_3Arg^{2+}]\left(1 + \frac{K_{a1}}{[H^+]} + \frac{K_{a1}K_{a2}}{[H^+]^2} + \frac{K_{a1}K_{a2}K_{a3}}{[H^+]^3}\right) \tag{2.12.7}$$

All the terms in in the parentheses in equation 2.12.7 are constant for a given pH, so we can calculate a value at each pH and to make it easier we can symbolize this value as A, allowing us to rewrite equation 2.12.7 as:

$$Arg_{tot} = [H_3Arg^{2+}]A \tag{2.12.8}$$

This allows us to write the fraction of each species as:

$$f(H_3Arg^{2+}) = \frac{[H_3Arg^{2+}]}{[H_3Arg^{2+}]A} = \frac{1}{A} \tag{2.12.9}$$

$$f(H_2Arg^{+}) = \frac{K_{a1}[H_3Arg^{2+}]}{[H^+][H_3Arg^{2+}]A} = \frac{K_{a1}}{[H^+]A} \tag{2.12.10}$$

$$f(HArg) = \frac{K_{a1}K_{a2}[H_3Arg^{2+}]}{[H^+]^2[H_3Arg^{2+}]A} = \frac{K_{a1}K_{a2}}{[H^+]^2A} \tag{2.12.11}$$

$$f(Arg)^{-} = \frac{K_{a1}K_{a2}K_{a3}[H_3Arg^{2+}]}{[H^+]^3[H_3Arg^{2+}]A} = \frac{K_{a1}K_{a2}K_{a3}}{[H^+]^3A} \tag{2.12.12}$$

These equations allow you to determine at what [H^+] or pH each conjugate pair are in equal concentration. For example setting equation 2.12.9 equal to equation 2.12.10 and solving for [H^+] yields:

$$\frac{1}{\cancel{A}} = \frac{K_{a1}}{[H^+]\ \cancel{A}} \implies [H^+] = K_{a1} \implies pH = pK_{a1} \tag{2.12.13}$$

Similar algebra shows that each conjugate pair make up equal fractions of the mixture each time the pH = pK_a. Calculation of the actual fraction show that they will each be close to 50% of the species in solution. See the plot of the calculated values (figure 2.12.1).

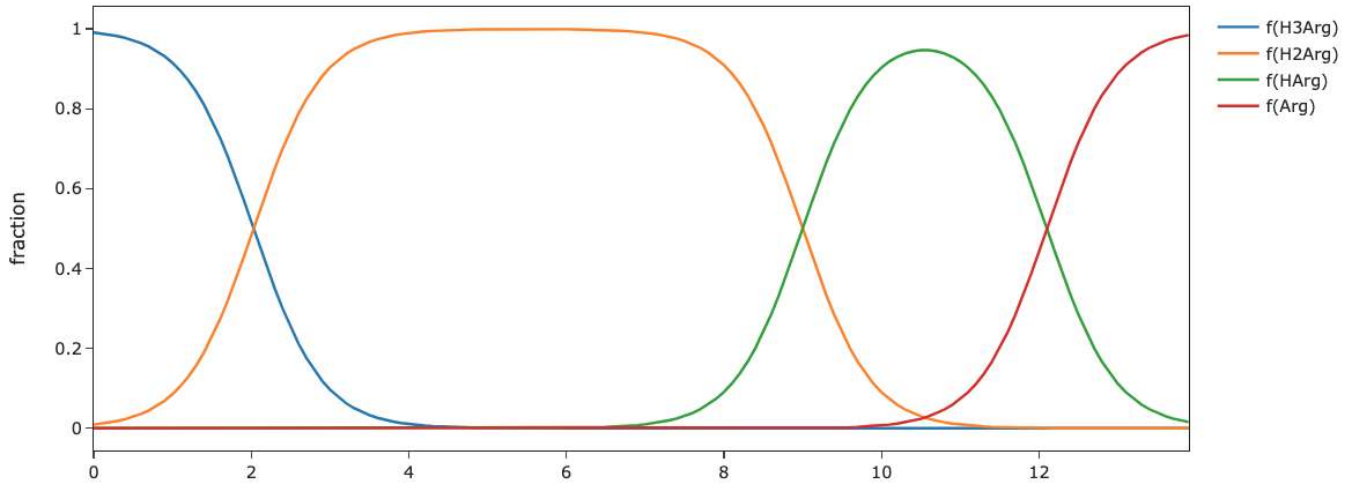


Figure 2.12.1: Fraction of each of the protonation states of arginine versus pH.

This page titled 2.12: Polyprotic Acids is shared under a CC BY-NC-SA 4.0 license and was authored, remixed, and/or curated by Jonathan Gutow.

- **14.5: Polyprotic Acids** by OpenStax is licensed CC BY 4.0. Original source: https://openstax.org/details/books/chemistry-2e.

2.13: Buffers

Based on OpenStax Buffers

2.13.1: Introduction

A solution containing appreciable amounts of a weak conjugate acid-base pair is called a buffer solution, or a **buffer**. Buffer solutions resist a change in pH when small amounts of a strong acid or a strong base are added (Figure 2.13.1). A solution of acetic acid and sodium acetate (CH_3COOH + CH_3COONa) is an example of a buffer that consists of a weak acid and its salt. An example of a buffer that consists of a weak base and its salt is a solution of ammonia and ammonium chloride ($NH_3(aq)$ + $NH_4Cl(aq)$).

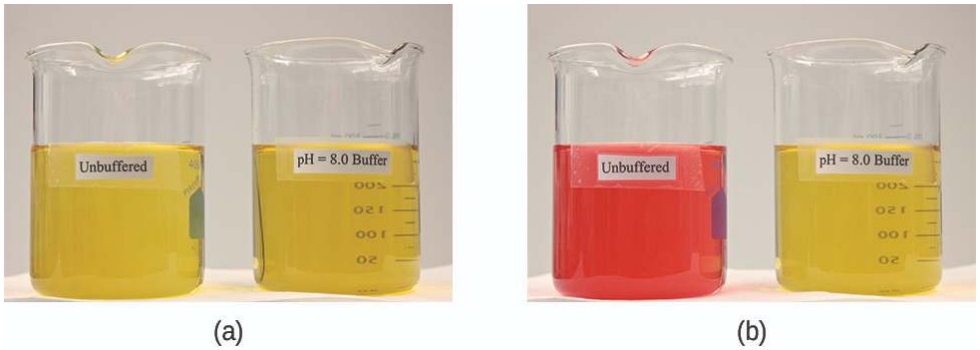


Figure 2.13.1: (a) The unbuffered solution on the left and the buffered solution on the right have the same pH (pH 8); they are basic, showing the yellow color of the indicator methyl orange at this pH. (b) After the addition of 1 mL of a 0.01-*M* HCl solution, the buffered solution has not detectably changed its pH but the unbuffered solution has become acidic, as indicated by the change in color of the methyl orange, which turns red at a pH of about 4. (credit: modification of work by Mark Ott)

Note

Although the term **buffer** usually refers to an acid-base buffer, it is possible to buffer the concentration of other species using appropriate equilibria.

2.13.2: How Buffers Work

To illustrate the function of a buffer solution, consider a mixture of roughly equal amounts of acetic acid and sodium acetate. The presence of a weak conjugate acid-base pair in the solution imparts the ability to neutralize modest amounts of added strong acid or base. For example, strong base added to this solution will neutralize hydronium ion, causing the acetic acid ionization equilibrium to shift to the right and generate additional amounts of the weak conjugate base (acetate ion):

$$\mathrm{CH_3CO_2H(aq) + H_2O(l) \rightleftharpoons H_3O^+(aq) + CH_3CO_2^-(aq)}$$

Likewise, strong acid added to this buffer solution will shift the above ionization equilibrium left, producing additional amounts of the weak conjugate acid (acetic acid). Figure 2.13.2 provides a graphical illustration of the changes in conjugate-partner concentration that occur in this buffer solution when strong acid and base are added. The buffering action of the solution is essentially a result of the added strong acid and base being converted to the weak acid and base that make up the buffer's conjugate pair. The weaker acid and base undergo only slight ionization, as compared with the complete ionization of the strong acid and base, and the solution pH, therefore, changes much less drastically than it would in an unbuffered solution.

Example 14.20: pH Changes in Buffered and Unbuffered Solutions

Acetate buffers are used in biochemical studies of enzymes and other chemical components of cells to prevent pH changes that might affect the biochemical activity of these compounds.

a. Calculate the pH of an acetate buffer that is a mixture with 0.10 *M* acetic acid and 0.10 *M* sodium acetate.
b. Calculate the pH after 1.0 mL of 0.10 NaOH is added to 100 mL of this buffer.
c. For comparison, calculate the pH after 1.0 mL of 0.10 *M* NaOH is added to 100 mL of a solution of an unbuffered solution with a pH of 4.74.

Solution

(a) Following the ICE approach to this equilibrium calculation yields the following:

	CH_3CO_2H + H_2O $\rightleftharpoons$	H_3O^+	+ $CH_3CO_2^-$
Initial concentration (*M*)	0.10	~0	0.10
Change (*M*)	−*x*	+*x*	+*x*
Equilibrium concentration (*M*)	0.10 − *x*	*x*	0.10 + *x*

Substituting the equilibrium concentration terms into the K_a expression, assuming $x \ll 0.10$, and solving the simplified equation for x yields

$$x = 1.8 \times 10^{-5}\ \text{M}$$

$$\left[\text{H}_3\text{O}^+\right] = 0 + x = 1.8 \times 10^{-5}\ \text{M}$$

$$pH = -\log\left[\text{H}_3\text{O}^+\right]$$

$$= -\log\left(1.8 \times 10^{-5}\right)$$

$$= 4.74$$

(b) Calculate the pH after 1.0 mL of 0.10 *M* NaOH is added to 100 mL of this buffer.

Adding strong base will neutralize some of the acetic acid, yielding the conjugate base acetate ion. Compute the new concentrations of these two buffer components, then repeat the equilibrium calculation of part (a) using these new concentrations.

$$0.0010\ \cancel{\text{L}} \times \left(\frac{0.10\ \text{mol NaOH}}{1\ \text{L}}\right) = 1.0 \times 10^{-4}\ \text{mol NaOH}$$

The initial molar amount of acetic acid is

$$0.100\ \cancel{\text{L}} \times \left(\frac{0.100\ \text{mol}\ \text{CH}_3\text{CO}_2\text{H}}{1\ \cancel{\text{L}}}\right) = 1.00 \times 10^{-2}\ \text{mol}\ \text{CH}_3\text{CO}_2\text{H}$$

The amount of acetic acid remaining after some is neutralized by the added base is

$$\left(1.0 \times 10^{-2}\right) - \left(0.01 \times 10^{-2}\right) = 0.99 \times 10^{-2}\ \text{mol}\ \text{CH}_3\text{CO}_2\text{H}$$

The newly formed acetate ion, along with the initially present acetate, gives a final acetate concentration of

$$\left(1.0 \times 10^{-2}\right) + \left(0.01 \times 10^{-2}\right) = 1.01 \times 10^{-2}\ \text{mol}\ \text{NaCH}_3\text{CO}_2$$

Compute molar concentrations for the two buffer components:

$$\left[\text{CH}_3\text{CO}_2\text{H}\right] = \frac{9.9 \times 10^{-3}\ \text{mol}}{0.101\ \text{L}} = 0.098\ \text{M}$$

$$\left[\text{NaCH}_3\text{CO}_2\right] = \frac{1.01 \times 10^{-2}\ \text{mol}}{0.101\ \text{L}} = 0.100\ \text{M}$$

Using these concentrations, the pH of the solution may be computed as in part (a) above, yielding pH = 4.75 (only slightly different from that prior to adding the strong base).

(c) For comparison, calculate the pH after 1.0 mL of 0.10 *M* NaOH is added to 100 mL of a solution of an unbuffered solution with a pH of 4.74.

The amount of hydronium ion initially present in the solution is

$$\left[\mathrm{H_3O^+}\right] = 10^{-4.74} = 1.8 \times 10^{-5}\ \mathrm{M}$$

$$\mathrm{mol\ H_3O^+} = (0.100\ \mathrm{L})\left(1.8 \times 10^{-5}\ \mathrm{M}\right) = 1.8 \times 10^{-6}\ \mathrm{mol\ H_3O^+}$$

The amount of hydroxide ion added to the solution is

$$molOH^- = (0.0010L)(0.10M) = 1.0 \times 10^{-4} mol\mathrm{OH^-}$$

The added hydroxide will neutralize hydronium ion via the reaction

$$\mathrm{H_3O^+(aq) + OH^-(aq) \leftharpoons 2\,H_2O(l)}$$

The 1:1 stoichiometry of this reaction shows that an excess of hydroxide has been added (greater molar amount than the initially present hydronium ion).

The amount of hydroxide ion remaining is

$$1.0 \times 10^{-4} mol - 1.8 \times 10^{-6} mol = 9.8 \times 10^{-5} molOH^-$$

corresponding to a hydroxide molarity of

$$\frac{9.8 \times 10^{-5}\ \mathrm{mol\ OH^-}}{0.101\ \mathrm{L}} = 9.7 \times 10^{-4} M$$

The pH of the solution is then calculated to be

$$pH = 14.00 - pOH = 14.00 - -\log\left(9.7 \times 10^{-4}\right) = 10.99$$

In this unbuffered solution, addition of the base results in a significant rise in pH (from 4.74 to 10.99) compared with the very slight increase observed for the buffer solution in part (b) (from 4.74 to 4.75).

? Exercise 2.13.1

Show that adding 1.0 mL of 0.10 M HCl changes the pH of 100 mL of a 1.8×10^{-5} M HCl solution from 4.74 to 3.00.

Answer

Initial pH of 1.8×10^{-5} M HCl;

$$\mathrm{pH} = -\log[\mathrm{H_3O^+}] = -\log[1.8 \times 10^{-5}] = 4.74$$

Moles of H_3O^+ in 100 mL 1.8×10^{-5} M HCl;

$$(1.8 \times 10^{-5}\ \mathrm{moles/L}) \times (0.100\ \mathrm{L} = 1.8 \times 10^{-6}\ \mathrm{mol}$$

Moles of H_3O^+ added by addition of 1.0 mL of 0.10 *M* HCl:

$$(0.10\ \mathrm{moles/L}) \times (0.0010\ \mathrm{L}) = 1.0 \times 10^{-4}\ \mathrm{mol}$$

Final pH after addition of 1.0 mL of 0.10 *M* HCl:

$$pH = -\log\left[\mathrm{H_3O^+}\right] = -\log\left(\frac{\text{total moles } \mathrm{H_3O^+}}{\text{total volume}}\right) = -\log\left(\frac{1.0 \times 10^{-4} mol + 1.8 \times 10^{-6}\ \mathrm{mol}}{101\ \mathrm{mL}\left(\frac{1\ \mathrm{L}}{1000\ \mathrm{mL}}\right)}\right) = 3.00$$

2.13.3: Buffer Capacity

Buffer solutions do not have an unlimited capacity to keep the pH relatively constant. Instead, the ability of a buffer solution to resist changes in pH relies on the presence of appreciable amounts of its conjugate weak acid-base pair. When enough strong acid or base is added to substantially lower the concentration of either member of the buffer pair, the buffering action within the solution is compromised.

The buffer capacity is the amount of acid or base that can be added to a given volume of a buffer solution before the pH changes significantly, usually by one unit. Buffer capacity depends on the amounts of the weak acid and its conjugate base that are in a buffer mixture. For example, 1 L of a solution that is 1.0 *M* in acetic acid and 1.0 *M* in sodium acetate has a greater buffer capacity than 1 L of a solution that is 0.10 *M* in acetic acid and 0.10 *M* in sodium acetate even though both solutions have the same pH. The first solution has more buffer capacity because it contains more acetic acid and acetate ion.

2.13.4: The Henderson-Hasselbalch Equation

The ionization-constant expression for a solution of a weak acid can be written as:

$$K_a = \frac{\left[\mathrm{H_3O^+}\right]\left[\mathrm{A^-}\right]}{[\mathrm{HA}]}$$

Rearranging to solve for $[H_3O^+]$ yields:

$$\left[\mathrm{H_3O^+}\right] = K_a \times \frac{[\mathrm{HA}]}{\left[\mathrm{A^-}\right]}$$

Taking the negative logarithm of both sides of this equation gives

$$-\log\left[\mathrm{H_3O^+}\right] = -\log K_a - \log\frac{[\mathrm{HA}]}{\left[\mathrm{A^-}\right]}$$

which can be written as

$$pH = pK_a + \log\frac{\left[\mathrm{A^-}\right]}{[\mathrm{HA}]} \tag{2.13.1}$$

where pK_a is the negative of the logarithm of the ionization constant of the weak acid (pK_a = −log K_a). This equation relates the pH, the ionization constant of a weak acid, and the concentrations of the weak conjugate acid-base pair in a buffered solution. This equation is often used in an approximate form 2.13.2, where the [A-] and [HA] are not solved for using an equilibrium calculation, but are assumed to be equal to the initial concentration of the salt containing the A- ion ($[salt]_i$) and the initial concentration of HA ($[HA]_i$) based on what was mixed into the solution. Many write equation 2.13.1 but utilize it as the approximate form, which is equivalent to the "small x" approximation in an equilibrium calculation.

$$pH = pK_a + \log\frac{[salt]_i}{[\mathrm{HA}]_i} \tag{2.13.2}$$

This last form is usually referred to as Henderson-Hasselbalch equation and used to estimate the pH of buffers.

2.13.4.1: What is ignored by the approximation

Based on "Buffer Solutions" by David Harvey.

We can derive a general buffer equation by considering the following reactions for a weak acid, HA, and the soluble salt of its conjugate weak base, NaA.

$$\mathrm{NaA}(s) \rightarrow \mathrm{Na^+}(aq) + \mathrm{A^-}(aq)$$
$$\mathrm{HA}(aq) + \mathrm{H_2O}(l) \rightleftharpoons \mathrm{H_3O^+}(aq) + \mathrm{A^-}(aq)$$
$$2\mathrm{H_2O}(l) \rightleftharpoons \mathrm{H_3O^+}(aq) + \mathrm{OH^-}(aq)$$

Because the concentrations of Na^+, A^-, HA, H_3O^+, and OH^- are unknown, we need five equations to define the solution's composition. Two of these equations are the equilibrium constant expressions for HA and H_2O.

$$K_a = \frac{\left[\mathrm{H_3O^+}\right]\left[\mathrm{A^-}\right]}{[\mathrm{HA}]} \tag{2.13.3}$$

$$K_w = \left[\mathrm{H_3O^+}\right]\left[\mathrm{OH^-}\right]$$

The remaining three equations are mass balance equations for HA and Na^+

$$C_{\mathrm{HA}} + C_{\mathrm{NaA}} = [\mathrm{HA}] + [\mathrm{A}^-] \tag{2.13.4}$$

$$C_{\mathrm{NaA}} = [\mathrm{Na}^+] \tag{2.13.5}$$

and a charge balance equation

$$[\mathrm{H_3O}^+] + [\mathrm{Na}^+] = [\mathrm{OH}^-] + [\mathrm{A}^-] \tag{2.13.6}$$

Substituting Equation 2.13.5 into Equation 2.13.6 and solving for [A⁻] gives

$$[\mathrm{A}^-] = C_{\mathrm{NaA}} - [\mathrm{OH}^-] + [\mathrm{H_3O}^+] \tag{2.13.7}$$

Next, we substitute Equation 2.13.7 into Equation 2.13.4, which gives the concentration of HA as

$$[\mathrm{HA}] = C_{\mathrm{HA}} + [\mathrm{OH}^-] - [\mathrm{H_3O}^+] \tag{2.13.8}$$

Finally, we substitute Equation 2.13.7 and Equation 2.13.8 into Equation 2.13.3 and solve for pH to arrive at a general equation for a buffer's pH.

$$\mathrm{pH} = \mathrm{p}K_{\mathrm{a}} + \log \frac{C_{\mathrm{NaA}} - [\mathrm{OH}^-] + [\mathrm{H_3O}^+]}{C_{\mathrm{HA}} + [\mathrm{OH}^-] - [\mathrm{H_3O}^+]}$$

If the initial concentrations of the weak acid, C_{HA}, and the weak base, C_{NaA}, are significantly greater than [H_3O^+] and [OH^-], then this becomes the usual approximate form of the Henderson-Hasselbach (equation 2.13.2), where $C_{NaA} = [salt]_i$ and $C_{HA} = [HA]_i$.

2.13.4.2: Henderson-Hasselbalch and buffer capacity

The buffer capacity is generally understood to be the amount of acid or base that can be added while changing the pH by a maximum of 1 pH unit. This means we want to see what happens to the [A-] to [HA] ratio when the pH changes by that much. An ideal buffer has the pH = pK_a, which implies we are interested in the case:

$$pH \pm 1 = pK_a \pm 1 = pK_a + log\frac{[A^-]}{[HA]}$$

Which simplifies to

$$\pm 1 = log\frac{[A-]}{[HA]} \implies 10^{\pm 1} = \frac{[A^-]}{[HA]}$$

So the buffer runs out when the ratio in the logarithm becomes 1/10 or 10/1.

Portrait of a Chemist: Lawrence Joseph Henderson and Karl Albert Hasselbalch

Lawrence Joseph Henderson (1878–1942) was an American physician, biochemist and physiologist, to name only a few of his many pursuits. He obtained a medical degree from Harvard and then spent 2 years studying in Strasbourg, then a part of Germany, before returning to take a lecturer position at Harvard. He eventually became a professor at Harvard and worked there his entire life. He discovered that the acid-base balance in human blood is regulated by a buffer system formed by the dissolved carbon dioxide in blood. He wrote an equation in 1908 to describe the carbonic acid-carbonate buffer system in blood. Henderson was broadly knowledgeable; in addition to his important research on the physiology of blood, he also wrote on the adaptations of organisms and their fit with their environments, on sociology and on university education. He also founded the Fatigue Laboratory, at the Harvard Business School, which examined human physiology with specific focus on work in industry, exercise, and nutrition.

In 1916, Karl Albert Hasselbalch (1874–1962), a Danish physician and chemist, shared authorship in a paper with Christian Bohr in 1904 that described the Bohr effect, which showed that the ability of hemoglobin in the blood to bind with oxygen was inversely related to the acidity of the blood and the concentration of carbon dioxide. The pH scale was introduced in 1909 by another Dane, Sørensen, and in 1912, Hasselbalch published measurements of the pH of blood. In 1916, Hasselbalch expressed Henderson's equation in logarithmic terms, consistent with the logarithmic scale of pH, and thus the Henderson-Hasselbalch equation was born.

This page titled 2.13: Buffers is shared under a CC BY-NC-SA 4.0 license and was authored, remixed, and/or curated by Jonathan Gutow.

- **14.6: Buffers** by OpenStax is licensed CC BY 4.0. Original source: https://openstax.org/details/books/chemistry-2e.
- **6.8: Buffer Solutions** by David Harvey is licensed CC BY-NC-SA 4.0.

CHAPTER OVERVIEW

3: Ions and Electrochemistry

3.1: Mean Ionic Activity Coefficients and the Debye-Hückel Model
3.2: Extending Debye-Hückel Theory to Higher Concentrations
3.3: Ion Transport
3.4: Review of Redox Chemistry
3.5: Half Cells and Standard Reduction Potentials
3.6: Cell potentials under non-standard conditions (Nernst equation)
3.7: Thermodynamics from Electrochemistry
3.8: Redox Examples

This page titled 3: Ions and Electrochemistry is shared under a CC BY-NC-SA 4.0 license and was authored, remixed, and/or curated by Jonathan Gutow.

3.1: Mean Ionic Activity Coefficients and the Debye-Hückel Model

3.1.1: Introduction

Solutions of ions behave very non-ideally because of the charge-charge interactions between the ions and interactions with the solvent. Thus to model the behavior of ions in solution requires using the ion activities rather than concentrations as can be done reasonably well for molecular solutes. In terms of activities the chemical potential of NaCl(aq) would be:

$$\mu_{NaCl} = \mu^o_{Na^+} + RTlna_{Na^+} + \mu^o_{Cl^-} + RTlna_{Cl^-} = \mu^o_{Na^+} + \mu^o_{Cl^-} + RTln\left(a_{Na^+}a_{Cl^-}\right) \tag{3.1.1}$$

If we write this in terms of activity coefficients we have:

$$\mu_{NaCl} = \mu^o_{Na^+} + \mu^o_{Cl^-} + RTln\left(\gamma_{Na^+}[Na^+]\gamma_{Cl^-}[Cl^-]\right) \tag{3.1.2}$$

where the convention is that [] is the concentration divided by the standard reference concentration. The problem is that you cannot get the positive ions without also getting the negative ions that balance the charge. This means the separate activities or activity coefficients cannot be measured. The solution is to measure and use a combined **mean activity coefficient**.

3.1.2: Combined (mean) activity coefficients

Based on these Wikipedia Articles: Activity Coefficients; Debye-Hückel Theory

For the case of NaCl(aq) the mean activity coefficient is defined as:

$$\gamma_{\pm}(NaCl) = \sqrt{\gamma_{Na^+}\gamma_{Cl^-}} \tag{3.1.3}$$

Substituting this into the equation for the total chemical potential of NaCl(aq):

$$\mu_{NaCl} = \mu^o_{Na^+} + \mu^o_{Cl^-} + RTln\left(\gamma^2_{\pm}[Na^+][Cl^-]\right) \tag{3.1.4}$$

More generally, the mean activity coefficient of an ionic compound of formula A_pB_q is given by

$$\gamma_{\pm} = \sqrt[p+q]{\gamma^p_{\mathrm{A}}\gamma^q_{\mathrm{B}}} \tag{3.1.5}$$

The behavior of this mean activity coefficient versus concentration can be understood theoretically. The Debye-Hückel theory and some extensions of it have proved to be useful for practical application.

3.1.3: Debye-Hückel Model

This theory explains the value of $\gamma_{\pm}$ in terms of the shielding of like charges from each other by the surrounding opposite charges and the impact of the dielectric constant of the solvent's impact on the electric field strength felt by each ion. This requires integration over the distrubution of ions. Figure 3.1.1 is a 2-d image of ions in solution. Note that any charge you choose is mostly surrounded by opposite charges.

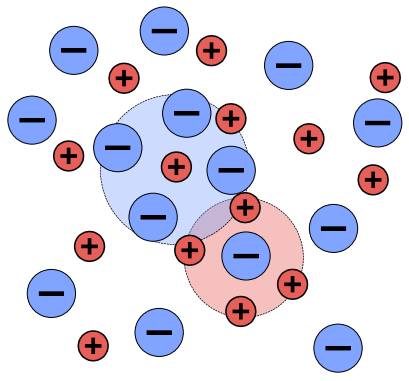


Figure 3.1.1: An idealized representation of a solution of a 1:1 electrolyte. (CC BY-SA 3.0 unported; Roland1952 via Wikipedia)

The combination of the higher probability that an ion is surrounded by oppositely charged ions and the dielectric constant of the solvent generally lowers the interaction strength between the ions. Thus like charges repel less and opposite charges are less

attracted to each other. This leads to slightly lower energies of the ions than if they were completely randomly distributed. Thus the chemical potential is less than would be found in an ideal solution. A careful mathematical analysis of this model by Debye and Hückel lead the the model named after them. At very low concentrations their model takes the form of the **Debye-Hückel limiting law**:

$$log_{10}\gamma_{\pm} = -A|z_{+}z_{-}|\sqrt{I} \tag{3.1.6}$$

where z_+ is the charge on the positive ions of the species, z_- the charge on the negative ions, A is a temperature dependent constant and I is the **ionic strength** (defined below). Beyond an ionic strength of about 10^{-3} a more complex version applies:

$$\log_{10}\gamma_{\pm} = -A|z_{+}z_{-}|\frac{\sqrt{I}}{1+B\sqrt{I}} \tag{3.1.7}$$

at room temperature in water for units of molarity or molality A ≈ 0.509 and B ≈ 3.2. Generally the values are arrived at empirically by fitting data in the units used for the experiment. At concentrations approaching 0.1 ionic strength and above extended versions of this and other models are used (see Extending Debye-Hückel).

Figure 3.1.2 shows how the first equation (limiting law) deviates from real data.

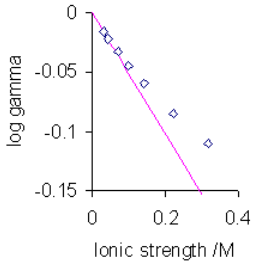


Figure 3.1.2: Experimental $\log\gamma_{\pm}$ values for KBr at 25°C (points) and Debye–Hückel limiting law (coloured line) (Public Domain; Petergans via Wikipedia)

The most significant aspect of equations 3.1.6 and 3.1.7 is the prediction that the mean activity coefficient is a function of *ionic strength* rather than the electrolyte concentration.

3.1.4: Ionic Strength

I*onic strength* (I) is defined as:

$$I = \frac{1}{2}\sum b_i z_i^2$$

where b_i is the molality of ion i and z_i is its charge coefficient. Note that highly charged ions (e.g. $z = 3+$) contribute strongly (nine times more than +1 ions), but the formula is *linear* in the molality.

Importance for Colloids

When a solid is formed by a reaction from solution it is sometimes possible that it remains dispersed as very small particles in the solvent. The sizes typically range in the nanometers This is why it has become fashionable to call them *nanoparticles*, although they had been known as *colloidal particles* since the mid nineteenth century. They are smaller than the wavelength of the visible reason. This causes liquids that contain them to remain *clear*, although they can at times be beautifully colored. A good example is the reduction of $AuCl_4^-$ with citrate to metallic gold. This produces clear wine red solutions, even at tiny gold concentrations.

$$2\,\mathrm{n\,AuCl_4(aq)^-} + \mathrm{n\,citrate^{3-}(aq)} + 2\,\mathrm{n\,H_2O(l)} \rightarrow$$
$$2\,\mathrm{n\,Au(colloid)} + 3\,\mathrm{n\,CH_2O(aq)} + 3\,\mathrm{n\,CO_2(g)} + 8\,\mathrm{n\,Cl^-(aq)} + 3\,\mathrm{n\,H^+(aq)}$$

The reason the gold does not precipitate completely is typically that the nanoparticle (AuNP) formed during the reaction are *charged* by the attachment of some of the ionic species in solution to its surface. This results in an charged particle with an atmosphere with a certain Debye length around it (Figure 3.1.3). This charged cloud prevents the particle form coalescing with other particles by electrostatic repulsion.

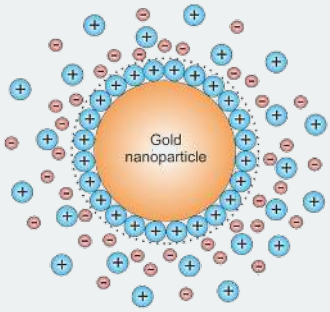


Figure 3.1.3: Potential difference as a function of distance from gold nanoparticle surface. (CC-SA-BY-3.0; Larryisgood)

Such a system is called a ***colloid.*** Of course these systems are ***metastable***. Often they have a pretty small threshold to crashing to a real precipitate under influence of the strong van der Waals interactions that the particles experience once they manage to get in close contact. Under the right conditions colloids can survive for a long time. Some gold colloids prepared by Faraday in the 1850's are still stable today.

It will be clear from the above that addition of a salt -particularly containing highly charged ions like 3+ or 3-- may destabilize the colloid because the ionic strength will changed drastically and this will affect the Debye length.

This page titled 3.1: Mean Ionic Activity Coefficients and the Debye-Hückel Model is shared under a CC BY-NC-SA 4.0 license and was authored, remixed, and/or curated by Jonathan Gutow.

- **25.6: The Debye-Hückel Theory** is licensed CC BY-NC-SA 4.0.

3.2: Extending Debye-Hückel Theory to Higher Concentrations

The equation for $\log \gamma_{\pm}$ predicted from Debye-Hückel theory is:

$$\log_{10} \gamma_{\pm} = -A|z_+ z_-| \frac{\sqrt{I}}{1 + B\sqrt{I}} \tag{3.2.1}$$

It gives satisfactory agreement with experimental measurements for low electrolyte concentrations, typically less than $10^{-2} mol/L$. Deviations from the theory occur at higher concentrations and with electrolytes that produce ions of higher charges, particularly asymmetrical electrolytes. These deviations occur because the model is oversimplified, so there is little to be gained by making small adjustments to the model. Instead, we must challenge the individual assumptions of the model:

- **Ions do not interact with each other**. Ion association may take place, particularly with ions of higher charge. This was followed up in detail by Niels Bjerrum. The Bjerrum length is the separation at which the electrostatic interaction between two ions is comparable in magnitude to kT.
- **Complete dissociation**. A weak electrolyte is one that is not fully dissociated. As such it has a dissociation constant. The dissociation constant can be used to calculate the extent of dissociation and hence, make the necessary correction needed to calculate activity coefficients.
- **Ions are spherical point charges that cannot be polarizable**. Ions, as all other atoms and molecules, have a finite size. Many ions, such as the nitrate ion NO_3^-, are not spherical. Polyatomic ions are polarizable.
- **The solvent composition does not matter**. The solvent is not a structureless medium but is made up of molecules. The water molecules in aqueous solution are both dipolar and polarizable. Both cations and anions have a strong primary solvation shell and a weaker secondary solvation shell. Ion–solvent interactions are ignored in Debye–Hückel theory.
- **Ionic radius is negligible**. At higher concentrations, the ionic radius becomes comparable to the radius of the ionic atmosphere.

Most extensions to the Debye–Hückel theory are empirical in nature. They usually allow the Debye–Hückel equation to be followed at low concentration and add further terms in some power of the ionic strength to fit experimental observations. Several approaches have been proposed to extend the validity of the Debye–Hückel theory.

3.2.1: Extended Debye-Hückel Equation

One such approach is the Extended Debye-Hückel Equation:

$$-log_{10}\gamma_{\pm} = \frac{A|z_+ z_-|\sqrt{I}}{1 + B\sqrt{I}} + CI$$

where γ is the activity coefficient, z is the integer charge of the ion I is the ionic strength of the aqueous solution, while A, B and C are adjustable parameters.

Other approaches include the Davies equation, Pitzer equations and specific ion interaction theory.

3.2.2: Davis Equation

The Davies equation is an empirical extension of Debye–Hückel theory which can be used to calculate activity coefficients of electrolyte solutions at relatively high concentrations at 25 °C. The equation, originally published in 1938, was refined by fitting to experimental data. The final form of the equation gives the mean molal activity coefficient $\gamma_{\pm}$ of an electrolyte that dissociates into ions having charges z1 and z2 as a function of ionic strength I:

$$-\log \gamma_{\pm} = 0.5|z_+ z_-| \left(\frac{\sqrt{I}}{1 + \sqrt{I}} - 0.30I \right).$$

The second term, 0.30 I, goes to zero as the ionic strength goes to zero, so the equation reduces to the Debye–Hückel equation at low concentration. However, as concentration increases, the second term becomes increasingly important, so the Davies equation can be used for solutions too concentrated to allow the use of the Debye–Hückel equation. For 1:1 electrolytes the difference between measured values and those calculated with this equation is about 2% of the value for 0.1 M solutions. The calculations become less precise for electrolytes that dissociate into ions with higher charges. Further discrepancies will arise if there is association between the ions, with the formation of ion pairs, such as $Mg^{2+}SO_4^{2-}$.

Plot of activity coefficients calculated using the Davies equation.

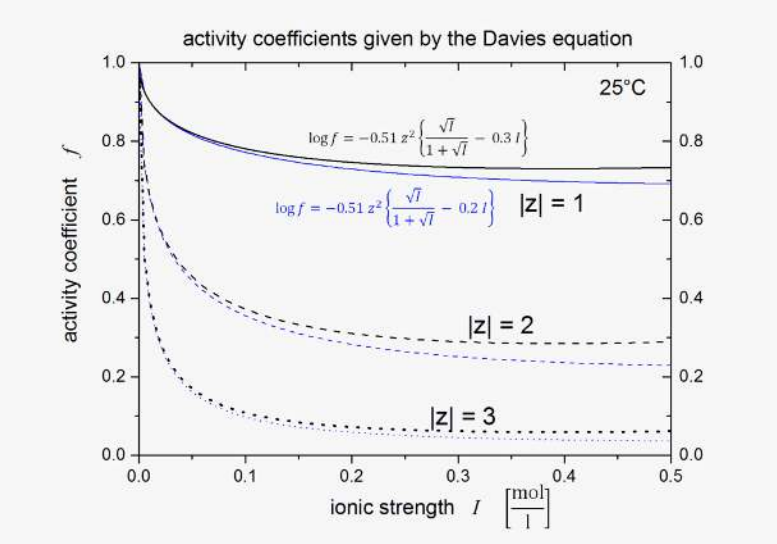


Figure 3.2.1: Semi-log plot of activity coefficients calculated using the Davies equation. (CC BY-SA 4.0; PChemiker via Wikipedia)

3.2.3: Pitzer Equations

Pitzer equations are important for the understanding of the behaviour of ions dissolved in natural waters such as rivers, lakes and sea-water. They were first described by physical chemist Kenneth Pitzer. The parameters of the Pitzer equations are linear combinations of parameters, of a virial expansion of the excess Gibbs free energy, which characterize interactions amongst ions and solvent. The derivation is thermodynamically rigorous at a given level of expansion. The parameters may be derived from various experimental data such as the osmotic coefficient, mixed ion activity coefficients, and salt solubility. They can be used to calculate mixed ion activity coefficients and water activities in solutions of high ionic strength for which the Debye–Hückel theory is no longer adequate.

An expression is obtained for the mean activity coefficient.

$$\ln \gamma_{\pm} = \frac{p \ln \gamma_M + q \ln \gamma_X}{p+q}$$

$$\ln \gamma_{\pm} = |z^+ z^-| f^{\gamma} + m \left(\frac{2pq}{p+q} \right) B^{\gamma}_{MX} + m^2 \left[2 \frac{(pq)^{3/2}}{p+q} \right] C^{\gamma}_{MX}$$

These equations were applied to an extensive range of experimental data at 25 °C with excellent agreement to about 6 mol kg−1 for various types of electrolyte. The treatment can be extended to mixed electrolytes and to include association equilibria. Values for the parameters β(0), β(1) and C for inorganic and organic acids, bases and salts have been tabulated. Temperature and pressure variation is also discussed.

3.2.4: Specific ion interaction theory

Specific ion Interaction Theory (SIT theory) is a theory used to estimate single-ion activity coefficients in electrolyte solutions at relatively high concentrations. It does so by taking into consideration interaction coefficients between the various ions present in solution. Interaction coefficients are determined from equilibrium constant values obtained with solutions at various ionic strengths. The determination of SIT interaction coefficients also yields the value of the equilibrium constant at infinite dilution.

The activity coefficient of the jth ion in solution is written as γ_j when concentrations are on the molal concentration scale and as yj when concentrations are on the molar concentration scale. (The molality scale is preferred in thermodynamics because molal concentrations are independent of temperature). The basic idea of SIT theory is that the activity coefficient can be expressed as

$$\log \gamma_j = -z_j^2 \frac{0.51\sqrt{I}}{1+1.5\sqrt{I}} + \sum_k \epsilon_{jk} m_k$$

where z is the electrical charge on the ion, I is the ionic strength, ε and b are interaction coefficients and m are concentrations. The summation extends over the other ions present in solution, which includes the ions produced by the background electrolyte. The first term in these expressions comes from Debye-Hückel theory. The second term shows how the contributions from "interaction" are dependent on concentration. Thus, the interaction coefficients are used as corrections to Debye-Hückel theory when concentrations are higher than the region of validity of that theory.

This page titled 3.2: Extending Debye-Hückel Theory to Higher Concentrations is shared under a CC BY-NC-SA 4.0 license and was authored, remixed, and/or curated by Jonathan Gutow via source content that was edited to the style and standards of the LibreTexts platform.

3.3: Ion Transport

3.3.1: Introduction

Ions moving around in batteries (galvanic cells) and across membranes in living cells are integral to energetic processes in both devices. There are significant dynamic (diffusion) contributions to these processes, but here we focus on the thermodynamics (energetics) of ions moving from one place to another, without accounting for things such as solvent viscosity or the size of the ions.

We will consider a simple model where there are two compartments separated by a membrane that is permeable to the ions in some way. For consistency with typical biochemical discussions of cell membranes we will refer to one side as the outside (extra-cellular) and the other as the inside (intra-cellular).

3.3.2: Concentration Gradient

Consider a single ion species that has a different concentration (activity, a) on the inside and outside. Using the convention of the inside as the "product", the chemical potential difference is then:

$$\Delta\mu = RTln\frac{a_{in}}{a_{out}} \tag{3.3.1}$$

3.3.3: Potential Gradient

In living cells there is also a potential gradient due to a charge imbalance associated with the separation of the positive and negative ions that maintain overall charge balance onto opposite sides of the membrane (electrically similar to a capacitor). Figure 3.3.1 illustrates the situation including some of the most important contributors to both concentration gradients and charge imbalance across a cell membrane.

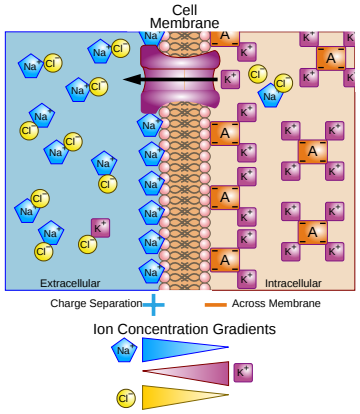


Figure 3.3.1: Although the system is electrically neutral overall, cells maintain a local charge imbalance across the cell membrane by separating counter ions on opposite sides of the membrane. In this figure the separated ions that cancel out each others' charges are the Na^+ (blue) and the large A^{4-} ions (orange). The large anions do not pass through the membrane (from https://commons.wikimedia.org).

The charge imbalance across the membrane leads to a potential difference across the membrane $\Delta\phi = \phi_{in} - \phi_{out}$. Moving a mole of species with a charge of z down this potential gradient (in the diagram moving a positive charge from the outside to the inside with a $\Delta\phi < 0$) results in a

$$\Delta\mu = zF\Delta\phi < 0 \tag{3.3.2}$$

.

3.3.4: Total chemical potential change on crossing the membrane

If we add the potential changes in equations 3.3.1 and 3.3.2 we arrive at the total chemical potential change on transporting a particular ion species from outside to inside the membrane:

$$\Delta\mu = RTln\frac{a_{in}}{a_{out}} + zF\Delta\phi \tag{3.3.3}$$

If this is negative, motion of the ion into the cell is a spontaneous process and will happen as long as there is a way for the ion to pass through the membrane. Since the central section of the membrane is made up of primarily non-polar hydrocarbon tails, ions usually only pass through the membrane via ion channels primarily formed from protein complexes. These ion channels come in many forms.

3.3.5: Ions Crossing Cell Membranes

Ion channels can be divided into three very general categories:

- **passive channels** which allow ions to pass through them in the spontaneous direction. Many of these are selective toward particular ions. Some of them also only pass ions in one direction.
- **channels that actively open and close** switch either because of a change in the membrane potential (important in nerve signaling) or when a ligand attaches to or detaches from the protein structure. Closing actively switched channels decreases the rate at which ions travel down the potential gradient.
- **ion pumps** use an energy source to move ions in the nonspontaneous direction across the membrane. These actively maintain the concentration and charge gradient across the membrane. These are usually protein complexes that couple the conversion of $\mathrm{ATP} \longrightarrow \mathrm{ADP}$ to the process of transport against the chemical potential.

An ion pump can effectively move an ion up the gradient as long as:

$$\Delta\mu = RTln\frac{a_{in}}{a_{out}} + zF\Delta\phi + \Delta_r G(\mathrm{ATP} \longrightarrow \mathrm{ADP}) < 0 \tag{3.3.4}$$

This page titled 3.3: Ion Transport is shared under a CC BY-NC-SA 4.0 license and was authored, remixed, and/or curated by Jonathan Gutow.

3.4: Review of Redox Chemistry

Learning Objectives

By the end of this section, you will be able to:

- Describe defining traits of redox chemistry
- Identify the oxidant and reductant of a redox reaction
- Balance chemical equations for redox reactions using the half-reaction method

Since reactions involving electron transfer are essential to the topic of electrochemistry, a brief review of redox chemistry is provided here that summarizes and extends the content of an earlier text chapter (see chapter on reaction stoichiometry). Readers wishing additional review are referred to the text chapter on reaction stoichiometry.

3.4.1: Oxidation Numbers

By definition, a redox reaction is one that entails changes in *oxidation number* (or *oxidation state*) for one or more of the elements involved. The oxidation number of an element in a compound is essentially an assessment of how the electronic environment of its atoms is different in comparison to atoms of the pure element. By this description, *the oxidation number of an atom in an element is equal to zero*. For an atom in a compound, *the oxidation number is equal to the charge the atom would have in the compound if the compound were ionic*. Consequential to these rules, *the sum of oxidation numbers for all atoms in a molecule is equal to the charge on the molecule*. To illustrate this formalism, examples from the two compound classes, ionic and covalent, will be considered.

Simple ionic compounds present the simplest examples to illustrate this formalism, since by definition the elements' oxidation numbers are numerically equivalent to ionic charges. Sodium chloride, NaCl, is comprised of Na^+ cations and Cl^- anions, and so oxidation numbers for sodium and chlorine are, +1 and −1, respectively. Calcium fluoride, CaF_2, is comprised of Ca^{2+} cations and F^- anions, and so oxidation numbers for calcium and fluorine are, +2 and −1, respectively.

Covalent compounds require a more challenging use of the formalism. Water is a covalent compound whose molecules consist of two H atoms bonded separately to a central O atom via polar covalent O−H bonds. The shared electrons comprising an O−H bond are more strongly attracted to the more electronegative O atom, and so it acquires a partial negative charge in the water molecule (relative to an O atom in elemental oxygen). Consequently, H atoms in a water molecule exhibit partial positive charges compared to H atoms in elemental hydrogen. The sum of the partial negative and partial positive charges for each water molecule is zero, and the water molecule is neutral.

Imagine that the polarization of shared electrons within the O−H bonds of water were 100% complete—the result would be *transfer* of electrons from H to O, and water would be an ionic compound comprised of O^{2-} anions and H^+ cations. And so, the oxidations numbers for oxygen and hydrogen in water are −2 and +1, respectively. Applying this same logic to carbon tetrachloride, CCl_4, yields oxidation numbers of +4 for carbon and −1 for chlorine. In the nitrate ion, NO_3^-, the oxidation number for nitrogen is +5 and that for oxygen is −2, summing to equal the 1− charge on the molecule:

$$(1N \text{ atom}) \left(\frac{+5}{N \text{ atom}} \right) + (3O \text{ atoms}) \left(\frac{-2}{O \text{ atom}} \right) = +5 + -6 = -1$$

Note: a more detailed discussion is available in the Classifying Chemical Reactions section of the OpenStax text.

3.4.2: Balancing Redox Equations

The unbalanced equation below describes the decomposition of molten sodium chloride:

$$\mathrm{NaCl(l)} \longrightarrow \mathrm{Na(l)} + \mathrm{Cl_2(g)} \qquad \text{(unbalanced)}$$

This reaction satisfies the criterion for redox classification, since the oxidation number for Na is decreased from +1 to 0 (it undergoes *reduction*) and that for Cl is increased from −1 to 0 (it undergoes *oxidation*). The equation in this case is easily balanced by inspection, requiring stoichiometric coefficients of 2 for the NaCl and Na:

$$2\,\mathrm{NaCl(l)} \longrightarrow 2\,\mathrm{Na(l)} + \mathrm{Cl_2(g)} \qquad \text{(balanced)}$$

Redox reactions that take place in aqueous solutions are commonly encountered in electrochemistry, and many involve water or its characteristic ions, $H^+(aq)$ and $OH^-(aq)$, as reactants or products. In these cases, equations representing the redox reaction can be very challenging to balance by inspection, and the use of a systematic approach called the *half-reaction method* is helpful.

Balancing REDOX reactions via the half-reaction Method

This approach involves the following steps:

1. Write skeletal equations for the oxidation and reduction half-reactions.
2. Balance each half-reaction for all elements except H and O.
3. Balance each half-reaction for O by adding H_2O.
4. Balance each half-reaction for H by adding H^+.
5. Balance each half-reaction for charge by adding electrons.
6. If necessary, multiply one or both half-reactions so that the number of electrons consumed in one is equal to the number produced in the other.
7. Add the two half-reactions and simplify.
8. If the reaction takes place in a basic medium, add OH^- ions the equation obtained in step 7 to neutralize the H^+ ions (add in equal numbers to both sides of the equation) and simplify.

The examples below demonstrate the application of this method to balancing equations for aqueous redox reactions.

Note: a more detailed discussion is available in the Classifying Chemical Reactions section of the OpenStax text.

Example 3.4.1: Balancing Equations for Redox Reactions in Acidic Solutions

Write the balanced equation representing reaction between solid copper and nitric acid to yield aqueous copper(II) ions and nitrogen monoxide gas.

Solution

Following the steps of the half-reaction method:

Step 1: Write skeletal equations for the oxidation and reduction half-reactions.

$$\begin{aligned} &\text{oxidation:} \quad \mathrm{Cu(s) \longrightarrow Cu^{2+}(aq)} \\ &\text{reduction:} \quad \mathrm{HNO_3(aq) \longrightarrow NO(g)} \end{aligned}$$

Step 2: Balance each half-reaction for all elements except H and O.

$$\begin{aligned} &\text{oxidation:} \quad \mathrm{Cu(s) \longrightarrow Cu^{2+}(aq)} \\ &\text{reduction:} \quad \mathrm{HNO_3(aq) \longrightarrow NO(g)} \end{aligned}$$

Step 3: Balance each half-reaction for O by adding H_2O.

$$\begin{aligned} &\text{oxidation:} \quad \mathrm{Cu(s) \longrightarrow Cu^{2+}(aq)} \\ &\text{reduction:} \quad \mathrm{HNO_3(aq) \longrightarrow NO(g) + \mathbf{2\,H_2O(l)}} \end{aligned}$$

Step 4: Balance each half-reaction for H by adding H^+.

$$\begin{aligned} &\text{oxidation:} \quad \mathrm{Cu(s) \longrightarrow Cu^{2+}(aq)} \\ &\text{reduction:} \quad \mathrm{\mathbf{3\,H^+(aq)} + HNO_3(aq) \longrightarrow NO(g) + 2\,H_2O(l)} \end{aligned}$$

Step 5: Balance each half-reaction for charge by adding electrons.

$$\begin{aligned} &\text{oxidation:} \quad \mathrm{Cu(s) \longrightarrow Cu^{2+}(aq) + \mathbf{2\,e^-}} \\ &\text{reduction:} \quad \mathrm{\mathbf{3\,e^-} + 3\,H^+(aq) + HNO_3(aq) \longrightarrow NO(g) + 2\,H_2O(l)} \end{aligned}$$

Step 6: If necessary, multiply one or both half-reactions so that the number of electrons consumed in one is equal to the number produced in the other.

$$\text{oxidation } (\times 3): \quad \mathbf{3}\,Cu(s) \longrightarrow \mathbf{3}\,Cu^{2+}(aq) + \mathbf{6}\ \cancel{2}e^-$$

$$\text{reduction } (\times 2): \quad \mathbf{6}\ \cancel{3}e^- + \mathbf{6}\ \cancel{3}H^+(aq) + \mathbf{2}\,HNO_3(aq) \longrightarrow \mathbf{2}\,NO(g) + \mathbf{4}\ \cancel{2}H_2O(l)$$

Step 7: Add the two half-reactions and simplify.

$$3\,Cu(s) + \cancel{6\,e^-} + 6\,H^+(aq) + 2\,HNO_3(aq) \longrightarrow 3\,Cu^{2+}(aq) + \cancel{6\,e^-} + 2\,NO(g) + 4\,H_2O(l)$$

$$3\,Cu(s) + 6\,H^+(aq) + 2\,HNO_3(aq) \longrightarrow 3\,Cu^{2+}(aq) + 2\,NO(g) + 4\,H_2O(l)$$

Step 8: If the reaction takes place in a basic medium, add OH^- ions the equation obtained in step 7 to neutralize the H^+ ions (add in equal numbers to both sides of the equation) and simplify.

This step not necessary since the solution is stipulated to be acidic.

The balanced equation for the reaction in an acidic solution is then

$$3\,Cu(s) + 6\,H^+(aq) + 2\,HNO_3(aq) \longrightarrow 3\,Cu^{2+}(aq) + 2\,NO(g) + 4\,H_2O(l)$$

? Exercise 3.4.1

The reaction above results when using relatively diluted nitric acid. If concentrated nitric acid is used, nitrogen dioxide is produced instead of nitrogen monoxide. Write a balanced equation for this reaction.

Answer

$$Cu(s) + 2\,H^+(aq) + 2\,HNO_3(aq) \longrightarrow Cu^{2+}(aq) + 2\,NO_2(g) + 2\,H_2O(l)$$

✔ Example 3.4.2: Balancing Equations for Redox Reactions in Basic Solutions

Write the balanced equation representing reaction between aqueous permanganate ion, , and solid chromium(III) hydroxide, $Cr(OH)_3$, to yield solid manganese(IV) oxide, MnO_2, and aqueous chromate ion, The reaction takes place in a basic solution.

Solution

Step 1: Write skeletal equations for the oxidation and reduction half-reactions.

$$\text{oxidation:} \quad Cr(OH)_3(s) \longrightarrow CrO_4^{2-}(aq)$$

$$\text{reduction:} \quad MnO_4^-(aq) \longrightarrow MnO_2(s)$$

Step 2: Balance each half-reaction for all elements except H and O.

$$\text{oxidation:} \quad Cr(OH)_3(s) \longrightarrow CrO_4^{2-}(aq)$$

$$\text{reduction:} \quad MnO_4^-(aq) \longrightarrow MnO_2(s)$$

Step 3: Balance each half-reaction for O by adding H_2O.

$$\text{oxidation:} \quad \mathbf{H_2O(l)} + Cr(OH)_3(s) \longrightarrow CrO_4^{2-}(aq)$$

$$\text{reduction:} \quad MnO_4^-(aq) \longrightarrow MnO_2(s) + \mathbf{2\,H_2O(l)}$$

Step 4: Balance each half-reaction for H by adding H^+.

$$\text{oxidation:} \quad H_2O(l) + Cr(OH)_3(s) \longrightarrow CrO_4^{2-}(aq) + \mathbf{5\,H^+(aq)}$$

$$\text{reduction:} \quad \mathbf{4\,H^+(aq)} + MnO_4^-(aq) \longrightarrow MnO_2(s) + 2\,H_2O(l)$$

Step 5: Balance each half-reaction for charge by adding electrons.

$$\text{oxidation:} \quad H_2O(l) + Cr(OH)_3(s) \longrightarrow CrO_4^{2-}(aq) + 5\,H^+(aq) + \mathbf{3\,e^-}$$

$$\text{reduction:} \quad \mathbf{3\,e^-} + 4\,H^+(aq) + MnO_4^-(aq) \longrightarrow MnO_2(s) + 2\,H_2O(l)$$

Step 6: If necessary, multiply one or both half-reactions so that the number of electrons consumed in one is equal to the number produced in the other.

This step is not necessary since the number of electrons is already in balance.

Step 7: Add the two half-reactions and simplify.

$$\cancel{H_2O(l)} + Cr(OH)_3(s) \longrightarrow CrO_4^{2-}(aq) + 5\cancel{1}^{1}\, H^+(aq) + \cancel{3e^-}$$

$$+ \quad \cancel{3e^-} + 4\,\cancel{H^+(aq)} + MnO_4^-(aq) \longrightarrow MnO_2(s) + 2\cancel{1}^{1}\, H_2O(l)$$

$$Cr(OH)_3(s) + MnO_4^-(aq) \longrightarrow CrO_4^{2-}(aq) + MnO_2(s) + H^+(aq) + H_2O(l)$$

Step 8: If the reaction takes place in a basic medium, add OH^- ions the equation obtained in step 7 to neutralize the H^+ ions (add in equal numbers to both sides of the equation) and simplify.

$$OH^-(aq) + Cr(OH)_3(s) + MnO_4^-(aq) \longrightarrow CrO_4^{2-}(aq) + MnO_2(s) + \cancel{H^+(aq)} + H_2O(l) + \cancel{OH^-(aq)}$$

after neutralizing the H^+, we get the balanced equation for the reaction in a basic solution

$$OH^-(aq) + Cr(OH)_3(s) + MnO_4^-(aq) \longrightarrow CrO_4^{2-}(aq) + MnO_2(s) + 2\,H_2O(l)$$

Exercise 3.4.2

Aqueous permanganate ion may also be reduced using aqueous bromide ion, Br^-, the products of this reaction being solid manganese(IV) oxide and aqueous bromate ion, BrO_3^-. Write the balanced equation for this reaction occurring in a basic medium.

Answer

$$H_2O(l) + 2\,MnO_4^-(aq) + Br^-(aq) \longrightarrow 2\,MnO_2(s) + BrO_3^-(aq) + 2\,OH^-(aq)$$

This page titled 3.4: Review of Redox Chemistry is shared under a CC BY-NC-SA 4.0 license and was authored, remixed, and/or curated by Jonathan Gutow.

- **17.1: Review of Redox Chemistry** by OpenStax is licensed CC BY 4.0. Original source: https://openstax.org/details/books/chemistry-2e.

3.5: Half Cells and Standard Reduction Potentials

3.5.1: Introduction

All redox reactions can formally be thought of as the sum of half-reactions. Some can also actually be run with the two half-reactions occurring in different locations. When this is possible they can be used to do electrical work by passing the electrons through a wire to exchange them rather than allowing direct exchange between the reactants. These two separate reaction containers are formally referred to as **half-cells**. A galvanic cell (generically called a battery*) is made of two connected half-cells that produce electrical energy as the two half-reactions proceed. Below is a cartoon (figure 3.5.1) of a galvanic cell based on the overall reaction $\mathrm{Cu} + 2\,\mathrm{Ag}^{+} \longrightarrow \mathrm{Cu}^{2+} + 2\,\mathrm{Ag}$. The two half-reactions are:

$$\mathrm{Cu} \longrightarrow \mathrm{Cu}^{2+} + 2\,\mathrm{e}^{-}\ (\text{oxidation}) \quad \text{and} \quad \mathrm{Ag}^{+} + \mathrm{e}^{-} \longrightarrow \mathrm{Ag}\ (\text{reduction})$$

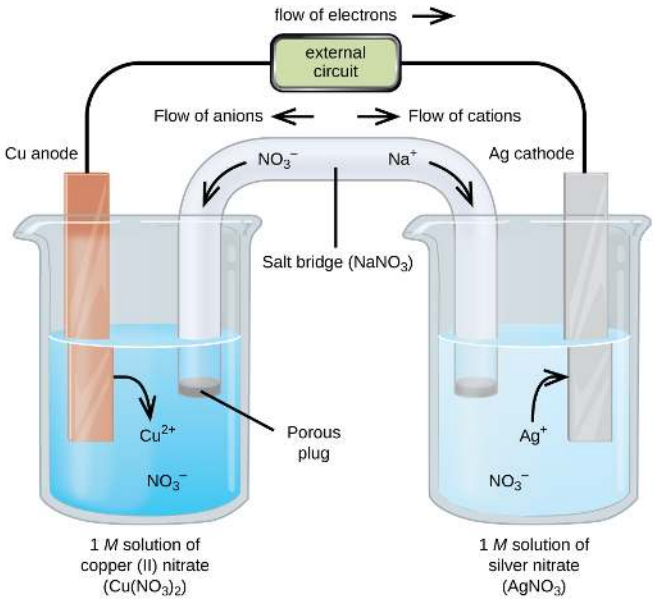


Figure 3.5.1 : A galvanic cell based on the spontaneous reaction between copper and silver(I) ions. From OpenStax.

*Definition: Battery

Technically a battery is made of multiple galvanic cells hooked together in series to produce a larger voltage or in parallel to produce more current at the same voltage as a single galvanic cell. A standard D battery is more properly called a D cell as it only contains a single galvanic cell. A 9V alkaline battery contains multiple galvanic cells stacked in series to produce the larger voltage. A single alkaline cell only produces about 1.5 V.

3.5.2: Standard Hydrogen Electrode

The voltage produced by a pair of half-cells connected in a galvanic cell is referred to as the **cell potential** and usually represented by the symbol **E**. Experimentation shows that the potentials of each half-reaction (half-cell) can be thought of as existing on a number line. Thus, if we choose an arbitrary half-cell as our reference state and set its potential to 0 V, we can define the potential of all other half-reactions relative to the reference electrode and calculate the potential of any galvanic cell as the difference between the potentials of each half-cell: $E_{cell} = E_2 - E_1$. The **standard hydrogen electrode** is this reference electrode.

The standard hydrogen electrode is constructed so that H_2 gas flows over an inert electrode made of platinum, and can interact with an acid solution which provides H^+ for the half reaction

$$2\,\mathrm{H}^{+}(\mathrm{aq}) + 2\,\mathrm{e}^{-} \longrightarrow \mathrm{H}_2(\mathrm{g})$$

Both H^+ and H_2 need to have unit activity (or fugacity), which if the solution and gas behave ideally means a concentration of 1 M and a pressure of 1 bar.

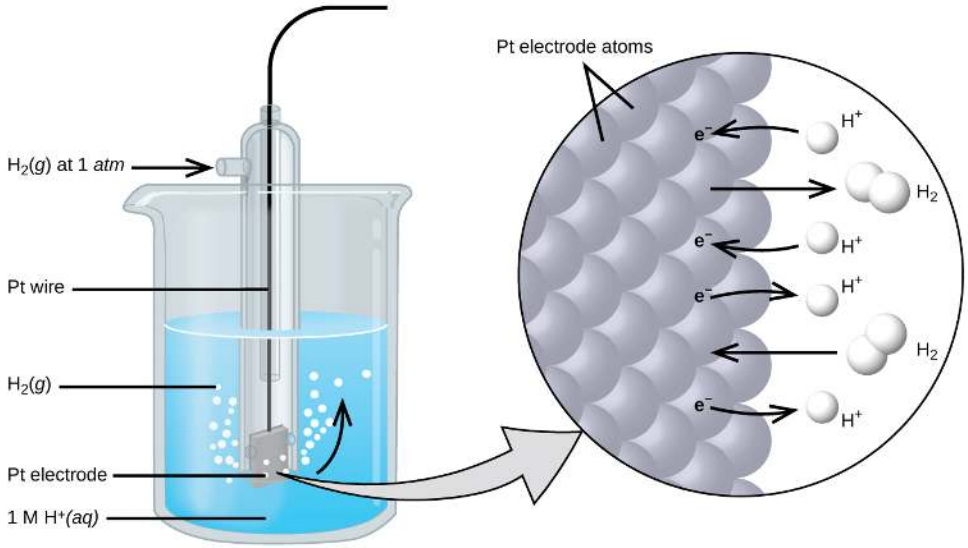


Figure 3.5.2: The standard hydrogen electrode (SHE). From OpenStax.

3.5.3: Standard cell potential (E^o_{cell}) and the spontaneous direction under standard conditions.

Using the **Standard Hydrogen Electrode** (SHE) as zero the half-cell potentials are usually tabulated for runing the half-reaction as a reduction (e- as reactants). A number of values are shown in Table P1 of the LibreTexts resources. When two half-cells are paired the half-reaction with the higher reduction potential goes spontaneously (as written) and the other runs in reverse.

Example 3.5.1: Cell Potential and Spontaneity

Which pair of reactants will produce a spontaneous reaction if everything is present in its standard state at 25 °C?

- Fe and Cu^{2+} or
- Fe^{2+} and Cu

Solution

The species with the highest standard reduction potential (Table P1) will force the other to oxidize.

From the table,

$$\mathrm{Cu}^{2+} + 2\,\mathrm{e}^- \rightarrow \mathrm{Cu} \quad E^o = 0.377V$$

$$\mathrm{Fe}^{2+} + 2\,\mathrm{e}^- \rightarrow \mathrm{Fe} \quad E^o = -0.440V$$

So the iron half-reaction will flip (so that iron is oxidizing) and the spontaneous reaction under standard conditions will be

$$Cu^{2+} + Fe \rightarrow Cu + Fe^{2+}$$

$E^o_{cell} = E^o_{Cu} - E^o_{Fe} = 0.377V - -0.440V = 0.777\,V$

Note

Applying a potential larger than the standard potential to the cell will turn the cell into an electrolytic cell running the reaction in the non-spontaneous direction. This is used to recharge batteries and purify many metals including Na. Some examples may be found in the OpenStax general chemistry text.

This page titled 3.5: Half Cells and Standard Reduction Potentials is shared under a CC BY-NC-SA 4.0 license and was authored, remixed, and/or curated by Jonathan Gutow.

- **10.3: Half Cells and Standard Reduction Potentials** by Patrick Fleming is licensed CC BY-NC-SA 4.0.

3.6: Cell potentials under non-standard conditions (Nernst equation)

3.6.1: Relation of E^o and ΔG^o

E^o is the cell potential under standard conditions. Applying this potential to the galvanic cell under standard conditions will bring the reaction to a halt as it will exactly oppose any flow of electrons. This suggests a relation between E^o and ΔG^o. We can derive the relation by considering the definition of electrical work from physics:

$$w_{elec} = CV \tag{3.6.1}$$

where C is the Coulombs of charge moved through the voltage potential and V is the magnitude of the potential change. When this work is done reversibly, we are balancing the potential exactly and can get the maximum work, which is just $-\Delta G$ under the current conditions. The (-) sign comes from the convention that released energy is negative. If we use E^o for the voltage we are under standard and reversible conditions so equation 3.6.1 becomes:

$$-\Delta G^o = CE^o \tag{3.6.2}$$

We usually calculate the free energy change with respect to a moles of a reactant. If we use n_e to represent the number of moles of electrons per unit of reaction and utilize the fact that there are F = 96485.33212 C/mol of electrons (F is the **Faraday constant**), we have C = n_eF. Substituting into equation 3.6.2:

$$-\Delta G^o = n_e F E^o \quad \text{or} \quad \Delta G^o = -n_e F E^o \tag{3.6.3}$$

This subscript 'e' is often dropped and other symbols are often used for n_e (most common is *v*).

3.6.2: The Nernst equation

The connection between ΔG and potential allows us to utilize our knowledge of concentration effects to develop an equation for how E_{cell} varies with concentrations (really the reactions quotient, Q). The resulting relation is the **Nernst equation**. First we remember that at nonstandard conditions:

$$\Delta G = \Delta G^o + RT \ln Q$$

then by analogy with equation 3.6.3:

$$\Delta G = -n_e F E = \Delta G^o + RT \ln Q$$

where we can substitute in for ΔG^o with equation 3.6.3 to get:

$$-n_e F E = -n_e F E^o + RT \ln Q \tag{3.6.4}$$

Dividing through by -n_eF produces the standard form of the **Nernst equation** showing the relationship of the cell potential to the reaction quotient:

$$E = E^o - \frac{RT}{n_e F} \ln Q \tag{3.6.5}$$

Since we know at equilibrium $\Delta G = -n_e F E = 0$ this makes it clear that when a galvanic cell (battery) is dead (the voltage, $E = 0$) it is at chemical equilibrium.

3.6.3: Concentration cells

Equation 3.6.5 has a very important implication. If you connect two half-cells of the same material but at different concentrations you will see a potential difference because of the concentration difference. If the two cells are the same $E^o = E_2^o - E_1^o = 0$ so the equation reduces to:

$$E = -\frac{RT}{n_e F} lnQ \tag{3.6.6}$$

This will give a non-zero voltage as long as Q ≠ 1. It also means that any ion that is at a different concentration in the two half-cells will generate a potential difference. Although spectator ions (the counter ions) are often ignored in calculations using the Nernst

equation, that is not completely correct as they do contribute to a concentration difference induced cell potential and impact the activity of all the ions through the ionic strength.

This idea is used in biochemical applications to assign contributions of specific ions to cell membrane potentials from differences in concentrations of the ion on each side of the membrane.

3.6.4: Calculating Cell Potentials

Using values measured relative to the SHE, it is fairly easy to calculate the standard cell potential of a given reaction. For example, consider the reaction

$$2\,\mathrm{Ag^+(aq) + Cu(s) \rightarrow 2\,Ag(s) + Cu^{2+}(aq)}$$

Before calculating the cell potential, we should review a few definitions. The anode half reaction, which is defined by the half-reaction in which oxidation occurs, is

$$\mathrm{Cu(s) \rightarrow Cu^{2+}(aq) + 2\,e^-}$$

And the cathode half-reaction, defined as the half-reaction in which reduction takes place, is

$$\mathrm{Ag^+(aq) + e^- \rightarrow Ag(s)}$$

Using **standard cell notation**, the conditions (such as the concentrations of the ions in solution) can be represented. In the standard cell notation, the anode is on the left-hand side, and the cathode on the right. The two are typically separated by a **salt bridge**, which is designated by a double vertical line. A single vertical line indicates a phase boundary. Hence for the reaction above, if the silver ions are at a concentration of 0.500 M, and the copper (II) ions are at a concentration of 0.100 M, the standard cell notation would be as shown in example 3.6.1.

Caution

For all the examples below we are using concentrations rather than activities. The ionic strength of the solutions in these examples are high enough that activities would need to be accounted for to get accurate results. Nonetheless, the general behavior as concentration varies is illustrated by these examples.

Example 3.6.1: Cell Potential Under nonstandard Conditions (ignoring the counter ions)

Calculate the cell potential at 25 °C for the cell indicated by

$$Cu(s)|Cu^{2+}(aq,\,0.100\,M)||Ag^{+}(aq,\,0.500\,M)|Ag(s)$$

Solution

In order to calculate the cell potential (E), the standard cell potential must first be obtained. The standard cell potential at 25 °C is given by

$$\begin{aligned} E_{cell} &= E^o_{cathode} - E^o_{anode} \\ &= 0.799\,V - 0.337\,V \\ &= 0.462\,V \end{aligned}$$

And for a cell at non-standard conditions, such as those indicated above, the Nernst equation can be used to calculate the cell potential. At 25 °C, The cell potential is given by

$$\begin{aligned} E_{cell} &= E^o_{cell} - \frac{RT}{nF}\ln\left(\frac{[Cu^{2+}]}{[Ag^+]^2}\right) \\ &= 0.462\,V - \frac{(8.314\,J/(mol\,K)(298\,K)}{2(96485\,C/mol)}\ln\left(\frac{0.100}{0.500^2}\right) \end{aligned}$$

Noting that $1\,J/C = 1\,V$,

$$E = 0.480\,V$$

Example 3.6.2: Cell Potential Under nonstandard Conditions (with the counter ions)

Calculate the cell potential at 25 °C for the cell indicated by

$$Cu(s)|Cu^{2+}(aq,\ 0.100\ M)||Ag^{+}(aq,\ 0.500\ M)|Ag(s)$$

Solution

If the other ions in solution are just the counter ions that make the overall charge in each half-cell neutral they can just be included in Q using the reaction stoichiometry. Because the concentrations on the two sides are different, they do not cancel out. Assuming a singly charged counter ion (eg. NO_3^-).

We have at 25 °C:

$$\begin{aligned} E_{cell} &= E^o_{cell} - \frac{RT}{nF}\ln\left(\frac{[Cu^{2+}][NO_3^-]^2_{Cu}}{[Ag^+]^2[NO_3^-]^2_{Ag}}\right) \\ &= 0.462\,V - \frac{(8.314\,J/(mol\,K)(298\,K)}{2(96485\,C/mol)}\ln\left(\frac{(0.100)(0.200)^2}{0.500^4}\right) \\ E &= 0.468\,V \end{aligned}$$

Example 3.6.3: Cell Potential under Non-Standard Conditions (ignoring the counter ions)

Calculate the cell potential at 25 °C for the cell defined by

$$Ni(s)|Ni^{2+}\ (aq,\ 0.500\ M)||Cu(s)|Cu^{2+}(aq,\ 0.100\ M)$$

Solution

We will use the Nernst equation. First, we need to determine E^o. Using Table P1, it is apparent that

$$\mathrm{Cu^{2+} + 2\,e^- \rightarrow Cu}$$

$E^o = 0.337\,V$

$$\mathrm{Ni^{2+} + 2\,e^- \rightarrow Ni}$$

with $E^o = -0.250\,V$

So copper, having the larger reduction potential will be the cathode half-reaction while forcing nickel to oxidize, making it the anode. So E^o for the cell will be given by

$$\begin{aligned} E_{cell} &= E^o_{cathode} - E^o_{anode} \\ &= 0.337\,V - (-0.250\,V) \\ &= 0.587\,V \end{aligned}$$

And the cell potential is then given by the Nernst Equation

$$\begin{aligned} E_{cell} &= E^o_{cell} - \frac{RT}{nF}\ln Q \\ &= 0.587 - \frac{(8.314\,J/(mol\,K)(298\,K)}{2(96485\,C/mol)}\ln\left(\frac{0.500}{0.100}\right) \\ &= 0.566\,V \end{aligned}$$

This page titled 3.6: Cell potentials under non-standard conditions (Nernst equation) is shared under a CC BY-NC-SA 4.0 license and was authored, remixed, and/or curated by Jonathan Gutow.

- **10.3: Half Cells and Standard Reduction Potentials** by Patrick Fleming is licensed CC BY-NC-SA 4.0.

3.7: Thermodynamics from Electrochemistry

3.7.1: Electrochemistry for indirect measurement of free energy

Many reactions (particularly biochemical) consist of multiple coupled half-reactions. It is often not possible to measure all of these half-reactions against one known half-cell to determine their reduction potentials. Many reduction potentials are arrived at indirectly using the fact that ΔG is a state function and thus so is E^o because $\Delta_r G = -n_e F E$. This means we can calculate an E^o by following any path that overall leads to the same electrochemical change. As a generic example consider three half-cell potentials $E_1 = E^o(A \longrightarrow B)$, $E_2 = E^o(B \longrightarrow C)$ and $E_3 = E^o(A \longrightarrow C)$. We know that:

$$\Delta G_1^o(A \longrightarrow B) + \Delta G_2^o(B \longrightarrow C) = \Delta G_3^o(A \longrightarrow C)$$

Using $\Delta_r G = -n_e F E$ to replace the free energies gives us:

$$-n_{e1} F E_1^o + -n_{e2} F E_2^o = -n_{e3} F E_3^o$$

Thus as long as we know two of the three cell potentials and all n_e's (moles e- in each reduction), we can solve for the third E^o. We could also solve for an unknown number of electrons transferred knowing all the potentials and two of the n_e's. The other possibility is to do a complete cycle so that $\Delta G_{overall}^o = 0$, which means that $E_{overall}^o = 0$. Then you can solve for the E^o of one reduction in the cycle knowing all the others.

Once E^o is known you can calculate equilibrium constants and ΔG from:

$$\Delta G^o = -n_e F E^o, \quad \Delta G^o = -RT ln K \quad \text{and} \quad E^o = \frac{RT}{n_e F} ln K \tag{3.7.1}$$

Example 3.7.1

Given the following half-reactions calculate the $E^o(Hg_2^{2+} + 2\,e^- \longrightarrow 2\,Hg(l))$.

$$Hg^{2+} + 2\,e^- \longrightarrow Hg(l) \quad E^o = 0.8535 \tag{3.7.2}$$

$$2\,Hg^{2+} + 2\,e^- \longrightarrow Hg_2^{2+} \quad E^o = 0.911 \tag{3.7.3}$$

Solution

By inspection two times the first reaction minus the second reaction gives us the desired overall reaction:

$$\begin{array}{l} 2(Hg^{2+} + 2\,e^- \longrightarrow Hg(l)) \quad \text{RXN 1} \\ \underline{-(2\,Hg^{2+} + 2\,e^- \longrightarrow Hg_2^{2+}) \quad \text{RXN 2}} \\ Hg_2^{2+} + 2\,e^- \longrightarrow 2\,Hg(l) \quad \text{RXN 3} \end{array}$$

The multiplication of RXN 1 by 2 means that there are n_{e1} = 4, while number electrons transferred in RXN 2 is unchanged at n_{e2} =2. Calling the desired reaction #3, we can write:

$$n_{e1} F E_1^o - n_{e2} F E_2^o = n_{e3} F E_3^o \implies 2E_3^o = 4E_1^o - 2E_2^o \tag{3.7.4}$$

So:

$$E_3^o = \frac{4(0.8535V) - 2(0.911V)}{2} = 0.796V \tag{3.7.5}$$

3.7.2: Getting to enthalpy and entropy

Electrochemical measurements of cell potentials versus temperature can be used to determine reaction free energies, entropies and enthalpies. This is because $\Delta_r G = -n_e F E$ under the current galvanic cell conditions. Thus measurement of E, directly gives us the Gibbs free energy. From general thermodynamics we know:

$$\left(\frac{\partial \Delta G}{\partial T}\right)_p = -\Delta S \tag{3.7.6}$$

Substituting in -n_eFE for ΔG yields:

$$nF\left(\frac{\partial E}{\partial T}\right)_p = \Delta S \tag{3.7.7}$$

So if we measure the slope of the potential at a given temperature we have the ΔS of the reaction. Because $\Delta G = \Delta H - T\Delta S$ we also get ΔH:

$$\Delta G + T\Delta S = \Delta H \tag{3.7.8}$$

If we are at standard conditions for all the reactants we get the standard Gibbs, entropy and enthalpy of reaction.

Example

Consider the following data for the Daniel cell (Buckbeei, Surdzial, & Metz, 1969) which is defined by the following reaction

$$Zn(s) + Cu^{2+}(aq) \rightleftharpoons Zn^{2+}(aq) + Cu(s)$$

T (°C)	0	10	20	25	30	40
E (V)	1.1028	1.0971	1.0929	1.0913	1.0901	1.0887

From a fit of the data to a quadratic function, the temperature dependence of

$$\left(\frac{\partial E^o}{\partial T}\right)_p$$

is easily established.

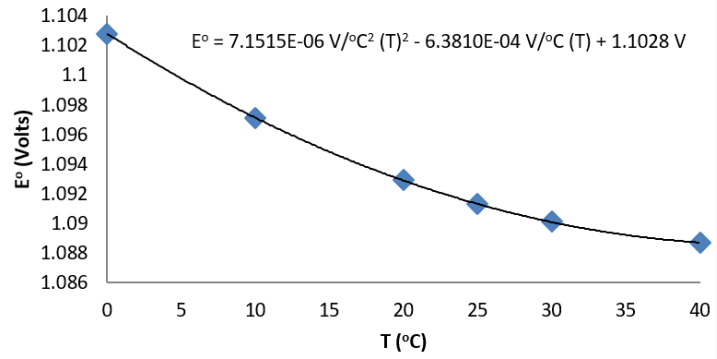


Figure 3.7.1: Temperature dependence of the cell potential for a Daniel cell.

The quadratic fit to the data results in

$$\left(\frac{\partial E^o}{\partial T}\right)_p = 3.8576 \times 10^{-6} \frac{V}{^\circ C^2}(T) - 6.3810 \times 10^{-4} \frac{V}{^\circ C}$$

So, at 25 °C,

$$\left(\frac{\partial E^o}{\partial T}\right)_p = -5.4166 \times 10^{-4} V/K$$

noting that K can be substituted for $^\circ C$ since in difference they have the same magnitude. So the entropy change calculated using equation 3.7.7 is

$$\Delta S = nF\left(\frac{\partial E^o}{\partial T}\right)_p = (2\,mol)(96485\,C/mol)(-5.4166 \times 10^{-4} V/K)$$

Because

$$1\,C \times 1\,V = 1\,J$$

The standard entropy change for the Daniel cell reaction at 25 °C is

$$\Delta S = -104.5\,J/(mol\,K).$$

It is the negative entropy change that leads to an increase in standard cell potential at lower temperatures.

This page titled 3.7: Thermodynamics from Electrochemistry is shared under a CC BY-NC-SA 4.0 license and was authored, remixed, and/or curated by Jonathan Gutow.

- **10.4: Entropy of Electrochemical Cells** by Patrick Fleming is licensed CC BY-NC-SA 4.0.

3.8: Redox Examples

3.8.1: Introduction

Many of the useful energetic reactions around us are examples of redox reactions. These include reactions such as:

the combustion of methane ($CH_4 + 2\,O_2 \longrightarrow CO_2 + 2\,H_2O$); many of the energy consuming and energy producing reactions in biological organisms; and the reactions in electrochemical energy sources such as batteries and fuel cells. A few examples are summarized in this section.

3.8.2: Oxidative phosphorylation and photophosphorylation

3.8.2.1: Electron Transport/Oxidative Phosphorylation

Mitocohondria are called the power plants of the cell because most of a cell's ATP is produced there, in a process referred to as oxidative phosphorylation. There are two parts to the process. The first is electrons from reduced energy carriers, such as NADH and FADH2, enter an electron transport system via protein complexes containing iron. As seen in the figure 3.8.1, electrons move from one complex to the next, not unlike the way they might move through an electrical circuit. The energy from the oxidation processes in this electron transport chain is used to pump protons and sodium ions out of the inner region of a mitochondrion, creating a concentration gradient and a membrane potential. The extra protons outside then flow down this gradient through the ATP Synthase complex to drive the production of ATP.

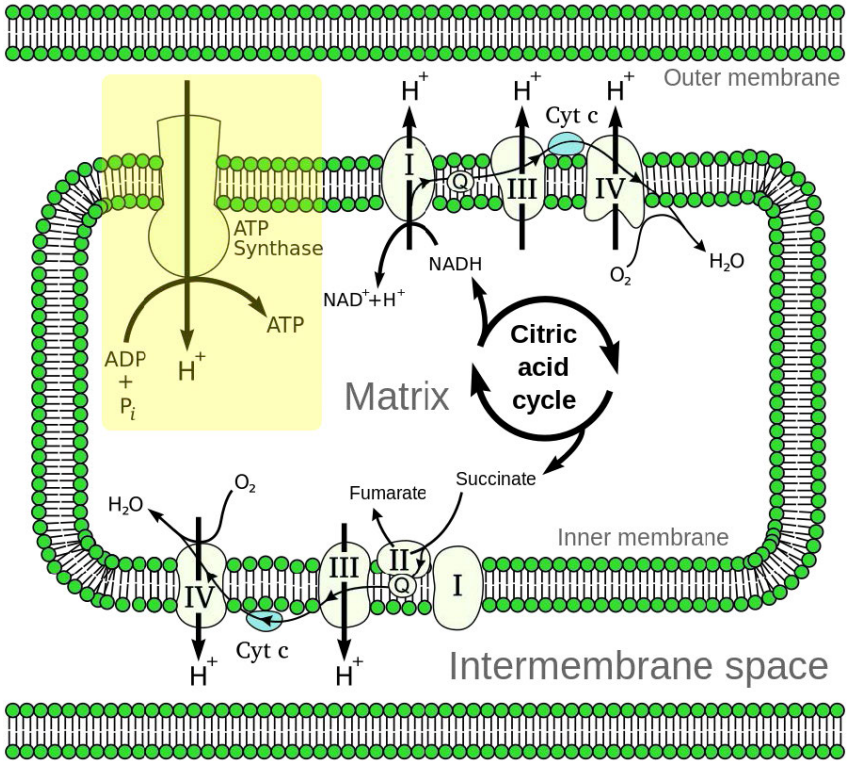


Figure 3.8.1: Cartoon of a mitochondrion, the oxidations occurring in the in the electron transport chain (I, II, III, IV) used to pump H^+ (also Na^+) out of the inner "Matrix" and the conversion of ADP to ATP by ATP Synthase using the energy from the membrane potential and the proton gradient.

When electrons pass through complexes I, III, and IV, protons are moved from the mitochondrial matrix (inside of mitochondrion) and deposited in the intermembrane space (between the inner and outer membranes of the mitochondrion). The effect of this redistribution is to increase the electrical and chemical potential across the membrane. The energetics of the oxidations are[1]:

Complex I: $H^+ + NADH + Q \longrightarrow NAD^+ + QH_2$, E^+ = + 0.42 V, $\Delta_r G^+$ = -81 kJ/mol

Complex II: $FADH_2 + Q \longrightarrow FAD + QH_2$, E^+ = + 0.32 V, $\Delta_r G^+$ = -62 kJ/mol

Complex III: $QH_2 + 2\,Fe^{3+}(Cytc) \longrightarrow Q + 2\,Fe^{2+}(Cytc) + H_2O$, E^+ = + 0.15 V, Δ_rG^+ = -29 kJ/mol

Complex IV: $2\,Fe^{2+}(Cytc) + 2\,H^+(\frac{1}{2})O_2 \longrightarrow Q + 2\,Fe^{3+}(Cytc) + H_2O$, E^+ = + 0.56 V, Δ_rG^+ = -108 kJ/mol

This is clearly enough energy to convert more than 1 ADP to ATP in the reaction:

$$ADP^{3-} + HPO_4^{2-} + H_3O^+ \longrightarrow ATP^{4-} + H_2O \quad \Delta_rG^+ = +31kJ/mol$$

The energy actually available for this last reaction by moving a mole of H^+ ions across the proton gradient and the membrane potential is:

$$\Delta G_m = RTln\frac{[H^+]_{in}}{[H^+]_{out}} + F\Delta\phi \tag{3.8.1}$$

Measurements suggest typical values are $\Delta\phi \approx 0.14V$ and $\Delta pH \approx -1$ ($\frac{[H^+]_{in}}{[H^+]_{out}} \approx 10$). Putting these values into equation 3.8.1 yields $\Delta G_m \approx 19$ kJ/mol. So at least 2 moles of protons must be transferred across the membrane to generate the 31 kJ/mol necessary to create a mole of ATP.

In summary, one can think of the electron transport system as charging the battery for oxidative phosphorylation by pumping protons out of the mitochondrion. The intact inner membrane of the mitochondrion keeps the protons out, except for those that re-enter through ATP Synthase. The ATP Synthase allows protons to re-enter the mitochondrial matrix and harvests their energy to make ATP.

References

1. P. Atkins, J. de Paula, *Physical Chemistry for the Life Sciences*, 2nd Ed. W.H. Freeman and Company, New York, 2011, p. 208.

3.8.2.2: Photophosphorylation

Photophosphorylation to make ATP is found only in cells that carry out photosynthesis. This process is similar to oxidative phosphorylation in several ways. A primary difference is the ultimate source of the energy for ATP synthesis. In oxidative phosphorylation, the energy comes from electrons produced by oxidation of biological molecules. In the case of photosynthesis, the energy comes from the light of the sun.

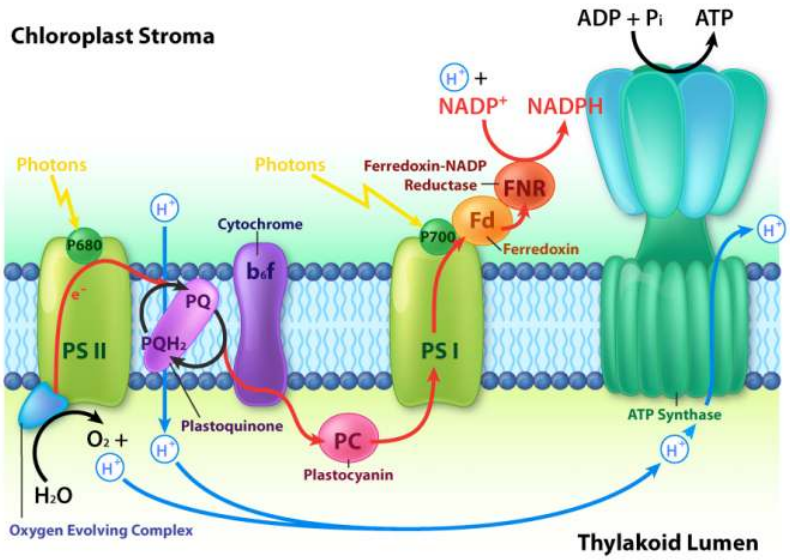


Figure 3.8.6: Photophosphorylation.

Photons from the sun interact with chlorophyll molecules in reaction centers in the chloroplasts of plants or membranes of photosynthetic bacteria. A schematic of the process is shown above. The similarities of photophosphorylation to oxidative phosphorylation include:

- an electron transport chain
- creation of a proton gradient
- harvesting energy of the proton gradient by making ATP

with the help of an ATP synthase. Some of the differences include:

- the source of the electrons – H_2O for photosynthesis versus $NADH/FADH_2$ for oxidative phosphorylation
- direction of proton pumping – into the thylakoid space of the chloroplasts versus outside the matrix of the mitochondrion
- movement of protons during ATP synthesis – out of the thylakoid space in photosynthesis versus into the mitochondrial matrix
- nature of the terminal electron acceptor – $NADP^+$ in photosynthesis versus O_2 in oxidative phosphorylation.

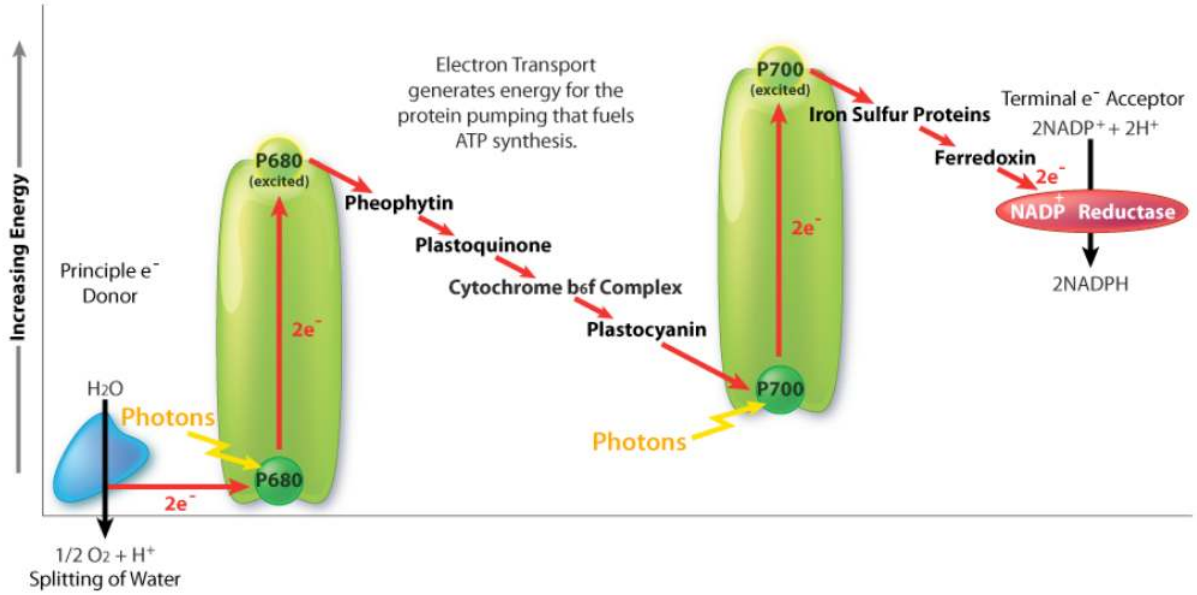


Figure 3.8.7: Electron movement in photosynthesis.

3.8.2.3: Electron Transport in Chloroplasts vs. Mitochondria

In some ways, the movement of electrons in chloroplasts during photosynthesis is opposite that of electron transport in mitochondria. In photosynthesis, water is the source of electrons and their final destination is $NADPH$. In mitochondria, $NADH/FADH_2$ are electron sources and H_2O is their final destination.

How do biological systems get electrons to go both ways? It would seem to be the equivalent of going to and from a particular place while always going downhill, since electrons will move according to potential. The answer is the captured energy of the photons, which elevates electrons in photosynthesis to an energy where they move “downhill” to their $NADPH$ destination in a Z-shaped scheme. The movement of electrons through this scheme in plants requires energy from photons in two places to “lift” the energy of the electrons sufficiently. Last, it should be noted that photosynthesis actually has two phases, referred to as the *light cycle* (described above) and the *dark cycle*, which is a set of chemical reactions that captures CO_2 from the atmosphere and “fixes” it, ultimately into glucose. The dark cycle is also referred to as the Calvin Cycle.

3.8.3: "Batteries"

The term "battery" is used in common speech to refer to any device that produces electrical energy via redox reactions. As chemists we differentiate between galvanic cells (a single electrochemical cell) and a battery (a connected collection of electrochemical cells). In this section we will concentrate on what happens in a single galvanic cell.

3.8.3.1: Single use batteries

A common primary battery is the dry cell, which uses a zinc can as both container and anode (“–” terminal) and a graphite rod as the cathode (“+” terminal). The Zn can is filled with an electrolyte paste containing manganese(IV) oxide, zinc(II) chloride, ammonium chloride, and water. A graphite rod is immersed in the electrolyte paste to complete the cell. The spontaneous cell reaction involves the oxidation of zinc:

$$\mathrm{Zn(s) \longrightarrow Zn^{2+}(aq) + 2\,e^-} \qquad \text{(anode)}$$

and the reduction of manganese(IV)

$$\mathrm{2\,MnO_2(s) + 2\,NH_4Cl(aq) + 2\,e^- \longrightarrow Mn_2O_3(s) + 2\,NH_3(aq) + H_2O(l) + 2\,Cl^-} \qquad \text{(cathode)}$$

which together yield the cell reaction:

$$2\,\mathrm{MnO_2(s)} + 2\,\mathrm{NH_4Cl(aq)} + \mathrm{Zn(s)} \longrightarrow \mathrm{Zn^{2+}(aq)} + \mathrm{Mn_2O_3(s)} + 2\,\mathrm{NH_3(aq)} + \mathrm{H_2O(l)} + 2\,\mathrm{Cl^-} \qquad \text{(cell)}$$

The voltage (*cell potential*) of a dry cell is approximately 1.5 V. Dry cells are available in various sizes (e.g., D, C, AA, AAA). All sizes of dry cells comprise the same components, and so they exhibit the same voltage, but larger cells contain greater amounts of the redox reactants and therefore are capable of transferring correspondingly greater amounts of charge. Like other galvanic cells, dry cells may be connected in series to yield batteries with greater voltage outputs, if needed.

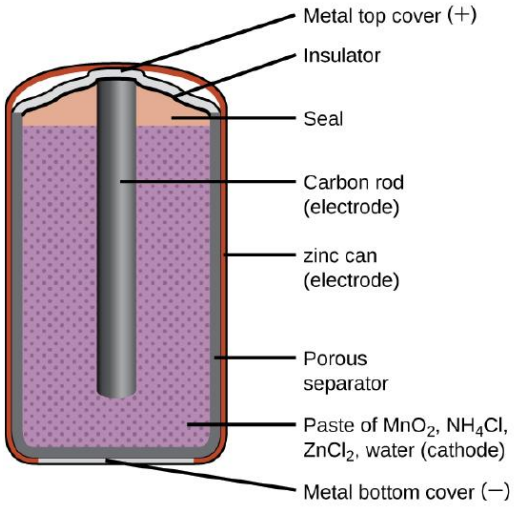


Figure 3.8.2: A schematic diagram shows a typical dry cell.

Link to Learning

Visit this site to learn more about zinc-carbon batteries.

Alkaline batteries (Figure 3.8.3) were developed in the 1950s to improve on the performance of the dry cell, and they were designed around the same redox couples. As their name suggests, these types of batteries use alkaline electrolytes, often potassium hydroxide. The reactions are

$$\begin{array}{ll} \text{anode:} & \mathrm{Zn(s) + 2\,OH^-(aq) \longrightarrow ZnO(s) + H_2O(l) + 2\,e^-} \\ \text{cathode:} & \mathrm{2\,MnO_2(s) + H_2O(l) + 2\,e^- \longrightarrow Mn_2O_3(s) + 2\,OH^-(aq)} \\ \hline \text{cell:} & \mathrm{Zn(s) + 2\,MnO_2(s) \longrightarrow ZnO(s) + Mn_2O_3(s)} \qquad E_{\text{cell}} = +1.43\ \text{V} \end{array}$$

An alkaline battery can deliver about three to five times the energy of a zinc-carbon dry cell of similar size. Alkaline batteries are prone to leaking potassium hydroxide, so they should be removed from devices for long-term storage. While some alkaline batteries are rechargeable, most are not. Attempts to recharge an alkaline battery that is not rechargeable often leads to rupture of the battery and leakage of the potassium hydroxide electrolyte.

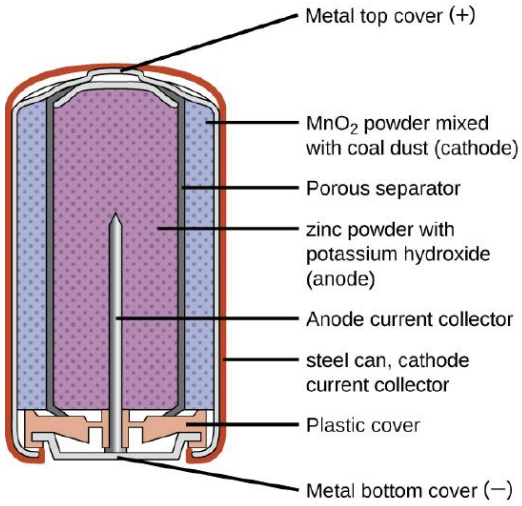


Figure 3.8.3: Alkaline batteries were designed as improved replacements for zinc-carbon (dry cell) batteries.

Link to Learning

Visit this site to learn more about alkaline batteries.

3.8.3.2: Rechargable batteries

Nickel-cadmium, or NiCd, batteries (Figure 3.8.4) consist of a nickel-plated cathode, cadmium-plated anode, and a potassium hydroxide electrode. The positive and negative plates, which are prevented from shorting by the separator, are rolled together and put into the case. This is a "jelly-roll" design and allows the NiCd cell to deliver much more current than a similar-sized alkaline battery. The reactions are

$$\begin{array}{lll} \text{anode:} & \mathrm{Cd(s) + 2\,OH^-(aq) \longrightarrow Cd(OH)_2(s) + 2\,e^-} & \\ \text{cathode:} & \mathrm{NiO_2(s) + 2\,H_2O(l) + 2\,e^- \longrightarrow Ni(OH)_2(s) + 2\,OH^-(aq)} & \\ \hline \text{cell:} & \mathrm{Cd(s) + NiO_2(s) + 2\,H_2O(l) \longrightarrow Cd(OH)_2(s) + Ni(OH)_2(s)} & E_{\text{cell}} \approx +1.2\ \text{V} \end{array}$$

When properly treated, a NiCd battery can be recharged about 1000 times. Cadmium is a toxic heavy metal so NiCd batteries should never be ruptured or incinerated, and they should be disposed of in accordance with relevant toxic waste guidelines.

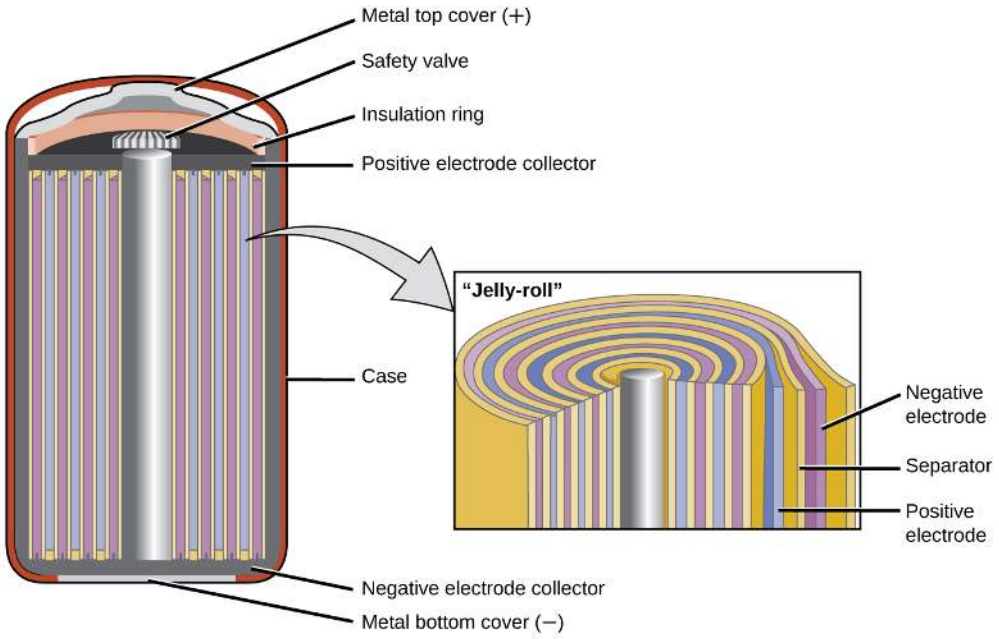


Figure 3.8.4: NiCd batteries use a "jelly-roll" design that significantly increases the amount of current the battery can deliver as compared to a similar-sized alkaline battery.

Link to Learning

Visit this site for more information about nickel cadmium rechargeable batteries.

Lithium ion batteries (Figure 3.8.5) are among the most popular rechargeable batteries and are used in many portable electronic devices. The reactions are

$$\begin{array}{lll} \text{anode:} & \mathrm{LiCoO_2 \longrightarrow Li_{1-x}CoO_2 + x\,Li^+ + x\,e^-} & \\ \text{cathode:} & \mathrm{x\,Li^+ + x\,e^- + x\,C_6 \longrightarrow x\,LiC_6} & \\ \hline \text{cell:} & \mathrm{LiCoO_2 + x\,C_6 \longrightarrow Li_{1-x}CoO_2 + x\,LiC_6} & E_{\text{cell}} \approx +3.7\,\text{V} \end{array}$$

The variable stoichiometry of the cell reaction leads to variation in cell voltages, but for typical conditions, *x* is usually no more than 0.5 and the cell voltage is approximately 3.7 V. Lithium batteries are popular because they can provide a large amount current, are lighter than comparable batteries of other types, produce a nearly constant voltage as they discharge, and only slowly lose their charge when stored.

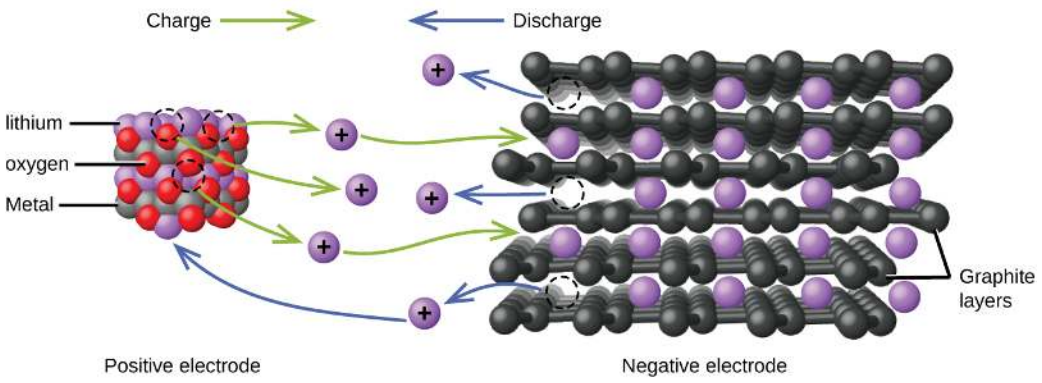


Figure 3.8.5: In a lithium ion battery, charge flows as the lithium ions are transferred between the anode and cathode.

https://chem.libretexts.org/@go/page/516017

Link to Learning

Visit this site for more information about lithium ion batteries.

The lead acid battery (Figure 3.8.6) is the type of secondary battery commonly used in automobiles. It is inexpensive and capable of producing the high current required by automobile starter motors. The reactions for a lead acid battery are

$$\begin{array}{ll} \text{anode:} & \mathrm{Pb(s) + HSO_4^-(aq) \longrightarrow PbSO_4(s) + H^+(aq) + 2\,e^-} \\ \text{cathode:} & \mathrm{PbO_2(s) + HSO_4^-(aq) + 3\,H^+(aq) + 2\,e^- \longrightarrow PbSO_4(s) + 2\,H_2O(l)} \\ \hline \text{cell:} & \mathrm{Pb(s) + PbO_2(s) + 2\,H_2SO_4(aq) \longrightarrow 2\,PbSO_4(s) + 2\,H_2O(l)} \qquad E_{\text{cell}} \approx +2\text{ V} \end{array}$$

Each cell produces 2 V, so six cells are connected in series to produce a 12-V car battery. Lead acid batteries are heavy and contain a caustic liquid electrolyte, $H_2SO_4(aq)$, but are often still the battery of choice because of their high current density. Since these batteries contain a significant amount of lead, they must always be disposed of properly.

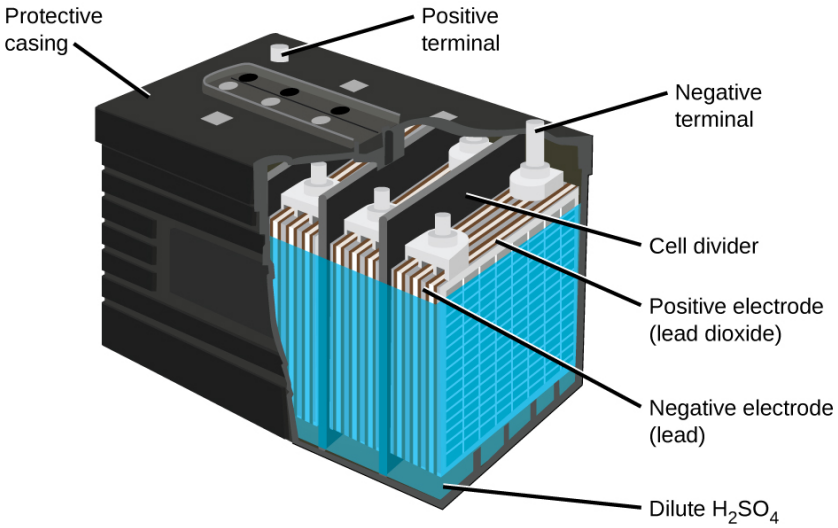


Figure 3.8.6: The lead acid battery in your automobile consists of six cells connected in series to give 12 V.

Link to Learning

Visit this site for more information about lead acid batteries.

3.8.3.3: Fuel cells

A fuel cell is a galvanic cell that uses traditional combustive fuels, most often hydrogen or methane, that are continuously fed into the cell along with an oxidant. (An alternative, but not very popular, name for a fuel cell is a *flow battery*.) Within the cell, fuel and oxidant undergo the same redox chemistry as when they are combusted, but via a catalyzed electrochemical that is significantly more efficient. For example, a typical hydrogen fuel cell uses graphite electrodes embedded with platinum-based catalysts to accelerate the two half-cell reactions:

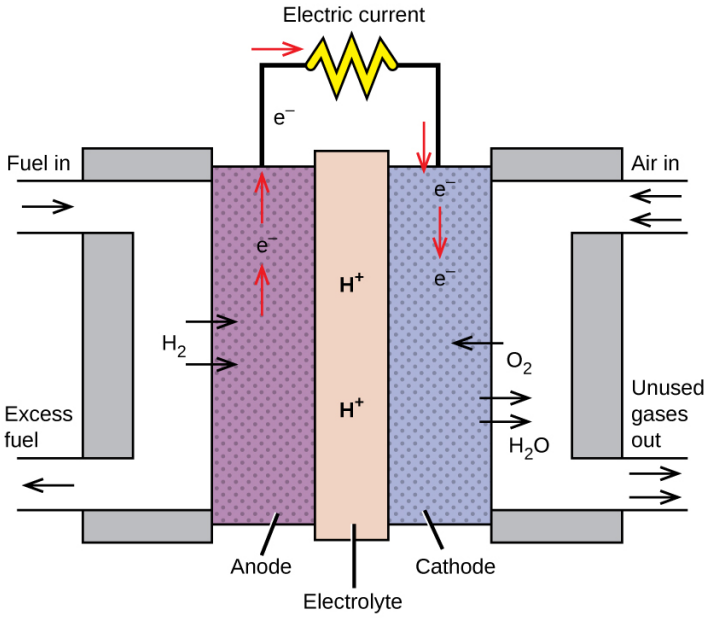


Figure 3.8.7: In this hydrogen fuel cell, oxygen from the air reacts with hydrogen, producing water and electricity.

$$\begin{array}{ll} \text{anode:} & 2\,H_2(g) \longrightarrow 4\,H^+(aq) + 4\,e^- \\ \text{cathode:} & O_2(g) + 4\,H^+(aq) + 4\,e^- \longrightarrow 2\,H_2O(g) \\ \hline \text{cell:} & 2\,H_2(g) + O_2(g) \longrightarrow 2\,H_2O(g) \qquad E_{\text{cell}} \approx +1.2\,\text{V} \end{array}$$

These types of fuel cells generally produce voltages of approximately 1.2 V. Compared to an internal combustion engine, the energy efficiency of a fuel cell using the same redox reaction is typically more than double (~20%–25% for an engine versus ~50%–75% for a fuel cell). Hydrogen fuel cells are commonly used on extended space missions, and prototypes for personal vehicles have been developed, though the technology remains relatively immature.

Link to Learning

Check out this link to learn more about fuel cells.

This page titled 3.8: Redox Examples is shared under a CC BY-NC-SA 4.0 license and was authored, remixed, and/or curated by Jonathan Gutow.

- **2.6: Cellular Phosphorylations** by Kevin Ahern & Indira Rajagopal is licensed CC BY-NC-SA 4.0. Original source: https://biochem.oregonstate.edu/undergraduate/educational-resources.
- **17.5: Batteries and Fuel Cells** by OpenStax is licensed CC BY 4.0. Original source: https://openstax.org/details/books/chemistry-2e.

CHAPTER OVERVIEW

4: Reaction Kinetics

4.1: Reaction Rates and Rate Laws
4.2: Measuring Reaction Rates
4.3: Determining Rate Laws
4.4: Integrated Rate Laws
4.5: Examples of Using Graphs to Determine Reaction Order
4.6: Temperature Dependence of Rate Constants

This page titled 4: Reaction Kinetics is shared under a CC BY-NC-SA 4.0 license and was authored, remixed, and/or curated by Jonathan Gutow.

4.1: Reaction Rates and Rate Laws

4.1.1: The Reaction Rate

The rate of a chemical reaction (or the **reaction rate**) can be defined by the time needed for a change in concentration to occur. But there is a problem in that this allows for the definition to be made based on concentration changes for either the reactants or the products. Plus, due to stoichiometric concerns, the rates at which the concentrations are generally different! Toward this end, the following convention is used.

For a general reaction

$$aA + bB \rightarrow cC + dD$$

the reaction rate can be defined by any of the ratios

$$\text{rate} = -\frac{1}{a}\frac{\Delta[A]}{dt} = -\frac{1}{b}\frac{\Delta[B]}{dt} = +\frac{1}{c}\frac{\Delta[C]}{dt} = +\frac{1}{d}\frac{\Delta[D]}{dt}$$

Or for infinitesimal time intervals

$$\text{rate} = -\frac{1}{a}\frac{d[A]}{dt} = -\frac{1}{b}\frac{d[C]}{dt} = +\frac{1}{c}\frac{d[C]}{dt} = +\frac{1}{d}\frac{d[D]}{dt}$$

Example 4.1.1:

Under a certain set of conditions, the rate of the reaction

$$\mathrm{N_2} + 3\,\mathrm{H_2} \rightarrow 2\,\mathrm{NH_3}$$

the reaction rate is $6.0 \times 10^{-4}\ M/s$. Calculate the time-rate of change for the concentrations of N_2, H_2, and NH_3.

Solution:

Due to the stoichiometry of the reaction,

$$\text{rate} = -\frac{d[N_2]}{dt} = -\frac{1}{3}\frac{d[H_2]}{dt} = +\frac{1}{2}\frac{d[NH_3]}{dt}$$

so

$$\frac{d[N_2]}{dt} = -6.0 \times 10^{-4}\ M/s$$

$$\frac{d[H_2]}{dt} = -2.0 \times 10^{-4}\ M/s$$

$$\frac{d[NH_3]}{dt} = 3.0 \times 10^{-4}\ M/s$$

Note: The time derivatives for the reactants are negative because the reactant concentrations are decreasing, and those of products are positive since the concentrations of products increase as the reaction progresses.

4.1.2: The Rate Law

As shown above, the rate of the reaction can be followed experimentally by measuring the rate of the loss of a reactant or the rate of the production of a product. The rate of the reaction is often related to the concentration of some or all of the chemical species present at a given time. An equation called the *rate law* is used to show this relationship. The rate law **cannot** be predicted by looking at the balanced chemical reaction but must be determined by experiment. For example, the rate law for the reaction

$$\mathrm{Cl_2(g) + CO(g) \rightarrow Cl_2CO(g)}$$

was experimentally determined to be

$$\text{rate} = k[Cl_2]^{3/2}[CO]$$

In this equation, k is the rate constant, and $[Cl_2]$ and $[CO]$ are the molar concentrations of Cl_2 and of CO. Each exponent is called the *order* of the given species. Thus, the rate law is 3/2 order in Cl_2 and first order in CO. The sum of the individual reactant orders is called the **reaction order**. This reaction has a reaction order of 5/2.

4.1.3: Contributors and Attributions

- Patrick E. Fleming (Department of Chemistry and Biochemistry; California State University, East Bay)
- Tom Neils (Grand Rapids Community College)
- J. Gutow (UW Oshkosh)

This page titled 4.1: Reaction Rates and Rate Laws is shared under a CC BY-NC-SA 4.0 license and was authored, remixed, and/or curated by Jonathan Gutow.

- **28.1: The Time Dependence of a Chemical Reaction is Described by a Rate Law** is licensed CC BY-NC-SA 4.0.

4.2: Measuring Reaction Rates

4.2.1: Introduction

Measuring reaction rates requires measuring the concentration of at least one species in a reaction versus time with a time resolution that is small compared to the rate at which the reaction proceeds. Any method of measuring concentration (nuclear magnetic resonance, mass spectrometry, gas chromatography, titration ...) can be used. However, spectroscopy methods are the most common.

4.2.2: Static Methods

In these cases the reaction is run in a container (ideally with stirring to maintain homogeneity). Some method where data can be collected quickly enough is used to monitor the concentration of species in the reaction. For a slow reaction that takes days this might be as simple as extracting a sample every hour and quantifying the concentrations via a titration or a gas chromatography measurement. For reactions that occur in a few minutes modern spectrometers work well if there is an absorbance that can be associated with a single species in the reaction. In this case the measurement depends on the Beer-Lambert Law to convert the absorbance (A) into the concentration of the species (c): $A = \epsilon \ell c$, where ϵ = the molar absorptivity (units: L/mol/cm) and ℓ = the path length through the sample in cm. A cartoon of such a setup is show in figure 4.2.1.

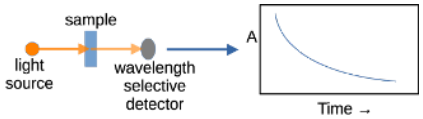


Figure 4.2.1: Cartoon of a spectrometer monitoring absorbance at a particular wavelength versus time. This can be applied in any wavelength range were the species of interest absorb light (UV, Vis, IR, NIR...).

Some absorbance spectroscopy methods can monitor the absorbance of multiple species simultaneously (e.g. NMR, FT-IR, diode-array based UV-Vis). In that case it is sometimes even possible to monitor the concentration of intermediate species formed and used up during the reaction.

4.2.3: Flow Methods

4.2.3.1: Continuous Flow

For reactions that take place in milliseconds, the standard approach since the 1950s has been to employ a flow technique of some kind. An early example was used to study fast gas-phase reactions in which one of the reactants is a free radical such as OH that can be produced by an intense microwave discharge acting on a suitable source gas mixture. This gas, along with the other reactant being investigated, is made to flow through a narrow tube at a known velocity.

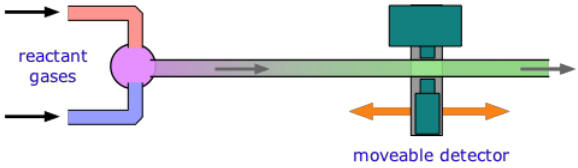


Figure 4.2.1: A continuous flow fast kinetic system.

If the distance between the point at which the reaction is initiated and the product detector is known, then the time interval can be found from the flow rate. By varying this distance, the time required to obtain the maximum yield can then be determined. Although this method is very simple in principle, it can be complicated in practice.

4.2.3.2: Stopped Flow

Owing to the rather large volumes required, continuous flow method is more practical for the study of gas-phase reactions than for solutions, for which the stopped-flow method described below is generally preferred. These are by far the most common means of studying fast solution-phase reactions over time intervals of down to a fraction of a millisecond. The use of reasonably simple devices is now practical even in student laboratory experiments. These techniques make it possible to follow not only changes in the concentrations of reactants and products, but also the buildup and decay of reaction intermediates.

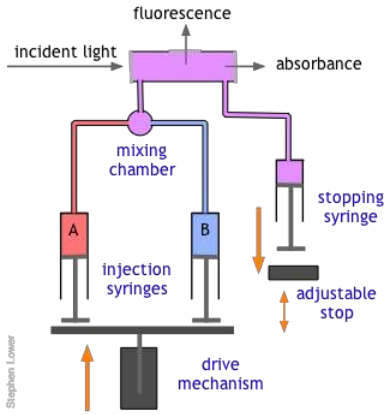


Figure 4.2.2: A stop flow fast kinetic system.

The basic stopped-flow apparatus consists of two or more coupled syringes that rapidly inject the reactants into a small mixing chamber and then through an observation cell that can be coupled to instruments that measure absorption, fluorescence, light scattering, or other optical or electrical properties of the solution. As the solution flows through the cell, it empties into a stopping syringe that, when filled, strikes a backstop that abruptly stops the flow. The volume that the stopping syringe can accept is adjusted so that the mixture in the cell has just become uniform and has reached a steady state; at this point, recording of the cell measurement begins and its change is followed.

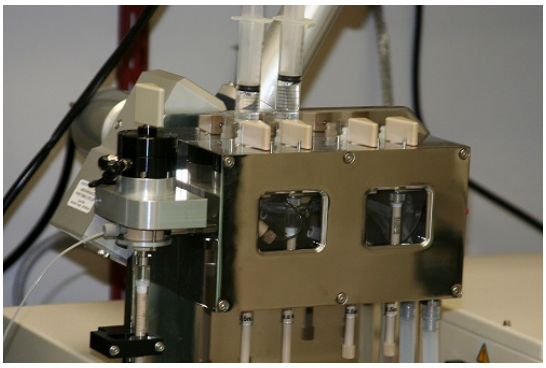


Figure 4.2.3: Stop-flow equipment at a biochemistry research laboratory for measuring rapid reactions and properties such as enzyme kinetics. from Wladimir Labeikovsky.

4.2.3.3: Quenched Flow

In a quenched-flow instrument, the reaction is stopped after a certain amount of time has passed after mixing. The stopping of the reaction is called quenching and it can be achieved by various means, for example by mixing with another solution, which stops the reaction (chemical quenching), quickly lowering the temperature (freeze quenching) or even by exposing the sample to light of a certain wavelength (optical quenching).

Of course, there are many reactions that cannot be followed by changes in light absorption or other physical properties that are conveniently monitored. In such cases, it is often practical to *quench* (stop) the reaction after a desired interval by adding an appropriate quenching agent. For example, an enzyme-catalyzed reaction can be stopped by adding an acid, base, or salt solution that denatures (destroys the activity of) the protein enzyme. Once the reaction has been stopped, the mixture is withdrawn and analyzed in an appropriate manner.

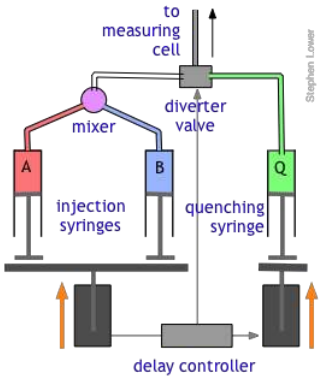


Figure 4.2.4: A quench flow fast kinetic system.

The quenched-flow technique works something like the stopped-flow method described above, with a slightly altered plumbing arrangement. The reactants A and B are mixed and fed directly through the diverter valve to the measuring cell, which is not shown in this diagram. After a set interval that can vary from a few milliseconds to 200 sec or more, the controller activates the quenching syringe and diverter valve, flooding the cell with the quenching solution.

4.2.4: Contributors and Attributions

- J. Gutow (UW Oshkosh)
- **Fast Reactions in Solution** by Stephen Lower is licensed CC BY-NC-SA 4.0. Original source: http://www.chem1.com/acad/webtext/virtualtextbook.html

---

This page titled 4.2: Measuring Reaction Rates is shared under a CC BY-NC-SA 4.0 license and was authored, remixed, and/or curated by Jonathan Gutow.

- **9.10: Fast Reactions in Solution** by Stephen Lower is licensed CC BY-NC-SA 4.0. Original source: http://www.chem1.com/acad/webtext/virtualtextbook.html.
- **28.1: The Time Dependence of a Chemical Reaction is Described by a Rate Law** is licensed CC BY-NC-SA 4.0.

4.3: Determining Rate Laws

4.3.1: Method of Initial Rates

The **method of initial rates** is a commonly used technique for deriving rate laws. As the name implies, the method involves measuring the initial rate of a reaction. The measurement is repeated for several sets of initial concentration conditions to see how the reaction rate varies. This might be accomplished by determining the time needed to exhaust a particular amount of a reactant (preferably one on which the reaction rate does not depend!) A typical set of data for a reaction

$$A + B \rightarrow products$$

might appear as follows:

Run	[A] (M)	[B] (M)	Rate (M/s)
1	0.0100	0.0100	0.0347
2	0.0200	0.0100	0.0694
3	0.0200	0.0200	0.2776

The analysis of this data involves taking the ratios of rates measured where one of the concentrations does not change. For example, assuming a rate law of the form

$$\text{rate} = k[A]^{\alpha}[B]^{\beta} \tag{4.3.1}$$

The ratio of runs i and j generate the following relationship.

$$\frac{\text{rate}_i}{\text{rate}_j} = \frac{k[A]_i^{\alpha}[B]_i^{\beta}}{k[A]_j^{\alpha}[B]_j^{\beta}}$$

So using runs 1 and 2,

$$\frac{0.0347\ M/s}{0.0694\ M/s} = \frac{\cancel{k}(0.01\ M/s)^{\alpha}\ \cancel{(0.01\ M/s)^{\beta}}}{\cancel{k}(0.02\ M/s)^{\alpha}\ \cancel{(0.01\ M/s)^{\beta}}}$$

this simplifies to

$$\frac{1}{2} = \left(\frac{1}{2}\right)^{\alpha}$$

So clearly, $\alpha = 1$ and the reaction is 1st order in A. Taking the ratio using runs 2 and 3 yields

$$\frac{0.0694\ M/s}{0.2776\ M/s} = \frac{\cancel{k}(0.02\ M)^{\alpha}\ \cancel{(0.01\ M)^{\beta}}}{\cancel{k}(0.02\ M)^{\alpha}\ \cancel{(0.02\ M)^{\beta}}}$$

This simplifies to

$$\frac{1}{4} = \left(\frac{1}{2}\right)^{\beta} \tag{4.3.2}$$

By inspection, one can conclude that $\beta = 2$, and that the reaction is second order in B. But if it is not so clear (as it might not be if the concentration is not incremented by a factor of 2), the value of β can be determined by taking the natural logarithm of both sides of the Equation 4.3.2.

$$\ln\frac{1}{4} = \ln\left(\frac{1}{2}\right)^{\beta}$$

$$= \beta \ln\left(\frac{1}{2}\right)$$

dividing both sides by $\ln(1/2)$

$$\frac{\ln\left(\frac{1}{4}\right)}{\ln\left(\frac{1}{2}\right)} = \beta \frac{\ln\left(\frac{1}{2}\right)}{\ln\left(\frac{1}{2}\right)}$$

or

$$\beta = \frac{-1.3863}{-0.69315} = 2$$

And so the rate law (Equation 4.3.1) can be expressed as

$$\text{rate} = k[A][B]^2$$

And is 1st order in A, 2nd order in B, and 3rd order overall. The rate constant can then be evaluated by substituting one of the runs into the rate law (or using all of the data and taking an average). Arbitrarily selecting the first run for this,

$$0.0347\ M/s = k(0.01\ M/s)(0.01\ M/s)^2$$

This results in a value of k

$$k = \frac{0.0347\ M/s}{(0.01\ M/s)(0.01\ M/s)^2} = 3.47 \times 10^5\ M^{-2}s^{-1}$$

It is useful to note that the units on k are consistent with a 3rd order rate law.

4.3.2: Pseudo-order (Isolation) Method

The initial rates method is often combined with the pseudo-order method. In this method all the reagents but one are used in large excess, so that no matter how far the reaction proceeds the concentration change for excess reagents is negligible (their concentrations are constant). This simplifies the interpretation of the data. Consider a reaction with a differential rate law of the form:

$$\text{rate} = k[A]^\alpha[B]^\beta \tag{4.3.3}$$

If B is in large excess then [B] ≈ $[B]_o$ at all times, where $[B]_o$ is the initial concentration of B. This implies that equation 4.3.3 rearranges to:

$$\text{rate} = k[A]^\alpha[B]_o^\beta = (k[B]_o^\beta)[A]^\alpha \tag{4.3.4}$$

The part in parentheses is all constants so can be considered an effective (often called apparent) rate constant, leading to:

$$\text{rate} = k_{app}[A]^\alpha \tag{4.3.5}$$

Taking the natural log of equation 4.3.5 yields:

$$ln(\text{rate}) = ln(k_{app}[A]^\alpha) \implies ln(\text{rate}) = ln(k_{app}) + \alpha ln([A]) \tag{4.3.6}$$

Thus, a plot of ln(rate) versus ln([A]) will be a straight line with the slope being the order with respect to [A], α. Reversing the process by using an excess of A can be used to solve for the order with respect to [B].

The rate constant is also easily extracted from the intercept, $\ln(k_{app})$:

$$ln(k_{app}) = ln(k[B]_o^\beta) \implies e^{ln(k_{app})} = k[B]_o^\beta \implies k = \frac{e^{ln(k_{app})}}{[B]_o^\beta} \tag{4.3.7}$$

Alternatively, the initial rates analysis method using just pairs of concentrations of A to solve for α could be applied, but then requires taking averages to get comparable results.

This method is also often combined with concentration versus time data rather than just the initial rates to determine rate laws.

4.3.3: Contributors and Attributions

- Patrick E. Fleming (Department of Chemistry and Biochemistry; California State University, East Bay)
- J. Gutow (UW Oshkosh)

This page titled 4.3: Determining Rate Laws is shared under a CC BY-NC-SA 4.0 license and was authored, remixed, and/or curated by Jonathan Gutow.

- **11.7: The Method of Initial Rates** by Patrick Fleming is licensed CC BY-NC-SA 4.0.
- **28.1: The Time Dependence of a Chemical Reaction is Described by a Rate Law** is licensed CC BY-NC-SA 4.0.

4.4: Integrated Rate Laws

4.4.1: Introduction

In reaction kinetic investigations the concentration versus time is usually monitored. Differential rate laws only describe the slope (rate of change) of the concentrations, not the concentration versus time. To compare more directly to measured values it is useful to consider **integrated rate laws**, which describe the concentration of species versus time. There are some simple cases where the differential rate laws can be integrated to generate the integrated rate laws.

Combined with pseudo-order (isolation) methods these can often be used to directly fit the observed concentration versus time to verify the order with respect to a particular reagent and extract apparent rate constants that can be combined with the known excess concentrations to extract the rate constant. This can require many fewer experiments than using the initial rates method.

4.4.2: Zeroth order reactions

If the reaction follows a zeroth order rate law, it can be expressed in terms of the time-rate of change of [A] (which will be negative since A is a reactant):

$$-\frac{d[A]}{dt} = k$$

In this case, it is straightforward to separate the variables. Placing time variables on the right and [A] on the left

$$d[A] = -k\,dt$$

In this form, it is easy to integrate. If the concentration of A is $[A]_0$ at time t = 0, and the concentration of A is [A] at some arbitrary time later, the form of the integral is

$$\int_{[A]_o}^{[A]} d[A] = -k\int_{t_o}^{t} dt$$

which yields

$$[A] - [A]_o = -kt$$

or

$$[A] = [A]_o - kt$$

This suggests that a plot of concentration as a function of time will produce a straight line, the slope of which is –k, and the intercept of which is $[A]_0$. If such a plot is linear, then the data are consistent with 0th order kinetics. If they are not, other possibilities must be considered.

4.4.3: First order reactions

A first order rate law would take the form

$$\frac{d[A]}{dt} = k[A]$$

Again, separating the variables by placing all of the concentration terms on the left and all of the time terms on the right yields

$$\frac{d[A]}{[A]} = -k\,dt$$

This expression is also easily integrated as before

$$\int_{[A]=0}^{[A]} \frac{d[A]}{[A]} = -k\int_{t=0}^{t=t} dt$$

Noting that

$$\frac{dx}{x} = d(\ln x)$$

The form of the integrated rate law becomes

$$\ln[A] - \ln[A]_o = kt$$

or

$$\ln[A] = \ln[A]_o - kt \tag{4.4.1}$$

This form implies that a plot of the natural logarithm of the concentration is a linear function of the time. And so a plot of ln[A] as a function of time should produce a linear plot, the slope of which is -k, and the intercept of which is $\ln[A]_0$.

It should also be noted that the integrated rate law (Equation 4.4.1) can be rewritten in exponential form by taking the exponetial of both sides:

$$[A] = [A]_o e^{-kt} \tag{4.4.2}$$

Because of this functional form, 1st order kinetics are sometimes referred to as exponential decay kinetics. Many processes, including radioactive decay of nuclides follow this type of rate law.

Note

With modern non-linear least squares fitting tools **data is best fit directly to equation** 4.4.2 rather than fitting ln[A] versus t with a line, which over emphasizes noise at later times.

If the goal is just to quickly determine if the order with respect to [A] is 1 (or close to it), then plotting ln[A] versus t to see if it looks linear is still reasonable.

Example 4.4.1:

Consider the following kinetic data. Use a graph to demonstrate that the data are consistent with first order kinetics. Also, if the data are first order, determine the value of the rate constant for the reaction.

Time (s)	0	10	20	50	100	150	200	250	300
[A] (M)	0.873	0.752	0.648	0.414	0.196	0.093	0.044	0.021	0.010

Solution

Plots of a direct fit to an exponential and the linearized version show how using the exponential is better:

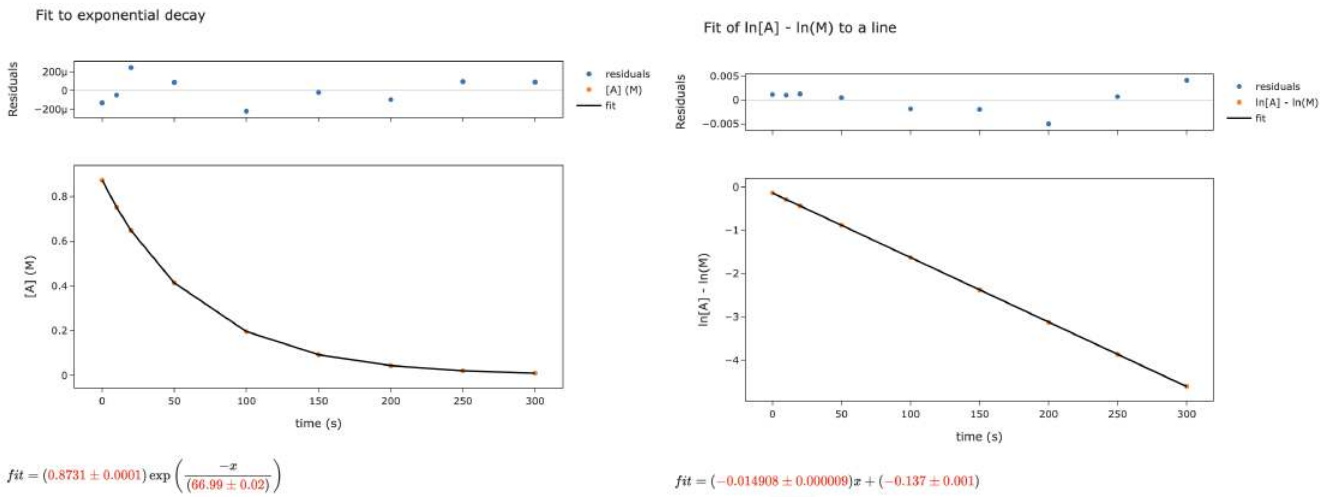


Figure 4.4.1: Comparison of fitting data from a first order process to an exponential and fitting the data to a line after taking the natural log. Note that in the natural log case the y-axis is actually a plot of the log of just the numeric part of the concentration. This is indicated by labeling the axis with ln[A]-ln(M) = ln(X.XX•M) - ln(M) = ln(X.XX) + ln(M) - ln(M) = ln(X.XX). Thus the graph is "offset" by whatever the value of ln(M) is, where 'M' stands for molarity.

From the exponential plot k= (0.014928 ± 0.000004) s^{-1} (the inverse of 66.99) and $[A]_o$ = (0.8731 ± 0.0001) M. From the linear fit k = (0.014908 ± 0.000009) s^{-1}, which is less certain than from the exponential fit. You can also see from the residuals in the linear fit that the disagreement between the fit and the experimental values is worse at long times than it is for the exponential fit.

4.4.4: Second order reactions

If the reaction follows a second order rate law, similar methodology can be employed. The rate can be written as

$$-\frac{d[A]}{dt} = k[A]^2 \tag{4.4.3}$$

The separation of concentration and time terms (this time keeping the negative sign on the left for convenience) yields

$$-\frac{d[A]}{[A]^2} = k\,dt$$

The integration then becomes

$$-\int_{[A]_o}^{[A]} \frac{d[A]}{[A]^2} = \int_{t=0}^{t} k\,dt \tag{4.4.4}$$

And noting that

$$-\frac{dx}{x^2} = d\left(\frac{1}{x}\right)$$

the result of integration Equation 4.4.4 is

$$\frac{1}{[A]} - \frac{1}{[A]_o} = kt$$

or

$$\frac{1}{[A]} = \frac{1}{[A]_o} + kt$$

And so a plot of $1/[A]$ as a function of time should produce a linear plot, the slope of which is k, and the intercept of which is $1/[A]_0$.

Other 2nd order rate laws are a little bit trickier to integrate, as the integration depends on the actual stoichiometry of the reaction being investigated. For example, for a reaction of the type

$$A + B \rightarrow P$$

If this has a simple second order rate law that depends in first order on each of the reactants

$$-\frac{d[A]}{dt} = k[A][B]$$

and

$$-\frac{d[B]}{dt} = k[A][B]$$

the integration will depend on the decrease of [A] and [B] (which will be related by the stoichiometry) which can be expressed in terms the concentration of the product [P].

$$[A] = [A]_o - [P] \tag{4.4.5}$$

and

$$[B] = [B]_o - [P] \tag{4.4.6}$$

The concentration dependence on A and B can then be eliminated if the rate law is expressed in terms of the production of the product.

$$\frac{d[P]}{dt} = k[A][B] \tag{4.4.7}$$

Substituting the relationships for $[A]$ and $[B]$ (Equations 4.4.5 and 4.4.6) into the rate law expression (Equation 4.4.7) yields

$$\frac{d[P]}{dt} = k([A]_o - [P])([B]_o - [P]) \tag{4.4.8}$$

Separation of concentration and time variables results in

$$\frac{d[P]}{([A]_o - [P])([B]_o - [P])} = k\,dt$$

Noting that at time $t = 0$, $[P] = 0$, the integrated form of the rate law can be generated by solving the integral

$$\int_{[A]_o}^{[A]} \frac{d[P]}{([A]_o - [P])([B]_o - [P])} = \int_{t=0}^{t} k\,dt$$

Consulting a table of integrals reveals that for $a \neq b$, [1]

$$\int \frac{dx}{(a-x)(b-x)} = \frac{1}{b-a}\ln\left(\frac{b-x}{a-x}\right)$$

Applying the definite integral (as long as $[A]_0 \neq [B]_0$) results in

$$\frac{1}{[B]_0 - [A]_0}\ln\left(\frac{[B]_0 - [P]}{[A]_0 - [P]}\right)\Bigg|_0^{[A]} = k\,t\Big|_0^t$$

$$\frac{1}{[B]_0 - [A]_0}\ln\left(\frac{[B]_0 - [P]}{[A]_0 - [P]}\right) - \frac{1}{[B]_0 - [A]_0}\ln\left(\frac{[B]_0}{[A]_0}\right) = k\,t \tag{4.4.9}$$

Substituting Equations 4.4.5 and 4.4.6 into Equation 4.4.9 and simplifying (combining the natural logarithm terms) yields

$$\frac{1}{[B]_0 - [A]_0}\ln\left(\frac{[B][A]_o}{[A][B]_o}\right) = kt$$

For this rate law, a plot of $\ln([B]/[A])$ as a function of time will produce a straight line, the slope of which is

$$m = ([B]_0 - [A]_0)k.$$

In the limit at $[A]_0 = [B]_0$, then $[A] = [B]$ at all times, due to the stoichiometry of the reaction. As such, the rate law becomes

$$\text{rate} = k[A]^2$$

which integrates as shown before to

$$\frac{1}{[A]} = \frac{1}{[A]_o} + kt$$

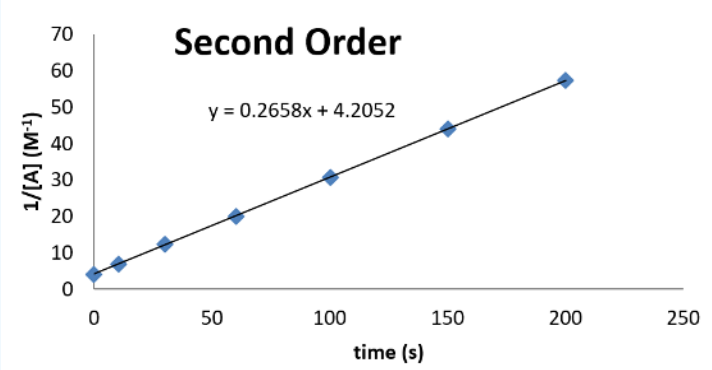
Example 4.4.2: Confirming Second Order Kinetics

Consider the following kinetic data. Use a graph to demonstrate that the data are consistent with second order kinetics. Also, if the data are second order, determine the value of the rate constant for the reaction.

time (s)	0	10	30	60	100	150	200
[A] (M)	0.238	0.161	0.098	0.062	0.041	0.029	0.023

Solution

The plot looks as follows:



From this plot, it can be seen that the rate constant is 0.2658 M^{-1} s^{-1}. The concentration at time $t = 0$ can also be inferred from the intercept.

4.4.5: Contributors and Attributions

- Patrick E. Fleming (Department of Chemistry and Biochemistry; California State University, East Bay)
- J. Gutow (UW Oshkosh)

1. This integral form can be generated by using the method of partial fractions. See (House, 2007) for a full derivation.

This page titled 4.4: Integrated Rate Laws is shared under a CC BY-NC-SA 4.0 license and was authored, remixed, and/or curated by Jonathan Gutow.

- **11.4: 0th order Rate Law** by Patrick Fleming is licensed CC BY-NC-SA 4.0.
- **11.5: 1st order rate law** by Patrick Fleming is licensed CC BY-NC-SA 4.0.
- **11.6: 2nd order Rate Laws** by Patrick Fleming is licensed CC BY-NC-SA 4.0.
- **28.1: The Time Dependence of a Chemical Reaction is Described by a Rate Law** is licensed CC BY-NC-SA 4.0.

4.5: Examples of Using Graphs to Determine Reaction Order

Learning Objectives

- To use graphs to analyze the kinetics of a reaction.

You learned that the integrated rate law for each common type of reaction (zeroth, first, or second order in a single reactant) can be plotted as a straight line. Using these plots offers an alternative to the methods described for showing how reactant concentration changes with time and determining reaction order. We will illustrate the use of these graphs by considering the thermal decomposition of NO_2 gas at elevated temperatures, which occurs according to the following reaction:

$$2NO_2(g) \xrightarrow{\Delta} 2NO(g) + O_2(g) \tag{4.5.1}$$

Experimental data for this reaction at 330°C are listed in Table 4.5.1; they are provided as $[NO_2]$, $\ln[NO_2]$, and $1/[NO_2]$ versus time to correspond to the integrated rate laws for zeroth-, first-, and second-order reactions, respectively.

Table 4.5.1: Concentration of NO_2 as a Function of Time at 330°C

Time (s)	$[NO_2]$ (M)	$\ln[NO_2]$	$1/[NO_2]$ (M^{-1})
0	1.00×10^{-2}	−4.605	100
60	6.83×10^{-3}	−4.986	146
120	5.18×10^{-3}	−5.263	193
180	4.18×10^{-3}	−5.477	239
240	3.50×10^{-3}	−5.655	286
300	3.01×10^{-3}	−5.806	332
360	2.64×10^{-3}	−5.937	379

The actual concentrations of NO_2 are plotted versus time in part (a) in Figure 4.5.1. Because the plot of $[NO_2]$ versus t is not a straight line, we know the reaction is not zeroth order in NO_2. A plot of $\ln[NO_2]$ versus t (part (b) in Figure 4.5.1) shows us that the reaction is not first order in NO_2 because a first-order reaction would give a straight line. Having eliminated zeroth-order and first-order behavior, we construct a plot of $1/[NO_2]$ versus t (part (c) in Figure 4.5.1). This plot is a straight line, indicating that the reaction is second order in NO_2.

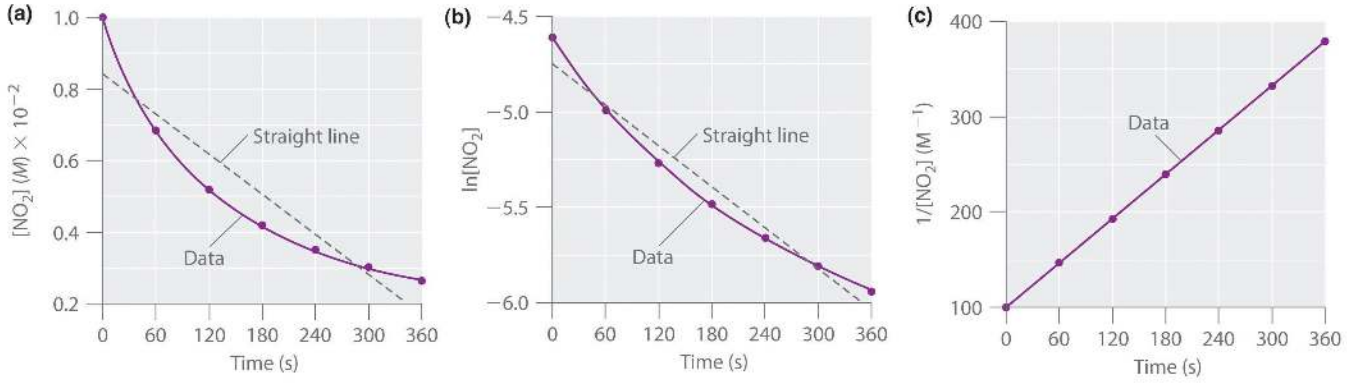


Figure 4.5.1: The Decomposition of NO_2. These plots show the decomposition of a sample of NO_2 at 330°C as (a) the concentration of NO_2 versus t, (b) the natural logarithm of $[NO_2]$ versus t, and (c) $1/[NO_2]$ versus t.

We have just determined the reaction order using data from a single experiment by plotting the concentration of the reactant as a function of time. Because of the characteristic shapes of the lines shown in Figure 4.5.2, the graphs can be used to determine the reaction order of an unknown reaction. In contrast, the method of initial rates required multiple experiments at different NO_2 concentrations as well as accurate initial rates of reaction, which can be difficult to obtain for rapid reactions.

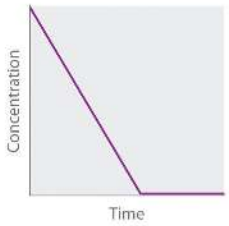
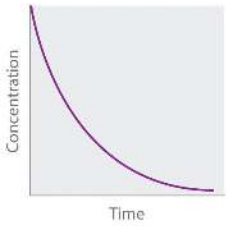
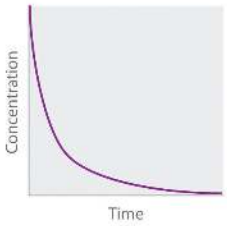
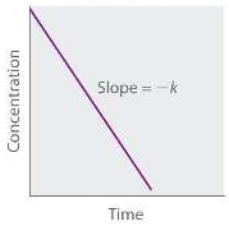
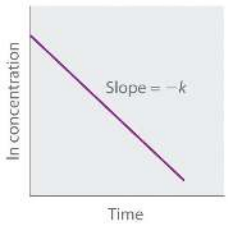
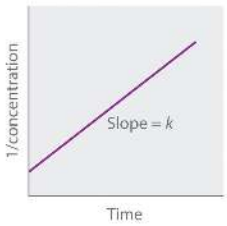
	Zeroth Order	First Order	Second Order
Differential rate law	$\text{Rate} = -\frac{\Delta[A]}{\Delta t} = k$	$\text{Rate} = -\frac{\Delta[A]}{\Delta t} = k[A]$	$\text{Rate} = -\frac{\Delta[A]}{\Delta t} = k[A]^2$
Concentration vs. time			
Integrated rate law	$[A] = [A]_0 - kt$	$[A] = [A]_0 e^{-kt}$ or $\ln[A] = \ln[A]_0 - kt$	$\frac{1}{[A]} = \frac{1}{[A]_0} + kt$
Straight-line plot to determine rate constant			
Relative rate vs. concentration	[A], *M* / Rate, M/s 1 / 1 2 / 1 3 / 1	[A], *M* / Rate, M/s 1 / 1 2 / 2 3 / 3	[A], *M* / Rate, M/s 1 / 1 2 / 4 3 / 9
Half-life	$t_{1/2} = \frac{[A]_0}{2k}$	$t_{1/2} = \frac{0.693}{k}$	$t_{1/2} = \frac{1}{k[A]_0}$
Units of *k*, rate constant	M/s	1/s	$M^{-1}\cdot s^{-1}$

Figure 4.5.2: Properties of Reactions That Obey Zeroth-, First-, and Second-Order Rate Laws

Example 4.5.1

Dinitrogen pentoxide (N_2O_5) decomposes to NO_2 and O_2 at relatively low temperatures in the following reaction:

$$2N_2O_5(soln) \rightarrow 4NO_2(soln) + O_2(g)$$

This reaction is carried out in a CCl_4 solution at 45°C. The concentrations of N_2O_5 as a function of time are listed in the following table, together with the natural logarithms and reciprocal N_2O_5 concentrations. Plot a graph of the concentration versus *t*, ln concentration versus *t*, and 1/concentration versus *t* and then determine the rate law and calculate the rate constant.

Time (s)	$[N_2O_5]$ (M)	$\ln[N_2O_5]$	$1/[N_2O_5]$ (M^{-1})
0	0.0365	−3.310	27.4
600	0.0274	−3.597	36.5
1200	0.0206	−3.882	48.5
1800	0.0157	−4.154	63.7
2400	0.0117	−4.448	85.5

Time (s)	$[N_2O_5]$ (M)	$\ln[N_2O_5]$	$1/[N_2O_5]$ (M^{-1})
3000	0.00860	−4.756	116
3600	0.00640	−5.051	156

Given: balanced chemical equation, reaction times, and concentrations

Asked for: graph of data, rate law, and rate constant

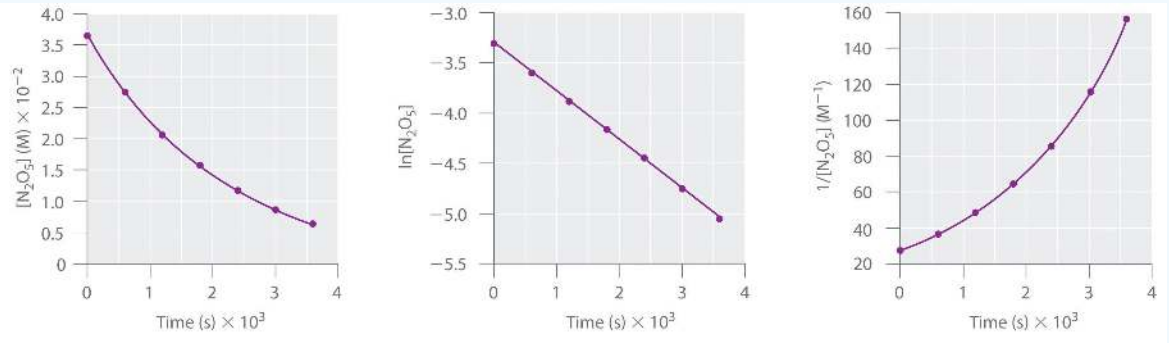
Strategy:

A Use the data in the table to separately plot concentration, the natural logarithm of the concentration, and the reciprocal of the concentration (the vertical axis) versus time (the horizontal axis). Compare the graphs with those in Figure 4.5.1 to determine the reaction order.

B Write the rate law for the reaction. Using the appropriate data from the table and the linear graph corresponding to the rate law for the reaction, calculate the slope of the plotted line to obtain the rate constant for the reaction.

Solution

A Here are plots of $[N_2O_5]$ versus t, $\ln[N_2O_5]$ versus t, and $1/[N_2O_5]$ versus t:



The plot of $\ln[N_2O_5]$ versus t gives a straight line, whereas the plots of $[N_2O_5]$ versus t and $1/[N_2O_5]$ versus t do not. This means that the decomposition of N_2O_5 is first order in $[N_2O_5]$.

B The rate law for the reaction is therefore

$$\text{rate} = k[N_2O_5]$$

Calculating the rate constant is straightforward because we know that the slope of the plot of ln[A] versus t for a first-order reaction is $-k$. We can calculate the slope using any two points that lie on the line in the plot of $\ln[N_2O_5]$ versus t. Using the points for t = 0 and 3000 s,

$$\begin{aligned}\text{slope} &= \frac{\ln[N_2O_5]_{3000} - \ln[N_2O_5]_0}{3000\ \text{s} - 0\ \text{s}} \\ &= \frac{(-4.756) - (-3.310)}{3000\ \text{s}} \\ &= -4.820 \times 10^{-4}\ \text{s}^{-1}\end{aligned}$$

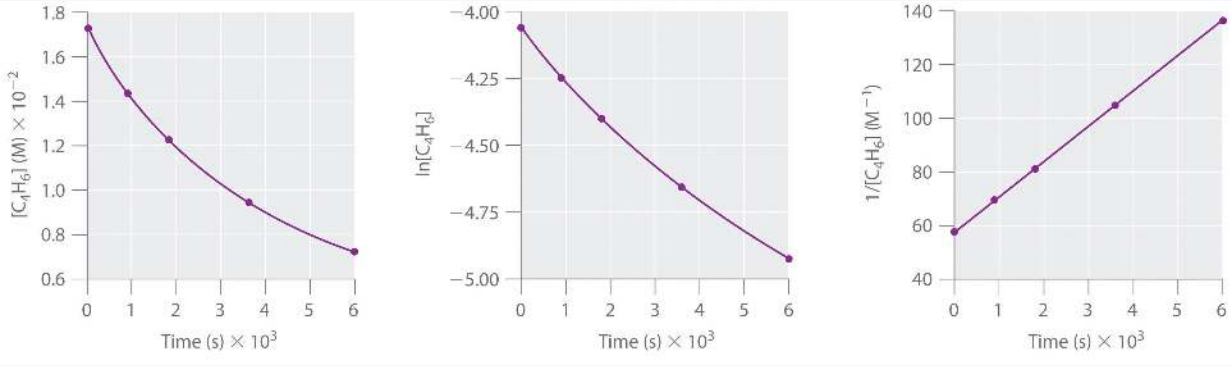
Thus $k = 4.820 \times 10^{-4}\ s^{-1}$.

? Exercise 4.5.1

1,3-Butadiene (CH_2=CH—CH=CH_2; C_4H_6) is a volatile and reactive organic molecule used in the production of rubber. Above room temperature, it reacts slowly to form products. Concentrations of C_4H_6 as a function of time at 326°C are listed in the following table along with $\ln[C_4H_6]$ and the reciprocal concentrations. Graph the data as concentration versus t, ln concentration versus t, and 1/concentration versus t. Then determine the reaction order in C_4H_6, the rate law, and the rate constant for the reaction.

Time (s)	$[C_4H_6]$ (M)	$\ln[C_4H_6]$	$1/[C_4H_6]$ (M^{-1})
0	1.72×10^{-2}	−4.063	58.1
900	1.43×10^{-2}	−4.247	69.9
1800	1.23×10^{-2}	−4.398	81.3
3600	9.52×10^{-3}	−4.654	105
6000	7.30×10^{-3}	−4.920	137

Answer



second order in C_4H_6; rate = $k[C_4H_6]^2$; $k = 1.3 \times 10^{-2}\ M^{-1}{\cdot}s^{-1}$

4.5.1: Summary

For a zeroth-order reaction, a plot of the concentration of any reactant versus time is a straight line with a slope of $-k$. For a first-order reaction, a plot of the natural logarithm of the concentration of a reactant versus time is a straight line with a slope of $-k$. For a second-order reaction, a plot of the inverse of the concentration of a reactant versus time is a straight line with a slope of k.

This page titled 4.5: Examples of Using Graphs to Determine Reaction Order is shared under a CC BY-NC-SA 4.0 license and was authored, remixed, and/or curated by Jonathan Gutow.

- **5.7: Using Graphs to Determine Integrated Rate Laws** by Anonymous is licensed CC BY-NC-SA 4.0.

4.6: Temperature Dependence of Rate Constants

In general, increases in temperature increase the rates of chemical reactions. It is easy to see why, since most chemical reactions depend on molecular collisions. The frequency with which molecules collide increases with increased temperature. But also, the kinetic energy of the molecules increases, which should increase the probability that a collision event will lead to a reaction. An empirical model was proposed by Arrhenius to account for this phenomenon. The **Arrhenius model** (Arrhenius, 1889) can be expressed as

$$k = Ae^{-E_a/RT} \tag{4.6.1}$$

Although the model is empirical, some of the parameters can be interpreted in terms of the energy profile of the reaction. E_a, for example, is the **activation energy**, which represents the energy barrier that must be overcome in a collision to lead to a reaction.

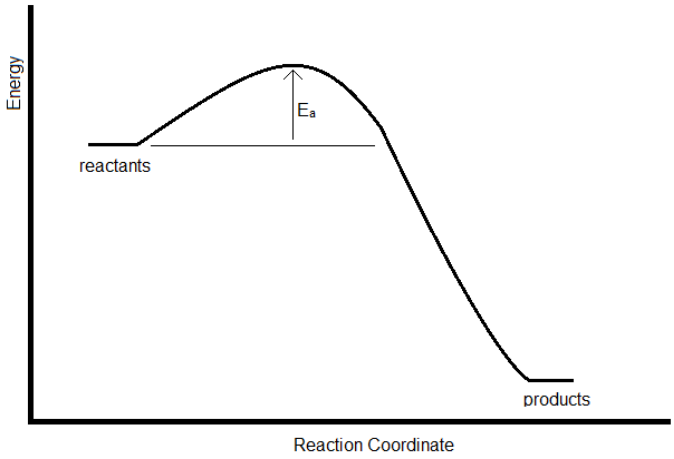


Figure 4.6.1: Reaction profile for an elementary step over an activated barrier of height E_a.

If the rate constant for a reaction is measured at two temperatures, the activation energy can be determined by taking the ratio. This leads to the following expression for the Arrhenius model:

$$\ln\left(\frac{k_1}{k_2}\right) = -\frac{E_a}{R}\left(\frac{1}{T_2} - \frac{1}{T_1}\right) \tag{4.6.2}$$

Example 4.6.1:

For a given reaction, the rate constant doubles when the temperature is increased form 25 °C to 35 °C. What is the Arrhenius activation energy for this reaction?

Solution

The energy of activation can be calculated from the Arrhenius Equation (Equation 4.6.2).

$$\ln\left(\frac{2k_1}{k_1}\right) = -\frac{E_a}{8.314\ \frac{J}{mol\ K}}\left(\frac{1}{308\ K} - \frac{1}{298\ K}\right)$$

From this reaction:

$$E_a = 52.9\ kJ/mol$$

Preferably, the rate constant is measured at several temperatures. Then the activation energy can be determined using all of the measurements by fitting them to a function. In this case E_a can be calculated from the derivative of the fitting function:

$$E_a = \frac{RT^2}{k}\frac{dk}{dT} = RT^2\frac{dlnk}{dT} \tag{4.6.3}$$

Derivation of general expression for E_a

Equation 4.6.3 is derived by taking the derivative with respect to temperature of the Arrhenius equation (4.6.1):

$$\frac{dk}{dT} = \left(\frac{d}{dT}\right) Ae^{-E_a/RT} = \frac{E_a Ae^{-\frac{E_a}{RT}}}{RT^2} \tag{4.6.4}$$

The blue part in 4.6.4 is just k. So this can be rewritten as:

$$\frac{dk}{dT} = \frac{kE_a}{RT^2} \tag{4.6.5}$$

Solving for E_a:

$$E_a = \frac{RT^2}{k}\frac{dk}{dT} = RT^2\frac{dlnk}{dT} \tag{4.6.6}$$

If E_a is temperature independent then a linear fit to the ln(k) versus 1/T can be used:

$$\ln(k) = -\frac{E_a}{RT} + \ln(A)$$

This can be done graphically by plotting the natural logarithm of the rate constant as a function of $1/T$ (with the temperature measured in K). For a well-behaved reactions over limited temperature ranges the result will be a line with a slope of $-E_a/R$.

There are some theoretical models (such as collision theory and transition state theory) which suggest the form of the Arrhenius model, but the model itself is purely empirical. A general feature, however, of the theoretical approaches is to interpret the activation energy as an energy barrier which a reaction must overcome in order to lead to a chemical reaction.

4.6.1: Contributors and Attributions

- Patrick E. Fleming (Department of Chemistry and Biochemistry; California State University, East Bay)
- J. Gutow (UW Oshkosh)

This page titled 4.6: Temperature Dependence of Rate Constants is shared under a CC BY-NC-SA 4.0 license and was authored, remixed, and/or curated by Jonathan Gutow.

- **11.9: Temperature Dependence** by Patrick Fleming is licensed CC BY-NC-SA 4.0.
- **28.1: The Time Dependence of a Chemical Reaction is Described by a Rate Law** is licensed CC BY-NC-SA 4.0.

CHAPTER OVERVIEW

5: Kinetic Mechanisms 1

5.1: Reaction Mechanisms
5.2: Relaxation Methods
5.3: Representative Reaction Mechanisms
5.4: The Rate Determining Step Approximation
5.5: The Equilibrium Approximation
5.6: The Steady-State Approximation

This page titled 5: Kinetic Mechanisms 1 is shared under a CC BY-NC-SA 4.0 license and was authored, remixed, and/or curated by Jonathan Gutow.

5.1: Reaction Mechanisms

A **reaction mechanism** is a set of **elementary reaction** steps, that when taken in aggregate define a chemical pathway that connects reactants to products. An elementary reaction is one that proceeds by a single process, such a molecular (or atomic) decomposition or a molecular collision. Typically, elementary reactions only come in **unimolecular**

$$A \rightarrow products$$

and **bimolecular**

$$A + B \rightarrow products$$

form. Occasionally, an elementary step that is **termolecular** (involving the simultaneous collision of three atoms or molecules)

$$A + B + C \rightarrow products$$

is postulated, but generally can be explained equally well as a pair of bimolecular steps acting in rapid succession, the first forming an energized complex, and the second stabilizing that complex chemically or physically.

$$A + B \rightarrow AB^*$$

$$AB^* + C \rightarrow AB + C^*$$

The wonderful property of elementary reactions is that the **molecularity** defines the order of the rate law for the reaction step.

The Requirements of a Reaction Mechanism

A valid reaction mechanism must satisfy three important criteria:

1. The sum of the steps must yield the overall stoichiometry of the reaction.
2. The mechanism must be consistent with the observed kinetics for the overall reaction.
3. The mechanism must account for the possibility of any observed side products formed in the reaction.

Example 5.1.1:

For the reaction

$$A + B \rightarrow C$$

is the following proposed mechanism valid?

$$A + A \xrightarrow{k_1} A_2$$

$$A_2 + B \xrightarrow{k_1} C + A$$

Solution

Adding both proposed reactions gives

$$2A + \cancel{A_2} + B \rightarrow \cancel{A_2} + C + \cancel{A}$$

Canceling those species that appear on both sides of the arrow leaves

$$A + B \rightarrow C$$

which is the reaction, so the mechanism is at least stoichiometrically valid. However, it would still have to be consistent with the observed kinetics for the reaction and account for any side-products that are observed.

This page titled 5.1: Reaction Mechanisms is shared under a CC BY-NC-SA 4.0 license and was authored, remixed, and/or curated by Jonathan Gutow.

- **12.1: Reaction Mechanisms** by Patrick Fleming is licensed CC BY-NC-SA 4.0.

5.2: Relaxation Methods

5.2.1: Explanation and Theory

Many reactions, especially those that take place in solution, occur too rapidly to follow by flow techniques, and can therefore only be observed when they are already at equilibrium. The classical examples of such reactions are two of the fastest ones ever observed, the dissociation of water

$$2H_2O \rightarrow H_3O^+ + OH^-$$

and the formation of the triiodide ion in aqueous solution

$$I^- + I_2 \rightarrow I_3^-$$

Reactions of these kinds could not be studied until the mid-1950s when techniques were developed to shift the equilibrium by imposing an abrupt physical change on the system.

For example, if the reaction A $\underset{k_{-1}}{\overset{k_1}{\rightleftharpoons}}$ B is endothermic, then according to the Le Chatelier principle, subjecting the system to a rapid jump in temperature will shift the equilibrium state to one in which the product B has a higher concentration. The composition of the system will than begin to shift toward the new equilibrium composition at a rate determined by the kinetics of the process. For this simple equilibrium, which is unimolecular in both directions, this can easily be interpreted in terms of a time dependent quantity x_t = the distance to the new equilibrium (at t = 0, $|x_t|$ is at its maximum). Representing the time dependent concentrations as $[A]_t$ and $[B]_t$ while using $[A]_e$ and $[B]_e$ as the new equilibrium concentrations we can write the time dependent concentrations in terms of x_t.

$$[A]_t = [A]_e + x_t \tag{5.2.1}$$

$$[B]_t = [B]_e - x_t \tag{5.2.2}$$

The rate laws for this equilibrium are:

$$\frac{d[A]_t}{dt} = -k_1[A]_t + k_{-1}[B]_t \tag{5.2.3}$$

$$\frac{d[B]_t}{dt} = k_1[A]_t - k_{-1}[B]_t \tag{5.2.4}$$

or

$$\text{rate} = -\frac{d[A]_t}{dt} = \frac{d[B]_t}{dt} = k_1[A]_t - k_{-1}[B]_t \tag{5.2.5}$$

Substituting into equation 5.2.5 the expressions for $[A]_t$ and $[B]_t$ (equations 5.2.1 and 5.2.2) in terms of x_t yields:

$$\text{rate} = -\frac{d([A]_e + x_t)}{dt} = k_1([A]_e + x_t) - k_{-1}([B]_e - x_t) \tag{5.2.6}$$

Recognizing that $\frac{d[A]_e}{dt} = 0$ because $[A]_e$ is a constant simplifies this to:

$$\text{rate} = -\frac{dx_t}{dt} = k_1[A]_e + k_1x_t - k_{-1}[B]_e + k_{-1}x_t \tag{5.2.7}$$

For any reaction at equilibrium the rate equals 0. Using the first rate law (equation 5.2.3) as an example:

$$\frac{d[A]_t}{dt} = 0 = -k_1[A]_e + k_{-1}[B]_e \tag{5.2.8}$$

which can be rearranged to:

$$k_{-1}[B]_e = k_1[A]_e \tag{5.2.9}$$

or

$$K_{eq} = \frac{[B]_e}{[A]_e} = \frac{k_1}{k_{-1}} \tag{5.2.10}$$

the concentration equilibrium constant. This relation between the concentration equilibrium constant and the ratios of the forward and reverse reactions is generally true for all reactions.

$k_{-1}[B]_e = k_1[A]_e$ (equation 5.2.9) can be used to replace $k_{-1}[B]_e$ in equation 5.2.7 yielding:

$$-\frac{dx_t}{dt} = k_1[A]_e + k_1 x_t - k_1[A]_e + k_{-1}x_t \tag{5.2.11}$$

which simplifies to:

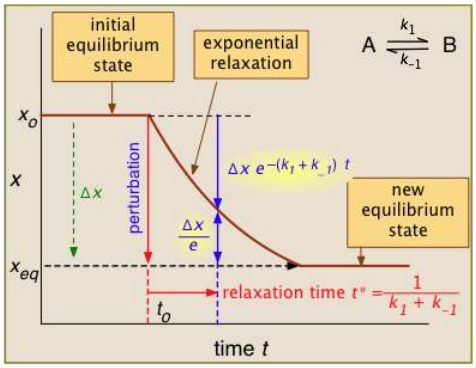
$$-\frac{dx_t}{dt} = k_1 x_t + k_{-1}x_t \implies \frac{dx_t}{dt} = -(k_1 + k_{-1})x_t \tag{5.2.12}$$

We recognize this as a first order process with the solution:

$$x_t = x_o exp\left(-(k_1 + k_{-1})t\right) = x_o exp\left(\frac{-t}{\tau}\right) \tag{5.2.13}$$

where $\tau = \frac{1}{k_1 + k_{-1}}$.

Although this derivation is for the unimolecular case, it can be shown that as long as x_o is small first order kinetics will be observed for reactions of other molecularities (see for example: 2.1.4: Relaxation Methods, but be aware there are many typos despite the correct conclusions). The cartoon below illustrates what data may look like.



Fitting the exponential decay directly yields τ. The measurements also give us K_{eq} (equation 5.2.10, the ratio of the two rate constants). This gives us two equations in two unknowns. It is left to the reader to show that these can be solved for the two rate constants yielding:

$$k_1 = \frac{K_{eq}}{(1 + K_{eq})\tau} \qquad k_{-1} = \frac{1}{(1 + K_{eq})\tau}$$

Similar analyses for higher order reactions yield somewhat more complicated expressions.

5.2.2: Examples

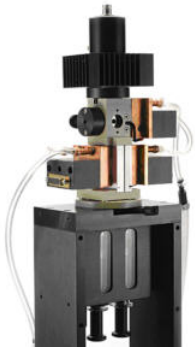
5.2.2.1: Temperature jumps



Manfred Eigen

This is the method that Manfred Eigen (Germany, 1927-) pioneered when, in the early 1960's, he measured the rate constant of what was then the fastest reaction ever observed:

$$H^+ + OH^- \rightarrow H_2O \quad k = 1.3 \times 10^{11}\ M^{-1}\ sec^{-1}$$



BioLogic rapid-mixing T-Jump System

Some ways of acheiving temperature jumps:

- **high-voltage electric discharge**: A capacitor, charged to 5-10 kV, is discharged through a solution to which an electrolyte has been added to provide a conductive path.
- **laser irradiation**: The sample is irradiated with a laser whose wavelength corresponds to an absorption peak in the sample. Infrared lasers are often used for this purpose.
- **mixing of two pre-equilibrated solutions**: Two solutions, otherwise identical but at different temperatures, are rapidly mixed in a stopped-flow type of apparatus. Although this method is not as fast, it has the advantage of allowing both negative and positive T-jumps. The device shown here uses 0.1-mL samples and provides jumps of up to ±40 C° over a few microseconds. Observation times, however, are limited to 1-2 milliseconds owing to thermal dissipation.

5.2.2.2: Pressure jumps

According to the Le Chatelier principle, a change in the applied pressure will shift the equilibrium state of any reaction which involves a change in the volume of a system. Aside from the obvious examples associated with changes in the number of moles of gases, there are many more subtle cases involving formation of complexes, hydration shells and surface adsorption, and phase changes. One area of considerable interest is the study of protein folding, which has implications in diseases such as Parkinson's and Alzheimer's.

The pressure-jump is applied to the cell through a flexible membrane that is activated by a high-pressure gas supply, or through an electrically-actuated piezoelectric crystal. This can produce P-jumps of around 1 GPa over sub-millisecond time intervals.

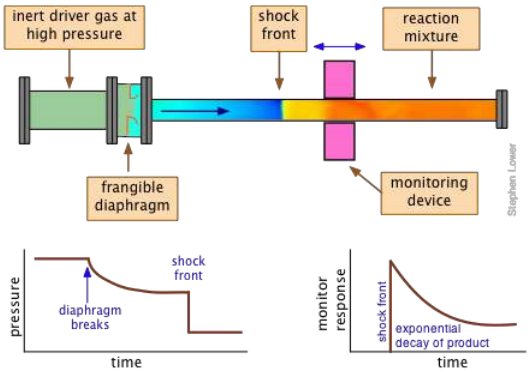
5.2.2.3: Shock tubes: extreme jumping

When a change in pressure propagates through a gas at a rate greater than the ordinary compressions and rarefactions associated with the travel of sound, a moving front (a *shock wave*) of very high pressure forms. This in turn generates an almost instantaneous rise in the temperature that can approach several thousand degrees in magnitude.

A shock tube is an apparatus in which shock waves can be generated and used to study the kinetics of gas-phase reactions that are otherwise inaccessible to kinetic measurements. Since all molecules tend to dissociate at high temperatures, shock tubes are widely used to study dissociation processes and the chemistry of the resulting fragments. For example, the shock-induced decomposition of carbon suboxide provides an efficient means of investigating carbon atom reactions:

$$C_3O_2 \rightarrow C + CO$$

Shock tube techniques are also useful for studying combustion reactions, including those that proceed explosively.



The shock tube itself consists of two sections separated by a breakable diaphragm of metal or plastic. One section is filled with a "driver" gas at a very high pressure, commonly helium, but often mixed with other inert gases to adjust the properties of the shock. The other, longer section of the tube contains the "driven" gas—the reactants—at a low pressure, usually less than 1 atmosphere.

The reaction is initiated by causing the diaphragm to rupture, either by means of a mechanical plunger or by raising the pressure beyond its bursting point. The kinetics of the reaction are monitored by means of an absorption or other optical monitoring device that is positioned at a location along the reaction tube that is appropriate to the time course of the reaction.

5.2.3: Contributors and Attributions

- Stephen Lower, Professor Emeritus (Simon Fraser U.) Chem1 Virtual Textbook
- Jonathan Gutow (UW Oshkosh)

This page titled 5.2: Relaxation Methods is shared under a CC BY-NC-SA 4.0 license and was authored, remixed, and/or curated by Jonathan Gutow via source content that was edited to the style and standards of the LibreTexts platform.

- **5.4: Resolving Kinetics- Faster Methods** by Stephen Lower is licensed CC BY-NC-SA 4.0. Original source: http://www.chem1.com/acad/webtext/virtualtextbook.html.

5.3: Representative Reaction Mechanisms

5.3.1: Introduction

A major goal in chemical kinetics is to determine the sequence of elementary reactions, or the reaction mechanism, that comprise complex reactions. For example, Sherwood Rowland and Mario Molina won the Nobel Prize in Chemistry in 1995 for proposing the elementary reactions involving chlorine radicals that contribute to the overall reaction of $O_3 \rightarrow O_2$ in the troposphere. In the following sections, we will derive rate laws for complex reaction mechanisms, including reversible, parallel and consecutive reactions.

5.3.2: Parallel Reactions

Consider the reaction in which chemical species A undergoes one of two irreversible first order reactions to form either species B or species C :

$$\mathrm{A} \xrightarrow{k_1} \mathrm{B} \tag{5.3.1}$$

$$\mathrm{A} \xrightarrow{k_2} \mathrm{C} \tag{5.3.2}$$

The overall reaction rate for the consumption of A can be written as:

$$\frac{d\left[\mathrm{A}\right]}{dt} = -k_1\left[\mathrm{A}\right] - k_2\left[\mathrm{A}\right] = -\left(k_1 + k_2\right)\left[\mathrm{A}\right] \tag{5.3.3}$$

Integrating $[\mathrm{A}]$ with respect to t, we obtain the following equation:

$$[\mathrm{A}] = [\mathrm{A}]_0 e^{-(k_1+k_2)t} \tag{5.3.4}$$

Plugging this expression into the equation for $\dfrac{d\left[\mathrm{B}\right]}{dt}$, we obtain:

$$\frac{d\left[\mathrm{B}\right]}{dt} = k_1\left[\mathrm{A}\right] = k_1[\mathrm{A}]_0 e^{-(k_1+k_2)t} \tag{5.3.5}$$

Integrating $[\mathrm{B}]$ with respect to t, we obtain:

$$[\mathrm{B}] = -\frac{k_1[\mathrm{A}]_0}{k_1+k_2}\left(e^{-(k_1+k_2)t}\right) + c_1 \tag{5.3.6}$$

At $t = 0$, $[\mathrm{B}] = 0$. Therefore,

$$c_1 = \frac{k_1[\mathrm{A}]_0}{k_1+k_2} \tag{5.3.7}$$

$$[\mathrm{B}] = \frac{k_1[\mathrm{A}]_0}{k_1+k_2}\left(1 - e^{-(k_1+k_2)t}\right) \tag{5.3.8}$$

Likewise,

$$[\mathrm{C}] = \frac{k_2[\mathrm{A}]_0}{k_1+k_2}\left(1 - e^{-(k_1+k_2)t}\right) \tag{5.3.9}$$

The ratio of $[\mathrm{B}]$ to $[\mathrm{C}]$ is simply:

$$\frac{[\mathrm{B}]}{[\mathrm{C}]} = \frac{k_1}{k_2} \tag{5.3.10}$$

An important parallel reaction in industry occurs in the production of ethylene oxide, a reagent in many chemical processes and also a major component in explosives. Ethylene oxide is formed through the partial oxidation of ethylene:

$$2\ C_2H_4 + O_2 \xrightarrow{k_1} 2\ C_2H_4O \tag{5.3.11}$$

However, ethylene can also undergo a combustion reaction:

$$C_2H_4 + 3\ O_2 \xrightarrow{k_2} 2\ CO_2 + 2\ H_2O \tag{5.3.12}$$

To select for the first reaction, the oxidation of ethylene takes place in the presence of a silver catalyst, which significantly increases k_1 compared to k_2. Figure 5.3.1 displays the concentration profiles for species A, B, and C in a parallel reaction in which $k_1 > k_2$.

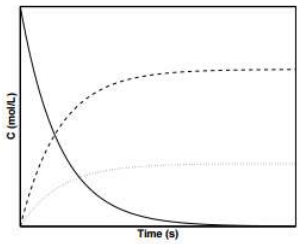


Figure 5.3.1: Plots of $[\mathrm{A}]$ (solid line), $[\mathrm{B}]$ (dashed line) and $[\mathrm{C}]$ (dotted line) over time for a parallel reaction.

5.3.3: Consecutive Reactions

Consider the following series of first-order irreversible reactions, where species A reacts to form an intermediate species, I, which then reacts to form the product, P:

$$\mathrm{A} \xrightarrow{k_1} \mathrm{I} \xrightarrow{k_2} \mathrm{P} \tag{5.3.13}$$

We can write the reaction rates of species A, I and P as follows:

$$\frac{d\left[\mathrm{A}\right]}{dt} = -k_1\left[\mathrm{A}\right] \tag{5.3.14}$$

$$\frac{d\left[\mathrm{I}\right]}{dt} = k_1\left[\mathrm{A}\right] - k_2\left[\mathrm{I}\right] \tag{5.3.15}$$

$$\frac{d\left[\mathrm{P}\right]}{dt} = k_2\left[\mathrm{I}\right] \tag{5.3.16}$$

As before, integrating $[\mathrm{A}]$ with respect to t leads to:

$$[\mathrm{A}] = [\mathrm{A}]_0 e^{-k_1 t} \tag{5.3.17}$$

The concentration of species I can be written as

$$[\mathrm{I}] = \frac{k_1[\mathrm{A}]_0}{k_2 - k_1}\left(e^{-k_1 t} - e^{-k_2 t}\right) \tag{5.3.18}$$

Then, solving for $[\mathrm{P}]$, we find that:

$$[\mathrm{P}] = [\mathrm{A}]_0\left[1 + \frac{1}{k_1 - k_2}\left(k_2 e^{-k_1 t} - k_1 e^{-k_2 t}\right)\right] \tag{5.3.19}$$

Figure 5.3.2 displays the concentration profiles for species A, I, and P in a consecutive reaction in which $k_1 = k_2$. As can be seen from the figure, the concentration of species I reaches a maximum at some time, $t_{\max}$. Oftentimes, species I is the desired product. Returning to the oxidation of ethylene into ethylene oxide, it is important to note another reaction in which ethylene oxide can decompose into carbon dioxide and water through the following reaction

$$C_2H_4O + \frac{5}{2}\ O_2 \xrightarrow{k_3} 2\ CO_2 + 2\ H_2O \tag{5.3.20}$$

Thus, to maximize the concentration of ethylene oxide, the oxidation of ethylene is only allowed proceed to partial completion before the reaction is stopped.

Finally, in the limiting case when $k_2 \gg k_1$, we can write the concentration of P as

$$[\mathrm{P}] \approx [\mathrm{A}]_0\left\{1 + \frac{1}{-k_2}k_2 e^{-k_1 t}\right\} = [\mathrm{A}]_0\left(1 - e^{-k_1 t}\right) \tag{5.3.21}$$

Thus, when $k_2 \gg k_1$, the reaction can be approximated as $\mathrm{A} \rightarrow \mathrm{P}$ and the apparent rate law follows 1st order kinetics.

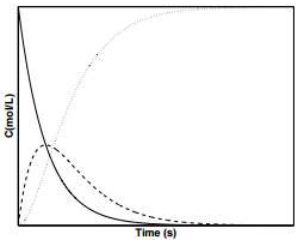


Figure 5.3.2: Plots of $[\mathrm{A}]$ (solid line), $[\mathrm{I}]$ (dashed line) and $[\mathrm{P}]$ (dotted line) over time for consecutive first order reactions.

5.3.4: Consecutive Reactions With an Equilibrium

Consider the reactions

$$\mathrm{A} \underset{k_{-1}}{\overset{k_1}{\rightleftharpoons}} \mathrm{I} \overset{k_2}{\rightarrow} \mathrm{P} \tag{5.3.22}$$

We can write the reaction rates as:

$$\frac{d[\mathrm{A}]}{dt} = -k_1[\mathrm{A}] + k_{-1}[\mathrm{I}] \tag{5.3.23}$$

$$\frac{d[\mathrm{I}]}{dt} = k_1[\mathrm{A}] - k_{-1}[\mathrm{I}] - k_2[\mathrm{I}] \tag{5.3.24}$$

$$\frac{d[\mathrm{P}]}{dt} = k_2[\mathrm{I}] \tag{5.3.25}$$

The exact solutions of these is straightforward, in principle, but rather involved, so we will just state the exact solutions, which are

$$[\mathrm{A}](t) = \frac{[\mathrm{A}]_0}{2\lambda}\left[(\lambda - k_1 + K)\, e^{-(k_1+K-\lambda)t/2} + (\lambda + k_1 - K)\, e^{-(k_1+K+\lambda)t/2}\right] \tag{5.3.26}$$

$$[\mathrm{I}](t) = \frac{k_1[\mathrm{A}]_0}{\lambda}\left[e^{-(k_1+K-\lambda)t/2} - e^{-(k_1+K+\lambda)t/2}\right] \tag{5.3.27}$$

$$[\mathrm{P}](t) = 2k_1k_2[\mathrm{A}]_0\left[\frac{2}{(k_1+K)^2 - \lambda^2} - \frac{1}{\lambda}\left(\frac{e^{-(k_1+K-\lambda)t/2}}{k_1+K-\lambda} - \frac{e^{-(k_1+K+\lambda)t/2}}{k_1+K+\lambda}\right)\right] \tag{5.3.28}$$

where

$$K = k_2 + k_{-1} \tag{5.3.29}$$

$$\lambda = \sqrt{(k_1 - K)^2 - 4k_1k_{-1}} \tag{5.3.30}$$

Notice that these solutions have similar functional forms to consecutive reactions without the equilibrium. The differences are essentially in the constant values in the expressions. We would still expect a build up and then decrease in the intermediate as the reactants are used up and final products are produced.

This page titled 5.3: Representative Reaction Mechanisms is shared under a CC BY-NC-SA 4.0 license and was authored, remixed, and/or curated by Jonathan Gutow.

- **1.20: Complex reaction mechanisms** by Mark Tuckerman is licensed CC BY-NC-SA 4.0.

5.4: The Rate Determining Step Approximation

The **rate determining step** approximation is one of the simplest approximations one can make to analyze a proposed mechanism to deduce the rate law it predicts. Simply stated, the rate determining step approximation says that a mechanism can proceed no faster than its slowest step. So, for example, if the reaction

$$A + B \rightarrow C$$

is proposed to follow the mechanism

$$\underbrace{A + A \overset{k_1}{\longrightarrow} A_2}_{\text{slow}}$$

$$\underbrace{A_2 \overset{k_2}{\longrightarrow} C + A}_{\text{fast}}$$

the rate determining step approximation suggests that the rate (expressed in terms of the appearance of product C) should be determined by the slow initial step, and so the rate law will be

$$\frac{d[C]}{dt} = k_1[A]^2$$

matching the order of the rate law to the molecularity of the slow step. Conversely, if the reaction mechanism is proposed as

$$\underbrace{A \overset{k_1}{\longrightarrow} A^*}_{\text{slow}}$$

$$\underbrace{A^* + B \overset{k_2}{\longrightarrow} C}_{\text{fast}}$$

the rate determining step approximation suggests that the rate of the reaction should be

$$\frac{d[C]}{dt} = k_1[A]$$

again, with the order of the rate law matching the molecularity of the rate determining step.

This page titled 5.4: The Rate Determining Step Approximation is shared under a CC BY-NC-SA 4.0 license and was authored, remixed, and/or curated by Jonathan Gutow.

- **12.4: The Rate Determining Step Approximation** by Patrick Fleming is licensed CC BY-NC-SA 4.0.

5.5: The Equilibrium Approximation

In many cases, the formation of a reactive intermediate (or even a longer lived intermediate) involves a reversible step. This is the case if the intermediate can decompose to reform reactants with a significant probability as well as moving on to form products. In many cases, this will lead to a pre-equilibrium condition in which the **equilibrium approximation** can be applied. An example of a reaction mechanism of this sort is

$$A + B \underset{k_{-1}}{\overset{k_1}{\rightleftharpoons}} AB$$

$$AB \xrightarrow{k_2} C$$

If the initial equilibrium is fast compared to the second step, one makes the assumption that the ratio of [AB] to [A][B] is always that expected at equilibrium. This results in the expression:

$$k_1[A][B] = k_{-1}[AB]$$

or

$$\frac{k_1[A][B]}{k_{-1}} = [AB]$$

This expression can be substituted into an expression for the rate of formation of the product C:

$$\frac{d[C]}{dt} = k_2[AB]$$

or

$$\frac{d[C]}{dt} = \frac{k_2 k_1}{k_{-1}}[A][B]$$

Which predicts a reaction rate law that is first order in A, first order in B, and second order overall. This is equivalent to making the steady state approximation and assuming that k_2 is negligible.

Example 5.5.1:

Given the following mechanism, apply the equilibrium approximation to the first step to predict the rate law suggested by the mechanism.

$$A + A \underset{k_{-1}}{\overset{k_1}{\rightleftharpoons}} A_2$$

$$A_2 + B \xrightarrow{k_2} C + A$$

Solution

If the equilibrium approximation is valid for the first step,

$$k_1[A]^2 = k_{-1}[A_2]$$

or

$$\frac{k_1[A]^2}{k_{-1}} \approx [A_2]$$

Plugging this into the rate equation for the second step

$$\frac{d[C]}{dt} = k_2[A_2][B]$$

yields

$$\frac{d[C]}{dt} = \frac{k_2 k_1}{k_{-1}}[A]^2[B]$$

Thus, the rate law has the form

$$\text{rate} = k'[A]^2[B]$$

which is second order in A, first order in B and third order over all, and in which the effective rate constant (k' is

$$k' = \frac{k_2 k_1}{k_{-1}}.$$

Sometimes, the equilibrium approximation can suggest rate laws that have negative orders with respect to certain species. For example, consider the following reaction

$$A + 2B \rightarrow 2C$$

A proposed mechanism for which might be

$$A + B \underset{k_{-1}}{\overset{k_1}{\rightleftharpoons}} I + C$$

$$I + B \xrightarrow{k_2} C$$

in which I is an intermediate. Applying the equilibrium approximation to the first step yields

$$k_1[A][B] = k_{-1}[I][C]$$

or

$$\frac{k_1[A][B]}{k_{-1}[C]} \approx [I]$$

Substituting this into an expression for the rate of formation of C, one sees

$$\frac{d[C]}{dt} = k_2[I][B]$$

or

$$\frac{d[C]}{dt} = \frac{k_1[A][B]}{k_{-1}[C]}[B] = \frac{k_2 k_1[A][B]}{k_{-1}[C]}$$

The rate law is then of the form

$$\text{rate} = k\frac{[A][B]^2}{[C]}$$

which is first order in A, second order in B, negative one order in C, and second order overall. Also,

$$k' = \frac{k_2 k_1}{k_{-1}}.$$

In this case, the negative order in C means that a buildup of compound C will cause the reaction to slow. These sort of rate laws are not uncommon for reactions with a reversible initial step that forms some of the eventual reaction product.

This page titled 5.5: The Equilibrium Approximation is shared under a CC BY-NC-SA 4.0 license and was authored, remixed, and/or curated by Jonathan Gutow.

- **12.6: The Equilibrium Approximation** by Patrick Fleming is licensed CC BY-NC-SA 4.0.

5.6: The Steady-State Approximation

One of the most commonly used and most attractive approximations is the **steady state approximation**. This approximation can be applied to the rate of change of concentration of a highly reactive (short lived) intermediate. The assumption is that the concentration of the intermediate, [I], holds a constant value over the duration of the observation of the reaction. The advantage here is that for such an intermediate (I),

$$\frac{d[I]}{dt} = 0$$

This often works well because intermediates are in such low concentration that even if [I] is changing d[I]/dt ≈ 0, because [I] is so small.

So long as one can write an expression for the rate of change of the concentration of the intermediate I, the steady state approximation allows one to solve for its constant concentration. For example, if the reaction

$$A + B \rightarrow C \tag{5.6.1}$$

is proposed to follow the mechanism

$$A + A \xrightarrow{k_1} A_2 \tag{5.6.2}$$

$$A_2 + B \xrightarrow{k_2} C + A \tag{5.6.3}$$

The time-rate of change of the concentration of the intermediate A_2 can be written as

$$\frac{d[A_2]}{dt} = k_1[A]^2 - k_2[A_2][B]$$

In the limit that the steady state approximation can be applied to A_2

$$\frac{d[A_2]}{dt} = k_1[A]^2 - k_2[A_2][B] \approx 0$$

or

$$[A_2] \approx \frac{k_1[A]^2}{k_2[B]}$$

So if the rate of the overall reaction is expressed as the rate of formation of the product C,

$$\frac{d[C]}{dt} = k_2[A_2][B]$$

the above expression for $[A_2]$ can be substituted

$$\frac{d[C]}{dt} = k_2\left(\frac{k_1[A]^2}{k_2[B]}\right)[B]$$

or

$$\frac{d[C]}{dt} = k_1[A]^2$$

and the reaction is predicted to be second order in $[A]$.

Alternatively, if the mechanism for Equation 5.6.1 is proposed to be

$$A \xrightarrow{k_1} A^* \tag{5.6.4}$$

$$A^* + B \xrightarrow{k_2} C \tag{5.6.5}$$

then the rate of change of the concentration of A^* is

$$\frac{[A^*]}{dt} = k_1[A] - k_2[A^*][B]$$

And if the steady state approximation holds, then

$$[A^*] \approx \frac{k_1[A]}{k_2[B]}$$

So the rate of production of C is

$$\frac{d[C]}{dt} = k_2[A^*][B] \tag{5.6.6}$$

$$= \cancel{k_2}\left(\frac{k_1[A]}{\cancel{k_2}\,[\cancel{B}]}\right)[\cancel{B}] \tag{5.6.7}$$

or

$$\frac{d[C]}{dt} = k_1[A]$$

and the rate law is predicted to be first order in A. In this manner, the plausibility of either of the two reaction mechanisms is easily deduced by comparing the predicted rate law to that which is observed. If the prediction cannot be reconciled with observation, then the scientific method eliminates that mechanism from consideration.

This page titled 5.6: The Steady-State Approximation is shared under a CC BY-NC-SA 4.0 license and was authored, remixed, and/or curated by Jonathan Gutow.

- **12.5: The Steady-State Approximation** by Patrick Fleming is licensed CC BY-NC-SA 4.0.

CHAPTER OVERVIEW

6: Molecular Level Models of Kinetics

6.1: Kinetics of Reactions in Solution
6.2: Kinetic vs. Thermodynamic Control of Reactions
6.3: Collision Theory
6.4: Transition State Theory
6.5: Reactions Involving Ions

This page titled 6: Molecular Level Models of Kinetics is shared under a CC BY-NC-SA 4.0 license and was authored, remixed, and/or curated by Jonathan Gutow.

6.1: Kinetics of Reactions in Solution

6.1.1: Introduction

Learning Objectives

Make sure you thoroughly understand the following essential ideas:

- Describe some of the major differences between the kinetics of reactions in the gas phase, compared with those in liquid solutions.
- What role do solvent cages play in solution kinetics?
- Explain the distinction between diffusion-control and activation-control of reaction rates in solutions.

Chemical reactions can occur in all phases of matter and at the interfaces between phases. Reactions in the liquid phase are particularly important in living organisms and the chemistry laboratory. Here we concentrate on a microscopic model of how reactions occur in liquid solutions. We will primarily compare them to reactions in the gas phase.

6.1.2: What's different about kinetics in liquid solutions?

Most of the added complications of kinetics and rate processes in liquid solutions arise from the *much higher density* of the liquid phase. In a typical gas at atmospheric pressure, the molecules occupy only about 0.2 per cent of the volume; the other 99.8 percent is empty space. In a liquid, molecules may take up more than half the volume, and the "empty" spaces are irregular and ever-changing as the solvent molecules undergo thermal motions of their own.

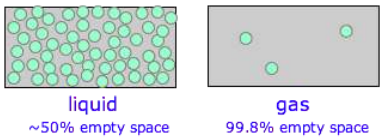


Figure 6.1.1: Liquid vs. Gases.

In a typical liquid solution, the solvent molecules massively outnumber the reactant solute molecules, which tend to find themselves momentarily (~10^{-11} sec) confined to a "hole" within the liquid. This trapping becomes especially important when the solvent is strongly hydrogen-bonded as is the case with water or alcohol.

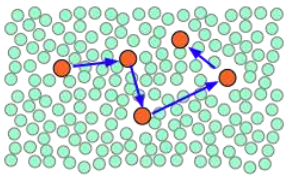
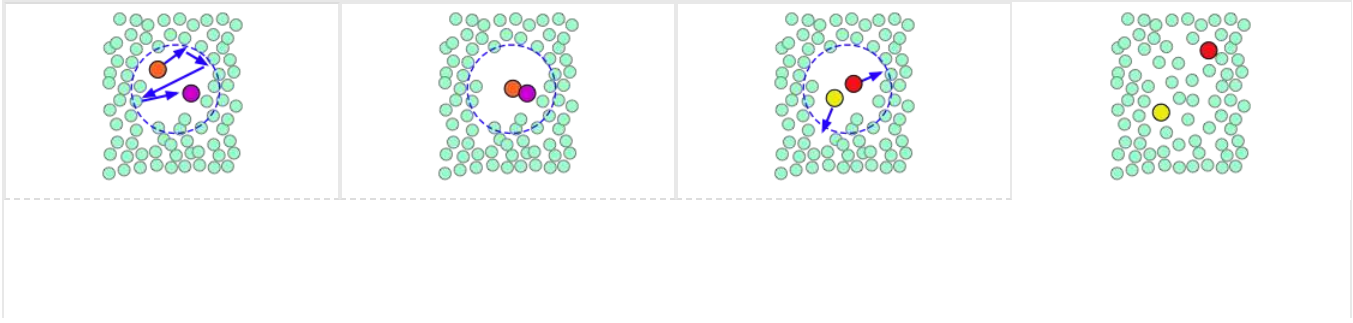


Figure 6.1.2: Brownian motion of a particle in solution

When thermal motions occasionally release a solute molecule from this trap, it will jump to a new location. The jumps are very fast (10^{-12} - 10^{-13} sec) and short (usually a few solvent-molecule diameters), and follow an entirely random pattern, very much as in **Brownian motion**. Consider a simple bimolecular process A + B → products. The reactant molecules will generally be jumping from hole to hole in the solvent matrix, only occasionally finding themselves in the same *solvent cage* (hole) where thermal motions are likely to bring them into contact.

Table 6.1.1: Solvent cages and encounter pairs



A pair of reactants end up in the same solvent cage, where they bounce around randomly and exchange kinetic energy with the solvent molecules.	Eventually the two reactants form an *encounter pair*. If they fail to react the first time, they have many more opportunities during the lifetime of the cage.	The products form and begin to move away from each other.	Finally, after about 10^{-11} sec, the solvent cage breaks up and the products diffuse away.

The process can be represented as

$$A + B \rightarrow \{AB\} \rightarrow \text{products} \tag{6.1.1}$$

in which the $\{AB\}$ term represents the caged reactants including the *encounter pair* and the activated complex.

Contrast this scenario with a similar reaction taking place in the gas phase; the molecules involved in the reaction will often be the only ones present, so a significant proportion of the collisions will be A-B encounters. However, if the collision should fail to be energetically or geometrically viable, the reactant molecules fly apart and are unlikely to meet again anytime soon. In a liquid, however, the solute molecules are effectively in a constant state of collision — if not with other reactants, then with solvent molecules which can exchange kinetic energy with the reactants. So once an A-B encounter pair forms, the two reactants get multiple whacks at each other, greatly increasing the probability that they will obtain the kinetic energy needed to kick them over the activation hump before the encounter pair disintegrates.

6.1.3: Limiting Cases: Diffusion-Controlled and Activation-Controlled Reactions

The encounter pair model introduces some new rate parameters:

$$\mathrm{A + B} \underset{k_{-1}}{\overset{k_1}{\rightleftharpoons}} \mathrm{AB} \xrightarrow{k_2} \mathrm{P} \tag{6.1.2}$$

The first step is an equilibrium between the reactants outside and inside the solvent cage. The rate constants k_1 reflects the rate of A and B diffusing together into the solvent cage to become an encounter pair, and k_{-1} the rate they diffuse back out, while k_2 is the rate at which the encounter pair becomes product. The values of the diffusion related constants are strongly dependent on the viscosity (and thus the temperature) of the solvent. (Note that k_1 is a second-order rate constant, while and k_{-1} and k_2 are first-order.)

Diffusion is the transport of a substance through a concentration gradient; that is, from a region of higher concentration to one of lower concentration. Think of the way the color of tea spreads out when a tea bag is immersed in hot water. Diffusion occurs because random thermal motions (figure 6.1.2) are statistically more likely to move molecules out of a region of higher concentration than in the reverse direction, simply because in the latter case fewer molecules are available to make the reverse trip. Eventually the concentrations become uniform and equilibrium is attained.

This mechanism leads to the following rate laws for formation of the encounter pair and the products:

$$\frac{d[\{AB\}]}{dt} = k_1[A][B] - k_{-1}[\{AB\}] - k_2[\{AB\}] \tag{6.1.3}$$

$$\frac{d[P]}{dt} = k_2[\{AB\}] \tag{6.1.4}$$

If we assume steady state in [{AB}] equation 6.1.3 becomes:

$$0 \approx k_1[A][B] - k_{-1}[\{AB\}]_{ss} - k_2[\{AB\}]_{ss} \tag{6.1.5}$$

Solving for $[\{AB\}]_{ss}$:

$$[\{AB\}]_{ss} \approx \frac{k_1}{k_{-1} + k_2}[A][B] \tag{6.1.6}$$

Substituting into equation 6.1.4 we get the dependence of the rate of product production on our rate constants and reactant concentrations:

$$\frac{d[P]}{dt} = k_2 \frac{k_1}{k_{-1} + k_2}[A][B] \tag{6.1.7}$$

There are two limiting cases:

6.1.3.1: Diffusion Controlled ($k_2 \gg k_{-1}$):

In this case the activation energy of the A+B reaction in the cage is very small or escape of molecules from the {AB} cage is difficult. This makes k_{-1} negligible in the denominator and equation 6.1.7 simplifies:

$$\frac{d[P]}{dt} = k_2 \frac{k_1}{k_{-1} + k_2}[A][B] \approx \cancel{k_2} \frac{k_1}{\cancel{k_2}}[A][B] \approx k_1[A][B] \tag{6.1.8}$$

So, the kinetics will be dominated by k_1, the rate the particles diffuse into the cage (by convention k_1 is often called k_d, where the subscript stands for diffusion). Such a process is said to be *diffusion controlled*. This suggest there is an upper-limit for bimolecular reactions in solution set by the diffusion process. A careful analysis[1] of the rate of two spherical particles diffusing together provides an estimate for k_1 (or k_d):

$$k_1 \approx \frac{8RT}{3\eta} \tag{6.1.9}$$

where R = gas constant, T = temperature in K and η = the solvent viscosity. For water at 25 ˚C η = 0.891 x 10^{-3}kgm^{-1}s^{-1} (0.891 cP), which yields $k_1 \approx$ 7.4 x 10^6 m^{3}mol^{-1}s^{-1} = 7.4 x 10^9 M^{-1}s^{-1}. So reactions with rate constants in water in the 10^{10} M^{-1}s^{-1} to 10^{11} M^{-1}s^{-1} are considered to be diffusion controlled, which in this model is the upper limit on the rate. An example is the acid-base reaction: $H^+ + OH^- \rightarrow H_2O$ for which k = 1.4×10^{11} dm^3 mol^{-1} s^{-1} at 298 K (reminder: 1 dm^3 = 1 L).

6.1.3.2: Activation Controlled ($k_2 \ll k_{-1}$):

Alternatively, if the activation energy of the A+B reaction in the cage dominates the kinetics, then k_2 in the denominator is negligible and equation 6.1.7 simplifies:

$$\frac{d[P]}{dt} = k_2 \frac{k_1}{k_{-1} + k_2}[A][B] \approx k_2 \frac{k_1}{k_{-1}}[A][B] \tag{6.1.10}$$

Thus the rate now depends on all three rate constants. These reactions have rates less than the *diffusion limited* reactions and are referred to as *activation controlled*. Keep in mind that the observed rate depends on the competition among the three processes. So the exact balance between the residence time of two particles in the cage (determined by k_1 and k_{-1}) and the average time it takes the molecules in the cage to absorb enough energy to overcome the activation energy and come together in the right orientation to react (k_2) determines the obseved rate.

6.1.4: References

1. P.W. Atkins, J. de Paula, *Physical Chemistry*, 10th Ed. (W.H. Freeman and Co. New York, 2014) P. 890.

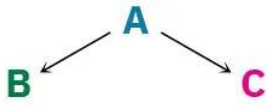
This page titled 6.1: Kinetics of Reactions in Solution is shared under a CC BY-NC-SA 4.0 license and was authored, remixed, and/or curated by Jonathan Gutow via source content that was edited to the style and standards of the LibreTexts platform.

- **17.5: Kinetics of Reactions in Solution** by Stephen Lower is licensed CC BY 3.0. Original source: http://www.chem1.com/acad/webtext/virtualtextbook.html.

6.2: Kinetic vs. Thermodynamic Control of Reactions

6.2.1: Qualitative Description

Imagine a reaction that can give either or both of two products, **B** and **C**.



Let's assume that B forms faster than C (in other words, $\Delta G_B^{\ddagger} < \Delta G_C^{\ddagger}$) but that C is more stable than B (in other words, $\Delta G_C^o > \Delta G_B^o$). An energy diagram for the two processes might look like that shown in Figure 6.2.1.

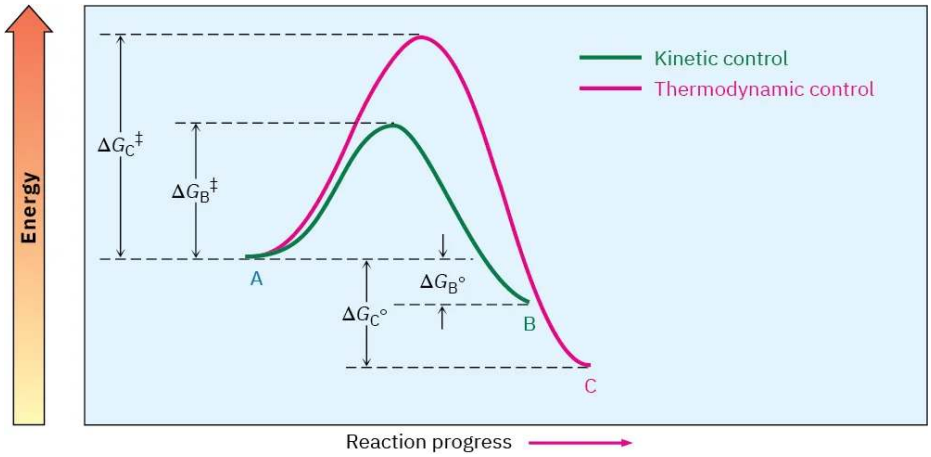


Figure 6.2.1: An energy diagram for two competing reactions in which the less stable product B forms faster than the more stable product C.

Let's first carry out the reaction at a lower temperature so that both processes are irreversible and no equilibrium is reached. Because **B** forms faster than **C**, **B** is the major product. It doesn't matter that **C** is more stable than **B**, because the two are not in equilibrium. *The product of an irreversible reaction depends only on relative rates, not on stability.* Such reactions are said to be under kinetic control.



Now let's carry out the same reaction at some higher temperature so that both processes are readily reversible and an equilibrium is reached. Because **C** is more stable than **B**, **C** is the major product obtained. It doesn't matter that **C** forms more slowly than **B**, because the two are in equilibrium. *The product of a readily reversible reaction depends only on stability, not on relative rates.* Such reactions are said to be under equilibrium control, or thermodynamic control.



In reality a reaction system is never completely irreversible, nor does it reach true equilibrium before infinite time has passed. However, because matter is particulate and our measurement precision is not infinite both limits are seen within our ability to make observations.

6.2.2: Quantitative Description

Rates depend on the activation barrier and not the reaction free energy change. This leads to situations where the thermodynamically most stable species in a set of coupled reactions is not the major product. This is easiest to understand by considering two equilibria starting from the same reactant A:

$$A \underset{k_{-1}}{\overset{k_1}{\rightleftharpoons}} P_1$$

$$A \underset{k_{-2}}{\overset{k_2}{\rightleftharpoons}} P_2$$

If both reactions are spontaneous ($\Delta G_r^o < 0$) and $\Delta G_r^o(A \rightarrow P_2) < \Delta G_r^o(A \rightarrow P_1)$ we would expect P_2 to dominate at equilibrium, because of the more negative ΔG. However, equilibrium may not be reached if $k_2 << k_1$. This can occur as shown in figure 6.2.2, if the barrier to reaction is much higher for the second reaction even if P_2 is more thermodynamically stable.

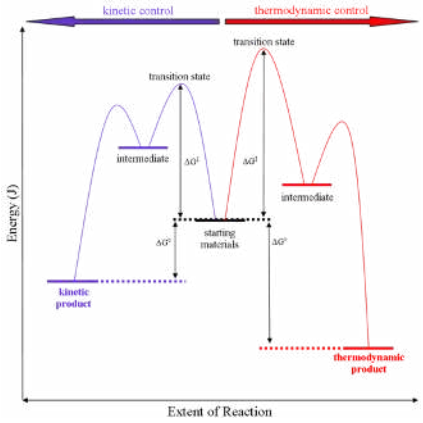


Figure 6.2.2: A cartoon of the free energy change of two competing pathways to different products from the same starting material, with an intermediate step between the starting materials and the final products. The right branch (red) corresponds to going to P_2 which is more stable, but via slower kinetics because of the higher activation barrier. Source:Nick024, CC0, via Wikimedia Commons.

Note that in both these spontaneous reactions $k_{-1} < k_1$ and $k_{-2} < k_2$ because the barrier is larger going back to A (the starting material). What this means is at short times and lower temperatures (less chance to establish equilibrium) the ratio of $[P_1]/[P_2] = k_1/k_2 > 1$ because $k_1 > k_2$. At higher temperatures or long times equilibrium will be established and the equilibrium ratio of the products will be observed:

$$\frac{[P_1]}{[P_2]} = \frac{K_1}{K_2} = \frac{k_1 k_{-2}}{k_{-1} k_2} = exp\left(\frac{-\Delta G_r^o(P_2 \rightarrow P_1)}{RT}\right)$$

It is often practical to select combinations of solvent and temperature that yield ratios of $k_1/k_2 >> 1$ (sometimes choices of solvent can even flip the relative barrier heights to get $k_2/k_1 >> 1$). Synthetic chemists regularly make use of this phenomenon to increase the yield of a desired product. Sometimes the thermodynamic product is enough more stable that raising the temperature or waiting long enough can dramatically shift the yield from primarily kinetic to primarily thermodynamic product. Removing the desired product as it is produced is another way of driving the reactions to the desired product.

6.2.3: Example

Electrophilic addition to a conjugated diene at or below room temperature normally leads to a mixture of products in which the 1,2 adduct predominates over the 1,4 adduct. When the same reaction is carried out at higher temperatures, however, the product ratio often changes and the 1,4 adduct predominates. For example, addition of HBr to 1,3-butadiene at 0 °C yields a 71 : 29 mixture of 1,2 and 1,4 adducts, but the same reaction carried out at 40 °C yields a 15 : 85 mixture. Furthermore, when the product mixture formed at 0 °C is heated to 40 °C in the presence of HBr, the ratio of adducts slowly changes from 71 : 29 to 15 : 85. Why?



1,3-Butadiene	1,2 Adduct	1,4 Adduct
At 0 °C:	71%	29%
At 40 °C:	15%	85%

At low temperature (0 °C), HBr adds to 1,3-butadiene under kinetic control to give a 71 : 29 mixture of products, with the more rapidly formed 1,2 adduct predominating. Because these low-temperature conditions don't allow the reaction to reach equilibrium, the product that forms faster predominates. At higher temperature (40 °C), however, the reaction occurs under thermodynamic control to give a 15 : 85 mixture of products, with the more stable 1,4 adduct predominating. The higher temperature allows the addition process to become reversible, so an equilibrium mixture of products results. Figure 6.2.2 shows this situation in an energy diagram.

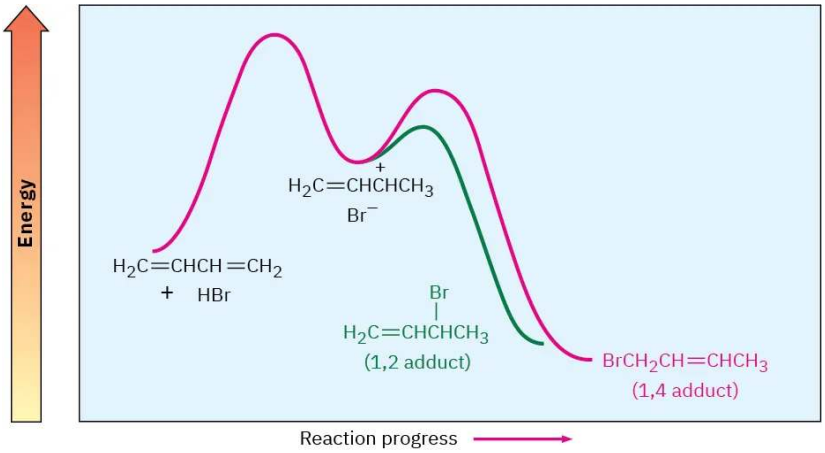


Figure 6.2.2: Energy diagram for the electrophilic addition of HBr to 1,3-butadiene. The 1,2 adduct is the kinetic product because it forms faster, but the 1,4 adduct is the thermodynamic product because it is more stable.

The electrophilic addition of HBr to 1,3-butadiene is a good example of how a change in experimental conditions can change the product of a reaction. The concept of thermodynamic control versus kinetic control is a useful one that we can sometimes take advantage of in the laboratory.

? Exercise 6.2.1

The 1,2 adduct and the 1,4 adduct formed by reaction of HBr with 1,3-butadiene are in equilibrium at 40 °C. Propose a mechanism by which the interconversion of products takes place.

Answer

Interconversion occurs by S_N1 dissociation to a common intermediate cation.

? Exercise 6.2.2

Why do you suppose 1,4 adducts of 1,3-butadiene are generally more stable than 1,2 adducts?

Answer

The double bond is more highly substituted.

This page titled 6.2: Kinetic vs. Thermodynamic Control of Reactions is shared under a CC BY-NC-SA 4.0 license and was authored, remixed, and/or curated by Jonathan Gutow via source content that was edited to the style and standards of the LibreTexts platform.

- **14.3: Kinetic vs. Thermodynamic Control of Reactions** by OpenStax is licensed CC BY-NC-SA 4.0. Original source: https://openstax.org/details/books/organic-chemistry.

6.3: Collision Theory

Collision Theory was first introduced in the 1910s by Max Trautz (Trautz, 1916) and William Lewis (Lewis, 1918) to try to account for the magnitudes of rate constants in terms of the frequency of molecular collisions, the collisional energy, and the relative orientations of the molecules involved in the collision.

The rate of a reaction, according to collision theory, can be expressed as

$$\text{rate} = Z_{ab}F \tag{6.3.1}$$

where Z_{AB} is the frequency of collisions between the molecules A and B involved in the reaction, and F is the fraction of those collisions that will lead to a reaction. The first term, Z_{AB}, can be taken from the kinetic molecular theory of gases (for a derivation see LibreTexts (Fleming) 2.6: Collisions with Other Molecules).

$$Z_{AB} = \sqrt{\frac{8k_BT}{\pi\mu}}\sigma_{AB}[A][B] \tag{6.3.2}$$

Where the first factor is the average relative velocity of the two particles, $\mu = m_Am_B/(m_A+m_B)$ is the reduced mass of the A-B collisional system, k_B = Boltzmann constant and T = temperature in Kelvin. σ_{AB} is the collisional cross section. [A] and [B] are the concentrations of A and B. The collision cross section σ_{AB} can be understood as the area of a circle that sweeps out the cylindrical volume within which spherical molecules with a center-to-center distance less than or equal to the sum of their radii collide. Those with centers farther apart do not collide (see figure 6.3.1). If A and B are hard spheres $\sigma_{AB} = \pi(r_A + r_B)^2$, where 'r' refers to the radius of a sphere.

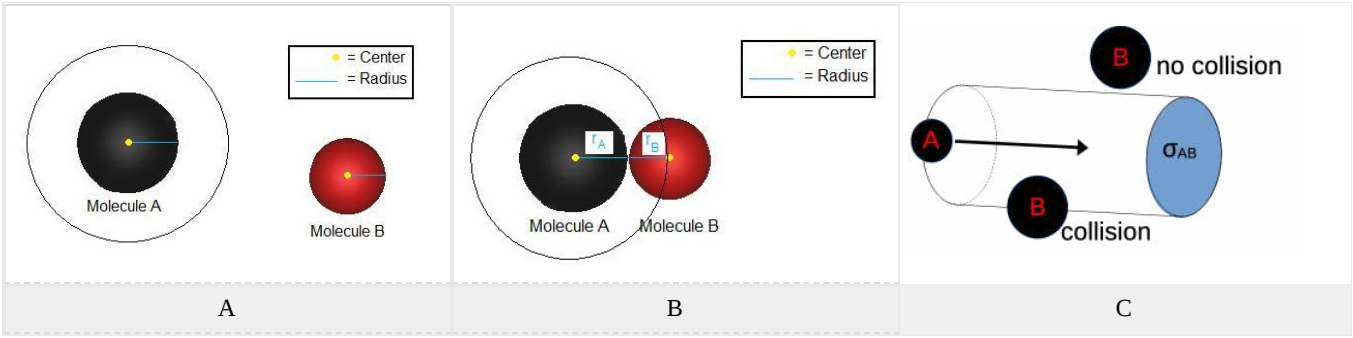


Figure 6.3.1: (A) no collision; (B) collision; (C) volume swept out by collision cross-section imagining only one particle moving.

The factor F has **two** important contributors, the energy of the collision and the orientation of the molecules when they collide. The factor F depends on the activation energy. Assuming a Boltzmann (or Boltzmann-like) distribution of energies, the fraction of molecular collisions that will have enough energy to overcome the activation barrier is given by

$$F = e^{-E_a/RT} \tag{6.3.3}$$

Combining Equations 6.3.2 and 6.3.3, the rate of the reaction (Equation 6.3.1) is predicted by

$$\text{rate} = \left(\frac{8k_BT}{\pi\mu}\right)^{1/2}\sigma_{AB}e^{-E_a/RT}[A][B]$$

So if the rate law can be expressed as a second order rate law

$$\text{rate} = k[A][B]$$

it is clear that the rate constant k is given by

$$k = \left(\frac{8k_BT}{\pi\mu}\right)^{1/2}\sigma_{AB}e^{-E_a/RT}$$

To account for the orientation dependence of collisions an *ad-hoc* **steric factor** (P, for the proportion of molecules with enough energy to react that meet in the right orientation) is often added to the pre-exponential factors yielding:

$$k = P\left(\frac{8k_BT}{\pi\mu}\right)^{1/2}\sigma_{AB}e^{-E_a/RT} \tag{6.3.4}$$

By comparison, the theory predicts the form of the **Arrhenius pre-expoential factor** to be

$$A = P\left(\frac{8k_BT}{\pi\mu}\right)^{1/2}\sigma_{AB}$$

Note this implies that A has a temperature dependence, ($\sqrt{T}$), so the Arrhenius equation is a simplification.

Given equation 6.3.4, if k and E_a are measured for molecules with a known collision cross section, σ_{AB}, P can be found. Generally 0 < P < 1. Occasionally, when charged species are involved P is found to be larger than 1.

Keep in mind that this model applies only to **bimolecular steps** in a mechanism.

6.3.1: References

1. Atkins, Peter and Julio de Paula. Physical Chemistry for the Life Sciences. 2006. New York, NY: W.H. Freeman and Company. pp.282-288, 290
2. Atkins, Peter. Concepts in Physical Chemistry. 1995. New York, NY: W.H. Freeman and Company. pp.193
3. Chang, Raymond. Physical Chemistry for the Biosciences. 2005. Sausalito, CA: University Science Books. pp.28

This page titled 6.3: Collision Theory is shared under a CC BY-NC-SA 4.0 license and was authored, remixed, and/or curated by Jonathan Gutow.

- **11.10: Collision Theory** by Patrick Fleming is licensed CC BY-NC-SA 4.0.
- **6.1.1: Collisional Cross Section** is licensed CC BY 4.0.

6.4: Transition State Theory

6.4.1: Introduction

Transition state theory was proposed in 1935 by Henry Erying, and further developed by Merrideth G. Evans and Michael Polanyi,[1] as another means of accounting for chemical reaction rates. It is based on the idea that a molecular collision that leads to reaction must pass through an intermediate state known as the transition state.

6.4.2: Concentration Formulation

For example, the reaction

$$A + BC \rightarrow AB + C$$

would have an intermediate (ABC) where the $B-C$ bond is partially broken, and the $A-B$ bond is partially formed.

$$\mathrm{A + B{-}C \rightleftharpoons (A{-}B{-}C)^{\ddagger} \longrightarrow A{-}B + C}$$

So the reaction is mediated by the formation of an activated complex (denoted with the double-dagger symbol ‡) and the decomposition of that complex into the reaction products. Using this theory, the rate of reaction can be expressed as the product of two factors

$$\text{rate} = (\text{transition state concentration}) \times (\text{decomposition frequency})$$

If the formation of the activated complex is considered to reach an equilibrium,

$$K^{\ddagger} = \frac{[ABC]^{\ddagger}}{[A][BC]}$$

So the concentration of the transition state complex can be expressed by

$$[ABC]^{\ddagger} = K^{\ddagger}[A][BC]$$

The overall rate then becomes:

$$\text{rate} = \nu K^{\ddagger}[A][BC] \tag{6.4.1}$$

where ν is the frequency the activated complex becomes products. This can be estimated from the average energy content of the vibrational coordinate corresponding to the reaction coordinate (breaking of B-C bond and shortening of the A-B bond in our model reaction). Statistical mechanics shows that the unknown frequency is related to the average energy in the vibrational mode, k_BT. Setting this equal to the energy of vibration $E = h\nu$ allows us to estimate the frequency factor:

$$E = h\nu = k_BT \implies \nu = \frac{k_BT}{h} \tag{6.4.2}$$

This derivation of the frequency is cheating a little. The frequency along the reaction coordinate actually cancels out and the only frequency left is the ratio of the the average mode energy to Planck's constant (k_bT/h). See reference 2.

Substituting for ν in equation 6.4.1:

$$\text{rate} = \frac{k_BT}{h} K^{\ddagger}[A][BC] \tag{6.4.3}$$

A full analysis[2] suggests there can be an additional transmission factor that may be less than 1 (κ) making the full version of the model (Eyring equation):

$$\text{rate} = \kappa \frac{k_BT}{h} K^{\ddagger}[A][BC] \tag{6.4.4}$$

Most of the time the assumption $\kappa \approx 1$ is made and equation 6.4.3 is used.

Note that in this formulation $K^{\ddagger}$ is a concentration and not a thermodynamic equilibrium constant. To convert to a thermodynamic equilibrium constant without units we would need to divide each concentration by the reference concentration (usually c^o = 1 M).

6.4.3: Thermodynamic Formulation

By rewriting this model in terms of thermodynamic functions, we can reformulate equation 6.4.3 in a more generally useful form. First we must explicitly include the reference concentration so that we are using thermodynamic values. This means $K^{\ddagger} = K_c^{\ddagger} c^o$. This implies that the $K^{\ddagger}$ that appears in equation 6.4.3 must be replaced by $K^{\ddagger}/c^o$ to make the equilibrium constant appearing in the expression a thermodynamic equilibrium constant. So equation 6.4.3 becomes:

$$\text{rate} = \frac{k_B T}{h} \frac{K^{\ddagger}}{c^o} [A][BC] \tag{6.4.5}$$

The equilibrium constant, $K^{\ddagger}$ can be expressed in terms of the free energy of formation of the complex, $\Delta G^{\ddagger}$:

$$K^{\ddagger} = e^{-\Delta G^{\ddagger}/R/T}$$

And so the reaction rate is given by

$$\text{rate} = \frac{k_B T}{h c^o} [A][BC] e^{-\Delta G^{\ddagger}/R/T}$$

Notice that the division by c^o ensures that the rate is in units of concentration per unit time.

And the rate constant for the second order reaction is thus given by

$$k = \frac{k_B T}{h c^o} e^{-\Delta G^{\ddagger}/R/T}$$

We can get a useful expression for comparison with the Arrhenius equation by expanding $\Delta G^{\ddagger}$ in terms of enthalpy and entropy:

$$k = \frac{k_B T}{h c^o} exp\left(-\frac{\Delta H^{\ddagger} - T\Delta S^{\ddagger}}{RT}\right) = \frac{k_B T}{h c^o} exp\left(\frac{\Delta S^{\ddagger}}{R}\right) exp\left(\frac{-\Delta H^{\ddagger}}{RT}\right) \tag{6.4.6}$$

In solution $\Delta H^{\ddagger} = E_a - RT$ and in the gas phase $\Delta H^{\ddagger} = E_a - 2RT$.[2] This can be derived from the general definition of $E_a = RT^2(\partial ln(k)/\partial T)$. Even at 1000 K, RT ≈ 8 kJ/mol. So near ambient temperatures for reactions with activation energies of 10's to 100's of kJ/mol the difference between the enthalpy of activation and the activation energy is not going to be large. However, to directly compare with the Arrhenius equation, k = Aexp(-E_a/R/T), we can make the substitutions as shown in the two equations below.

Gas Phase:

$$k = \frac{k_B T}{h c^o} exp\left(\frac{\Delta S^{\ddagger}}{R}\right) exp(2) exp\left(\frac{-E_a}{RT}\right) \tag{6.4.7}$$

Liquid Phase:

$$k = \frac{k_B T}{h c^o} exp\left(\frac{\Delta S^{\ddagger}}{R}\right) exp(1) exp\left(\frac{-E_a}{RT}\right) \tag{6.4.8}$$

The blue parts of the expressions are the pre-exponential factors. Notice that they include $e^{\Delta S^{\ddagger}/R}$. As two molecules come together the entropy change on going to the transition state is negative making the contribution from entropy to the A factor less then 1, reducing the A factor. If this negative entropy change is more negative than would simply be expected from two colliding particles, this is called a "tight" transition state and is equivalent to a steric factor in the collision model of less than 1 (some collision orientations do not lead to reaction).

Notice that this formulation includes temperature dependence in the A factor through the explicit temperature and the temperature dependence of the entropy of activation.

6.4.4: References

1. K.J. Laidler, J.H. Meiser, B.C. Sanctuary *Physical Chemistry*, 4th Ed. (Houghton Mifflin Co. Boston, 2003) P. 390.

2. P.W. Atkins, J. de Paula, *Physical Chemistry*, 10th Ed. (W.H. Freeman and Co. New York, 2014) Pp. 894 - 899.

This page titled 6.4: Transition State Theory is shared under a CC BY-NC-SA 4.0 license and was authored, remixed, and/or curated by Jonathan Gutow.

- **11.11: Transition State Theory** by Patrick Fleming is licensed CC BY-NC-SA 4.0.

6.5: Reactions Involving Ions

6.5.1: Introduction

When ions react charged particles must come together. Thus we would expect a reaction between two like charged molecules to be disfavored compared to neutral species or opposite charges, because the like charges will repel, the opposite charges will attract, and the neutral species will experience no electrostatic forces (unless they are polar). For reactions in solution we would also expect the dielectric constant, polarizability and polarity of the solvent, and the presence of other ions to impact the reaction kinetics when polar or charged species are involved.

6.5.2: Impact of dielectric constant

In solution our model of a reaction is: $\mathrm{A}+\mathrm{B} \underset{k_{-1}}{\overset{k_1}{\rightleftharpoons}} \{\mathrm{AB}\} \overset{k_2}{\longrightarrow} \mathrm{P}$, where {AB} is the encounter pair, which also includes the transition state of the reaction. If A and B are charged the rate they come together in the first step will be impacted by the dielectric constant of the solvent.

The interaction potential between charged particles is proportional to $1/\epsilon$, where ϵ is the dielectric constant (relative permittivity) of the solvent. So for two molecules of the same charge in water ($\epsilon \approx 80$) they are more likely to come together than in methanol ($\epsilon \approx 33$), because methanol reduces the repulsion between the particles less than water. The situation is reversed for oppositely charged particles, since methanol reduces the attraction less than water leading to higher probability of forming {AB} for oppositely charged species in methanol. Thus, in the diffusion limited case higher dielectric constant will lead to faster reactions for like charges and slower reactions for opposite charges. An additional implication is that reactions between oppositely charged species in the diffusion limit may be faster than the limit estimated for neutral species in the same solvent.

Despite the fact that the solvent dielectric constant is expected to have minimal impact on the rate of the second step because in the encounter pair there is little or no solvent between the two species, the effects are the same in the activation controlled limit. In this limit the rate is:

$$\frac{d[P]}{dt} \approx k_2[\{AB\}] \tag{6.5.1}$$

k_2 is not impacted by the dielectric constant but the impact on the initial equilibrium is the same, either reducing or increasing the concentration of the encounter pair, [{AB}], as argued above.

6.5.3: Impact of solvent polarity or polarizability

If a solvent is polar or easily polarized it will stabilize charged species and to a lesser degree polar species. The more localized and larger the charge the greater the stabilization. Surrounding an ion with oriented dipoles (or polarized species) also reduces the strength of the interactions (either repulsive or attractive) between two charged particles. So, oppositely charged particles are less strongly attracted and same charged particles are less strongly repelled. Thus, one expects that the trends in reaction rate for increasing solvent polarity and increasing dielectric constant to be the same. However, there is an additional factor due to the significant overall stabilization of the charged particles.

Like charges: Since the stabilization increases with increased charge density when two like charges form an even more highly charged transition state the transition state is stabilized more than the reactants. This reduces the activation energy, $\Delta G^{\ddagger}$, as the solvent polarity or polarizability grows, increasing the reaction rate. So the impact is in the same direction as the reduced repulsion from the shielding. See figure 6.5.1.

Opposite charges: In this case the transition state will be less stabilized than the separate reactants, because the charges will partially or completely cancel out in the transition state. This means the as the solvent polarity or polarizability grows, the activation energy will increase, decreasing the reaction rate. Again the impact is in the same direction as the reduced attraction from the shielding. See figure 6.5.1.

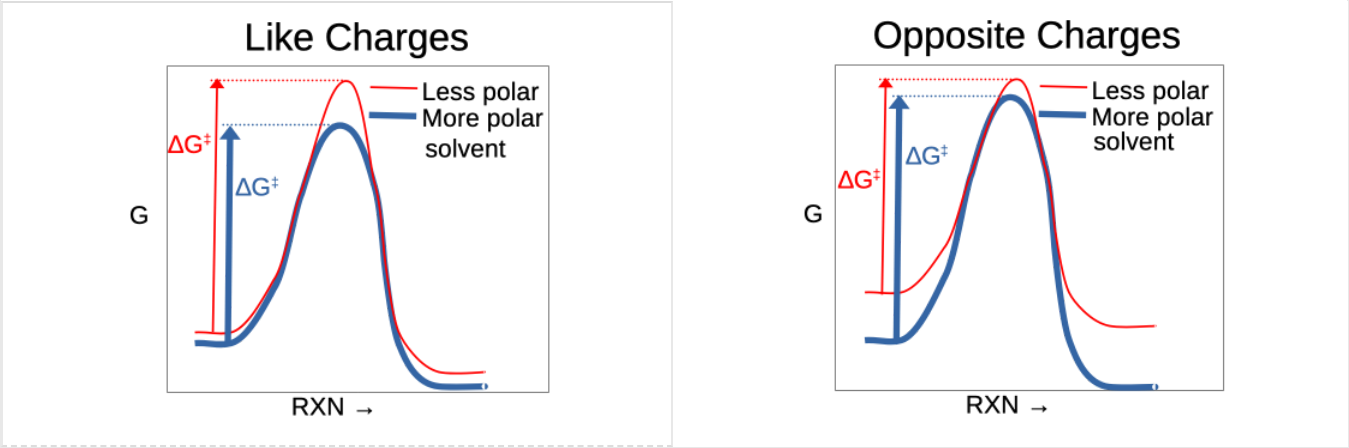


Figure 6.5.1: Impact of solvent polarity on the activation energy when charged particles react. For like charges the activation free energy change is reduced in the more polar solvent, increasing the reaction rate (blue). For opposite charges the activation free energy is increased in the more polar solvent, reducing the reaction rate (blue). Note that in the right-hand figure, if the opposite charges cancel out to make the transition state neutral and non-polar the free energy of the transition state may be exactly the same in the less and more polar solvents.

6.5.4: Impact of other ions (ionic strength)

If there are more ions in solution each ion is more likely to be surrounded by a local atmosphere of oppositely charged ions. For more details see a discussion of ionic activity/ionic strength (e.g. 5.2: The Debye-Hückel Theory). This means that any pair of particles are shielded from each other. Thus, like charged reactants can approach each other more easily and oppositely charged species are not attracted as strongly. Highly charged species are also more stabilized then species with lesser charges. Thus the arguments are parallel to those for polar solvents. Higher ion concentration (ionic strength):

- increases the rate of reactions between like charged species;
- and decreases the rate of reaction between oppositely charged species.

This is often referred to as the **kinetic salt effect**.

6.5.5: Quantitative model of ionic strength impact

Using transition state theory and the Debye-Hückel model for ion activities one can develop an approximate quantitative model for how reaction rates depend upon ionic strength.[1] Our model reaction mechanism is the same as from transition state theory:

$$\mathrm{A} + \mathrm{B} \rightleftharpoons \mathrm{C}^{\ddagger} \longrightarrow \mathrm{P}$$

If we assume an equilibrium between the charged reactants and the activated complex (transition state), $C^{\ddagger}$, then we have:

$$K = \frac{a_{C^{\ddagger}}}{a_A a_B} = \frac{\gamma_{C^{\ddagger}}}{\gamma_A \gamma_B} \frac{[C^{\ddagger}]c^o}{[A][B]} = K_{\gamma} \frac{[C^{\ddagger}]c^o}{[A][B]} \tag{6.5.2}$$

Where a_i = activity of i, γ_i = the activity coefficient of i, and c^o is the reference concentration (usually 1 M). Solving for $[C^{\ddagger}]$:

$$[C^{\ddagger}] = \frac{K}{K_{\gamma} c^o}[A][B] \tag{6.5.3}$$

The rate of formation of products from the activated complex is:

$$\frac{d[P]}{dt} = k^{\ddagger}[C^{\ddagger}] = k^{\ddagger} \frac{K}{K_{\gamma} c^o}[A][B] \tag{6.5.4}$$

From 6.5.4 we identify the overall rate constant for the reaction k_r as:

$$k_r = k^{\ddagger} \frac{K}{K_{\gamma} c^o} \tag{6.5.5}$$

We identify the reference rate k_r^o as the rate when K_γ = 1:

$$k_r^o = k^\ddagger \frac{K}{c^o} \implies k_r = \frac{k_r^o}{K_\gamma} \tag{6.5.6}$$

Now we use the Debye-Hückel limiting law to estimate the activity coefficients of the charged species. For a single ion the theory predicts the following for the $\log_{10}$ of the activity coefficient:

$$log\gamma_i = -Az_i^2\sqrt{I} \tag{6.5.7}$$

where z_i = charge on the species i, and I = the ionic strength of the solution. Clearly we need to look at the $\log_{10}$ of k_r:

$$logk_r = logk_r^o - logK_\gamma = logk_r^o + log\gamma_A + log\gamma_B - log\gamma_{C^\ddagger} \tag{6.5.8}$$

Substituting in with equation 6.5.7 for each of the activity coefficient logs:

$$logk_r = logk_r^o - A(z_A^2 + z_B^2 - (z_A + z_B)^2)\sqrt{I} = logk_r^o + 2Az_Az_B\sqrt{I} \tag{6.5.9}$$

This equation matches the qualitative predictions that higher ionic strength will lead to a higher rate constant if the charges on A and B are the same and a lower rate constant if they are different. Note that a plot of log k_r versus $\sqrt{I}$ allows one to extract the reference rate (from the intercept) and the product of the two charges from the slope. Thus if you only know the charge on one of the species involved in the rate limiting step you can get the other from the slope.

6.5.6: References

1. P.W. Atkins, J. de Paula, *Physical Chemistry*, 10th Ed. (W.H. Freeman and Co. New York, 2014) Pp. 900 - 901.

This page titled 6.5: Reactions Involving Ions is shared under a CC BY-NC-SA 4.0 license and was authored, remixed, and/or curated by Jonathan Gutow.

- **17.5: Kinetics of Reactions in Solution** by Stephen Lower is licensed CC BY 3.0. Original source: http://www.chem1.com/acad/webtext/virtualtextbook.html.

CHAPTER OVERVIEW

7: Kinetic Mechanisms 2

7.1: Numerical Modeling of Mechanisms
7.2: The Michaelis-Menten Mechanism
7.3: The Lindemann Mechanism
7.4: Chain Reactions
7.5: Catalysis (ozone example)
7.6: Oscillating Reactions
7.7: Diffusion
7.8: Membrane Diffusion
7.9: Ion Mobilities
7.10: Transport Across Cell Membranes
7.11: Kinetics of Electron Transfer Reactions

This page titled 7: Kinetic Mechanisms 2 is shared under a CC BY-NC-SA 4.0 license and was authored, remixed, and/or curated by Jonathan Gutow.

7.1: Numerical Modeling of Mechanisms

7.1.1: Introduction

In many cases complicated mechanisms cannot be analytically integrated to determine the time profiles of all the species involved and approximation methods (pre-equilibrium, steady-state, etc...) do not provide an adequate model to make useful predictions. Figuring out which pollutants are the most important to control to reduce smog is one example where good models for the kinetics and time evolution of the species involved is essential. There are two primary methods used for numerical modeling of reaction mechanisms: numerical integration; and stochastic modeling. Numerical integration works well as long as samples are large enough that the discrete (particulate) nature of matter can be ignored, and the system is not chaotic.

7.1.2: Numerical Integration

In this case the differential rate laws are used to propagate the reaction mechanism in small time steps. For this discussion we will illustrate the simple Euler method.[1,2] Consider the following kinetic mechanism:

$$\mathrm{A} + \mathrm{B} \underset{k_{-1}}{\overset{k_1}{\rightleftharpoons}} \mathrm{I} \xrightarrow{k_2} \mathrm{P}$$

The differential rate laws for each of the species are:

$$\frac{d[A]}{dt} = \frac{d[B]}{dt} = k_{-1}[I] - k_1[A][B]$$

$$\frac{d[I]}{dt} = k_1[A][B] - k_{-1}[I] - k_2[I]$$

$$\frac{d[P]}{dt} = k_2[I]$$

If at time zero (t = 0) we have [A] = $[A]_o$, [B] = $[B]_o$, [I] = $[I]_o$, and [P] = $[P]_o$ we can substitute these into the rate laws to calculate any of the rates (slopes) at t = 0. For example:

$$\left.\frac{d[A]}{dt}\right|_o = \left.\frac{d[B]}{dt}\right|_o = k_{-1}[I]_o - k_1[A]_o[B]_o$$

The value of $[A]_{0+\Delta t}$ (concentration after time Δt has passed) can be approximated by adding the slope multiplied by the size of the Δt step to $[A]_o$:

$$[A]_{\Delta t} \approx [A]_o + \Delta t \left.\frac{d[A]}{dt}\right|_o \tag{7.1.1}$$

We can then repeat this process for all the species to get $[B]_{0+\Delta t}$, $[I]_{0+\Delta t}$, and $[P]_{0+\Delta t}$. If Δt is small enough these will be good estimates of the values. The new values can then be used in the rate laws to calculate new slopes at time 0 + Δt (e.g. $d[A]/dt|_{0+\Delta t}$). The process is then repeated using the new slopes and concentrations to estimate the concentration after the next time step. Thus, the concentration of $[A]_{n\Delta t}$, the concentration of A at time nΔt, where n is the number of steps taken is:

$$[A]_{n\Delta t} \approx [A]_{(n-1)\Delta t} + \Delta t \left.\frac{d[A]}{dt}\right|_{(n-1)\Delta t} \tag{7.1.2}$$

The issue here is that if the steps are too big the estimated concentrations rapidly deviate from the actual values (see figure 7.1.1). There are more robust methods, such as the Bulirsch–Stoer algorithm[3], which extend the Euler method by adjusting the step size and making more sophisticated estimates of how the the derivatives change with time.

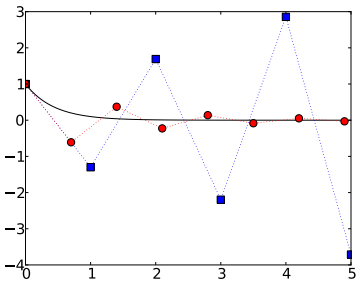


Figure 7.1.1: Illustration of how a large step size can lead to a poor estimate of the actual integrated curve. Black curve is exact, blue squares are the larger time step and red dots are the smaller time step. From Jitse Niesen, CC0, via Wikimedia Commons.

Another serious problem with numerical integration for modeling chemical reactions is that it ignores the fact that matter is particulate. It allows reactions to involve fractions of a molecule. This is not a serious problem for large samples, but can give very wrong answers for reactions occurring in small volumes with only a few molecules or in cases where reactions oscillate, in which case the difference between a whole molecule and 1/2 molecule (which is physically 0 molecules) is significant.

7.1.3: Stochastic Modeling

Stochastic modeling treats each reaction event separately through the probability that a particular molecule or pair of molecules will react. Because this method deals with discrete reaction events, it also properly accounts for the fact that you cannot have a fraction of a molecule (e.g. (1/8) H_2O) involved in a reaction. The discrete nature of matter becomes important when dealing with small numbers of molecules in small volumes as seen inside of cellular organelles. These situations can lead to very different overall outcomes each time the process happens. One of the first good descriptions of the stochastic method was published by Gillespie in 1977.[4] We will not delve into the details of the implementation here, but figure 7.1.2 illustrates the important difference between using numerical integration, which does not allow for fluctuations seen in small samples and the stochastic method which does.

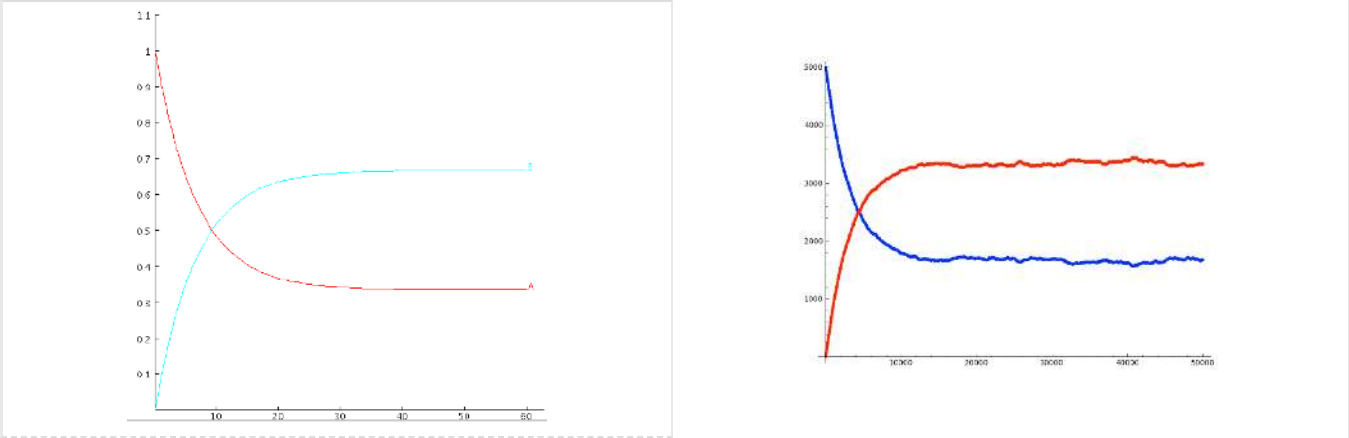


Figure 7.1.2: The left image illustrates a reaction approaching equilibrium using numerical integration. The right image is the same approach to equilibrium using stochastic methods. Notice that the stochastic method shows realistic statistical fluctuations around the final equilibrium amounts of the species.

7.1.4: References

1. "Euler Method", Wikipedia.org (https://en.wikipedia.org/wiki/Euler_method), accessed April 2025.

2. "Numerical methods for ordinary differential equations", Wikipedia.org (https://en.wikipedia.org/wiki/Numerical_methods_for_ordinary_differential_equations), accessed April 2025.

3. "Bulirsch–Stoer algorithm", Wikipedia.org (https://en.wikipedia.org/wiki/Bulirsch%E2%80%93Stoer_algorithm), accessed April 2025.

4. D. T. Gillespie, J. Phys. Chem. 1977, 81(25), 1977, 2340–2361. https://doi.org/10.1021/j100540a008.

This page titled 7.1: Numerical Modeling of Mechanisms is shared under a CC BY-NC-SA 4.0 license and was authored, remixed, and/or curated by Jonathan Gutow.

7.2: The Michaelis-Menten Mechanism

7.2.1: Introduction

The **Michaelis-Menten** mechanism (Michaelis & Menten, 1913) is one which many enzyme catalyzed reactions follow. The basic mechanism involves an enzyme (E, a biological catalyst) and a substrate (S) which must connect to form an enzyme-substrate complex (ES) in order for the substrate to be degraded (or augmented) to form a product (P). The overall reaction is

$$S \rightarrow P$$

And the simple two-step mechanism is given by

$$E + S \underset{k_{-1}}{\overset{k_1}{\rightleftharpoons}} ES \tag{7.2.1}$$

$$ES \xrightarrow{k_2} P \tag{7.2.2}$$

Notice that the enzyme is necessary for the reaction to proceed, but is not part of the overall stoichiometry (as is the case for any catalyst!).

7.2.2: Equilibrium Approximation Derivation

Applying the equilibrium approximation to the first step

$$k_1[E][S] \approx k_{-1}[ES] \tag{7.2.3}$$

And using a mass conservation relationship on the enzyme (noting that the enzyme must be either in its bare form (E) or complexed with a substrate (ES)):

$$[E]_o = [E] + [ES]$$

or

$$[E] = [E]_o - [ES]$$

Substituting this into the equilibrium expression (Equation 7.2.3) yields

$$k_1([E]_o - [ES])[S] = k_{-1}[ES]$$

Solving this expression for $[ES]$ stepwise reveals

$$k_1[E]_o[S] - k_1[ES][S] = k_{-1}[ES]$$

$$k_1[E]_o[S] = k_{-1}[ES] + k_1[ES][S]$$

$$= (k_{-1} + k_1)[ES]$$

$$\frac{k_1[E]_o[S]}{k_1[S] + k_{-1}} = [ES]$$

Substituting this into the expression for the rate of production of the product P

$$\frac{d[P]}{dt} = k_2[ES] \tag{7.2.4}$$

yields

$$\frac{d[P]}{dt} = \frac{k_2 k_1[E]_o[S]}{k_1[S] + k_{-1}}$$

Multiplying the top and bottom of the expression on the right hand side by $1/k_1$ gives the result

$$\frac{d[P]}{dt} = \frac{k_2[E]_o[S]}{[S] + \frac{k_1}{k_{-1}}}$$

The ratio of k_{-1}/k_1 is the equilibrium constant that describes the dissociation of the enzyme-substrate complex, K_d in Equation 7.2.1. Noting that $k_2[E]_0$ gives the maximum rate (V_{max}), and that $\frac{d[P]}{dt}$ is the observed reaction rate, the rate law takes the form

$$\text{rate} = \frac{V_{max}[S]}{K_d + [S]}$$

In the limit that the substrate concentration is large compared to K_d (i.e., $K_d + [S] \approx [S]$), the reaction ends up zeroth order in substrate.

$$\text{rate} = \frac{V_{max}[S]}{K_d + [S]} \approx \frac{V_{max}\ \cancel{[S]}}{\cancel{[S]}} = V_{max}$$

Hence, adding more substrate to the system under this limiting condition will have no effect on the observed rate. This is characteristic of a bottleneck in the mechanism, which would happen if there is a shortage of enzyme sites to which the substrate can attach.

In the other extreme, in which K_d is very large compared to the substrate concentration (i.e., $K_d + [S] \approx K_d$), the reaction become first order in substrate.

$$\text{rate} = \frac{V_{max}[S]}{K_d + [S]} \approx \frac{V_{max}[S]}{K_d} = \frac{V_{max}}{K_d}[S]$$

7.2.3: Steady-State Approximation Derivation

In an alternate derivation (Briggs & Haldane, 1925) using the steady state approximation applied to the enzyme-substrate complex

$$\frac{[ES]}{dt} = k_1[E][S] - k_{-1}[ES] - k_2[ES] \approx 0$$

Solving for $[ES]$ gives the result

$$[ES] = \frac{k_1[E][S]}{k_{-1} + k_2}$$

or

$$[ES] = \frac{[E][S]}{K_m}$$

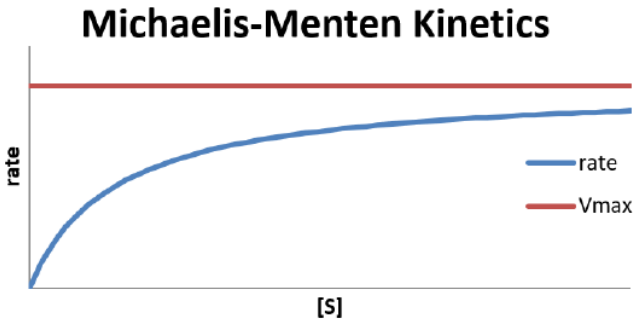
where

$$K_m = \frac{k_{-1} + k_2}{k_1}$$

K_M is the **Michaelis constant**, which is affected by a number of factors, including pH, temperature, and the nature of the substrate itself. Proceeding as before, though the conservation of mass relationship and substitution into the expression for rate (Equation 7.2.4) results in

$$\frac{d[P]}{dt} = \frac{V_{max}[S]}{K_m + [S]}$$

The advantage to this approach is that it accounts for the loss of ES complex due to the production of products as well as the decomposition to reform the reactants E and S. As before, in the limit that $[S] \gg K_M$, the reaction reaches its maximum rate (V_{max}) and becomes independent of any concentrations. However in the limit that $[S] \ll K_M$, the reaction becomes 1st order in $[S]$.



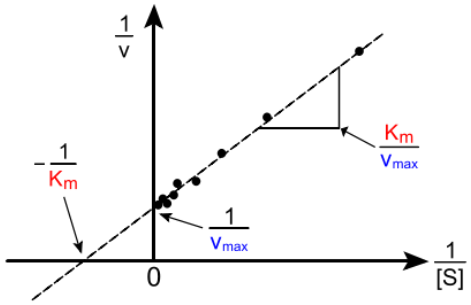
The Michalis constant and V_{max} parameters can be extracted in a number of ways. In the Lineweaver-Burk (Lineweaver & Burk, 1934) method, the reciprocal of the rate law is used to create a linear relationship.

$$\frac{1}{\text{rate}} = \frac{K_m + [S]}{V_{max}[S]}$$

or

$$\frac{1}{\text{rate}} = \frac{K_m}{V_{max}}\frac{1}{[S]} + \frac{1}{V_{max}}$$

So a plot of $1/rate$ as a function of $1/[S]$ results in a straight line, the slope of which is equal to K_M/V_{max} and the intercept is $1/V_{max}$. This is called a Lineweaver–Burk plot.



An example of a Lineweaver-Burk plot. (CC BY-SA 3.0; Diberri).

This page titled 7.2: The Michaelis-Menten Mechanism is shared under a CC BY-NC-SA 4.0 license and was authored, remixed, and/or curated by Jonathan Gutow.

- **12.8: The Michaelis-Menten Mechanism** by Patrick Fleming is licensed CC BY-NC-SA 4.0.

7.3: The Lindemann Mechanism

7.3.1: Introduction

The **Lindemann mechanism** (Lindemann, Arrhenius, Langmuir, Dhar, Perrin, & Lewis, 1922) is a useful one to demonstrate some of the techniques we use for relating chemical mechanisms to rate laws. In this mechanism, a reactant is collisionally activated to a highly energetic form that can then go on to react to form products.

$$A + A \underset{k_1}{\overset{k_{-1}}{\rightleftharpoons}} A^* + A$$

$$A^* \xrightarrow{k_2} P$$

As written in this mechanism it is assumed that the energy is removed from A^* by collision. If it leaves via photon emission, than the reaction with rate constant k_{-1} is unimolecular rather than bimolecular.

7.3.2: Steady-state Analysis

If the steady state approximation is applied to the intermediate A^*

$$\frac{d[A^*]}{dt} = k_1[A]^2 - k_{-1}[A^*][A] - k_2[A^*] \approx 0$$

an expression can be derived for $[A^*]$.

$$[A^*] = \frac{k_1[A]^2}{k_{-1}[A] + k_2}$$

Substituting this into an expression for the rate of the production of the product P

$$\frac{d[P]}{dt} = k_2[A^*]$$

yields

$$\frac{d[P]}{dt} = \frac{k_2 k_1[A]^2}{k_{-1}[A] + k_2}$$

In the limit that $k_{-1}[A] \ll k_2$, the rate law becomes first order in $[A]$ since $k_{-1}[A] + k_2 \approx k_{-1}[A]$.

$$\frac{d[P]}{dt} = \frac{k_2 k_1}{k_{-1}}[A]$$

This will happen if the second step is very slow (and is the rate determining step), such that the reverse of the first step "wins" in the competition for [A*]. However, in the other limit, that $k_2 \gg k_{-1}[A]$, the reaction becomes second order in $[A]$ since $k_{-1}[A] + k_2 \approx k_2$.

$$\frac{d[P]}{dt} = k_1[A]^2$$

which is consistent with the forward reaction of the first step being the rate determining step, since A^* is removed from the reaction (through the formation of products) very quickly as soon as it is formed.

7.3.3: Third-body Collisions

Sometimes, the **third-body collision** is provided by an inert species M, perhaps by filling the reaction chamber with a heavy non-reactive species, such as Ar. In this case, the mechanism becomes

$$A + M \underset{k_1}{\overset{k_{-1}}{\rightleftharpoons}} A^* + M$$

$$A^* \xrightarrow{k_2} P$$

In the limit that $[A^*]$ can be treated using the steady state approximation, where [M] = concentration of all colliding species (e.g. [A] + [Ar], assuming [A*] is negligible) we get:

$$[A^*] = \frac{k_1[A][M]}{k_{-1}[M] + k_2}$$

and the rate of production of the product becomes

$$\frac{d[P]}{dt} = k_2 \frac{k_1[M][A]}{k_{-1}[M] + k_2}$$

If the concentration of the third body collider is constant ([Ar] >> [A]), it is convenient to define an **effective rate constant**, k_{uni}.

$$k_{uni} = \frac{k_2 k_1[M]}{k_{-1}[M] + k_2}$$

The utility is that important information about the individual step rate constants can be extracted by plotting $1/k_{uni}$ as a function of $1/[M]$.

$$\frac{1}{k_{uni}} = \frac{k_{-1}}{k_2 k_1} + k_2 \left(\frac{1}{[M]}\right)$$

The plot should yield a straight line, the slope of which gives the value of k_2, and the intercept gives $(k_{-1}/k_2 k_1)$.

This page titled 7.3: The Lindemann Mechanism is shared under a CC BY-NC-SA 4.0 license and was authored, remixed, and/or curated by Jonathan Gutow.

- **12.7: The Lindemann Mechanism** by Patrick Fleming is licensed CC BY-NC-SA 4.0.

7.4: Chain Reactions

A large number of reactions proceed through a series of steps that can collectively be classified as a **chain reaction**. The reactions contain steps that can be classified as

- **initiation step** – a step that creates the intermediates from stable species
- **propagation step** – a step that consumes an intermediate, but creates a new one
- **termination step** – a step that consumes intermediates without creating new ones

These types of reactions are very common when the intermediates involved are radicals. An example, is the reaction

$$H_2 + Br_2 \rightarrow 2HBr$$

The observed rate law for this reaction is

$$\text{rate} = \frac{k[H_2][Br_2]^{3/2}}{[Br_2] + k'[HBr]} \tag{7.4.1}$$

A proposed mechanism is

$$Br_2 \underset{k_{-1}}{\overset{k_1}{\rightleftharpoons}} 2Br^{\cdot} \tag{7.4.2}$$

$$2Br^{\cdot} + H_2 \underset{k_{-2}}{\overset{k_2}{\rightleftharpoons}} HBr + H^{\cdot} \tag{7.4.3}$$

$$H^{\cdot} + Br_2 \xrightarrow{k_3} HBr + Br^{\cdot} \tag{7.4.4}$$

Based on this mechanism, the rate of change of concentrations for the intermediates ($H^{\cdot}$ and $Br^{\cdot}$) can be written, and the steady state approximation applied.

$$\frac{d[H^{\cdot}]}{dt} = k_2[Br^{\cdot}][H_2] - k_{-2}[HBr][H^{\cdot}] - k_3[H^{\cdot}][Br_2] = 0$$

$$\frac{d[Br^{\cdot}]}{dt} = 2k_1[Br_2] - 2k_{-1}[Br^{\cdot}]^2 - k_2[Br^{\cdot}][H_2] + k_{-2}[HBr][H^{\cdot}] + k_3[H^{\cdot}][Br_2] = 0$$

Adding these two expressions cancels the terms involving k_2, k_{-2}, and k_3. The result is

$$2k_1[Br_2] - 2k_{-1}[Br^{\cdot}]^2 = 0$$

Solving for $Br^{\cdot}$

$$Br^{\cdot} = \sqrt{\frac{k_1[Br_2]}{k_{-1}}}$$

This can be substituted into an expression for the $H^{\cdot}$ that is generated by solving the steady state expression for $d[H^{\cdot}]/dt$.

$$[H^{\cdot}] = \frac{k_2[Br^{\cdot}][H_2]}{k_{-2}[HBr] + k_3[Br_2]}$$

so

$$[H^{\cdot}] = \frac{k_2\sqrt{\frac{k_1[Br_2]}{k_{-1}}}[H_2]}{k_{-2}[HBr] + k_3[Br_2]}$$

Now, armed with expressions for $H^{\cdot}$ and $Br^{\cdot}$, we can substitute them into an expression for the rate of production of the product HBr:

$$\frac{d[HBr]}{dt} = k_2[Br^{\cdot}][H_2] + k_3[H^{\cdot}][Br_2] - k_{-2}[H^{\cdot}][HBr]$$

After substitution and simplification, the result is

$$\frac{d[HBr]}{dt} = \frac{2k_2\left(\frac{k_1}{k_{-1}}\right)^{1/2}[H_2][Br_2]^{1/2}}{1+\frac{k_{-1}}{k_3}\frac{[HBr]}{[Br_2]}}$$

Multiplying the top and bottom expressions on the right by $[Br_2]$ produces

$$\frac{d[HBr]}{dt} = \frac{2k_2\left(\frac{k_1}{k_{-1}}\right)^{1/2}[H_2][Br_2]^{3/2}}{[Br_2]+\frac{k_{-1}}{k_3}[HBr]}$$

which matches the form of the rate law found experimentally (Equation 7.4.1)! In this case,

$$k = 2k_2\sqrt{\frac{k_1}{k_{-1}}}$$

and

$$k' = \frac{k_{-2}}{k_3}$$

This page titled 7.4: Chain Reactions is shared under a CC BY-NC-SA 4.0 license and was authored, remixed, and/or curated by Jonathan Gutow.

- **12.9: Chain Reactions** by Patrick Fleming is licensed CC BY-NC-SA 4.0.

7.5: Catalysis (ozone example)

There are many examples of reactions that involve catalysis. One that is of current importance to the chemistry of the environment is the catalytic decomposition of ozone (Fahey, 2006). The overall reaction

$$O_3 + O^{\cdot} \longrightarrow 2\,O_2$$

can be catalyzed by atomic chlorine by the following mechanism.

$$O_3 + Cl \xrightarrow{k_1} ClO + O_2 \qquad \text{(step 1)}$$

$$ClO + O \xrightarrow{k_2} Cl + O_2 \qquad \text{(step 2)}$$

The rate of change of the intermediate (ClO) concentration is given by

$$\frac{d[ClO]}{dt} = k_1[O_3][Cl] - k_2[ClO][O]$$

Applying the steady state approximation to this relationship and solving for $[ClO]$ produces

$$[ClO] = \frac{k_1[O_3][Cl]}{k_2[O]} \qquad (7.5.1)$$

The rate of production of O_2 (which is two times the rate of the reaction) is given by

$$\frac{d[O_2]}{dt} = k_1[O_3][Cl] + k_2[ClO][O]$$

Substituting the expression for $[ClO]$ (Equation 7.5.1) into the above expression yields

$$\begin{aligned}\frac{d[O_2]}{dt} &= k_1[O_3][Cl] + k_2\left(\frac{[k_1O_3][Cl]}{k_2[O]}\right)[O] \\ &= k_1[O_3][Cl] + k_1[O_3][Cl] \\ &= 2k_1[O_3][Cl]\end{aligned}$$

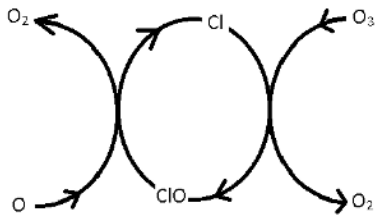
And so the rate of the reaction is predicted to be first order in $[O_3]$, first order in the catalyst $[Cl]$, and second order overall.

$$\text{rate} = k[O_3][Cl]$$

This demonstrates classic catalysis, where the Cl is not used up, but increasing its concentration increases the overall rate. If the concentration of the catalyst is constant, the reaction kinetics will reduce to first order.

$$\text{rate} = k[O_3]$$

This catalytic cycle can be represented in the following diagram:



On the left, atomic oxygen picks up an oxygen atom from ClO to form O_2 and generate a Cl atom, which can then react with O_3 to form ClO and an O_2 molecule. The closed loop in the middle is characteristic of the catalytic cycle involving Cl and ClO. Further, since Cl acts as a catalyst, it can decompose many O_3 molecules without being degraded through side reactions.

The introduction of chlorine atoms into the upper atmosphere is a major environmental problem, leading to the annual thinning and eventual opening of the ozone layer over Antarctica. The source of chlorine is from the decomposition of chlorofluorocarbons

which are sued as refrigerants and propellants due to their incredible stability near the Earth's surface. However, in the upper atmosphere, these compounds are subjected to ultraviolet radiation emitted by the sun and decompose to form the radicals responsible for the catalytic decomposition of ozone. The world community addressed this issue by drafting the **Montreal Protocol (Secretariat, 2015)**, which focused on the emission of ozone-destroying compounds. The result of this action has been a stabilization and possible decrease in the size and degree of depletion seen in the Antartic ozone hole (see NASA ozone watch, September images). This is one example science-guided political, industrial, and economic policies leading to positive changes for our environment.

It is noteworthy that one reason for the success of this was many commercial enterprises saw a big market for products to replace the chlorine containing CFC products that were the source of the stratospheric chlorine. Thus, they may not have fought as strongly against the regulations phasing out CFCs.

This page titled 7.5: Catalysis (ozone example) is shared under a CC BY-NC-SA 4.0 license and was authored, remixed, and/or curated by Jonathan Gutow.

- **12.10: Catalysis** by Patrick Fleming is licensed CC BY-NC-SA 4.0.

7.6: Oscillating Reactions

7.6.1: Introduction

In most cases, the conversion of reactants into products is a fairly smooth process, in that the concentrations of the reactants decrease in a regular manner, and those of the products increase in a similar regular manner. However, some reactions can show irregular behavior in this regard. One particularly peculiar (but interesting!) phenomenon is that of **oscillating reactions**, in which reactant concentrations can rise and fall as the reaction progresses. One way this can happen is when the products of the reaction (or one of the steps) catalyzes the reaction (or one of the steps. This process is called **autocatalysis**.

An example of an autocatalyzed mechanism is the **Lotka-Voltera mechanism**. This is a three-step mechanism defined as follows:

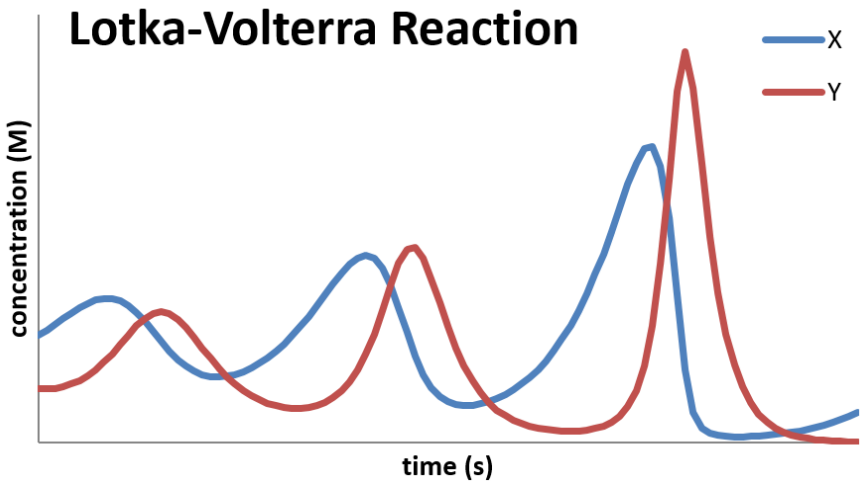
$$A + X \xrightarrow{k_1} X + X$$

$$X + Y \xrightarrow{k_2} Y + Y$$

$$Y \xrightarrow{k_3} B$$

In this reaction, the concentration of reactant A is held constant by continually adding it to the reaction mixture. The first step is **autocatalyzed**, so as it proceeds, it speeds up. However, an increase in the production of X by the first reaction increases the rate of the second reaction as well, which is also autocatalyzed. Finally, the removal of Y through the third reaction brings things to a halt, until the first reaction can again produce a build up of X to start the cycle over.

A plot of the concentration of X and Y as a function of time looks as follows:



This mechanism follows kinetics predicted by what is called the **predator-prey** relationship. In this case, X represents the "prey" and Y represents the "predator". The population of the predator cannot build up unless there is a significant population of prey on which the predators can feed. Likewise, the population of predators decreases when the population of the prey falls. And finally, there is a lag, as the rise and decline of the prey population controls the rise and fall of the predator population. The equations have been studied extensively and have applications not just in chemical kinetics, but in biology, economics, and elsewhere.

7.6.2: Steady-state approximation applied to Lotka-Volterra reaction[1]

Species A being added to keep [A] constant implies that [A] = $[A]_o$, an unchanging constant.

The rate laws are:

$$\frac{d[X]}{dt} = k_1[A]_o[X] - k_2[X][Y]$$

$$\frac{d[Y]}{dt} = k_2[X][Y] - k_3[Y]$$

If [X] is in steady state:

$$0 = k_1[A]_o[X] - k_2[X][Y] = [X](k_1[A]_o - k_2[Y])$$

Which has two possible solutions: [X] = 0 or [Y] = $k_1[A]_o/k_2$. Applying the steady state to [Y] yields:

$$0 = k_2[X][Y] - k_3[Y] = [Y](k_2[X] - k_3) \implies [Y] = 0 \text{ or } [X] = \frac{k_3}{k_2}$$

So we now have two steady-state solutions for each species:

$$[X] = \frac{k_3}{k_2} \text{ or } [X] = 0$$

$$[Y] = \frac{k_1[A]_o}{k_2} \text{ or } [Y] = 0$$

This means that the reaction could oscillate between the two extremes for each species. Having multiple steady-state solutions for species is a hallmark of reactions that can oscillate. This is an example of an unstable (bistable) system. Reference 1 has a more detailed mathematical analysis of the time behavior where the oscillations are modeled as small excursions from the steady-state conditions $[Y]_{ss} = k_1[A]_o/k_2$ and $[X]_{ss} = k_3/k_2$.

7.6.3: References

1. J. I. Steinfeld, J.S Francisco, W. L. Hase *Chemical Kinetics and Dynamics* (Prentice-Hall, Inc, Englewood Cliffs, New Jersey, 1989) Sec. 5.3.

7.6.4: Contributors

- Patrick Fleming (CSU Eastbay)
- Jonathan Gutow (UW Oshkosh)

This page titled 7.6: Oscillating Reactions is shared under a CC BY-NC-SA 4.0 license and was authored, remixed, and/or curated by Jonathan Gutow.

- **12.11: Oscillating Reactions** by Patrick Fleming is licensed CC BY-NC-SA 4.0.

7.7: Diffusion

7.7.1: Introduction

We are now going to start a new set of topics that involve the dynamics of molecular transport. A significant fraction of how molecules move spatially in biophysics is described macroscopically by “diffusion” and microscopically through its counterpart “Brownian motion”. Diffusion refers to the phenomenon by which concentration and temperature gradients spontaneously disappear with time, and the properties of the system become spatially uniform. As such, diffusion refers to the transport of mass and energy in a nonequilibrium system that leads toward equilibrium. Brownian motion is also a spontaneous process observed in equilibrium and non-equilibrium systems. It refers to the random motion of molecules in fluids that arises from thermal fluctuations of the environment that rapidly randomize the velocity of particles. Much of the molecular transport in biophysics over nanometer distances arises from diffusion.

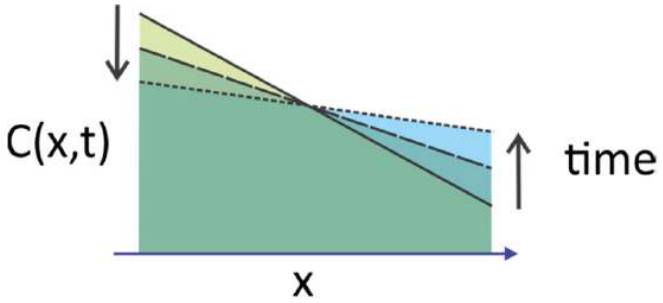


Figure 7.7.1: Cartoon of the evolution of a concentration gradient versus time.

This can be contrasted with directed motion, which requires the input of energy and is crucial for transporting cargo to targets over micron-scale distances. Here we will start by describing diffusion in continuum systems.

7.7.2: Fick's First Law

We will describe the time evolution of spatially varying concentration distributions $C(x,t)$ as they evolve toward equilibrium. These are formalized in two laws that were described by Adolf Fick (1855).[1] Fick’s first law is the “common sense law” that is in line with everyone’s physical intuition. Molecules on average will tend to diffuse from regions of higher concentration to regions of lower concentration. Therefore we say that the flux of molecules through a surface, J, is proportional to the concentration gradient across that surface.

$$J = -D\frac{\partial C}{\partial x} \tag{7.7.1}$$

J is more accurately called a flux density, since it has units of concentration or number density per unit area and time. The proportionality constant between flux density J (mol m^{-2} s^{-1}) and concentration gradient (mol m^{-4}) which sets the timescale for the process is the diffusion constant D (m^2 s^{-1}). The negative sign assures that the flux points in the direction of decreasing concentration. This relationship follows naturally, when we look at the two concentration gradients in the figure. Both C and C' have a negative gradient that will lead to a flux in the positive direction. C will give a bigger flux than C' because there is more probability for flow to right. The gradient disappears and the concentration distribution becomes constant and time invariant at equilibrium. Note, in a general sense $\partial C/\partial x$ can be considered the leading term in an expansion of C in x.

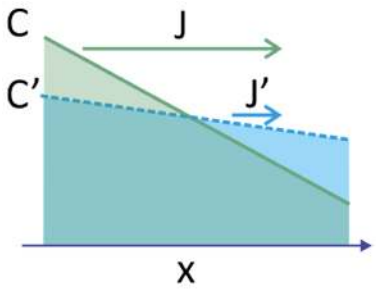


Figure 7.7.2: Cartoon of flux density relation to concentration gradient.

7.7.3: Fick's Second Law

Fick's second law extends the first law by adding an additional constraint based on the conservation of mass. Consider diffusive transport along x in a pipe with cross-sectional area a, and the change in the total number of particles within a disk of thickness Δx over a time period Δt.

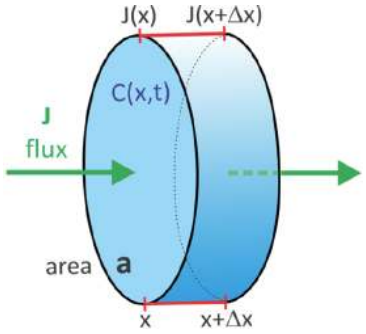


Figure 7.7.3: Cartoon illustrating the relation between flux in and out of a thin slab. If the concentration is changing over time the two fluxes are not equal.

If we take this disk to be thin enough that the concentration is a constant at any moment in time, then the total number of particles in the slab at that time is obtained from the concentration times the volume:

$$N = aC(t)\Delta x$$

Within the time interval Δt the concentration can change and therefore the total number of particles within the disk changes by an amount

$$\Delta N = a\{C(t+\Delta t) - C(t)\}\Delta x$$

Now, the change in the number of particles is also dependent on the fluxes of molecules at the two surfaces of the disk. The number of molecules passing into one surface of the disk is $-aJ\,\Delta\,t$, and therefore the net change in the number of molecules during Δt is obtained from the difference of fluxes between the left and right surfaces of the disk:

$$\Delta N = -a\,J(x+\Delta x) - J(x)\Delta t$$

Setting these two calculations of ΔN equal to each other, we see that the flux and concentration gradients for the disk are related as

$$\{C(t+\Delta t) - C(t)\}\Delta x = -\{J(x+\Delta x) - J(x)\}\Delta t$$

or rewriting this in differential form

$$\frac{\partial C}{\partial t} = -\frac{\partial J}{\partial x} \tag{7.7.2}$$

This important relationship is known as a continuity expression. Substituting eq. (7.7.1) into this expression leads to **Fick's Second Law**

$$\frac{\partial C}{\partial t} = -\frac{\partial}{\partial x}\left(-D\frac{\partial C}{\partial x}\right) = D\frac{\partial^2 C}{\partial x^2} \tag{7.7.3}$$

This is the diffusion equation in one dimension. So the rate of change of the concentration with respect to time is proportional to the second derivative (curvature) of the concentration. A positive curvature (dip in the spatial concentration distribution) leads to an increase in the concentration in the low concentration regions. Likewise the curvature of a high concentration region will be negative, predicting a decrease of the concentration in the high concentration regions. As expected over time the concentration will even out as shown in the figure 7.7.4 below.

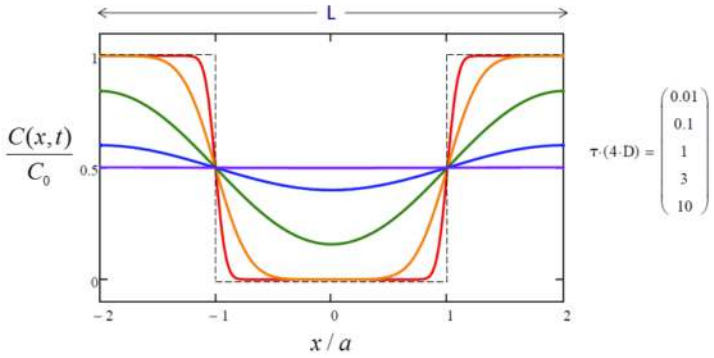


Figure 7.7.4: Concentration profile versus time for an initial square hole in the concentration (dashed line). Red curve is the first small time step, orange the next, then green, then blue and finally purple is after the longest time.

7.7.4: Diffusion from a Point Source

As our first example of how concentration distributions evolve diffusively, we consider the time-dependent concentration profile when the concentration is initially all localized to one point in space, x = 0. The initial condition is

$$C(x, t = 0) = C_0 \delta(x)$$

and the solution to eq. (10.1.3) is

$$C(x,t) = \frac{C_0}{\sqrt{4\pi Dt}} e^{-x^2/4Dt} \tag{7.7.4}$$

The concentration profile has a Gaussian form which is centered on the origin, ⟨x⟩ = 0, with the mean square displacement broadening with time as:

$$\langle x^2 \rangle = 2Dt$$

$\langle x^2 \rangle = 2Dt$

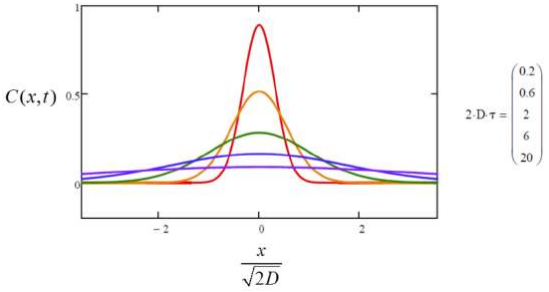


Figure 7.7.5: Concentration profile versus time given an initial concentration at x = 0. Red is closest to t = 0 and purple is the longest time.

Diffusive transport has no preferred direction. Concentration profiles spread evenly in the positive and negative direction, and the highest concentration observed will always be at the origin and have a value $C_{max} = C_0/\sqrt{4\pi Dt}$. Viewing time-dependent concentrations in space reveal that they reach a peak at $t_{max} = x^2/2D$, before decaying at $t^{-1/2}$ (dashed line below).

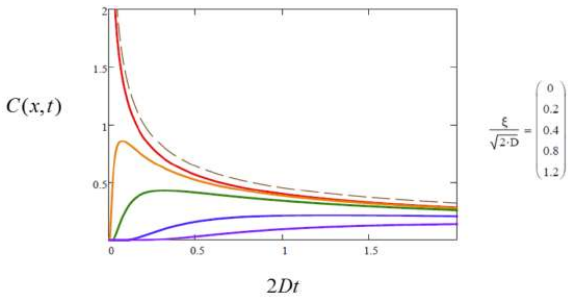


Figure 7.7.6: Time profile of concentration at different distances x from x = 0. Dashed line is x = 0, red is slightly more than zero, purple is farthest from zero.

When we solve for 3D diffusion from a point source at the origin in an isotropic medium in which D is identical for diffusion in the x, y, and z dimensions,

$$C(x,y,z,t) = \frac{C_0}{(4\pi Dt)^{3/2}} e^{-r^2/4Dt} \tag{7.7.5}$$

where $r^2 = x^2 + y^2 + z^2$.

Calculating the mean square displacement from x = y = z = 0.

$$\begin{aligned} \langle r^2 \rangle &= \frac{\int_0^\infty dr\, r^2 C(r,t)}{\int_0^\infty dr\, C(r,t)} \\ &= 6Dt \end{aligned}$$

or in d dimensions, $\langle r^2 \rangle = d(2Dt)$.

7.7.5: Diffusion Constants

The value of the diffusion constant will depend on how easily the species move through the medium. As temperature increases molecules have more energy and thus would be expected to more easily escape the attraction of neighbors as the diffuse to a new location. So the diffusion rate and diffusion coefficient are expected to increase with increasing temperature. To a good approximation we expect it to follow an Arrhenius like law with an activation energy for a diffusive step:

$$D = D_o exp\left(\frac{-E_a}{RT}\right) \tag{7.7.6}$$

The viscosity of the medium also impacts the diffusion coefficient, with diffusion rates decreasing with more viscous solutions. For spherical particles the Stokes-Einstein relation provides a useful estimate of how D depends on viscosity η and effective radius (R_{eff}, this depends on the solvent and the species, ions often carry around a solvent shell).[3]

$$D = \frac{k_B T}{6\pi\eta R_{eff}} \tag{7.7.7}$$

Typical diffusion constants for biologically relevant molecules in water are shown in the graph below, varying from small molecules such as O_2 and glucose in the upper left to proteins and viruses in the lower right.

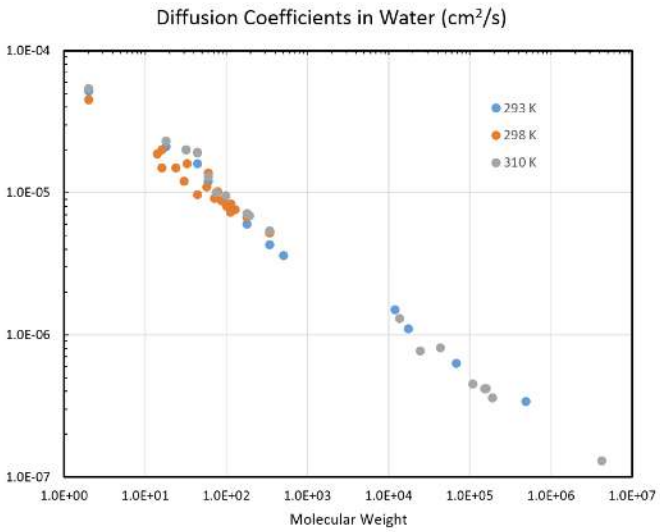


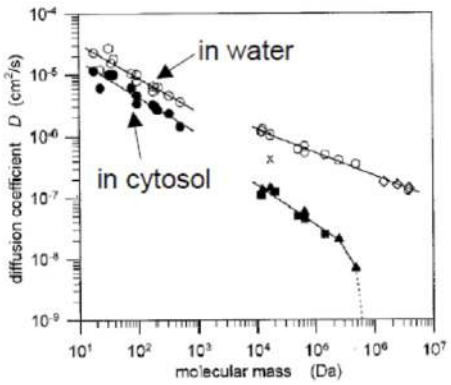
Figure 7.7.7: Diffusion coefficients in water by molecular weight. Notice this is a log-log plot. Also note that the y-axis units are cm^2/s, not the SI units of m^2/s.

- For a typical globular protein, typically diffusion coefficients are:

$$\text{in water D} \sim 10^{-10}\ m^2/s$$
$$\text{in cells D} \sim 10^{-12}\ m^2/s$$
$$\text{in lipids D} \sim 10^{-14}\ m^2/s$$

$$\begin{aligned} \langle r^2 \rangle^{1/2} &= 1\mu m, \quad t \sim 0.4 \text{sec in cells} \\ &= 10\mu m, \quad t \sim 40 \text{ sec in cells} \end{aligned}$$

- Ions in water at room temperature usually have a diffusion coefficient of 10^{-9} to $10^{-11}\ m^2/s$.
- Lipids:
  - Self-diffusion $10^{-12}\ m^2/s$
  - Tracer molecules in lipid bilayers 10^{-11} to $10^{-12}\ m^2/s$



7.7.6: Contributors

- Andrei Tokmakoff (U. Chicago)
- J. Gutow (UW Oshkosh) - simplifications and edits, addition of temperature and viscosity dependence.

7.7.7: References

1. A. Fick, Ueber diffusion, Ann. Phys. 170, 59–86 (1855).
2. This equation assumes that D is a constant, but if it is a function of space: $C = \nabla(D\nabla C)$. In three dimensions, Fick's First Law and the continuity expression are: $J(r,t) = vC(r,t) - D\nabla C(r,t)$ and $dC(r,t)/dt = -\nabla \cdot J(r,t)$ where v is the

velocity of the fluid. These expressions emphasize that flux density and velocity are vectors, whereas concentration field is a scalar.

3. P.W. Atkins, J. de Paula, *Physical Chemistry*, 10th Ed. (W.H. Freeman and Co. New York, 2014) P. 803.

This page titled 7.7: Diffusion is shared under a CC BY-NC-SA 4.0 license and was authored, remixed, and/or curated by Jonathan Gutow via source content that was edited to the style and standards of the LibreTexts platform.

- **10.1: Continuum Diffusion** by Andrei Tokmakoff is licensed CC BY-NC-SA 4.0. Original source: https://tdqms.uchicago.edu.
- **10.2: Solving the Diffusion Equation** by Andrei Tokmakoff is licensed CC BY-NC-SA 4.0. Original source: https://tdqms.uchicago.edu.

7.8: Membrane Diffusion

7.8.1: Introduction

Membranes provide barriers to molecular flow between regions. In living systems this allows the maintenance of the concentration gradients used to do useful work and separates molecules so that they cannot react. In industrial processes such as reverse osmosis, this allows us to generate pure water by doing work to push water up a concentration gradient while preventing contaminants (mostly ions) from passing through the membrane. We will focus on the situation of semi-permeable membranes such as found in living cells. The simplest system to model is one where a species can pass through the membrane but a constant relative concentration is maintained on either side by processes that produce the species on one side and use it up on the other at the rate it passes through the membrane. This is illustrated in figure 7.8.1 showing different concentrations (C_l and C_r) on the left and right of the membrane. This means that the concentrations are not changing with time, making Fick's second law easier to solve:

$$0 = \frac{\partial C}{\partial t} = D\frac{\partial^2 C}{\partial x^2} \tag{7.8.1}$$

This is a steady-state situation.

7.8.2: Diffusion through a Membrane[1]

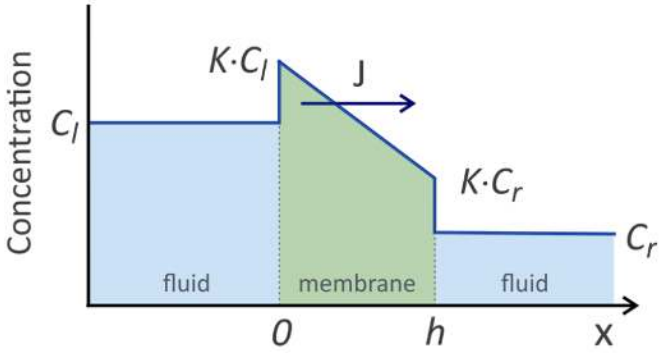


Figure 7.8.1: Cartoon of a membrane (green region) separating two regions of differing constant concentrations (C_l and C_r) of a species that can pass through the membrane, but with some resistance.

In this model, the membrane thickness is h, and the concentrations of the diffusing molecule in the fluid on left and right side of membrane are C_l and C_r. The species (usually a small molecule) can have a different solubility in the fluid and the membrane, which is quantified by the partition coefficient between membrane and fluid:

$$K_p = \frac{C_{\text{membrane}}}{C_{\text{fluid}}} \implies C_{\text{membrane}} = K_p C_{\text{fluid}}$$

K_p can vary between 10^3 and 10^{-7} depending on the nature of the species and membrane composition.

For the steady-state diffusion equation $\partial^2 C/\partial x^2 = 0$, means that the first derivative of the C must be a constant. A functional form that has this property is a line. Thus solutions take the form $C(x) = A_1 x + A_2$. At x = 0 (left side of the membrane) $C(0) = K_P C_l = A_2$. Then setting $C(h) = K_P C_r = A_1(h) + K_P C_l$, we can solve for A_1.

$$A_1 = \frac{K_p(C_r - C_l)}{h} \qquad A_2 = K_p C_l$$

Thus, in the membrane

$$C(x) = x\left(\frac{K_p(C_r - C_l)}{h}\right) + K_p C_l \quad \text{and} \quad \frac{\partial C}{\partial x} = \frac{K_p(C_r - C_l)}{h} \tag{7.8.2}$$

By substituting into Fick's first law we can write the transmembrane flux density of the small molecule across the membrane as

$$J = -D_{mol}\frac{\partial C}{\partial x} = \frac{-K_p D_{mol}\Delta C}{h} \tag{7.8.3}$$

The membrane permeability is equivalent to the volume of small molecule solution that diffuses across a given area of the membrane per unit time, and is defined as

$$P_m \equiv \frac{J}{-\Delta C} = \frac{K_p D_{mol}}{h} \tag{7.8.4}$$

The membrane resistance to flow is R = 1/P_m, and the rate of transport across the membrane is dn/dt = J A, where A is area.

This linear relationship in equation 7.8.4 between P_m and K_p, also known as the **Overton relation**, has been verified for thousands of molecules. For small molecules with molecular weight <50, P_m can vary from 10^{1} to 10^{-6} cm s^{-1}. It varies considerably even for water across different membrane systems, but its typical value for a phospholipid vesicle is 10^{-3} cm s^{-1}. Some of the highest values (>50 cm s^{-1}) are observed for O_2. Cations such as Na^+ and K^+ have permeabilities of ~5×10^{-14} cm s^{-1}, and small peptides have values of 10^{-9}–10^{-6} cm s^{-1}.

7.8.3: Facilitated diffusion of membrane insoluble molecules[2]

As noted above some species (e.g. small peptides and ions) have very small membrane permeabilities (K_p, the solubility in the membrane is small). Ion transport across membranes is mostly mediated by active and passive ion channels. Other molecules may have their transport across the membrane facilitated by complexing with another species forming a more membrane soluble complex. In this case the maximum rate of flux across the membrane is limited by the availability of the transporter molecule that forms the membrane soluble complex.

Consider the equilibrium between the insoluble molecule A and a transporter molecule T and their membrane soluble complex AT:

$$\mathrm{A} + \mathrm{T} \rightleftharpoons \mathrm{AT} \quad K = \frac{[AT]c^o}{[A][T]}$$

where c^o is the standard concentration, which converts the equilibrium constant to the unitless thermodynamic equilibrium constant. If the total concentration of T is $[T]_o$ = [T] + [AT] => [T] = $[T]_o$ - [AT], then substituting in for [T] in K and solving for [AT] we get:

$$[AT] = \frac{[A][T]_o}{[A] + \frac{c^o}{K}} \tag{7.8.5}$$

This shows that at high concentration of [A], [AT] saturates at [AT]≈$[T]_o$. There are no more transporter molecules to form complexes with any added A. So unlike the case for membrane soluble molecules where the flux J (equation 7.8.3) across the membrane is proportional to the concentration difference between the two sides, in this case the flux will plateau when [A] >> c^o/K on the high concentration side of the membrane. Observation of the flux rate reaching a plateau with increasing concentration of a molecule on one side of the membrane is indicative of facilitated (mediated) transport. See figure 7.8.2.

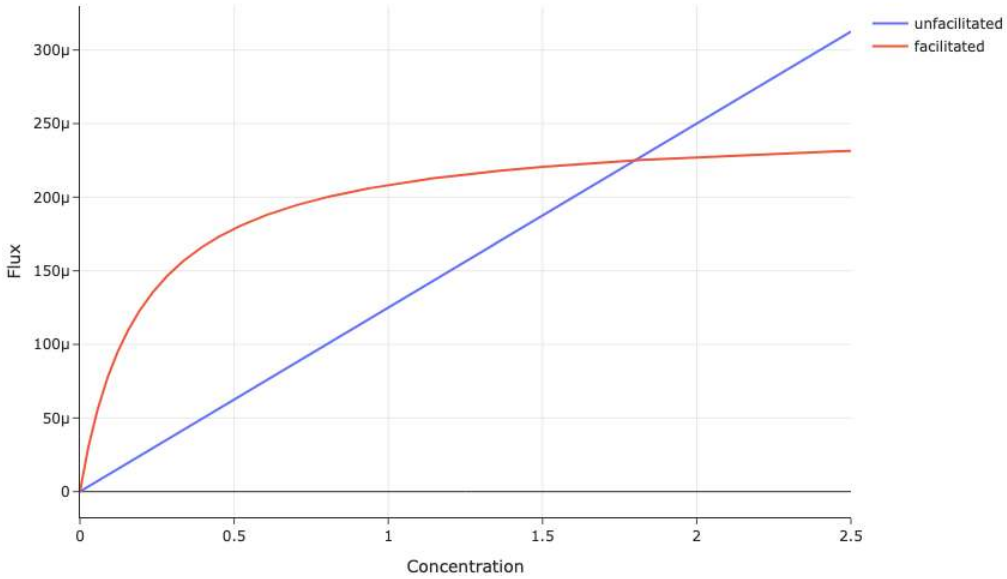


Figure 7.8.2: Flux versus concentration on the high concentration side of a membrane for facilitated (mediated) and unfacilitated diffusion across the membraned. The units are arbitrary.

7.8.4: Reference

1. A. Walter and J. Gutknecht, Permeability of small nonelectrolytes through lipid bilayer membranes, J. Membr.Biol. 90, 207–217 (1986).
2. Atkins, Peter and Julio de Paula. Physical Chemistry for the Life Sciences. 2011. New York, NY: W.H. Freeman and Company. P. 289.

7.8.5: Contributors

- Andrei Tokmakoff (U. Chicago)
- J. Gutow (UW Oshkosh)

This page titled 7.8: Membrane Diffusion is shared under a CC BY-NC-SA 4.0 license and was authored, remixed, and/or curated by Jonathan Gutow via source content that was edited to the style and standards of the LibreTexts platform.

- **10.3: Steady-State Solutions** by Andrei Tokmakoff is licensed CC BY-NC-SA 4.0. Original source: https://tdqms.uchicago.edu.
- **10.1: Continuum Diffusion** by Andrei Tokmakoff is licensed CC BY-NC-SA 4.0. Original source: https://tdqms.uchicago.edu.

7.9: Ion Mobilities

7.9.1: Introduction

Just like all particles in solution ions move around randomly due to the exchange of energy and momentum with the surrounding molecules (primarily solvent). However, if an electric field is applied (e.g. a potential between two electrodes or across a membrane) they will have a tendency to make more of their random jumps in position in the direction of the more negative potential (if positive ions) or the more positive potential (if negative ions). How fast they move on average in one direction is determined by the force exerted by the electric field and how freely the ions can move in the solution.

7.9.2: Ion mobility[1]

An isolated ion in an electric field *E* will accelerate due to the force on the particle. In a solution this acceleration will stop when it reaches a velocity where the frictional forces exactly counter the force of acceleration. At this point the ion has a steady drift speed, which we will denote by *s*. This speed is proportional to the strength of the electric field. The proportionality constant is called the ion mobility and often denoted by *u* (equation 7.9.1).

$$s = uE \implies u = s/E \tag{7.9.1}$$

Stoke's law for a spherical particle of radius, R_{eff}, (which in water contains some or all of the solvation shell of waters) in a medium with viscosity η tells us the frictional retarding force versus speed:

$$f = 6\pi\eta R_{eff} s \tag{7.9.2}$$

The force it counter balances is f = z*eE*, where z = charge on the particle and *e* = charge of +1 in Coulombs. Setting these forces equal we have:

$$zeE = 6\pi\eta R_{eff} s \implies s = \frac{zeE}{6\pi\eta R_{eff}} \tag{7.9.3}$$

Substituting this into equation 7.9.1 we get an an alternative expression for mobility:

$$u = s/E = \frac{ze}{6\pi\eta R_{eff}} \tag{7.9.4}$$

Thus the mobility increases with the charge on the ion, but is decreased by increasing viscosity and effective size.

Some example mobilities are provided in table 7.9.1.

Table 7.9.1: Mobilities of some common ions in water at 298 K with units of 10^{-8} $m^2s^{-1}V^{-1}$.

Cations	mobility	Anions	mobility
H^+	36.23	OH^-	20.64
Li^+	4.01	F^-	5.74
Na^+	5.19	Cl^-	7.92
K^+	7.62	Br^-	8.09
Rb^+	8.06	I^-	7.96
Cs^+	8.00	CO_3^{2-}	7.46
Mg^{2+}	5.50	NO_3^-	7.41
Ca^{2+}	6.17	SO_4^{2-}	8.29

7.9.3: Anomoulous mobilities

A quick glance at table 7.9.1 makes it obvious that the mobilities of protons and hydroxide ions are much higher than would be expected compared to the other ions. This is explained by the **Grotthus mechanism**. Rather than these ions diffusing through the solution under the influence of the electric field they only have to transfer a hydrogen bond to their nearest neighbor in the correct direction while their nearest neighbor simultaneously does the same thing. This means the effective charge can be transferred through a long chain of water molecules were each proton moves only a short distance, but simultaneously. See the figure.

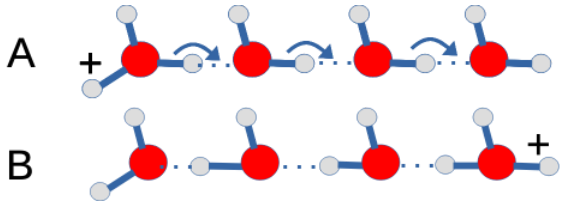


Figure 7.9.1: Cartoon illustrating the Grotthus mechanism. Dashed lines indicate hydrogen bonds. A) + charge at the left end of the chain, with arrows indicating the synchronous shifting of the hydrogen bonding network in this short chain of molecules. B) the situation after the shift, which has moved the + charge from one end of the chain to the other in the time it takes to flip the hydrogen bonds.

The fact that the mobilities of H^+ and OH^- are 5 - 10 times that of the other small + charged ions suggest that the length of the transfer chains are in the 5 - 10 molecule range.

7.9.4: Analytical uses

Since the mobility of molecules is proportional to their charge and inversely proportional to R_{eff} and the viscosity of the medium molecules can be separated in an electric field by placing them near the electrode that repels them in a medium of relatively high viscosity. The larger the molecule (more massive) the less distance they will move in a given time. This technique is used extensively for separating charged DNA and protein fragments, using flat gels (e.g. polyacrylamide gel electrophoresis, PAGE) and capillary electrophoresis for smaller ionic species.

This page titled 7.9: Ion Mobilities is shared under a CC BY-NC-SA 4.0 license and was authored, remixed, and/or curated by Jonathan Gutow.

7.10: Transport Across Cell Membranes

Source: BiochemFFA_3_2.pdf. The entire textbook is available for free from the authors at http://biochem.science.oregonstate.edu/content/biochemistry-free-and-easy

7.10.1: Introduction

Ions generally cross cell membranes via ion channels.

Ion channels can be divided into three very general categories:

- **passive channels** which allow ions to pass through them in the spontaneous direction. Many of these are selective toward particular ions. Some of them also only pass ions in one direction.
- **channels that actively open and close** switch either because of a change in the membrane potential (important in nerve signaling) or when a ligand attaches to or detaches from the protein structure. Closing actively switched channels decreases the rate at which ions travel down the potential gradient.
- **ion pumps** use an energy source to move ions in the nonspontaneous direction across the membrane. These actively maintain the concentration and charge gradient across the membrane. These are usually protein complexes that couple the conversion of $\mathrm{ATP} \longrightarrow \mathrm{ADP}$ to the process of transport against the chemical potential.

An ion pump can effectively move an ion up the gradient as long as:

$$\Delta\mu = RTln\frac{a_{in}}{a_{out}} + zF\Delta\phi + \Delta_r G(\mathrm{ATP} \longrightarrow \mathrm{ADP}) < 0 \tag{7.10.1}$$

See the electrochemical discussion of ion transport for more energetics details.

7.10.2: Selective passive ion channels

Ion channels are pore-forming membrane proteins in the membranes of all cells that regulate movement of selected ions across a membrane (Figures 7.10.1 & 7.10.2). They help to establish the resting membrane potential and to affect action potentials and other electrical signals. They are very important in the process of nerve transmission. Ion channels control the flow of ions across secretory and epithelial cells, and consequently help to regulate cell volume by affecting osmotic pressure.

Ion channels are essential features of almost all cells, functioning as selective “tunnels” that restrict movement through them to ions with specific characteristics (typically size). The size of the opening is very narrow (usually one or two atoms wide) and is able to select even against ions that are too small.

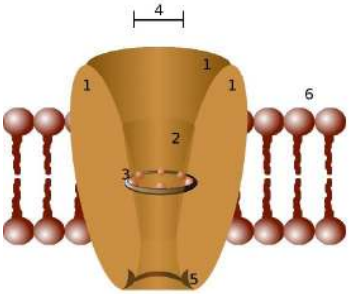


Figure (\\PageIndex{1}\): Schematic structure of an ion channel protein - 1 = General structure / 2 = Entrance / 3 = Selectivity filter / 4 = Effective diameter / 5 = Controllable opening (Note from AG: what does not seem right about this picture?)

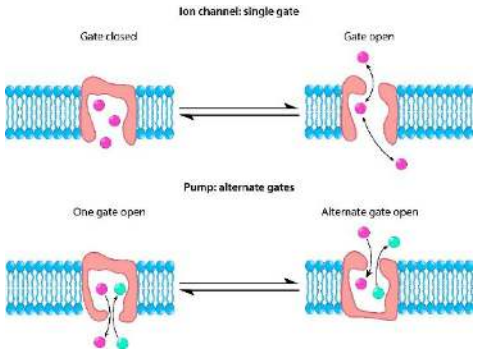


Figure 7.10.2: Two types of ion channel - single and double gates - Image by Pehr Jacobson

Control mechanisms

Ion channels are controlled by mechanisms that include voltage, ligands, light, temperature, and mechanical deformation (stretch activated). Ligand-gated ion channels (LGICs) are transmembrane proteins which open to selectively allow ions such as Na^+, K^+, Ca^{++}, or Cl^- to pass through the membrane in response to the binding of a ligand messenger.

Sound waves cause mechanical deformation of hair cells in the ear. This results in the opening of ion channels and initiation of a nerve signal to the brain.

Sodium ion channels in the tongue for sugar receptors open in response to binding of sucrose, allowing sodium concentration in the nerve cell to increase and initiate a nerve signal to the brain. In this case, the default for the gate is to be closed and it opens in response to binding of a ligand (sucrose).

In light sensing cells of the eye, calcium gates are open by default, but stimulation by light causes them to close, triggering a series of events that result in a signal being sent the brain about the perception of light. Thus, in this case, the stimulus (light) causes an open channel to close.

Moving the other direction, nerve signals originating in the brain travel to muscle tissue and through a complicated set of exchanges, result in the opening of calcium gates of muscle cells, increasing the concentration of calcium and stimulating muscular contraction.

Voltage gated channels are essential for transmission of nerve signals.

Ion movement through channels

The ability of ion channels to select against ions too large is intuitive - the size of the opening in the ion channel simply isn't big enough for a larger ion to fit through the opening. Potassium, for example, passes through sodium channels rarely because the opening is too small.

Potassium channels that are selective for potassium ions must be big enough to allow potassium to enter, but if size were the only selection means, then sodium ions would also readily pass through potassium channels, since sodium ions (0.95 Å) are smaller than potassium ions (1.33 Å). In order for potassium channels to select against sodium ions and favor potassium ions, other considerations come into play.

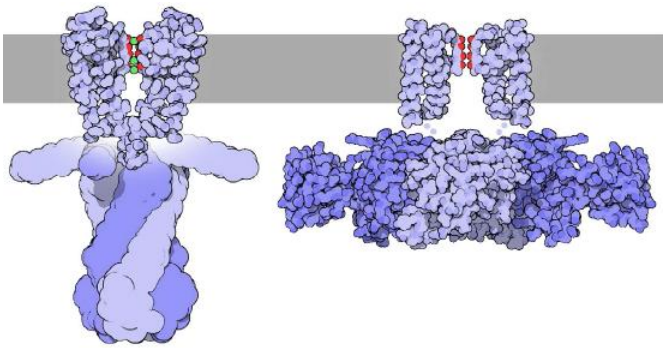


Figure 7.10.3: A potassium channel closed (left) and open (right) - David Goodsell - "Molecule of the Month: Potassium Channels". (from Wikipedia)

Hydration shell

To understand this unique selectivity, it is important to understand how ions move through channels. Before an ion can pass through a channel, it must first be dissociated from (stripped of) the water molecules in its hydration shell - water molecules surrounding ions in aqueous solutions (Figure 7.10.4). This process requires an input of energy.

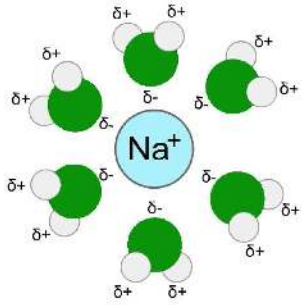


Figure 7.10.4: Sodium surrounded by water molecules in a hydration shell

Comparable to enzymes

Just as enzymes lower the activation energy of enzymatic reactions and thus allow them to more readily occur, so too do channel proteins lower the energy requirements for a molecule to traverse a lipid bilayer. In the absence of the channel protein, the dehydration energy is mostly prohibitive for most polar molecules to occur, so very few make it across the lipid bilayer without the channel protein. This is why ion channel/transport proteins are so important to the cell.

After the water has been stripped, the ion can pass through the channel and when it arrives at the other side of the channel, the diffusing ion becomes rehydrated, thus regaining the energy that was required initially to strip away the water molecules from the ion.

Selectivity of the potassium channel

The potassium channel (Figure 7.10.5) uses the dimensions of the potassium ion precisely to shepherd it through the channel. The sodium ion, which has different dimensions has a more difficult time making it through the channel despite its smaller size. The reason this is rooted in the energy required for dehydration.

For potassium ions, after the water has been stripped off, precisely positioned carbonyl groups along the channel help to stabilize the ion as it moves. The sodium ion, on the other hand is too small and does not make efficient connections with carbonyl groups and thus has a more difficult path. Because of this, the energy difference between dehydration and rehydration of a sodium ion in a potassium channel is more energetically unfavorable than the same process for a potassium ion. The lower effective activation energy for dehydration of the potassium ion in the channel leads to the selectivity.

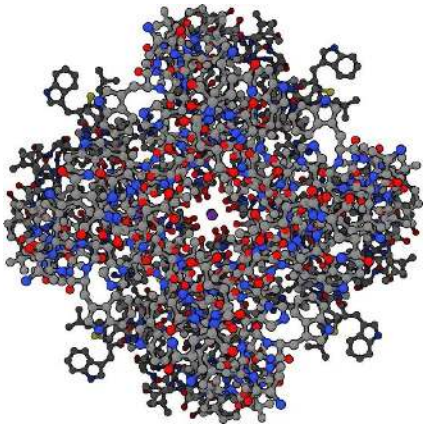


Figure 7.10.5: A potassium ion (center) transiting the potassium channel - David Goodsell

Note

Ions only flow down the concentration gradient through these types of channels. Because they are often unidirectional they will not contribute to ion flow in the opposite direction even if that is down the concentration gradient.

7.10.3: Active transport of ions

During active transport, at least one molecule is being moved against a concentration gradient. A common, but not exclusive, energy source is ATP (see Na+/K+ ATPase), but other energy sources are also employed. For example, the sodium-glucose transporter uses a sodium gradient as a force for actively transporting glucose into a cell. Thus, it is important to know that not all active transport uses ATP energy.

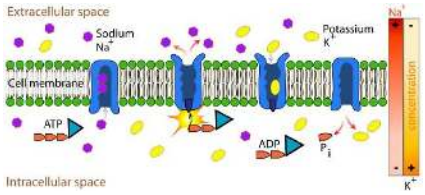


Figure 7.10.6: An overview of active transport by the Na+K+ ATPase

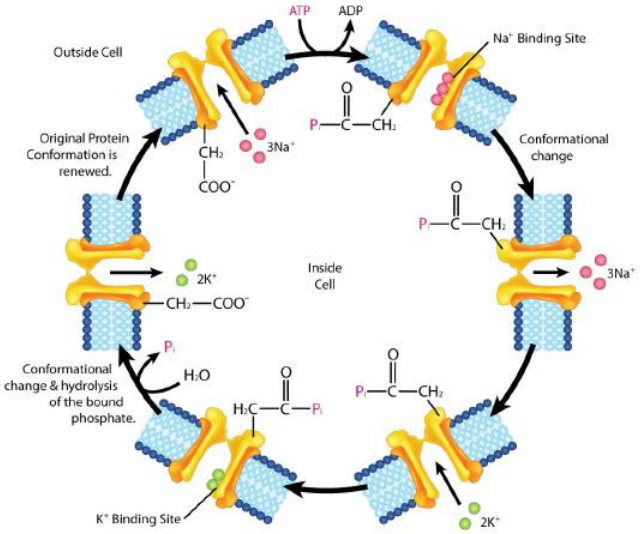


Figure 7.10.7: Sequential steps in the active transport of ions by theNa+K+ ATPase - Wikipedia (Note from AG: do not worry about details of this transporter, just focus on the general idea/summary)

7.10.3.1: Example: Na+/K+ ATPase

An important integral membrane transport protein is the Na+/K+ ATPase antiport (Figures 7.10.6 and 7.10.7), which moves three sodium ions out of the cell and two potassium ions into the cell with each cycle of action. In each case, the movement of ions is against the concentration gradient. Since three positive charges are moved out for each two positive charges moved in, the system is electrogenic.

The protein uses the energy released during ATP hydrolysis to create ion gradients that are important both in maintaining cellular osmotic pressure and (in nerve cells) for creating the sodium and potassium gradients necessary for signal transmission. Failure of the system to function results in swelling of the cell due to movement of water into the cell through osmotic pressure. The transporter expends about one fifth of the ATP energy of animal cells.

The cycle of action occurs as follows:

1. Pump binds ATP followed by binding of 3 Na+ ions from cytoplasm of cell
2. ATP hydrolysis results in phosphorylation of aspartate residue of pump. ADP is released
3. Phosphorylated pump undergoes conformational change to expose Na+ ions to exterior of cell. Na+ ions are released.
4. Pump binds 2 extracellular K+ ions.

5. Pump dephosphorylates causing it to expose K+ ions to cytoplasm as pump returns to original shape.
6. Pump binds 3 Na+ ions, binds ATP and releases 2 K+ ions to restart process

The Na+/K+ ATPase is classified as a P-type ATPase. This category of pump is notable for having a phosphorylated aspartate intermediate and is present across the biological kingdoms - bacteria, archaeans, and eukaryotes.

This page titled 7.10: Transport Across Cell Membranes is shared under a CC BY-NC-SA 4.0 license and was authored, remixed, and/or curated by Kevin Ahern, Indira Rajagopal, & Taralyn Tan.

This page titled 7.10: Transport Across Cell Membranes is shared under a CC BY-NC-SA 4.0 license and was authored, remixed, and/or curated by Jonathan Gutow.

- **3.2: Transport in Membranes** by Kevin Ahern, Indira Rajagopal, & Taralyn Tan is licensed CC BY-NC-SA 4.0. Original source: http://biochem.science.oregonstate.edu/content/biochemistry-free-and-easy.

7.11: Kinetics of Electron Transfer Reactions

7.11.1: Introduction

A large fraction of energetic reactions of importance to our technology and living organisms can be classified as redox reactions (reactions involving electron transfer). These reactions involve steps where an electron is transferred between a donor and an acceptor. One example are the electron transfers that occur at the electrodes of electrochemical cells. Another example is photosynthesis where an electron freed by the absorption of a photon undergoes multiple transfers to generate a large physical separation between the original electron donor and the electron, thereby reducing the probability of recombination before the energy can be used in another process. We can gain some insight into these types of processes through the **Marcus theory**.

As the model involves a reaction between a donor (D) and an acceptor (A) the mechanism involves the two species coming together and then transferring the electron:

$$\mathrm{D} + \mathrm{A} \underset{k_{-e}}{\overset{k_e}{\rightleftharpoons}} \mathrm{DA}$$

$$\mathrm{DA} \underset{k_{-et}}{\overset{k_{et}}{\rightleftharpoons}} \mathrm{D^+A^-}$$

$$\mathrm{D^+A^-} \underset{k_{-d}}{\overset{k_d}{\rightleftharpoons}} \mathrm{D^+ + A^-}$$

where $k_{\pm e}$ are the rate constants for formation of an encounter pair and its separation, $k_{\pm et}$ are the forward and reverse electron transfer rates, and $k_{\pm d}$ are the forward and reverse dissociation rates for the charged species. In many cases these reactions are diffusion limited, the second two processes proceed rapidly compared to the rate the two initial species come together. However, in systems where the reaction is not diffusion limited the kinetics of the second reaction become important. Slow electron transfer and donor acceptor pairs held at fixed distances in inorganic complexes, proteins and extended biochemical structures are some examples.

In activation limited cases with slow electron transfer, the first reaction can be treated as a pre-equilibrium and the overall rate (assuming negligible back reactions in steps 2 and 3) will be:

$$\text{rate} \approx k_{et} \frac{K_e^{\ddagger}}{c^o}[A][D] \tag{7.11.1}$$

which implies an observed bimolecular rate of:

$$k_{obs} \approx k_{et} \frac{K_e^{\ddagger}}{c^o} \tag{7.11.2}$$

7.11.2: Marcus Theory[1]

Marcus theory models the rate constant of the forward electron transfer (k_{et}). This theory was developed in the later half of the 1950s primarily by Rudi A. Marcus, who received the Nobel prize in chemistry for this work in 1992. The model is grounded in Transition State Theory. Because the complex is already formed we have a unimolecular reaction:

$$\mathrm{DA} \rightleftharpoons \mathrm{DA^{\ddagger}} \overset{k_t}{\longrightarrow} \mathrm{D^+A^-}$$

with an equilibrium constant for the formation of the activated complex (indicated by ‡), $K^{\ddagger} = e^{-\Delta G^{\ddagger}/R/T}$. The observed rate constant of electron transfer is then the rate constant of the second step (k_t) multiplied by the equilibrium constant for formation of the transition state.

$$k_{et} = k_t e^{-\Delta G^{\ddagger}/R/T}$$

The rate constant of the transfer (k_t) once in the activated complex (transition state) is dictated by the rate (probability) that the electron will jump the distance between the donor (D) location and the acceptor (A) location. This is a quantum tunneling process which is dependent on the separation distance. From quantum mechanical calculations and observations using scanning tunneling

microscopes this distance dependence is known to drop off exponentially with distance. Calling the edge-to-edge jump (tunneling) distance r and β the distance decay rate for tunneling probability the rate of electron transfer becomes:

$$k_{et} = e^{-\beta r} e^{-\Delta G^{\ddagger}/R/T} \tag{7.11.3}$$

Because the geometry of DA may be different than D^+A^- the transition state geometry is distorted from that of just D in contact with A. Marcus theory is able to account for this by representing the $\Delta G^{\ddagger}$ as having two components; ΔG^o the standard Gibbs energy of electron transfer (overall reaction); and λ the reorganization energy. The way they contribute to $\Delta G^{\ddagger}$ is approximated using the assumption that the reaction potential energy curve can be modeled by overlapping parabolas (see reference 1 for a more detailed discussion):

$$\Delta G^{\ddagger} = \frac{(\Delta G^o + \lambda)^2}{4\lambda} \tag{7.11.4}$$

Combining this with equation 7.11.3 we get:

$$k_{et} = e^{-\beta r} \exp\left(-\frac{(\Delta G^o + \lambda)^2}{4\lambda RT}\right) \tag{7.11.5}$$

If the same donor and acceptor are fixed at different distances from each other in a protein or by some other covalent linkages, $\Delta G^{\ddagger}$ will be constant. In that case we can take the log of equation 7.11.3 to get:

$$ln k_{et} = -\beta r - \frac{\Delta G^{\ddagger}}{RT} = -\beta r - \text{constant} \tag{7.11.6}$$

so a plot of ln k_{et} versus r gives a straight line with a slope of $-\beta$. In vacuum it is found that 28 nm^{-1}<β< 35 nm^{-1} while in proteins 9.0 nm^{-1} < β< 16 nm^{-1}. The smaller values for proteins indicated that the probability of a jump decays less rapidly with distance. This agrees with the observation that large electron transfer distances on the order of 2 nm are observed for donor acceptor pairs in proteins.

If the distance is held constant and the donor acceptor pair is changed the variation in k_{et} can be interpreted in terms of variation in ΔG^o and λ. Because the sum of ΔG^o and λ is squared in equations 7.11.4 and 7.11.5 this means the numerator, $(\Delta G^o + \lambda)^2 \geq 0$, making $\Delta G^{\ddagger} \geq 0$. With the negative sign in the exponential this means that the maximum for k_{et} will be reached when $\Delta G^o + \lambda = 0$. This has been verified in experiments.[2]

7.11.3: Marcus Cross Relation

The Marcus cross relation provides a way of estimating k_{et} from self exchange rates, the rate of electron exchange between identical species:

$$A + A \xrightarrow{k_{AA}} A^+ + A^- \quad \text{and} \quad D + D \xrightarrow{k_{DD}} D^+ + D^-$$

The final estimate when $|\Delta G^o| \ll \lambda$ is (see below for a justification of this approximate relationship):

$$k_{et} \approx \sqrt{k_{DD} k_{AA} K_{DA}} \tag{7.11.7}$$

where K_{DA} is the equilibrium constant for $D + A \rightleftharpoons D^+ + A^-$. K_{DA} is easily obtained from redox potentials since $\Delta G^o = -n_e F E^o$, where n_e = number moles electrons transferred in the reaction, F = Faraday's constant and E^o = the redox potential of the reaction. Thus:

$$K_{DA} = \exp\left(\frac{-\Delta G^o}{RT}\right) = \exp\left(\frac{n_e F E^o}{RT}\right)$$

Time resolved measurements of the self exchange rate constants can thus be combined with the known redox potential of a reaction to estimate the electron transfer rates as long as the reorganization energy is significant compared to the redox free energy change using equation 7.11.7. When this is not true an additional factor, which is difficult to estimate must be included.

Justification of approximate Marcus Cross Relation

Equation 7.11.5 can be expanded to:

$$k_{et} = e^{-\beta r} \exp\left(-\frac{\Delta G^{o\,2} + 2\lambda\Delta G^o + \lambda^2}{4\lambda RT}\right) \tag{7.11.8}$$

$$= e^{-\beta r} \exp\left(-\frac{1}{4RT}\left(\frac{\Delta G^{o\,2}}{\lambda} + \frac{2\lambda\Delta G^o}{4\lambda} + \frac{\lambda^2}{\lambda}\right)\right) \tag{7.11.9}$$

When $|\Delta G^o| \ll \lambda$ the $\Delta G^{o\,2}/\lambda$ term is negligible compared to the other two and can be dropped leading to:

$$k_{et} \approx e^{-\beta r} \exp\left(-\frac{1}{4RT}\left(\frac{2\lambda\Delta G^o}{\lambda} + \frac{\lambda^2}{\lambda}\right)\right) \tag{7.11.10}$$

$$\approx e^{-\beta r} \exp\left(-\frac{\Delta G^o}{2RT} - \frac{\lambda}{4RT}\right) \tag{7.11.11}$$

$$\approx e^{-\beta r} \exp\left(-\frac{\lambda}{4RT}\right) \exp\left(-\frac{\Delta G^o}{2RT}\right) \tag{7.11.12}$$

The last exponential is the square root of the overall equilibrium constant ($K_{DA}^{1/2}$), leading to:

$$k_{et} \approx e^{-\beta r} \exp\left(-\frac{\lambda}{4RT}\right) \sqrt{K_{DA}} \tag{7.11.13}$$

If we assume that the exchange energy λ and distances (r) can be approximated as the averages of the values in the self exchange reactions this becomes:

$$k_{et} \approx \exp\left(-\beta\frac{r_{DD} + r_{AA}}{2}\right) \exp\left(-\frac{\lambda_{DD} + \lambda_{AA}}{8RT}\right) \sqrt{K_{DA}} \tag{7.11.14}$$

$$\approx \exp\left(-\beta\frac{r_{DD}}{2}\right) \exp\left(-\frac{\lambda_{DD}}{8RT}\right) \exp\left(-\beta\frac{r_{AA}}{2}\right) \exp\left(-\frac{\lambda_{AA}}{8RT}\right) \sqrt{K_{DA}} \tag{7.11.15}$$

The blue pair of exponentials are $\sqrt{k_{DD}}$ and the red pair are $\sqrt{k_{AA}}$ because ΔG^o for the self exchange reactions is 0 (see equation 7.11.5). This recovers equation 7.11.7.

7.11.4: References

1. P.W. Atkins, J. de Paula, *Physical Chemistry*, 10th Ed. (W.H. Freeman and Co. New York, 2014) Pp. 1114-1021.
2. J. R. Miller *et al*. J. Am. Chem Soc. 106, 3047 (1984).

This page titled 7.11: Kinetics of Electron Transfer Reactions is shared under a CC BY-NC-SA 4.0 license and was authored, remixed, and/or curated by Jonathan Gutow.

CHAPTER OVERVIEW

8: Quantum Chemistry Fundamentals

8.1: Failures of Classical Physics
8.2: The Schrödinger Wave Equation
8.3: Particle in a One-Dimensional Box
8.4: Tunneling
8.5: Particle in a 2-Dimensional Box
8.6: Particle on a Ring
8.7: The Schrödinger Wave Equation for the Hydrogen Atom
8.8: Many-Electron Atoms and the Periodic Table
8.9: Harmonic Oscillator

This page titled 8: Quantum Chemistry Fundamentals is shared under a CC BY-NC-SA 4.0 license and was authored, remixed, and/or curated by Jonathan Gutow.

8.1: Failures of Classical Physics

Imagine being a scientist in the year 1900. At the time, there was significant debate in society as to whether or not science was a valuable discipline for study. The argument was that Isaac Newton and others had already solved all of the important problems of physics and as such, there was nothing more to be learned. There were still a few problems remaining that didn't work perfectly according to Newtonian physics, but the prevailing thought was that it was a simple matter of finding the one small piece that people were missing and the entire package would be complete. As it turned out, they couldn't have been more incorrect!

Every new detail that was discovered on these pesky problems seemed to indicate something that was not commensurate with Newtonian physics at all. And the deeper investigators looked, the more perplexing the problems became – and the further from classical physics the solutions took them.

But the modeling of these problems formed the foundations of a new quantum theory. That theory, while completely counter-intuitive to scientists of the time, is now engrained in every aspect of how we think of the atomic and molecular nature of matter. As such, no study of chemistry is complete without exploring this bizarre world of quantum mechanics. So sit back, relax, and enjoy the story of the origins of the quantum theory.

8.1.1: Max Planck and Blackbody Radiation

One of the problems that perplexed scientists at the turn of the 20th century was that of the description of black-body radiation. The term "Black Body" was introduced by Gustav Kirchhoff in 1860. It refers to an object that absorbs all light that falls on it (i.e. it reflects no light.) The thermal radiation emitted by a black body is called **black body radiation**.

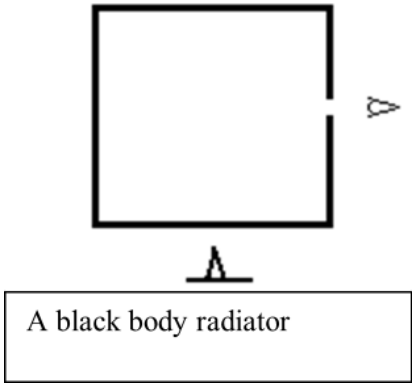


Figure 8.1.1

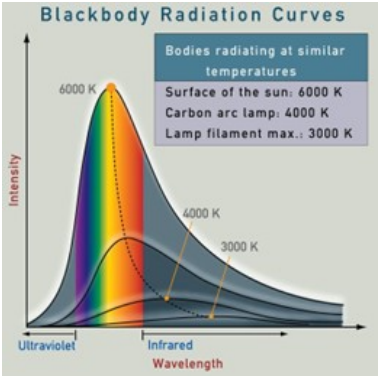


Figure 8.1.2

Black-body radiation is the light that is given off from a body that glows from being hot. Examples of blackbody radiators include incandescent light bulbs and the sun. In the laboratory, a black body radiator can be constructed by painting the inside of a metal box black (so that light is not reflected inside) and heating the box. The light given off by the box will be black body radiation.

The emission spectrum of a black-body radiator was well established and reproducible. The intensity increases at all wavelengths and the maximum intensity shifts to shorter wavelengths at higher temperatures. But while the experimental result was well

established and agreed upon, there was no theoretical model that predicted the result. Existing classical models could predict either the long-wavelength side of the spectrum or the short wavelength side, but not both.

Max Planck (1858-1947) produced the first theory that could predict both sides of the spectrum. He did this by making a ridiculous assumption about the nature of light. Despite the prevailing classical theories of the wave-nature of light and numerous experimental observations confirming these theories, Planck decided to model a light beam as a shower of energy packets (which he called Quanta) where the energy was proportional to the frequency of the light wave.

$$E = h\nu$$

In this model, E is the energy of a quantum, h is a constant of proportionality and ν is the frequency of the light wave.

This dual nature of light (having properties of both particles and waves) was revolutionary, and was thus met with great skepticism. Planck's model, published in 1901 [1], can be expressed by

$$I(\nu, T) = \frac{2h\nu^3}{c^2}\left(\frac{1}{e^{\frac{h\nu}{k_B T}} - 1}\right)$$

in which I is the intensity, T the temperature and c the speed of light, successfully described both sides of the black body radiation curve. It also provided a value of h, the constant of proportionality of

$$h = 6.36 \times 10^{-34} J \cdot s$$

Planck was awarded the Nobel Prize in Physics in 1918 for this theory. But while interesting, Planck's theory only provided one possible explanation of the black body radiation problem. But without corroboration from other experiments involving other phenomena, Planck's theory of light quanta would not have gained any meaningful attention. That corroboration came in a paper published by Albert Einstein describing a quantum theory of the photoelectric effect.

8.1.2: Albert Einstein and the Photoelectric Effect

When Planck published his paper in 1901, Albert Einstein was working as a scientific expert in the Swiss patent office while working to secure a professorship in physics. He read Planck's paper. Through studying Planck's work, Einstein was able to apply a quantum theory of light to make sense out of another well-established, but as of then not understood experiment, the photoelectric effect.

The photoelectric effect involves shining light on the polished surface of metal under a vacuum. If the light has a wavelength shorter than a threshold value (characteristic of the individual metal), electrons are emitted from the surface.

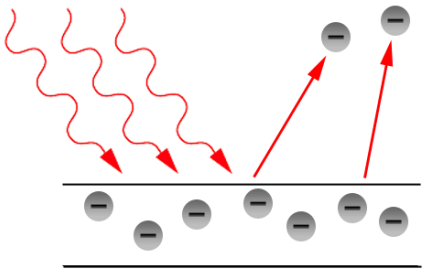


Figure 8.1.3

The challenge to understanding the result came from changing the intensity of the light. Classical physics tells us that the energy of a wave is determined by its amplitude, or in the case of light, the intensity. An increase in the intensity of incident light, therefore, should lead to an increase in the kinetic energy possessed by the emitted electrons. However, the kinetic energy of the electrons seemed to be a function not of the intensity of the light, but rather it's frequency. Einstein was able to explain [2] this using Planck's theory that light consisted of a shower of quant, each of which was a packet of energy the magnitude of which was proportional to the frequency of the light. ($E_{photon} = h\nu$)

In Einstein's model, the kinetic energy of the photoelectrons was determined as the difference between the photon energy and the "work function" or the energy necessary to rip an electron from the surface of the metal.

$$E_{kin} = h\nu - \varepsilon$$

In this case, each quantum of light, or photon, can produce one photoelectron. If the energy of the photons are too small (less than ε), no photoelectrons are produced. But at frequencies that exceeded the threshold value, the kinetic energy was a linear function of the light frequency, with the slope of that line giving a value for Planck's constant of proportionality. Einstein's model provided a separate measurement for Planck's constant but yielded an identical result. At this point, the scientific community could no longer ignore this new quantum theory of light. Einstein was awarded the Nobel Prize in Physics in 1921 for explaining the photoelectric effect.

8.1.2.0.1: Johannes Balmer and the Emission Spectrum of Hydrogen

In 1885, J.J. Balmer [3](a high school teacher and amateur scientist) wrote about the series of lines in the visible emission spectrum of atomic hydrogen. The lines formed a pattern

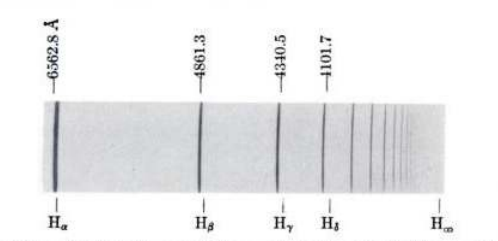


Figure 8.1.4

where the spacing decreased in decreasing wavelength and seemed to converge on a series limit. The wavelengths (λ) of lines in this spectrum fit the pattern:

$$\lambda = G\left(\frac{n^2}{n^2-4}\right)$$

where $G = 3647.053\mathring{A}$, or the series limit, and $n = 3, 4, 5, \ldots$.

In modern terms, this expression is given as

$$\frac{1}{\lambda} = \tilde{\nu} = R_H\left(\frac{1}{n_l^2} - \frac{1}{n_u^2}\right)$$

where $R_H$is known as the "Rydberg constant" for hydrogen, and has the value given by $R_H = 109677.581cm^{-1}$. Also, $n_l < n_u$ and either value must obey $n = 1, 2, 3, \ldots$.

In Balmer's paper, the expression is purely empirical (meaning it is based only on observation and not tied to any theoretical value.) While he was unable to provide any theory for the pattern he had derived from data, he did state that such a simple pattern could not be a coincidence.

The job of theoretical physics was to derive a theory of the H-atom that would yield energy levels, transitions between which would produce the observed spectrum and the simple pattern determined by Balmer. The first quantum theory of the hydrogen atom was proposed by Niel's Bohr (who was born in 1885 – the year that Balmer's paper was published!) Bohr's model is consistent with the wave nature of matter predicted by Louis de Broglie.

8.1.3: Louis de Broglie and wave nature of matter

Louis de Broglie (1892-1987) was intrigued by the notion that light, which every sensible physicist knew propagated as waves, could be described as though it was a stream of particles. Not to be outdone, he decided to examine the ramifications of doing something equally preposterous – treat something everyone knew was a particle, as a wave. de Broglie proposed that all particles would behave with a wave nature, and would have a wavelength determined by their momentum and Planck's constant.

$$\lambda = \frac{h}{p} = \frac{h}{mv}$$

Based on this theory, de Broglie predicted in his 1923 Ph.D. dissertation that interference patterns could be observed in electron beams diffracted by regular patterns, much in the same way that such results could be seen with light waves or water waves. This phenomenon was observed in electron beams diffracted off of nickel surfaces in 1927 [4]. de Broglie was awarded the Nobel Prize in physics in 1929 for the work in his dissertation – the first time the prize was awarded for a PhD thesis!

8.1.4: Niels Bohr and the Hydrogen Atom

Niels Bohr (1885-1962) was the first person to offer a quantum theory of the hydrogen atom that satisfactorily predicted the patterns seen in the emission spectra of atomic hydrogen. Basically, Bohr suggested that the electron in a hydrogen atom orbited the nucleus (a proton) in a circle, the circumference of which had to be an integral multiple of de Broglie wavelengths. (Bohr's model was actually published in 1913 [5] – 10 years before de Broglie's Nobel Prize winning thesis, but it is easily explained based on the de Broglie principle.)

Bohr suggested that the angular momentum of an orbiting electron had to be an integral multiple of Planck's constant divided by 2π.

$$mvr = \frac{nh}{2\pi} = n\hbar$$

This expression is easily rearranged to yield the de Broglie relationship:

$$mvr = \frac{nh}{2\pi}$$
$$2\pi\, r = \frac{nh}{mv} = n\lambda$$

Based on this relationship, and balancing the electrostatic attractive forces with the centripetal force acting on the orbiting electron, Bohr was able to derive the value of the Rydberg constant for hydrogen and predict the pattern seen in the emission spectrum of hydrogen.

While the theory does a remarkable job of describing the empirical model of Balmer, it has many shortcomings as well. For example, a charged electron orbiting a charged proton should eventually see its orbit decay and the electron will crash into the proton. Clearly this does not happen, contrary to the predictions of classical physics. Also, the Bohr theory is not applicable to atoms that have more than one electron, meaning it has not real application on most of the atoms in which chemists have interest. None the less, Bohr's foothold into the quantum world was important. And some important aspects of a quantum theory can be easily demonstrated using the model as well.

8.1.5: Heisenberg, Schrödinger and Dirac

While quantum mechanics is most often taught (and will be discussed in this text) in terms of the formalisms of Erwin Schrödinger (1887-1961), the first formal theory was derived by Werner Heisenberg (1901-1976) in 1925 (he was awarded the Nobel Prize in physics in 1932 for this theory) using a matrix formalism. Schrödinger's methodology uses integrals and eigenvalue-eigenfunction relationships and was first published in 1926. Schrödinger was awarded the Nobel Prize in Physics in 1933. Two years later, he proposed the famous "Schrödinger's Cat" thought experiment (after consulting with Albert Einstein, who never fully excepted quantum mechanics) aimed at disproving the very theory that had won Schrödinger the Nobel Prize. Schrödinger clearly lamented his contributions to the scientific foofaraw that quantum theory would become. In particular, he was dissatisfied by the notion of "quantum jumps" that were needed to describe electronic transitions in the hydrogen atom. In one heated debate with Niels Bohr, Schrödinger exasperated

If we are going to have to put up with these damn quantum jumps, I'm sorry that I ever had anything to do with quantum theory. [6]

Paul Dirac's (1902-1984) seminal textbook on quantum theory published in 1930 showed that the formalisms of Heisenberg and Schrödinger were mathematically identical. Dirac shared the 1933 Nobel Prize with Schrödinger. Among the many significant contributions that Dirac made, was a January 1928 paper in the *Proceedings of the Royal Society* that helped to explain the nature of electron spin. The consequences of his relativistic interpretation of the nature of an electron also predicted the existence of antimatter.

There is a lot more to the story of the development of quantum theory and a great many colorful characters involved. While this text will focus on the applications of quantum theory to understand molecular behavior rather than the history of its development, the history of the science is definitely something about which reading is extremely worthwhile.

Also, given the efforts towards a unified field theory in physics, there is no time that studying quantum mechanics could be more valuable. In the development of these theories, quantum mechanics and relativity often struggle against one another, but it is quantum mechanics that always seems to win these struggles. As such, quantum theory is bound to play an enormous role as modern physics continues to evolve. It is my sincerest hope that this introduction will not only provide a background required to make sense out of modern chemistry, but also whet the appetite for more knowledge and understanding on this fascinating subject.

---

[1] M. Planck, "On the Law of Distribution of Energy in the Normal Spectrum," Annalen der Physik, vol. 4, p. 553, 1901. W310W9405

[2] A. Einstein, "On a Heuristic Viewpoint Concerning the Production and Transformation of Light," Annalen der Physik, vol. 17, pp. 132-148, 1905. W310W9405

[3] J. J. Balmer, "Hinweis auf die Spektrallinien des Wasserstoffs," Annalen der Physik und Chemie, vol. 25, pp. 80-85, 1885. W310W9405

[4] C. Davisson and L. Germer, "Diffraction of Electrons by a Crystal of Nickel," Physical Review, vol. 30, pp. 705-740, 1927. W310W9405

[5] N. Bohr, "On the Constitution of Atoms and Molecules, Part I," Philosphical Magazine, vol. 26, pp. 1-24, 1913. W310W9405

[6] J. Baggot, The Meaning of Quantum Theory, New York: Oxford Science Publications, 1992, p. 28.W310W9405

This page titled 8.1: Failures of Classical Physics is shared under a CC BY-NC-SA 4.0 license and was authored, remixed, and/or curated by Jonathan Gutow.

- **1.4: Failures of Classical Physics** by Patrick Fleming is licensed CC BY-NC-SA 4.0.

8.2: The Schrödinger Wave Equation

Beginning in the early 20th century, physicists began to acknowledge that matter--much like electromagnetic radiation--possessed wave-like behaviors. While electromagnetic radiation were well understood to obey Maxwell's Equations, matter obeyed no known equations.

8.2.1: Introduction

In 1926, the Austrian physicist Erwin Schrödinger formulated what came to be known as the (time-dependent) Schrödinger Equation:

$$i\hbar\frac{\partial}{\partial t}\Psi(\vec{r},t)=\frac{-\hbar}{2m}\nabla^2\Psi(\vec{r},t)+V(\vec{r})\Psi(\vec{r},t) \tag{8.2.1}$$

Where t = time, $\vec{r}$ = position in 3-D space, Ψ = wavefunction of the particle, $V(\vec{r})$ = position dependent potential energy of the particle, m = particle mass and $\nabla^2=\partial^2/\partial x^2+\partial^2/\partial y^2+\partial^2/\partial z^2$. Equation 8.2.1 effectively describes matter as a wave that fluctuates with both displacement and time. The imaginary portion of the equation dictates its time dependence. For many purposes time dependence can be ignored and the equation simplifies to:

$$\frac{-\hbar^2}{2m}\nabla^2\Psi(\vec{r})+V(\vec{r})\Psi(\vec{r})=E\Psi(\vec{r}) \tag{8.2.2}$$

Which in one dimension reduces to:

$$\frac{-\hbar^2}{2m}\frac{\partial\Psi(x)^2}{\partial x^2}+V(x)\Psi(x)=E\Psi(x) \tag{8.2.3}$$

Although the time-independent Schrödinger Equation can be useful to describe a matter wave in free space, we are most interested in waves when confined to a small region, such as an electron confined in a small region around the nucleus of an atom.

The wavefunctions that are solutions to this equation are limited. There are four general aspects that are applicable to an acceptable wavefunction:

1. An acceptable wavefunction will be the solution of the Schrödinger equation (either Equations 8.2.1 or 8.2.2).
2. An acceptable wavefunction must be normalizable (scalable to integrate to 1 over all of space) so will approaches zero as position approaches infinity.
3. An acceptable wavefunction must be a continuous function of position (Figure 8.2.1).
4. An acceptable wavefunction will have a continuous slope (Figure 8.2.2).

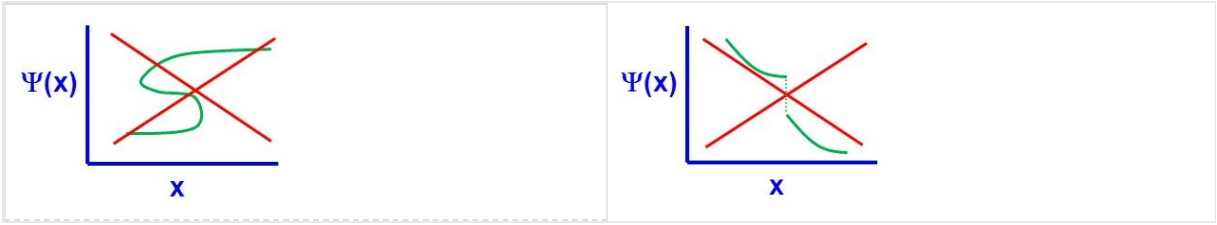


Figure 8.2.1 : Two unacceptable wavefunctions. (left) This is not a single-valued function and (right) this is a non-continuous function

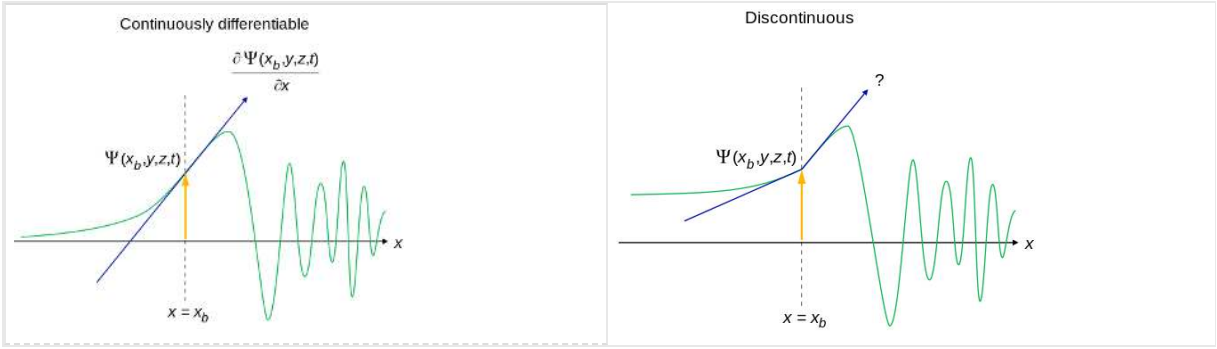


Figure 8.2.2 : Wavefunction continuity in space

8.2.2: Interpretation of the Wavefunction

Since wavefunctions can in general be complex functions, the physical significance cannot be found from the function itself because the $\sqrt{-1}$ is not a property of the physical world. Rather, the physical significance is found in the product of the wavefunction and its complex conjugate, i.e. the absolute square of the wavefunction, which also is called the square of the modulus.

$$\psi^*(\vec{r},t)\psi(\vec{r},t) = |\psi(\vec{r},t)|^2 \tag{8.2.4}$$

where $\vec{r}$ is a vector (x, y, z) specifying a point in three-dimensional space. The square is used, rather than the modulus itself, just like the intensity of a light wave depends on the square of the electric field. At one time it was thought that for an electron described by the wavefunction $\psi(\vec{r})$, the quantity $e\psi^*(\vec{r}_i)\psi(\vec{r}_i)d\tau$ was the amount of charge to be found in the volume $d\tau$ located at $\vec{r}_i$. However, Max Born found this interpretation to be inconsistent with the results of experiments.

The Born interpretation, which generally is accepted today, is that $\psi^*(\vec{r}_i)\psi(\vec{r}_i)\,d\tau$ is the probability that the electron is in the volume dτ located at $\vec{r}_i$. The Born interpretation therefore calls the wavefunction the probability amplitude, the absolute square of the wavefunction is called the probability density. The probability density times a volume element in three-dimensional space ($d\tau$) is the probability of finding the electron. The idea that we can understand the world of atoms and molecules only in terms of probabilities is disturbing to some, who are seeking more satisfying descriptions through ongoing research.

8.2.3: Normalization of the Wavefunction

A probability is a real number between 0 and 1. An outcome of a measurement which has a probability 0 is an impossible outcome, whereas an outcome which has a probability 1 is a certain outcome. The probability of a measurement of x yielding a result between $-\infty$ and $+\infty$ is

$$P_{x\in-\infty:\infty}(t) = \int_{-\infty}^{\infty} |\psi(x,t)|^2 dx. \tag{8.2.5}$$

However, a measurement of x *must* yield a value between $-\infty$ and $+\infty$, since the particle has to be located somewhere. It follows that $P_{x\in-\infty:\infty}(t) = 1$, or

$$\int_{-\infty}^{\infty} |\psi(x,t)|^2 dx = 1, \tag{8.2.6}$$

which is generally known as the *normalization condition* for the wavefunction.

Example 8.2.1: Normalizing a Gaussian wavefunction

Normalize the wavefunction of a Gaussian wave packet, centered on $x = x_o$, and of characteristic width σ: i.e.,

$$\psi(x) = \psi_0 \mathrm{e}^{-(x-x_0)^2/(4\sigma^2)}. \tag{8.2.7}$$

Solution

To determine the normalization constant ψ_0, we simply substitute Equation 8.2.7 into Equation 8.2.6, to obtain

$$|\psi_0|^2 \int_{-\infty}^{\infty} \mathrm{e}^{-(x-x_0)^2/(2\sigma^2)} dx = 1. \tag{8.2.8}$$

Changing the variable of integration to $y = (x - x_0)/(\sqrt{2}\sigma)$, we get

$$|\psi_0|^2 \sqrt{2}\sigma \int_{-\infty}^{\infty} \mathrm{e}^{-y^2} dy = 1. \tag{8.2.9}$$

However,

$$\int_{-\infty}^{\infty} \mathrm{e}^{-y^2} dy = \sqrt{\pi}, \tag{8.2.10}$$

which implies that

$$|\psi_0|^2 = \frac{1}{(2\pi\sigma^2)^{1/2}}. \tag{8.2.11}$$

Hence, a general **normalized** Gaussian wavefunction takes the form

$$\psi(x) = \frac{e^{\mathrm{i}\phi}}{(2\pi\sigma^2)^{1/4}} e^{-(x-x_0)^2/(4\sigma^2)} \tag{8.2.12}$$

where ϕ is an arbitrary real phase-angle.

8.2.4: Contributors and Attributions

- David M. Hanson, Erica Harvey, Robert Sweeney, Theresa Julia Zielinski ("Quantum States of Atoms and Molecules")

This page titled 8.2: The Schrödinger Wave Equation is shared under a CC BY-NC-SA 4.0 license and was authored, remixed, and/or curated by Jonathan Gutow.

- **11.7: The Schrödinger Wave Equation** is licensed CC BY-NC-SA 4.0.

8.3: Particle in a One-Dimensional Box

A particle in a 1-dimensional box is a fundamental quantum mechanical approximation describing the translational motion of a single particle confined inside an infinitely deep well from which it *cannot* escape.

8.3.1: Introduction

The particle in a box problem is a common application of a quantum mechanical model to a simplified system consisting of a particle moving horizontally within an infinitely deep well from which it cannot escape. The solutions to the problem give possible values of E and ψ that the particle can possess. E represents allowed energy values and $\psi(x)$ is a wavefunction, which when squared gives us the probability of locating the particle at a certain position within the box at a given energy level.

recipe for Quantum Mechanics

To solve the problem for a particle in a 1-dimensional box, we must follow our *Big, Big recipe for Quantum Mechanics*:

1. Define the Potential Energy, V
2. Solve the Schrödinger Equation
3. Solve for the wavefunctions
4. Solve for the allowed energies

8.3.2: Step 1: Define the Potential Energy V

The potential energy is *0 inside the box* (V=0 for 0<x<L) and *goes to infinity at the walls of the box* (V=∞ for x<0 or x>L). We assume the walls have infinite potential energy to ensure that the particle has zero probability of being at the walls or outside the box. Doing so significantly simplifies our later mathematical calculations as we employ these **boundary conditions** when solving the Schrödinger Equation.

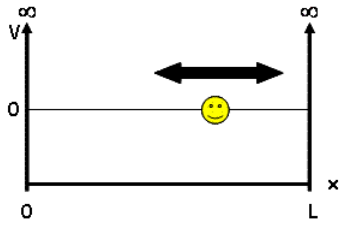


Figure 8.3.1: Cartoon of a particle trapped in a 1-D infinite potential of length L.

8.3.3: Step 2: Solve the Schrödinger Equation

The time-independent Schrödinger equation for a particle of mass m moving in one direction with energy E is

$$-\frac{\hbar^2}{2m}\frac{d^2\psi(x)}{dx^2}+V(x)\psi(x)=E\psi(x) \tag{8.3.1}$$

with

- $\hbar$ is the reduced Planck constant where $\hbar=\frac{h}{2\pi}$
- m is the mass of the particle
- $\psi(x)$ is the stationary time-independent wavefunction
- $V(x)$ is the potential energy as a function of position
- E is the energy, a real number

This equation can be modified for a particle of mass m free to move parallel to the x-axis with zero potential energy (V = 0 everywhere) resulting in the quantum mechanical description of free motion in one dimension:

$$-\frac{\hbar^2}{2m}\frac{d^2\psi(x)}{dx^2}=E\psi(x) \tag{8.3.2}$$

This equation has been well studied and gives a general solution of:

$$\psi(x) = A\sin(kx) + B\cos(kx) \tag{8.3.3}$$

where A, B, and k are constants.

8.3.4: Step 3: Define the Wavefunction

The solution to the Schrödinger equation we found above is the general solution for a 1-dimensional system. We now need to apply our **boundary conditions** to find the solution to our particular system. According to our boundary conditions, the probability of finding the particle at $x = 0$ or $x = L$ is zero. When $x = 0$, then $\sin(0) = 0$ and $\cos(0) = 1$; therefore, B *must equal 0* to fulfill this boundary condition giving:

$$\psi(x) = A\sin(kx) \tag{8.3.4}$$

We can now solve for our constants (A and k) systematically to define the wavefunction.

8.3.4.1: **Solving for k**

Differentiate the wavefunction with respect to x:

$$\frac{d\psi}{dx} = kA\cos(kx) \tag{8.3.5}$$

Differentiate the wavefunction again with respect to x:

$$\frac{d^2\psi}{dx^2} = -k^2 A\sin(kx) \tag{8.3.6}$$

Since $\psi(x) = A\sin(kx)$, then

$$\frac{d^2\psi}{dx^2} = -k^2\psi \tag{8.3.7}$$

Substituting this for the second derivative in the Schrödinger equation (8.3.2) yields:

$$-\frac{\hbar^2}{2m}k^2\psi(x) = E\psi(x) \tag{8.3.8}$$

If we then solve for k, we find:

$$k = \left(\frac{8\pi^2 mE}{h^2}\right)^{1/2} \tag{8.3.9}$$

Now we plug k into our wavefunction (Equation 8.3.4):

$$\psi = A\sin\left(\frac{8\pi^2 mE}{h^2}\right)^{1/2} x \tag{8.3.10}$$

8.3.4.2: **Solving for A**

To determine A, we have to apply the boundary conditions again. Recall that the *probability of finding a particle at $x = 0$ or $x = L$ is zero.*

When x = L:

$$0 = A\sin\left(\frac{8\pi^2 mE}{h^2}\right)^{1/2} L \tag{8.3.11}$$

This is only true when

$$\left(\frac{8\pi^2 mE}{h^2}\right)^{1/2} L = n\pi \tag{8.3.12}$$

where $n = 1, 2, 3, \ldots$

Plugging this back in gives us:

$$\psi = A \sin \frac{n\pi}{L} x \tag{8.3.13}$$

To determine A, recall that the total probability of finding the particle inside the box is 1, meaning there is no probability of it being outside the box. When we find the probability and set it equal to 1, we are *normalizing* the wavefunction.

$$\int_0^L \psi^2 dx = 1 \tag{8.3.14}$$

For our system, the normalization looks like:

$$A^2 \int_0^L \sin^2\left(\frac{n\pi}{L}\right) x \, dx = 1 \tag{8.3.15}$$

Using the solution for this integral from an integral table, we find our normalization constant, A:

$$A = \sqrt{\frac{2}{L}} \tag{8.3.16}$$

Which results in the normalized wavefunctions for a particle in a 1-dimensional box:

$$\psi_n = \sqrt{\frac{2}{L}} \sin \frac{n\pi}{L} x \tag{8.3.17}$$

where $n = 1, 2, 3, \ldots$

8.3.5: Step 4: Determine the Allowed Energies

Solving for the energy of each ψ requires substituting Equation 8.3.17 into Equation 8.3.2 to get the allowed energies for a particle in a box:

$$E_n = \frac{n^2 h^2}{8mL^2} \tag{8.3.18}$$

Equation 8.3.18 is a very important result and tells us that:

1. The energy of a particle is quantized.
2. The lowest possible energy of a particle is **NOT** zero. This is called the **zero-point energy** and means the particle can never be at rest because it always has some kinetic energy.

Zero point energy is one manifestation of the **Heisenberg Uncertainty Principle**, which states that you cannot know a particle's exact momentum and exact position simultaneously.

8.3.6: Heisenberg uncertainty principle[2]

The Heisenberg uncertainty principle is a general quantum phenomenon, where certain pairs of physical quantities cannot be measured exactly simultaneously. In other words, the quantities are coupled in such a way that the uncertainty in one is related to the uncertainty in the other quantity. These pairs are called **complementary observables**. Momentum and position are one set of complementary observables. In the case of momentum and position of a particle the Heisenberg uncertainty principle quantifies this relationship as:

$$\Delta x \Delta p \geq \frac{\hbar}{2} \tag{8.3.19}$$

where Δx is the uncertainty in position and Δp is the uncertainty in momentum. Thus, for a particle confined to a 1-D box of length L ($\Delta x \approx L$):

$$\Delta p \gtrsim \frac{\hbar}{2L} \tag{8.3.20}$$

Since kinetic energy is expressed in terms of momentum by the equation $KE = \frac{p^2}{2m}$ this means a confined particle must have some non-zero amount of kinetic energy to satisfy the Heisenberg uncertainty principle.

8.3.7: What does all this mean?

The wavefunction for a particle trapped in an infinite 1-D well are sine waves with nodes at the walls as shown in figure $8.3.2a$.

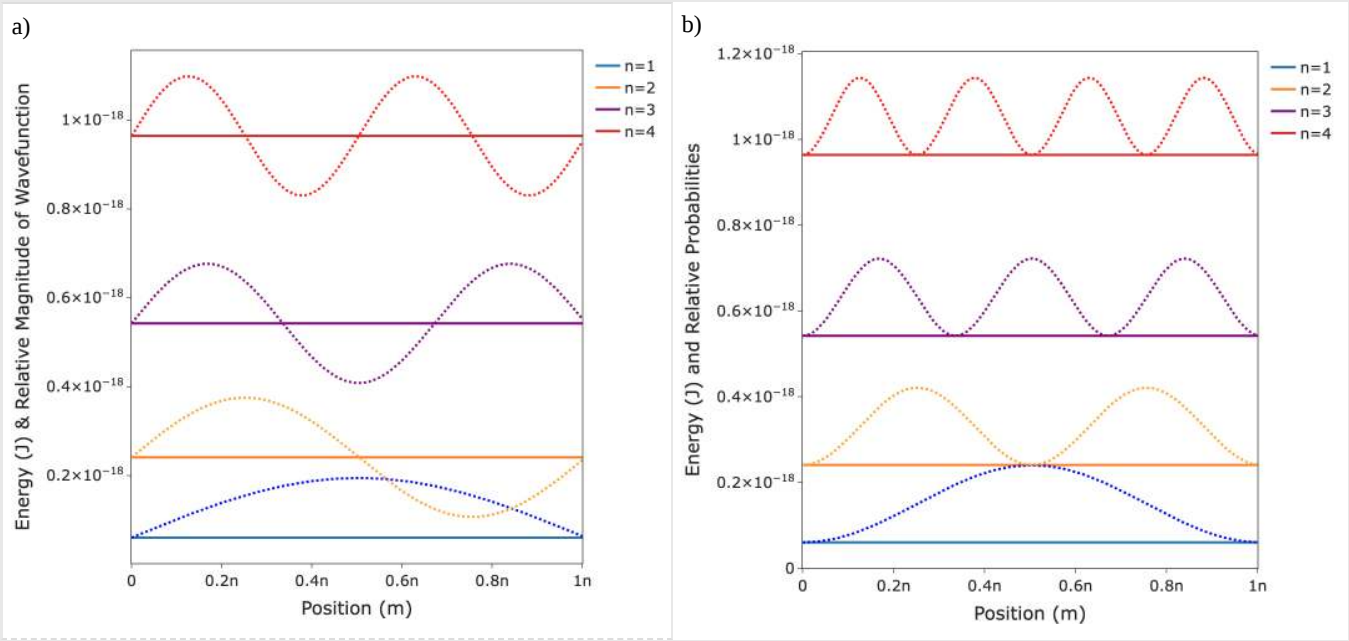


Figure $8.3.2$: Calculated energies, wavefunctions and probability densities for an electron in a 1.0 nm long infinite well. a) Energy levels and wavefunctions. b) Energy levels and probability densities.

The probability of finding a particle at a certain spot in the box is determined by squaring ψ. The probability distributions for a trapped particle are shown in figure $8.3.2b$.

Notice:

- The lowest energy (n=1) quantum state has energy > 0, the **zero-point energy**. This is a characteristic of localized particles.
- The number of **nodes** (places where the particle has zero probability of being located) increases with increasing energy level, n.
- The spacing between energy levels increases as n increases. This can be made quantitative by deriving the expression for the separation between neighboring levels.

$$\Delta E = E_{n+1} - E_n = \frac{(n+1)^2 h^2}{8mL^2} - \frac{n^2 h^2}{8mL^2} = (2n+1)\frac{h^2}{8mL^2} \tag{8.3.21}$$

Other potentials have different energy spacing patterns.

Example 8.3.1

What is the ΔE between the $n = 4$ and $n = 5$ states for an F_2 molecule trapped within in a one-dimension well of length 3.0 cm? At what value of n does the energy of the molecule reach ¼k_BT at 450 K, and what is the separation between this energy level and the one immediately above it?

Solution

Since this is a one-dimensional particle in a box problem, the particle has only kinetic energy (V = 0), so the permitted energies are:

$$E_n = \frac{n^2h^2}{8mL^2}$$

with $n = 1, 2, \ldots$

The energy difference between $n = 4$ and $n = 5$ is then

$$\Delta E = E_5 - E_4 = \frac{5^2h^2}{8mL^2} - \frac{4^2h^2}{8mL^2}$$

Using Equation 8.3.18 with the mass of F_2 (37.93 amu = $6.3 \times 10^{-26}\ kg$) and the length of the box ($L = 3 \times 3.0 \times 10^{-2}\ \text{m}^2$:

$$\Delta E = \frac{9h^2}{8mL^2} = \frac{9(6.626 \times 10^{-34}\ \text{kg} \cdot \text{m}^2 \cdot \text{s}^{-1})^2}{8(6.30938414 \times 10^{-26}\ \text{kg})(3.0 \times 10^{-2}\ \text{m}^2)^2}$$

$$\Delta E = 8.70 \times 10^{-39}\ J$$

The n value for which the energy reaches $\frac{1}{4}k_BT$:

$$\frac{n^2h^2}{8mL^2} = \frac{1}{4}k_BT$$

$$n = 1.79 \times 10^9$$

The separation between $n+1$ and n:

$$\Delta E = E_{n+1} - E_n = \frac{(n+1)^2h^2 - (n)^2h^2}{8mL^2}$$

$$\Delta E = \frac{(2n+1)h^2}{8mL^2}$$

$$\Delta E = 3.47 \times 10^{-30}\ J$$

Example 8.3.2: Modeling a linear conjugated system

The particle-on-a-line model provides a reasonable approximation for the electronic states of the π electrons in conjugated chains (nearly linear). Consider hexatriene (=–=–=). We can estimate the transition energy between the highest occupied molecular orbital (HOMO) and lowest unoccupied molecular orbital (LUMO) using this model. The lowest energy photon absorbed by the electronic system (longest wavelength) would be this transition.

Solution

There are 6 π electrons. Each orbital (quantum state) can hold two electrons. So the HOMO is the n = (# π electrons)/2 = 3.

Thus we are looking for the transition energy between the n = 3 and n = 4 states:

$$\Delta E = E_4 - E_3 = \frac{4^2h^2}{8mL^2} - \frac{3^2h^2}{8mL^2} = \frac{7h^2}{8mL^2}$$

Using an average C–C bond length of roughly 140 pm give L ≈ 700 pm. The mass of an electron is 9.109 X 10^{-31} kg which yields:

$$\Delta E = \frac{7(6.626 \times 10^{-34} Js)^2}{8(9.109 \times 10^{-31} kg)(700 \times 10^{-12} m)^2} = 8.61 \times 10^{-19} J$$

Which corresponds to a wavelength of about 218 nm, well into the UV.

8.3.8: Important Facts to Learn from the Particle in the Box

- The energy of a particle is quantized. This means it can only take on discreet energy values.

- The lowest possible energy for a confined particle is **NOT** zero (even at 0 K). This means the particle *always* has some kinetic energy.
- The square of the wavefunction is related to the probability of finding the particle in a specific position for a given energy level.
- The probability changes with increasing energy of the particle and depends on the position in the box.
- In classical physics, the probability of finding the particle is independent of the energy and the same at all points in the box.

8.3.9: Helpful Links

- Provides a live quantum mechanical simulation of the particle in a box model and allows you to visualize the solutions to the Schrödinger Equation: www.falstad.com/qm1d/

8.3.10: References

1. Chang, Raymond. *Physical Chemistry for the Biosciences*. Sansalito, CA: University Science, 2005.
2. Levine, Ira. *Quantum Chemistry*, 4th Ed. (Prentice-Hall, Inc. Englewood Cliffs, New Jersey, 1991) Pp. 80 - 83.

This page titled 8.3: Particle in a One-Dimensional Box is shared under a CC BY-NC-SA 4.0 license and was authored, remixed, and/or curated by Jonathan Gutow.

- **11.8: Particle in a One-Dimensional Box** by Delmar Larsen is licensed CC BY-NC-SA 4.0.

8.4: Tunneling

8.4.1: Introduction

Tunneling is a quantum mechanical phenomenon where a particle is able to penetrate through a finite potential energy barrier that is higher in energy than the particle's kinetic energy. This amazing property of microscopic particles plays important roles in explaining several physical phenomena including radioactive decay. Additionally, the principle of tunneling lead to the development of Scanning Tunneling Microscope (STM) which had a profound impact on chemical, biological and material science research.

8.4.2: Violating Classical Mechanics

Consider a ball rolling from one valley to another over a hill (Figure 8.4.1). If the ball has enough energy (E) to overcome the potential energy (V) at the top of the barrier between each valley, then it can roll from one valley to the other. This is the classical picture and is controlled by the simple Law of Conservation of Energy approach taught in beginning physics courses. However, If the ball does not have enough kinetic energy ($E < V$), to overcome the barrier it will never roll from one valley to the other. In contrast, when quantum effects are taken into account, the ball can "tunnel" through the barrier to the other valley, even if its kinetic energy is less than the potential energy of the barrier to the top of one of the hills.

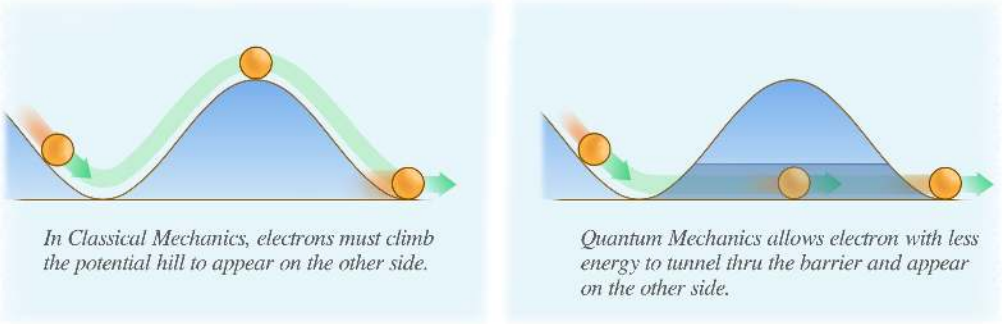


Figure 8.4.1: Contrasting classical (over the barrier) motion vs. quantum (through the barrier) motion. (CC BY-NC 4.0; Ümit Kaya via LibreTexts)

The Heisenberg Uncertainty Principle in Action

The reason for the difference between classical and quantum motion comes from wave-particle nature of matter. One interpretation of this duality involves the Heisenberg uncertainty principle, which defines a limit on how precisely the position and the momentum of a particle can be known at the same time. This implies that there are no solutions with a probability of exactly zero (or one), though a solution may approach infinity if, for example, the calculation for its position was taken as a probability of 1, the other, i.e. its speed, would have to be infinity. Hence, the probability of a given particle's existence on the opposite side of an intervening barrier is non-zero, and such particles will appear on the 'other' (a semantically difficult word in this instance) side with a relative frequency proportional to this probability.

Microscopic particles such as protons, or electrons behave differently as a consequence of wave-particle duality. Consider a particle with energy E that is confined in a box which has a barrier of height V. Classically, the box will prevent these particles from escaping because the kinetic energy of these particles to low to get over the barrier. However, if the thickness of the barrier is thin, the particles have some probability of penetrating through the barrier **without** sufficient energy and appear on the other side of the box (Figure 8.4.2).

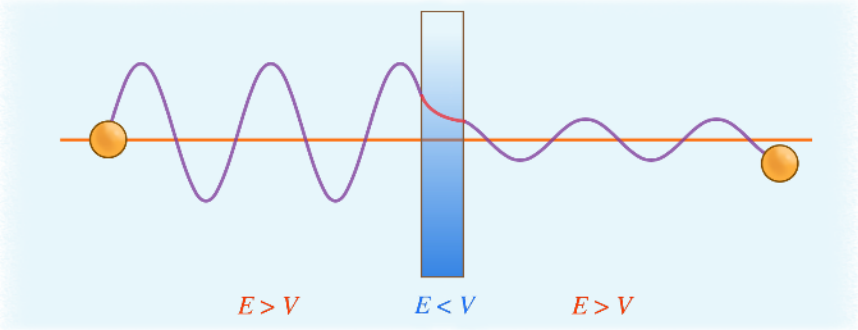


Figure 8.4.2: Quantum tunneling through a barrier. The energy of the tunneled particle is the same but the amplitude is decreased. (CC BY-NC 4.0; Ümit Kaya via LibreTexts)

When it reaches a barrier it cannot overcome, a particle's wave function changes from sinusoidal to exponentially diminishing in form. The solution for the Schrödinger equation in such a medium (Figure 8.4.2; blue region) is:

$$\psi = Ne^{-\beta x} \tag{8.4.1}$$

where

- N is a normalization constant and
- $\beta = \sqrt{\frac{2m(V-E)}{\hbar^2}}$

For a quantum particle to *appreciably* tunnel through a barrier three conditions must be met (Figure 8.4.2):

1. The height of the barrier must be **finite** and the thickness of the barrier should be **thin**.
2. The potential energy of the barrier exceeds the kinetic energy of the particle ($E < V$).
3. The particle has wave properties because the wavefunction is able to penetrate through the barrier. This suggests that quantum tunneling only apply to microscopic objects such protons or electrons and does not apply to macroscopic objects.

If these conditions are met, there would be some probability of finding the particles on the other side of the barrier. Beginning as a sinusoidal wave, a particle begins tunneling through the barrier and goes into exponential decay until it exits the barrier and gets transmitted out the other side as a final sinusoidal wave with a smaller amplitude. The act of tunneling decreases the wave amplitude due the reflection of the incident wave when it comes into the contact with the barrier but does not affect the wave equation.

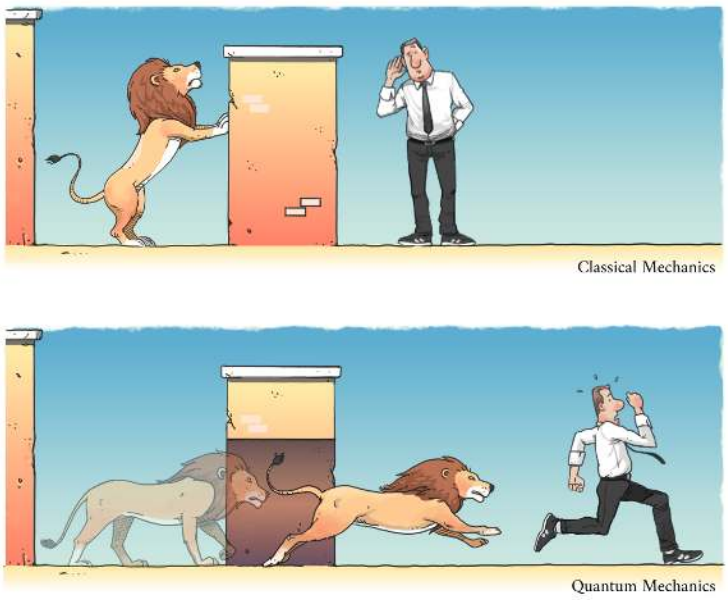


Figure 8.4.3: Quantum tunnelling of a lion through a barrier is a quantum effect with no classical analog. (CC BY-NC 4.0; Ümit Kaya via LibreTexts)

The probability, P, of a particle tunneling through the potential energy barrier is derived from the Schrödinger Equation by calculating the ratio of the probabilities ($|\psi^2|$) of a particle traveling towards the barrier on the left and the particle traveling away from the barrier on the right. This yields:

$$P \approx \exp\left(\frac{-4a\pi}{h}\sqrt{2m(V-E)}\right) \tag{8.4.2}$$

with $E < V$

where

- V is the potential barrier,
- E is the kinetic energy possessed by the particle, and
- a is the thickness of the barrier.
- m is mass of the particle
- h is Planks Constant ($6.626 \times 10^{-34} m^2 kg/s$)

Therefore, the probability of an object tunneling through a barrier decreases with the object's increasing mass and with the increasing gap between the energy of the object and the energy of the barrier. This explains how tunneling is frequent at the nanoscale, but negligible at the macroscopic level. Equation 8.4.2 argues that the probability of tunneling decreases exponentially with the square root of the particles mass (particles with a small mass can effectively tunnel through barriers more easily than those with larger mass) and the thickness of the barrier (a).

Example 8.4.1

An electron having total kinetic energy E of 4.50 eV approaches a rectangular energy barrier with $V = 5.00\,eV$ and $L = 950\,pm$. Classically, the electron cannot pass through the barrier because $E < V$. Calculate probability of tunneling of this electron through the barrier.

Solution

This is a straightforward application of Equation 8.4.2.

$$P \approx \exp\left(\frac{-4a\pi}{h}\sqrt{2m(V-E)}\right)$$

The electronvolt (eV) is a unit of energy that is equal to approximately $1.6 \times 10^{-19}\ J$, which is the conversion used below.

The mass of an electron is $9.10 \times 10^{-31}\ kg$

$$P \approx \exp\left[\left(-\frac{(4)(950 \times 10^{-12}\ m)(\pi)}{6.6260 \times 10^{-34} m^2 kg/s}\right)\sqrt{(2)(9.10 \times 10^{-31}\ kg)(5.00 - 4.50\ \cancel{eV})(1.60 \times 10^{-19} J/\ \cancel{eV})}\right]$$

$$= \exp^{-6.88} = 1.03 \times 10^{-3}$$

There is a ~0.1% probability of the electrons tunneling though the barrier.

8.4.3: Alpha Decay Radioactivity

Protons and neutrons in a nucleus have kinetic energy, but it is about 8 MeV less than that needed to get out from attractive nuclear potential (Figure 8.4.4). Hence, they are bound by an average of 8 MeV per nucleon. The slope of the hill outside the bowl is analogous to the repulsive Coulomb potential for a nucleus, such as for an α particle outside a positive nucleus. In α decay, two protons and two neutrons spontaneously break away as a ^{4}He unit. Yet the protons and neutrons do not have enough kinetic energy to classically get over the rim.

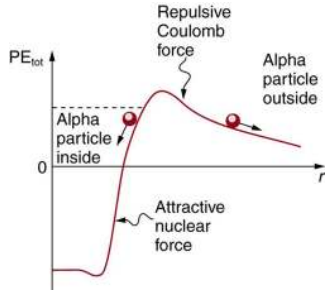


Figure 8.4.4: Nucleons within an atomic nucleus are bound or trapped by the attractive nuclear force, as shown in this simplified potential energy curve. An particle outside the range of the nuclear force feels the repulsive Coulomb force. The α particle inside the nucleus does not have enough kinetic energy to get over the rim, yet it does manage to get out by quantum mechanical tunneling. (CC BY; OpenStax)

The α article tunnels through a region of space it is forbidden to be in, and it comes out of the side of the nucleus. Like an electron making a transition between orbits around an atom, it travels from one point to another without ever having been in between (Figure 8.4.5). The wave function of a quantum mechanical particle varies smoothly, going from within an atomic nucleus (on one side of a potential energy barrier) to outside the nucleus (on the other side of the potential energy barrier). Inside the barrier, the wave function does not become zero but decreases exponentially, and we do not observe the particle inside the barrier. The probability of finding a particle is related to the square of its wave function, and so there is a small probability of finding the particle outside the barrier, which implies that the particle can tunnel through the barrier.

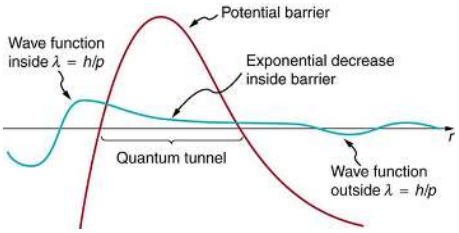


Figure 8.4.5: The wave function representing a quantum mechanical particle must vary smoothly, going from within the nucleus (to the left of the barrier) to outside the nucleus (to the right of the barrier). Inside the barrier, the wave function does not abruptly become zero; rather, it decreases exponentially. Outside the barrier, the wave function is small but finite, and there it smoothly becomes sinusoidal. Owing to the fact that there is a small probability of finding the particle outside the barrier, the particle can tunnel through the barrier. (CC BY; OpenStax)

8.4.4: Scanning Tunneling Microscopy (STM)

A metal tip usually made out of tungsten is placed a very small distance above a conducting or semiconducting surface. This distance acts as a potential barrier for tunneling. The space between the tip and the surface normally is vacuum. When electrons tunnel from the metal tip to the surface, a current is created and monitored by a computer (Figure 8.4.6). The current depends on the distance between the tip and the surface, which is controlled by a piezoelectric cylinder. If there is a strong current, the tip will

move away from the surface. The increase of the potential barrier will decrease the probability of tunneling and decrease the current. If the current becomes too weak, the tip moves closer to the surface. The potential barrier will be reduced and the current will increase. The variations in the current or the voltage applied to the piezoelectric cylinder as the tip moves over the sample are used to construct a topological image of the scanned surface.

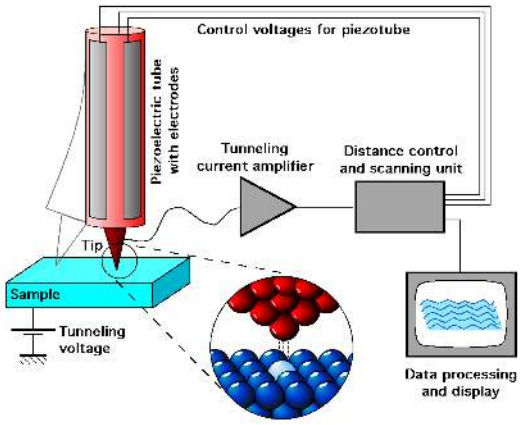


Figure 8.4.6: Schematic diagram of a scanning tunneling microscope. (CC BY-SA 2.0 Austria; Michael Schmid via Wikipedia).

8.4.5: References

1. Chang, Raymond. *Physical Chemistry for the Biosciences*. Sansalito, CA: University Science, 2005. Print.
2. Engel, Thomas. Quantum Chemistry and Spectroscopy.Upper Saddle River, NJ. Pearson, 2006. Print.

8.4.6: Contributors and Attributions

- Paul Flowers (University of North Carolina - Pembroke), Klaus Theopold (University of Delaware) and Richard Langley (Stephen F. Austin State University) with contributing authors. Textbook content produced by OpenStax College is licensed under a Creative Commons Attribution License 4.0 license. Download for free at http://cnx.org/contents/85abf193-2bd...a7ac8df6@9.110).
- J. Gutow (University of Wisconsin Oshkosh).

This page titled 8.4: Tunneling is shared under a CC BY-NC-SA 4.0 license and was authored, remixed, and/or curated by Jonathan Gutow.

- **Tunneling** is licensed CC BY 4.0.

8.5: Particle in a 2-Dimensional Box

Learning Objectives

- Manipulate probability, energy, and transition problems involving multidimensional wavefunctions
- Apply the Separation of Variables to solve a multi-dimensional Schrödinger equation
- Manipulate problems with multiple quantum numbers
- To be introduced to the concepts of non-singular nodes (e.g., nodal lines)
- To be introduced to the concept of degeneracy

8.5.1: Introduction

Let us now consider the Schrödinger Equation for an electron confined to a two dimensional box, $0 < x < a$ and $0 < y < b$. That is to say, within this rectangle the electron wavefunction behaves as a free particle ($V(x, y) = 0$), but the walls are impenetrable so the wavefunction $\psi(x, y, t) = 0$ at the walls.

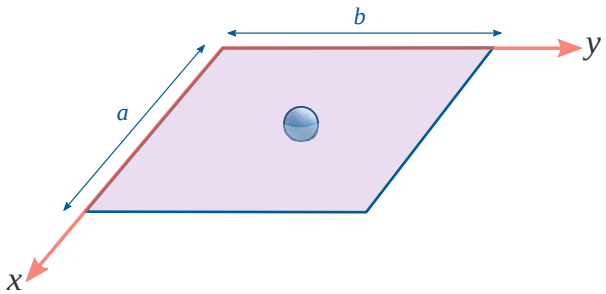


Figure 8.5.1: A particle in a $a \times b$ 2-dimensional box with infinite height can only be found within the box (highlighted). (CC BY-NC; Ümit Kaya)

Extending the (time-independent) Schrödinger equation for a one-dimensional system

$$-\frac{\hbar^2}{2m}\frac{d^2\psi(x)}{d\,x^2} + V(x)\psi(x) = E\psi(x) \tag{8.5.1}$$

to a two-dimensional system is not difficult

$$-\frac{\hbar^2}{2m}\left(\frac{\partial^2\psi(x,y)}{\partial x^2} + \frac{\partial^2\psi(x,y)}{\partial y^2}\right) + V(x,y)\psi(x,y) = E\psi(x,y). \tag{8.5.2}$$

Equation 8.5.2 can be simplified for the particle in a 2D box since we know that $V(x, y) = 0$ within the box and $V(x, y) = \infty$ outside the box, ii.e.

$$V(x,y) = \begin{cases} 0 & 0 \le x \le a \text{ and } 0 \le y \le b \\ \infty & x < 0 \text{ and } x > a \\ \infty & y < 0 \text{ and } y > b \end{cases}$$

So Equation 8.5.2 becomes

$$-\frac{\hbar^2}{2m}\left(\frac{\partial^2\psi(x,y)}{\partial x^2} + \frac{\partial^2\psi(x,y)}{\partial y^2}\right) = E\psi(x,y). \tag{8.5.3}$$

Since the Hamiltonian (i.e. left side of Equation 8.5.3) is the sum of two terms with independent (separate) variables, we try a product wavefunction like in the Separation of Variables approach used to separate time-dependence from the spatial dependence previously. Within this approach we express the 2-D wavefunction as a product of two independent 1-D components

$$\psi(x,y) = X(x)Y(y). \tag{8.5.4}$$

This ansatz separates Equation 8.5.3 into two independent one-dimensional Schrödinger equations

$$-\frac{\hbar^2}{2m}\left(\frac{d^2X(x)}{dx^2}\right) = \varepsilon_x X(x). \tag{8.5.5}$$

$$-\frac{\hbar^2}{2m}\left(\frac{d^2Y(y)}{dy^2}\right) = \varepsilon_y Y(y). \tag{8.5.6}$$

where the total energy of the particle is the sum of the energies from each one-dimensional Schrödinger equation

$$E = \varepsilon_x + \varepsilon_y \tag{8.5.7}$$

The differential equations in Equations 8.5.5 and 8.5.6 are familiar as they were found for the particle in a 1-D box previously. They have the general solution

$$X(x) = A_x \sin(k_x x) + B_x \cos(k_x x) \tag{8.5.8}$$

$$Y(y) = A_y \sin(k_y y) + B_y \cos(k_y y) \tag{8.5.9}$$

8.5.2: Applying Boundary Conditions

The general solutions in Equations 8.5.8 and 8.5.9 can be simplified to address boundary conditions dictated by the potential, i.e., $\psi(0, y) = 0$ and $\psi(x, 0) = 0$. Therefore, $B_x = 0$ and $B_y = 0$.

Thus, we can combine Equations 8.5.8, 8.5.9, and 8.5.4 to construct the wavefunction $\psi(x, y)$ for a particle in a 2D box of the form

$$\psi(x, y) = N \sin\left(\sqrt{\frac{2m\varepsilon_x}{\hbar^2}}x\right) \sin\left(\sqrt{\frac{2m\varepsilon_y}{\hbar^2}}y\right) \tag{8.5.10}$$

We still need to satisfy the remaining boundary conditions $\psi(a, y) = 0$ and $\psi(x, b) = 0$. To save writing we will consider the square well potential where a = b = L and generalize to a ≠ b later.

$$N \sin\left(\sqrt{\frac{2m\varepsilon_x}{\hbar^2}}L\right) \sin\left(\sqrt{\frac{2m\varepsilon_y}{\hbar^2}}y\right) = 0 \tag{8.5.11}$$

and

$$N \sin\left(\sqrt{\frac{2m\varepsilon_x}{\hbar^2}}x\right) \sin\left(\sqrt{\frac{2m\varepsilon_y}{\hbar^2}}L\right) = 0 \tag{8.5.12}$$

Equation 8.5.11 can be satisfied if

$$\sin\left(\sqrt{\frac{2m\varepsilon_x}{\hbar^2}}L\right) = 0 \tag{8.5.13}$$

independent of the value of y, while Equation 8.5.12 can be satisfied if

$$\sin\left(\sqrt{\frac{2m\varepsilon_y}{\hbar^2}}L\right) = 0 \tag{8.5.14}$$

independent of the value of x. These are the same conditions that we encountered for the one-dimensional box, hence we already know the sin function in each case can be zero in many places. In fact, these two conditions are satisfied if

$$\sqrt{\frac{2m\varepsilon_x}{\hbar^2}}L = n_x\pi \tag{8.5.15}$$

and

$$\sqrt{\frac{2m\varepsilon_y}{\hbar^2}}L = n_y\pi \tag{8.5.16}$$

which yield the allowed values of ε_x and ε_y as

$$\varepsilon_{n_x} = \frac{\hbar^2 \pi^2}{2mL^2} n_x^2 \tag{8.5.17}$$

and

$$\varepsilon_{n_y} = \frac{\hbar^2 \pi^2}{2mL^2} n_y^2 \tag{8.5.18}$$

We need two different integers n_x and n_y because the conditions are completely independent and can be satisfied by any two different (or similar) values of these integers. The allowed values of the total energy are now given by

$$E_{n_x,n_y} = \frac{\hbar^2 \pi^2}{2mL^2} (n_x^2 + n_y^2) \tag{8.5.19}$$

Note that the allowed energies now depend on two integers n_x and n_y rather than one. These arise from the *two* independent boundary conditions in the x and y directions. As in the one-dimensional box, the values of n_x and n_y are both restricted to the natural numbers $1, 2, 3, \ldots$Note, therefore, that the ground state energy $E_{1,1}$ is

$$E_{1,1} = \frac{\hbar^2 \pi^2}{mL^2} \tag{8.5.20}$$

is larger than for the one-dimensional box because of the contributions from kinetic energy in the x and y directions.

Once the conditions on ε_{n_x} and ε_{n_y} are substituted into Equation 8.5.10, the wavefunctions become

$$\psi_{n_x,n_y}(x,y) = N \sin\left(\frac{n_x \pi x}{L}\right) \sin\left(\frac{n_y \pi y}{L}\right) \tag{8.5.21}$$

The constant N is now determined by the normalization condition

$$\begin{aligned} \int_0^L \int_0^L |\psi_{n_x,n_y}(x,y)|^2 dx\, dy &= 1 \\ N^2 \int_0^L \sin^2\left(\frac{n_x \pi x}{L}\right) dx \int_0^L \sin^2\left(\frac{n_y \pi y}{L}\right) dy &= 1 \\ N^2 \frac{L}{2} \cdot \frac{L}{2} &= 1 \\ N &= \frac{2}{L} \end{aligned}$$

so that the complete normalized 2D wavefunction is

$$\psi_{n_x,n_y}(x,y) = \frac{2}{L} \sin\left(\frac{n_x \pi x}{L}\right) \sin\left(\frac{n_y \pi y}{L}\right) \tag{8.5.22}$$

The Separability of the Hamiltonian

Because the Halmiltonian in Equation 8.5.3 can be expressed as a simple sum of independent terms, the solutions can be expressed as simple **products** of the one-dimensional solution (Equation 8.5.22) with energies that are expressed as the **sum** of one-dimensional energies (Equation 8.5.19). This observation extends to higher dimensional wavefunctions as demonstrated later.

The wavefunctions in Equation 8.5.22 are somewhat more difficult that 1-D analogs to visualize because they are two dimensional. Nevertheless, we can still visualize them, and Figure 8.5.2 shows the following wavefunctions: $\psi_{1,1}(x,y)$, $\psi_{2,1}(x,y)$ and $\psi_{2,2}(x,y)$.

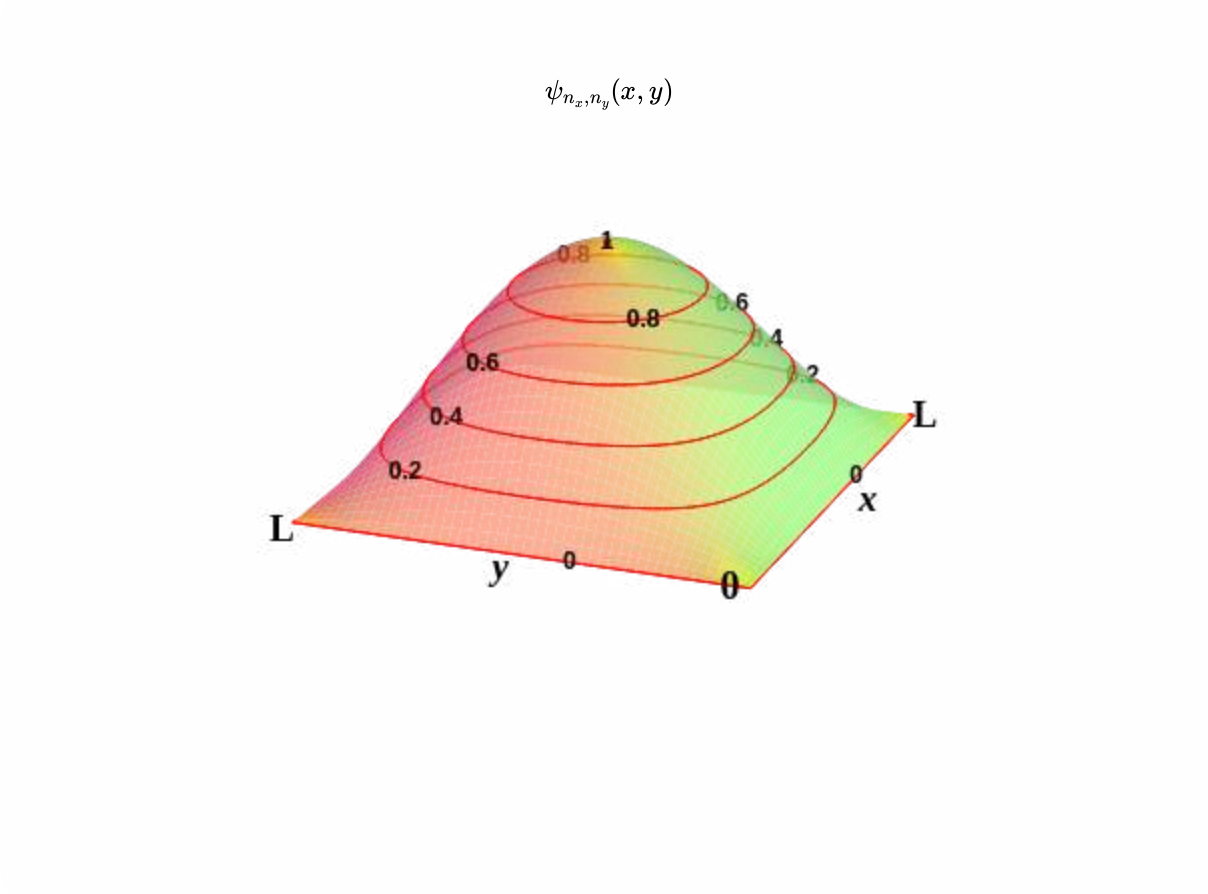


Figure 8.5.2: *Visualizing the first six wavefunctions for a particle in a two-dimensional square box ($L_x = L_y = L$). Use the slide bar to independently change either n_x or n_y quantum number and see the changing wavefunction.*

It is important to note that the wavefunctions can be either positive or negative, even though the associated probability density $p_{n_x,n_y}(x,y) = |\psi_{n_x,n_y}(x,y)|^2$ is strictly positive.

$\psi_{n_x,n_y}(x,y)$ $|\psi_{n_x,n_y}(x,y)|^2$

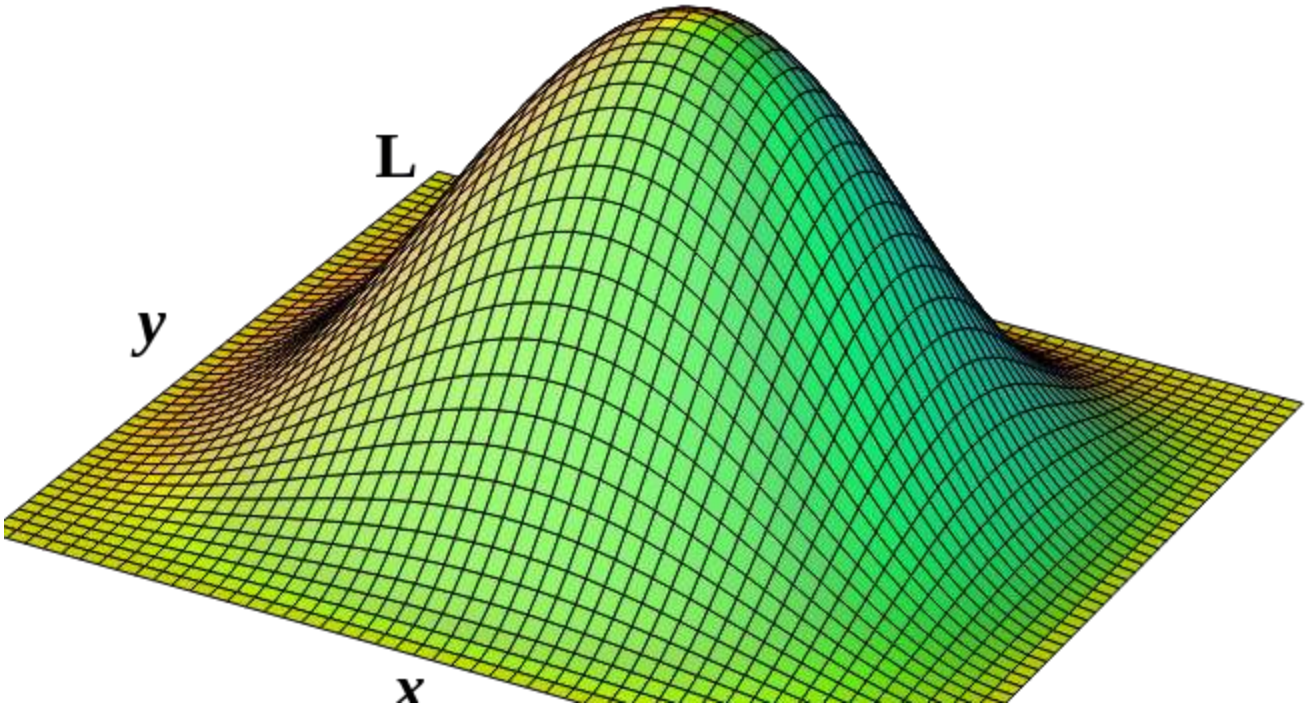


Figure 8.5.3: *Visualizing the first six wavefunctions and associated probability densities for a particle in a two-dimensional square box ($L_x = L_y = L$). Use the slide bar to independently change either n_x or n_y quantum number and see the changing wavefunction.*

Unlike in the one-dimensional analoge, where nodes in the wavefunction are points where $\psi_n(x) = 0$, here entire lines can be nodal (called *nodal lines)*. For example, in the state $\psi_{2,1}(x,y)$, there is a nodal line at $\psi_{2,1}(L/2,y)$. Along the entire line $x = L/2$, the wavefunction is 0 independent of the value of y. The wavefunction $\psi_{2,2}(x,y)$ has two nodal lines when $x = L/2$ and when $y = L/2$. The sign of the wavefunction and its nodal structure will play central roles later when we consider chemical bonding.

The fact that the wavefunction $\psi_{n_x n_y}(x,y)$ is a product of one-dimensional wavefunctions:

$$\psi_{n_x n_y}(x,y) = \psi_{n_x}(x)\psi_{n_y}(y) \tag{8.5.23}$$

makes the calculation of probabilities rather easy. The probability that a measurement the particle's position will yield a value of $x \in [a,b]$ and $y \in [c,d]$ is

$$\begin{aligned} P(x \in [a,b] \text{ and } y \in [c,d]) &= \int_a^b dx \int_c^d dy |\psi_{n_x n_y}(x,y)|^2 \\ &= \int_a^b dx \int_c^d dy \psi^2_{n_x}(x)\psi^2_{n_y}(y) \\ &= \left[\int_a^b \psi^2_{n_x}(x)dx\right]\left[\int_c^d \psi^2_{n_y}(y)dy\right] \end{aligned} \tag{8.5.24}$$

Example 8.5.1: Probability

For a particle in a two-dimensional square box of length L, if the particle is in the $\psi_{1,2}(x,y)$ state, what is the probability that a measurement of the particle's position will yield $x \in [0, L/2]$ and $y \in [0, L/2]$?

Solution

Substituting the limits of integration into Equation 8.5.24, we have

$$\begin{aligned} P(x \in [0, L/2] \; and \; y \in [0, L/2] \; &= \left[\int_0^{L/2} \psi_1^2(x) dx\right] \left[\int_0^{L/2} \psi_2^2(y) dy\right] \\ &= \left[\frac{2}{L}\int_0^{L/2} \sin^2\left(\frac{\pi x}{L}\right) dx\right] \left[\frac{2}{L}\int_0^{L/2} \sin^2\left(\frac{2\pi y}{L}\right) dy\right] \\ &= \left[\frac{2}{L}\frac{L}{4}\right] \left[\frac{2}{L}\frac{L}{4}\right] \\ &= \frac{1}{4} \end{aligned}$$

This can be graphically confirmed by exploring the probability densities in Figure 8.5.2 for the $\psi_{1,2}(x,y)$ state.

Exercise 8.5.1

For a particle in a two-dimensional square box of length L, if the particle is in the state $\psi_{2,3}(x,y)$, what is the probability that a measurement of the particle's position will yield $x \in [0, L/2]$ and $y \in [0, L/3]$?

Answer

$$P = \frac{1}{6}$$

Confirmed this by exploring the probability densities in Figure 8.5.2for the $\psi_{2,3}(x,y)$ state.

Note that if the box were rectangular rather than square, then instead of having a length of L on both sides, there would be two different lengths L_x and L_y. The formulas for the energies and wavefunctions become only slightly more complicated:

$$E_{n_x,n_y} = \frac{\hbar^2\pi^2}{2m}\left(\frac{n_x^2}{L_x^2} + \frac{n_y^2}{L_y^2}\right) \tag{8.5.25}$$

instead of Equation 8.5.19 and

$$\psi_{n_x,n_y}(x,y) = \frac{2}{\sqrt{L_x L_y}} \sin\left(\frac{n_x \pi x}{L_x}\right) \sin\left(\frac{n_y \pi y}{L_y}\right) \tag{8.5.26}$$

instead of Equation 8.5.22.

8.5.3: Degeneracy

Two distinct wavefunctions are said to be *degenerate* if they correspond to the same energy. If the sides *a*, *b* of the rectangle are such that *a*/*b* is irrational (the general case), there will be no degeneracies. The *most* degenerate case is the square, $L_x = L_y$, for which clearly $E_{m,n} = E_{n,m}$. Degeneracies in quantum physics are most often associated with symmetries in this way. Figure 8.5.4 shows the wavefunctions (3,2) and (2,3) for a rectangle. These are contour maps for the time-independent solution, with white being the highest point. These two wavefunctions do not correspond to the same energy, although they would, of course, for a square.

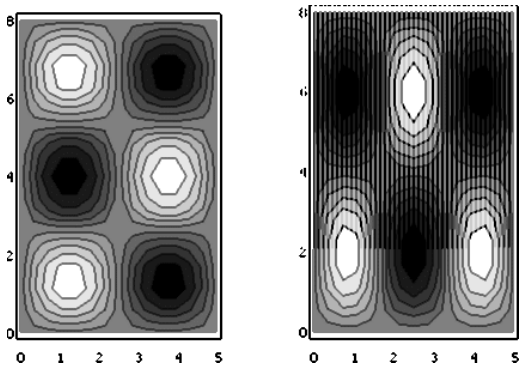


Figure 8.5.4: Contours of the $n_x = 2$ and $n_y = 3$ wavefunction (left) and $n_x = 3$ and $n_y = 2$ wavefunction (right).

The energy of the particle in a 2-D square box (i.e., $L_x = L_y = L$) in the **ground state** is given by Equation 8.5.25 with $n_x = 1$ and $n_y = 1$. This energy (E_{11}) is hence

$$E_{1,1} = \frac{2\hbar^2\pi^2}{2mL^2} \tag{8.5.27}$$

For the ground state of the particle in a 2D box, there is one wavefunction (and no other) with this specific energy; the ground state and the energy level are said to be **non-degenerate**. However, in the 2-D box potential, the energy of a state depends upon the sum of the squares of the two quantum numbers. The particle having a particular value of energy in the excited state *may* has several different stationary states or wavefunctions. If so, these states and energy eigenvalues are said to be **degenerate**.

For the first excited state, three combinations of the quantum numbers $(n_x,\ n_y)$ are $(2,\ 1)$ and $(1, 2)$. The sum of squares of the quantum numbers in each combination is same (equal to 5). Each waveunction has same energy:

$$E_{2,1} = E_{1,2} = \frac{5\hbar^2\pi^2}{2mL^2} \tag{8.5.28}$$

Corresponding to these combinations three different wavefunctions and **two** different states are possible. Hence, the first excited state is said to be doubly degenerate. The number of independent wavefunctions for the stationary states with *a shared energy* is called as the **degree of degeneracy** of the energy level. The value of energy levels with the corresponding combinations and sum of squares of the quantum numbers

$$n^2\ = n_x^2 + n_y^2 \tag{8.5.29}$$

as well as the degree of degeneracy are depicted in Table 8.5.1.

Table 8.5.1: Degeneracy properties of the particle in a 2-D box with $L_x = L$ and $L_y = L$.

$n_x^2 + n_y^2$	Combinations of Degeneracy (n_x, n_y)			Total Energy (E_{n_x,n_y})	Degree of Degeneracy
2	(1, 1)			$\frac{2\hbar^2\pi^2}{2mL^2}$	1
5	(2, 1)	(1, 2)		$\frac{5\hbar^2\pi^2}{2mL^2}$	2
8	(2, 2)			$\frac{8\hbar^2\pi^2}{2mL^2}$	1
10	(3, 1)	(1, 3)		$\frac{10\hbar^2\pi^2}{2mL^2}$	2
13	(3, 2)	(2, 3)		$\frac{13\hbar^2\pi^2}{2mL^2}$	2
18	(3,3)			$\frac{18\hbar^2\pi^2}{2mL^2}$	1

Note that all the states above would be non-degenerate if $L_x \neq L_y$. However, a degeneracy will be "accidentally" observed for states that fulfill this requirement:

$$\frac{n_x^2}{L_x^2} = \frac{n_y^2}{L_y^2}. \tag{8.5.30}$$

Example 8.5.2: Transition Energy

An electron in a 2D infinite potential well needs to absorb electromagnetic wave with wavelength 4040 nm (IR radiation) to be excited from lowest excited state to next higher energy state. What is the length of the box if this potential well is a square ($L_x = L_y = L$)?

Solution

The energy of a particle in a 2-D well is given by Equation 8.5.25:

$$E_{n_x,n_y} = \frac{\hbar^2\pi^2}{2m}\left(\frac{n_x^2}{L_x^2} + \frac{n_y^2}{L_y^2}\right)$$

and for a square well $L_x = L_y = L$ this simplifies to Equation 8.5.19:

$$E_{n_x,n_y} = \frac{\hbar^2\pi^2}{2mL^2}\left(n_x^2 + n_y^2\right)$$

When the electron absorbs an electromagnetic wave and it transitions from one state (e.g., $(n_x = 1, n_y = 2)$ or $(n_x = 2, n_y = 1)$ since are degenerate states as Table 8.5.1 demonstrates) to a higher energetic state, e.g., $(n_x = 2, n_y = 2)$.

The energy of the lowest excited state is $\frac{5h^2}{8mL^2}$ and the energy of the next higher excited state is $\frac{8h^2}{8mL^2}$, so we can equate the difference in energies of these state to the energy of the absorbed photon

$$\begin{aligned} h\nu &= E_{2,1} - E_{1,1} \\ &= \frac{5\hbar^2\pi^2}{2mL^2} - \frac{2\hbar^2\pi^2}{2mL^2} \\ &= \frac{3\hbar^2\pi^2}{2mL^2} \end{aligned}$$

Converting frequency (ν) to wavelength (λ):

$$\nu = \frac{c}{\lambda}$$

results in an expresstion relating wavelength of absorbed light to box length L:

$$\frac{hc}{\lambda} = \frac{3\hbar^2\pi^2}{2mL^2}$$

and solving for L

$$L = \sqrt{\frac{3\hbar^2\pi^2}{2mhc}\lambda}$$

or

$$\begin{aligned} L &= \sqrt{\frac{3\hbar\pi}{4mc}\lambda} \\ &= 1.91\,nm \end{aligned}$$

Exercise 8.5.2

An electron in a 2D infinite potential well needs to absorb electromagnetic wave with wavelength 4040 nm to be excited from $(n_x = 2, n_y = 2)$ state to the $(n_x = 3, n_y = 3)$ state.

a. What is the length of the box if this potential well is a square ($L_x = L_y = L$)?
b. How many wavefunction exist between these two states (do not count the start or ending states)

Answer a

$L = 3.5\, nm$

Answer b

From the energies in Table 8.5.1, four wavefunctions exist between $(n_x = 2, n_y = 2)$ state to the $(n_x = 3, n_y = 3)$ state. However, due to degeneracy, only two possible energies exist.

8.5.4: Contributors and Attributions

- Mark Tuckerman (New York University)
- Michael Fowler (Beams Professor, Department of Physics, University of Virginia)

This page titled 8.5: Particle in a 2-Dimensional Box is shared under a CC BY-NC-SA 4.0 license and was authored, remixed, and/or curated by Jonathan Gutow.

- **Particle in a 2-Dimensional Box** by Mark E. Tuckerman is licensed CC BY-NC-SA 4.0.

8.6: Particle on a Ring

Learning Objectives

- To be familiar with a quantum system with angular symmetry.
- To be introduced to quantum angular momentum

8.6.1: Introduction

The case of a quantum particle confined a one-dimensional ring is similar to the particle in a 1D box. Consider a variant of the one-dimensional particle in a box problem in which the x-axis is bent into a ring of radius R. We can write the same Schrödinger equation

$$\frac{-\hbar^2}{2m}\frac{d^2\psi(x)}{dx^2} = E\psi(x) \tag{8.6.1}$$

There are no boundary conditions in this case since the x-axis closes upon itself. A more appropriate independent variable for this problem is the angular position on the ring given by, $\phi = x/R$. The Schrödinger equation would then read

$$-\frac{\hbar^2}{2mR^2}\frac{d^2\psi(\phi)}{d(\phi)^2} = E\psi(\phi) \tag{8.6.2}$$

8.6.2: Solving for the wavefunctions (eigenfunctions)

The kinetic energy of a body rotating in the xy-plane can be expressed as

$$E = \frac{J_z^2}{2I} \tag{8.6.3}$$

where $I = mR^2$ is the moment of inertia and J_z, the *z*-component of angular momentum. (Since $J = r \times p$, if $\boldsymbol{r}$ and $\boldsymbol{p}$ lie in the *xy*-plane, $\boldsymbol{J}$ points in the *z*-direction. The Schrödinger Equation (8.6.2\ can now be rewritten as:

$$-\frac{\hbar^2}{2I}\frac{d^2\psi(\phi)}{d(\phi)^2} = \frac{J_z^2}{2I}\psi(\phi) \tag{8.6.4}$$

or

$$-\frac{d^2\psi(\phi)}{d(\phi)^2} = \frac{J_z^2}{\hbar^2}\psi(\phi) \tag{8.6.5}$$

This is usually simplified further by setting the ratio $\frac{J_z^2}{\hbar^2} = m_l^2$. Yielding

$$-\frac{d^2\psi(\phi)}{d(\phi)^2} = m_l^2\psi(\phi) \tag{8.6.6}$$

Do not confuse the variable m_l with the mass of the particle!

By remembering that the derivative of e^{ax} is ae^{ax} and the derivative of that would give us a^2e^{ax} we can realize that the wavefunctions (ψ) that satisfy equation 8.6.6 are of the form:

$$\psi(\phi) = \text{const}\, e^{\pm im\phi} \tag{8.6.7}$$

For this wavefunction to be physically acceptable, it must be *single-valued*. Since ϕ increased by any multiple of 2π represents the same point on the ring, we must have

$$\psi(\phi + 2\pi) = \psi(\phi) \tag{8.6.8}$$

and therefore

$$e^{im_l(\phi+2\pi)} = e^{im_l\phi} \tag{8.6.9}$$

This requires that

$$e^{2\pi i m_l} = 1$$

which is true only if m_l is an integer:

$$m_l = 0, \pm 1, \pm 2... \tag{8.6.10}$$

Rearranging the definition of m_l^2 gives us $J_z^2 = \hbar^2 m_l^2$, which can be substituted into equation 8.6.3, giving the quantized energy values

$$E_{m_l} = \frac{\hbar^2}{2I} m_l^2 = \frac{\hbar^2}{2mR^2} m_l^2 \tag{8.6.11}$$

In contrast to the particle in a box, the eigenfunctions corresponding to $+m_l$ and $-m_l$ (Equation 8.6.7) are *linearly independent*, so both must be accepted. Therefore all eigenvalues, except E_0, are two-fold (or doubly) degenerate. The eigenfunctions can all be written in the form const $e^{im_l\phi}$, with m_l allowed to take either **positive and negative** values (or 0), as in equation 8.6.10. The normalized eigenfunctions are

$$\psi_{m_l}(\phi) = \frac{1}{\sqrt{2\pi}} e^{\pm i m_l \phi} \tag{8.6.12}$$

and can be verified to satisfy the normalization condition containing the complex conjugate

$$\int_0^{2\pi} \psi^*_{m_l}(\phi)\psi_{m_l}(\phi)d\phi = 1$$

where we have noted that $\psi^*_{m_l}(\phi) = (2\pi)^{-1/2} e^{-im_l\phi}$. The mutual orthogonality of the functions also follows easily, for

$$\int_0^{2\pi} \psi^*_{m'} \psi_{m_l}(\phi)d\phi = \frac{1}{2\pi}\int_0^{2\pi} e^{i(m_l - m'_l)\phi} d\phi \tag{8.6.13}$$

$$= \frac{1}{2\pi}\int_0^{2\pi} [\cos(m_l - m'_l)\phi + i\sin(m_l - m'_l)\phi]d\phi = 0 \tag{8.6.14}$$

for $m'_l \neq m_l$.

This is a instance of a fundamental result in quantum mechanics, that any measured component of angular momentum is restricted to integral multiples of $\hbar$. The Bohr theory of the hydrogen atom can be derived from this principle alone.

Example 8.6.1: Free Electron Model for Aromatic Molecules

The benzene molecule consists of a ring of six carbon atoms around which six delocalized *pi*-electrons can circulate. A variant of the FEM for rings predicts the ground-state electron configuration which we can write as $1\pi^2 2\pi^4$, as shown here:

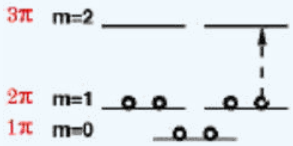


Figure 8.6.1: Free electron model for benzene. Dotted arrow shows the lowest-energy excitation.

The enhanced stability the benzene molecule can be attributed to the complete shells of π-electron orbitals, analogous to the way that noble gas electron configurations achieve their stability. Naphthalene, apart from the central C-C bond, can be modeled as a ring containing 10 electrons in the next closed-shell configuration$1\pi^2 2\pi^4 3\pi^4$. These molecules fulfill Hückel's "4*N*+2 rule" for aromatic stability. The molecules cyclobutadiene $(1\pi^2 2\pi^2)$ and cyclooctatetraene$(1\pi^2 2\pi^4 3\pi^2)$, even though they consist of rings with alternating single and double bonds, do *not* exhibit aromatic stability since they contain partially-filled orbitals.

The longest wavelength absorption in the benzene spectrum can be estimated according to this model as

$$\frac{hc}{\lambda} = E_2 - E_1 = \frac{\hbar^2}{2mR^2}(2^2 - 1^2)$$

The ring radius R can be approximated by the C-C distance in benzene, 1.39 Å. We predict $\lambda \approx$ 210 nm, whereas the experimental absorption has $\lambda_{max} \approx$ 268 nm.

8.6.3: Understanding the quantization in terms of wavelengths[1]

de Bröglie used essentially the following argument to explain why Bohr's model of electrons orbiting a nucleus yield quantized values. We will use this argument to arrive at the quantization and energies of a particle-on-a-ring without formally solving Schrödinger's equations. We, again, start with the energy of a particle of a mass m rotating at a fixed speed at distance R around the origin. In terms of angular momentum about the z axis (J_z) the energy can be expressed as:

$$E = \frac{J_z^2}{2mR^2} = \frac{J_z^2}{2I} \tag{8.6.15}$$

- J_z is the angular momentum in z-axis and
- mR^2 is the particle's moment of inertia I on the z-axis.

We then use the de Broglie equation ($\lambda = \frac{h}{p} \implies p = \frac{h}{\lambda}$) to quantize the energy of rotation. This is done by expressing the angular momentum in wavelengths. Because the rotation is in the xy-plane, J_z = pR, where p is the linear momentum in the deBroglie equation:

$$J_z = pR = \frac{hR}{\lambda} \tag{8.6.16}$$

Because the particle must exist on the line its wavelength must be an integer multiple of the circumference, otherwise it would destructively interfere with itself as the phase of the wave shifts on each circuit around the ring. This is equivalent to the requirement to be single valued expressed in equations 8.6.8 and 8.6.9. Figure 8.6.2 illustrates this where the circumference has been unwrapped to form a line.

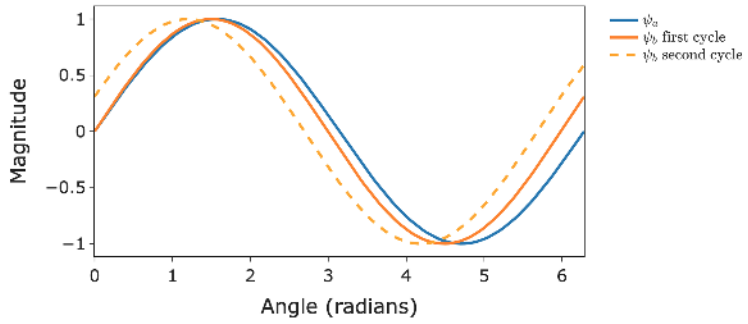


Figure 8.6.2: Two waves on a ring that has been unwrapped to a line for clarity at the angle $\phi = 0 = 2\pi$. One that has a wavelength equal to the circumference so that it creates a standing wave on the ring (ψ_a) and one that has a wavelength that is not an integer fraction of the circumference so shifts on each circuit around the ring and destructively interferes with itself (ψ_b).

Thus the only allowed wavelengths (those that create standing waves) are:

$$\lambda = \frac{2\pi R}{m_l}$$

where m_l is an integer. This can be substituted into equation 8.6.16 to yield:

$$J_z = pR = \frac{m_l h}{2\pi}$$

when this is substituted int equation 8.6.15 for J_z, we get:

$$E = \frac{m_l^2 h^2}{8\pi^2 I} = \frac{\hbar^2}{2I} m_l^2 \tag{8.6.17}$$

This is the same result as in equation 8.6.11.

8.6.4: References

1. Atkins, Peter, and Julio de Paula. Physical Chemistry for the Life Sciences. New York. Oxford University Press. 2006, p 358.

This page titled 8.6: Particle on a Ring is shared under a CC BY-NC-SA 4.0 license and was authored, remixed, and/or curated by Jonathan Gutow.

- **Particle on a Ring** by Seymour Blinder, Stephanie Montenegro is licensed CC BY-NC-SA 4.0.

8.7: The Schrödinger Wave Equation for the Hydrogen Atom

8.7.1: Introduction (Schrödinger equation for 1 e- system)

The hydrogen atom, consisting of an electron and a proton, is a two-particle system, and the internal motion of two particles around their center of mass is equivalent to the motion of a single particle with a reduced mass ($m = \frac{m_1 m_2}{m_1+m_2}$). This reduced particle is located at $\vec{r}$, where $\vec{r}$ is the vector specifying the position of the electron relative to the position of the proton. The length r of $\vec{r}$ is the distance between the proton and the electron, and the direction of r is given by the orientation of the vector pointing from the proton to the electron. Since the proton is much more massive than the electron, we will assume that the reduced mass equals the electron mass and the proton is located at the center of mass.

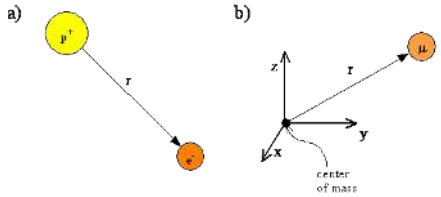


Figure 8.7.1: a) The proton (p^+) and electron (e^-) of the hydrogen atom. b) Equivalent reduced particle with reduced mass μ at distance r from center of mass.

Starting with the general Schrödinger equation:

$$\frac{-\hbar^2}{2m}\nabla^2\Psi(\vec{r}) + V(\vec{r})\Psi(\vec{r}) = E\Psi(\vec{r}) \tag{8.7.1}$$

we need an expression for the potential. This is just Coulomb attraction and depends only on the separation distance r:

$$V(r) = -\frac{e^2}{4\pi\epsilon_0 r} \tag{8.7.2}$$

where r is the distance between the electron and the proton. The Coulomb potential energy depends inversely on the distance between the electron and the nucleus and does not depend on any angles. Such a potential is called a central potential. Substituting in to equation 8.7.1 this gives us:

$$\frac{-\hbar^2}{2m}\nabla^2\Psi(\vec{r}) + \frac{e^2}{4\pi\epsilon_0 r}\Psi(\vec{r}) = E\Psi(\vec{r}) \tag{8.7.3}$$

Because of the spherical symmetry of the equation it turns out to be better to switch from Cartesian coordinates x, y, z to spherical coordinates in terms of a radius r, as well as angles ϕ, which is measured from the positive x axis in the xy plane and may be between 0 and 2π, and θ, which is measured from the positive z axis towards the xy plane and may be between 0 and π.

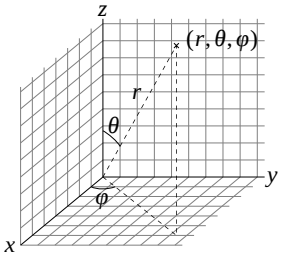


Figure 8.7.2: Spherical Coordinates

This generates a much more complicated, but easier to solve equation:

$$\left\{-\frac{\hbar^2}{2\mu r^2}\left[\frac{\partial}{\partial r}\left(r^2\frac{\partial}{\partial r}\right) + \frac{1}{\sin\theta}\frac{\partial}{\partial\theta}\left(\sin\theta\frac{\partial}{\partial\theta}\right) + \frac{1}{\sin^2\theta}\frac{\partial^2}{\partial\varphi^2}\right] - \frac{e^2}{4\pi\epsilon_0 r}\right\}\psi(r,\theta,\varphi) = E\psi(r,\theta,\varphi) \tag{8.7.4}$$

The second two terms in the square brackets of this equation only depend on the angles. This lead people to try separating the equation into two parts, one that depends on the angles (θ and φ) and one that depends on the distance (r). This does work, just as the wavefunction for a particle in a multidimensional box can be represented as the product of wavefunctions that depend on each coordinate separately.

8.7.2: Solutions

The solutions to this equation take the form of products of two functions as shown in equation 8.7.5.

$$\psi_{nlm_l}(r,\theta,\varphi) = R_n(r)Y_{lm}(\theta,\varphi) \tag{8.7.5}$$

The $Y_{lm_l}(\theta,\varphi)$ are a the Spherical Harmonic functions (Table M4), which were well known before quantum mechanics was developed. The Spherical Harmonic functions provide information about the angular probability distribution of the electron around the proton, and the radial function $R_n(r)$ describes how far the electron is away from the proton.

The state of the electron is specified by the three quantum numbes n, l, and m_l. For this case of a single electron atom the energy E_n depends only on n, although the other quantum numbers are required for the full description of the wavefunction:

$$E_n = -\frac{m_e e^4}{8\epsilon_0^2 h^2 n^2} \tag{8.7.6}$$

with $n = 1, 2, 3 \ldots \infty$.

It is found that the possible values of l are constrained by n and the possible values of m_l are constrained by l. We will see when we consider multi-electron atoms that these constraints explain the features of the Periodic Table. In other words, the Periodic Table is a manifestation of the Schrödinger model and the physical constraints imposed to obtain the solutions to the Schrödinger equation for the hydrogen atom.

8.7.3: The Three Quantum Numbers

Schrödinger's approach requires three quantum numbers (n, l, and m_l) to specify a wavefunction for the electron. The quantum numbers provide information about the spatial distribution of an electron. Although n can be any positive integer (NOT zero), only certain values of l and m_l are allowed for a given value of n.

The principal quantum number (n): This quantum number indicates the energy of the electron (equation 8.7.6) and the average distance of an electron from the nucleus. n is restricted to the positive integers:

$$n = 1,\ 2,\ 3,\ 4,\ \ldots \tag{8.7.7}$$

As n increases for a given atom, so does the average distance of an electron from the nucleus. A negatively charged electron that is, on average, closer to the positively charged nucleus is attracted to the nucleus more strongly than an electron that is farther out in space. This means that electrons with higher values of n are easier to remove from an atom. All wave functions that have the same value of n are said to constitute a principal ***shell***, because those electrons have similar average distances from the nucleus. The principal quantum number n corresponds to the n used by Bohr to describe electron orbits and by Rydberg to describe atomic energy levels.

The Azimuthal Quantum Number (l): This quantum number indicates the shape of the region of space occupied by an electron and the electrons total orbital angular momentum. The allowed values of l are integers that depend on the value of n and can range from 0 to n − 1:

$$l = 0,\ 1, . , 2,\ 3,\ .\ .\ (n-1) \tag{8.7.8}$$

For example, if n = 1, l can be only 0; if n = 2, l can be 0 or 1; and so forth. For a given atom, all wave functions that have the same values of both n and l form a ***subshell***. The regions of space occupied by electrons in the same subshell usually have the same shape, but they are oriented differently in space.

The total angular momentum of the electron has the value:

$$J = \sqrt{l(l+1)}\hbar \tag{8.7.9}$$

Thus the angular momentum of the electron is quantized.

The Magnetic Quantum Number (m_l): This quantum number indicates the orientation of the region of space occupied by an electron with respect to an applied magnetic field. The allowed integer values of m_l depend on the value of l and can range from $-l$ to l:

$$m = -l,\ -l+1,\ .\ .\ .0,\ \ .\ .\ .l-1, l \tag{8.7.10}$$

For example, if $l = 0$, m_l can be only 0; if l = 1, m_l can be −1, 0, or +1; and if l = 2, m_l can be −2, −1, 0, +1, or +2.

Each wave function with an allowed combination of n, l, and m_l values describes an ***atomic orbital***, a particular spatial distribution for an electron. For a given set of quantum numbers, each principal shell has a fixed number of subshells, and each subshell has a fixed number of orbitals.

Because the electron is charged and has an angular momentum it can interact with a magnetic field. If the direction of the magnetic field is taken to be along the z-axis then the component (projection) of the angular momentum along the z-axis is:

$$J_z = m_l\hbar \tag{8.7.11}$$

This is the same quantization of J_z as seen for the particle on a ring.

Example 8.7.1: Number of subshells

How many subshells and orbitals are contained within the principal shell with n = 4?

Strategy

- Given: value of n
- Asked for: number of subshells and orbitals in the principal shell

Step 1: Given n = 4, calculate the allowed values of l. From these allowed values, count the number of subshells.

Step 2: For each allowed value of l, calculate the allowed values of m_l. The sum of the number of orbitals in each subshell is the number of orbitals in the principal shell.

Solution

Step 1: We know that l can have all integral values from 0 to n − 1. If n = 4, then l can equal 0, 1, 2, or 3. Because the shell has four values of l, it has four subshells, each of which will contain a different number of orbitals, depending on the allowed values of ml.

Step 2: For l = 0, ml can be only 0, and thus the l = 0 subshell has only one orbital. For l = 1, m_l can be 0 or ±1; thus the l = 1 subshell has three orbitals. For l = 2, ml can be 0, ±1, or ±2, so there are five orbitals in the l = 2 subshell. The last allowed value of l is l = 3, for which ml can be 0, ±1, ±2, or ±3, resulting in seven orbitals in the l = 3 subshell. The total number of orbitals in the n = 4 principal shell is the sum of the number of orbitals in each subshell and is equal to n_2:

$$\underset{(l=0)}{1} + \underset{(l=1)}{3} + \underset{(l=2)}{5} + \underset{(l=3)}{7} = 16 \text{ orbitals} = (4 \text{ principal shells})^2$$

Exercise 8.7.1

How many subshells and orbitals are in the principal shell with $n = 3$?

Answer: three subshells; nine orbitals

Rather than specifying all the values of n and l every time we refer to a subshell or an orbital, chemists use an abbreviated system with lowercase letters to denote the value of l for a particular subshell or orbital:

l	0	1	2	3
Designation	*s*	*p*	*d*	*f*

The principal quantum number is named first, followed by the letter *s*, *p*, *d*, or *f* as appropriate. These orbital designations are derived from corresponding spectroscopic characteristics of lines involving them: sharp, *p*rinciple, *d*iffuse, and *f*undamental. A 1*s* orbital has $n = 1$ and $l = 0$; a 2*p* subshell has $n = 2$ and $l = 1$ (and has three 2*p* orbitals, corresponding to $m_l = −1$, 0, and +1); a 3*d* subshell has $n = 3$ and $l = 2$ (and has five 3*d* orbitals, corresponding to $m_l = −2$, −1, 0, +1, and +2); and so forth.

We can summarize the relationships between the quantum numbers and the number of subshells and orbitals as follows (Table 8.7.1):

- Each principal shell has n subshells. For $n = 1$, only a single subshell is possible (1*s*); for $n = 2$, there are two subshells (2*s* and 2*p*); for $n = 3$, there are three subshells (3*s*, 3*p*, and 3*d*); and so forth. Every shell has an *ns* subshell, any shell with $n \geq 2$ also has an *np* subshell, and any shell with $n \geq 3$ also has an *nd* subshell. Because a 2*d* subshell would require both $n = 2$ and $l = 2$, which is not an allowed value of l for $n = 2$, a 2*d* subshell does not exist.
- Each subshell has $2l + 1$ orbitals. This means that all *ns* subshells contain a single *s* orbital, all *np* subshells contain three *p* orbitals, all *nd* subshells contain five *d* orbitals, and all *nf* subshells contain seven *f* orbitals.

Note

Each principal shell has n subshells, and each subshell has $2l + 1$ orbitals.

Table 8.7.1: Allowed values of n, l, and m_l through n = 4

n	l	Subshell Designation	m_l	Number of Orbitals in Subshell	Number of Orbitals in Shell
1	0	1*s*	0	1	1
2	0	2*s*	0	1	4
	1	2*p*	−1, 0, 1	3	
3	0	3*s*	0	1	9
	1	3*p*	−1, 0, 1	3	
	2	3*d*	−2, −1, 0, 1, 2	5	
4	0	4*s*	0	1	16
	1	4*p*	−1, 0, 1	3	
	2	4*d*	−2, −1, 0, 1, 2	5	
	3	4*f*	−3, −2, −1, 0, 1, 2, 3	7	

8.7.4: The Radial Component

The first six radial functions are provided in Table 8.7.2. Note that the functions in the table exhibit a dependence on Z, the atomic number of the nucleus. Other one electron systems have electronic states analogous to those for the hydrogen atom, and inclusion of the charge on the nucleus allows the same wavefunctions to be used for all one-electron systems. For hydrogen, $Z = 1$ and for helium, $Z = 2$.

Table 8.7.2: Hydrogen-like atomic wavefunctions for n values $1, 2, 3$: Z is the atomic number of the nucleus, and $\rho = \frac{Zr}{a_0}$, where a_0 is the Bohr radius and r is the radial variable.

n	l	m_l	Radial Component
1	0	0	$\psi_{100} = \frac{1}{\sqrt{\pi}}\left(\frac{Z}{a_0}\right)^{\frac{3}{2}} e^{-\rho}$
2	0	0	$\psi_{200} = \frac{1}{\sqrt{32\pi}}\left(\frac{Z}{a_0}\right)^{\frac{3}{2}} (2-\rho)e^{\frac{-\rho}{2}}$
2	1	0	$\psi_{210} = \frac{1}{\sqrt{32\pi}}\left(\frac{Z}{a_0}\right)^{\frac{3}{2}} \rho e^{-\rho/2}\cos(\theta)$
2	1	± 1	$\psi_{21\pm 1} = \frac{1}{\sqrt{64\pi}}\left(\frac{Z}{a_0}\right)^{\frac{3}{2}} \rho e^{-\rho/2}\sin(\theta)$
3	0	0	$\psi_{300} = \frac{1}{81\sqrt{3\pi}}\left(\frac{Z}{a_0}\right)^{\frac{3}{2}} (27-18\rho+2$
3	1	0	$\psi_{310} = \frac{1}{81}\sqrt{\frac{2}{\pi}}\left(\frac{Z}{a_0}\right)^{\frac{3}{2}} (6r-\rho^2)e^{-\rho/}$
3	1	± 1	$\psi_{31\pm 1} = \frac{1}{81\sqrt{\pi}}\left(\frac{Z}{a_0}\right)^{\frac{3}{2}} (6\rho-\rho^2)e^{-r/}$
3	2	0	$\psi_{320} = \frac{1}{81\sqrt{6\pi}}\left(\frac{Z}{a_0}\right)^{\frac{3}{2}} \rho^2 e^{-\rho/3}(3cos^2$
3	2	± 1	$\psi_{32\pm 1} = \frac{1}{81\sqrt{\pi}}\left(\frac{Z}{a_0}\right)^{\frac{3}{2}} \rho^2 e^{-\rho/3}\sin(\theta$
3	2	± 2	$\psi_{32\pm 2} = \frac{1}{162\sqrt{\pi}}\left(\frac{Z}{a_0}\right)^{\frac{3}{2}} \rho^2 e^{-\rho/3}\sin^2($

Visualizing the variation of an electronic wavefunction with r, θ, and ϕ is important because the absolute square of the wavefunction depicts the charge distribution (electron probability density) in an atom or molecule. The charge distribution is central to chemistry because it is related to chemical reactivity. For example, an electron deficient part of one molecule is attracted to an electron rich region of another molecule, and such interactions play a major role in chemical interactions ranging from substitution and addition reactions to protein folding and the interaction of substrates with enzymes.

Plots of the radial functions, R(r), for the 1s, 2s, and 2p orbitals plotted in figure 8.7.2 (left). The quantity $R(r)^* R(r)$ gives the radial probability density; i.e., the probability density for the electron to be at a point located the distance r from the proton. Radial probability densities for three types of atomic orbitals are plotted in figure 8.7.2 (middle). The probability of finding an electron at a particular distance from the nucleus is the integral of $R(r)^* R(r)$ over the surface of the sphere of radius r, $P(r) = 4\pi r^2 R(r)^* R(r)$, which is plotted in figure 8.7.2 (right).

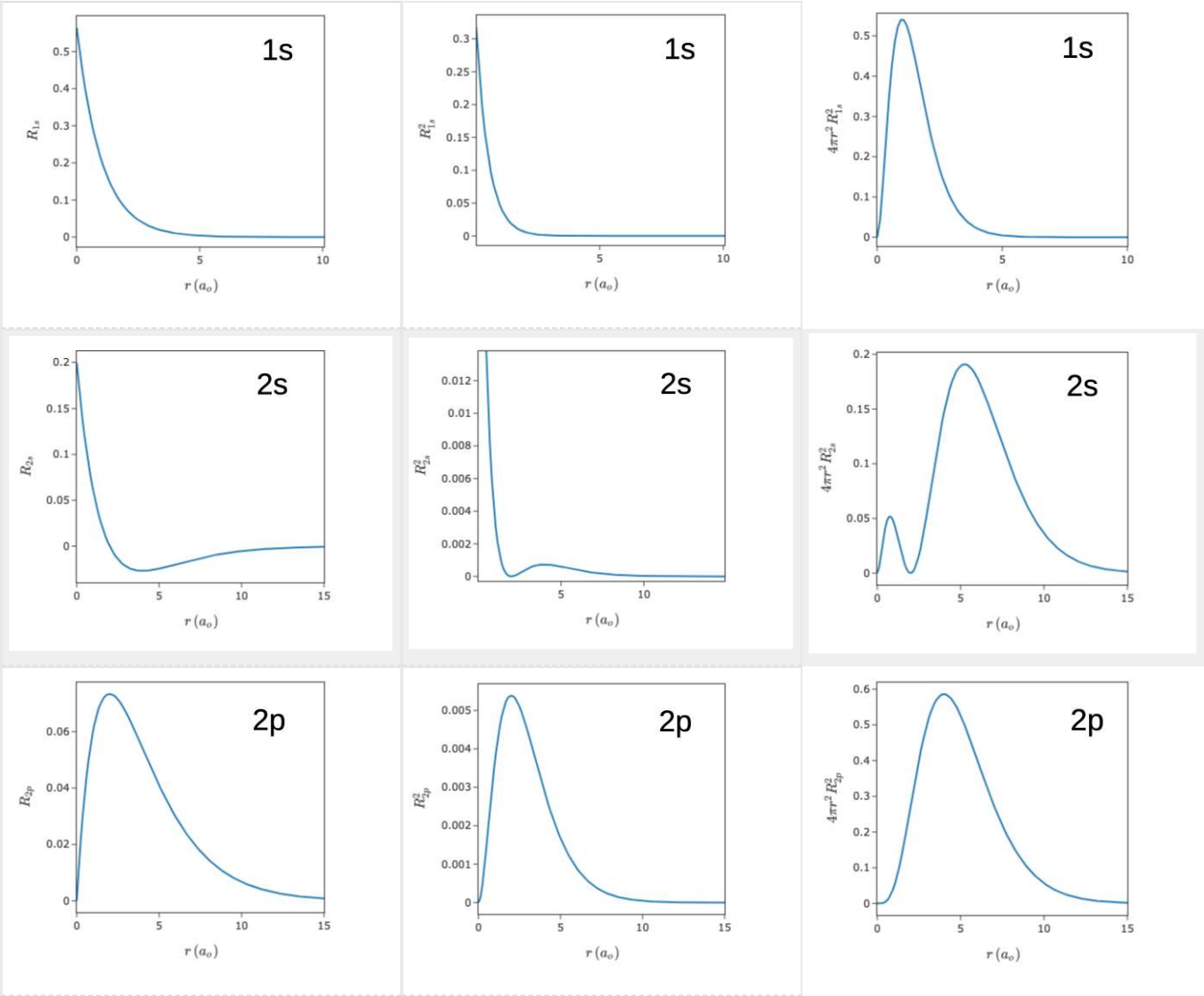


Figure 8.7.2: (left) **Radial function**, R(r), for the 1s, 2s, and 2p orbitals. (middle) **Radial probability densities** for the 1s, 2s, and 2p orbitals.(right) **Radial distribution functions** for the 1s, 2s, and 2p orbitals. Units on the x-axis are Bohrs = 0.529 Å = a_o.

For the hydrogen atom, the peak in the radial probability plot (right colum in figure 8.7.2) occurs at r = 0.529 Å (52.9 pm), which is exactly the radius calculated by Bohr for the n = 1 orbit. Thus the *most probable radius* obtained from quantum mechanics is identical to the radius calculated by classical mechanics. In Bohr's model, however, the electron was assumed to be at this distance 100% of the time, whereas in the Schrödinger model, it is at this distance only some of the time. The difference between the two models is attributable to the wavelike behavior of the electron and the Heisenberg uncertainty principle.

> Notice that because the surface area of a sphere with radius of zero is zero, **there is no probability of finding the electron at the nucleus** (r = 0). See the right hand column in figure 8.7.2. This quantum prediction can be thought of as an explanation for why atoms do not collapse into a single uncharged particle.

Figure 8.7.3 compares the electron probability densities for the hydrogen 1*s*, 2*s*, and 3*s* orbitals in 3-D. Note that all three are spherically symmetrical. For the 2*s* and 3*s* orbitals, however (and for all other *s* orbitals as well), the electron probability density does not fall off smoothly with increasing *r*. Instead, a series of minima and maxima are observed in the radial probability plots (part (c) in Figure 8.7.3). The minima correspond to spherical nodes (regions of zero electron probability), which alternate with spherical regions of nonzero electron probability.

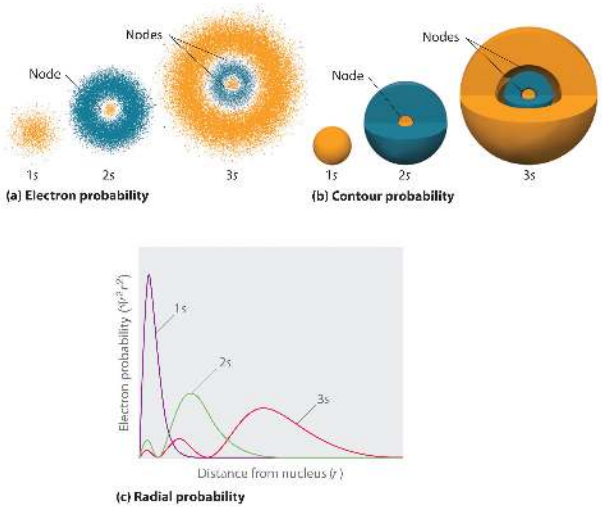


Figure 8.7.3: Probability Densities for the 1 s, 2 s, and 3*s* Orbitals of the Hydrogen Atom. (a) The electron probability density in any plane that contains the nucleus is shown. Note the presence of circular regions, or nodes, where the probability density is zero. (b) Contour surfaces enclose 90% of the electron probability, which illustrates the different sizes of the 1*s*, 2*s*, and 3*s* orbitals. The cutaway drawings give partial views of the internal spherical nodes. The orange color corresponds to regions of space where the phase of the wave function is positive, and the blue color corresponds to regions of space where the phase of the wave function is negative. (c) In these plots of electron probability as a function of distance from the nucleus (*r*) in all directions (radial probability), the most probable radius increases as*n* increases, but the 2*s* and 3*s* orbitals have regions of significant electron probability at small values of *r*.

8.7.5: The Angular Component

The angular component of the wavefunction $Y_{lm_l}(\theta,\phi)$ in Equation 8.7.5 does much to give an orbital its distinctive shape. Y is typically normalized so the the integral of Y^2 over the unit sphere is equal to one. In this case, Y^2 serves as a probability function. The probability function can be interpreted as the probability that the electron will be found on the ray emitting from the origin that is at angles (θ,ϕ) from the axes. The probability function can also be interpreted as the probability distribution of the electron being at position (θ,ϕ) on a sphere of radius *r*, given that it is *r* distance from the nucleus. $Y_{l,m_l}(\theta,\phi)$ are also the wavefunction solutions to Schrödinger's equation for a rigid rotor consisting of rotating bodies, for example a diatomic molecule. These are called Spherical Harmonic functions (Table M4).

8.7.5.1: s Orbitals (l=0)

Three things happen to *s* orbitals as *n* increases (figure 8.7.3):

1. They become larger, extending farther from the nucleus.
2. They contain more nodes. This is similar to a standing wave that has regions of significant amplitude separated by nodes, points with zero amplitude.
3. For a given atom, the *s* orbitals also become higher in energy as *n* increases because of their increased distance from the nucleus.

Orbitals are generally drawn as three-dimensional surfaces that enclose 90% of the electron density. Although such drawings show the relative sizes of the orbitals, they do not normally show the spherical nodes in the 2*s* and 3*s* orbitals because the spherical nodes lie inside the 90% surface. Fortunately, the positions of the spherical nodes are not important for chemical bonding.

8.7.5.2: p Orbitals (l=1)

Only *s* orbitals are spherically symmetrical. As the value of *l* increases, the number of orbitals in a given subshell increases, and the shapes of the orbitals become more complex. Because the 2*p* subshell has $l = 1$, with three values of m_l (−1, 0, and +1), there are three 2*p* orbitals).

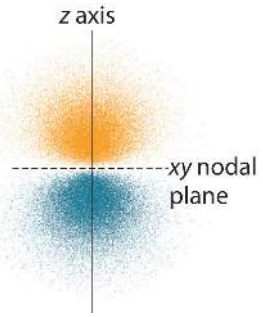


Figure 8.7.4: Illustration of a slice through a p_z orbital, where the dot density indicates the relative probability of finding the electron. The colors correspond to regions of space where the phase of the wave function is positive (orange) and negative (blue).

The electron probability distribution for one of the hydrogen 2*p* orbitals is shown in Figure 8.7.4. Because this orbital has two lobes of electron density arranged along the *z* axis, with an electron density of zero in the *xy* plane (i.e., the *xy* plane is a nodal plane), it is a $2p_z$ orbital. As shown in Figure 8.7.5, the other two 2*p* orbitals have identical shapes, but they lie along the *x* axis ($2p_x$) and *y* axis ($2p_y$), respectively. Note that each *p* orbital has just one nodal plane. In each case, the phase of the wave function for each of the 2*p* orbitals is positive for the lobe that points along the positive axis and negative for the lobe that points along the negative axis. It is important to emphasize that these signs correspond to the *phase* of the wave that describes the electron motion, *not* to positive or negative charges.

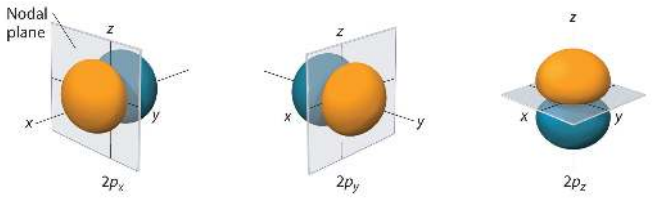


Figure 8.7.5: The Three Equivalent 2 p Orbitals of the Hydrogen Atom. The surfaces shown enclose 90% of the total electron probability for the $2p_x$, $2p_y$, and $2p_z$ orbitals. Each orbital is oriented along the axis indicated by the subscript and a nodal plane that is perpendicular to that axis bisects each 2*p* orbital. The phase of the wave function is positive (orange) in the region of space where *x*, *y*, or *z* is positive and negative (blue) where *x*, *y*, or *z* is negative.

Just as with the *s* orbitals, the size and complexity of the *p* orbitals for any atom increase as the principal quantum number *n* increases. The shapes of the 90% probability surfaces of the 3*p*, 4*p*, and higher-energy *p* orbitals are, however, essentially the same as those shown in figure 8.7.5, but with additional radial nodes.

Note: Orbitals specified by m_l are not the same as those usually labeled p_x, p_y or p_z

The p_x, p_y and p_z orbitals are **not the solutions to the Schrödinger equation associated with m_l = -1, 0 and 1**. They are valid wavefunctions built from linear combinations of the m_l = -1, 0, 1 wavefunctions in order to get real valued functions. See the table of Spherical Harmonics and Real Valued Spherical Harmonics.

8.7.5.3: d Orbitals (l=2)

Subshells with $l = 2$ have five *d* orbitals; the first principal shell to have a *d* subshell corresponds to $n = 3$. The five *d* orbitals have m_l values of −2, −1, 0, +1, and +2. The surfaces enclosing the 90% probability of finding the electron for the five real-valued linear combinations of the complex orbitals specified by m_l are shown in figure 8.7.6.

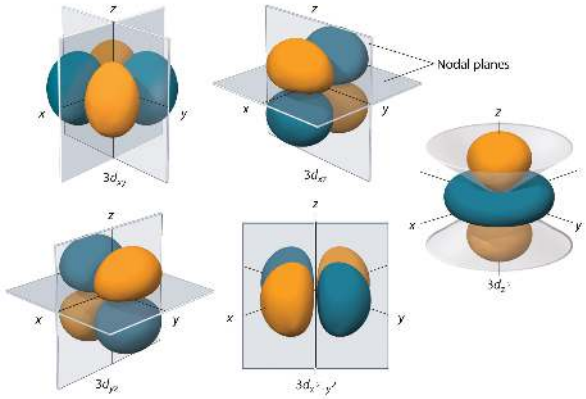


Figure 8.7.6: The five equivalent 3d orbitals of the hydrogen atom. The surfaces shown enclose 90% of the total electron probability for the five hydrogen 3d orbitals. Four of the five 3d orbitals consist of four lobes arranged in a plane that is intersected by two perpendicular nodal planes. These four orbitals have the same shape but different orientations. The fifth 3d orbital, $3d_{z^2}$, has a distinct shape even though it is mathematically equivalent to the others. The phase of the wave function for the different lobes is indicated by color: orange for positive and blue for negative.

The hydrogen 3d orbitals have more complex shapes than the 2p orbitals. All five 3d orbitals contain two nodal surfaces, as compared to one for each p orbital and zero for each s orbital. In three of the d orbitals, the lobes of electron density are oriented between the x and y, x and z, and y and z planes; these orbitals are referred to as the $3d_{xy}$, $3d_{xz}$, and $3d_{yz}$ orbitals, respectively. A fourth d orbital has lobes lying along the x and y axes; this is the $3d_{x_2-y_2}$ orbital. The fifth 3d orbital, called the $3d_{z^2}$ orbital, has a unique shape: it looks like a $2p_z$ orbital combined with an additional doughnut of electron probability lying in the xy plane. Despite its peculiar shape, the $3d_{z^2}$ orbital is mathematically equivalent to the other four and has the same energy. In contrast to p orbitals, the phase of the wave function for d orbitals is the same for opposite pairs of lobes. As shown in Figure 8.7.6, the phase of the wave function is positive for the two lobes of the dz^2 orbital that lie along the z axis, whereas the phase of the wave function is negative for the doughnut of electron density in the xy plane. Like the s and p orbitals, as n increases, the size of the d orbitals increases, but the overall shapes remain similar to those depicted in figure 8.7.6.

8.7.5.4: f Orbitals (l=3)

Principal shells with n = 4 can have subshells with l = 3 and m_l values of −3, −2, −1, 0, +1, +2, and +3. These subshells consist of seven *f* orbitals. Each *f* orbital has three nodal surfaces, so their shapes are complex (not shown).

8.7.6: Energies

As noted previously, the energy for a single electron atom depend only on n, the principle quantum number. The solutions reproduce the same quantized expression for hydrogen atom energy levels that was obtained from the Bohr model of the hydrogen atom.

$$E = -\frac{Z^2}{n^2} Rhc \tag{8.7.12}$$

or

$$E_n = -\frac{Z^2 \mu e^4}{8\epsilon_0^2 h^2 n^2} \tag{8.7.13}$$

The relative energies of the atomic orbitals with $n \leq 4$ for a hydrogen atom are plotted in Figure 8.7.7; note that the orbital energies depend on *only* the principal quantum number n and are all less than zero, indicating attraction to the nucleus. Consequently, the energies of the 2*s* and 2*p* orbitals of hydrogen are the same; the energies of the 3*s*, 3*p*, and 3*d* orbitals are the same; and so forth. The orbital energies obtained for hydrogen using quantum mechanics are exactly the same as the allowed energies calculated by Bohr. In contrast to Bohr's model, however, which allowed only one orbit for each energy level, quantum mechanics predicts that there are *4* orbitals with different electron density distributions in the n = 2 principal shell (one 2*s* and three 2*p* orbitals), *9* in the n = 3 principal shell, and *16* in the n = 4 principal shell.

> For a single electron atom, the energy of that electron is a function of only the principal quantum number (Equation 8.7.12).

The different values of l and m_l for the individual orbitals within a given principal shell are not important for understanding the emission or absorption spectra of the hydrogen atom under most conditions, but they do explain the splittings of the main lines that are observed when hydrogen atoms are placed in a magnetic field. As we have just seen, however, quantum mechanics also predicts that in the hydrogen atom, all orbitals with the same value of n (e.g., the three 2*p* orbitals) are degenerate, meaning that they have the same energy. Figure 8.7.7 shows that the energy levels become closer and closer together as the value of n increases, as expected because of the $1/n^2$ dependence of orbital energies.

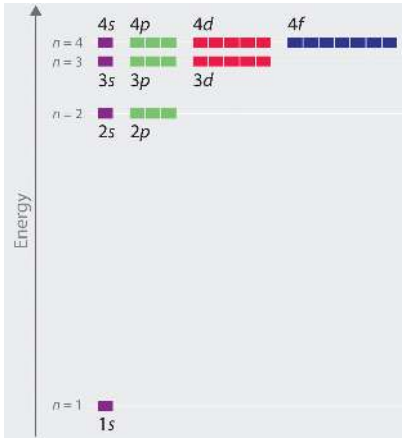


Figure 8.7.7: Orbital energy level diagram for the hydrogen atom. Each box corresponds to one orbital. Note that the difference in energy between orbitals decreases rapidly with increasing values of n.

In general, both energy and radius decrease as the nuclear charge increases. Thus the most stable orbitals (those with the lowest energy) are those closest to the nucleus. For example, in the ground state of the hydrogen atom, the single electron is in the 1s orbital, whereas in the first excited state, the atom has absorbed energy and the electron has been promoted to one of the n = 2 orbitals. In ions with only a single electron, the energy of a given orbital depends on only n, and all subshells within a principal shell, such as the p_x, p_y, and p_z orbitals, are degenerate.

Note: Bohr vs. Schrödinger

It is interesting to compare the results obtained by solving the Schrödinger equation with Bohr's model of the hydrogen atom. There are several ways in which the Schrödinger model and Bohr model differ.

1. First, and perhaps most strikingly, the Schrödinger model does not produce well-defined orbits for the electron. The wavefunctions only give us the probability for the electron to be at various directions and distances from the proton.
2. Second, the quantization of angular momentum is different from that proposed by Bohr. Bohr proposed that the angular momentum is quantized in integer units of $\hbar$, while the Schrödinger model leads to an angular momentum of $(l(l+1)\hbar^2)^{\frac{1}{2}}$.

3. Third, the quantum numbers appear naturally during solution of the Schrödinger equation while Bohr had to postulate the existence of quantized energy states. Although more complex, the Schrödinger model leads to a better correspondence between theory and experiment over a range of applications that was not possible for the Bohr model.

8.7.7: Electron Spin: The Fourth Quantum Number

The quantum numbers n, l, m_l are not sufficient to fully characterize the physical state of the electrons in an atom. In 1926, Otto Stern and Walther Gerlach carried out an experiment that could not be explained in terms of the three quantum numbers n, l, m_l and showed that there is, in fact, another quantum-mechanical degree of freedom that needs to be included in the theory. The experiment is illustrated in the Figure 8.7.8. A beam of atoms (e.g. hydrogen or silver atoms) is sent through a spatially inhomogeneous magnetic field with a definite field gradient toward one of the poles. It is observed that the beam splits into two beams as it passes through the field region.

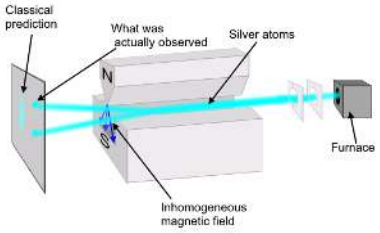


Figure 8.7.8: The Stern-Gerlach apparatus. from Wikipedia

The fact that the beam splits into 2 beams suggests that the electrons in the atoms have a degree of freedom capable of coupling to the magnetic field. That is, an electron has an *intrinsic magnetic moment* M arising from a degree of freedom that has no classical analog. The magnetic moment must take on only 2 values according to the Stern-Gerlach experiment. The intrinsic property that gives rise to the magnetic moment is called *spin*, S; unlike position and momentum, which have clear classical analogs, spin does not. The implication of the Stern-Gerlach experiment is that we need to include a fourth quantum number, m_s in our description of the physical state of the electron. That is, in addition to give its principle, angular, and magnetic quantum numbers, we also need to say if it is a spin-up electron or a spin-down electron.

Note: Spin is a Quantum Phenomenon

Unlike position and momentum, which have clear classical analogs, spin does not. Spin may be thought of as a relativistic phenomenon. Solutions to the relativistic form of the wave equation for an electron (Dirac equation) do require the inclusion of a spin quantum number.[1] This is related to the relativistic effect that leads to the generation of a magnetic field by moving charged particles.[2] For most situations it is not necessary to use the relativistic formulation and spin is just added as an extra quantum number with two values.

George Uhlenbeck (1900–1988) and Samuel Goudsmit (1902–1978), proposed that the splittings were caused by an electron spinning about its axis, much as Earth spins about its axis. When an electrically charged object spins, it produces a magnetic moment parallel to the axis of rotation, making it behave like a magnet. Electrons are not spinning as they are a wave, but they do have a magnetic moment. The name electron spin stuck, despite not being particularly accurate.

The magnetic moment has two possible orientations, described by the fourth quantum number, m_s = +½ (up) and m_s = −½ (down). The subscript *s* is for spin. An electron behaves like a magnet that has one of two possible orientations, aligned either with the magnetic field or against it. The implications of electron spin for chemistry were recognized almost immediately by an Austrian physicist, Wolfgang Pauli (1900–1958; Nobel Prize in Physics, 1945), who determined that each orbital can contain no more than two electrons. This is usually referred to as **the Pauli exclusion principle**.

Pauli Exclusion Principle

No two electrons in an atom can have the same values of all four quantum numbers (n, l, m_l, m_s).

By giving the values of *n*, *l*, and m_l, we specify a particular orbital (e.g., 1*s* with *n* = 1, *l* = 0, m_l = 0). Because m_s has only two possible values (+½ or −½), two electrons, *and only two electrons*, can occupy any given orbital, one with spin up and one with spin down. With this information, we can proceed to construct the entire periodic table, which was originally based on the physical and chemical properties of the known elements.

Example 8.7.2

List all the allowed combinations of the four quantum numbers (n, l, m_l, m_s) for electrons in a 2*p* orbital and predict the maximum number of electrons the 2*p* subshell can accommodate.

Given: orbital

Asked for: allowed quantum numbers and maximum number of electrons in orbital

Strategy:

- Step 1: List the quantum numbers (n, l, m_l) that correspond to an $n = 2p$ orbital. List all allowed combinations of (n, l, m_l).
- Step 2: Build on these combinations to list all the allowed combinations of (n, l, m_l, m_s).
- Step 3: Add together the number of combinations to predict the maximum number of electrons the $2p$ subshell can accommodate.

Solution:

Step 1: For a $2p$ orbital, we know that $n = 2$, $l = n - 1 = 1$, and $m_l = -l$, $(-l + 1)$,…, $(l - 1)$, l. There are only three possible combinations of (n, l, m_l): (2, 1, 1), (2, 1, 0), and (2, 1, −1).

Step 2: Because m_s is independent of the other quantum numbers and can have values of only +½ and −½, there are six possible combinations of (n, l, m_l, m_s): (2, 1, 1, +½), (2, 1, 1, −½), (2, 1, 0, +½), (2, 1, 0, −½), (2, 1, −1, +½), and (2, 1, −1, −½).

Step 3: Hence the $2p$ subshell, which consists of three $2p$ orbitals ($2p_x$, $2p_y$, and $2p_z$), can contain a total of six electrons, two in each orbital.

? Exercise 8.7.2

List all the allowed combinations of the four quantum numbers (n, l, m_l, m_s) for a $6s$ orbital, and predict the total number of electrons it can contain.

Answer: (6, 0, 0, +½), (6, 0, 0, −½); two electrons

8.7.8: References

1. Leonard I. Schiff, *Quantum Mechanics*, 3rd Ed. (McGraw-Hill, New York, 1968) Pp. 480 - 481.
2. Paul Lorain and Dale Corson, *Electromagnetic Fields and Waves*, 2nd Ed. (W. H. Freeman and Co. New York, 1970) Chpt 6.

8.7.9: Contributors and Attributions

- David M. Hanson, Erica Harvey, Robert Sweeney, Theresa Julia Zielinski ("Quantum States of Atoms and Molecules")
- J. Gutow (UW Oshkosh)

This page titled 8.7: The Schrödinger Wave Equation for the Hydrogen Atom is shared under a CC BY-NC-SA 4.0 license and was authored, remixed, and/or curated by Jonathan Gutow.

- **11.10: The Schrödinger Wave Equation for the Hydrogen Atom** by David M. Hanson, Erica Harvey, Robert Sweeney, Theresa Julia Zielinski is licensed CC BY-NC-SA 4.0.

8.8: Many-Electron Atoms and the Periodic Table

8.8.1: Introduction

Quantum mechanics can account for the periodic structure of the elements, by any measure a major conceptual accomplishment for any theory. Although accurate computations become increasingly more challenging as the number of electrons increases, the general patterns of atomic behavior can be predicted with remarkable accuracy.

Figure 8.8.1 shows a schematic representation of a helium atom with two electrons whose coordinates are given by the vectors $\mathbf{r_1}$ and $\mathbf{r_2}$. The electrons are separated by a distance $r_{12} = |\mathbf{r_1} - \mathbf{r_2}|$. The origin of the coordinate system is fixed at the nucleus. As with the hydrogen atom, the nuclei for multi-electron atoms are so much heavier than an electron that the nucleus is assumed to be the center of mass. Fixing the origin of the coordinate system at the nucleus allows us to exclude translational motion of the center of mass from our quantum mechanical treatment.

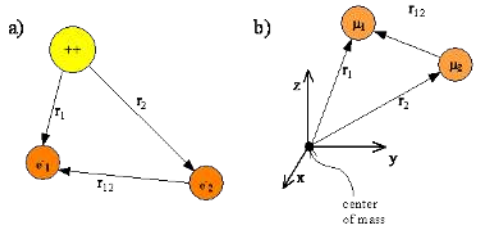


Figure 8.8.1 **:** a) The nucleus (++) and electrons (e-) of the helium atom. b) Equivalent reduced particles with the center of mass (approximately located at the nucleus) at the origin of the coordinate system. Note that μ_1 and $\mu_2 \approx m_e$.

The Schrödinger equation operator for the hydrogen atom serves as a reference point for writing the Schrödinger equation for atoms with more than one electron. Start with the same general form we used for the hydrogen atom Hamiltonian

$$\hat{H}\psi = (\hat{T} + \hat{V})\psi = E\psi \tag{8.8.1}$$

which includes a kinetic energy term, $\hat{T}$, for each electron and a potential energy term for the attraction of each negatively charged electron for the positively charged nucleus and a potential energy term for the mutual repulsion of each pair of negatively charged electrons, $\hat{V}$. The He atom Schrödinger equation is

$$\left(-\frac{\hbar^2}{2m_e}(\nabla_1^2 + \nabla_2^2) + V(r_1) + V(r_2) + V(r_{12})\right)\psi = E\psi \tag{8.8.2}$$

where

$$V(r_1) = -\frac{2e^2}{4\pi\epsilon_0 r_1} \tag{8.8.3}$$

$$V(r_2) = -\frac{2e^2}{4\pi\epsilon_0 r_2} \tag{8.8.4}$$

$$V(r_{12}) = +\frac{e^2}{4\pi\epsilon_0 r_{12}} \tag{8.8.5}$$

Equation 8.8.2 can be extended to any atom or ion by including terms for the additional electrons and replacing the He nuclear charge +2 with a general charge Z; e.g.

$$V(r_1) = -\frac{Ze^2}{4\pi\epsilon_0 r_1} \tag{8.8.6}$$

Equation 8.8.2 then becomes

$$\left(-\frac{\hbar^2}{2m_e}\sum_i \nabla_i^2 + \sum_i V(r_i) + \sum_{i\neq j} V(r_{ij})\right)\psi = E\psi \tag{8.8.7}$$

Given what we have learned from the previous quantum mechanical systems we've studied, we predict that exact solutions to the multi-electron Schrödinger equation would consist of a family of multi-electron wavefunctions, each with an associated energy

eigenvalue. These wavefunctions and energies would describe the ground and excited states of the multi-electron atom, just as the hydrogen wavefunctions and their associated energies describe the ground and excited states of the hydrogen atom. We would predict quantum numbers to be involved, as well.

The fact that electrons interact through their electron-electron repulsion means that an exact wavefunction for a multi-electron system would be a single function that depends **simultaneously** upon the coordinates of all the electrons; i.e., a multi-electron wavefunction:

$$\Psi(r_1, r_2, \cdots r_i) \tag{8.8.8}$$

Unfortunately, the electron-electron repulsion terms make it impossible to find an exact solution to the Schrödinger equation for many-electron atoms. The most basic ansatz to the exact solutions involve writing a multi-electron wavefunction as a **simple product of single**-electron wavefunctions

$$\psi(r_1, r_2, \cdots, r_i) = \varphi_1(r_1)\varphi_2(r_2)\cdots\varphi_i(r_i) \tag{8.8.9}$$

Obtaining the energy of the atom in the state described by that wavefunction as the **sum** of the energies of the one-electron components.

By writing the multi-electron wavefunction as a product of single-electron functions in Equation 8.8.9, we conceptually transform a multi-electron atom into a collection of individual electrons located in individual orbitals whose spatial characteristics and energies can be separately identified. For atoms these single-electron wavefunctions are called atomic orbitals. For molecules, as we will see in the next chapter, they are called molecular orbitals. While a great deal can be learned from such an analysis, it is important to keep in mind that such a discrete, compartmentalized picture of the electrons is an approximation, albeit a powerful one.

8.8.2: Electron Configurations

The specific arrangement of electrons in orbitals of an atom determines many of the chemical properties of that atom and is formulated via the *Aufbau* principle, which means "building-up" in German. Aufbau principles determine the order in which atomic orbitals are filled as the atomic number is increased. For the hydrogen atom, the order of increasing orbital energy is given by 1*s* < 2*s* = 2*p* < 3*s* = 3*p* = 3*d*, etc. The dependence of energy on *n* alone leads to extensive degeneracy, which is however removed for orbitals in many-electron atoms. Thus 2*s* lies below 2*p*, as already observed in helium. Similarly, 3*s*, 3*p* and 3*d* increase energy in that order, and so on. The 4*s* is lowered sufficiently that it becomes comparable to 3*d*. The general ordering of atomic orbitals is summarized in the following scheme:

$$\begin{aligned} 1s < 2s < 2p < 3s < 3p < 4s \sim 3d < 4p < 5s \sim 4d \\ < 5p < 6s \sim 5d \sim 4f < 6p < 7s \sim 6d \sim 5f \end{aligned} \tag{8.8.10}$$

and illustrated in Figure 8.8.2. This provides enough orbitals to fill the ground states of all the atoms in the periodic table. For orbitals designated as comparable in energy, e.g., 4*s* ∼ 3*d*, the actual order depends which other orbitals are occupied. The energy of atomic orbitals increases as the principal quantum number, n, increases. In any atom with two or more electrons, the repulsion between the electrons makes energies of subshells with different values of l differ so that the energy of the orbitals increases within a shell in the order *s* < *p* < *d* < *f*. Figure 8.8.2 depicts how these two trends in increasing energy relate. The 1*s* orbital at the bottom of the diagram is the orbital with electrons of lowest energy. The energy increases as we move up to the 2*s* and then 2*p*, 3*s*, and 3*p* orbitals, showing that the increasing *n* value has more influence on energy than the increasing l value for small atoms. However, this pattern does not hold for larger atoms. The 3*d* orbital is higher in energy than the 4*s* orbital. Such overlaps continue to occur frequently as we move up the chart.

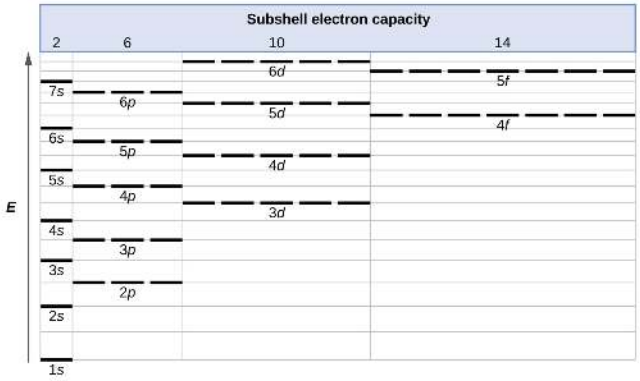


Figure 8.8.2: Generalized energy-level diagram for atomic orbitals in an atom with two or more electrons (not to scale).

Electrons in successive atoms on the periodic table tend to fill low-energy orbitals first. The arrangement of electrons in the orbitals of an atom is called the electron configuration of the atom. We describe an electron configuration with a symbol that contains three pieces of information (Figure 8.8.3):

1. The number of the principal quantum shell, *n*,
2. The letter that designates the orbital type (the subshell, *l*), and
3. A superscript number that designates the number of electrons in that particular subshell.

For example, the notation $2p^4$ (read "two–p–four") indicates four electrons in a *p* subshell (l = 1) with a principal quantum number (n) of 2. The notation $3d^8$ (read "three–d–eight") indicates eight electrons in the *d* subshell (i.e., l = 2) of the principal shell for which n = 3.

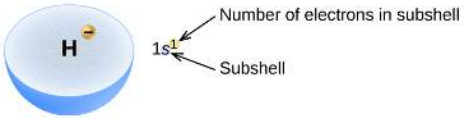


Figure 8.8.3: The diagram of an electron configuration specifies the subshell (n and l value, with letter symbol) and superscript number of electrons.

To determine the electron configuration for any particular atom, we can “build” the structures in the order of atomic numbers. Beginning with hydrogen, and continuing across the periods of the periodic table, we add one proton at a time to the nucleus and one electron to the proper subshell until we have described the electron configurations of all the elements. This procedure is called the Aufbau principle, from the German word *Aufbau* (“to build up”). Each added electron occupies the subshell of lowest energy available (in the order shown in Figure 8.8.2), subject to the limitations imposed by the allowed quantum numbers according to the Pauli exclusion principle. Electrons enter higher-energy subshells only after lower-energy subshells have been filled to capacity. Figure 8.8.4 illustrates a pictorial way to remember the filling order for atomic orbitals. It is usually easier to just read it off from position in the periodic table after remembering which parts of the table are filling which subshells (figure \PageIndex{5}\).

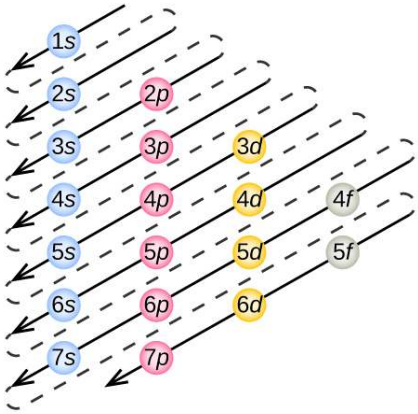


Figure 8.8.4: The arrow leads through each subshell in the appropriate filling order for electron configurations. This chart is straightforward to construct. Simply make a column for all the s orbitals with each n shell on a separate row. Repeat for p, d, and f. Be sure to only include orbitals allowed by the quantum numbers (no 1p or 2d, and so forth). Finally, draw diagonal lines from top to bottom as shown.

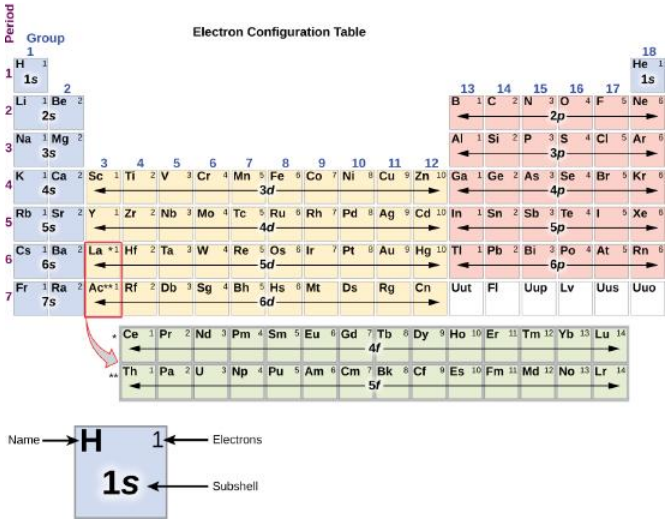
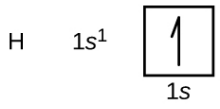


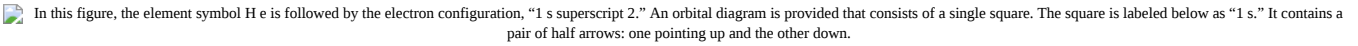
Figure 8.8.5: Regions of shell filling in the periodic table: blue filling s orbitals; pink filling p orbitals; yellow filling d orbitals; and green filling f orbitals.

We will now construct the ground-state electron configuration and orbital diagram for a selection of atoms in the first and second periods of the periodic table. Orbital diagrams are pictorial representations of the electron configuration, showing the individual orbitals and the pairing arrangement of electrons. We start with a single hydrogen atom (atomic number 1), which consists of one proton and one electron. Referring to either Figure 8.8.4, we would expect to find the electron in the 1*s* orbital. By convention, the $m_s = +\frac{1}{2}$ value is usually filled first. The electron configuration and the orbital diagram are:



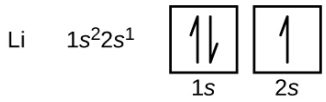
Following hydrogen is the noble gas helium, which has an atomic number of 2. The helium atom contains two protons and two electrons. The first electron has the same four quantum numbers as the hydrogen atom electron (n = 1, l = 0, m_l = 0, $m_s = +\frac{1}{2}$). The second electron also goes into the 1*s* orbital and fills that orbital. The second electron has the same n, l, and m_l quantum numbers, but must have the opposite spin quantum number, $m_s = -\frac{1}{2}$. This is in accord with the Pauli exclusion principle: No two electrons in the same atom can have the same set of four quantum numbers. For orbital diagrams, this means two arrows go in

each box (representing two electrons in each orbital) and the arrows must point in opposite directions (representing paired spins). The electron configuration and orbital diagram of helium are:

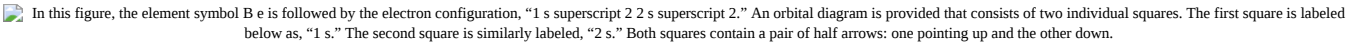

In this figure, the element symbol H e is followed by the electron configuration, “1 s superscript 2.” An orbital diagram is provided that consists of a single square. The square is labeled below as “1 s.” It contains a pair of half arrows: one pointing up and the other down.

The $n = 1$ shell is completely filled in a helium atom.

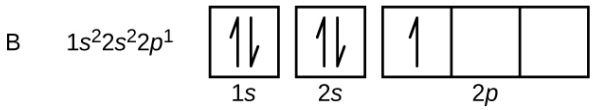
The next atom is the alkali metal lithium with an atomic number of 3. The first two electrons in lithium fill the 1*s* orbital and have the same sets of four quantum numbers as the two electrons in helium. The remaining electron must occupy the orbital of next lowest energy, the 2*s* orbital (Figure 8.8.4). Thus, the electron configuration and orbital diagram of lithium are:



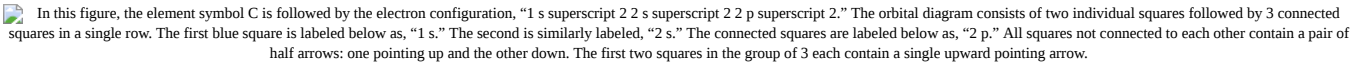
An atom of the alkaline earth metal beryllium, with an atomic number of 4, contains four protons in the nucleus and four electrons surrounding the nucleus. The fourth electron fills the remaining space in the 2*s* orbital.


In this figure, the element symbol B e is followed by the electron configuration, “1 s superscript 2 2 s superscript 2.” An orbital diagram is provided that consists of two individual squares. The first square is labeled below as, “1 s.” The second square is similarly labeled, “2 s.” Both squares contain a pair of half arrows: one pointing up and the other down.

An atom of boron (atomic number 5) contains five electrons. The $n = 1$ shell is filled with two electrons and three electrons will occupy the $n = 2$ shell. Because any *s* subshell can contain only two electrons, the fifth electron must occupy the next energy level, which will be a 2*p* orbital. There are three degenerate 2*p* orbitals ($m_l = -1, 0, +1$) and the electron can occupy any one of these *p* orbitals. When drawing orbital diagrams, we include empty boxes to depict any empty orbitals in the same subshell that we are filling.



Carbon (atomic number 6) has six electrons. Four of them fill the 1*s* and 2*s* orbitals. The remaining two electrons occupy the 2*p* subshell. We now have a choice of filling one of the 2*p* orbitals and pairing the electrons or of leaving the electrons unpaired in two different, but degenerate, *p* orbitals. The orbitals are filled as described by Hund’s rule: the lowest-energy configuration for an atom with electrons within a set of degenerate orbitals is that having the maximum number of unpaired electrons. Thus, the two electrons in the carbon 2*p* orbitals have identical *n*, *l*, and m_s quantum numbers and differ in their m_l quantum number (in accord with the Pauli exclusion principle). The electron configuration and orbital diagram for carbon are:


In this figure, the element symbol C is followed by the electron configuration, “1 s superscript 2 2 s superscript 2 2 p superscript 2.” The orbital diagram consists of two individual squares followed by 3 connected squares in a single row. The first blue square is labeled below as, “1 s.” The second is similarly labeled, “2 s.” The connected squares are labeled below as, “2 p.” All squares not connected to each other contain a pair of half arrows: one pointing up and the other down. The first two squares in the group of 3 each contain a single upward pointing arrow.

Nitrogen (atomic number 7) fills the 1*s* and 2*s* subshells and has one electron in each of the three 2*p* orbitals, in accordance with Hund’s rule. These three electrons have unpaired spins. Oxygen (atomic number 8) has a pair of electrons in any one of the 2*p* orbitals (the electrons have opposite spins) and a single electron in each of the other two. Fluorine (atomic number 9) has only one 2*p* orbital containing an unpaired electron. All of the electrons in the noble gas neon (atomic number 10) are paired, and all of the orbitals in the $n = 1$ and the $n = 2$ shells are filled. The electron configurations and orbital diagrams of these four elements are:

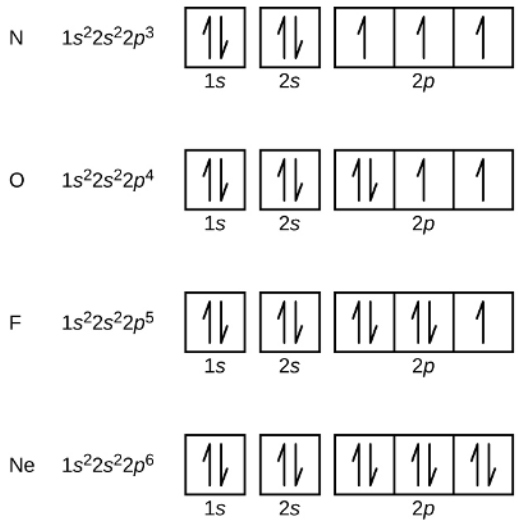


Figure 8.8.6). Since the core electron shells correspond to noble gas electron configurations, we can abbreviate electron configurations by writing the noble gas that matches the core electron configuration, along with the valence electrons in a condensed format. For our sodium example, the symbol [Ne] represents core electrons, (1 $s^2 2s^2 2p^6$) and our abbreviated or condensed configuration is [Ne]$3s^1$.

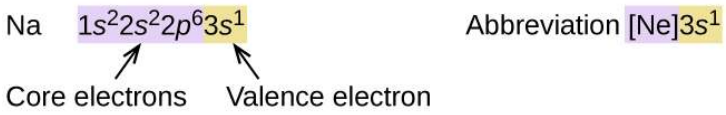


Figure 8.8.7: A core-abbreviated electron configuration (right) replaces the core electrons with the noble gas symbol whose configuration matches the core electron configuration of the other element.

Similarly, the abbreviated configuration of lithium can be represented as [He]$2s^1$, where [He] represents the configuration of the helium atom, which is identical to that of the filled inner shell of lithium. Writing the configurations in this way emphasizes the similarity of the configurations of lithium and sodium. Both atoms, which are in the alkali metal family, have only one electron in a valence *s* subshell outside a filled set of inner shells.

$$\begin{aligned} \text{Li} &: [\text{He}]\, 2s^1 \\ \text{Na} &: [\text{Ne}]\, 3s^1 \end{aligned} \tag{8.8.11}$$

The alkaline earth metal magnesium (atomic number 12), with its 12 electrons in a [Ne]$3s^2$ configuration, is analogous to its family member beryllium, [He]$2s^2$. Both atoms have a filled *s* subshell outside their filled inner shells. Aluminum (atomic number 13), with 13 electrons and the electron configuration [Ne]$3s^2 3p^1$, is analogous to its family member boron, [He]$2s^2 2p^1$.

The electron configurations of silicon (14 electrons), phosphorus (15 electrons), sulfur (16 electrons), chlorine (17 electrons), and argon (18 electrons) are analogous in the electron configurations of their outer shells to their corresponding family members carbon, nitrogen, oxygen, fluorine, and neon, respectively, except that the principal quantum number of the outer shell of the heavier elements has increased by one to $n = 3$. Figure

Beginning with the transition metal scandium (atomic number 21), additional electrons are added successively to the 3*d* subshell. This subshell is filled to its capacity with 10 electrons (remember that for $l = 2$ [*d* orbitals], there are $2l + 1 = 5$ values of m_l, meaning that there are five *d* orbitals that have a combined capacity of 10 electrons). The 4*p* subshell fills next. Note that for three series of elements, scandium (Sc) through copper (Cu), yttrium (Y) through silver (Ag), and lutetium (Lu) through gold (Au), a total of 10 *d* electrons are successively added to the $(n - 1)$ shell next to the *n* shell to bring that $(n - 1)$ shell from 8 to 18 electrons. For two series, lanthanum (La) through lutetium (Lu) and actinium (Ac) through lawrencium (Lr), 14 *f* electrons ($l = 3$, $2l + 1 = 7$ m_l values; thus, seven orbitals with a combined capacity of 14 electrons) are successively added to the $(n - 2)$ shell to bring that shell from 18 electrons to a total of 32 electrons.

Example 8.8.1

Quantum Numbers and Electron Configurations What is the electron configuration and orbital diagram for a phosphorus atom? What are the four quantum numbers for the last electron added?

Solution

The atomic number of phosphorus is 15. Thus, a phosphorus atom contains 15 electrons. The order of filling of the energy levels is 1*s*, 2*s*, 2*p*, 3*s*, 3*p*, 4*s*, . . . The 15 electrons of the phosphorus atom will fill up to the 3*p* orbital, which will contain three electrons:



The last electron added is a 3*p* electron. Therefore, $n = 3$ and, for a *p*-type orbital, $l = 1$. The m_l value could be –1, 0, or +1. The three *p* orbitals are degenerate, so any of these m_l values is correct. For unpaired electrons, convention assigns the value of $+\frac{1}{2}$ for the spin quantum number; thus, $m_s = +\frac{1}{2}$.

Exercise 8.8.1

Identify the atoms from the electron configurations given:

a. $[Ar]4s^2 3d^5$
b. $[Kr]5s^2 4d^{10} 5p^6$

Answer

(a) Mn (b) Xe

8.8.3: Effective Charge, Shielding and Penetration

For an atom or an ion with only a single electron, we can calculate the potential energy by considering only the electrostatic attraction between the positively charged nucleus and the negatively charged electron. When more than one electron is present, however, the total energy of the atom or the ion depends not only on attractive electron-nucleus interactions but also on repulsive electron-electron interactions. When there are two electrons, the repulsive interactions depend on the positions of *both* electrons at a given instant, but because we cannot specify the exact positions of the electrons, it is impossible to exactly calculate the repulsive interactions. Consequently, we must use approximate methods to deal with the effect of electron-electron repulsions on orbital energies.

If an electron is far from the nucleus (i.e., if the distance *r* between the nucleus and the electron is large), then at any given moment, most of the other electrons will be *between* that electron and the nucleus. Hence the electrons will cancel a portion of the positive charge of the nucleus and thereby decrease the attractive interaction between it and the electron farther away. As a result, the electron farther away experiences an effective nuclear charge (Z_{eff}) that is *less* than the actual nuclear charge Z (Figure 8.8.6). This effect is called electron shielding.

As the distance between an electron and the nucleus approaches infinity, Z_{eff} approaches a value of 1 because all the other $(Z - 1)$ electrons in the neutral atom are, on the average, between it and the nucleus. If, on the other hand, an electron is very close to the nucleus, then at any given moment most of the other electrons are farther from the nucleus and do not shield the nuclear charge. At $r \approx 0$, the positive charge experienced by an electron is approximately the full nuclear charge, or $Z_{eff} \approx Z$. At intermediate values of *r*, the effective nuclear charge is somewhere between 1 and *Z*: $1 \le Z_{eff} \le Z$. Thus the actual Z_{eff} experienced by an electron in a given orbital depends not only on the spatial distribution of the electron in that orbital but also on the distribution of all the other electrons present. This leads to large differences in Z_{eff} for different elements, as shown in Figure 2.5.1 for the elements of the first three rows of the periodic table. Notice that only for hydrogen does $Z_{eff} = Z$, and only for helium are Z_{eff} and *Z* comparable in magnitude.

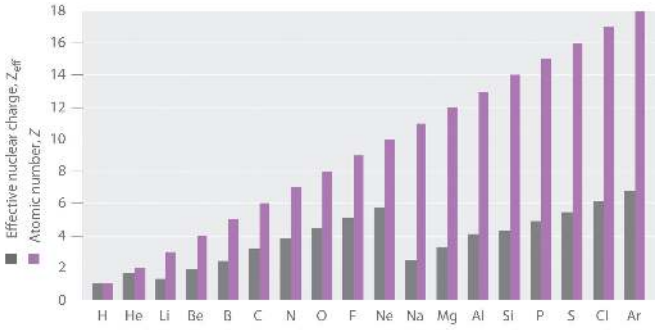


Figure 8.8.6: Relationship between the Effective Nuclear Charge Z_{eff} and the Atomic Number Z for the Outer Electrons of the Elements of the First Three Rows of the Periodic Table. Except for hydrogen, Z_{eff} is *always* less than Z, and Z_{eff} increases from left to right as you go across a row.

Because of the effects of shielding and the different radial distributions of orbitals with the same value of n but different values of l, the different subshells are not degenerate in a multielectron atom. For a given value of n, the ns orbital is always lower in energy than the np orbitals, which are lower in energy than the nd orbitals, and so forth. As a result, some subshells with higher principal quantum numbers are actually lower in energy than subshells with a lower value of n; for example, the 4s orbital is lower in energy than the 3d orbitals for most atoms.

Note

Except for the single electron containing hydrogen atom, in every other element Z_{eff} is always less than Z.

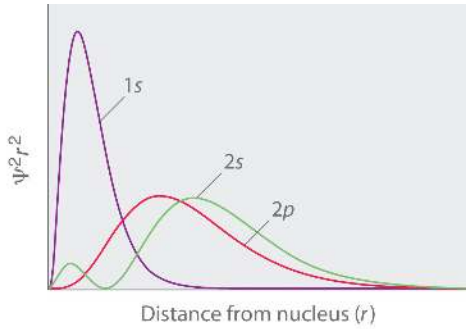


Figure 8.8.7: Orbital Penetration. A comparison of the radial probability distribution of the 2 s and 2p orbitals for various states of the hydrogen atom shows that the 2s orbital penetrates inside the 1s orbital more than the 2p orbital does. Consequently, when an electron is in the small inner lobe of the 2s orbital, it experiences a relatively large value of Z_{eff}, which causes the energy of the 2s orbital to be lower than the energy of the 2p orbital.

8.8.4: Ionization Energy

Ionization energy is the energy required to remove an electron from a neutral atom in its gaseous phase. Conceptually, ionization energy is the opposite of electronegativity. The lower this energy is, the more readily the atom becomes a cation (positively charged). Alternatively, one can say that as ionization energy increases the likelihood of creating a cation drops. Generally, elements on the right side of the periodic table have a higher ionization energy because their valence shell is nearly filled. Elements on the left side of the periodic table have low ionization energies because of their willingness to lose electrons and become cations. Thus, ionization energy increases from left to right on the periodic table.

Another factor that affects ionization energy is *electron shielding*. Electron shielding describes the ability of an atom's inner electrons to shield its positively-charged nucleus from its valence electrons. When moving to the right of a period, the number of electrons increases and the strength of shielding increases. As a result, it is easier for valence shell electrons to ionize, and thus the ionization energy decreases down a group. Electron shielding is also known as *screening*.

Note

- The ionization energy of the elements within a period generally increases from left to right. This is due to valence shell stability.
- The ionization energy of the elements within a group generally decreases from top to bottom. This is due to electron shielding.
- The noble gases possess very high ionization energies because of their full valence shells as indicated in the graph. Note that helium has the highest ionization energy of all the elements.

Some elements have several ionization energies; these varying energies are referred to as the first ionization energy, the second ionization energy, third ionization energy, etc. The first ionization energy is the energy required to remove the outermost, or highest, energy electron, the second ionization energy is the energy required to remove any subsequent high-energy electron from a gaseous cation, etc. Below are the chemical equations describing the first and second ionization energies:

First Ionization Energy:

$$X_{(g)} \rightarrow X^{+}_{(g)} + e^{-} \tag{8.8.12}$$

Second Ionization Energy:

$$X^{+}_{(g)} \rightarrow X^{2+}_{(g)} + e^{-} \tag{8.8.13}$$

Generally, any subsequent ionization energies (2nd, 3rd, etc.) follow the same periodic trend as the first ionization energy.

Ionization energies decrease as atomic radii increase. This observation is affected by n (the principal quantum number) and Z_{eff} (based on the atomic number and shows how many protons are seen in the atom) on the ionization energy (I). The relationship is given by the following equation:

$$I = \frac{R_H Z^2_{eff}}{n^2} \tag{8.8.14}$$

- Across a period, Z_{eff} *increases* and n (principal quantum number) *remains the same*, so the ionization energy *increases*.
- Down a group, n *increases* and Z_{eff} *increases slightly;* the ionization energy *decreases*.

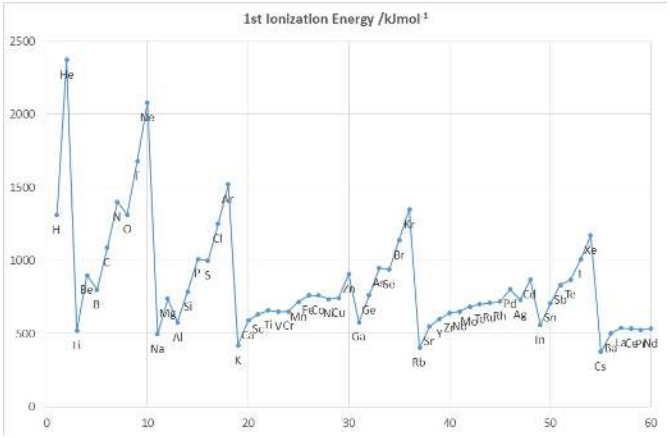


Figure 8.8.8: Periodic trends in ionization energy.

The periodic structure of the elements is evident for many physical and chemical properties, including chemical valence, atomic radius, electronegativity, melting point, density, and hardness. The classic prototype for periodic behavior is the variation of the first ionization energy with atomic number, which is plotted in Figure 8.8.8.

8.8.5: Electron Affinity

The electron affinity (EA) of an element E is defined as minus the internal energy change associated with the gain of an electron by a gaseous atom, at 0 K :

$$E_{(g)} + e^{-} \rightarrow E^{-}_{(g)} \tag{8.8.15}$$

Unlike ionization energies, which are always positive for a neutral atom because energy is required to remove an electron, electron affinities can be positive (energy is released when an electron is added), negative (energy must be added to the system to produce an anion), or zero (the process is energetically neutral).

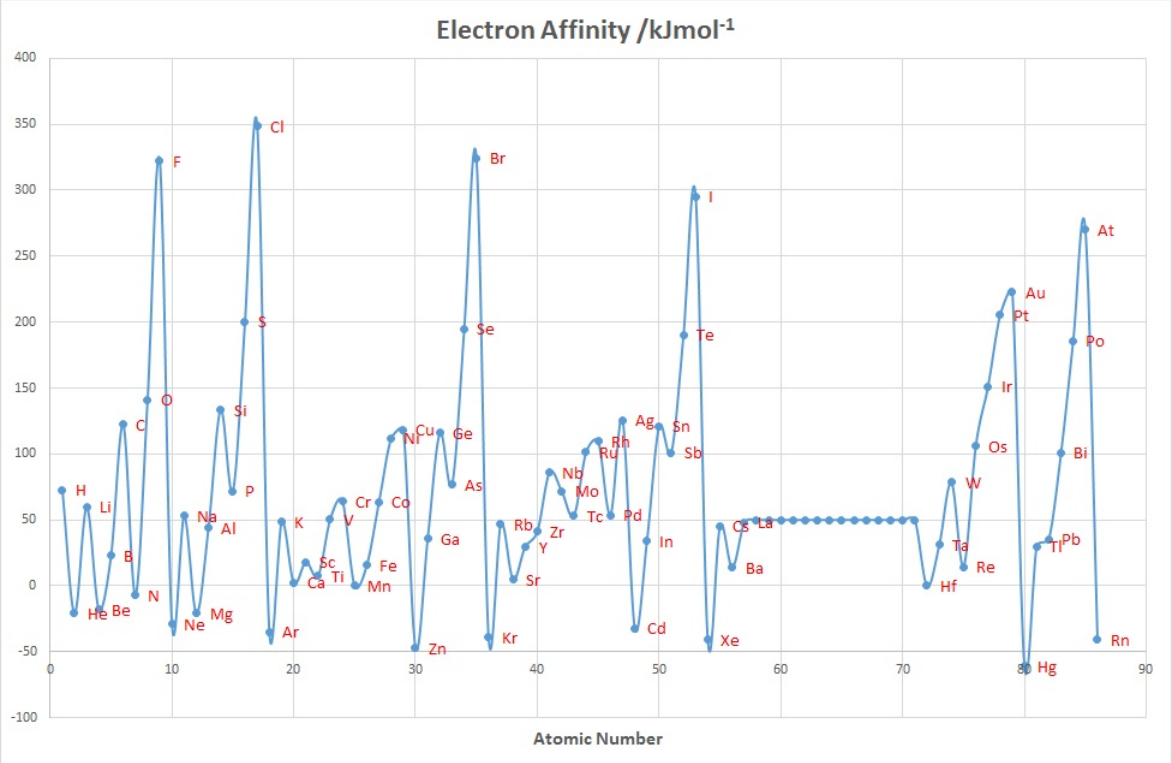


Figure* 8.8.9*: *Periodic trends in electron affinities.*

The periodic trends of electron affinity (Figure 8.8.9) shows that chlorine has the most positive electron affinity of any element, which means that more energy is released when an electron is added to a gaseous chlorine atom than to an atom of any other element, EA= 348.6 kJmol^{-1} and the Group 17 elements have the largest values overall. The addition of a second electron to an element is expected to be much less favored since there will be repulsion between the negatively charged electron and the overall negatively charged anion. For example, for O the values are:

$$O_{(g)} + e^{\rightarrow} O^{-}_{(g)} \quad EA = +141\ kJmol^{-1} \tag{8.8.16}$$

$$O^{-}_{(g)} + e^{-} \rightarrow O^{2-})(g) \quad EA = -798\ kJmol^{-1} \tag{8.8.17}$$

David M. Hanson, Erica Harvey, Robert Sweeney, Theresa Julia Zielinski ("Quantum States of Atoms and Molecules")

This page titled 8.8: Many-Electron Atoms and the Periodic Table is shared under a CC BY-NC-SA 4.0 license and was authored, remixed, and/or curated by Jonathan Gutow.

- **11.11: Many-Electron Atoms and the Periodic Table** is licensed CC BY-NC-SA 4.0.

8.9: Harmonic Oscillator

8.9.1: Introduction

The harmonic oscillator is a model which has several important applications in both classical and quantum mechanics. It serves as a prototype in the mathematical treatment of such diverse phenomena as elasticity, acoustics, AC circuits, molecular and crystal vibrations, electromagnetic fields and optical properties of matter.

8.9.2: Classical Oscillator

A simple realization of the harmonic oscillator in classical mechanics is a particle which is acted upon by a restoring force proportional to its displacement from its equilibrium position. Considering motion in one dimension, this means

$$F = -kx \tag{8.9.1}$$

Such a force might originate from a spring which obeys Hooke's law, as shown in Figure 8.9.1. According to Hooke's law, which applies to real springs for sufficiently small displacements, the restoring force is proportional to the displacement—either stretching or compression—from the equilibrium position.

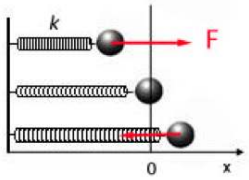


Figure 8.9.1: Spring obeying Hooke's law.

The *force constant* k is a measure of the stiffness of the spring. The variable x is chosen equal to zero at the equilibrium position, positive for stretching, negative for compression. The negative sign in Equation 8.9.1 reflects the fact that F is a *restoring* force, always in the opposite sense to the displacement x.

Applying Newton's second law to the force from Equation 8.9.1, we find x

$$F = m\frac{d^2x}{dx^2} = -kx \tag{8.9.2}$$

where m is the mass of the body attached to the spring, which is itself assumed massless. This leads to a differential equation of familiar form, although with different variables:

$$\ddot{x}(t) + \omega^2 x(t) = 0 \tag{8.9.3}$$

with

$$\omega^2 \equiv \frac{k}{m} \tag{8.9.4}$$

The dot notation (introduced by Newton himself) is used in place of primes when the independent variable is time. The general solution to Equation 8.9.3 is

$$x(t) = A\sin\omega t + B\cos\omega t \tag{8.9.5}$$

which represents periodic motion with a sinusoidal time dependence. This is known as *simple harmonic motion* and the corresponding system is known as a *harmonic oscillator*. The oscillation occurs with a constant angular frequency

$$\omega = \sqrt{\frac{k}{m}} \text{ radians per second} \tag{8.9.6}$$

This is called the *natural frequency* of the oscillator. The corresponding *circular (or angular) frequency* in Hertz (cycles per second) is

$$\nu = \frac{\omega}{2\pi} = \frac{1}{2\pi}\sqrt{\frac{k}{m}} \text{ Hz} \tag{8.9.7}$$

The general relation between force and potential energy in a conservative system in one dimension is

$$F = \frac{-dV}{dx} \tag{8.9.8}$$

Thus the potential energy of a harmonic oscillator is given by

$$V(x) = \frac{1}{2}kx^2 \tag{8.9.9}$$

which has the shape of a parabola, as drawn in Figure 8.9.2. A simple computation shows that the oscillator moves between positive and negative turning points $\pm x_{max}$ where the total energy E equals the potential energy $\frac{1}{2}kx_{max}^2$ while the kinetic energy is momentarily zero. In contrast, when the oscillator moves past $x = 0$, the kinetic energy reaches its maximum value while the potential energy equals zero.

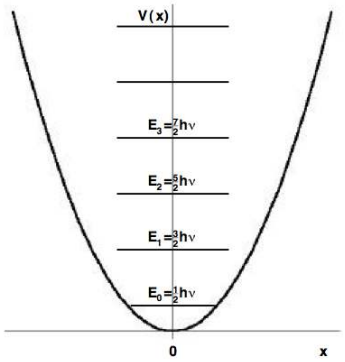


Figure 8.9.2: Potential energy function and first few energy levels for harmonic oscillator.

8.9.3: Harmonic Oscillator in Quantum Mechanics

Given the potential energy in Equation 8.9.9, we can write down the Schrödinger equation for the one-dimensional harmonic oscillator:

$$-\frac{\hbar^2}{2m}\frac{d^2\psi(x)}{dx^2} + \frac{1}{2}kx^2\psi(x) = E\psi(x) \tag{8.9.10}$$

This equation is challenging to solve for ψ because the potential varies with position and is less than infinity in all of space. This means the particle can be found at any x between $\pm\infty$. Solutions for it have been found by others by what are essentially sophisticated guess and check methods. The results are:

$$\psi_n(x) = \left(\frac{\sqrt{\alpha}}{2^n n!\sqrt{\pi}}\right)^{1/2} H_n(\sqrt{\alpha}x)e^{-\alpha x^2/2} \tag{8.9.11}$$

where

$$\alpha = \sqrt{\frac{mk}{\hbar^2}} \tag{8.9.12}$$

and $H_n(\xi)$, with $\xi = \sqrt{\alpha}x$ represents the Hermite polynomial of degree n. The first few Hermite polynomials are

$$H_0(\xi) = 1 \tag{8.9.13}$$

$$H_1(\xi) = 2\xi \tag{8.9.14}$$

$$H_2(\xi) = 4\xi^2 - 2 \tag{8.9.15}$$

$$H_3(\xi) = 8\xi^3 - 12\xi \tag{8.9.16}$$

The four lowest harmonic-oscillator eigenfunctions are plotted in Figure 8.9.3. Note the topological resemblance to the corresponding particle-in-a-box eigenfunctions.

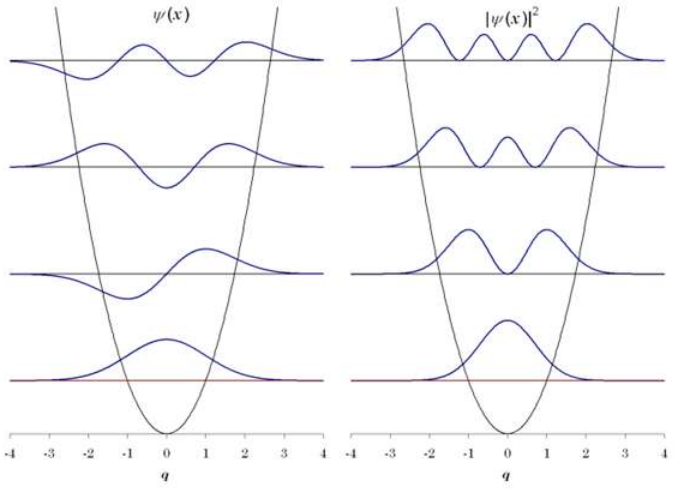


Figure 8.9.3: Harmonic oscillator eigenfunctions for n=0, 1, 2, 3 and probability densities. **Two things to note**: these wavefunctions do not reach zero until x = ±∞; a particle represented by any of these wavefunctions have a probability of being in the classically forbidden regions where the energy is less than the potential energy (the particle exhibits tunneling).

The eigenvalues are given by the simple formula

$$E_n = \left(n + \frac{1}{2}\right)\hbar\omega \tag{8.9.17}$$

where ω is as defined in equation 8.9.6. These energy levels are drawn in Figure 8.9.2, on the same scale as the potential energy. The ground-state energy $E_0 = \frac{1}{2}\hbar\omega$ is greater than the classical value of zero, again a consequence of the uncertainty principle. This means that the oscillator is always oscillating.

Note that the difference between successive energy eigenvalues has a constant value

$$\Delta E = E_{n+1} - E_n = \hbar\omega = h\nu \tag{8.9.18}$$

This is reminiscent of Planck's formula for the energy of a photon. It comes as no surprise then that the quantum theory of radiation has the structure of an assembly of oscillators, with each oscillator representing a mode of electromagnetic waves of a specified frequency.

8.9.4: Contributors and Attributions

- Seymour Blinder (Professor Emeritus of Chemistry and Physics at the University of Michigan, Ann Arbor)
- Jonathan Gutow (UW Oshkosh).

This page titled 8.9: Harmonic Oscillator is shared under a CC BY-NC-SA 4.0 license and was authored, remixed, and/or curated by Jonathan Gutow.

- **Harmonic Oscillator** is licensed CC BY-NC-SA 4.0.

CHAPTER OVERVIEW

9: Molecular Quantum Mechanics

9.1: The Born-Oppenheimer Approximation Simplifies the Schrödinger Equation for Molecules
9.2: Valence Bond Theory
9.3: Hybridization of Atomic Orbitals
9.4: Molecular Orbital Theory
9.5: Diatomic Molecules With More Than s Orbitals
9.6: Hückel MO Model of Conjugation
9.7: Benzene and Aromaticity
9.8: Numerical QM Methods

This page titled 9: Molecular Quantum Mechanics is shared under a CC BY-NC-SA 4.0 license and was authored, remixed, and/or curated by Jonathan Gutow.

9.1: The Born-Oppenheimer Approximation Simplifies the Schrödinger Equation for Molecules

Learning Objectives

- Understand the need to introduce an approximation like the Born-Oppenheimer approximation to solve multi-electron systems
- Understand the basis of parameterization involved in using the Born-Oppenheimer approximation

9.1.1: Introduction

Using quantum mechanics to predict the chemical bonding patterns, optimal geometries, and physical and chemical properties of molecules is a large and active field of research known as *molecular quantum mechanics* or more commonly as *quantum chemistry*. Quantum chemistry calculations allow the geometries of molecules to be computed as well as a wide range of properties. Quantum chemistry can also be combined with classical mechanics in what is often referred to as quantum mechanical molecular dynamics (QM/MD) calculations, in which the electrons are treated using quantum mechanics but the nuclei are treated as classical particles. Quantum mechanics is used to calculate the internuclear forces but then these forces are used in Newton's Second Law to study the motion of the nuclei during chemical reactions. This gives us a microscopic window into the specific motions, the complex dance, executed by the nuclei during a simple or complex chemical process.

The methods of quantum chemistry have become very sophisticated, and there are various software packages that can be downloaded for carrying out the calculations of quantum chemistry. It should be noted that these packages use a series of approximations to solve the Schrödinger equation because for all but the simplest of molecules, exact solutions are not available.

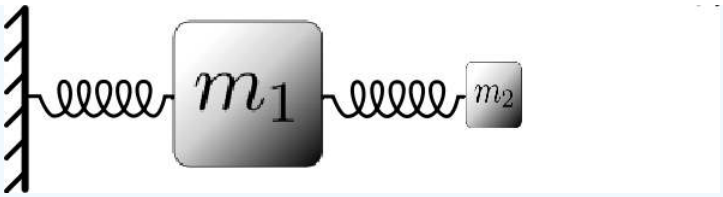
9.1.2: The Born-Oppenheimer Approximation

The Born-Oppenheimer approximation is one of the basic concepts underlying the description of the quantum states of molecules. This approximation makes it possible to separate the motion of the nuclei and the motion of the electrons. This is not a new idea for us. We already made use of this approximation in the particle-in-a-box model when we explained the electronic absorption spectra of conjugated systems without considering the motion of the nuclei. Here we will examine more closely the significance and consequences of this important approximation. Note, in this discussion nuclear refers to the atomic nuclei as parts of molecules not to the internal structure of the nucleus.

The Born-Oppenheimer approximation neglects the motion of the atomic nuclei when describing the electrons in a molecule. The physical basis for the Born-Oppenheimer approximation is the fact that the mass of an atomic nucleus in a molecule is much larger than the mass of an electron (more than 1000 times). Because of this difference, the nuclei move much more slowly than the electrons. In addition, due to their opposite charges, there is a mutual attractive force of Ze^2/r^2 acting on an atomic nucleus and an electron. This force causes both particles to be accelerated. Since the magnitude of the acceleration is inversely proportional to the mass, a = F/m, the acceleration of the electrons is large and the acceleration of the atomic nuclei is small; the difference is a factor of more than 2000. Consequently, the electrons are moving and responding to forces very quickly, and the nuclei are not. You can imagine running a 100-yard dash against someone whose acceleration is a 2000 times greater than yours. That person could literally run circles around you.

Example 9.1.1 : Coupled Oscillators with Dissimilar Masses

If two particles interact in some way, and one is much heavier than the other, the light particle will move essentially as a "slave" of the heavy particle. That is, it will simply follow the heavy particle wherever it goes, *and*, it will move rapidly in response to the heavy particle motion. As an illustration of this phenomenon, consider the simple mechanical system pictured below:



(CC BY-SA 3.0 Unported; Jim.belk via Wikipedia).

Considering this as a classical system, we expect that the motion will be dominated by the large heavy particle (m_1), which is attached to a fixed wall by a spring. The small, light particle (m_2, which is attached to the heavy particle by a spring will simply follow the heavy particle and execute rapid oscillations around it.

So a good approximation is to describe the electronic states of a molecule by thinking that the nuclei are not moving, i.e. that they are stationary. The nuclei, however, can be stationary at different positions so the electronic wavefunction can depend on the positions of the nuclei even though their motion is neglected.

Now we look at the mathematics to see what is done in solving the Schrödinger equation after making the Born-Oppenheimer approximation. The Hamiltonian has contributions from the kinetic, $\hat{T}$, and potential, $\hat{V}$, energies of the nuclei and the electrons:

$$\hat{H}(\vec{r},\vec{R}) = \hat{T}_{nuc}(\vec{R}) + \hat{T}_{elec}(\vec{r}) + \hat{V}_{nuc}(\vec{R}) + \hat{V}_{elec}(\vec{r}) + \hat{V}_{elec-nuc}(\vec{r},\vec{R}) \tag{9.1.1}$$

where $\vec{R}$ are nuclear coordinates and $\vec{r}$ are electronic coordinates. Notice that the term for the nuclear kinetic energy only depends on the position of the nuclei. The Born-Oppenheimer approximation is mathematically equivalent to assuming the nuclei have no kinetic energy so the effective Hamiltonian which we refer to as $\hat{H}_{elec}$ only contains the last four terms in equation 9.1.1. For a diatomic molecule with a single electron (e.g. H_2^+) this effective Hamiltonian is:

$$\hat{H}_{elec}(\vec{r},\vec{R}) = \frac{-\hbar^2}{2m_e}\nabla^2 + \frac{e^2}{4\pi\epsilon_o}\left(\frac{z_A z_B}{r_{AB}} + 0 + \frac{-z_A}{r_A} + \frac{-z_B}{r_B}\right) \tag{9.1.2}$$

where z_i is the charge on nucleus i, r_{AB} is the internuclear distance and r_i is the distance of the electron from nucleus i. The gradient ∇ term is the kinetic energy of the electrons. The remaining terms are the potential of interaction of the charged particles. The 0 valued term is where the potential from interaction with other electrons would be if there were more than one. Thus, the electronic wavefunction $\phi_e(\vec{r},\vec{R})$ is found as a solution to the electronic Schrödinger equation

$$\hat{H}_{elec}(\vec{r},\vec{R})\phi_e(\vec{r},\vec{R}) = E_e(R)\phi_e(\vec{r},\vec{R}) \tag{9.1.3}$$

Even though the nuclear kinetic energy terms are neglected, the Born-Oppenheimer approximation still takes into account the variation in the positions of the nuclei in determining the electronic energy and the resulting electronic wavefunction depends upon the nuclear positions, R. As a result of the Born-Oppenheimer approximation, the molecular wavefunction can be written as a product

$$\psi_{ne}(\vec{r},\vec{R}) = X_{ne}(\vec{R})\phi_e(\vec{r},\vec{R}) \tag{9.1.4}$$

This product wavefunction is called the Born-Oppenheimer wavefunction. The function $X_{ne}(\vec{R})$ is the vibrational wavefunction, which is a function of the nuclear coordinates R and depends upon both the vibrational and electronic quantum numbers or states, n and e, respectively. The electronic function, $\phi_e(\vec{r},\vec{R})$, is a function of both the nuclear and electronic coordinates, but only depends upon the electronic quantum number or electronic state, e. Translational and rotational motion is not included here. The translational and rotational wavefunctions simply multiply the vibrational and electronic functions in Equation 9.1.4 to give the complete molecular wavefunction when the translational and rotational motions are not coupled to the vibrational and electronic motion.

9.1.3: Potential Energy Curves and Surfaces

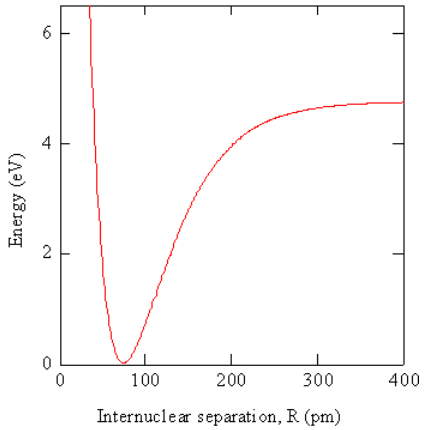


Figure 9.1.1 : The potential energy function for a diatomic molecule.

In practice the electronic Schrödinger equation is solved using approximations at particular values of R to obtain the wavefunctions ϕ_e and potential energies $V_e(R)$. The potential energies can be graphed as illustrated in Figure 9.1.1 .

The graph in Figure 9.1.1 is the energy of a diatomic molecule as a function of internuclear separation, which serves as the potential energy function for the nuclei. When R is very large there are two atoms that are weakly interacting. As R becomes smaller, the interaction becomes stronger, the energy becomes a large negative value, and we say a bond is formed between the atoms. At very small values of R, the internuclear repulsion is very large so the energy is large and positive. This energy function controls the motion of the nuclei. The equilibrium position of the nuclei is where this function is a minimum, i.e. at $R = R_0$.

While the potential energy function, $V_e(R)$, for a diatomic molecule is a 1-D curve (Figure 9.1.1), molecules with more than two atoms will have multi-dimensional **potential energy surfaces** with 3N-6 (or 3N-5 for linear molecule) dimensions for the number of internal degrees of freedom.

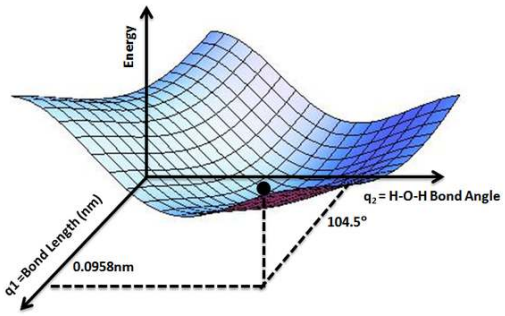


Figure 9.1.2 : The potential energy surface for a water molecule: Shows the energy minimum corresponding to optimized molecular structure for water- O-H bond length of 0.0958 nm and H-O-H bond angle of 104.5°. from Wikipeda (AimNature)

The potential energy surface concept can be used to theoretically explore properties of structures composed of atoms, for example, finding the minimum energy shape of a molecule or computing the rates of a chemical reaction. Qualitatively the reaction coordinate diagrams (one-dimensional slices through the potential energy surfaces) have numerous applications. Chemists use reaction coordinate diagrams as both an analytical and pedagogical aid for rationalizing and illustrating kinetic and thermodynamic events. The purpose of energy profiles and surfaces is to provide a qualitative representation of how potential energy varies with molecular motion for a given reaction or process.

9.1.4: Summary

In this section we started with the Schrödinger equation for a diatomic molecule and separated it into two equations, an electronic Schrödinger equation and a nuclear Schrödinger equation. In order to make the separation, we had to make an approximation. We had to neglect the effect of the nuclear kinetic energy on the electrons. The fact that this assumption works can be traced to the fact that the nuclear masses are much larger than the electron mass. We then used the solution of the electronic Schrödinger equation to provide the potential energy function for the nuclear motion. The solution to the nuclear Schrödinger equation provides the vibrational wavefunctions and energies.

Contributors and Attributions

- David M. Hanson, Erica Harvey, Robert Sweeney, Theresa Julia Zielinski ("Quantum States of Atoms and Molecules")
- Jonathan Gutow (UW Oshkosh)

This page titled 9.1: The Born-Oppenheimer Approximation Simplifies the Schrödinger Equation for Molecules is shared under a CC BY-NC-SA 4.0 license and was authored, remixed, and/or curated by Jonathan Gutow.

- **9.1: The Born-Oppenheimer Approximation Simplifies the Schrödinger Equation for Molecules** is licensed CC BY-NC-SA 4.0.

9.2: Valence Bond Theory

9.2.1: Introduction

Valence bond (VB) theory is one of two basic theories, along with molecular orbital (MO) theory, that were developed to use the methods of quantum mechanics to explain chemical bonding. It focuses on how the atomic orbitals of the dissociated atoms combine to give individual chemical bonds when a molecule is formed. In contrast, molecular orbital theory, which will be discussed elsewhere, predicts wavefunctions that cover the entire molecule.

The simplest case to consider is the hydrogen molecule, H_2. When we say that the two hydrogen nuclei share their electrons to form a covalent bond, what we mean in VB theory terms is that the two spherical 1*s* orbitals (the grey spheres in Figure 9.2.1) overlap and contain two electrons.

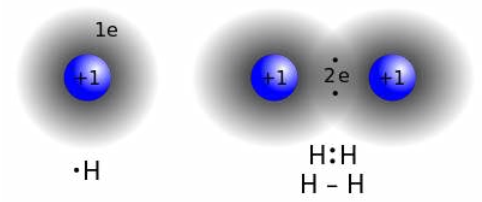


Figure 9.2.1: These two electrons are now attracted to the positive charge of both of the hydrogen nuclei, with the result that they serve as a sort of 'chemical glue' holding the two nuclei together. from Wikipedia (credit: Jacek FH)

How far apart are the two nuclei? If they are too far apart, their respective 1*s* orbitals cannot overlap, and thus no covalent bond can form - they are still just two separate hydrogen atoms. As they move closer and closer together, orbital overlap begins to occur, and a bond begins to form. This lowers the **potential energy** of the system, as new, *attractive* positive-negative electrostatic interactions become possible between the nucleus of one atom and the electron of the second (Figure 9.2.2). However, something else is happening at the same time: as the atoms get closer, the *repulsive* positive-positive interaction between the two nuclei also begins to increase.

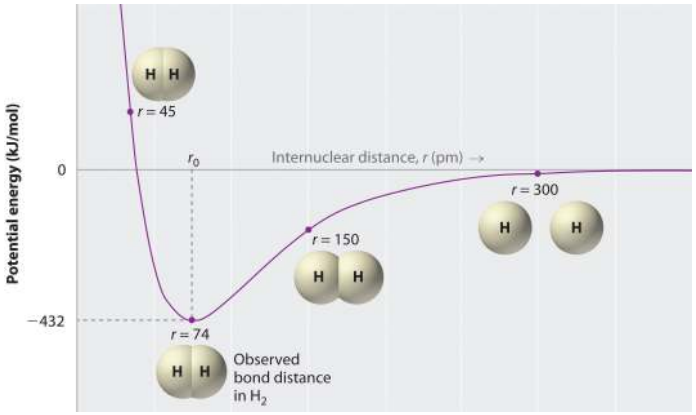


Figure 9.2.2: A plot of potential energy versus internuclear distance for the interaction between two gaseous hydrogen atoms. At long distances, both attractive and repulsive interactions are small. As the distance between the atoms decreases, the attractive electron–proton interactions dominate, and the energy of the system decreases. At the observed bond distance, the repulsive electron–electron and proton–proton interactions just balance the attractive interactions, preventing a further decrease in the internuclear distance. At very short internuclear distances, the repulsive interactions dominate, making the system less stable than the isolated atoms.

At first this repulsion is more than offset by the attraction between nuclei and electrons, but at a certain point, as the nuclei get even closer, the repulsive forces begin to overcome the attractive forces, and the potential energy of the system rises quickly. When the two nuclei are 'too close', we have an unstable, high-energy situation. There is a defined optimal distance between the nuclei in which the potential energy is at a minimum, meaning that the combined attractive and repulsive forces add up to the greatest overall attractive force. This optimal internuclear distance is the **bond length**; the distance is 74 pm for H_2. Likewise, the difference in potential energy between the lowest energy state (at the optimal internuclear distance) and the state where the two atoms are completely separated is called the **bond dissociation energy,** or, more simply**, bond strength**; the H_2 bond strength is 435 kJ/mol.

A comparison of some bond lengths and energies is shown in Table 9.2.1. We can find many of these bonds in a variety of molecules, and this table provides average values. For example, breaking the first C–H bond in CH_4 requires 439.3 kJ/mol, while breaking the first C–H bond in $H–CH_2C_6H_5$ (a common paint thinner) requires 375.5 kJ/mol.

Table 9.2.1: Representative Bond Energies and Lengths

Bond	Length (pm)	Energy (kJ/mol)		Bond	Length (pm)	Energy (kJ/mol)
H–H	74	436		C–O	140.1	358
H–C	106.8	413		C = O	119.7	745
H–N	101.5	391		C ≡ O	113.7	1072
H–O	97.5	467		H–Cl	127.5	431
C–C	150.6	347		H–Br	141.4	366
C = C	133.5	614		H–I	160.9	298
C ≡ C	120.8	839		O–O	148	146
C–N	142.1	305		O = O	120.8	498
C = N	130.0	615		F–F	141.2	159
C ≡ N	116.1	891		Cl–Cl	198.8	243

Example 9.2.1: A Morse Potential Approximation

The Morse potential, named after physicist Philip M. Morse, is a convenient interatomic interaction approximation for the potential energy of a diatomic molecule.

$$V(r) = D_e \left[1 - e^{-\beta(r-r_e)}\right]^2$$

Here r is the distance between the atoms, r_e is the equilibrium bond distance, D_e is the well depth (defined relative to the dissociated atoms), and β controls the 'width' of the potential (the smaller β is, the larger the well). For H_2, the equilibrium bond length $r_e = 74.1\ pm$, the bond energy $D_e = 7.61 \times 10^{-19} J$, and the Morse potential parameter $\beta = 0.0193\ pm^{-1}$.

The force on the system is given by

$$F(r) = -\frac{dV(r)}{dr}$$

Calculate the force for H_2 and explain the status of the system (e.g., compressing, expanding, or stationary) at:

a. 45 pm,
b. 74 pm,
c. 150 pm, and
d. 500 pm.

9.2.2: Overlap

Valence bond theory describes a covalent bond as the overlap of half-filled atomic orbitals (each containing a single electron) that yield a pair of electrons shared between the two bonded atoms. We say that orbitals on two different atoms overlap when a portion of one orbital and a portion of a second orbital occupy the same region of space. According to valence bond theory, a covalent bond results when two conditions are met:

1. an orbital on one atom overlaps an orbital on a second atom and
2. the single electrons in each orbital combine to form an electron pair.

The mutual attraction between this negatively charged electron pair and the two atoms' positively charged nuclei serves to physically link the two atoms through a force we define as a covalent bond. The strength of a covalent bond depends on the extent

of overlap of the orbitals involved. Orbitals that overlap extensively form bonds that are stronger than those that have less overlap.

In addition to the distance between two orbitals, the orientation of orbitals also affects their overlap (other than for two *s* orbitals, which are spherically symmetric). Greater overlap is possible when orbitals are oriented such that they overlap on a direct line between the two nuclei. Figure 9.2.3 illustrates this for two *p* orbitals from different atoms; the overlap is greater when the orbitals overlap end to end rather than at an angle.

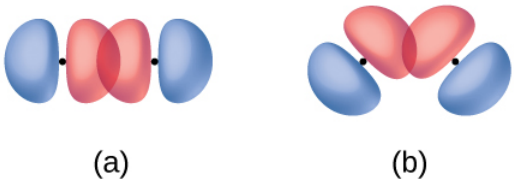


Figure 9.2.3: (a) The overlap of two p orbitals is greatest when the orbitals are directed end to end. (b) Any other arrangement results in less overlap. The dots indicate the locations of the nuclei.

The overlap of two *s* orbitals (as in H_2), the overlap of an *s* orbital and a *p* orbital (as in HCl), and the end-to-end overlap of two *p* orbitals (as in Cl_2) all produce sigma bonds (σ bonds), as illustrated in Figure 9.2.4. A σ bond is a covalent bond in which the electron density is concentrated in the region along the internuclear axis; that is, a line between the nuclei would pass through the center of the overlap region. Single bonds in Lewis structures are described as σ bonds in valence bond theory.

Three diagrams are shown and labeled “a,” “b,” and “c.” Diagram a shows two spherical orbitals lying side by side and overlapping. Diagram b shows one spherical and one peanut-shaped orbital lying near one another so that the spherical orbital overlaps with one end of the peanut-shaped orbital. Diagram c shows two peanut-shaped orbitals lying end to end so that one end of each orbital overlaps the other.

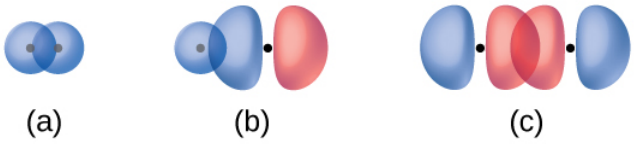


Figure 9.2.4: Sigma (σ) bonds form from the overlap of the following: (a) two s orbitals, (b) an s orbital and a p orbital, and (c) two p orbitals. The dots indicate the locations of the nuclei.

A pi bond (π bond) is a type of covalent bond that results from the side-by-side overlap of two *p* orbitals, as illustrated in Figure 9.2.5. In a π bond, the regions of orbital overlap lie on opposite sides of the internuclear axis. Along the axis itself, there is a node, that is, a plane with no probability of finding an electron.

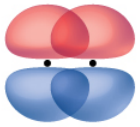
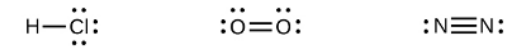


Figure 9.2.5: Pi (π) bonds form from the side-by-side overlap of two p orbitals. The dots indicate the location of the nuclei.

While all single bonds are σ bonds, multiple bonds consist of both σ and π bonds. As the Lewis structures below suggest, O_2 contains a double bond, and N_2 contains a triple bond. The double bond consists of one σ bond and one π bond, and the triple bond consists of one σ bond and two π bonds. Between any two atoms, the first bond formed will always be a σ bond, but there can only be one σ bond in any one location. In any multiple bond, there will be one σ bond, and the remaining one or two bonds will be π bonds. These bonds are described in more detail later in this chapter.

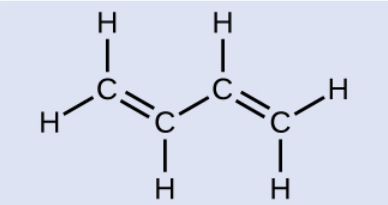


One σ bond	One σ bond	One σ bond
No π bonds	One π bond	Two π bonds

As seen in Table 9.2.2, an average carbon-carbon single bond is 347 kJ/mol, while in a carbon-carbon double bond, the π bond increases the bond strength by 267 kJ/mol. Adding an additional π bond causes a further increase of 225 kJ/mol. We can see a similar pattern when we compare other σ and π bonds. Thus, each individual π bond is generally weaker than a corresponding σ bond between the same two atoms. In a σ bond, there is a greater degree of orbital overlap than in a π bond.

Counting σ and π Bonds

Butadiene, C_6H_6, is used to make synthetic rubber. Identify the number of σ and π bonds contained in this molecule.



Butadiene

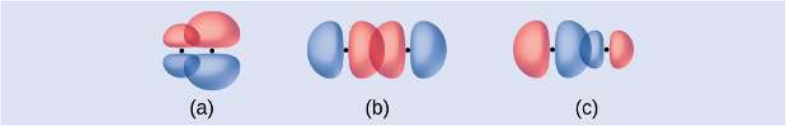
Solution

There are six σ C–H bonds and one σ C–C bond, for a total of seven from the single bonds. There are two double bonds that each have a π bond in addition to the σ bond. This gives a total nine σ and two π bonds overall.

Exercise 9.2.2

Identify each illustration as depicting a σ or π bond:

a. side-by-side overlap of a 4*p* and a 2*p* orbital
b. end-to-end overlap of a 4*p* and 4*p* orbital
c. end-to-end overlap of a 4*p* and a 2*p* orbital



Answer

(a) is a π bond with a node along the axis connecting the nuclei while (b) and (c) are σ bonds that overlap along the axis.

9.2.3: The Valence Bond Wavefunction

In the hydrogen molecule, VB theory uses two electrons (electron 1 and electron 2) in two 1s atomic orbitals (ψ_a and ψ_b) on the hydrogen atoms (atom a and atom b). The simplest description of a H_2 molecule with two electrons and two nuclei is

$$\psi_{simple} = \psi_a(1)\psi_b(2) \tag{9.2.1}$$

Equation 9.2.1 means electron 1 is in ψ_a of atom a and electron 2 is in ψ_b on the atom b. Where ψ_a and ψ_b may be the $1s$ orbitals as the simplest wavefunction ($n = 1$, $l = 0$, $m_l = 0$). The ψ_{simple} wavefunction predicts an energy that is about 6% of the experimental value at a bond length of 0.90 Å, which is considerably longer than the experimental value of 0.74 Å (Table 9.2.1). However, Equation 9.2.1 does not address the *indistinguishability* of the problem, i.e, we **cannot** distinguished each electron from the other.

Distinguishable vs. Indistinguishable Particles

Assume you have two particle A and B in states 1 and 2. If the two particle are *distinguishable*, then by exchanging the particles A and B, you will obtain a new state that will have the same properties as the old state. However, for *indistinguishable* particles, exchanging A and B is a transformation that does nothing and you have the same physical state. This means that for indistinguishable particles, particle labels are unphysical and they represent a redundancy in describing the physical state.

To account for the indistinguishable nature of the two electrons in the system, a covalent wavefunction that is better than Equation 9.2.1 can be constructed (ignoring spin effect):

$$\psi_{covalent} = \psi_a(1)\psi_b(2) + \psi_a(2)\psi_b(1) \tag{9.2.2}$$

Equation 9.2.2 means electron 1 is sometimes in ψ_a on atom a and electron 2 is on the atom b (left term of right hand side of equation) and sometime electron 1 is sometimes in ψ_b on atom b and electron 2 is in ψ_a on the atom a (right term of right hand side of equation). Notice that in contrast to equation 9.2.1, if the two electron labels are switched, the wavefunction in equation 9.2.2 does not change. The potential energy curve for the $\psi_{covalent}$ wavefunction predicts a bond energy that is about 72% at a bond length of 0.87 Å (Table 9.2.2), so the $\psi_{covalent}$ wavefunction is more accurate than ψ_{simple}.

To be more accurate within VB theory, the possibility that both electrons may be on atom a ($\psi_a(1)\psi_a(2)$) or on atom b ($\psi_b(1)\psi_b(2)$) should also be taken into account. This introduces an ionic contribution:

$$\psi_{ionic} = \psi_a(1)\psi_a(2) + \psi_b(2)\psi_b(1) \tag{9.2.3}$$

Notice that equation 9.2.3 addresses indistinguishability since the wavefunction is unchanged if the two electron labels are switched. The more complete VB wavefunction is a linear combination of both $\psi_{covalent}$ and ψ_{ionic}:

$$\psi_{AB} = \Psi_{covalent} + \lambda\psi_{ionic} \tag{9.2.4}$$

where λ quantifies the amount of ionic character to the bond, e.g., if $\lambda = 0$, then the bond is purely covalent. The potential energy curve for the ψ_{AB} wavefunction predicts a bond energy that is ~80% of the experimental value and a reasonably accurate bond length of 0.77 pm (Table 9.2.2). Additional tinkering with the wavefunction leads to even better results, but is beyond the scope of this discussion. It should be noted that the wavefunctions in equations 9.2.2, 9.2.3, and 9.2.4 are unnormalized.

Table 9.2.2: Valence Bond Theory Results for H_2

Wavefunction	Bond Energy (kJ mol^{-1})	Bond Length (Å)
Experiment	435	0.74
ψ_{simple}	25	0.90
$\psi_{covalent}$	301	0.87
ψ_{AB}	335	0.77

Two-Atom Bonds

The central gist of VB theory is that a covalent bond is formed between the **two** atoms by the overlap of half filled valence **atomic orbitals** of each atom containing one unpaired electron.

Linus Pauling used the pair bonding ideas of Lewis together with Heitler–London theory to develop two key concepts in VB theory: **resonance** and **orbital hybridization**. These will be addressed in later.

9.2.4: Summary

Valence bond theory describes bonding as a consequence of the overlap of two separate atomic orbitals on different atoms that creates a region with one pair of electrons shared between the two atoms. When the orbitals overlap along an axis containing the nuclei, they form a σ bond. When they overlap in a fashion that creates a node along this axis, they form a π bond.

9.2.5: Contributors and Attributions

- Organic Chemistry With a Biological Emphasis by Tim Soderberg (University of Minnesota, Morris)
- Paul Flowers (University of North Carolina - Pembroke), Klaus Theopold (University of Delaware) and Richard Langley (Stephen F. Austin State University) with contributing authors. Textbook content produced by OpenStax College is licensed under a Creative Commons Attribution License 4.0 license. Download for free at http://cnx.org/contents/85abf193-2bd...a7ac8df6@9.110).
- http://physics.stackexchange.com
- J. Gutow (UW Oshkosh)

This page titled 9.2: Valence Bond Theory is shared under a CC BY-NC-SA 4.0 license and was authored, remixed, and/or curated by Jonathan Gutow.

- **12.2: Valence Bond Theory** is licensed CC BY-NC-SA 4.0.

9.3: Hybridization of Atomic Orbitals

9.3.1: Introduction

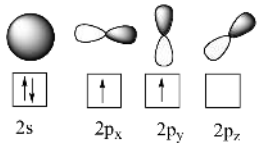
Hybridization was introduced to explain molecular structure when the valence bond theory failed to correctly predict them. It is experimentally observed that bond angles in organic compounds are close to 109°, 120°, or 180°. According to Valence Shell Electron Pair Repulsion (VSEPR) theory, electron pairs repel each other and the bonds and lone pairs around a central atom are generally separated by the largest possible angles.

In this section, we will use a model called **valence bond theory** to describe bonding in molecules. In this model, bonds are considered to form from the overlapping of two atomic orbitals on different atoms, each orbital containing a single electron. In looking at simple inorganic molecules such as H_2 or HF, our present understanding of s and p atomic orbitals will suffice. In order to explain the bonding in organic molecules, however, we will need to introduce the concept of **hybrid orbitals**.

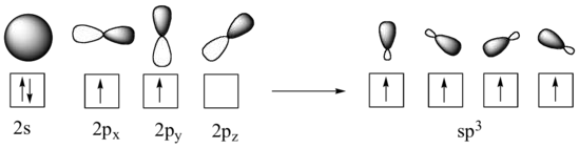
Interactive website on hybrid orbitals.

9.3.2: Hybrid orbitals: sp^3 hybridization and tetrahedral bonding

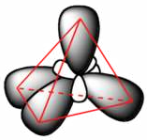
Now let's turn to methane, the simplest organic molecule. Recall the valence electron configuration of the central carbon:



This picture, however, is problematic. How does the carbon form four bonds if it has only two half-filled *p* orbitals available for bonding? A hint comes from the experimental observation that the four C-H bonds in methane are arranged with tetrahedral geometry about the central carbon, and that each bond has the same length and strength. In order to explain this observation, valence bond theory relies on a concept called **orbital hybridization**. In this picture, the four valence orbitals of the carbon (one 2*s* and three 2*p* orbitals) combine mathematically (remember: orbitals are described by equations) to form four equivalent **hybrid orbitals**, which are named **sp^3 orbitals** because they are formed from mixing one s and three p orbitals. In the new electron configuration, each of the four valence electrons on the carbon occupies a single sp^3 orbital.

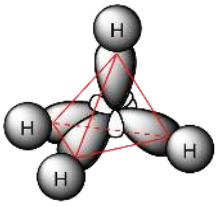


The sp^3 hybrid orbitals, like the *p* orbitals of which they are partially composed, are oblong in shape, and have two lobes of opposite sign. Unlike the *p* orbitals, however, the two lobes are of very different size. The larger lobes of the sp^3 hybrids are directed towards the four corners of a tetrahedron, meaning that the angle between any two orbitals is 109.5°.



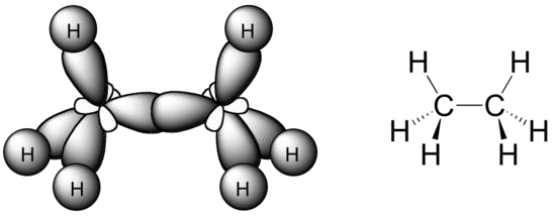
This geometric arrangement makes perfect sense if you consider that it is precisely this angle that allows the four orbitals (and the electrons in them) to be as far apart from each other as possible. This is simply a restatement of the Valence Shell Electron Pair Repulsion (VSEPR) theory that you learned in General Chemistry: electron pairs (in orbitals) will arrange themselves in such a way as to remain as far apart as possible, due to negative-negative electrostatic repulsion.

Each C-H bond in methane, then, can be described as an overlap between a half-filled 1*s* orbital in a hydrogen atom and the larger lobe of one of the four half-filled sp^3 hybrid orbitals in the central carbon. The length of the carbon-hydrogen bonds in methane is 1.09 Å (1.09×10^{-10} m).

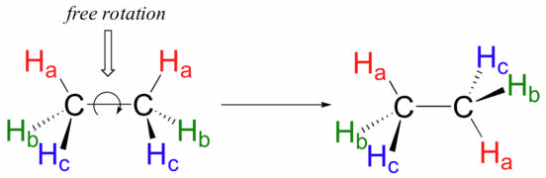


interactive 3D model of the bonding in methane

In the ethane molecule, the bonding picture according to valence orbital theory is very similar to that of methane. Both carbons are sp^3-hybridized, meaning that both have four bonds arranged with tetrahedral geometry. The carbon-carbon bond, with a bond length of 1.54 Å, is formed by overlap of one sp^3 orbital from each of the carbons, while the six carbon-hydrogen bonds are formed from overlaps between the remaining sp^3 orbitals on the two carbons and the 1*s* orbitals of hydrogen atoms. All of these are sigma bonds.

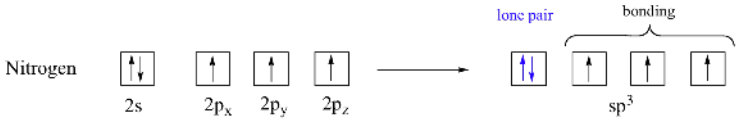


Because they are formed from the end-on-end overlap of two orbitals, *sigma bonds are free to rotate*. This means, in the case of ethane molecule, that the two methyl (CH_3) groups can be pictured as two wheels on a hub, each one able to rotate freely with respect to the other.

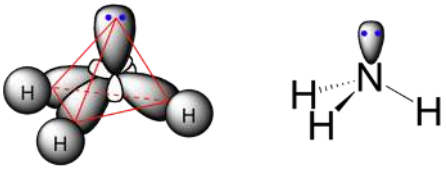


Rotational freedom in sigma bonds leads to the multiple conformations of organic molecules.

The sp^3 bonding picture is also used to described the bonding in amines, including ammonia, the simplest amine. Just like the carbon atom in methane, the central nitrogen in ammonia is sp^3-hybridized. With nitrogen, however, there are five rather than four valence electrons to account for, meaning that three of the four hybrid orbitals are half-filled and available for bonding, while the fourth is fully occupied by a (non-bonding) pair of electrons.

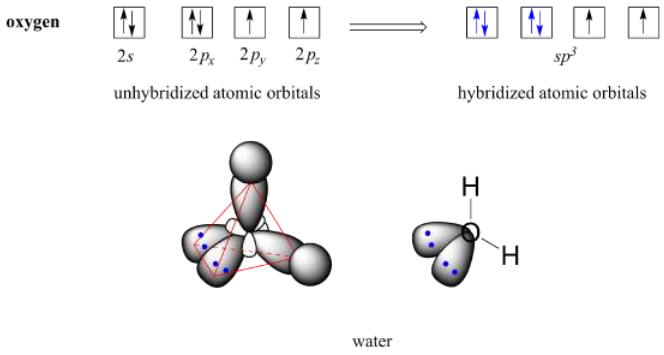


The bonding arrangement here is also tetrahedral: the three N-H bonds of ammonia can be pictured as forming the base of a trigonal pyramid, with the fourth orbital, containing the lone pair, forming the top of the pyramid.



Recall from your study of VSEPR theory in General Chemistry that the lone pair, with its slightly greater repulsive effect, 'pushes' the three N-H sigma bonds away from the top of the pyramid, meaning that the H-N-H bond angles are slightly less than tetrahedral, at 107.3˚ rather than 109.5˚.

VSEPR theory also predicts, accurately, that a water molecule is 'bent' at an angle of approximately 104.5˚. It would seem logical, then, to describe the bonding in water as occurring through the overlap of sp^3-hybrid orbitals on oxygen with 1sorbitals on the two hydrogen atoms. In this model, the two nonbonding lone pairs on oxygen would be located in sp^3 orbitals.



? Exercise

Draw, in the same style as the figures above, an orbital picture for the bonding in methylamine.

Solution

9.3.3: Mathematical form of sp^3 hybrids[1]

The four unnormalized hybrid sp^3 orbitals are the following combinations of the valence s and p orbitals:

$$h_1 = s + p_x + p_y + p_z \qquad h_2 = s - p_x - p_y + p_z$$

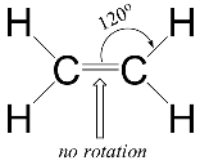
$$h_3 = s - p_x + p_y - p_z \qquad h_2 = s + p_x - p_y - p_z$$

Live 3-D view based on quantum computations: https://cms.gutow.uwosh.edu/gutow/Orbitals/N/sp3%20hybrid.shtml

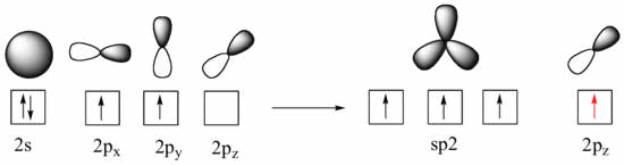
9.3.4: Formation of pi bonds - sp^2 and sp hybridization

The valence bond theory, along with the hybrid orbital concept, does a very good job of describing double-bonded compounds such as ethene. Three experimentally observable characteristics of the ethene molecule need to be accounted for by a bonding model:

1. Ethene is a planar (flat) molecule.
2. Bond angles in ethene are approximately 120°, and the carbon-carbon bond length is 1.34 Å, significantly shorter than the 1.54 Å single carbon-carbon bond in ethane.
3. There is a significant barrier to rotation about the carbon-carbon double bond.

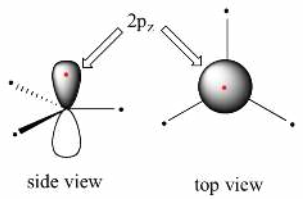


Clearly, these characteristics are not consistent with an sp^3 hybrid bonding picture for the two carbon atoms. Instead, the bonding in ethene is described by a model involving the participation of a different kind of hybrid orbital. Three atomic orbitals on each carbon – the 2*s*, $2p_x$ and $2p_y$ orbitals – combine to form three sp^2 hybrids, leaving the $2p_z$ orbital unhybridized.

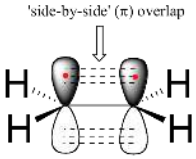


The three sp^2 hybrids are arranged with trigonal planar geometry, pointing to the three corners of an equilateral triangle, with angles of 120°between them. The unhybridized $2p_z$ orbital is *perpendicular* to this plane (in the next several figures, sp^2 orbitals

and the sigma bonds to which they contribute are represented by lines and wedges; only the $2p_z$ orbitals are shown in the 'space-filling' mode).



The carbon-carbon double bond in ethene consists of one sigma bond, formed by the overlap of two sp^2 orbitals, and a second bond, called a **π (pi) bond**, which is formed by the *side-by-side* overlap of the two unhybridized $2p_z$ orbitals from each carbon.

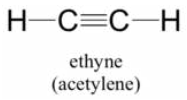


interactive model

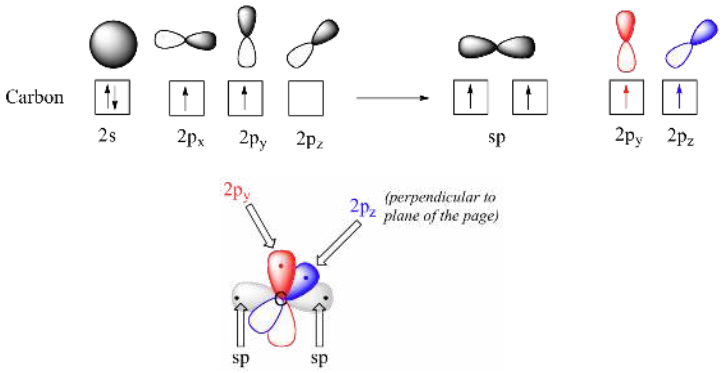
another interactive model

The pi bond does *not* have cylindrical symmetry about the bond. Because they are the result of side-by-side overlap (rather then end-to-end overlap like a sigma bond), *pi bonds are not free to rotate.* If rotation about this bond were to occur, it would involve disrupting the side-by-side overlap between the two $2p_z$ orbitals that make up the pi bond. The presence of the pi bond thus 'locks' the six atoms of ethene into the same plane.

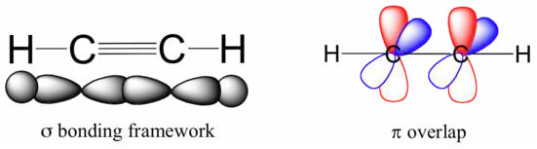
Finally, the hybrid orbital concept applies well to triple-bonded groups, such as alkynes and nitriles. Consider, for example, the structure of ethyne (common name acetylene), the simplest alkyne.



This molecule is linear: all four atoms lie in a straight line. The carbon-carbon triple bond is only 1.20Å long. In the hybrid orbital picture of acetylene, both carbons are **sp-hybridized**. In an sp-hybridized carbon, the 2*s* orbital combines with the $2p_x$ orbital to form two sp hybrid orbitals that are oriented at an angle of 180°with respect to each other (eg. along the x axis). The $2p_y$ and $2p_z$ orbitals remain unhybridized, and are oriented perpendicularly along the y and z axes, respectively.



The C-C sigma bond, then, is formed by the overlap of one sp orbital from each of the carbons, while the two C-H sigma bonds are formed by the overlap of the second sp orbital on each carbon with a 1*s* orbital on a hydrogen. Each carbon atom still has two half-filled $2p_y$ and $2p_z$ orbitals, which are perpendicular both to each other and to the line formed by the sigma bonds. These two perpendicular pairs of *p* orbitals form two pi bonds between the carbons, resulting in a triple bond overall (one sigma bond plus two pi bonds).



another view

9.3.5: Mathematical form of sp and sp^2 hybrid[1]

sp

The two unnormalized sp hybrids are:

$$h_1 = s + p_z \qquad h_2 = s - p_z \tag{9.3.1}$$

Giving two orbitals with their major lobes pointing 180˚ apart. By convention these lobes are chosen to point along the z-axis.

Live 3-D view based on quantum computations: https://cms.gutow.uwosh.edu/gutow/Orbitals/N/sp%20hybrid.shtml

sp^2

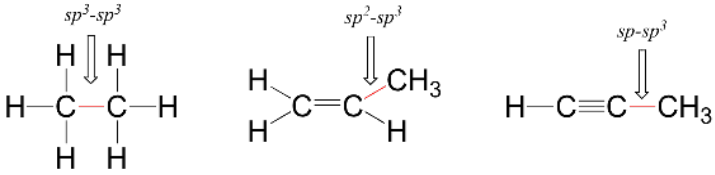
The three unnormalized sp^2 hybrids are:

$$h_1 = s + \sqrt{1/2}p_y \qquad h_2 = s + \sqrt{3/2}p_x - \sqrt{1/2}p_z \qquad h_3 = s - \sqrt{3/2}p_x - \sqrt{1/2}p_z \tag{9.3.2}$$

Live 3-D view based on quantum computations: https://cms.gutow.uwosh.edu/gutow/Orbitals/N/sp2%20hybrid.shtml

9.3.6: Hybridization and bond lengths

The hybrid orbital concept nicely explains another experimental observation: single bonds adjacent to double and triple bonds are progressively shorter and stronger than 'normal' single bonds, such as the one in a simple alkane. The carbon-carbon bond in ethane (structure A below) results from the overlap of two sp^3 orbitals.



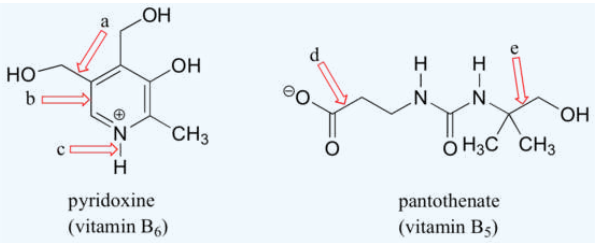
In alkene B, however, the carbon-carbon single bond is the result of overlap between an sp^2 orbital and an sp^3 orbital, while in alkyne C the carbon-carbon single bond is the result of overlap between an sp orbital and an sp^3 orbital. These are all single bonds, but the bond in molecule C is shorter and stronger than the one in B, which is in turn shorter and stronger than the one in A.

The explanation here is relatively straightforward. An sp orbital is composed of one *s* orbital and one *p* orbital, and thus it has 50% *s* character and 50% *p* character. sp^2 orbitals, by comparison, have 33% *s* character and 67% *p* character, while sp^3 orbitals have 25% *s* character and 75% *p* character. Because of their spherical shape, 2*s* orbitals are smaller, and hold electrons closer and 'tighter' to the nucleus, compared to 2*p* orbitals. Consequently, bonds involving sp + sp^3 overlap (as in alkyne C) are shorter and stronger than bonds involving sp^2 + sp^3 overlap (as in alkene B). Bonds involving sp^3-sp^3overlap (as in alkane A) are the longest and weakest of the group, because of the 75% '*p*' character of the hybrids.

Example

For each of the bonds indicated by arrows a-e in the figures below, describe the bonding picture by completing this sentence:

"The sigma bond indicated by this arrow is formed by the overlap of an _____ orbital of a _____atom and an _____orbital of a _____atom."



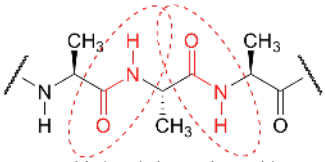
Solution

9.3.7: Resonance

The valence bond model does not account well for electron delocalization. Just as with Lewis structures this is accounted for by making resonance hybrids. In this case the overall wavefunction is a weighted linear combination of the valence bond wavefunctions for all of the resonance hybids:

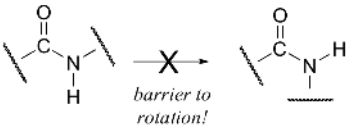
$$\Psi_{resonance\ hybrid} = a\psi_1 + b\psi_2 + \ldots$$

An example of where this is important is in peptide bonds that link amino acids to form polypeptides and proteins.

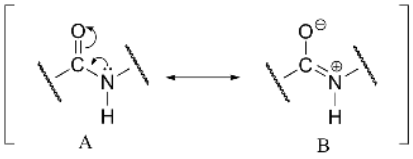


peptide bonds in a polypeptide

Critical to the structure of proteins is the fact that, although it is conventionally drawn as a single bond, the C-N bond in a peptide linkage has a significant barrier to rotation, almost as if it were a double bond.



This, along with the observation that the bonding around the peptide nitrogen has trigonal planar geometry, strongly suggests that the nitrogen is sp^2-hybridized. An important resonance contributor has a C=N double bond and a C-O single bond, with a separation of charge between the oxygen and the nitrogen.



Although B is a minor contributor due to the separation of charges, it is still very relevant in terms of peptide and protein structure – our proteins would simply not fold up properly if there was free rotation about the peptide C-N bond.

9.3.8: Contributors and Attributions

1. P. Atkins, J. De Paula, *Physical Chemistry for the Life Sciences*, 2ed. (W.H. Freeman and Company, New York, 2011) Pp. 369 - 372.

- Organic Chemistry With a Biological Emphasis by Tim Soderberg (University of Minnesota, Morris)
- Jonathan Gutow (UW Oshkosh)

This page titled 9.3: Hybridization of Atomic Orbitals is shared under a CC BY-NC-SA 4.0 license and was authored, remixed, and/or curated by Jonathan Gutow.

- **12.3: Hybridization of Atomic Orbitals** is licensed CC BY-NC-SA 4.0.
- **12.7: Resonance and Electron Delocalization** is licensed CC BY-NC-SA 4.0.

9.4: Molecular Orbital Theory

9.4.1: Introduction

None of the approaches we have described so far can adequately explain why some compounds are colored and others are not, why some substances with unpaired electrons are stable, and why others are effective semiconductors. These approaches also cannot describe the nature of resonance. Such limitations led to the development of a new approach to bonding in which electrons are *not* viewed as being localized between the nuclei of bonded atoms but are instead delocalized throughout the entire molecule. Just as with the valence bond theory, the approach we are about to discuss is based on a quantum mechanical model.

Previously, we described the electrons in isolated atoms as having certain spatial distributions, called *orbitals*, each with a particular *orbital energy*. Just as the positions and energies of electrons in *atoms* can be described in terms of *atomic orbitals* (AOs), the positions and energies of electrons in *molecules* can be described in terms of molecular orbitals (MOs) A particular spatial distribution of electrons in a molecule that is associated with a particular orbital energy. As the name suggests, molecular orbitals are not localized on a single atom but extend over the entire molecule. Consequently, the molecular orbital approach, called molecular orbital theory is a *delocalized* approach to bonding.

Although the molecular orbital theory is computationally demanding, the principles on which it is based are similar to those we used to determine electron configurations for atoms. The key difference is that in molecular orbitals, the electrons are allowed to interact with more than one atomic nucleus at a time. Just as with atomic orbitals, we create an energy-level diagram by listing the molecular orbitals in order of increasing energy. We then fill the orbitals with the required number of valence electrons according to the Pauli principle. This means that each molecular orbital can accommodate a maximum of two electrons with opposite spins.

9.4.2: The Hydrogen Molecule-Ion

Molecular orbital theory is a conceptual extension of the orbital model, which was so successfully applied to atomic structure. As was once playfully remarked, "a molecule is nothing more than an atom with more nuclei." This may be overly simplistic, but we do attempt as far as possible, to exploit analogies with atomic structure. Our understanding of atomic orbitals began with the exact solutions of a prototype problem – the hydrogen atom. We will begin our study of homonuclear diatomic molecules beginning with another exactly solvable prototype, the hydrogen molecule-ion H_2^+. This species actually has a transient existence in electrical discharges through hydrogen gas and has been detected by mass spectrometry. It also has been detected in outer space. The Schrödinger equation for H_2^+ can be solved exactly within the Born-Oppenheimer approximation. For fixed internuclear distance *R*, this reduces to a problem of one electron in the field of two protons, designated A and B. We can write

$$\hat{H}_{elec}(\vec{r},R)=\frac{-\hbar^2}{2m_e}\nabla^2+\frac{e^2}{4\pi\epsilon_o}\left(\frac{z_Az_B}{R}+\frac{-z_A}{r_A}+\frac{-z_B}{r_B}\right)=\frac{-\hbar^2}{2m_e}\nabla^2+\frac{e^2}{4\pi\epsilon_o}\left(\frac{1}{R}+\frac{-1}{r_A}+\frac{-1}{r_B}\right) \tag{9.4.1}$$

So, the Schrödinger equation to solve is:

$$\hat{H}_{elec}(\vec{r},R)\phi_e(\vec{r},R)=E_e(R)\phi_e(\vec{r},R) \tag{9.4.2}$$

where r_A and r_B are the distances from the electron to protons A and B, respectively. This equation was solved by Burrau (1927), after separating the variables in prolate spheroidal coordinates.

9.4.3: Molecular Orbitals Involving Only *ns* Atomic Orbitals

We begin our discussion of molecular orbitals with the simplest molecule, H_2, formed from two isolated hydrogen atoms, each with a $1s^1$ electron configuration. As discussed before, electrons can behave like waves. In the molecular orbital approach, the overlapping atomic orbitals are described by mathematical equations called *wave functions*. The 1*s* atomic orbitals on the two hydrogen atoms interact to form two new molecular orbitals, one produced by taking the *sum* of the two H 1*s* wave functions, and the other produced by taking their *difference*:

$$\begin{aligned} MO(1) &= AO(atom\ A) + AO(atom B) \\ MO(1) &= AO(atom\ A) - AO(atom B) \end{aligned} \tag{9.4.3}$$

The molecular orbitals created from the sum and the difference of two wavefunctions (atomic orbitals) from Equation 9.4.3 are called Linear Combinations of Atomic Orbitals (LCAOs). A molecule **must** have as many molecular orbitals as there are atomic orbitals.

Adding two atomic orbitals corresponds to *constructive* interference between two waves, thus reinforcing their intensity; the internuclear electron probability density is *increased*. The molecular orbital corresponding to the sum of the two H 1*s* orbitals is called a σ_{1s} combination (pronounced "sigma one ess") (part (a) and part (b) in Figure 9.4.1). The sigma (σ) orbital has cylindrical symmetry about the internuclear axis; that is, all cross-sections perpendicular to the internuclear axis are circles. The subscript 1*s* denotes the atomic orbitals from which the molecular orbital was derived.

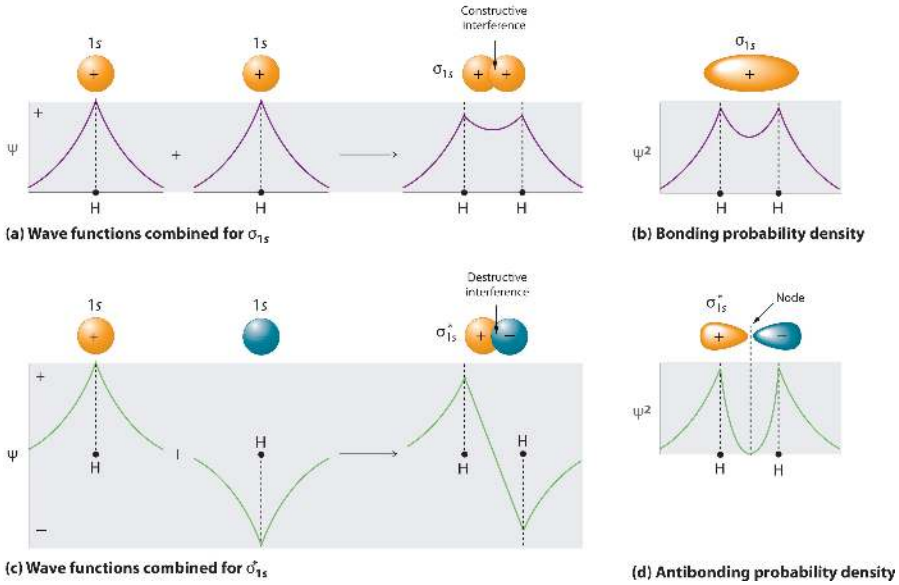


Figure 9.4.1: Molecular Orbitals for the H_2 Molecule**.** (a) This diagram shows the formation of a bonding σ_{1s} molecular orbital for H_2 as the sum of the wave functions (Ψ) of two H 1*s* atomic orbitals. (b) This plot of the square of the wave function (Ψ^2) for the bonding σ_{1s} molecular orbital illustrates the increased electron probability density between the two hydrogen nuclei. (Recall that the probability density is proportional to the *square* of the wave function.) (c) This diagram shows the formation of an antibonding σ^*_{1s} *molecular orbital for* H_2 *as the difference of the wave functions (Ψ) of two H 1s atomic orbitals. (d) This plot of the square of the wave function* (Ψ^2) *for the* σ^*_{1s} *antibonding molecular orbital illustrates the node corresponding to zero electron probability density between the two hydrogen nuclei.*

$$\sigma_{1s} \approx 1s\,(A) + 1s\,(B) \tag{9.4.4}$$

The ≈ sign is used rather than an = sign because we are ignoring certain constants that are not important to our argument. This is the bonding orbital, which is lower energy than the two non-interacting 1s orbitals. The decrease in energy can be thought of as arising from the added electron density between the nuclei, which reduces the repulsion of the nuclei by shielding them from each other.

Conversely, subtracting one atomic orbital from another corresponds to *destructive* interference between two waves, which reduces their intensity and causes a *decrease* in the internuclear electron probability density (part (c) and part (d) in Figure 9.4.1). The resulting pattern contains a *node* where the electron density is zero. The molecular orbital corresponding to the difference is called σ^*_{1s} ("sigma one ess star"). This sigma star (σ*) orbital is an antibonding molecular orbital in which there is a region of zero electron probability (a nodal plane) perpendicular to the internuclear axis.

$$\sigma^\star_{1s} \approx 1s\,(A) - 1s\,(B) \tag{9.4.5}$$

Key Ideas

- A molecule must have as many molecular orbitals as there are atomic orbitals.
- Antibonding orbitals contain a node perpendicular to the internuclear axis; bonding orbitals do not.

9.4.4: Energy-Level Diagrams

Because electrons in the σ_{1s} orbital interact simultaneously with both nuclei, they have a lower energy than electrons that interact with only one nucleus. This means that the σ_{1s} molecular orbital has a *lower* energy than either of the hydrogen 1*s* atomic orbitals.

Conversely, electrons in the σ^*_{1s} orbital interact with only one hydrogen nucleus at a time. In addition, they are farther away from the nucleus than they were in the parent hydrogen 1*s* atomic orbitals. Consequently, the σ^*_{1s} molecular orbital has a *higher* energy than either of the hydrogen 1*s* atomic orbitals. The σ_{1s} (bonding) molecular orbital is *stabilized* relative to the 1*s* atomic orbitals, and the σ^*_{1s} (antibonding) molecular orbital is *destabilized*. The relative energy levels of these orbitals are shown in the energy-level diagram (a schematic drawing that compares the energies of the molecular orbitals (bonding, antibonding, and nonbonding) with the energies of the parent atomic orbitals) in Figure 9.4.2

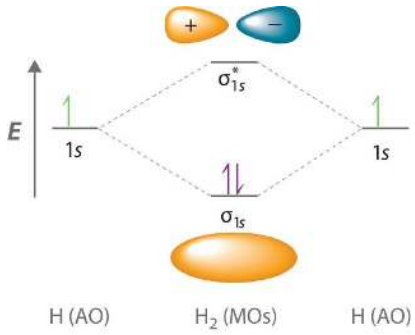


Figure 9.4.2: Molecular Orbital Energy-Level Diagram for H_2. The two available electrons (one from each H atom) in this diagram fill the bonding σ_{1s} molecular orbital. Because the energy of the σ_{1s} molecular orbital is lower than that of the two H 1*s* atomic orbitals, the H_2 molecule is more stable (at a lower energy) than the two isolated H atoms.

> A bonding molecular orbital is *always* lower in energy (more stable) than the component atomic orbitals, whereas an antibonding molecular orbital is *always* higher in energy (less stable).

To describe the bonding in a homonuclear diatomic molecule (a molecule that consists of two atoms of the same element) such as H_2, we use molecular orbitals; that is, for a molecule in which two identical atoms interact, we insert the total number of valence electrons into the energy-level diagram (Figure 9.4.2). We fill the orbitals according to the Pauli principle and Hund's rule: each orbital can accommodate a maximum of two electrons with opposite spins, and the orbitals are filled in order of increasing energy. Because each H atom contributes one valence electron, the resulting two electrons are exactly enough to fill the σ_{1s} bonding molecular orbital. The two electrons enter an orbital whose energy is lower than that of the parent atomic orbitals, so the H_2 molecule is more stable than the two isolated hydrogen atoms. Thus molecular orbital theory correctly predicts that H_2 is a stable molecule. Because bonds form when electrons are concentrated in the space between nuclei, this approach is also consistent with concept of electron-pair bonds.

9.4.5: Bond Order in Molecular Orbital Theory

In the Lewis electron structures, the number of electron pairs holding two atoms together was called the *bond order*. In the molecular orbital approach, bond order is defined as one-half the *net* number of bonding electrons:

$$bond\ order = \frac{number\ of\ bonding\ electrons - number\ of\ antibonding\ electrons}{2} \tag{9.4.6}$$

To calculate the bond order of H_2, we see from Figure 9.4.2 that the σ_{1s} (bonding) molecular orbital contains two electrons, while the σ^*_{1s} (antibonding) molecular orbital is empty. The bond order of H_2 is therefore

$$\frac{2-0}{2} = 1 \tag{9.4.7}$$

This result corresponds to the single covalent bond predicted by Lewis dot symbols. Thus molecular orbital theory and the Lewis electron-pair approach agree that a single bond containing two electrons has a bond order of 1. Double and triple bonds contain four or six electrons, respectively, and correspond to bond orders of 2 and 3.

We can use energy-level diagrams such as the one in Figure 9.4.2 to describe the bonding in other pairs of atoms and ions where *n* = 1, such as the H_2^+ ion, the He_2^+ ion, and the He_2 molecule. Again, we fill the lowest-energy molecular orbitals first while being sure not to violate the Pauli principle or Hund's rule.

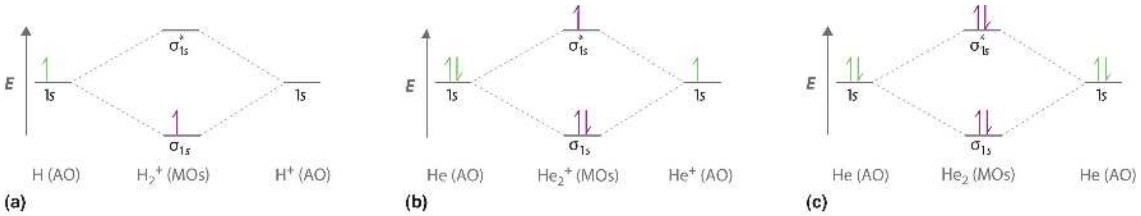


Figure 9.4.3: Molecular Orbital Energy-Level Diagrams for Diatomic Molecules with Only 1 s Atomic Orbitals. (a) The H_2^+ ion, (b) the He_2^+ ion, and (c) the He_2 molecule are shown here.

Part (a) in Figure 9.4.3 shows the energy-level diagram for the H_2^+ ion, which contains two protons and only one electron. The single electron occupies the σ_{1s} bonding molecular orbital, giving a $(\sigma_{1s})^1$ electron configuration. The number of electrons in an orbital is indicated by a superscript. In this case, the bond order is (1-0)/2=1/2 Because the bond order is greater than zero, the H_2^+ ion should be more stable than an isolated H atom and a proton. We can therefore use a molecular orbital energy-level diagram and the calculated bond order to predict the relative stability of species such as H_2^+. With a bond order of only 1/2 the bond in H_2^+ should be weaker than in the H_2 molecule, and the H–H bond should be longer. As shown in Table 9.4.1, these predictions agree with the experimental data.

Part (b) in Figure 9.4.3 is the molecular orbital energy-level diagram for He_2^+. This ion has a total of three valence electrons. Because the first two electrons completely fill the σ_{1s} molecular orbital, the Pauli principle states that the third electron must be in the $\sigma_{1s}^\star$ antibonding orbital, giving a $(\sigma_{1s})^2(\sigma_{1s}^\star)^1$ electron configuration. This electron configuration gives a bond order of (2-1)/2=1/2. As with H_2^+, the He_2^+ ion should be stable, but the He–He bond should be weaker and longer than in H_2. In fact, the He_2^+ ion can be prepared, and its properties are consistent with our predictions (Table 9.4.1).

Table 9.4.1: Molecular Orbital Electron Configurations, Bond Orders, Bond Lengths, and Bond Energies for some Simple Homonuclear Diatomic Molecules and Ions

Molecule or Ion	Electron Configuration	Bond Order	Bond Length (pm)	Bond Energy (kJ/mol)
H_2^+	$(\sigma_{1s})^1$	1/2	106	269
H_2	$(\sigma_{1s})^2$	1	74	436
He_2^+	$(\sigma_{1s})^2(\sigma_{1s}^\star)^1$	1/2	108	251
He_2	$(\sigma_{1s})^2(\sigma_{1s}^\star)^2$	0	not observed	not observed

Finally, we examine the He_2 molecule, formed from two He atoms with $1s^2$ electron configurations. Part (c) in Figure 9.4.3 is the molecular orbital energy-level diagram for He_2. With a total of four valence electrons, both the σ_{1s} bonding and $\sigma_{1s}^\star$ antibonding orbitals must contain two electrons. This gives a $(\sigma_{1s})^2(\sigma_{1s}^\star)^2$ electron configuration, with a predicted bond order of $(2-2)\div 2 = 0$, which indicates that the He_2 molecule has no net bond and is not a stable species. Experiments show that the He_2 molecule is actually *less* stable than two isolated He atoms due to unfavorable electron–electron and nucleus–nucleus interactions.

In molecular orbital theory, *electrons in antibonding orbitals effectively cancel the stabilization resulting from electrons in bonding orbitals*. Consequently, any system that has equal numbers of bonding and antibonding electrons will have a bond order of 0, and it is predicted to be unstable and therefore not to exist in nature. In contrast to Lewis electron structures and the valence bond approach, molecular orbital theory is able to accommodate systems with an odd number of electrons, such as the H_2^+ ion.

Note

In contrast to Lewis electron structures and the valence bond approach, molecular orbital theory can accommodate systems with an odd number of electrons.

Example 9.4.1

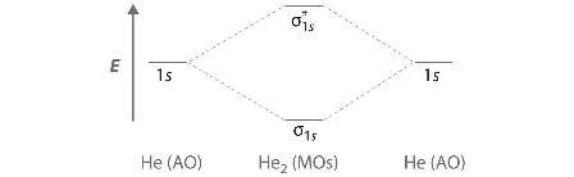
Use a molecular orbital energy-level diagram, such as those in Figure 9.4.3, to predict the bond order in the He_2^{2+} ion. Is this a stable species?

Strategy:

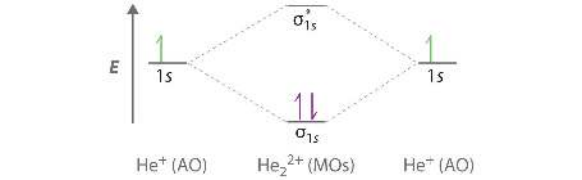
A. Combine the two He valence atomic orbitals to produce bonding and antibonding molecular orbitals. Draw the molecular orbital energy-level diagram for the system.
B. Determine the total number of valence electrons in the He_2^{2+} ion. Fill the molecular orbitals in the energy-level diagram beginning with the orbital with the lowest energy. Be sure to obey the Pauli principle and Hund's rule while doing so.
C. Calculate the bond order and predict whether the species is stable.

Solution:

A Two He 1*s* atomic orbitals combine to give two molecular orbitals: a σ_{1s} bonding orbital at lower energy than the atomic orbitals and a $\sigma_{1s}^{\star}$ antibonding orbital at higher energy. The bonding in any diatomic molecule with two He atoms can be described using the following molecular orbital diagram:



B The He_2^{2+} ion has only two valence electrons (two from each He atom minus two for the +2 charge). We can also view He_2^{2+} as being formed from two He^{+} ions, each of which has a single valence electron in the 1*s* atomic orbital. We can now fill the molecular orbital diagram:



The two electrons occupy the lowest-energy molecular orbital, which is the bonding (σ_{1s}) orbital, giving a $(\sigma_{1s})^2$ electron configuration. To avoid violating the Pauli principle, the electron spins must be paired. **C** So the bond order is

$$\frac{2-0}{2}=1$$

He_2^{2+} is therefore predicted to contain a single He–He bond. Thus it should be a stable species.

? Exercise 9.4.1

Use a molecular orbital energy-level diagram to predict the valence-electron configuration and bond order of the H_2^{2-} ion. Is this a stable species?

Answer:

H_2^{2-} has a valence electron configuration of $(\sigma_{1s})^2(\sigma_{1s}^{\star})^2$ with a bond order of 0. It is therefore predicted to be unstable.

So far, our discussion of molecular orbitals has been confined to the interaction of valence orbitals, which tend to lie farthest from the nucleus. When two atoms are close enough for their valence orbitals to overlap significantly, the filled inner electron shells are largely unperturbed; hence they do not need to be considered in a molecular orbital scheme. Also, when the inner orbitals are completely filled, they contain exactly enough electrons to completely fill both the bonding and antibonding molecular orbitals that arise from their interaction. Thus the interaction of filled shells always gives a bond order of 0, so filled shells are not a factor when predicting the stability of a species. This means that we can focus our attention on the molecular orbitals derived from valence atomic orbitals.

A molecular orbital diagram that can be applied to any **homonuclear diatomic molecule**. The diagram for two identical alkali metal atoms (Li_2 and Cs_2, for example) is shown in part (a) in Figure 9.4.4, where M represents the metal atom. Only two energy levels are important for describing the valence electron molecular orbitals of these species: a σ_{ns} bonding molecular orbital and a σ^{*}_{ns} antibonding molecular orbital. Because each alkali metal (M) has an ns^1 valence electron configuration, the M_2 molecule has

two valence electrons that fill the σ_{ns} bonding orbital. As a result, a bond order of 1 is predicted for all homonuclear diatomic species formed from the alkali metals (Li_2, Na_2, K_2, Rb_2, and Cs_2). The general features of these M_2 diagrams are identical to the diagram for the H_2 molecule in Figure 9.4.2. Experimentally, all are found to be stable in the gas phase, and some are even stable in solution.

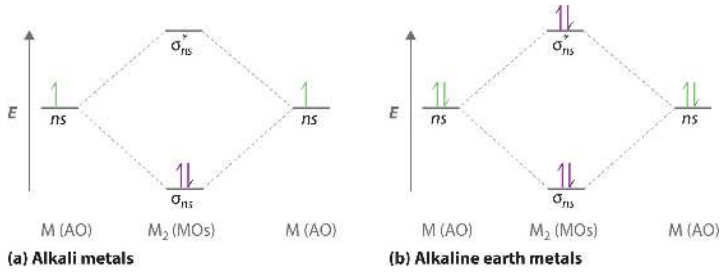


Figure 9.4.4: Molecular Orbital Energy-Level Diagrams for Alkali Metal and Alkaline Earth Metal Diatomic (M_2) Molecules. (a) For alkali metal diatomic molecules, the two valence electrons are enough to fill the σ_{ns} (bonding) level, giving a bond order of 1. (b) For alkaline earth metal diatomic molecules, the four valence electrons fill both the σ_{ns} (bonding) and the σ_{ns}* (nonbonding) levels, leading to a predicted bond order of 0.

Similarly, the molecular orbital diagrams for homonuclear diatomic compounds of the alkaline earth metals (such as Be_2), in which each metal atom has an ns^2 valence electron configuration, resemble the diagram for the He_2 molecule in part (c) in Figure 9.4.3 As shown in part (b) in Figure 9.4.4, this is indeed the case. All the homonuclear alkaline earth diatomic molecules have four valence electrons, which fill both the σ_{ns} bonding orbital and the σ_{ns}* antibonding orbital and give a bond order of 0. Thus Be_2, Mg_2, Ca_2, Sr_2, and Ba_2 are all expected to be unstable, in agreement with experimental data. In the solid state, however, all the alkali metals and the alkaline earth metals exist as extended lattices held together by metallic bonding. At low temperatures, Be_2 is stable.

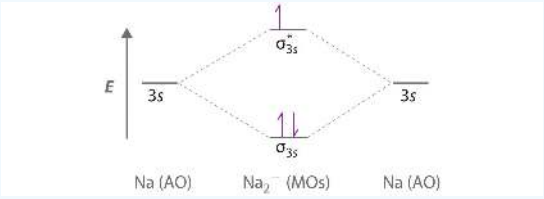
Example 9.4.2

Use a qualitative molecular orbital energy-level diagram to predict the valence electron configuration, bond order, and likely existence of the Na_2^- ion.

Solution:

A Because sodium has a [Ne]$3s^1$ electron configuration, the molecular orbital energy-level diagram is qualitatively identical to the diagram for the interaction of two 1*s* atomic orbitals.

B The Na_2^- ion has a total of three valence electrons (one from each Na atom and one for the negative charge), resulting in a filled σ_{3s} molecular orbital, a half-filled σ_{3s}* and a $(\sigma_{3s})^2(\sigma^\star_{3s})^1$ electron configuration.



C The bond order is (2-1)÷2=1/2 With a fractional bond order, we predict that the Na_2^- ion exists but is highly reactive.

Exercise 9.4.2

Use a qualitative molecular orbital energy-level diagram to predict the valence electron configuration, bond order, and likely existence of the Ca_2^+ ion.

Answer: Ca_2^+ has a $(\sigma_{4s})^2(\sigma^\star_{4s})^1$ electron configurations and a bond order of 1/2 and should exist.

9.4.6: Contributors

- Seymour Blinder (Professor Emeritus of Chemistry and Physics at the University of Michigan, Ann Arbor)
- Jonathan Gutow (UW Oshkosh)

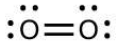
This page titled 9.4: Molecular Orbital Theory is shared under a CC BY-NC-SA 4.0 license and was authored, remixed, and/or curated by Jonathan Gutow.

- **12.5: Molecular Orbital Theory** is licensed CC BY-NC-SA 4.0.

9.5: Diatomic Molecules With More Than s Orbitals

9.5.1: Introduction

For almost every covalent molecule that exists, we can now draw the Lewis structure, predict the electron-pair geometry, predict the molecular geometry, and come close to predicting bond angles. However, one of the most important molecules we know, the oxygen molecule O_2, presents a problem with respect to its Lewis structure. We would write the following Lewis structure for O_2:



This electronic structure adheres to all the rules governing Lewis theory. There is an O=O double bond, and each oxygen atom has eight electrons around it. However, this picture is at odds with the magnetic behavior of oxygen. By itself, O_2 is not magnetic, but it is attracted to magnetic fields. Thus, when we pour liquid oxygen past a strong magnet, it collects between the poles of the magnet and defies gravity. Such attraction to a magnetic field is called paramagnetism, and it arises in molecules that have unpaired electrons. And yet, the Lewis structure of O_2 indicates that all electrons are paired. How do we account for this discrepancy?

Magnetic susceptibility measures the force experienced by a substance in a magnetic field. When we compare the weight of a sample to the weight measured in a magnetic field (Figure 9.5.1), paramagnetic samples that are attracted to the magnet will appear heavier because of the force exerted by the magnetic field. We can calculate the number of unpaired electrons based on the increase in weight.

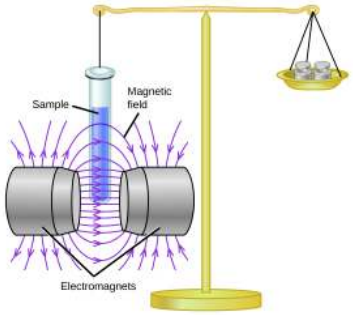


Figure 9.5.1: A Gouy balance compares the mass of a sample in the presence of a magnetic field with the mass with the electromagnet turned off to determine the number of unpaired electrons in a sample.

Experiments show that each O_2 molecule has two unpaired electrons. The Lewis-structure and valence bond models do not predict the presence of these two unpaired electrons. Unlike oxygen, the apparent weight of most molecules decreases slightly in the presence of an inhomogeneous magnetic field. Materials in which all of the electrons are paired are diamagnetic and weakly repel a magnetic field. Paramagnetic and diamagnetic materials do not act as permanent magnets. Only in the presence of an applied magnetic field do they demonstrate attraction or repulsion.



***Video* 9.5.1:** *Water, like most molecules, contains all paired electrons. Living things contain a large percentage of water, so they demonstrate diamagnetic behavior. If you place a frog near a sufficiently large magnet, it will levitate. You can see videos of diamagnetic floating frogs,*

strawberries, and more (https://www.youtube.com/watch?v=A1vyB-O5i6E)

Molecular orbital theory (MO theory) provides an explanation of chemical bonding that accounts for the paramagnetism of the oxygen molecule. It also explains the bonding in a number of other molecules, such as violations of the octet rule and molecules with more complicated bonding (beyond the scope of this text) that are difficult to describe with Lewis structures. Additionally, it provides a model for describing the energies of electrons in a molecule and the probable location of these electrons. Unlike valence bond theory, which uses hybrid orbitals that are assigned to one specific atom, MO theory uses the combination of atomic orbitals to yield molecular orbitals that are delocalized over the entire molecule rather than being localized on its constituent atoms. MO theory also helps us understand why some substances are electrical conductors, others are semiconductors, and still others are insulators. Table 9.5.1 summarizes the main points of the two complementary bonding theories. Both theories provide different, useful ways of describing molecular structure.

Table 9.5.1 : Comparison of Bonding Theories

Valence Bond Theory	Molecular Orbital Theory
considers bonds as localized between one pair of atoms	considers electrons delocalized throughout the entire molecule
creates bonds from overlap of atomic orbitals (*s*, *p*, *d*…) and hybrid orbitals (*sp*, sp^2, sp^3…)	combines atomic orbitals to form molecular orbitals (σ, σ*, π, π*)
forms σ or π bonds	creates bonding and antibonding interactions based on which orbitals are filled
predicts molecular shape based on the number of regions of electron density	predicts the arrangement of electrons in molecules
needs multiple structures to describe resonance	

9.5.2: Molecular Orbitals Formed from *ns* and *np* Atomic Orbitals

Atomic orbitals other than *ns* orbitals can also interact to form molecular orbitals. Because individual *p*, *d*, and *f* orbitals are not spherically symmetrical, however, we need to define a coordinate system so we know which lobes are interacting in three-dimensional space. Recall that for each *np* subshell, for example, there are np_x, np_y, and np_z orbitals. All have the same energy and are therefore degenerate, but they have different spatial orientations.

Just as with *ns* orbitals, we can form molecular orbitals from *np* orbitals by taking their mathematical sum and difference. When two positive lobes with the appropriate spatial orientation overlap, as illustrated for two np_z atomic orbitals in part (a) in Figure 9.5.2, it is the mathematical *difference* of their wave functions that results in *constructive* interference, which in turn increases the electron probability density between the two atoms. The difference therefore corresponds to a molecular orbital called a σ_{np_z} *bonding molecular orbital* because, just as with the σ orbitals discussed previously, it is symmetrical about the internuclear axis (in this case, the *z*-axis):

$$\sigma_{np_z} = np_z\,(A) - np_z\,(B) \tag{9.5.1}$$

The other possible combination of the two np_z orbitals is the mathematical sum:

$$\sigma_{np_z} = np_z\,(A) + np_z\,(B) \tag{9.5.2}$$

In this combination, shown in part (b) in Figure 9.5.2, the positive lobe of one np_z atomic orbital overlaps the negative lobe of the other, leading to *destructive* interference of the two waves and creating a node between the two atoms. Hence this is an antibonding molecular orbital. Because it, too, is symmetrical about the internuclear axis, this molecular orbital is called a σ_{np_z} *antibonding molecular orbital*. Whenever orbitals combine, *the bonding combination is always lower in energy* (more stable) than the atomic orbitals from which it was derived, and *the antibonding combination is higher in energy* (less stable).

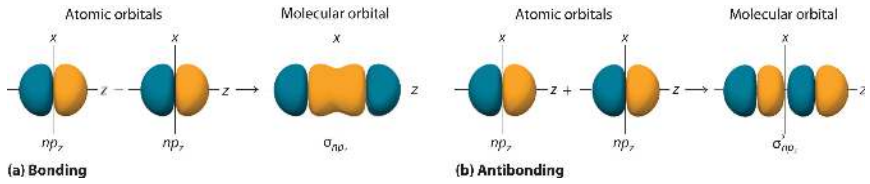


Figure 9.5.2: Formation of Molecular Orbitals from np_z Atomic Orbitals on Adjacent Atoms.(a) By convention, in a linear molecule or ion, the *z*-axis always corresponds to the internuclear axis, with +*z* to the right. As a result, the signs of the lobes of the np_z atomic orbitals on the two atoms alternate − + − +, from left to right. In this case, the σ (bonding) molecular orbital corresponds to the mathematical *difference*, in which the overlap of lobes with the same sign results in increased probability density between the nuclei. (b) In contrast, the σ* (antibonding) molecular orbital corresponds to the mathematical *sum*, in which the overlap of lobes with opposite signs results in a nodal plane of zero probability density perpendicular to the internuclear axis.

> Overlap of atomic orbital lobes with the *same sign* produces a bonding molecular orbital, regardless of whether it corresponds to the sum or the difference of the atomic orbitals.

The remaining *p* orbitals on each of the two atoms, np_x and np_y, do not point directly toward each other. Instead, they are perpendicular to the internuclear axis. If we arbitrarily label the axes as shown in Figure 9.5.3, we see that we have two pairs of *np* orbitals: the two np_x orbitals lying in the plane of the page, and two np_y orbitals perpendicular to the plane. Although these two pairs are equivalent in energy, the np_x orbital on one atom can interact with only the np_x orbital on the other, and the np_y orbital on one atom can interact with only the np_y on the other. These interactions are side-to-side rather than the head-to-head interactions characteristic of σ orbitals. Each pair of overlapping atomic orbitals again forms two molecular orbitals: one corresponds to the arithmetic sum of the two atomic orbitals and one to the difference. The sum of these side-to-side interactions increases the electron probability in the region above and below a line connecting the nuclei, so it is a bonding molecular orbital that is called a pi (π) orbital (a bonding molecular orbital formed from the side-to-side interactions of two or more parallel np atomic orbitals). The difference results in the overlap of orbital lobes with opposite signs, which produces a nodal plane perpendicular to the internuclear axis; hence it is an antibonding molecular orbital, called a pi star (π*) orbital. An antibonding molecular orbital is formed from the difference of the side-to-side interactions of two or more parallel *np* atomic orbitals, creating a nodal plane perpendicular to the internuclear axis. These orbitals are represented by the following linear combinations of the atomic orbitals:

$$\pi_{np_x} = np_x\,(A) + np_x\,(B) \tag{9.5.3}$$

$$\pi^{\star}_{np_x} = np_x\,(A) - np_x\,(B) \tag{9.5.4}$$

The two np_y orbitals can also combine using side-to-side interactions to produce a bonding π_{np_y} molecular orbital and an antibonding $\pi^{\star}_{np_y}$ molecular orbital. Because the np_x and np_y atomic orbitals interact in the same way (side-to-side) and have the same energy, the π_{np_x} and π_{np_y} molecular orbitals are a degenerate pair, as are the $\pi^{\star}_{np_x}$ and $\pi^{\star}_{np_y}$ molecular orbitals.

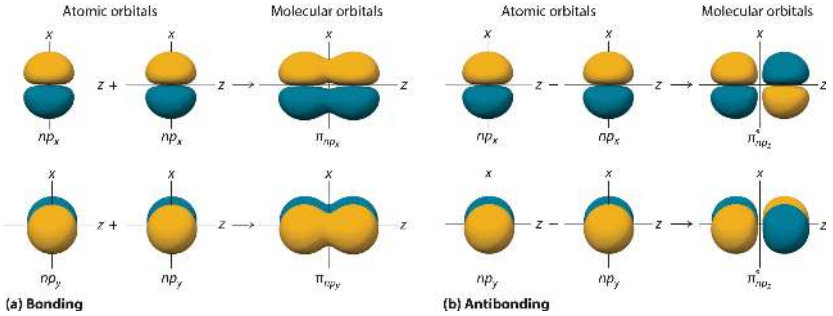


Figure 9.5.3: Formation of π Molecular Orbitals from np_x and np_y Atomic Orbitals on Adjacent Atoms.(a) Because the signs of the lobes of both the np_x and the np_y atomic orbitals on adjacent atoms are the same, in both cases the mathematical sum corresponds to a π (bonding) molecular orbital. (b) In contrast, in both cases, the mathematical difference corresponds to a π* (antibonding) molecular orbital, with a nodal plane of zero probability density perpendicular to the internuclear axis.

Figure 9.5.4 is an energy-level diagram that can be applied to two identical interacting atoms that have three *np* atomic orbitals each. There are six degenerate *p* atomic orbitals (three from each atom) that combine to form six molecular orbitals, three bonding and three antibonding. The bonding molecular orbitals are lower in energy than the atomic orbitals because of the increased stability associated with the formation of a bond. Conversely, the antibonding molecular orbitals are higher in energy, as shown. Generally as shown in the diagram, the energy difference between the σ and σ* molecular orbitals is significantly greater than the difference between the two π and π* sets. The reason for this is that the atomic orbital overlap and thus the strength of the interaction are greater for a σ bond than a π bond, which means that the σ molecular orbital is more stable (lower in energy) than the π molecular orbitals. There are instances (e.g. homonuclear diatomics formed from period 2 atoms Li through N), where the π orbitals are lower in energy than the σ_p orbital.

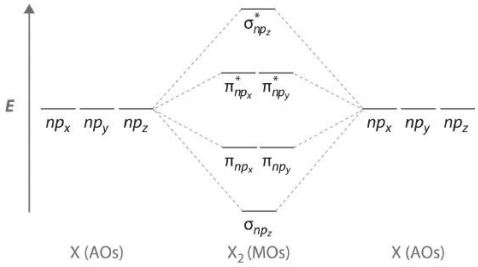


Figure 9.5.4: The Relative Energies of the σ and π Molecular Orbitals Derived from np_x, np_y, and np_z Orbitals on Identical Adjacent Atoms. Because the two np_z orbitals point directly at each other, their orbital overlap is greater, so the difference in energy between the σ and σ* molecular orbitals is greater than the energy difference between the π and π* orbitals.

Although many combinations of atomic orbitals form molecular orbitals, we will discuss only one other interaction: an *ns* atomic orbital on one atom with an np_z atomic orbital on another. As shown in Figure 9.5.5, the sum of the two atomic wave functions (*ns* + np_z) produces a σ bonding molecular orbital. Their difference (*ns* − np_z) produces a σ* antibonding molecular orbital, which has a nodal plane of zero probability density perpendicular to the internuclear axis.

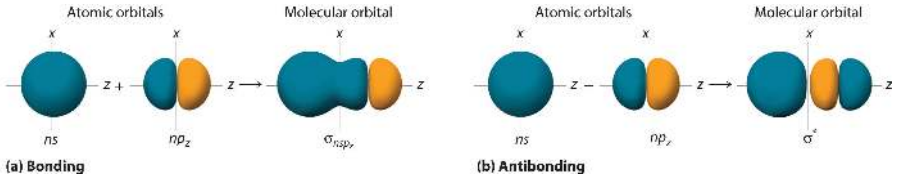


Figure 9.5.5: Formation of Molecular Orbitals from an ns Atomic Orbital on One Atom and an np_z Atomic Orbital on an Adjacent Atom.(a) The mathematical sum results in a σ (bonding) molecular orbital, with increased probability density between the nuclei. (b) The mathematical difference results in a σ* (antibonding) molecular orbital, with a nodal plane of zero probability density perpendicular to the internuclear axis.

9.5.3: Second Row Diatomic Molecules

If we combine the splitting schemes for the 2s and 2p orbitals, we can predict bond order in all of the diatomic molecules and ions composed of elements in the first complete row of the periodic table. Remember that only the valence orbitals of the atoms need be considered; as we saw in the cases of dilithium, the inner orbitals remain tightly bound and retain their localized atomic character.

We now describe examples of systems involving period 2 homonuclear diatomic molecules, such as N_2, O_2, and F_2. When we draw a molecular orbital diagram for a molecule, there are four key points to remember:

1. The number of molecular orbitals produced is the same as the number of atomic orbitals used to create them (the law of conservation of orbitals).
2. As the overlap between two atomic orbitals increases, the difference in energy between the resulting bonding and antibonding molecular orbitals increases.
3. When two atomic orbitals combine to form a pair of molecular orbitals, the bonding molecular orbital is stabilized about as much as the antibonding molecular orbital is destabilized.
4. The interaction between atomic orbitals is greatest when they have the same energy.

> The number of molecular orbitals is **always** equal to the total number of atomic orbitals we started with.

We illustrate how to use these points by constructing a molecular orbital energy-level diagram for F_2. We use the diagram in part (a) in Figure 9.5.6; the $n = 1$ orbitals (σ_{1s} and σ_{1s}*) are located well below those of the $n = 2$ level and are not shown. As illustrated in the diagram, the σ_{2s} and σ_{2s}* molecular orbitals are much lower in energy than the molecular orbitals derived from the 2*p* atomic orbitals because of the large difference in energy between the 2*s* and 2*p* atomic orbitals of fluorine. The lowest-energy molecular orbital derived from the three 2*p* orbitals on each F is σ_{2p_z} and the next most stable are the two degenerate orbitals, π_{2p_x} and π_{2p_y}. For each bonding orbital in the diagram, there is an antibonding orbital, and the antibonding orbital is destabilized by about as much as the corresponding bonding orbital is stabilized. As a result, the $\sigma^{\star}_{2p_z}$ orbital is higher in energy than either of the degenerate $\pi^{\star}_{2p_x}$ and $\pi^{\star}_{2p_y}$ orbitals. We can now fill the orbitals, beginning with the one that is lowest in energy.

Each fluorine has 7 valence electrons, so there are a total of 14 valence electrons in the F_2 molecule. Starting at the lowest energy level, the electrons are placed in the orbitals according to the Pauli principle and Hund's rule. Two electrons each fill the σ_{2s} and σ_{2s}* orbitals, 2 fill the σ_{2p_z} orbital, 4 fill the two degenerate π orbitals, and 4 fill the two degenerate π^* orbitals, for a total of 14 electrons. To determine what type of bonding the molecular orbital approach predicts F_2 to have, we must calculate the bond order. According to our diagram, there are 8 bonding electrons and 6 antibonding electrons, giving a bond order of $(8 - 6) \div 2 = 1$. Thus F_2 is predicted to have a stable F–F single bond, in agreement with experimental data.

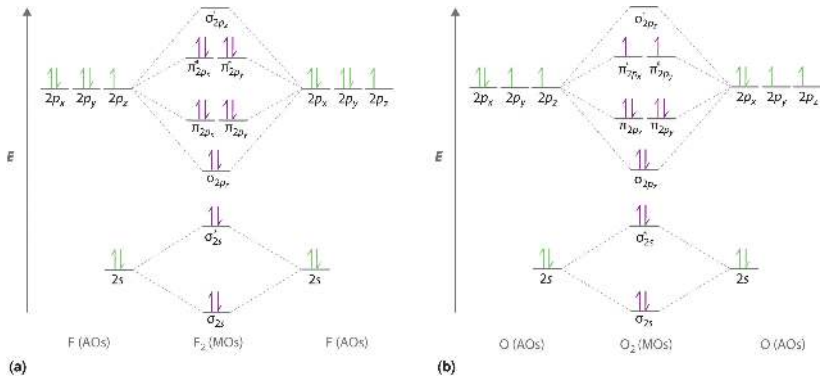


Figure 9.5.6: Molecular Orbital Energy-Level Diagrams for Homonuclear Diatomic Molecules.(a) For F_2, with 14 valence electrons (7 from each F atom), all of the energy levels except the highest, $\sigma^{\star}_{2p_z}$ are filled. This diagram shows 8 electrons in bonding orbitals and 6 in antibonding orbitals, resulting in a bond order of 1. (b) For O_2, with 12 valence electrons (6 from each O atom), there are only 2 electrons to place in the $\left(\pi^{\star}_{np_x}, \pi^{\star}_{np_y}\right)$ pair of orbitals. Hund's rule dictates that one electron occupies each orbital, and their spins are parallel, giving the O_2 molecule two unpaired electrons. This diagram shows 8 electrons in bonding orbitals and 4 in antibonding orbitals, resulting in a predicted bond order of 2.

We now turn to a molecular orbital description of the bonding in O_2. It so happens that the molecular orbital description of this molecule provided an explanation for a long-standing puzzle that could not be explained using other bonding models. To obtain the molecular orbital energy-level diagram

for O_2, we need to place 12 valence electrons (6 from each O atom) in the energy-level diagram shown in part (b) in Figure 9.5.6. We again fill the orbitals according to Hund's rule and the Pauli principle, beginning with the orbital that is lowest in energy. Two electrons each are needed to fill the σ_{2s} and σ_{2s}* orbitals, 2 more to fill the σ_{2p_z} orbital, and 4 to fill the degenerate $\pi^{\star}_{2p_x}$ and $\pi^{\star}_{2p_y}$ orbitals. According to Hund's rule, the last 2 electrons must be placed in separate π^* orbitals with their spins parallel, giving two unpaired electrons. This leads to a predicted bond order of $(8 - 4) \div 2 = 2$, which corresponds to a double bond, in agreement with experimental data: the O–O bond length is 120.7 pm, and the bond energy is 498.4 kJ/mol at 298 K.

The two unpaired electrons in the degenerate $\pi*$ highest occupied molecular orbitals explain why oxygen molecules are paramagnetic as described in the introduction.

The magnetic properties of O_2 are not just a laboratory curiosity; they are absolutely crucial to the existence of life. Because Earth's atmosphere contains 20% oxygen, all organic compounds, including those that compose our body tissues, should react rapidly with air to form H_2O, CO_2, and N_2 in an exothermic reaction. Fortunately for us, however, this reaction is very, very slow. The reason for the unexpected stability of organic compounds in an oxygen atmosphere is that virtually all organic compounds, as well as H_2O, CO_2, and N_2, have only paired electrons, whereas oxygen has two unpaired electrons. Thus the reaction of O_2 with organic compounds to give H_2O, CO_2, and N_2 would require that at least one of the electrons on O_2 change its spin during the reaction. This would require a large input of energy, an obstacle that chemists call a *spin barrier*. Consequently, reactions of this type are usually exceedingly slow. If they were not so slow, all organic substances, including this book and you, would disappear in a puff of smoke!

For period 2 diatomic molecules to the left of N_2 in the periodic table, a slightly different molecular orbital energy-level diagram is needed because the σ_{2p_z} molecular orbital is slightly *higher* in energy than the degenerate π_{np_x} and π_{np_y} orbitals. The difference in energy between the 2*s* and 2*p* atomic orbitals increases from Li_2 to F_2 due to increasing nuclear charge and poor screening of the 2*s* electrons by electrons in the 2*p* subshell. The bonding interaction between the 2*s* orbital on one atom and the $2p_z$ orbital on the other is most important when the two orbitals have similar energies. This interaction decreases the energy of the σ_{2s} orbital and increases the energy of the σ_{2p_z} orbital. Thus for Li_2, Be_2, B_2, C_2, and N_2, the σ_{2p_z} orbital is higher in energy than the $\pi_{2p_{x,y}}$ orbitals, as shown in Figure 9.5.7 Experimentally, it is found that the energy gap between the *ns* and *np* atomic orbitals *increases* as the nuclear charge increases (Figure 9.5.7). This leads to the σ_{2p_z} molecular orbital shifting down in energy as we move right in the periodic table, resulting in it being lower energy than the $\pi_{2p_{x,y}}$ pair when we reach O and F.

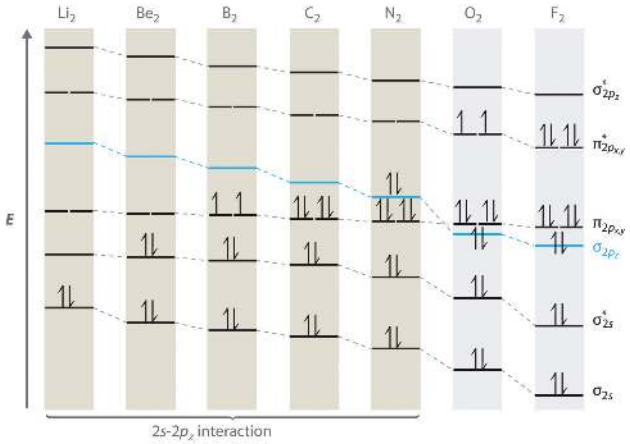


Figure 9.5.7: Molecular Orbital Energy-Level Diagrams for the Diatomic Molecules of the Period 2 Elements. Unlike earlier diagrams, only the molecular orbital energy levels for the molecules are shown here. For simplicity, the atomic orbital energy levels for the component *atoms* have been omitted. For Li_2 through N_2, the σ_{2p_z} *orbital is higher in energy than the* $\pi_{2p_{x,y}}$ *orbitals. In contrast, the* σ_{2p_z} *orbital is lower in energy than the* $\pi_{2p_{x,y}}$ *orbitals for* O_2 *and* F_2 *due to the increase in the energy difference between the 2s and 2p atomic orbitals as the nuclear charge increases across the row.*

Completing the diagram for N_2 in the same manner as demonstrated previously, we find that the 10 valence electrons result in 8 bonding electrons and 2 antibonding electrons, for a predicted bond order of 3, a triple bond. Experimental data show that the N–N bond is significantly shorter than the F–F bond (109.8 pm in N_2 versus 141.2 pm in F_2), and the bond energy is much greater for N_2 than for F_2 (945.3 kJ/mol versus 158.8 kJ/mol, respectively). Thus the N_2 bond is much shorter and stronger than the F_2 bond, consistent with what we would expect when comparing a triple bond with a single bond.

✔ Example 9.5.1

Use a qualitative molecular orbital energy-level diagram to predict the electron configuration, the bond order, and the number of unpaired electrons in S_2, a bright blue gas at high temperatures.

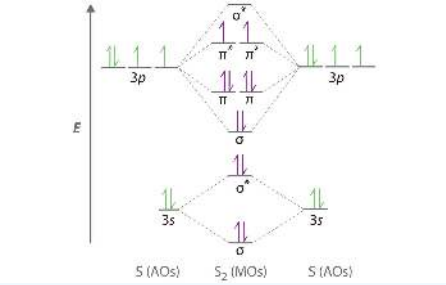
Strategy:

A. Write the valence electron configuration of sulfur and determine the type of molecular orbitals formed in S_2. Predict the relative energies of the molecular orbitals based on how close in energy the valence atomic orbitals are to one another.
B. Draw the molecular orbital energy-level diagram for this system and determine the total number of valence electrons in S_2.
C. Fill the molecular orbitals in order of increasing energy, being sure to obey the Pauli principle and Hund's rule.
D. Calculate the bond order and describe the bonding.

Solution:

A Sulfur has a [Ne]$3s^2 3p^4$ valence electron configuration. To create a molecular orbital energy-level diagram similar to those in Figure 9.5.6 and Figure 9.5.7, we need to know how close in energy the 3*s* and 3*p* atomic orbitals are because their energy separation will determine whether the $\pi_{3p_{x,y}}$ or the σ_{3p_z}> molecular orbital is higher in energy. Because the *ns*–*np* energy gap *increases* as the nuclear charge increases (Figure 9.5.7), the σ_{3p_z} molecular orbital will be lower in energy than the $\pi_{3p_{x,y}}$ pair.

B The molecular orbital energy-level diagram is as follows:



Each sulfur atom contributes 6 valence electrons, for a total of 12 valence electrons.

C Ten valence electrons are used to fill the orbitals through π_{3p_z} and π_{3p_y}, leaving 2 electrons to occupy the degenerate $\pi^*_{3p_x}$ and $\pi^*_{3p_y}$ pair. From Hund's rule, the remaining 2 electrons must occupy these orbitals separately with their spins aligned. With the numbers of electrons written as superscripts, the electron configuration of S_2 is $(\sigma_{3s})^2(\sigma^*_{3s})^2(\sigma_{3p_z})^2(\pi_{3p_{x,y}})^4(\pi_{3p^*_{x,y}})^2$ with 2 unpaired electrons. The bond order is $(8-4)\div 2 = 2$, so we predict an S=S double bond.

? Exercise 9.5.1

Use a qualitative molecular orbital energy-level diagram to predict the electron configuration, the bond order, and the number of unpaired electrons in the peroxide ion (O_2^{2-}).

Answer

$(\sigma_{2s})^2(\sigma^*_{2s})^2(\sigma_{2p_z})^2(\pi_{2p_{x,y}})^4(\pi_{2p^*_{x,y}})^4$ bond order of 1; no unpaired electrons

9.5.4: Molecular Orbitals for Heteronuclear Diatomic Molecules

Diatomic molecules with two different atoms are called heteronuclear diatomic molecules. When two nonidentical atoms interact to form a chemical bond, the interacting atomic orbitals do not have the same energy. If, for example, element B is more electronegative than element A ($\chi_B > \chi_A$), the net result is a "skewed" molecular orbital energy-level diagram, such as the one shown for a hypothetical A–B molecule in Figure 9.5.8. The atomic orbitals of element B are uniformly lower in energy than the corresponding atomic orbitals of element A because of the enhanced stability of the electrons in element B. The molecular orbitals are no longer symmetrical, and the energies of the bonding molecular orbitals are more similar to those of the atomic orbitals of B. Hence the electron density of bonding electrons is likely to be closer to the more electronegative atom. In this way, molecular orbital theory can describe a polar covalent bond.

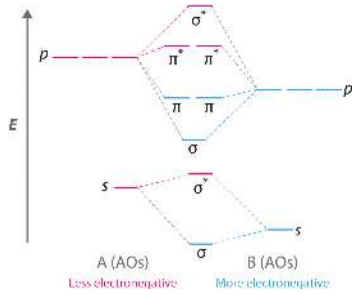


Figure 9.5.8: Molecular Orbital Energy-Level Diagram for a Heteronuclear Diatomic Molecule AB, Where $\chi_B > \chi_A$. The bonding molecular orbitals are closer in energy to the atomic orbitals of the more electronegative B atom. Consequently, the electrons in the bonding orbitals are not shared equally between the two atoms. On average, they are closer to the B atom, resulting in a polar covalent bond.

> A molecular orbital energy-level diagram is always skewed toward the more electronegative atom.

9.5.4.1: An Odd Number of Valence Electrons: NO

Nitric oxide (NO) is an example of a heteronuclear diatomic molecule. The reaction of O_2 with N_2 at high temperatures in internal combustion engines forms nitric oxide, which undergoes a complex reaction with O_2 to produce NO_2, which in turn is responsible for the brown color we associate with air pollution. Recently, however, nitric oxide has also been recognized to be a vital biological messenger involved in regulating blood pressure and long-term memory in mammals.

Because NO has an odd number of valence electrons (5 from nitrogen and 6 from oxygen, for a total of 11), its bonding and properties cannot be successfully explained by either the Lewis electron-pair approach or valence bond theory. The molecular orbital energy-level diagram for NO (Figure 9.5.9) shows that the general pattern is similar to that for the O_2 molecule (Figure 9.5.7). Because 10 electrons are sufficient to fill all the bonding molecular orbitals derived from 2*p* atomic orbitals, the 11th electron must occupy one of the degenerate π^* orbitals. The predicted bond order for NO is therefore (8-3) ÷ 2 = 2 1/2 . Experimental data, showing an N–O bond length of 115 pm and N–O bond energy of 631 kJ/mol, are consistent with this description. These values lie between those of the N_2 and O_2 molecules, which have triple and double bonds, respectively. As we stated earlier, molecular orbital theory can therefore explain the bonding in molecules with an odd number of electrons, such as NO, whereas Lewis electron structures cannot.

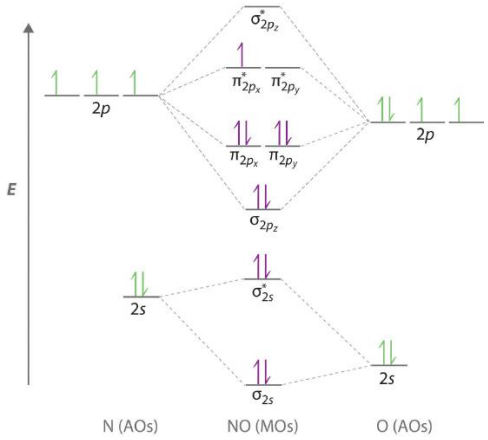


Figure 9.5.9: Molecular Orbital Energy-Level Diagram for NO. Because NO has 11 valence electrons, it is paramagnetic, with a single electron occupying the $\left(\pi^*_{2p_x}, \pi^*_{2p_y}\right)$ pair of orbitals.

Molecular orbital theory can also tell us something about the *chemistry* of NO. As indicated in the energy-level diagram in Figure 9.5.9, NO has a single electron in a relatively high-energy molecular orbital. We might therefore expect it to have similar reactivity as alkali metals such as Li and Na with their single valence electrons. In fact, NO is easily oxidized to the NO^+ cation, which is isoelectronic with N_2 and has a bond order of 3, corresponding to an N≡O triple bond.

9.5.5: Nonbonding Molecular Orbitals

Molecular orbital theory is also able to explain the presence of lone pairs of electrons. Consider, for example, the HCl molecule, whose Lewis electron structure has three lone pairs of electrons on the chlorine atom. Using the molecular orbital approach to describe the bonding in HCl, we can see from Figure 9.5.10 that the 1*s* orbital of atomic hydrogen is closest in energy to the 3*p* orbitals of chlorine. Consequently, the filled Cl 3*s* atomic orbital is not involved in bonding to any appreciable extent, and the only important interactions are those between the H 1*s* and Cl 3*p* orbitals. Of the three *p* orbitals, only one, designated as $3p_z$, can interact with the H 1*s* orbital. The $3p_x$ and $3p_y$ atomic orbitals have no net overlap with the 1*s* orbital on hydrogen, so they are not involved in bonding. Because the energies of the Cl 3*s*, $3p_x$, and $3p_y$ orbitals do not change when HCl forms,

they are called **nonbonding molecular orbitals**. A nonbonding molecular orbital occupied by a pair of electrons is the molecular orbital equivalent of a lone pair of electrons. By definition, electrons in nonbonding orbitals have no effect on bond order, so they are not counted in the calculation of bond order. Thus the predicted bond order of HCl is (2 − 0) ÷ 2 = 1. Because the σ bonding molecular orbital is closer in energy to the Cl $3p_z$ than to the H 1*s* atomic orbital, the electrons in the σ orbital are concentrated closer to the chlorine atom than to hydrogen. A molecular orbital approach to bonding can therefore be used to describe the polarization of the H–Cl bond to give $H^{\delta+} - Cl^{\delta-}$.

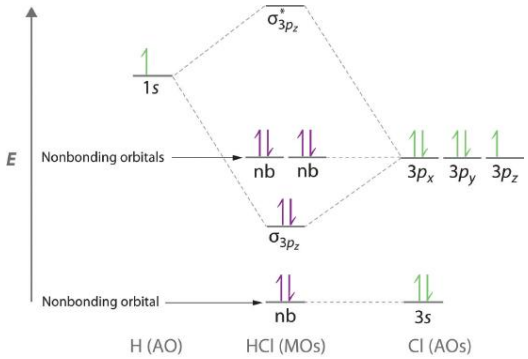


Figure 9.5.10: Molecular Orbital Energy-Level Diagram for HCl. The hydrogen 1 s atomic orbital interacts most strongly with the $3p_z$ orbital on chlorine, producing a bonding/antibonding pair of molecular orbitals. The other electrons on Cl are best viewed as nonbonding. As a result, only the bonding σ orbital is occupied by electrons, giving a bond order of 1.

Electrons in nonbonding molecular orbitals have **no effect** on bond order.

Example 9.5.2

Use a "skewed" molecular orbital energy-level diagram like the one in Figure 9.5.8 to describe the bonding in the cyanide ion (CN^-). What is the bond order?

Given: chemical species

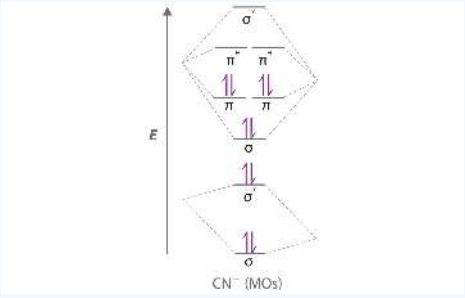
Asked for: "skewed" molecular orbital energy-level diagram, bonding description, and bond order

Strategy:

A. Calculate the total number of valence electrons in CN^-. Then place these electrons in a molecular orbital energy-level diagram like Figure 9.5.8 in order of increasing energy. Be sure to obey the Pauli principle and Hund's rule while doing so.
B. Calculate the bond order and describe the bonding in CN^-.

Solution:

A The CN^- ion has a total of 10 valence electrons: 4 from C, 5 from N, and 1 for the −1 charge. Placing these electrons in an energy-level diagram like Figure 9.5.8 fills the five lowest-energy orbitals, as shown here:



Because $\chi_N > \chi_C$, the atomic orbitals of N (on the right) are lower in energy than those of C.

B The resulting valence electron configuration gives a predicted bond order of (8 − 2) ÷ 2 = 3, indicating that the CN^- ion has a triple bond, analogous to that in N_2.

Exercise 9.5.2

Use a qualitative molecular orbital energy-level diagram to describe the bonding in the hypochlorite ion (OCl^-). What is the bond order?

Answer

> All molecular orbitals except the highest-energy σ* are filled, giving a bond order of 1.

Although the molecular orbital approach reveals a great deal about the bonding in a given molecule, the procedure quickly becomes computationally intensive for molecules of even moderate complexity. Furthermore, because the computed molecular orbitals extend over the entire molecule, they are often difficult to represent in a way that is easy to visualize. Therefore we do not use a pure molecular orbital approach to describe the bonding in molecules or ions with more than two atoms. Instead, we use a valence bond approach and a molecular orbital approach to explain, among other things, the concept of resonance, which cannot adequately be explained using other methods.

This page titled 9.5: Diatomic Molecules With More Than s Orbitals is shared under a CC BY-NC-SA 4.0 license and was authored, remixed, and/or curated by Jonathan Gutow.

- **12.6: Diatomic Molecules** is licensed CC BY-NC-SA 4.0.

9.6: Hückel MO Model of Conjugation

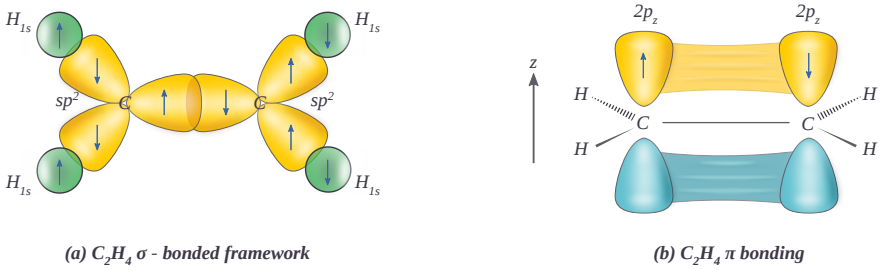
Learning Objectives

- Demonstrate how Hückel's theory approximates the full molecular orbital picture of molecules by treating the σ-bonding and π-bonding networks independently.

9.6.1: Introduction

Molecular orbital theory has been very successfully applied to large conjugated systems, especially those containing chains of carbon atoms with alternating single and double bonds. An approximation introduced by Hückel in 1931 considers only the delocalized *p* electrons moving in a framework of π-bonds. This is, in fact, a more sophisticated version of a free-electron model.

The simplest hydrocarbon to consider that exhibits π bonding is ethylene (ethene), which is made up of four hydrogen atoms and two carbon atoms. Experimentally, we know that the H–C–H and H–C–C angles in ethylene are approximately 120°. This angle suggests that the carbon atoms are sp^2 hybridized, which means that a singly occupied sp^2 orbital on one carbon overlaps with a singly occupied *s* orbital on each H and a singly occupied sp^2 lobe on the other C. Thus each carbon forms a set of three σ bonds: two C–H (sp^2 + *s*) and one C–C (sp^2 + sp^2) (part (a) of Figure 9.6.1).



(a) C_2H_4 σ - bonded framework *(b) C_2H_4 π bonding*

Figure 9.6.1 : (a) The σ-bonded framework is formed by the overlap of two sets of singly occupied carbon sp^2 hybrid orbitals and four singly occupied hydrogen 1s orbitals to form electron-pair bonds. This uses 10 of the 12 valence electrons to form a total of five σ bonds (four C–H bonds and one C–C bond). (b) One singly occupied unhybridized $2p_z$ orbital remains on each carbon atom to form a carbon–carbon π bond. (Note: by convention, in planar molecules the axis perpendicular to the molecular plane is the *z*-axis.) (CC BY-NC; Ümit Kaya via LibreTexts)

The Hückel approximation is used to determine the energies and shapes of the π molecular orbitals in conjugated systems. Within the Hückel approximation, the covalent bonding in these hydrocarbons is separated into two independent "frameworks": the σ-bonding framework and the the π-bonding framework. Only π electron molecular orbitals are included because these determine the general properties of these molecules; the σ electrons are ignored. This is referred to as *sigma-pi separability* and is justified by the orthogonality of σ and π orbitals in planar molecules. For this reason, the Hückel method is limited to planar systems. The Hückel approximation focuses only on the formation of π bonds, given that the σ bonding framework has already been formed.

Conjugated Systems

A conjugated system has a region of overlapping p-orbitals, bridging the interjacent single bonds, that allow a *delocalization* of π electrons across all the adjacent aligned p-orbitals. These π electrons do not belong to a single bond or atom, but rather to a group of atoms.

9.6.2: π system of ethylene

The σ-bonding occurs via the mixing of the electrons in the sp^2 hybrid orbitals on carbon and the electrons in the $1s$ atomic orbitals of the four hydrogen atoms (Figure 9.6.1 (a)). The π-bonding framework results from the unhybridized $2p_z$ orbitals (Figure 9.6.1 (b)). The independence of these two frameworks is demonstrated in the resulting molecular orbital diagram in Figure 9.6.2.

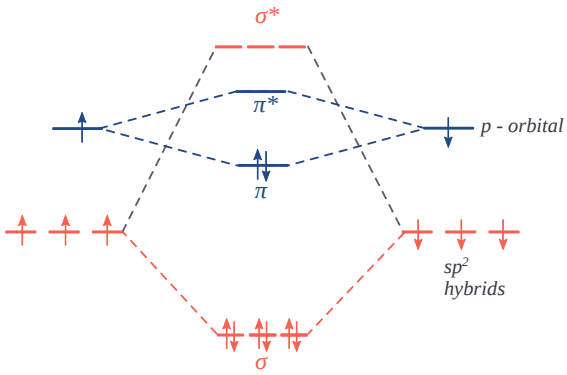


Figure 9.6.2 : Molecular orbitals demonstrating the sigma-pi separability of the π-bonding framework (blue) and the σ-bonding frameworks (red) of ethylene. (CC BY-NC; Ümit Kaya via LibreTexts)

In Hückel theory the molecular orbitals ψ_i can be described as a linear combination of the $2p_z$ atomic orbitals ϕ at each carbon with their corresponding $\{c_i\}$ coefficients:

$$\psi_i = c_1\phi_1 + c_2\phi_2 \tag{9.6.1}$$

Substituting this into the Schrödinger equation:

$$\hat{H}\psi_i = E_i\psi_i$$

with $\hat{H}$ the Hamiltonian and E_i the energy corresponding to the molecular orbital to give:

$$\hat{H}c_1\phi_1 + \hat{H}c_2\phi_2 = Ec_1\phi_1 + Ec_2\phi_2 \tag{9.6.2}$$

Notice that the E is for the hybrid orbital, so does not have a subcript. If Equation 9.6.2 is left multiplied by ϕ_1^* (and integrated), then

$$\int_{allspace} \phi_1^*\hat{H}c_1\phi_1 + \phi_1^*\hat{H}c_2\phi_2 d\tau = \int_{allspace} \phi_1^*Ec_1\phi_1 + \phi_1^*Ec_2\phi_2 d\tau$$

Utilizing the fact that the c's and E are constants this rearranges to:

$$c_1\int_{allspace} \phi_1^*\hat{H}\phi_1 d\tau + c_2\int_{allspace} \phi_1^*\hat{H}\phi_2 d\tau = Ec_1\int_{allspace} \phi_1^*\phi_1 d\tau + Ec_2\int_{allspace} \phi_1^*\phi_2 d\tau$$

Using H_{ik} to represent the integrals with Hamiltonians in them and S_{ik} to represent **overlap integrals** (no Hamiltonian between the wavefunctions) of orbital i and k this can be written more compactly as:

$$c_1H_{11} + c_2H_{12} = c_1ES_{11} + c_2ES_{12}$$

collecting all the terms on one side yields the first of a system of equations in the coefficients:

$$c_1(H_{11} - ES_{11}) + c_2(H_{12} - ES_{12}) = 0 \tag{9.6.3}$$

The same analysis but starting by left multiplying by ϕ_2^* and integrating over all of space leads to the second:

$$c_1(H_{21} - ES_{21}) + c_2(H_{22} - ES_{22}) = 0 \tag{9.6.4}$$

Nontrivial solutions, $c_i \neq 0$, only exist for the coefficients if the determinant of the matrix of the integral quantities in parentheses (the secular determinant) is equal to zero.

$$\begin{vmatrix} H_{11} - ES_{11} & H_{12} - ES_{12} \\ H_{21} - ES_{21} & H_{22} - ES_{22} \end{vmatrix} = 0 \tag{9.6.5}$$

All diagonal Hamiltonian integrals H_{ii} are called **Coulomb integrals** and those of type H_{ik} are called **resonance integrals**. Both integrals are negative and the resonance integrals determines the strength of the bonding interactions. The S_{ik} integrals are called the **overlap integrals** and **S_{ii} = 1 for normalized wavefunctions**. The equations described in 9.6.3 and 9.6.4 are called the **secular equations**.

Everything in Equation 9.6.5 is a known number except E. Since the secular determinant for ethylene is a 2×2 matrix, finding E, requires solving a quadratic equation (after expanding the determinant):

$$(H_{11} - ES_{11})(H_{22} - ES_{22}) - (H_{21} - ES_{21})(H_{12} - ES_{12}) = 0$$

There will be two values of E which satisfy this equation and they are the molecular orbital energies. For ethylene, one will be the bonding energy and the other the antibonding energy for the π-orbitals formed by the combination of the two carbon $2p_z$ orbitals (Equation 9.6.1). However, if more than two ϕ atomic orbitals were used, e.g., in a bigger molecule, then more energies would be estimated by solving the secular determinant.

Math Review 9.6.1: Determinants

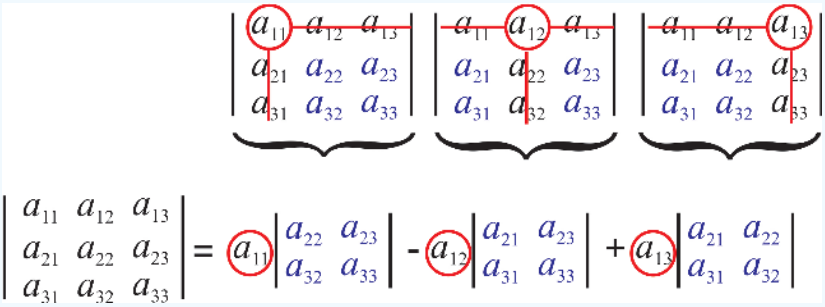
A 2 X 2 determinant is calculated as follows:

$$\begin{vmatrix} a & b \\ c & d \end{vmatrix} = ad - cb \tag{9.6.6}$$

A 3 X 3 determinant is calculated as follows:

$$\begin{vmatrix} a_{11} & a_{12} & a_{13} \\ a_{21} & a_{22} & a_{23} \\ a_{31} & a_{32} & a_{33} \end{vmatrix} = a_{11} \begin{vmatrix} a_{22} & a_{23} \\ a_{32} & a_{33} \end{vmatrix} - a_{12} \begin{vmatrix} a_{21} & a_{23} \\ a_{31} & a_{33} \end{vmatrix} + a_{13} \begin{vmatrix} a_{21} & a_{22} \\ a_{31} & a_{32} \end{vmatrix} \tag{9.6.7}$$

This drawing indicates how you pick the sub-determinants:



For more on determinants see: https://chem.libretexts.org/Bookshel...A_Determinants .

9.6.3: Applying the Hückel approximations

Solving the secular determinant is simplified in the Hückel method via the following four assumptions:

1. All overlap integrals S_{ik} with k ≠ i are set equal to zero. This is quite reasonable since the $\pi-$ orbitals are directed perpendicular to the direction of their bonds (Figure 9.6.1). This assumption is often call neglect of differential overlap (NDO).
2. All resonance integrals H_{ik} between non-neighboring atoms are set equal to zero.
3. All resonance integrals H_{ik} between neighboring atoms are equal and set to β.
4. All coulomb integrals H_{ii} are set equal to α.

These assumptions are mathematically expressed as

$$H_{11} = H_{22} = \alpha$$

$$H_{12} = H_{21} = \beta$$

Assumptions 1 means that the overlap integral between any two atomic orbitals on different atoms is 0. Thus:

$$S_{11} = S_{22} = 1$$

$$S_{12} = S_{21} = 0$$

The Hückel assumptions reduces Equation 9.6.5 to:

$$\begin{vmatrix} \alpha - E & \beta \\ \beta & \alpha - E \end{vmatrix} = 0 \tag{9.6.8}$$

if Equation 9.6.8 is divided by β:

$$\begin{vmatrix} \frac{\alpha - E}{\beta} & 1 \\ 1 & \frac{\alpha - E}{\beta} \end{vmatrix} = 0 \tag{9.6.9}$$

and then a new variable x is defined

$$x = \frac{\alpha - E}{\beta} \tag{9.6.10}$$

then Equation 9.6.9 simplifies to

$$\begin{vmatrix} x & 1 \\ 1 & x \end{vmatrix} = 0$$

The trivial solution gives both wavefunction coefficients equal to zero and the other (nontrivial) solution is determined by solving the secular determinant

$$\begin{vmatrix} x & 1 \\ 1 & x \end{vmatrix} = (x-1)(x+1) = 0$$

so $x = \pm 1$.

Knowing that $E = \alpha - x\beta$ from Equation 9.6.10, the energy levels can be found to be

$$E = \alpha - \pm 1 \times \beta$$

or

$$E = \alpha \mp \beta$$

Since β is negative, the two energies are ordered (Figure 9.6.3)

- For π_1: $E_1 = \alpha + \beta$
- For π_2: $E_2 = \alpha - \beta$

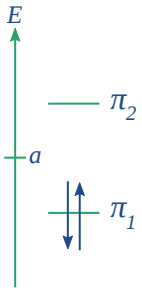


Figure 9.6.3 : π energies of ethylene with occupation. (CC BY-NC; Ümit Kaya via LibreTexts)

To extract the coefficients attributed to these energies, the corresponding E values can be substituted back into the secular equations 9.6.3 and 9.6.4 and combined with the normalization requirement. For the lower energy state ($E_1 = \alpha + \beta$)

$$c_1(H_{11} - ES_{11}) + c_2(H_{12} - ES_{12}) = c_1(\alpha - (\alpha + \beta)) + c_2(\beta - (\alpha + \beta)(0)) = c_1(-\beta)) + c_2\beta = 0 \tag{9.6.11}$$

and

$$c_1(H_{21} - ES_{21}) + c_2(H_{22} - ES_{22}) = c_1(\beta - (\alpha + \beta)(0)) + c_2(\alpha - (\alpha + \beta)) = c_1\beta - c_2\beta = 0 \tag{9.6.12}$$

This gives $c_1 = c_2$ and the molecular orbitals attributed to this energy is then (based off of Equation 9.6.1):

$$\psi_1 = N_1(\phi_1 + \phi_2) \tag{9.6.13}$$

where N_1 is the normalization constant for this molecular orbital; this is the **bonding** molecular orbital.

For the higher energy molecular substituting in the energy gives $c_1 = -c_2$ and the molecular orbitals attributed to this energy is then:

$$\psi_2 = N_2(\phi_1 - \phi_2) \tag{9.6.14}$$

where N_2 is the normalization constant for this molecular orbital; this is the **anti-bonding** molecular orbital.

Normalization of ψ_1, remembering the ϕ are real and S_{ik} = 0 when i ≠ k, leads to:

$$1 = \int_{\text{all space}} \psi_1^* \psi_1 d\tau = \int_{\text{all space}} N_1(\phi_1 + \phi_2) N_1(\phi_1 + \phi_2) d\tau = N_1^2(S_{11} + S_{22}) = 2N_1^2$$

and similarly for ψ_2:

$$1 = 2N_2^2$$

Thus:

$$N_1 = N_2 = \frac{1}{\sqrt{2}}$$

These molecular orbitals form the π-bonding framework and since each carbon contributes one electron to this framework, only the lowest molecular orbital (ψ_1) is occupied (Figure 9.6.4) in the ground state. The corresponding electron configuration is then π_1^2.

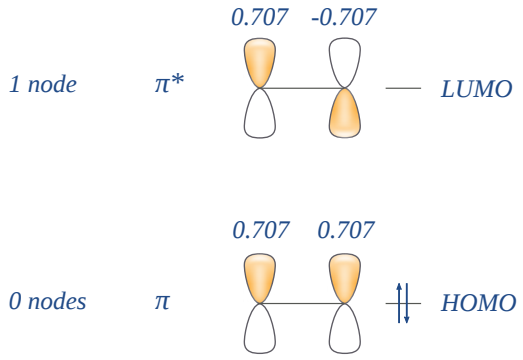


Figure 9.6.4 : Schemetic representation of the π molecular orbitals framework for ethylene . Notice that the antibonding molecular orbital has one more node than the bonding molecular orbital as expected since it is higher in energy. (CC BY-NC; Ümit Kaya via LibreTexts)

Note

HOMO *and* ***LUMO*** *are acronyms for highest occupied molecular orbital and lowest unoccupied molecular orbital, respectively and are often referred to as frontier orbitals. The energy difference between the HOMO and LUMO is termed the HOMO–LUMO gap.*

The 3-D calculated π molecular orbitals based on more sophisticated quantum calculations are shown in Figure 9.6.5.

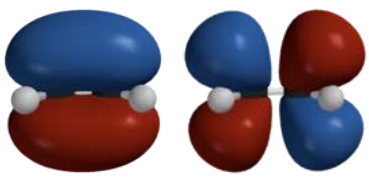


Figure 9.6.5: Calculated π molecular orbitals for ethylene . (left) the bonding orbital ψ_1 and (right) the antibonding ψ_2 orbital.

Limitations of Hückel Theory

Hückel theory was developed in the 1930's when computers were unavailable and a simple mathematical approaches were very important for understanding experiment. Although the assumptions in Hückel theory are drastic they enabled the early calculations of molecular orbitals to be performed with mechanical calculators or by hand. Hückel Theory can be extended to address other types of atoms in conjugated molecules (e.g., nitrogen and oxygen). Moreover, it can be extended to also treat σ orbitals and this "Extended Hückel Theory" is still used today. Despite the utility of Hückel Theory, it is highly qualitative and we should remember the limitations of Hückel Theory:

- Hückel Theory is very approximate
- Hückel Theory cannot calculate energies accurately (electron-electron repulsion is not calculated)
- Hückel Theory typically overestimates predicted dipole moments

Hückel Theory is best used to provide simplified models for understanding chemistry and for a detailed understanding modern *ab initio* molecular methods are required.

9.6.4: Hückel model applied to butadiene

Butadiene $H_2C{=}CH{-}CH{=}CH_2$, has two conjugated bonds. Thus four carbons are involved in the π system. By analogy with ethylene we can set up a secular matrix to solve, where we place x down the diagonal and 1 in the matrix elements representing neighboring p orbitals. The rows and columns of the determinant can be thought of as numbered by orbital positions (on atoms 1, 2, 3, or 4) as suggested in this table:

Atom Numbers	1	2	3	4
1	x	1	0	0
2	1	x	1	0
3	0	1	x	1
4	0	0	1	x

This leads to the determinant:

$$\begin{vmatrix} x & 1 & 0 & 0 \\ 1 & x & 1 & 0 \\ 0 & 1 & x & 1 \\ 0 & 0 & 1 & x \end{vmatrix} = 0 \tag{9.6.15}$$

This is essentially the connection matrix for the butadiene molecule. Each pair of connected atoms is represented by 1, each non-connected pair by 0 and each diagonal element by x. Expansion of the determinant in Equation 9.6.15 gives the 4th order polynomial equation

$$x^4 - 3x^2 + 1 = 0 \tag{9.6.16}$$

While solving 4th order equations typically require numerical estimation, Equation 9.6.16 can be further simplified by recognizing that it is a quadratic equation in terms of x^2. Therefore, the roots are

$$x^2 = \frac{3 \pm \sqrt{5}}{2}$$

or $x = \pm\, 0.618$ and $x = \pm\, 1.618$. Since α and β are negative, these molecular orbital energies can ordered in terms of energy (from lowest to highest):

$$E_1 = \alpha + 1.618\beta \tag{9.6.17}$$

$$E_2 = \alpha + 0.618\beta \tag{9.6.18}$$

$$E_3 = \alpha - 0.618\beta \tag{9.6.19}$$

$$E_4 = \alpha - 1.618\beta \tag{9.6.20}$$

This sequence of energies is displayed in the energy diagram of Figure 9.6.6.

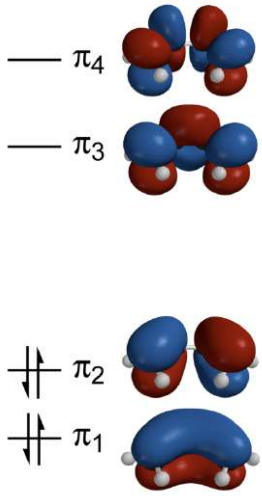


Figure 9.6.6 : The π molecular orbital energies from Hückel theory for butadiene with ground-state configuration. Structures calculated and images produced using HF/6-31G* (Public Domain; Ben Mills).

Each p atomic orbital of carbon contributes a single electron to the π manifold, so the ground-state occupation of the resulting four π electrons have a $\pi_1^2\pi_2^2$ configuration (Figure 9.6.6). The the total π-electron energy is then determined by adding up the energies in Equations 9.6.17-9.6.20 and scaling by their occupations to get

$$\begin{aligned} E_\pi(\text{butadiene}) &= 2\times E_1 + 2\times E_2 + 0\times E_3 + 0\times E_4 \\ &= 2(\alpha + 1.618\beta) + 2(\alpha + 0.618\beta) \\ &= 4\alpha + 4.472\beta \end{aligned} \tag{9.6.21}$$

If the bonding of butadiene were described only as two localized double bond as in its dominant valence-bond structure, then its π-electron energy would be given by twice the E_π predicted for the ethlyene molecule:

$$\begin{aligned} E_\pi(\text{butadiene}) &= 2\times E_\pi(\text{ethylene}) \\ &= 2\times 2(\alpha + \beta) \\ &= 4\alpha + 4\beta \end{aligned} \tag{9.6.22}$$

Comparing Equation 9.6.21 with Equation 9.6.22, the total π energy of butadiene lies lower than the total π energy of two double bonds by 0.472β(the σ bond does not contribute). This difference is known as the **delocalization energy**; a typical estimate of β is around -75 kJ/mol, which results in a *delocalization energy* for butadiene of -35 kJ/mol.

> *The delocalization energy is the extra stabilization resulting from the electrons extending over the whole molecule.*

Delocalization Energy in Valence Bond Theory

Delocalization energy is intrinsic to molecular orbital theory, since it results from breaking the two-center bond concept with the molecular orbitals that spread over more that just one pair of atoms. However, within the two-center theory of valence bond theory, the delocalization energy results from a stabilization energy attributed to resonance. Several conventional valence bond resonance structures can be written for 1,3-butadiene, four of which are shown in Figure 9.6.7. However, while the top left structure dominates, the other resonance structures also contribute to describing the total molecule and hence predict a corresponding stabilization energy akin to the delocalization energy in molecular orbital theory.

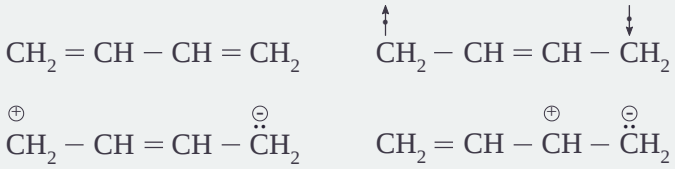


Figure 9.6.7 : Several resonance structures that can be written for 1,3-butadiene. The resonance structure in the upper left dominates, but does not exclusively describe the system since a delocalization energy is experimentally observed compared to two ethylene molecules. (CC BY-NC; Ümit Kaya via LibreTexts)

In general, the true description of the bonding within the valence bond theory is a superposition of resonance structures with amplitudes that are determined via a variational optimization to find the lowest possible energy for the valence bond wavefunctions.

Solving the secular equations (not shown) gives the weighting coefficients for the individual p orbital contributions to the molecular orbitals:

$$\psi_1 = 0.37p_1 + 0.60p_2 + 0.60p_3 + 0.37p_4 \tag{9.6.23}$$

$$\psi_3 = 0.60p_1 + 0.37p_2 - 0.37p_3 - 0.60p_4 \tag{9.6.24}$$

$$\psi_3 = 0.60p_1 - 0.37p_2 - 0.37p_3 + 0.60p_4 \tag{9.6.25}$$

$$\psi_4 = 0.37p_1 - 0.60p_2 + 0.60p_3 - 0.37p_4 \tag{9.6.26}$$

These are depicted in Figure 9.6.8 and using *ab intio* methods in Figure 9.6.6.

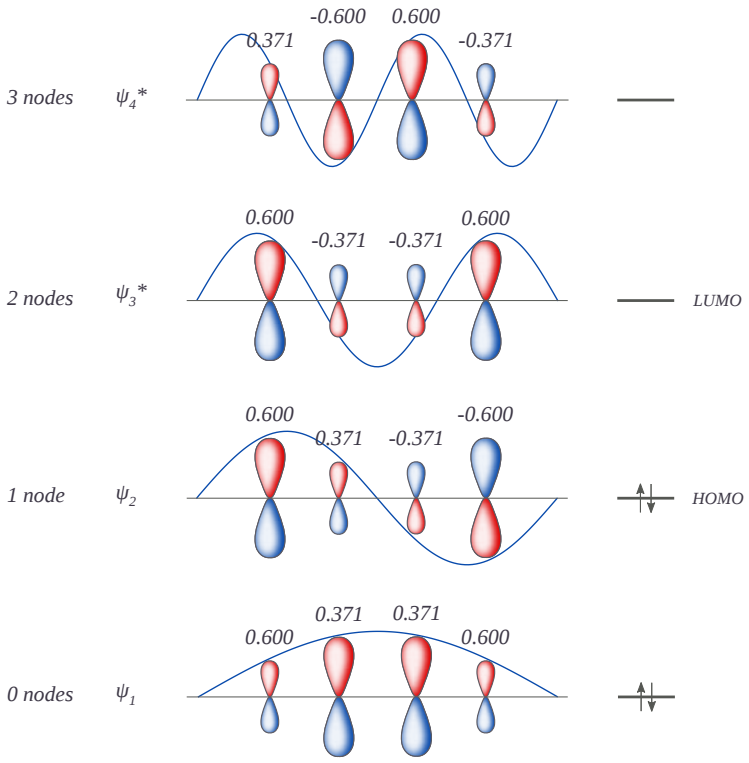


Figure 9.6.8 : Energy level diagram and decomposition of the π molecular orbitals of butadiene. This is shown three-dimensionally in Figure 9.6.6. Note how the nodal structure of these wavefunctions are analogous to the particle-on-a-line nodal structure. (CC BY-NC; Ümit Kaya via LibreTexts)

Note the correlation of the energy of the π molecular orbitals of butadiene to the number of nodes in the wavefunction; this is the general trend observed in previous systems like the particle in the box and atomic orbitals.

9.6.5: Contributors

- Seymour Blinder (Professor Emeritus of Chemistry and Physics at the University of Michigan, Ann Arbor)
- Delmar Larsen (UC Davis)
- Wikipedia
- StackExchange (Philipp)
- Jonathan Gutow (UW Oshkosh)

This page titled 9.6: Hückel MO Model of Conjugation is shared under a CC BY-NC-SA 4.0 license and was authored, remixed, and/or curated by Jonathan Gutow.

- **10.5: The pi-Electron Approximation of Conjugation** is licensed CC BY-NC-SA 4.0.
- **10.6: Butadiene is Stabilized by a Delocalization Energy** by Delmar Larsen is licensed CC BY-SA 4.0.

9.7: Benzene and Aromaticity

Learning Objectives

- Apply Hückel theory to describing the pi bonding in cyclical conjugated system
- Identify the origin of aromaticity within Hückel theory to describe extra stabilization in certain cyclical conjugated systems

9.7.1: Introduction

The previous sections addressed the π orbitals of linear conjugated system. Here we address conjugated systems of **cyclic conjugated hydrocarbons** with the general formula of CnHn where n is the number of carbon atoms in the ring. The molecule from this important class of organic molecule that you are most familiar with is benzene ($\mathrm{C_6H_6}$) with $n = 6$, although many other molecules exist like cyclobutadiene ($\mathrm{C_4H_4}$) with $n = 4$ (Figure $9.7.1$).

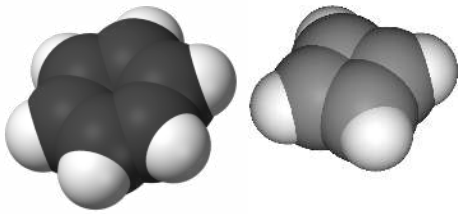


Figure $9.7.1$: Space-filling model of benzene (left) and cyclobutadiene (right). Carbon atoms are indicated in black, while hydrogen atoms are indicated in white. (Public domain; Benjah-bmm27 and Edgar181, respectively).

Structure of Benzene

The structure of benzene is an interesting historical topic. In 1865, the German chemist Friedrich August Kekulé published a paper suggesting that the structure of benzene contained a ring of six carbon atoms with alternating single and double bonds. Within this argument, two resonance structures can be formulated.

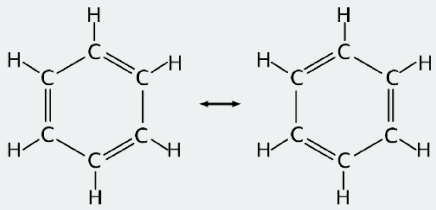


Figure $9.7.2$: Resonance structures of benzene.

However, X-ray diffraction shows that all six carbon-carbon bonds in benzene are of the same length, at 140 pm. The C–C bond lengths are greater than a double bond (135 pm), but shorter than a typical single bond (147 pm). This means that neither of the structures in Figure $9.7.2$ are correct and the true 'structure' of benzene is a mixture of the two. As discussed previously, that such a valence bond perspective results in a **delocalization energy** within a molecular orbital approach.

9.7.2: Applying the Hückel model

Aromatic systems provide the most significant applications of Hückel theory. For benzene, we find the secular determinant

$$\begin{vmatrix} x & 1 & 0 & 0 & 0 & 1 \\ 1 & x & 1 & 0 & 0 & 0 \\ 0 & 1 & x & 1 & 0 & 0 \\ 0 & 0 & 1 & x & 1 & 0 \\ 0 & 0 & 0 & 1 & x & 1 \\ 1 & 0 & 0 & 0 & 1 & x \end{vmatrix} = 0 \tag{9.7.1}$$

Notice the 1's in the bottom left and upper right corners, indicating that atoms 1 and 6 are connected.

There are the six roots $x = \pm 2, \pm 1, \pm 1$. This corresponds to the following energies (ordered from most stable to least since $\beta < 0$):

- $E_1 = \alpha + 2\beta$
- $E_2 = \alpha + \beta$
- $E_3 = \alpha + \beta$
- $E_4 = \alpha - \beta$
- $E_5 = \alpha - \beta$
- $E_6 = \alpha - 2\beta$

The two pairs of $E = \alpha \pm \beta$ energy levels are two-fold degenerate (Figure 9.7.3).

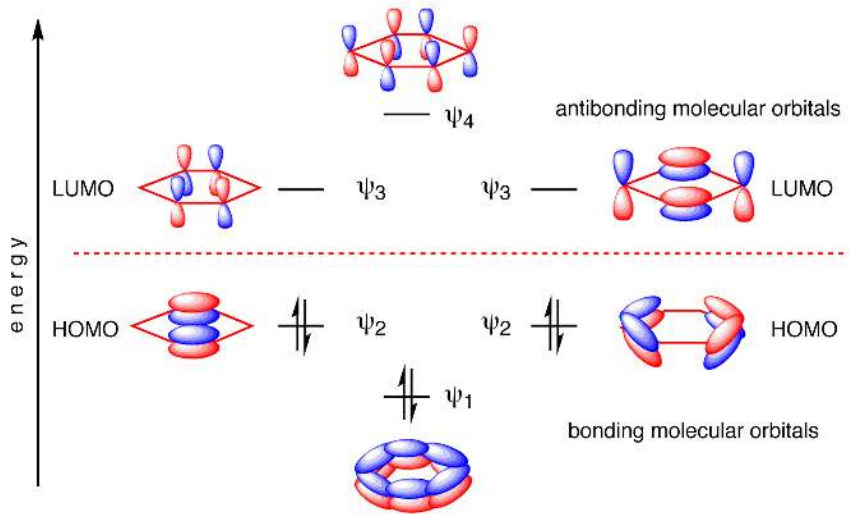


Figure 9.7.3 : The π molecular orbitals for benzene. The dashed lines represent the energy of an isolated p orbitals and all orbitals below this line are bonding. All orbitals above it are antibonding. (CC BY-NC-SA 4.0; Nick Greeves via ChemTube3D)

The resulting wavefunctions are below (expanded in terms of carbon $|2p\rangle$ atomic orbitals).

$$
\begin{aligned}
|\psi_1\rangle &= \frac{1}{\sqrt{6}}[2p_{z1} + 2p_{z2} + 2p_{z3} + 2p_{z4} + 2p_{z5} + 2p_{z6}] \\
\psi_2 &= \frac{1}{\sqrt{4}}[2p_{z2} + 2p_{z3} - 2p_{z4} - 2p_{z5}] \\
\psi_3 &= \frac{1}{\sqrt{3}}\left[2p_{z1} + \frac{1}{2}2p_{z2} - \frac{1}{2}2p_{z3} - 2p_{z4} - \frac{1}{2}2p_{z5} + \frac{1}{2}2p_{z6}\right] \\
\psi_4 &= \frac{1}{\sqrt{4}}[2p_{z2} - 2p_{z3} + 2p_{z4} - 2p_{z5}] \\
\psi_5 &= \frac{1}{\sqrt{3}}\left[2p_{z1} - \frac{1}{2}2p_{z2} - \frac{1}{2}2p_{z3} + 2p_{z4} - \frac{1}{2}2p_{z5} - \frac{1}{2}2p_{z6}\right] \\
\psi_6 &= \frac{1}{\sqrt{6}}[2p_{z1} - 2p_{z2} + 2p_{z3} - 2p_{z4} + 2p_{z5} - 2p_{z6}]
\end{aligned}
$$

Each of the carbons in benzene contributes one electron to the π-bonding framework (Figure 9.7.3). This means that all bonding molecular orbitals are fully occupied and benzene then has an electron configuration of $\pi_1^2\pi_2^2\pi_3^2$. With the three lowest molecular orbitals occupied, the total π-bonding energy is

$$
\begin{aligned}
E_{tot}(\text{benzene}) &= 2(\alpha + 2\beta) + 4(\alpha + \beta) \\
&= 6\alpha + 8\beta
\end{aligned} \tag{9.7.2}
$$

Since the energy of a localized double bond is $2(\alpha + \beta)$, as determined from the analysis of ethylene, the delocalization energy of benzene is

$$\begin{aligned}\Delta E &= E_{tot}(\text{benzene}) - 3E_{tot}(\text{ethylene}) \\ &= (6\alpha + 8\beta) - 3 \times 2(\alpha + \beta) \\ &= 2\beta\end{aligned}$$

The experimental thermochemical value is -152 kJ mol^{-1}.

9.7.3: Aromaticity

In general, cyclic polyenes are only closed shell (i.e., each electron paired up) and extra stable with $(4n+2)\pi$ electrons (n=0,1,2…). These special molecules have the highest delocalization energies and are said to be "aromatic". For benzene this is 2β (Equation 9.7.2), which is the energy by which the delocalized π electrons in benzene are more stable than those in three isolated double bonds.

Hückel's Rule

A stable, closed-shell conjugated cyclic structure is obtained for molecules with $(4n+2)\pi$ electrons with n=2, 6, 10, ... electrons.

Evidence for the enhanced thermodynamic stability of benzene was obtained from measurements of the heat released when double bonds in a six-carbon ring are hydrogenated (hydrogen is added catalytically) to give cyclohexane as a common product.

$$\mathrm{C_6H_6 + 3\,H_2 \longrightarrow C_6H_{12}}$$

In the following diagram cyclohexane represents a low-energy reference point. Addition of hydrogen to cyclohexene produces cyclohexane and releases heat amounting to 11.9 kJ mol^{-1}. If we take this value to represent the energy cost of introducing one double bond into a six-carbon ring, we would expect a cyclohexadiene to release 23.9 kJ mol^{-1} on complete hydrogenation, and 1,3,5-cyclohexatriene to release 35.9 kJ mol^{-1}. These heats of hydrogenation ΔH_{hyd} reflect the relative thermodynamic stability of the compounds (Figure 9.7.4).

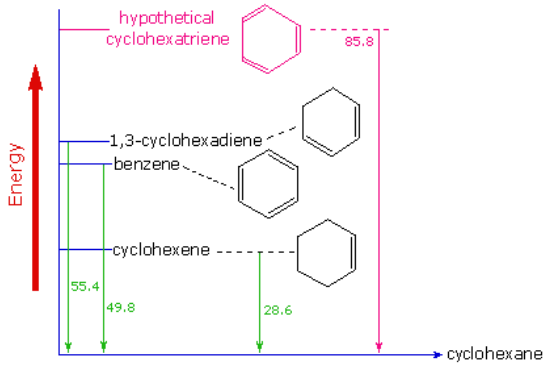


Figure 9.7.4 : Experimental evidence for aromatic stabilization energy in benzene from the heat of hydrogenation. Energies are in kcal/mol. (CC BY-NC-SA 4.0; William Resuch);

In practice, 1,3-cyclohexadiene is slightly more stable than expected, by about 8.1 kJ mol^{-1}, presumably due to conjugation of the double bonds. Benzene, however, is an extraordinary 15 kJ mol^{-1} more stable than expected. This additional stability is a characteristic of all aromatic compounds.

This page titled 9.7: Benzene and Aromaticity is shared under a CC BY-NC-SA 4.0 license and was authored, remixed, and/or curated by Jonathan Gutow.

- **10.7: Benzene and Aromaticity** by William Reusch is licensed CC BY-NC-SA 4.0.

9.8: Numerical QM Methods

9.8.1: Introduction

Quantum mechanical computations can be performed to estimate many properties of molecules: shape, charge distribution, dipole moments, spectroscopic properties, ionization energies, reactivity and much more. Realistic computations require significant computing power combined with sophisticated numerical methods that have been undergoing continuous development since the 1960s. The current state of the art *ab initio* (from first principles) methods come in two flavors **Hartree-Fock self consistent field methods** (HF-SCF) and **Density functional theory methods** (DFT). These methods are *ab initio* in the sense that they do not require any empirical (measured values) other than basic physical constants. This contrasts with semi-empirical methods, many of which are extensions of the Hückel method beyond π orbitals. In semi-empirical methods many of the necessary integrals are replaced with constants that have been adjusted to get results (e.g. molecular geometries) that match those of a particular set of molecules. Some of these semi-empirical methods (e.g. the extended Hückel) are used to make initial guesses at the electron distribution to begin an *ab initio* computation.

Both methods utilize the **Born-Oppenheimer** approximation to separate the nuclear and electronic parts of the calculation. They also depend on the **variational principle**, the provable assertion that the best guess at the ground state wavefunction is the lowest energy that can be achieved by adjusting parameters in a guessed wavefunction. Thus an optimized wavefunction provides an upper bound to the energy of the actual wavefunction.

Although it is now possible for anybody who can draw a Lewis structure to purchase or download software to do these types of computations, there are myriad pitfalls and ways to get results that are very far from what is observed experimentally. Care must be taken when doing these types of calculations and should generally be undertaken and interpreted with the assistance of an expert in quantum computations.

9.8.2: Hartree-Fock self consistent field methods (HF-SCF)[1]

This method is based on the molecular orbital approximation, where each electron is assumed to be represented by a single electron wavefunction consisting of a linear combination of atomic orbitals (LCAO). So a single electron wavefunction is of the form:

$$\phi_j = c_{j1}\psi_1 + c_{j2}\psi_2 + c_{j3}\psi_3 \ldots \tag{9.8.1}$$

where ϕ_j is the single electron wavefunction, the ψ_k are the atomic orbitals on all the atoms and the c_{jk} are the coefficients that scale the contribution of each of the atomic orbitals to the overall wavefunction. To make the computations numerically tractable, the ψ_k are built from sums of 3-D gaussians rather than using the functional forms of the s, p, d, etc. from the exact solution of the one electron atom. The overall wavefunction is then taken as a product of these wavefunctions in the same way as for a multi-electron atom.

$$\Psi_{molec} = \phi_1\phi_2\phi_3\phi_4 \ldots \tag{9.8.2}$$

The Hartree-Fock method accounts for the interaction of the electrons in the different molecular orbitals, ϕ_j, by adding a potential term to the Hamiltonian that is the average electrostatic potential experienced by an electron in orbital j because of the probability distribution of the all the other electrons. This is then used to optimize the coefficients in equation 9.8.1. In order to start a calculation you must have an initial guess for the orbitals and their occupations. Most HF-SCF use an extended version of the Hückel method for this initial guess. Glossing over the details of setting up the complex secular equations for these large systems, the HF-SCF procedure can be outlined as follows:

1. Guess an initial geometry.
2. Choose a basis set (the ψ_q in equation 9.8.1).
3. Use a method such as extended Hückel to generate an initial set of orbital energies and occupations.
4. Start the SCF process:
    a. Choose a wavefunction ϕ_k to focus on.
    b. Calculate the average electrostatic potential experienced by an electron in orbital ϕ_k using the current wavefunctions for all the other occupied orbitals and the nuclear positions.
    c. Adjust ϕ_k to minimize its energy in the electrostatic field.
    d. Choose a new ϕ_k to concentrate on and repeat (b) and (c) until the total energy has reached a minimum within the precision requested.

e. This process may iterate through all the ϕ multiple times.

5. Move the nuclei and restart SCF (step 4) until the total energy is minimized within the precision requested.

The SCF part of this process keeps adjusting the wavefunctions until they stop changing. This generally works, but there is no guarantee that the SCF process will converge to an optimal set of ϕ_k. In large systems and with large basis sets the SCF process can start oscillating. Significant effort has gone into developing techniques to improve convergence (a couple of common techniques are Damping and DIIS). Another issue with this method (and any simple MO calculation) is that it ignores electron correlation to the extent that the average electrostatic potential does not account for the fact that any chosen pair of electrons repels each other, so will have some correlation of their movement. The result is that HF-SCF energies are expected to be higher than the true energy, where electron correlation is taken into account. Extensions to the HF-SCF that include variable contributions from alternative (excited) electron configurations can correct for this but are computationally very expensive. There are many versions of these configuration interaction extensions (e.g. CI, MCSCF, CASSCF, CC). Some of these configuration interaction methods come in specialized flavors designed to calculate a specific molecular property such as ionization energies (IP-EOMCCSD), that are sensitive to electron correlations.

9.8.3: Density functional theory methods (DFT)[2]

The basic idea behind density functional theory methods is to calculate the electron density at a grid of points in the system rather than the quantum states (orbitals) of each of the electrons. Rather than having to account for 3 coordinates for each electron, you only have to account for the electron density at each point in 3-D space. It has been proven that describing the electron density is adequate to determine the overall system energy and in the exact form of DFT the variational principle applies (for a chosen basis set the minimum energy is the best estimate of the actual value). Because only the overall electron density is calculated rather than individual wavefunctions, this method is generally much less computationally intensive.

DFT methods were originally developed for solid state computations where the number of nuclei and electrons are very large. All practical implementations require an empirical function (the "functionals") that is guessed at to perform the calculation. It was not until the early 1990s that people began to guess at functionals able to yield reasonable agreement with properties of small molecules. Since then a large amount of work has been directed at improving these guessed functionals. In theory these functionals have to account for electron correlations and the non-classical behavior of electrons, but as of yet only guesses as to the form of these functionals are available.

The outline of the procedure for DFT calculations is similar to HF-SCF except that the SCF process optimizes the electron density rather than each orbital.

DFT is rapidly evolving and can be a good method for calculating molecular parameters. However, the quality of the results is highly dependent on the choice of functional (an early popular one was B3YLP, which is no longer recommended for most computations). Different functionals give better results for different kinds of computations. Another issue with DFT computations is that they are sensitive to the spacing chosen between points on the 3-D grid at which the electron densities are computed.

9.8.4: Examples of output from quantum computations

Modern quantum software produces lots of information about a molecular species. The most obvious are the shapes of the molecules, their orbitals and the orbital energies. Combined with modern graphics software this can help chemists visualize what molecules look like and how they might interact. The figure below shows some images for methyl fluoride.

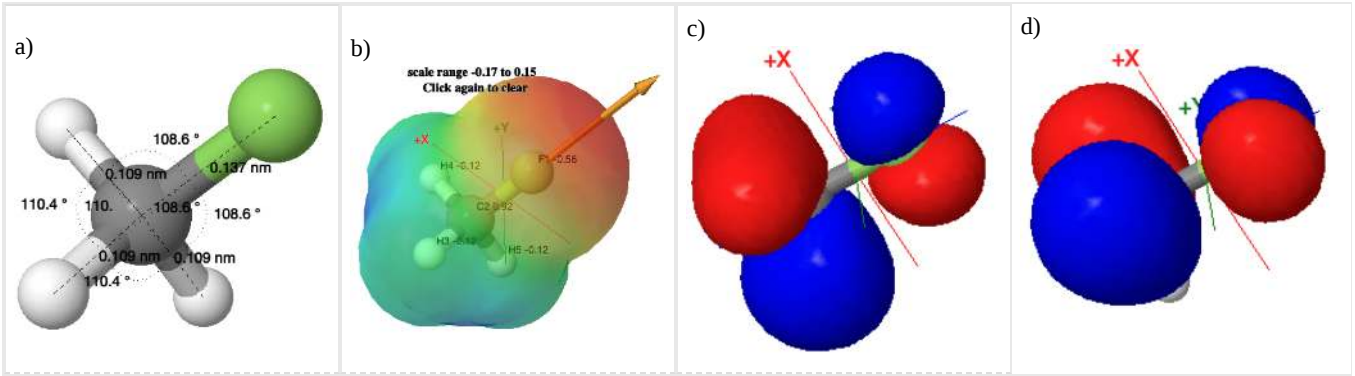


Figure 9.8.1: HF-SCF calculations using an ACCD basis set on fluoromethane: a) geometry; b) electrostatic potential, partial charges and vector representing the dipole moment; c) & d) the two degenerate HOMO orbitals.

We can compare the computed bond lengths in figure 9.8.1a with experimental values listed in the NIST computational chemistry comparison database. The listed bond lengths are r_{CH} = 0.1087 nm, r_{CF} = 0.1383 nm and bond angles are a_{HCH} = 110.2˚ and a_{HCF} = 108.73˚. There are slight discrepencies from the experimental geometry, but they are very small, suggesting the ACCD basis set gives a reasonable approximation to the structure of the molecule. The dipole moment and electrostatic potential map (figure 9.8.1b) are consistent with what we would expect from the much higher electronegativity of F compared to the other atoms in the molecule. In figure 9.8.1 c & d we can visually see that the two degenerate HOMO orbitals involve primarily p-type orbitals on the F atom, but on the methyl end the orbitals involve combinations of p-type orbitals on the C and s-type orbitals on the hydrogens. These fractional contributions to the MOs can be understood more quantitatively by examining the numerical coefficients multiplying the AO contributions to the MOs.

The figure below is a calculation on a fragment of a cold virus showing where it is in close contact (bullseyes) with the cell surface receptor molecule it uses to enter the cell.

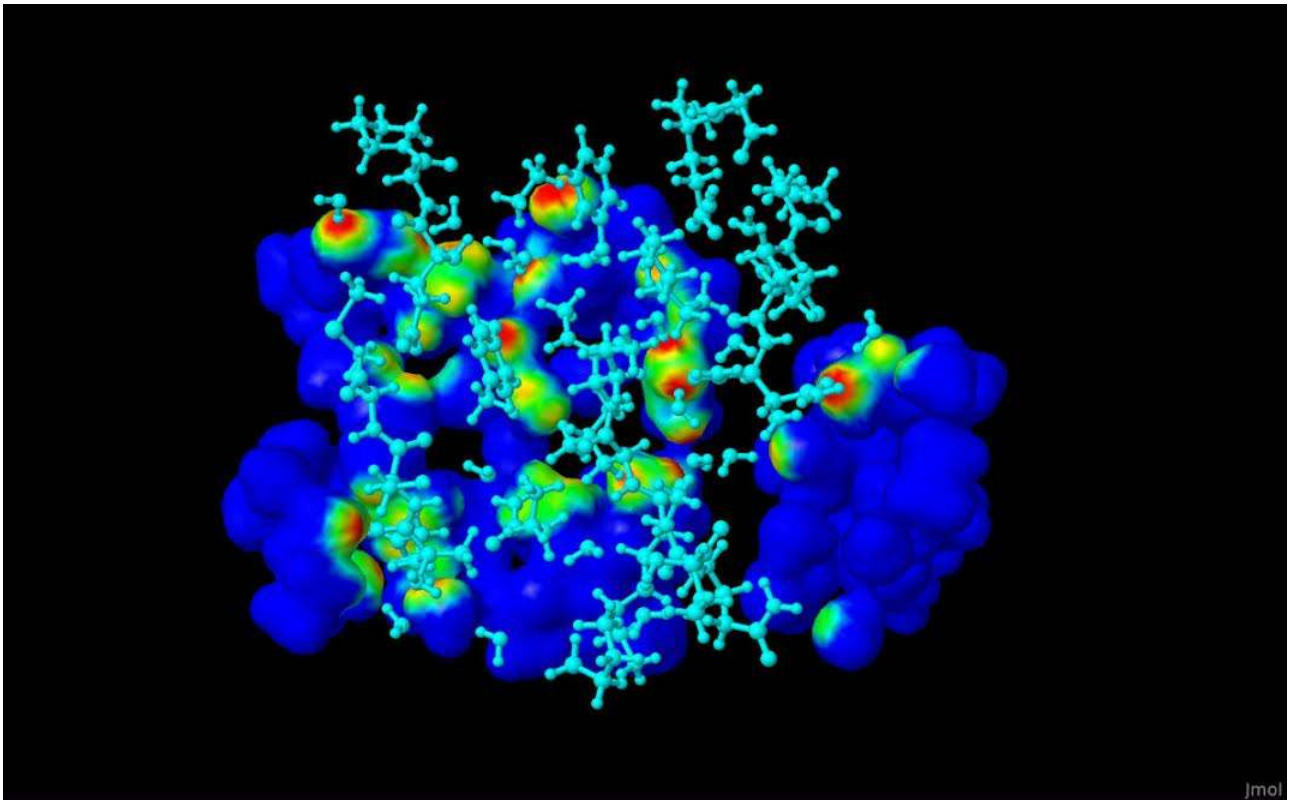


Figure 9.8.2: The binding site on the rhinovirus capsid in contact with the receptor it uses to enter the cell.

MO calculations can also be used to generate estimates of UV-Vis, NMR, IR and Raman spectra as well. Unless great care is taken the generated spectra will have peaks significantly shifted from the experimental values. Even with these shifts they can often be used to assign the origin of peaks in the spectra to particular spectroscopic transitions. See the figure below for a comparison of an experimental and simulated IR spectrum for methylfluoride.

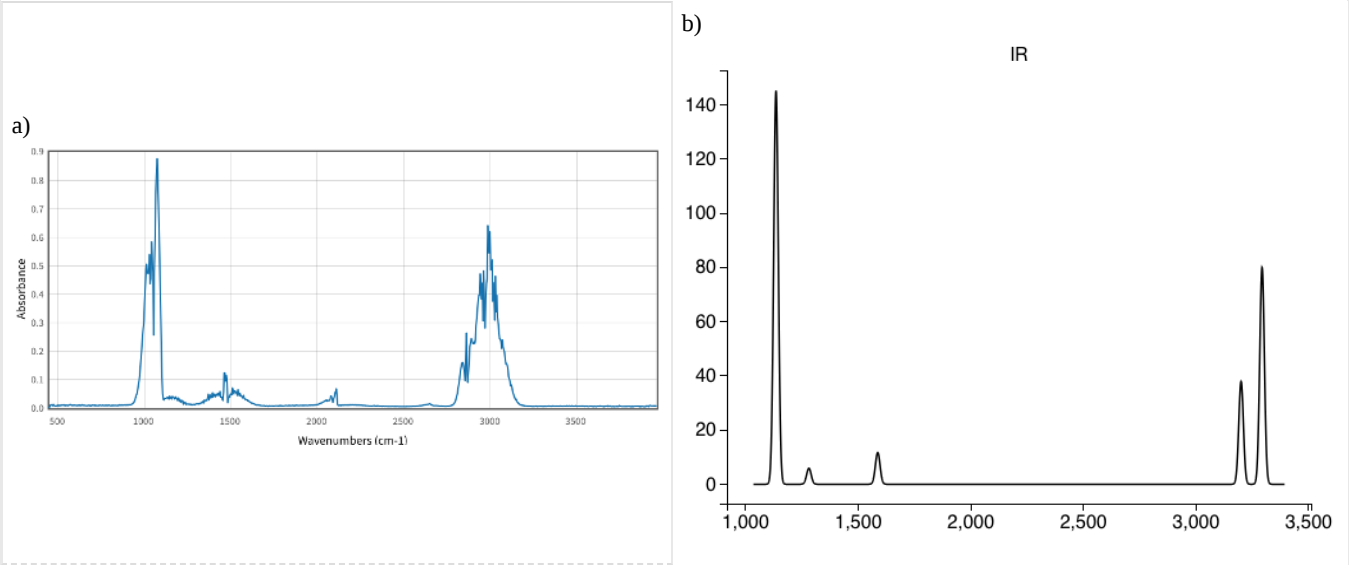


Figure 9.8.3: a) Experimental IR spectrum (from NIST Chemistry Webbook); b) Simulated spectrum generated from a GAMESS computation on methylfluoride using the ACCD basis set. Notice that the C-H stretching wavenumbers seen at about 3000 cm^{-1} in the experimental spectrum are much too high in the simulated spectrum. This reflects the fact that the simulation assumes a harmonic vibrational potential, while the C-H bond stretch is extremely anharmonic leading to more closely spaced quantum states and a lower energy vibrational transition.

9.8.5: References

1. C. J. Cramer *Essentials of Computational Chemistry*, 2nd Ed. (John Wiley & Sons, Ltd, Hoboken, NJ, 2004) Ch. 4.

2. C. J. Cramer *Essentials of Computational Chemistry*, 2nd Ed. (John Wiley & Sons, Ltd, Hoboken, NJ, 2004) Ch. 8.

9.8.6: Contributors

- Jonathan Gutow (UW Oshkosh)

This page titled 9.8: Numerical QM Methods is shared under a CC BY-NC-SA 4.0 license and was authored, remixed, and/or curated by Jonathan Gutow.

CHAPTER OVERVIEW

10: Aggregates and Macromolecules

10.1: Mass Spectrometry
10.2: X-Ray Crystallography
10.3: Cryo-Electron Microscopy
10.4: Intermolecular Forces
10.5: Structure of Gases, Liquids and Glasses
10.6: Macromolecules
10.7: Simulations

This page titled 10: Aggregates and Macromolecules is shared under a CC BY-NC-SA 4.0 license and was authored, remixed, and/or curated by Jonathan Gutow.

10.1: Mass Spectrometry

10.1.1: Introduction

Mass spectrometry (MS) is used widely in chemistry and biochemistry to identify molecules. Measuring the mass-to-charge ratio (m/z) of an ion can allow identification of the species the ion came from. This page starts by describing the three basic functional blocks of a mass spectrometer (ion source, mass filter and detector). Then focuses on particular versions of the building blocks most applicable to large molecules and macromolecules.

10.1.2: Parts of a mass spectrometer

There are three basic functional blocks to a mass spectrometer: the ion source; a mass analyzer/filter; and a detector as shown in figure 10.1.1.[1]

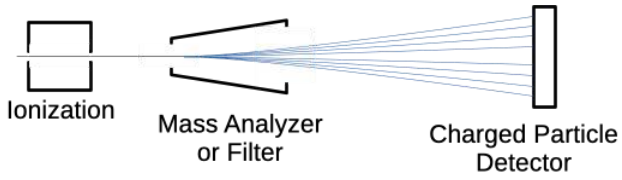


Figure 10.1.1: A cartoon block diagram of the parts of a mass spectrometer. The sample enters the ionization region at the left. Once ionized the particles enter the mass analyzer and are sorted in some way by their mass-to-charge ratio (m/z) before being detected.

For small to medium molecules that can be readily volatilized (up to a few hundred amu) the samples are often separated via physical characteristics using gas chromatography (GC). The gaseous output from the GC is then fed into the ionization region of the mass spectrometer. When molecules other than the carrier gas come out of the GC signal is detected (figure 10.1.2*a*). Since most mass spectrometers can collect the mass spectrum of a sample in less than a second, the mass spectra can represent different time slices of the GC output. Thus the m/z peaks from each time slice can be used to help figure out what came out of the GC at each particular time (figure 10.1.2*b*).

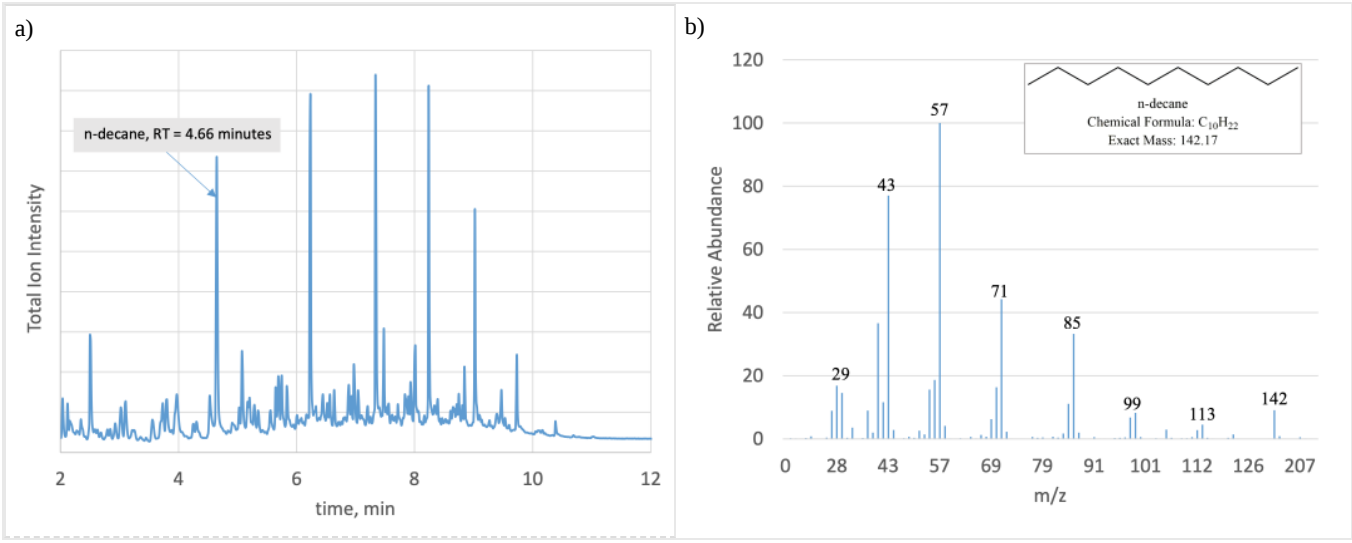


Figure 10.1.2: a) the total ion count versus time GC trace for jet fuel (JP-8); b) the mass spectrum of the decane peak. In this case the ionization was done by exposing the molecules to electrons boiling off of a filament (electron impact ionization or 'EI'). Notice that the molecules are broken into many characteristic smaller ions. From reference 2 (https://tsapps.nist.gov/publication/...?pub_id=926655).

Most larger molecules decompose on vaporization so getting their mass spectra are more difficult requiring specialized vaporization and ionization techniques such as Electrospray Ionization (ESI) and Matrix Assisted Laser Desorption and Ionization

(MALDI), as well as very high resolution MS techniques to differentiate between large ions that vary by less than 1 part in 10,000 in mass.

10.1.3: Techniques for generating ions of large molecules

Because large molecules tend to decompose at temperatures high enough to volatilize them, alternative methods for getting them into the gas phase and ionized are used. Two of the most important methods are Electrospray Ionization (ESI) and Matrix Assisted Laser Desorption and Ionization (MALDI).

10.1.3.1: ESI

Electrospray Ionization (ESI) for MS was first reported in the late 1960s, but was primarily developed in the 1980s. J.B. Fenn received the Nobel Prize in Chemistry for this work, but a number of others were involved and described similar results at the same time (https://en.wikipedia.org/wiki/Electrospray_ionization).[3]

As illustrated in figure 10.1.3 a solution containing low concentrations of the high molecular weight analyte are ejected from a capillary held at a large voltage difference compared to a target. Charged droplets and eventually single ions are created as the droplets disperse and move towards the target. The target contains an aperture through which the created ions can enter the low pressure regions of the mass spectrometer. The illustration shows a system set up to create positive ions.

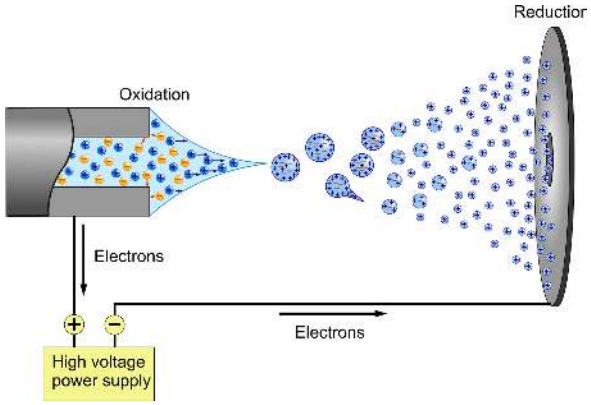


Figure 10.1.3: Diagram of electrospray ionization in positive mode: under high voltage, the liquid leaving the capillary tip emits a jet of liquid drops. The solvent from the droplets progressively evaporates, leaving them more and more charged. When the repulsion due to charging exceeds the attractions (reaches the Rayleigh limit) the droplet explosively dissociates, leaving a stream of charged (positive) ions.[3] Image courtesy of Andreas Dahlin, CC BY 2.0, via Wikimedia Commons.

The solvent used is primarily water, but additional small organic molecules and acids are added to optimize droplet formation and provide protons. This ionization technique commonly produces multiply charged ions (eg. +2, +3 ...) in addition to singly charged ions. The charge is usually in the form of associated protons or other cations (e.g. Na^+).[3]

10.1.3.2: MALDI

This technique was developed in the 1980s. In 1987 K. Tanaka and co-workers at Shimadzu Corp. demonstrated a matrix that allowed the ionization of intact proteins up to about 34 kDa. Tanaka received part of the 2002 Nobel Prize in Chemistry for this work. Others rapidly found matrices that allowed ionization of much larger intact molecules. Commercial instruments became available for purchase in the 1990s.[4]

As illustrated in figure 10.1.4 the macromolecule of interest is embedded in a solid matrix of a small molecule that strongly absorbs the wavelength of the laser. A short pulse of laser light ablates (removes from the surface) the small molecules through rapid heating. In the process the macromolecules are carried intact into the gas phase as well. With the proper choice of matrix molecules positive charges can transfer to the macromolecules creating the desired gas phase macromolecular ions.

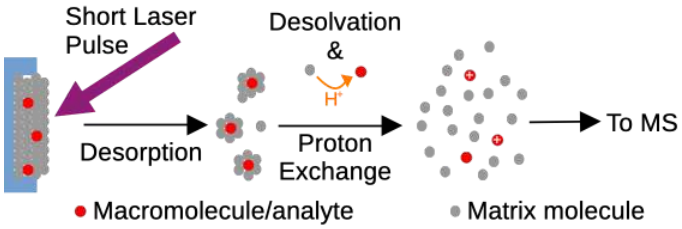


Figure 10.1.4: Cartoon of the MALDI process. The matrix is rapidly heated by the pulsed laser, leading to a cloud of vaporized matrix molecules and the entrained macromolecules. Charges (usually protons) are transferred from the matrix to the macromolecules yielding charged macromolecules. The pulse of charged macromolecules are then transferred to the mass analyzer section, usually using a voltage difference to accelerate the charged particles.

Different matrix molecules are used depending on the species. Nicotinic acid, sinapic acid and ferulic acid have been used with proteins. Gentisic acid has been applied to peptides and nucleotides. Sinapic acid and α-cyano-4-hydroxycinnamic acid have been used for lipids. The analyte and matrix molecules are dissolved in a volatile solvent mixture usually containing water plus species such as acetonitrile, methanol and acetone. A drop is placed in a well on a metal target and the solvent is allowed to evaporate. Once the samples have solidified, they are placed in the evacuated ionization chamber. A pulse from the laser is focused on the sample spot producing a short pulse of ionized macromolecules. This technique typically produces more singly charged ions, but ions with multiple charges are observed and recognizable by the fact that their m/z ratio is an integer fraction of the largest m/z of the species.[4]

10.1.4: High resolving power mass filters

For small relatively easy to volatilize molecules as might be separated using gas chromatography the most common mass analyzer/filter is the quadrupole mass filter. The practical limit of a quadrupole for differentiating two molecules with a mass difference of 1 amu (Dalton) is a molecular mass of less than 1000 - 1200 amu. This is inadequate for macromolecules which have masses > 10,000 amu. For this reason most macromolecular mass spectrometry uses time-of-flight or ion cyclotron resonance traps to differentiate masses within a sample. These can differentiate masses that vary by 1 amu in 50,000 or more.[2]

10.1.4.1: Time-of-flight[5]

This technique has been in use since the 1940's, but enhancements to electronics, ion sources (MALDI, in particular) and the development of **reflectron** time-of-flight techniques have improved the mass resolution to the point where time-of-flight is applicable to mass spectrometry of macromolecules.

As illustrated in figure 10.1.5 a clump (short pulse) of ions is accelerated through a fixed voltage. This imparts the same kinetic energy to all ions with the same charge. The accelerated ions are then allowed to travel through an evacuated tube with no electric field (the "drift region"). Lighter ions travel faster for the same total kinetic energy, thus reaching the detector at the end of the drift region before heavier ions. The time of arrival can be used to determine the mass of the ions.



Figure 10.1.5: Cartoon of a simple linear time-of-flight mass spectrometer. By K. K. Murray, CC BY-SA 4.0, via Wikimedia Commons.

When a charged particle is accelerated by a constant electric field (*E*) through a distance (*d*) it experiences a total potential change of *V* = *zeEd*, where *z* is the charge and *e* is the fundamental unit of charge in Coulombs. All of this potential change is in the form of kinetic energy:

$$KE = \frac{1}{2}mv^2 = zeEd \implies v = \sqrt{\frac{2zeEd}{m}} \tag{10.1.1}$$

The drift time is just the length of the drift region ℓ divided by the speed (v):

$$t = \ell\left(\frac{m}{2zeEd}\right)^{1/2} = \ell\left(\frac{m}{2zeV}\right)^{1/2} = k\left(\frac{m}{z}\right)^{1/2} \tag{10.1.2}$$

For any given instrument setting everything but *m/z* is constant. These constants can be combined into a single constant yielding the final form of equation 10.1.2. Thus, a plot of *t* vs *m/z* (or *m/z* vs *t*) yields a straight line and the instrument can be calibrated using a sample containing known masses. In practice the zero-time is usually set by the generation of the ions (e.g. the laser pulse) and not when the ions enter the drift region. So, there is a zero offset (non-zero y-intercept) and the flight time takes the form of:

$$t = k\left(\frac{m}{z}\right)^{1/2} + C \tag{10.1.3}$$

Where C accounts for the time offset.

Because the initially created ions have a distribution of velocities before acceleration, ions of a single *m/z* ratio have a spread of velocities in the drift region. This reduces the resolution of the instrument. Many modern instruments correct for this by using a reflectron geometry as illustrated in figure 10.1.6. The ions that are traveling faster penetrate more deeply into the refectron electric field region than the slower ions. The difference in path length causes ions of the same *m/z* to arrive at the detector at the same time despite their initial differences in velocity.

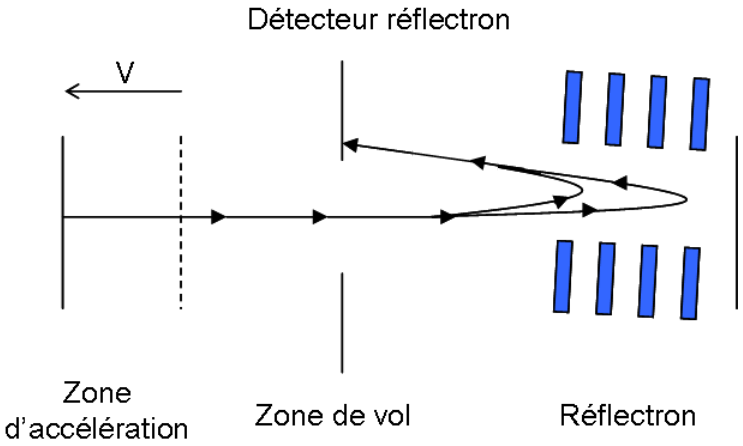


Figure 10.1.6: Cartoon of a reflectron time-of-flight mass spectrometer. By Elisemarion 16:08, 7 June 2007 (UTC), CC BY-SA 3.0, via Wikimedia Commons.

10.1.4.2: Ion traps

There are two ion traps that are regularly used to measure mass differences between large ions: **ion cyclotron resonance traps**[6] and **orbitraps**[7]. They achieve the necessary resolution by trapping the ions in a way that causes them to oscillate back and forth within the trap at a frequency related to the *m/z* ratio of the ions. The high resolution is achieved because trapping and detection are combined. The ion oscillation frequency is measured over relatively long periods of time, leading to very high precision and thus high mass resolving ability. The longer the period of time the ions are trapped the higher the resolution. The signal measured contains frequency components from all the ions in the trap. Modern instruments use the Fourier-transform[8] to convert the signal into individual frequency (*m/z*) contributions.

There are other types of ion traps, but they are generally not used for resolving small mass differences between large ions.

10.1.5: Detectors[1]

Based on "Microchannel plate detector" from Wikipedia.

The most common detector in mass spectrometers is the **microchannel plate** (**MCP**) which can detect single particles. It is closely related to an electron multiplier, as both intensify single particles or photons by the multiplication of electrons via secondary emission. Because a microchannel plate detector has many separate channels, it can provide spatial resolution.

A microchannel plate is a slab made from resistive material (most often glass) 0.5 to 2mm thick with a regular array of tiny tubes (microchannels) leading from one face to the other. The microchannels are typically 5-20 micrometers in diameter, parallel to each

other and enter the plate at a small angle to the surface (8-13° from normal). See figure 10.1.7.

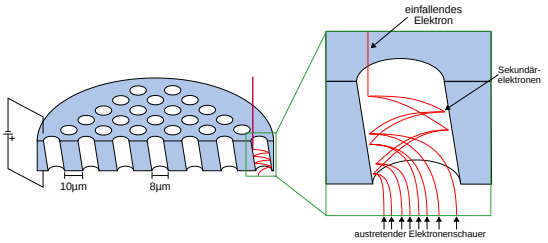


Figure 10.1.7: Schematic diagram of the operation of a microchannel plate. By Andreas 06, Public domain, via Wikimedia Commons.

The microchannel plate functions as a particle amplifier, turning a single impinging particle into a cloud of electrons. By applying a strong electric field across the MCP, each individual microchannel becomes a continuous-dynode electron multiplier. The electrons exit the channels on the opposite side of the plate, where they are collected on an anode. Some anodes are designed to allow spatially resolved ion collection, producing an image of the particles or photons incident on the plate.

> Note that high resolution ion traps detect the image currents created in electrodes by the spacial oscillations of the trapped ions, rather than detecting when the ions collide with a detector.

10.1.6: References

1. Wikipedia: https://en.wikipedia.org/wiki/Mass_spectrometry#Parts_of_a_mass_spectrometer.

2. Lovestead, T. and Urness, K. (2019), Gas Chromatography - Mass Spectrometry (GC-MS), ASM Handbook, Volume 10: Materials Characterization, [online], https://tsapps.nist.gov/publication/get_pdf.cfm?pub_id=926655.

3. "Electrospray Ionization", Wikipedia.org, https://en.wikipedia.org/wiki/Electrospray_ionization.

4. "Matrix-Assited Laser Desorption/Ionization", Wikipedia.org, https://en.wikipedia.org/wiki/Matrix...ion/ionization.

5. "Time-of-flight MS", Wikipedia.org, https://en.wikipedia.org/wiki/Time-of-flight_mass_spectrometry.

6. "Fourier-transform ion cyclotron resonance", Wikipedia.org, https://en.wikipedia.org/wiki/Fourie...tron_resonance.

7. "Orbitrap", Wikipedia.org, https://en.wikipedia.org/wiki/Orbitrap.

8. "Fourier transform", Wikipedia.org, https://en.wikipedia.org/wiki/Fourier_transform.

This page titled 10.1: Mass Spectrometry is shared under a CC BY-NC-SA 4.0 license and was authored, remixed, and/or curated by Jonathan Gutow.

10.2: X-Ray Crystallography

10.2.1: Introduction

X-Ray crystallography can provide precise information on the geometry of molecules and molecular aggregates. However, it requires solid crystalline samples and for the most precise information the crystals must be nearly free of flaws in the repeating structure. We begin with an overview of X-Ray diffraction.

The size of the unit cell and the arrangement of atoms in a crystal may be determined from measurements of the *diffraction* of X-rays by the crystal, termed X-ray crystallography. Diffraction is the change in the direction of travel experienced by an electromagnetic wave when it encounters a physical barrier whose dimensions are comparable to those of the wavelength of the light. X-rays are electromagnetic radiation with wavelengths about as long as the distance between neighboring atoms in crystals (on the order of a few Å).

When a beam of monochromatic X-rays strikes a crystal, its rays are scattered in all directions by the atoms within the crystal. When scattered waves traveling in the same direction encounter one another, they undergo *interference*, a process by which the waves combine to yield either an increase or a decrease in amplitude (intensity) depending upon the extent to which the combining waves' maxima are separated (see Figure 10.2.18).

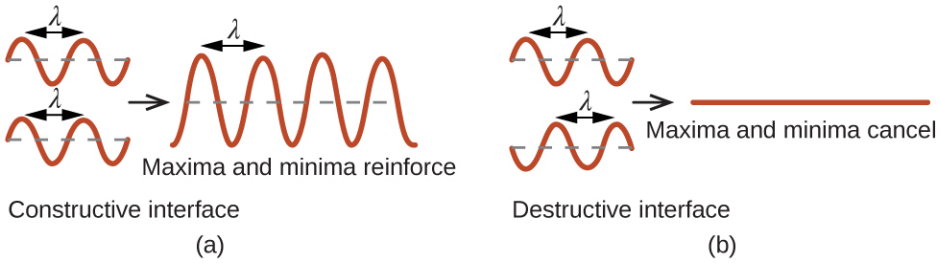


Figure 10.2.18: Light waves occupying the same space experience interference, combining to yield waves of greater (a) or lesser (b) intensity, depending upon the separation of their maxima and minima.

When X-rays of a certain wavelength, λ, are scattered by atoms in adjacent crystal planes separated by a distance, d, they may undergo constructive interference when the difference between the distances traveled by the two waves prior to their combination is an integer factor, n, of the wavelength. This condition is satisfied when the angle of the diffracted beam, θ, is related to the wavelength and interatomic distance by the equation:

$$n\lambda = 2d\sin\theta \tag{10.2.1}$$

This relation is known as the **Bragg equation** in honor of W. H. Bragg, the English physicist who first explained this phenomenon. Figure 10.2.19 illustrates two examples of diffracted waves from the same two crystal planes. The figure on the left depicts waves diffracted at the Bragg angle, resulting in constructive interference, while that on the right shows diffraction and a different angle that does not satisfy the Bragg condition, resulting in destructive interference.

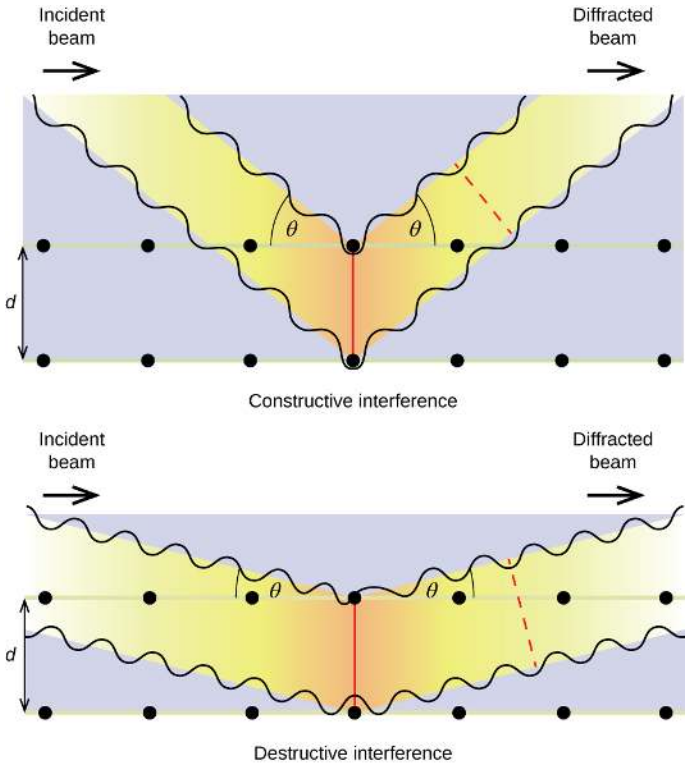


Figure 10.2.19: The diffraction of X-rays scattered by the atoms within a crystal permits the determination of the distance between the atoms. The top image depicts constructive interference between two scattered waves and a resultant diffracted wave of high intensity. The bottom image depicts destructive interference and a low intensity diffracted wave.

Link to Learning

Visit this site for more details on the Bragg equation and a simulator that allows you to explore the effect of each variable on the intensity of the diffracted wave.

An X-ray diffractometer, such as the one illustrated in Figure 10.2.20, may be used to measure the angles at which X-rays are diffracted when interacting with a crystal as described earlier. From such measurements, the Bragg equation may be used to compute distances between atoms as demonstrated in the following example exercise.

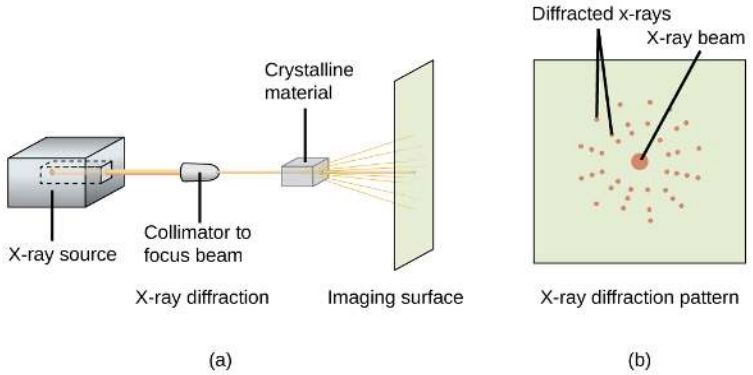


Figure 10.2.20: (a) In a diffractometer, a beam of X-rays strikes a crystalline material, producing (b) an X-ray diffraction pattern that can be analyzed to determine the crystal structure.

Example 10.2.6: Using the Bragg Equation

In a diffractometer, X-rays with a wavelength of 0.1315 nm were used to produce a diffraction pattern for copper. The first order diffraction ($n = 1$) occurred at an angle $\theta = 25.25°$. Determine the spacing between the diffracting planes in copper.

10.2.1.1: Solution

The distance between the planes is found by solving the Bragg equation (Equation 10.2.1), $n\lambda = 2d\sin\theta$, for d.

This gives:

$$d = \frac{n\lambda}{2\sin\theta} = \frac{1(0.1315nm)}{2\sin(25.25^\circ)} = 0.154nm$$

Exercise 10.2.6

A crystal with spacing between planes equal to 0.394 nm diffracts X-rays with a wavelength of 0.147 nm. What is the angle for the first order diffraction?

Answer

10.8°

Portrait of a Chemist: X-ray Crystallographer Rosalind Franklin

The discovery of the structure of DNA in 1953 by Francis Crick and James Watson is one of the great achievements in the history of science. They were awarded the 1962 Nobel Prize in Physiology or Medicine, along with Maurice Wilkins, who provided experimental proof of DNA's structure. British chemist Rosalind Franklin made invaluable contributions to this monumental achievement through her work in measuring X-ray diffraction images of DNA. Early in her career, Franklin's research on the structure of coals proved helpful to the British war effort. After shifting her focus to biological systems in the early 1950s, Franklin and doctoral student Raymond Gosling discovered that DNA consists of two forms: a long, thin fiber formed when wet (type "B") and a short, wide fiber formed when dried (type "A"). Her X-ray diffraction images of DNA (Figure 10.2.21) provided the crucial information that allowed Watson and Crick to confirm that DNA forms a double helix, and to determine details of its size and structure. Franklin also conducted pioneering research on viruses and the RNA that contains their genetic information, uncovering new information that radically changed the body of knowledge in the field. After developing ovarian cancer, Franklin continued to work until her death in 1958 at age 37. Among many posthumous recognitions of her work, the Chicago Medical School of Finch University of Health Sciences changed its name to the Rosalind Franklin University of Medicine and Science in 2004, and adopted an image of her famous X-ray diffraction image of DNA as its official university logo.

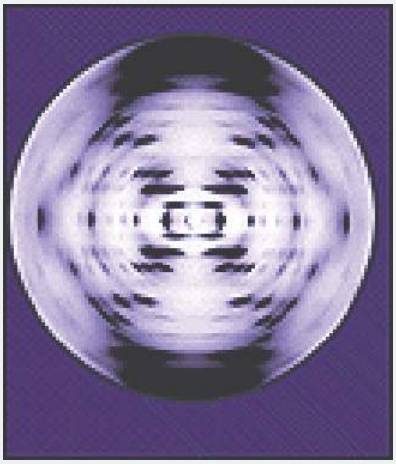


Figure 10.2.21: This illustration shows an X-ray diffraction image similar to the one Franklin found in her research. (credit: National Institutes of Health)

10.2.2: Crystal Systems

Unit cells need not be cubes, but they *must* be parallel-sided, three-dimensional figures. A general example is shown in Figure 10.2.4 Such a cell can be described in terms of the lengths of three adjacent edges, *a*, *b*, and *c*, and the angles between them, α, β, and γ.

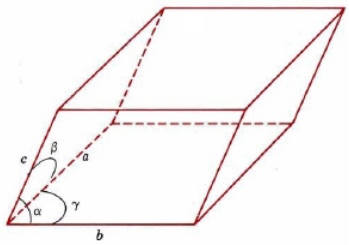


Figure 10.2.4 A generalized unit cell with sides a, b, and c, and angles α, β, and γ.

Crystals are usually classified as belonging to one of fourteen Bravais lattices, depending on the shape of the unit cell and the number of atoms in the unit cell. These fourteen systems are shown in Figure 10.2.5 below. Figure 10.2.6 lists the details about each of the lattice systems.

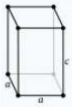
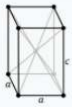
Crystal family	Lattice system	Point group (Schönflies notation)	14 Bravais lattices			
			Primitive (P)	Base-centered (S)	Body-centered (I)	Face-centered (F)
Triclinic (a)		C_i	 aP			
Monoclinic (m)		C_{2h}	 mP	 mS		
Orthorhombic (o)		D_{2h}	 oP	 oS	 oI	 oF
Tetragonal (t)		D_{4h}	 tP		 tI	
Hexagonal (h)	Rhombohedral	D_{3d}	 hR			
	Hexagonal	D_{6h}	 hP			
Cubic (c)		O_h	 cP		 cI	 cF

Figure 10.2.5: The seven lattice systems and fourteen Bravais lattices. (Wikipedia contributors. (2021, September 2). Bravais lattice. In Wikipedia, The Free Encyclopedia. Retrieved 01:22, October 3, 2021, from https://en.Wikipedia.org/w/index.php?title=Bravais_lattice&oldid=1042012012)

Crystal family	Lattice system	Volume	Axial distances (edge lengths)[7]	Axial angles[7]	Corresponding examples
Triclinic		$abc\sqrt{1-\cos^2\alpha-\cos^2\beta-\cos^2\gamma+2\cos\alpha\cos\beta\cos\gamma}$	(All remaining cases)		$K_2Cr_2O_7$, $CuSO_4{\cdot}5H_2O$, H_3BO_3
Monoclinic		$abc\sin\beta$	$a \neq c$	$\alpha = \gamma = 90°, \beta \neq 90°$	Monoclinic sulphur, $Na_2SO_4{\cdot}10H_2O$, $PbCrO_3$
Orthorhombic		abc	$a \neq b \neq c$	$\alpha = \beta = \gamma = 90°$	Rhombic sulphur, KNO_3, $BaSO_4$
Tetragonal		a^2c	$a = b \neq c$	$\alpha = \beta = \gamma = 90°$	White tin, SnO_2, TiO_2, $CaSO_4$
Hexagonal	Rhombohedral	$a^3\sqrt{1-3\cos^2\alpha+2\cos^3\alpha}$	$a = b = c$	$\alpha = \beta = \gamma \neq 90°$	Calcite ($CaCO_3$), cinnabar (HgS)
	Hexagonal	$\frac{\sqrt{3}}{2}a^2c$	$a = b$	$\alpha = \beta = 90°, \gamma = 120°$	Graphite, ZnO, CdS
Cubic		a^3	$a = b = c$	$\alpha = \beta = \gamma = 90°$	NaCl, zinc blende, copper metal, KCl, Diamond, Silver

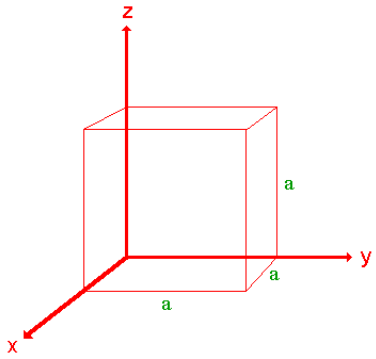
Figure 10.2.6: The six lattice parameters are the three axial distances $(a, b, \text{and } c)$ and the three axial angles $(\alpha, , \beta, \text{and } \gamma)$. (Wikipedia contributors. (2021, September 2). Bravais lattice. In Wikipedia, The Free Encyclopedia. Retrieved 01:22, October 3, 2021, from https://en.Wikipedia.org/w/index.php?title=Bravais_lattice&oldid=1042012012)

The simplest lattice system is the cubic system, in which all edges of the unit cell are equal and all angles are 90°. The tetragonal and orthorhombic systems also feature rectangular cells, but the edges are not all equal. In the remaining systems, some or all of the angles are not 90°. The least symmetrical is the triclinic, in which no edges are equal and no angles are equal to each other or to 90°.

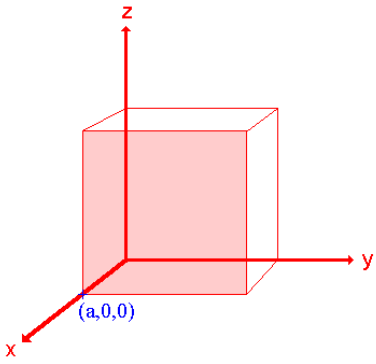
10.2.3: Miller indices

Miller indices are a convenient way to keep track of planes in crystals. They also map the spacing between planes in a convenient way into Bragg's law.

The following treatment of the procedure used to assign the Miller Indices is a simplified one (it may be best if you simply regard it as a "recipe") and only a **cubic** crystal system (one having a cubic unit cell with dimensions *a* x *a* x *a*) will be considered.



The procedure is most easily illustrated using an example so we will first consider the following surface/plane:



Step 1: *Identify the intercepts on the x- , y- and z- axes.*

In this case the intercept on the x-axis is at $x = a$ (at the point (a,0,0)), but the surface is parallel to the *y*- and *z*-axes - strictly therefore there is no intercept on these two axes but we shall consider the intercept to be at infinity (∞) for the special case where the plane is parallel to an axis. The intercepts on the *x*- , *y*- and *z*-axes are thus

Intercepts: ***a*** **,** ∞ **,** ∞

Step 2: Specify the intercepts in fractional co-ordinates

Co-ordinates are converted to fractional co-ordinates by dividing by the respective cell-dimension - for example, a point (*x*,*y*,*z*) in a unit cell of dimensions *a* x *b* x *c* has fractional co-ordinates of (*x*/*a* , *y*/*b* , *z*/*c*). In the case of a cubic unit cell each co-ordinate will simply be divided by the cubic cell constant , *a* . This gives

Fractional Intercepts: ***a*****/*****a*** **,** ∞**/*****a*****,** ∞**/*****a*** i.e. **1 ,** ∞ **,** ∞

Step 3: Take the reciprocals of the fractional intercepts

This final manipulation generates the Miller Indices which (by convention) should then be specified without being separated by any commas or other symbols. The Miller Indices are also enclosed within standard brackets (….) when one is specifying a unique

surface such as that being considered here.

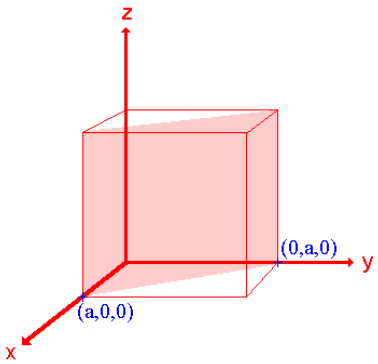
The reciprocals of 1 and ∞ are 1 and 0 respectively, thus yielding

Miller Indices: **(100)**

So the surface/plane illustrated is the (100) plane of the cubic crystal.

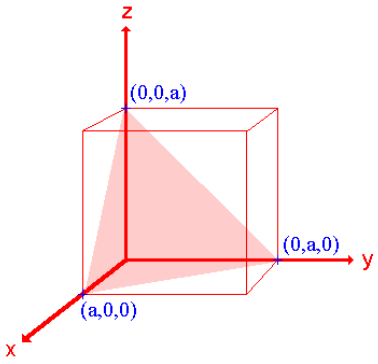
Other Examples

1. The (110) surface



Assignment
Intercepts: *a* , *a* , ∞
Fractional intercepts: 1 , 1 , ∞
Miller Indices: **(110)**

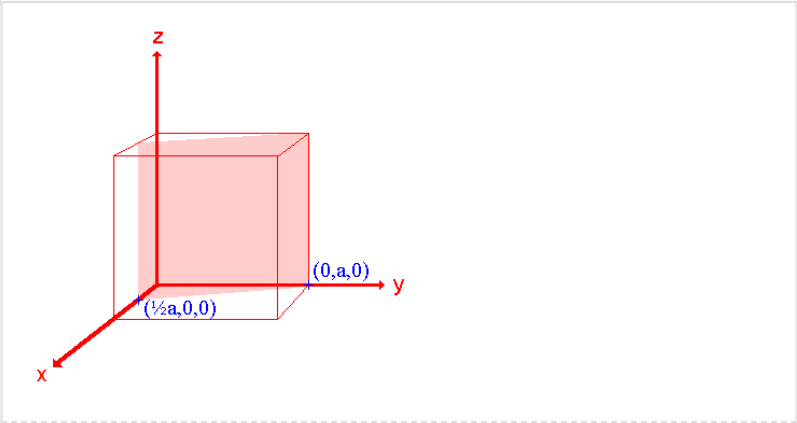
2. The (111) surface



Assignment
Intercepts: *a* , *a* , *a*
Fractional intercepts: 1 , 1 , 1
Miller Indices: **(111)**

The (100), (110) and (111) surfaces considered above are the so-called low index surfaces of a cubic crystal system (the "low" refers to the Miller indices being small numbers - 0 or 1 in this case). These surfaces have a particular importance but there an infinite number of other planes that may be defined using Miller index notation. We shall just look at one more …

3. The (210) surface



Assignment
Intercepts: ½ *a* , *a* , ∞
Fractional intercepts: ½ , 1 , ∞
Miller Indices: **(210)**

Further notes:

i. in some instances the Miller indices are best multiplied or divided through by a common number in order to simplify them by, for example, removing a common factor. This operation of multiplication simply generates a parallel plane which is at a different distance from the origin of the particular unit cell being considered. e.g. (200) is transformed to (100) by dividing through by 2 .
ii. if any of the intercepts are at negative values on the axes then the negative sign will carry through into the Miller indices; in such cases the negative sign is actually denoted by overstriking the relevant number. e.g. (00 -1) is instead denoted by $(00\bar{1})$.
iii. in the *hcp* crystal system there are four principal axes; this leads to four Miller Indices e.g. you may see articles referring to an *hcp* (0001) surface. It is worth noting, however, that the intercepts on the first three axes are necessarily related and not completely independent; consequently the values of the first three Miller indices are also linked by a simple mathematical relationship.

The symbol d is used to designate the perpendicular spacing between adjacent planes. Table 10.2.1 shows the equations for calculating the value of d for four of the seven crystal systems.

Table 10.2.1: Equations for calculating the spacing between adjacent planes, d

System	Equation for d
cubic	$\frac{1}{d^2} = \frac{h^2+k^2+l^2}{a^2}$
tetragonal	$\frac{1}{d^2} = \frac{h^2+k^2}{a^2} + \frac{l^2}{c^2}$
hexagonal	$\frac{1}{d^2} = \frac{4}{3}\left(\frac{h^2+hk+k^2}{a^2}\right) + \frac{l^2}{c^2}$
orthorhombic	$\frac{1}{d^2} = \frac{h^2}{a^2} + \frac{k^2}{b^2} + \frac{l^2}{c^2}$

Example 10.2.1

If a tetragonal unit cell has dimensions a = b = 501 pm and c = 451 pm, calculate the perpendicular distance between the 111 planes.

Solution

For a tetragonal unit cell

$$\frac{1}{d^2} = \frac{h^2+k^2}{a^2} + \frac{l^2}{c^2}.$$

Thus,

$$\frac{1}{d^2} = \frac{1+1}{(501\text{ pm})^2} + \frac{1}{(451\text{ pm})^2}$$
$$= 1.29 \times 10^{-5}\text{ pm}^{-2}.$$

Then $d = 279$ pm

10.2.4: Miller indices and Bragg's law

A second way to analyze the x-ray diffraction is to use Bragg's law. Diffraction of an x-ray beam by crystalline solids occurs when the light interacts with the electron cloud surrounding the atoms of the solid. Because of the periodic crystalline structure of a solid, it is possible to describe it as a series of planes with an equal interplanar distance. As an x-ray beam hits the surface of the crystal at an angle θ, some of the light will be diffracted at that same angle away from the solid (Figure 10.2.5). The remainder of the light will travel into the crystal and some of that light will interact with the second plane of atoms. Some of the light will be diffracted at an angle $theta$, and the remainder will travel deeper into the solid. This process will repeat for the many planes in the crystal. The x-ray beams travel different path lengths before hitting the various planes of the crystal, so after diffraction, the beams will interact constructively only if the path length difference is equal to an integer number of wavelengths (just like in the normal diffraction case above). In the figure below, the difference in path lengths of the beam striking the first plane and the beam striking the second plane is equal to BG + GF. So, the two diffracted beams will constructively interfere (be in phase) only if $BG + GF = n\lambda$. Basic trigonometry will tell us that the two segments are equal to one another with the interplanar distance times the sine of the angle θ. So we get:

$$BG = BC = d\sin\theta \tag{10.2.2}$$

Thus,

$$2d\sin\theta = n\lambda \tag{10.2.3}$$

This equation is known as Bragg's Law, named after W. H. Bragg and his son, W. L. Bragg; who discovered this geometric relationship in 1912. Bragg's Law relates the distance between two planes in a crystal and the angle of reflection to the x-ray wavelength. The x-rays that are diffracted off the crystal have to be in-phase in order to be observed. Only certain angles that satisfy the following condition will register:

$$\sin\theta = \frac{n\lambda}{2d} \tag{10.2.4}$$

For historical reasons, the resulting diffraction spectrum is represented as intensity vs. 2θ.

Example 10.2.1

Cesium metal has a body-centered cubic crystal structure with a unit cell length of 605.0 pm. Use the Bragg equation to determine the first two observed diffraction angles from the 110 planes when the wavelength of the x-rays is 154.4 pm.

Solution

From section 31.2.3, we found that the interplanar distance for cubic cells can be calculated using the equation

$$\frac{1}{d^2} = \frac{h^2+k^2+l^2}{a^2}$$

If we square equation 31.3.10 we get

$$\sin^2\theta = \frac{n^2\lambda^2}{4d^2}$$

Combining these two equations, we get

$$\sin^2\theta = \frac{n^2\lambda^2}{4a^2}(h^2+k^2+l^2)$$

The smallest diffraction angle occurs when $n = 1$

$$\sin^2\theta = \frac{(1^2)(154.4\ ,pm)^2}{4(605.0)^2}(1^2+1^2+0^2) = 0.03257$$

Thus, θ = 10.40°

The next largest diffraction angle occurs when $n = 2$

$$\sin^2\theta = \frac{(2^2)(154.4\ ,pm)^2}{4(605.0)^2}(1^2+1^2+0^2) = 0.1303$$

Thus, θ = 21.16°

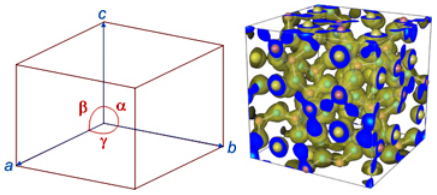
In the next section, we will discuss the factors that determine the phase and the amplitude of the multiple scattered x-rays produced during diffraction.

10.2.5: Beyond simple crystals

The crystals that are used to determine structure usually do not have simple cubic lattices and often parts of a molecule may reside in separate unit cells. Those complications are minor compared to the fact that, because the X-rays are scattered by the electron density, portions of the molecule scatter with different intensities and phases (fraction of the way through the wave cycle). What this means is that the scattering pattern is the result of a much more complicated interference process than modeled by the simple Bragg's law.

In order to know (or to see) the internal structure of a crystal we have to solve a mathematical function known as the "electron density;" a function that is defined at every point in the **unit cell**.

The function of electron density, represented by the letter ***ρ***, has to be solved at each point within the unit cell given by the coordinates (***x, y, z***), referred to the unit cell axes. At those points where this function takes maximum values (estimated in terms of electrons per cubic Angstrom) is where atoms are located. That means that if we are able to calculate this function, we will "see" the atomic structure of the crystal.



$$\rho(xyz) = \frac{1}{V}\sum_{\substack{hkl\\-\infty}}^{+\infty} |F(hkl)|\ .\ e^{-2\pi i[hx+ky+lz-\phi(hkl)]}$$

Formula 1. *Function defining the electron density in a point of the unit cell given by the coordinates (x, y, z). From* : Crystallography in a Nutshell (Ripoll and Cano)

- *F(hkl) represents the resultant diffracted beams of all atoms contained in the unit cell in a given direction. These magnitudes (actually waves), one for each diffracted beam, are known as structure factors. Their moduli are directly related to the diffracted intensities.*
- *h, k, l are the Miller indices of the diffracted beams (the reciprocal points) and Φ(hkl) represent the phases of the structure factors. V represents the volume of the unit cell. The function has limitations due to the extent to which the diffraction pattern is observed. The number of observed structure factors is finite, and therefore the synthesis will only be approximate and may show some truncation effects.*

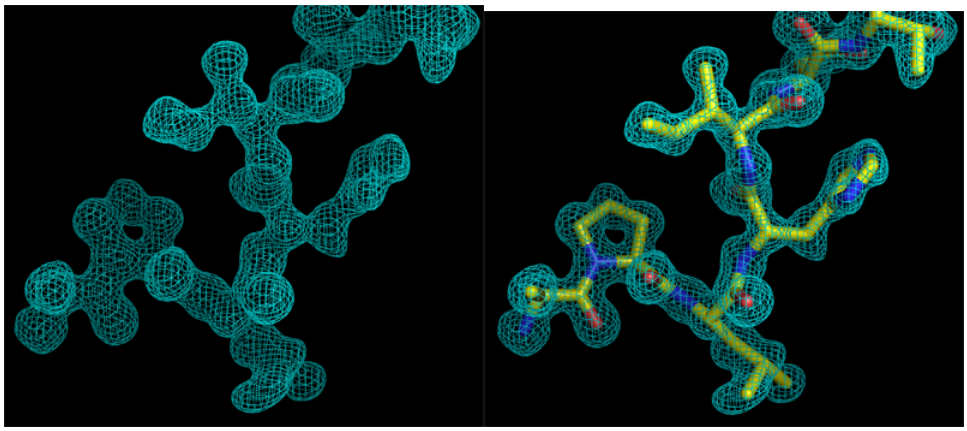


Figure 10.2.6: Left: *Appearance of a zone of the electron density map of a protein crystal, before it is interpreted.* Right: *The same electron density map after its interpretation in terms of a peptidic fragment. From:* Crystallography in a Nutshell (Ripoll and Cano)

The equation above (***Formula 1***) represents the ***Fourier transform*** between the ***real or direct space*** (where the atoms are, represented by the function ***ρ***) and the ***reciprocal space*** (the X-ray pattern) represented by the ***structure factor amplitudes*** and their ***phases***. Formula 1 also shows the holistic character of diffraction, because in order to calculate the value of the electron density in a ***single point*** of coordinates ***(xyz)*** it is necessary to use ***the contributions of all structure factors*** produced by the crystal diffraction.

The intensities of the overall scattering is known, but the individual phases necessary to use the formula are not known. There are a number of ways to figure out the phases to use. For small molecules direct methods where constraints on the possible phases based on statistics and possibly the existence of certain common structures are used. For Macromolecules this does not work well. In those cases a common approach is to use **isomorphous replacement**, where some atoms in the unit cell are replaced by heavy atoms that dominate the scattering and allow referencing the phase to their scattering. Sometimes a structure can be solved by using a known closely related structure (maybe similar peptide sequence) as a starting point for refining the phase guesses and thus the structure.

For more complete details of what is involved in interpreting X-ray scattering data see: Crystallography in a Nutshell (Ripoll and Cano)

This page titled 10.2: X-Ray Crystallography is shared under a CC BY-NC-SA 4.0 license and was authored, remixed, and/or curated by Jonathan Gutow.

- **10.6: Lattice Structures in Crystalline Solids** by OpenStax is licensed CC BY 4.0. Original source: https://openstax.org/details/books/chemistry-2e.
- **31.1: The Unit Cell is the Fundamental Building Block of a Crystal** is licensed CC BY-NC-SA 4.0.
- **31.2: The Orientation of a Lattice Plane is Described by its Miller Indices** is licensed CC BY-NC-SA 4.0.
- **31.3: The Spacing Between Lattice Planes Can Be Determined from X-Ray Diffraction Measurements** is licensed CC BY-NC-SA 4.0.
- **1.7: Structural Resolution** by Martín Martínez Ripoll & Félix Hernández Cano is licensed CC BY-NC 4.0. Original source: https://www.xtal.iqfr.csic.es/Cristalografia/index-en.html.

10.3: Cryo-Electron Microscopy

10.3.1: Introduction[1,2]

Prior to 1990 X-ray crystallography was the only method available to determine the detailed structure of macromolecules. But crystallography requires being able to grow crystals of the macromolecule, thus many biological and macromolecular structures could not be investigated at atomic resolution as scientists were unable to crystallize them. Additionally, the structure of the molecule in a crystal may be different from in solution. In 1990 Richard Henderson and colleagues produced an atomic resolution structure of the membrane protein bacteriorhodopsin in a 2D crystal using a cryogenically cooled sample in an electron microscope. This demonstrated the feasibility of generating atomic resolution macromolecular structures from electron microscopy using cryogenically cooled samples. Simultaneously, Jacques Dubochet developed a method for creating a layer of biomacromolecules in glassy ice (non-crystalline), suggesting that the 'in solution' structure could be observed. Joachim Frank developed the computational tools necessary to convert the electron scattering pattern from a randomly oriented layer of macromolecules into structures. However, it was not until 2013 that the combined improvements in electron sources, electron optics, electron detectors and software made approaching atomic resolution using cryo-EM nearly as routine as for X-ray crystallography. Jacques Dubochet, Joachim Frank and Richard Henderson were awarded the 2017 Nobel Prize in Chemistry for "developing cryo-electron microscopy for the high-resolution structure determination of biomolecules in solution".

10.3.2: Experimental Technique[1]

A concentrated sample of the macromolecule or aggregate in water is transferred to a metal mesh appropriate for insertion into the transmission electron microscope (TEM). The sample is then rapidly immersed in liquid ethane at 77 K (liquid nitrogen temperature, originally it was shot in using something akin to a bow). The ethane has enough heat capacity to rapidly cool the water solution, freezing the water into a glass (an amorphous solid with nearly the same arrangement as the initial liquid). This sample is then inserted into the vacuum chamber of a TEM. While maintaining the low temperature the sample is exposed to a low intensity, but high kinetic energy (short wavelength) electron beam. The scattering of the beam by the macromolecules is recorded for later interpretation. The process is summarized in figure 10.3.1.

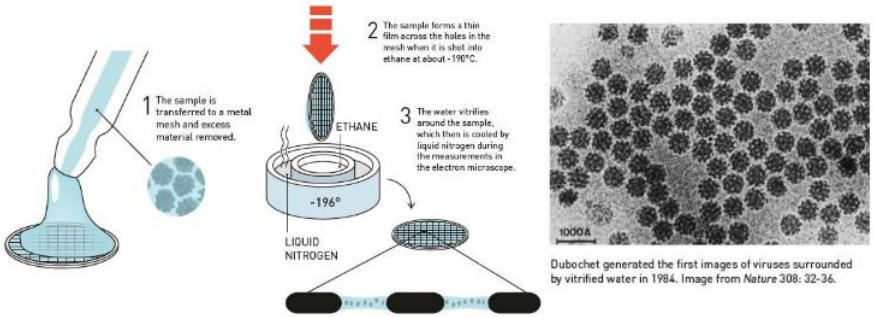


Figure 10.3.1: Illustration of the process used by Dubochet and co-workers to get the first cryo-EM images of viruses in vitrified (glassy) water. From reference 1, direct link to original image: https://www.nobelprize.org/uploads/2...ets-method.jpg. © Johan Jarnestad/The Royal Swedish Academy of Science.

As the electron micrograph included in the figure shows the contrast between the viral particles and the surrounding vitrified water is large. This is because glassy water does not scatter electrons strongly. Slower cooling methods that allow water to form crystalline ice have lower contrast and can sometimes disrupt the structure of aggregates. In addition, keeping the sample so cold reduces the rate of damage to the sample from the high energy electrons. These two effects allow significant improvements in the signal to noise because the scattering can be collected over a longer period of time and most of the scattering is due to the macromolecules/aggregates of interest.

10.3.3: Data Interpretation[1]

Once the scattering pattern has been collected it must be interpreted to provide the structure. The process is similar to interpreting the scattering from X-Ray crystallography, except that the sample is not crystalline. This means that the macromolecules or aggregates are randomly oriented and each generates a different scattering pattern that depends on their orientation. Joachim Frank worked out the mathematical tools to figure out how to group molecules of the same orientation in a thing film (2D) to average

their scattering for better signal to noise, as well as how to account for their varied orientation in the thin film. This allows combining the high resolution 2D data to get high resolution 3D data for molecular structure. A cartoon illustrating the process is shown in figure 10.3.2

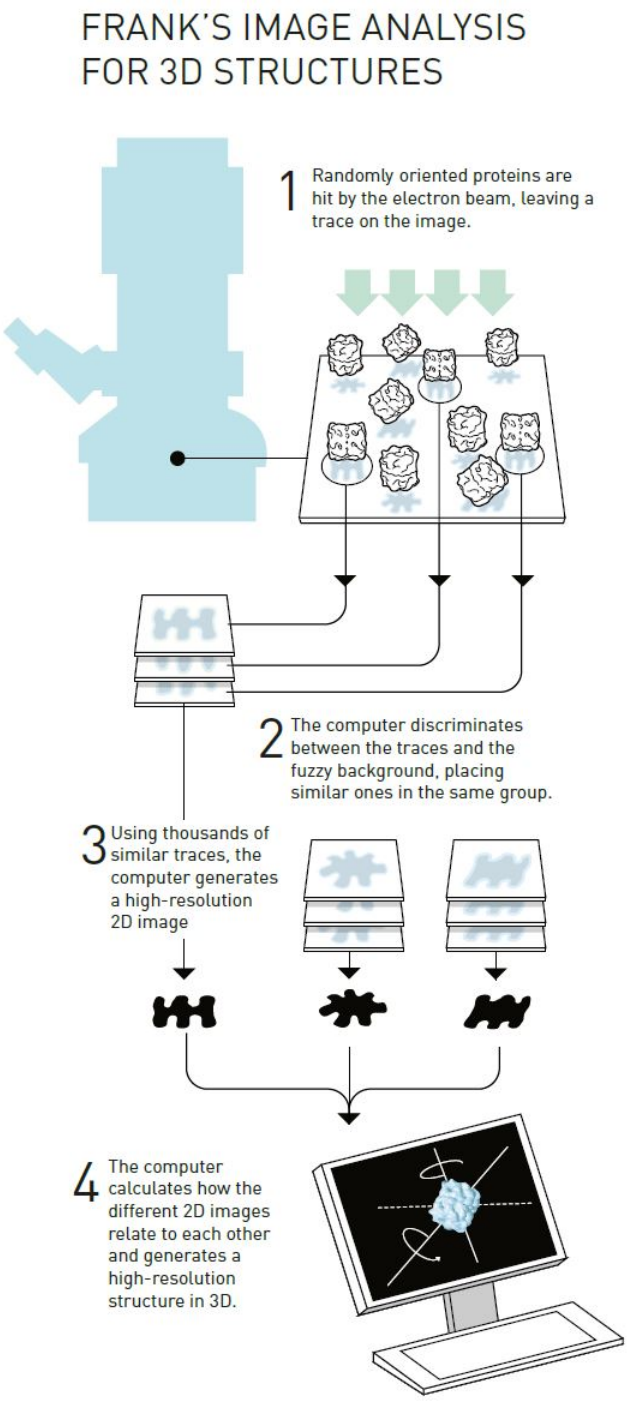


Figure 10.3.2 Illustration of how cryoEM data is interpreted to generate 3D structures. From reference 1, direct link to original image: https://www.nobelprize.org/uploads/2...-structure.jpg. © Johan Jarnestad/The Royal Swedish Academy of Science.

10.3.4: References

1. "The Nobel Prize in Chemistry 2017: Popular Science Background", The Royal Swedish Academy of Sciences. Available at: https://www.nobelprize.org/prizes/ch...r-information/ and https://www.nobelprize.org/uploads/2...rize2017-1.pdf.

2. Peter Brzezinski, "Scientific Background on the Nobel Prize in Chemistry 2017: The Development of Cryo-Electron Microscopy", The Royal Swedish Academy of Sciences. Available at: https://www.nobelprize.org/uploads/2...rize2017-1.pdf

This page titled 10.3: Cryo-Electron Microscopy is shared under a CC BY-NC-SA 4.0 license and was authored, remixed, and/or curated by Jonathan Gutow.

10.4: Intermolecular Forces

10.4.1: Introduction

Intermolecular forces are the attractions and repulsions between chemical species that occur without changing the chemical identity of the species or breaking bonds. Generally the interactions occur at a longer distance than bonding (intramolecular) interactions. This separation is somewhat arbitrary as intermolecular attractions may be the forces that bring two molecules together in the proper orientation to react. Intermolecular forces can be used to explain non-ideality of gases, why some molecules are found as liquids at room temperature while others are gases and solids. These forces are also key in maintaining the shapes of many molecular aggregates (e.g. micelles, biomembranes and protein structures).

Intermolecular forces are generally divided into the categories of: charge-charge; dipole-dipole; and polarizability interactions; with the added inclusion of hydrogen-bonds.

10.4.2: Charge-charge interactions

From electrostatics the interaction potential between charges is just Coulomb's law:

$$V = \frac{q_1 q_2}{4\pi\epsilon r} \tag{10.4.1}$$

where q_i = charge in Coulombs on particle i, ϵ = the permittivity of the medium separating the charges, and r = distance between the two particles. Thus opposite charges attract (V < 0) and same charges repel (V > 0). The strength of this interaction falls off as 1/r.

10.4.3: Dipoles

10.4.3.1: Dipole moments

A dipole moment $\vec{\mu}$ is a vector quantity that can be used to describe the average directionality and magnitude of the electric field created by separated charges. In the simple case of two separate charges it is calculated as follows:

$$\vec{\mu} = q\vec{r} \tag{10.4.2}$$

where q is the magnitude of the separated charge +q at one end of the vector $\vec{r}$ and -q at the other end. The SI units for this are Coulomb meters, but a more molecularly useful unit is the Debye (1 D = 3.335 x 10^{-30} C m).

As vector quantities dipole moments can be vector summed together to get an overall dipole moment. Thus although each C=O bond in CO_2 has a dipole moment overall the molecule has zero dipole moment because the bond-dipole vectors sum to zero as shown in figure 10.4.1.

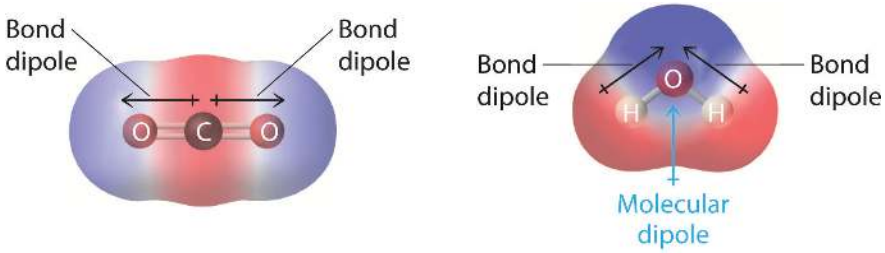


Figure 10.4.1: Cartoons illustrating the cancelation of dipoles in CO_2 when added, while the bond dipoles in H_2O sum to an overall dipole.

10.4.3.2: Dipole-charge interactions

When a charged particle interacts with a dipole the interaction will be attractive or repulsive depending on the orientation of the dipole as illustrated in figure 10.4.2

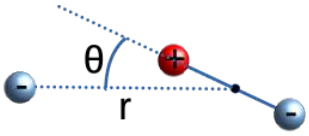


Figure 10.4.2: Cartoon of a dipole interacting with a charge. In this case the (+) end of the dipole is closer to the (-) point charge so the interaction will be overall attractive.

This orientation dependence of the interaction potential is quantitatively described by:

$$V = \frac{\mu q cos\theta}{4\pi\epsilon r^2} \tag{10.4.3}$$

where μ is the dipole moment magnitude, q is the charge of the single point charge, and r is the distance to the center of the dipole. Notice that this interaction falls off as $1/r^2$, which is much more rapid that the decrease for charge-charge interactions.

10.4.3.3: Dipole-dipole interactions

For two dipoles the interaction also depends on their orientation as illustrated in figure 10.4.3

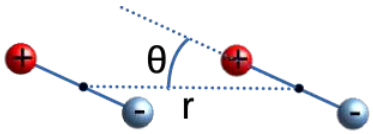


Figure 10.4.3: Cartoon of two interacting dipoles.

If the dipoles are maintained in a parallel orientation and only θ and r are allowed to vary (imagine taking the left dipole in figure 10.4.3 and moving it around without changing its orientation) the interaction potential may be described by the equation[1]:

$$V = \frac{\mu_1\mu_2(1-3cos^2\theta)}{4\pi\epsilon r^3} \tag{10.4.4}$$

Which falls off as $1/r^3$, even faster than charge-charge and charge-dipole interactions.

In liquids and gases the dipoles can rotate. If they rotate completely freely they would spend an equal amount of time in attractive and repulsive orientations leading to an overall average interaction energy of zero. However, because attractive orientations are lower energy, and thus favored, molecules spend more time in attractive orientations. By accounting for the Boltzmann distribution of energies it is possible to derive a quantitative expression for the thermally averaged interaction of two dipoles. The result is[1]:

$$V = -\frac{2\mu_1^2\mu_2^2}{3(4\pi\epsilon)^2kTr^6} \tag{10.4.5}$$

This falls off as $1/r^6$, the most rapid decrease yet described.

10.4.4: Polarizability

Neutral nonpolar species have arrangements of electrons in their electron clouds that exhibit inversion symmetry through the center of the species (the electron density $\rho(x,y,z) = \rho(-x,-y,-z)$). When in the presence of an electric field, their electron clouds can be distorted (Figure 10.4.1). The ease of this distortion is the polarizability of the atom or molecule. The created distortion of the electron cloud causes the originally nonpolar molecule or atom to acquire a dipole moment. This induced dipole moment is related to the polarizability of the molecule or atom and the strength of the electric field by the following equation:

$$\mu_{ind} = \alpha E \tag{10.4.6}$$

where E denotes the strength of the electric field and α is the polarizability of the atom or molecule with units of C m^2V^{-1}.

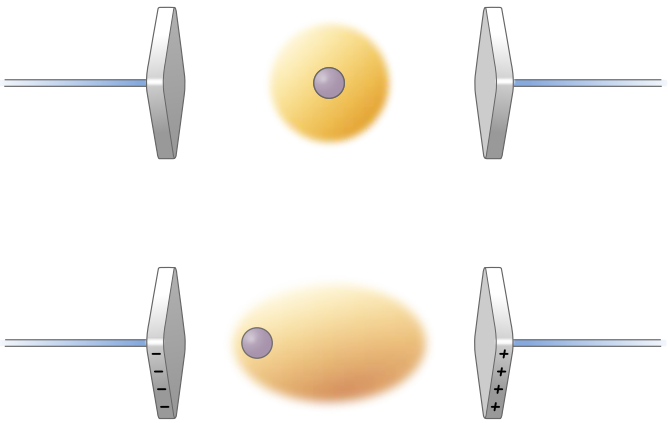


Figure 10.4.1: A neutral nonpolar species's electron cloud is distorted by an externally applied electric field. (top) Before the electric field is turned on the electron cloud is isotropically distributed. (bottom) Once the electric field is turned on, an induced dipole moment is generated. If we turn off the electric field, the dipole moment goes away (not shown). (CC BY-NC 4.0; Ümit Kaya via LibreTexts).

In general, polarizability correlates with the interaction between electrons and the nucleus. The amount of electrons in a molecule affects how tight the nuclear charge can control the overall charge distribution. Atoms with fewer electrons will have smaller, denser electron clouds, as there is a strong interaction between the few electrons in the atoms' orbitals and the positively charged nucleus. There is also less shielding in atoms with fewer electrons contributing to the stronger interaction of the outer electrons and the nucleus. With the electrons held tightly in place in these smaller atoms, these atoms are typically not easily polarized by external electric fields. In contrast, large atoms with many electrons, such as negative ions with excess electrons, are easily polarized. These atoms typically have very diffuse electron clouds and large atomic radii that limit the interaction of their external electrons and the nucleus.

Factors that Influence Polarizability

The relationship between polarizability and the factors of electron density, atomic radii, and molecular orientation is as follows:

1. The greater the number of electrons, the less control the nuclear charge has on charge distribution, and thus the increased polarizability of the atom.
2. The greater the distance of electrons from nuclear charge, the less control the nuclear charge has on the charge distribution, and thus the increased polarizability of the atom.
3. Molecular orientation with respect to an electric field can affect polarizability (labeled Orientation-dependent), except for molecules that are: tetrahedral, octahedral or icosahedral (labeled Orientation-independent). This factor is more important for unsaturated molecules that contain areas of electron-dense regions, such as 2,4-hexadiene. Greatest polarizability in these molecules is achieved when the electric field is applied parallel to the molecule rather than perpendicular to the molecule.

The relationship between polarizability and dispersion forces can be seen in the following equation, which can be used to quantify the interaction between two like nonpolar atoms or molecules (e.g., A with A):

$$V(r) = \frac{-3}{4}\frac{\alpha'^2 I}{r^6} \tag{10.4.7}$$

where r is the distance between the atoms or molecules, I is the **first ionization energy** of the atom or molecule, and α is the polarizability constant expressed in units of m^3.

This expression of α is related to α' by the following equation:

$$\alpha' = \frac{\alpha}{4\pi\epsilon_o} \tag{10.4.8}$$

To quantify the interaction between unlike atoms or molecules (A and B), Equation 10.4.7becomes:

$$V(r) = \frac{-3}{2}\frac{I_A I_B}{I_A + I_B}\frac{\alpha'_A \alpha'_B}{r^6} \tag{10.4.9}$$

1. Petrucci, Ralph H., et al. General Chemistry: Principles and Modern Applications.Upper Saddle River, NJ: Prentice Hall, 2007
2. Chang, Raymond. "Chapter 13: Intermolecular Forces/ Ion-Induced Dipole and Dipole-Induced Dipole Interactions/ Dispersion, or London, Interactions." *Physical Chemistry for the Biosciences*. Sansalito, CA: University Science, 2005. 495-98. Print.
3. Housecroft, Catherine E., and Alan G. Sharpe. "Chapter 6: Structures and Energetics of Metallic and Ionic Solids." *Inorganic Chemistry*. Harlow [etc.: Prentice Hall, 2008. 173-74. Print.
4. Miessler, Gary L., and Donald A. Tarr. "Chapter 6: Acid-Base and Donor-Acceptor Chemistry." *Inorganic Chemistry*. Upper Saddle River, NJ: Pearson Education, 2004. 183-86. Print

10.4.5: Hydrogen bonding

Hydrogen bonds (H-bonds) were originally proposed to explain anomalous attractions between certain molecules. Many think of H-bonds as extra strong dipole interactions, they are now believed to have significant quantum mechanical covalent bonding characteristics.

10.4.5.1: Evidence

Many elements form compounds with hydrogen. If you plot the boiling points of the compounds of the group 14 elements with hydrogen, you find that the boiling points increase as you go down the group.

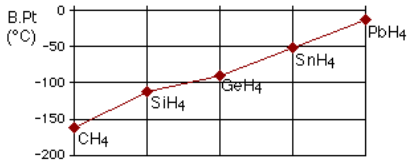


Figure 1: Boiling points of group 14 elemental halides.

The increase in boiling point happens because the molecules are getting larger with more electrons, and so van der Waals dispersion forces become greater. If you repeat this exercise with the compounds of the elements in groups 15, 16, and 17 with hydrogen, something odd happens.

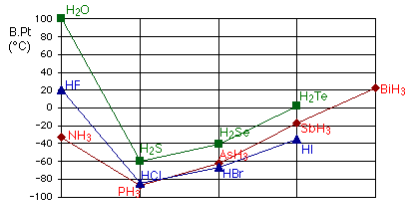


Figure 2: Boiling points of group 15-17 elemental halides.

Although the same reasoning applies for group 4 of the periodic table, the boiling point of the compound of hydrogen with the first element in each group is abnormally high. In the cases of NH_3, H_2O and HF there must be some additional intermolecular forces of attraction, requiring significantly more heat energy to break the IMFs. These relatively powerful intermolecular forces are described as hydrogen bonds.

So a hydrogen bond is formed between a molecule on which a hydrogen is bonded to N, O or F and another molecule containing N, O, or F that can interact.

10.4.5.2: Models

The simplest model for a hydrogen bond is that the hydrogen which has a significant partial positive charge forms a weak (sometimes called "partial") bond to a N, O or F that has a significant negative partial charge. One can visualize this as the hydrogen forming a partial bond with a set of lone-pair electrons on the N, O or F. Symbolically this can be illustrated as $\mathrm{X{-}H + : YR \longrightarrow X{-}H : YR}$, where X and Y are an N, O or F.

As indicated by the very ordered geometry of solid water, hydrogen bonds are extremely directional. This suggests that they may have significant covalent character, which Compton Scattering and computational studies support.[2] A pictorial visualization of this quantum interaction is shown in the figure below. The X-H molecule frontier orbitals are the bonding and anti-bonding orbitals formed from combining the H 1s orbital with valences orbitals of X (primarily p). The bonding orbital is occupied by an electron pair, the anti-bonding is unoccupied. The species Y has non-bonding orbitals containing pairs of electrons. If one of those non-bonding orbitals interacts with the bonding and anti-bonding orbitals on the XH species three new molecular orbitals are created. The lowest energy is an all in-phase orbital with electron density shared across X, H and Y. In the middle is an orbital with a node at the H, which is non-bonding. The highest energy is anti-bonding and has two nodes. There are only four electrons available amoung these three orbitals so they occupy the lowest two creating a weak covalent bond because of the lower energy of the molecular orbital spanning X, H and Y.

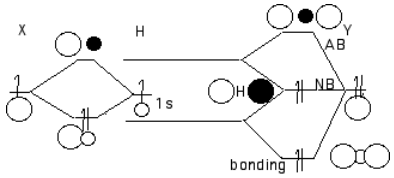


Figure 10.4.7: Cartoon of the formation of the weak covalent hydrogen bond.

10.4.6: Overall models of interactions

Ionic interactions (charge-charge) and hydrogen bonding are very strong interactions being roughly 200 - 300 kJ/mol and ~ 20 kJ/mol respectively. They are usually considered separately from the other interactions. Ignoring these interactions we can summarize the interactions encountered by many molecules as:

- dipole-dipole which fall off a $1/r^3$ (non-rotating) and $1/r^6$(rotating).
- dispersion which fall off as $1/r^6$. Note: this includes interactions of permanent dipoles with polarizable molecules.

The key thing to note is that for liquids and gases where molecules are rotating both of these contributions fall off as $1/r^6$. This matches well with the observed distance dependence of intermolecular attraction.

If molecules get very close together, they begin to repel mostly due to the Pauli exclusion principle, which means that pairs of electrons cannot occupy the same quantum states. This repulsion increases rapidly with decreasing separation. A good model for the distance dependence of the repulsions is $\exp(-r/r_o)$, where r_o is a reference distance that sets the stepness of the repulsive wall. So combining these suggests that intermolecular interactions can be broadly modeled as:

$$V = C_e exp\left(\frac{-r}{r_o}\right) - \frac{C_6}{r^6} \tag{10.4.10}$$

Thus, combined with the attractions there is a distance of separation where the energy is minimum, much like the equilibrium bond length in a diatomic molecule, but generally at a much larger distance. This exp-6 potential (equation 10.4.10) is not as commonly used as the less realistic, but mathematically more convenient Lennard-Jones potential.

The Lennard-Jones model consists of two 'parts'; a steep repulsive term, and smoother attractive term, representing the London dispersion forces. Apart from being an important model in itself, the Lennard-Jones potential frequently forms one of the 'building blocks' of many force fields. It is worth mentioning that the 12-6 Lennard-Jones model is not the most faithful representation of the potential energy surface, but rather its use is widespread due to its computational expediency. The Lennard-Jones Potential is given by the following equation:

$$V(r) = 4\epsilon\left[\left(\frac{\sigma}{r}\right)^{12} - \left(\frac{\sigma}{r}\right)^{6}\right] \tag{10.4.11}$$

or is sometimes expressed as:

$$V(r) = \frac{A}{r^{12}} - \frac{B}{r^6} \tag{10.4.12}$$

where

- V is the intermolecular potential between the two atoms or molecules.

- ϵ is the well depth and a measure of how strongly the two particles attract each other.
- σ is the distance at which the intermolecular potential between the two particles is zero (Figure 10.4.8). σ gives a measurement of how close two nonbonding particles can get
- r is the distance of separation between both particles (measured from the center of one particle to the center of the other particle).
- $A = 4\epsilon\sigma^{12}$, $B = 4\epsilon\sigma^{6}$
- Minimum value of V at $r = r_{min} = 2^{1/6}\sigma$. This separation allows an estimate of the *van der Waals radius*, which is defined as one-half of the internuclear distance between nonbonding particles.

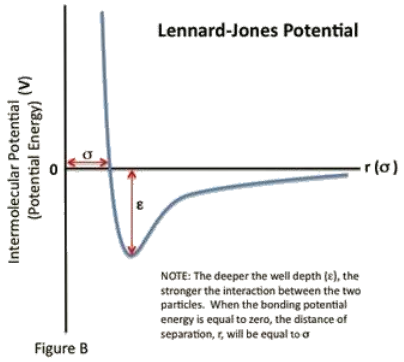


Figure 10.4.8: The Lennard-Jones potential describes both the attraction and repulsion between nonionic particles. The first part of the equation, the short-ranged σ/r^{12} term describes the repulsive forces between particles while the latter part of the equation and the longer-ranged σ/r^{6} term denotes the attraction.

Example 10.4.1: The van der Waals Radius

The ϵ and σ values for Xenon (Xe) are found to be 1.77 kJ/mol and 4.10 Angstroms, respectively. Determine the van der Waals radius for the Xenon atom.

Solution

Recall that the van der Waals radius is equal to one-half of the internuclear distance between nonbonding particles. Because σ gives a measure of how close two non-bonding particles can be, the van der Waals radius for Xenon (Xe) is given by:

$$r = 2^{1/6}\frac{\sigma}{2} = 2^{1/6}\frac{4.10\mathring{A}}{2} = 2.30\mathring{A}$$

10.4.7: References

1. P.W. Atkins, J. de Paula, Physical Chemistry, 10th Ed. (W.H. Freeman and Co. New York, 2014) Pp. 668-669.

2. B. Barbiellini, A. Shukla, PHYSICAL REVIEW B 66, 235101 2002

10.4.8: Contributors

- Jonathan Gutow (UW Oshkosh)
- See below for sections included from other LibreText pages.

This page titled 10.4: Intermolecular Forces is shared under a CC BY-NC-SA 4.0 license and was authored, remixed, and/or curated by Jonathan Gutow.

- **Polarizability** by Dana Reusser, Delmar Larsen, Kelly Cox is licensed CC BY 4.0.
- **Hydrogen Bonding** by Jim Clark, Jose Pietri is licensed CC BY-NC-SA 4.0.
- **Lennard-Jones Potential** by Rabia Naeem is licensed CC BY 4.0.

10.5: Structure of Gases, Liquids and Glasses

10.5.1: Introduction

The molecules in liquids and gases are in constant random motion. Thus one might expect that there would be no order in the arrangement of molecules. In an ideal gas of molecules without volume this is true. When there is any distance dependent interaction energy there is some structure. Glassy solids are also randomly arranged over macroscopic distances, but often have local order. This limited structuring is usually described by the radial distribution function.

10.5.2: Radial distribution function

Based on "Radial distribution function" from Wikipedia.org.

The **radial distribution function**, (or **pair correlation function**) g(r) in a system of particles (atoms, molecules, colloids, etc.), describes how density varies as a function of distance from a reference particle. If a given particle is taken to be at the origin "O", and if $\rho = N/V$ is the average number density of particles, then the local time-averaged density at a distance r from "O" is $\rho g(r)$. This simplified definition holds for a homogeneous and isotropic system. In simplest terms it is a measure of the probability of finding a particle at a distance of r away from a given reference particle, relative to that for an ideal gas. The general algorithm involves determining how many particles are within a distance of r and r+dr away from a particle (figure 10.5.1a). Radial distribution functions can be experimentally determined from the radially symmetric neutron and x-ray scattering seen from gases, liquids and glassy solids.

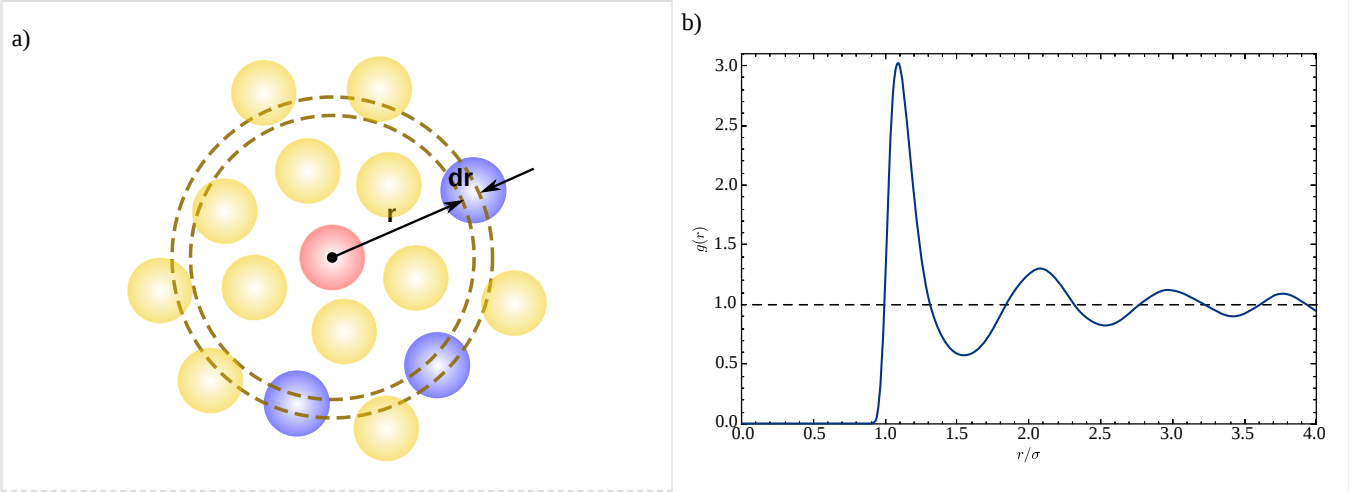


Figure 10.5.1: a) What g(r) represents. The red particle is the reference particle, and the blue particles are those whose centers are within the circular shell, dotted in orange. Source:The original uploader was Wiki47222 at Wikimedia Commons., Public domain, via Wikimedia Commons. b) A computed g(r) for a Lennard-Jones liquid. Source:Grigory Sarnitskiy, Public domain, via Wikimedia Commons

The radial distribution function is usually determined by calculating the distance between all particle pairs and binning them into a histogram. The histogram is then normalized with respect to an ideal gas, where particle histograms are completely uncorrelated. For three dimensions, this normalization is the number density of the system ρ multiplied by the volume of the spherical shell, which symbolically can be expressed as $\rho\, 4\pi r^2 dr$.

The computed example in figure 10.5.1b illustrates the typical characteristics of a radial distribution function. There is an initial large peak in probability of finding a particle which is the first "solvation" shell. Later peaks are less intense as g(r) washes out to the average value of 1 expected for a completely random distribution. Generally in liquid systems the peaks move to larger r and wash out more quickly as temperature increases. In the case of water, with its strong hydrogen bonds, the first peak persists essentially up to the boiling point, indicating water clusters are not completely disrupted.

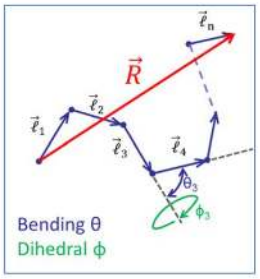
This page titled 10.5: Structure of Gases, Liquids and Glasses is shared under a CC BY-NC-SA 4.0 license and was authored, remixed, and/or curated by Jonathan Gutow.

10.6: Macromolecules

10.6.1: Introduction

The relative positions of atoms in macromolecules (polymers) are restricted by the bonding in the molecules. However, because bond angles are somewhat flexible and there is nearly free rotation about any single bonds, macromolecules can take on many conformations and often rapidly shift among them. We will start with a simple physical model for how these long chains can behave. As examples of real molecules we will look briefly at biologically important macromolecules and biological molecular aggregates.

10.6.2: Segment Models[1]



- $(n+1)$ beads linked by n segments or bonds of length ℓ.
- Each bead has a position $\vec{r_i}$.
- Each bond is assigned a vector, $\vec{\ell_i} = \vec{r_i} - \vec{r_{i-1}}$.
- The bending angle between adjacent segments i and $(i+1)$ is θ_i: $\cos\theta = \vec{\ell_i} \cdot \vec{\ell_{i-1}}$
- For each bending angle there is an associated dihedral angle ϕ_i defined as the rotation of segment $(i+1)$ out of the plane defined by segments i and $(i-1)$.
- There are $n-1$ separate bending and dihedral angles.

10.6.3: Statistical Variables for Macromolecules

10.6.3.1: End-to-end distance

The **contour length** is the full length of the polymer along the contour of the chain:

$$R_C = n\ell$$

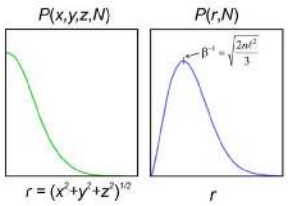
Each polymer chain has the same contour length, but varying dimensions in space that result from conformational flexibility.

10.6.3.2: Freely Jointed Chain

The freely jointed chain describes a macromolecule as a backbone for which all possible θ and ϕ are equally probable, and there are no correlations between segments. It is known as an "ideal chain" because there are no interactions between beads or excluded volume, and configuration of the polymer backbone follows a random walk. The freely jointed chain is also known as a **Gaussian random coil**, because the statistics of its configuration are fully described by $\langle R \rangle$ and $\langle R^2 \rangle$, the first two moments of a Gaussian end-to-end probability distribution $P(R)$. We can also express this as a radial probability density that gives the probability of finding the end of a chain at a radius between r and $r+dr$ from the origin (for a more complete derivation see: 7.1: Segment Models):

$$P(r,n) = 4\pi r^2 \left(\frac{3}{2\pi n\ell^2}\right)^{3/2} \exp\left[-\frac{3}{2}\frac{r^2}{n\ell^2}\right] \tag{10.6.1}$$

The units of $P(r,n)$ are inverse length. For the freely jointed chain, we see that $\beta^{-1} = \sqrt{2n\ell^2/3}$ is the most probable end-to-end distance.



From this the root-mean-square value for R can be calculated:

$$R_{rms} = \langle R^2 \rangle^{1/2} = \sqrt{n}\ell$$

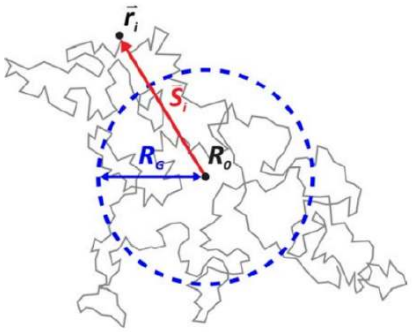
One way to picture this is that the chain is constantly moving, with very low probability of the ends being close together. R_{rms} can be thought of as one measure of the time averaged size of the random coil.

Note

In its most probable configuration (or set of configurations) the random coil has its maximum entropy. Stretching out or compressing the polymer (increasing or decreasing R) lowers the entropy of the chain. This is one contribution to the tendency of a rubber band to shorten after being stretched.

10.6.3.3: Radius of Gyration

The **radius of gyration** is another important structural variable that is closely related to experimental observables. In can be thought of as the radius of an infinitesimally thick sphere with the same moment of inertia as the polymer. It is essentially a mass weighted average distance from the center-of-mass of the polymer.



This proves useful for branched polymers and heteropolymers (such as proteins). For a freely jointed chain this can be computed to be:

$$R_g = \ell\sqrt{\frac{n}{6}} \tag{10.6.2}$$

10.6.3.4: More realistic models

It is possible but much more difficult to analyze more realistic models that constrain things like bond angles and diheadral angles. For further discussion see: 7.1: Segment Models.

10.6.4: Biological polymers

10.6.4.1: Proteins

Proteins are the primary catalysts in biological systems and also participate in many mechanical biological processes (e.g. the motor protein actin). These macromolecules consist of chains of amino acids (peptides). There are 20 common amino acids found in living organisms on Earth of the general chemical formula $H_2NCHRCOOH$. They form condensation polymer chains as indicated in figure 10.6.1.

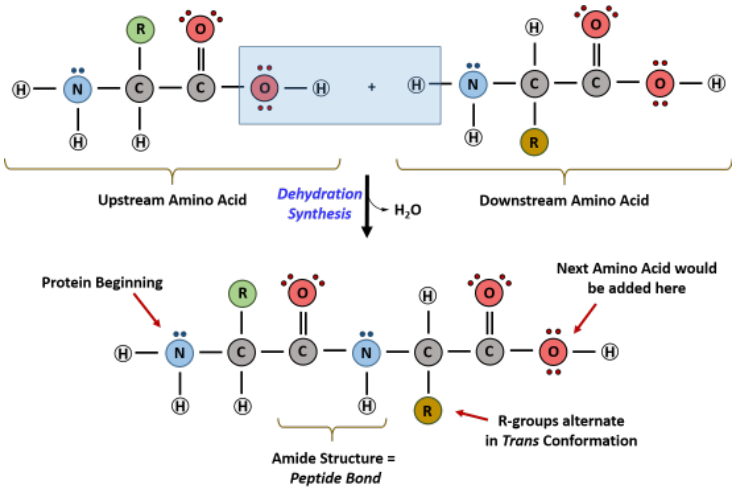


Figure 10.6.1: Cartoon of formation of a dipeptide. Source: https://bio.libretexts.org/Bookshelves/Biochemistry/Fundamentals_of_Biochemistry_(Jakubowski_and_Flatt)/01%3A_Unit_I-_Structure_and_Catalysis/03%3A_Amino_Acids_Peptides_and_Proteins/3.2%3A_The_Structure_of_Proteins-_An_Overview and https://wou.edu/chemistry/files/2017/05/protein-synthesis.png

The sequence of these connected peptides is referred to as the **primary structure**.

The **secondary structure** of a protein are repetitive structures such as **α-helices** and **β-sheets** held in their shape by hydrogen bonds between the NH on one amino acid and the C=O of a number of amino acids away in the chain. There are other motifs, but these are the primary one.

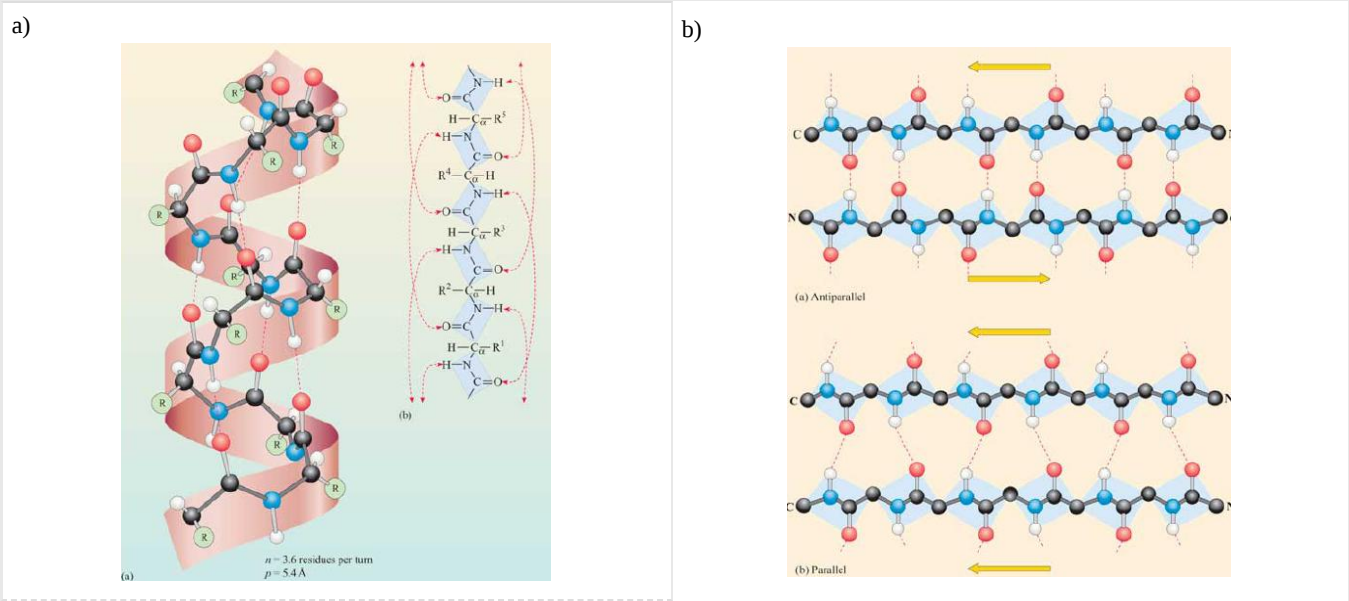


Figure 10.6.2: a) Cartoon of an α-helix fragment of a protein. Originally from: https://www.open.edu/openlearn/scien...-section-1.3.1. b) Cartoon of a β-sheet. Originally from: https://www.open.edu/openlearn/scien...-section-1.3.2.

Proteins further fold up into their overall 3-D or **tertiary structure** because of additional interactions between chains and interactions with the surrounding medium (primarily water). For proteins that are not embedded in membranes the balance of hydrophobic, hydrophilic and hydrogen bonding interactions with water tend to expose polar and hydrogen bonding sites on the outside of the protein. The exact structure is driven by a combination of the order in which interactions form and the thermodynamic tendency towards approaching the lowest free energy configuration. This combination of kinetic and thermodynamic control of conformation has made predicting protein structures challenging.

Proteins also often aggregate in to larger structures. This kind of structure is referred to as **quarternary structure**.

10.6.4.2: Nucleic Acids

Nucleic acids are large polymers formed by linking nucleotides together and are found in every cell. **Deoxyribonucleic acid (DNA)** is the nucleic acid that stores genetic information. If all the DNA in a typical mammalian cell were stretched out end to end, it would extend more than 2 m. **Ribonucleic acid (RNA)** is the nucleic acid responsible for using the genetic information encoded in DNA to produce the thousands of proteins found in living organisms. Nucleotides are joined together through the phosphate group of one nucleotide connecting in an ester linkage to the OH group on the third carbon atom of the sugar unit of a second nucleotide. This unit joins to a third nucleotide, and the process is repeated to produce a long nucleic acid chain (Figure 10.6.3). The backbone of the chain consists of alternating phosphate and sugar units (2-deoxyribose in DNA and ribose in RNA). The purine and pyrimidine bases branch off this backbone.

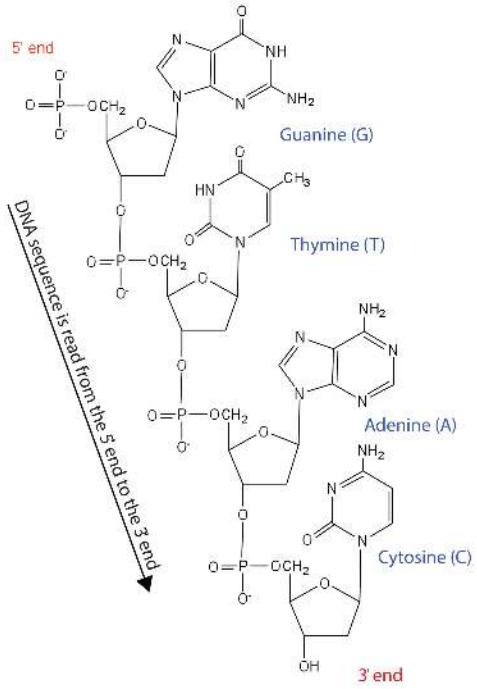


Figure 10.6.3 Structure of a Segment of DNA. A similar segment of RNA would have OH groups on each C2′, and uracil would replace thymine.

Like proteins, nucleic acids have a **primary structure** that is defined as the sequence of their nucleotides. Unlike proteins, which have 20 different kinds of amino acids, there are only 4 different kinds of nucleotides in nucleic acids.

The three-dimensional structure of DNA was the subject of an intensive research effort in the late 1940s to early 1950s. Initial work revealed that the polymer had a regular repeating structure. In 1950, Erwin Chargaff of Columbia University showed that the molar amount of adenine (A) in DNA was always equal to that of thymine (T). Similarly, he showed that the molar amount of guanine (G) was the same as that of cytosine (C). Chargaff drew no conclusions from his work, but others soon did.

At Cambridge University in 1953, James D. Watson and Francis Crick announced that they had a model for the **secondary structure** of DNA. Using the information from Chargaff's experiments (as well as other experiments) and data from the X ray studies of Rosalind Franklin (which involved sophisticated chemistry, physics, and mathematics), Watson and Crick worked with models that were not unlike a child's construction set and finally concluded that DNA is composed of two nucleic acid chains running **antiparallel** to one another. Their model showed, the two chains are twisted to form a **double helix**—a structure that can be compared to a spiral staircase, with the phosphate and sugar groups (the backbone of the nucleic acid polymer) representing the outside edges of the staircase. The purine and pyrimidine bases face the inside of the helix, with guanine always opposite cytosine and adenine always opposite thymine. These specific base pairs, referred to as complementary bases, are the steps, or treads, in our staircase analogy (Figure 10.6.4).

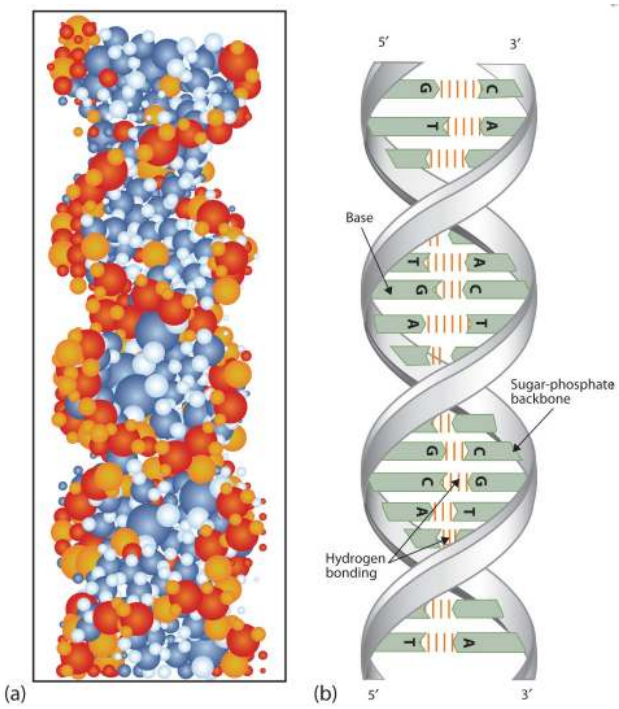


Figure 10.6.4 DNA Double Helix. (a) This represents a computer-generated model of the DNA double helix. (b) This represents a schematic representation of the double helix, showing the complementary bases.

DNA is quite flexible and further folds around itself and proteins (many of which control the reading of genetic information) to form more condensed structures.

10.6.4.3: Polysaccharides

Polysaccharides, as their name implies, are made by joining together many sugars. The functions for polysaccharides are varied. They include energy storage, structural strength, and lubrication. Polysaccharides involved in energy storage include the plant polysaccharides, amylose and amylopectin. The polysaccharide involved in energy storage in animals is called **Glycogen** and it is mostly found in the muscles and liver.

Amylose is the simplest of the polysaccharides, being comprised solely of glucose units joined in an alpha 1-4 linkage. Amylose is broken down by the enzyme alpha-amylase, found in saliva. Amylopectin is related to amylose in being composed only of glucose, but it differs in how the glucose units are joined together. Alpha 1-4 linkages predominate, but every 30-50 residues, a 'branch' arises from an alpha 1-6 linkage. Branches make the structure of amylopectin more complex than that of amylose.

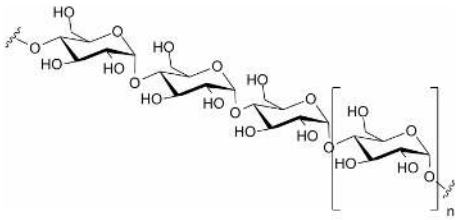


Figure 8.5.1: Amylose.

Glycogen is a polysaccharide that is physically related to amylopectin in being built only of glucose and in having a mix of alpha 1-4 and alpha 1-6 bonds. Glycogen, however, has many more alpha 1-6 branches than amylopectin, with such bonds occurring about every 10 residues. One might wonder why such branching occurs more abundantly in animals than in plants. A plausible explanation is based on the method by which these molecules are broken down. The breakdown of these polysaccharides is catalyzed by enzymes, known as phosphorylases, that clip glucose residues from the ends of glycogen chains and attach a phosphate to them in the process, producing glucose-1-phosphate. More highly branched polysaccharides have more ends to clip, and this translates to more glucose-1-phosphates that can be removed simultaneously by numerous phosphorylases. Since glucose is used for energy by muscles, glucose concentrations can be increased faster the more branched the glycogen is. Plants, which are immobile do not have needs for such immediate release of glucose and thus have less need for highly branched polysaccharides.

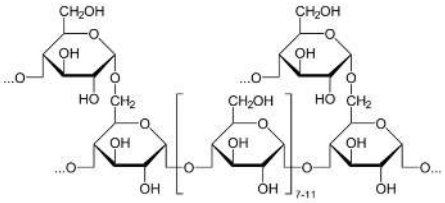


Figure 8.5.2: *Glycogen Structure*

Another important polysaccharide containing only glucose is **cellulose**. It is a polymer of glucose used to give plant cell walls structural integrity and has the individual units joined solely in a beta 1-4 configuration. That simple structural change makes a radical diff erence in its digestibility. Humans are unable to break down cellulose and it passes through the digestive system as roughage. Ruminant animals, such as cattle, however have bacteria in their rumens that contain the enzyme cellulase. It breaks the beta 1-4 links of the glucoses in cellulose to release the sugars for energy.

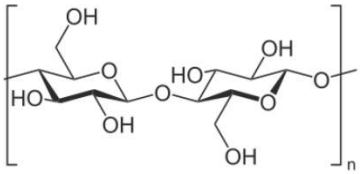


Figure 8.5.3: *The repeating structure of cellulose.*

Another polysaccharide used for structural integrity is known as **chitin**. Chitin makes up the exoskeleton of insects and is a polymer of a modified form of glucose known as N-acetyl-glucosamine.

Yet another category of polysaccharides are the **glycosaminoglycans** (also called mucopolysaccharides), some examples of which include keratan sulfate, heparin, hyaluronic acid, and chondroitin sulfate. The polysaccharide compounds are linked to proteins, but differ from glycoproteins in having a much larger contingent of sugar residues and, further, the sugars are considerably more chemically modified. Each of them contains a repeating unit of a disaccharide that contains at least one negatively charged residue. The result is a polyanionic substance that, in its interactions with water, makes for a “slimy" feel. Glycosaminoglycans are found in snot, and in synovial fluid, which lubricates joints. Heparin is a glycosaminoglycan that helps to prevent blood from clotting.

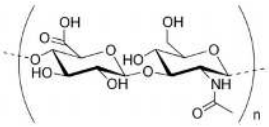


Figure 8.5.4: *The repeating unit of a glycosaminoglycan structure.*

10.6.5: Biological aggregates

10.6.5.1: Amphiphile (surfactant) aggregates

If amphiphilic molecules (those having a long hydrophobic "tail" connected to a polar, ionic or zwitterionic "head" group) are put in a polar solvent such as water, they aggregate into ordered groups that minimize the free energy of the system. These aggregates can take on many shapes, but the key ones as shown in figure 10.6.5 are **micelles**, **bilayers**, and **liposomes**.

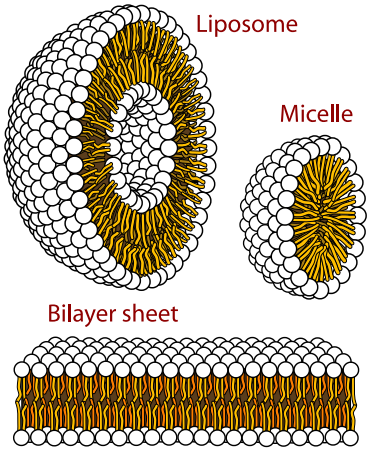


Figure 10.6.5: Cross sectional views of a micelle, bilayer and liposome, where the white spheres indicate the polar head group and the squiggly lines represent the non-polar hydrocarbon tails. Source: LadyofHats, Public domain, via Wikimedia Commons.

Micelles and the other forms are seen only above the critical micelle concentration (CMC) and the Kraft temperature. Under these conditions the free energy of the system is minimized by the formation of these aggregates that expose primarily polar groups to the surrounding solvent and place the hydrophobic tails in contact with each other. The spherical micelle shape is favored by single tail chains with relatively large head group size. As the surfactant parameter (equation 10.6.3) gets larger less spherical shapes, liposomes, bilayers and other shapes are observed.

$$N_s = \frac{V_{tail}}{A_{head}\,\ell} = \frac{A_{tail}}{A_{head}} \tag{10.6.3}$$

where V is volume, A is cross-sectional area and ℓ is the length of the tail. So as the average cross-sectional area of the tail increases relative to the cross-sectional area of the head group N_s increases. Some rough guidelines for how shape varies with the value of N_s is shown in table 10.6.1.[2]

Table 10.6.1: Micelle shape dependence on the surfactant parameter (N_s).

N_s	< 0.33	0.33 - 0.50	0.50 - 1.00	1.00	> 1.00
Shape	spherical	cylindrical rods	liposomes (vesicles)	"planar" bilayers	reverse micelles and other shapes

These are extremely dynamic structures with surfactants diffusing within the structures and leaving and joining the aggregate. In bilayers the diffusion is primarily in the plane of the bilayer (2-D) with the surfactants on the two faces unlikely to trade places. The diffusion constant in a typical phospholipid bilayer (cell membrane) is many times smaller than in water. A typical phospholipid diffuses about 1 µm/min.

10.6.5.2: Cell membranes

Cell membranes are complex aggregates that consist of a phospholipid bilayer with protein aggregates and other molecules embedded in them. Again, their stability depends on the balance between the entropy of the arrangement and the enthalpies of interactions between all the involved particles. Understanding how they behave is a current area of intense theoretical and experimental study.

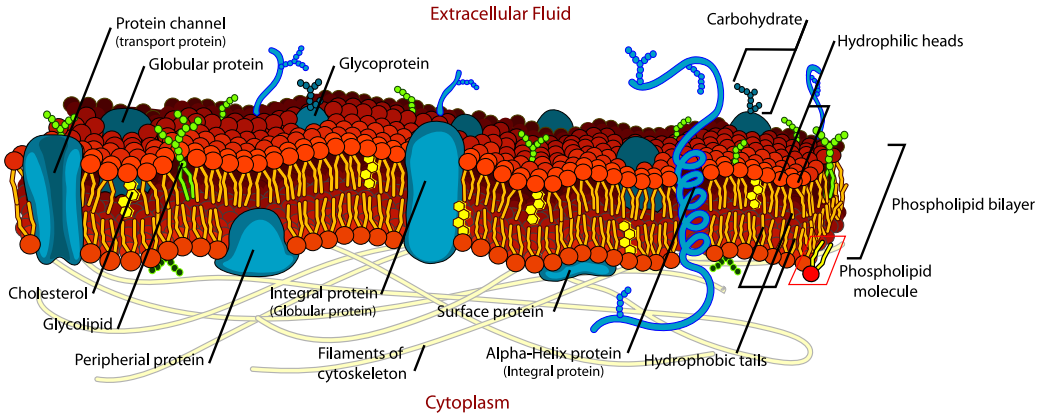


Figure 10.6.6 Cartoon of a phospholipid (biological) membrane. Source: LadyofHats, Public domain, via Wikimedia Commons

A more detailed discussion may be found at https://bio.libretexts.org/Bookshelves/Biochemistry/Fundamentals_of_Biochemistry_(Jakubowski_and_Flatt)/01%3A_Unit_I-_Structure_and_Catalysis/10%3A_Lipids/10.03%3A_Membrane_Bilayer_and_Monolayer_Assemblies_-_Structures_and_Dynamics.

10.6.6: References

1. C. R. Cantor and P. R. Schimmel, *Biophysical Chemistry Part III: The Behavior of Biological Macromolecules*. (W. H. Freeman, San Francisco, 1980), Ch. 18.; K. Dill and S. Bromberg, *Molecular Driving Forces: Statistical Thermodynamics in Biology, Chemistry, Physics, and Nanoscience*. (Taylor & Francis Group, New York, 2010); P. J. Flory, *Principles of Polymer Chemistry*. (Cornell University Press, Ithaca, 1953).
2. P.W. Atkins, J. De Paula, *Physical Chemistry for the Life Sciences*, 2nd Ed. (W. H. Freeman and Co. New York, 2011) P. 449.

10.6.7: Contributors

- A. Tokmakoff (U. Chicago)
- Dr. Kevin Ahern and Dr. Indira Rajagopal (Oregon State University)
- Jonathan Gutow (UW Oshkosh)
- Tanesha Osborne

This page titled 10.6: Macromolecules is shared under a CC BY-NC-SA 4.0 license and was authored, remixed, and/or curated by Jonathan Gutow.

- **7.1: Segment Models** by Andrei Tokmakoff is licensed CC BY-NC-SA 4.0. Original source: https://tdqms.uchicago.edu.
- **19.2: Nucleic Acid Structure** by Anonymous is licensed CC BY-NC-SA 3.0. Original source: https://2012books.lardbucket.org/books/introduction-to-chemistry-general-organic-and-biological.
- **9.2: Nucleic Acid Structure** by Tanesha Osborne is licensed CC BY-NC-SA 4.0.

10.7: Simulations

10.7.1: Introduction

Computer simulations are often used to understand and predict the behavior and structure of molecules. With modern computers it is practical to perform simulations involving macromolecules. This section provides brief descriptions of molecular dynamics simulations (MD) for predicting behavior and machine learning (ML/AI) for the prediction of macromolecular structures.

10.7.2: Molecular dynamics

Classical molecular dynamics (MD) simulations attempt to track the time evolution of the positions and velocities of the atoms and thereby the molecules in a system. In theory with the exact interaction potentials and adequate computing power, one could simulate the motion of all the species involved in a chemical reaction, diffusion across a membrane, folding of a protein, etc. These simulations essentially calculate the physical trajectory of all the simulated particles versus time. This is essentially the same problem as numerical simulation of chemical kinetics except for the scale of the problem. The position vector $\vec{q}$ and rate of change of $\vec{q}$ along the three coordinates (velocity) must be kept track of and updated at each time step. This requires being able to calculate the force on each particle based on the position of all the other particles. This is done by taking the partial derivative of the potential V (e.g. $\partial V/dx$, $\partial V/dx$, $\partial V/dx$, hereafter represented as $\partial V/\partial q$). So at each time step one calculates a new position q and velocity (dq/dt) using Newton's equations:

$$q(t+\delta t) = q_0 + \left(\frac{dq}{\delta t}\right)_0 dt \tag{10.7.1}$$

$$\frac{dq}{dt}(t+\delta t) = \left(\frac{dq}{dt}\right)_0 - \delta t\left[\left(\frac{\partial V}{\partial q}\right)_0 \frac{1}{m_q}\right]. \tag{10.7.2}$$

Here m_q is the mass of the particle. Just as with numerical integration of chemical concentrations versus time there are sophisticated algorithms for efficiently calculating the values after the next time step.

10.7.2.1: Force fields (the potential)

Let's interrupt our discussion of MD propagation of coordinates and velocities to examine the ingredients that usually appear in the force fields mentioned above. In Figure 10.7.1, we see a molecule in which various intramolecular and intermolecular interactions are introduced.

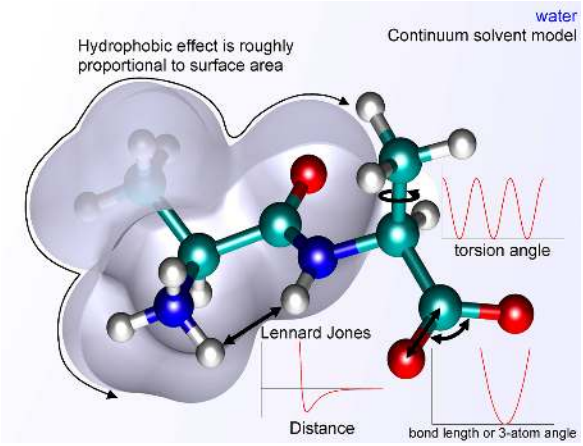


Figure 10.7.1: Depiction of a molecule in which bond-stretching, bond-bending, intramolecular van der Waals, and intermolecular solvation potentials are illustrated.

The total potential of a system containing one or more such molecules in the presence of a solvent (e.g., water) it typically written as a sum of intramolecular potentials (one for each molecule in the system) and intermolecular potentials. The total potential experienced by a particle thus has the following generic form:

$$V = V_{stretch} + V_{bend} + V_{torsion} + V_{Coulomb} + V_{vanderWaals} \tag{10.7.3}$$

The covalent interactions describing how the energy varies with bond stretching, bond bending, and dihedral angle distortion are depicted are:

$$V_{stretch} = \sum_{bonds} (1/2)k_{f,stretch}\,(R - R_e)^2 \tag{10.7.4}$$

$$V_{bend} = \sum_{angles} (1/2)k_{f,bend}(\theta - \theta_e)^2 \tag{10.7.5}$$

$$V_{torsion} = \sum_{dihedrals} \sum_{\eta} \frac{V_\eta}{2}(1 + cos(\eta\phi - \gamma)) \tag{10.7.6}$$

where η is the periodicity of the dihedral rotation (e.g 2 = cis-trans), V_η is the barrier height for torsion, γ is the phase.

The non-covalent interactions describing electrostatic and van der Waals interactions among the atoms in the molecule are

$$V_{\text{noncovalent}} = \sum_{i<j}^{\text{atoms}} \left[\frac{A_{i,j}}{r_{i,j}^{12}} - \frac{B_{i,j}}{r_{i,j}^{6}} + \frac{q_i q_j}{\varepsilon r_{i,j}} \right]. \tag{10.7.7}$$

These functional forms would be used to describe how the energy $V(q)$ changes with the bond lengths (r) and angles (θ, ϕ) within, for example, each of the molecules shown in figure 10.7.1 (let's call them solute molecules) as well as for any water molecules that may be present (if these molecules are explicitly included in the MD simulation).

The interactions among the solute and solvent molecules are also often expressed in a form involving electrostatic and van der Waals interactions between pairs of atoms- one on one molecule (solute or solvent) and the other on another molecule (solute or solvent). Usually hydrogen bonding is included in this as a primarily electrostatic interaction.

$$V_{\text{intermolecular}} = \sum_{i<j}^{\text{atoms}} \left[\frac{A_{i,j}}{r_{i,j}^{12}} - \frac{B_{i,j}}{r_{i,j}^{6}} + \frac{q_i q_j}{\varepsilon r_{i,j}} \right]. \tag{10.7.8}$$

The Cartesian forces on any atom within a solute or solvent molecule are then computed for use in the MD simulation by using the chain rule to relate derivatives with respect to Cartesian coordinates to derivatives of the above intramolecular and intermolecular potentials with respect to the interatomic distances and the angles appearing in them.

Because water is such a ubiquitous component in condensed-phase chemistry, much effort has been devoted to generating highly accurate intermolecular potentials to describe the interactions among water molecules. In the popular TIP3P and TIP4P models, the water-water interaction is given by

$$V = \frac{A}{r_{OO}^{12}} - \frac{B}{r_{OO}^{6}} + \sum_{i,j} \frac{k q_i q_j}{r_{i,j}}. \tag{10.7.9}$$

where r_{OO} is the distance between the oxygen atoms of the two water molecules in Å, and indices i and j run over 3 or 4 sites, respectively, for TIP3P or TIP4P, with i labeling sites on one water molecule and j labeling sites on the second water molecule. The parameter k is 332.1 Å kcal mol^{-1}. A and B are conventional Lennard-Jones parameters for oxygen atoms and q_i is the magnitude of the partial charge on the ith site. In Figure 10.7.2, we show how the 3 or 4 sites are defined for these two models.

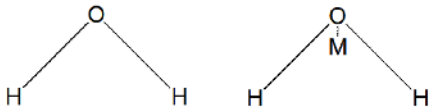


Figure 10.7.2: Location of the 3 or 4 sites used in the TIP3P and TIP4P models.

Typical values for the parameters are given in the table below.

	r_{OH}(Å)	HOH angle degrees	r_{OM}(Å)	A (Å^{12} kcal/mol)	B (Å^{6} kcal/mol)	q_O or q_M	q_H
TIP3P	0.9572	104.52		582 x10^3	595	-0.834	0.417
TIP4P	0.9672	104.52	0.15	600 x10^3	610	-1.04	0.52

In the TIP3P model, the three sites reside on the oxygen and two hydrogen centers. For TIP4P, the fourth site is called the M-site and it resides off the oxygen center a distance of 0.15 along the bisector of the two O-H bonds as shown in Figure 10.7.2 In using either the TIP3P or TIP4P model, the intramolecular bond lengths and angles are often constrained to remain fixed; when doing so, one is said to be using a rigid water model.

There are variants to these two 3-site and 4-site models that, for example, include van der Waals interactions between H atoms on different water molecules, and there are models including more than 4 sites, and models that allow for the polarization of each water molecule induced by the dipole fields (as represented by the partial charges) of the other water molecules and of solute molecules. The more detail and complexity one introduces, the more computational effort is needed to perform MD simulations. In particular, water molecules that allow for polarization are considerably more computationally demanding because they often involve solving self-consistently for the polarization of each molecule by the charge and dipole potentials of all the other molecules, with each dipole potential including both the permanent and induced dipoles of that molecule. This web page provides links to numerous software packages that use these kinds of force fields to carry out MD simulations. These links also offer more detailed information about the performance of various force fields as well as giving values for the parameters used in those force fields.

The parameter values are usually obtained by

1. fitting the intramolecular or intermolecular functional form (e.g., as shown above) to energies obtained in electronic structure calculations at a large number of geometries, or
2. adjusting them to cause MD simulations employing the force field to reproduce certain thermodynamic properties (e.g., radial distribution functions, solvation energies, vaporization energies, diffusion constants), or some combination of both. It is important to observe that the kind of force fields discussed above have limitations beyond issues of accuracy. In particular, they are not designed to allow for bond breaking and bond forming, and they represent the Born-Oppenheimer energy of one (most often the ground) electronic state. There are force fields explicitly designed to include chemical bonding changes, but most MD packages do not include them. When one is interested in treating a problem that involves transitions from one electronic state to another (e.g., in spectroscopy or when the system undergoes a surface hop near a conical intersection), it is most common to use a combined QM-MM approach. A QM treatment of the portion of the system that undergoes the electronic transition is combined with a force-field (MM) treatment of the rest of the system to carry out the MD simulation.

10.7.2.2: Practical considerations

By applying one of the time-propagation algorithms to all of the coordinates and momenta of the N molecules at time t, one generates a set of new coordinates $q(t+\delta t)$ and new velocities $dq/dt(t+\delta t)$ appropriate to the system at time $t+dt$. Using these new coordinates and momenta as q_0 and $(dq/\delta t)_0$ and evaluating the forces $-(\partial V/\partial q)_0$ at these new coordinates, one can again use the propagation equations to generate another finite-time-step set of new coordinates and velocities. Through the sequential application of this process, one generates a sequence of coordinates and velocities that simulate the system's behavior.

These MD simulations are difficult to carry out in a parallel manner. One can certainly execute many different classical trajectories on many different computer nodes, which when averaged can provide values for average (thermodynamic) outcomes. However, to distribute one trajectory over many nodes is difficult. The primary difficulty is that, for each time step, all N of the molecules undergo movement to new coordinates and momenta. To compute the forces on all N molecules requires on the order of N^2 calculations (e.g., when pairwise additive potentials are used).

Another factor that complicates MD simulations has to do with the wide range of times scales that may be involved. For example, for one to use a time step dt short enough to follow high-frequency motions (e.g., O-H stretching) in a simulation of an ion or polymer in water solvent, dt must be of the order of 10^{-15} s. To then simulate the diffusion of an ion or the folding of a polymer in the liquid state, which might require 10^{-4} s or longer, one would have to carry out 10^{11} MD steps. In the table below we illustrate the wide range of time scales that characterize various events that one might want to simulate using some form of MD, and we give a sense of what was practical using MD simulations in the year 2010. Since that time things have not improved much. This may seem counter to the massive improvement in computer usability, but because these calculations do not parallelize well the explosion in number of cpu cores with only an increase in cpu speed of 2 to 3 has not helped much.

Examples of dynamical processes taking place over timescales ranging from 10^{-15} s through hundreds of seconds, each of which one may wish to simulate using MD.

10^{-15} -10^{-14} s	10^{-12} s	10^{-9} s	10^{-6} s	10^{-3} s	110 s

10^{-15} -10^{-14} s	10^{-12} s	10^{-9} s	10^{-6} s	10^{-3} s	110 s
C-H, N-H, O-H bond vibration	Rotation of small molecule	Routinely accessible time duration for atomistic MD simulation	Time duration for heroic atomistic MD simulation	Time duration achievable using coarse-graining techniques	Time needed for protein folding

Because one can not afford to carry out simulations covering 10^{-3} -100 s using time steps needed to follow bond vibrations 10^{-15} s, it is necessary to devise strategies to focus on motions whose time frame is of primary interest while ignoring or approximating faster motions. For example, when carrying out long-time MD simulations, one can ignore the high-frequency intramolecular motions by simply not including these coordinates and momenta in the Netwonian dynamics (e.g., as one does when using a rigid-water model discussed earlier). In other words, one simply freezes certain bond lengths and angles. Of course, this is an approximation whose consequences must be tested and justified, and would certainly not be a wise step to take if those coordinates played a key role in the dynamical process being simulated. Another approach, called coarse graining involves replacing the fully atomistic description of selected components of the system by a much-simplified description involving significantly fewer spatial coordinates and momenta.

Quite impressive simulations can be made using some approximations. For example see this simulation of a COVID virus particle in a water drop.

10.7.3: Machine learning (AI) prediction 3D protein structure

Based on: https://bio.libretexts.org/Bookshelves/Biochemistry/Fundamentals_of_Biochemistry_(Jakubowski_and_Flatt)/01%3A_Unit_I-_Structure_and_Catalysis/04%3A_The_Three-Dimensional_Structure_of_Proteins/4.14%3A_Predicting_Structure_from_Sequence_and_Sequence_from_Structure_Function_(New_10%2F%2F24)#The_Protein_Folding_Problem__Sequence_to_3D_Structure

Protein structure can be experimentally analyzed and the 3D structure of a protein determined using NMR, X-ray crystallography, and cryo-EM. Now, using sequence and structural databases (like the PDB with over 227,000 structures), we can often predict the 3D structure of a protein just from its linear sequence by comparing the sequence of a protein of unknown tertiary structure to homologous proteins (by sequence) whose 3D structures are known. Machine learning and artificial intelligence have extended earlier and simpler "homology modeling" attempts to allow structural predictions for millions of protein sequences using programs such as RoseTTAFold and AlphaFold. RoseTTAFold and AlphaFold produce high-quality structure predictions when trained using the vast sequence information in the Protein Data Bank. Embedded in those linear sequences is a large amount of hidden (to the human eye) evolutionary information that machine learning and AI can harness to predict 3D structures. The key appears to be that particular sequences lead to the same sequential steps with similar balances between the kinetics and thermodynamics as the proteins fold. These AI tools work less well when very limited sequence comparisons are available.

In general (for smaller proteins), the protein folding problem, the prediction of structure from sequence, appears to have been "solved". The Nobel Prize in Chemistry in 2024 was awarded to Demis Hassabis and John M. Jumper from Google DeepMind for developing AlphaFold and David Baker for developing RoseTTaFold and other powerful techniques described below. (For more details on how this works see, Chapter 4.13: Predicting Structure and Function of Biomolecules Through Natural Language Processing Tools)

A comparison of protein structures obtained using these programs with known 3D structures obtained through X-ray crystallography or other techniques shows them almost identical. Different metrics can be used to compare predicted structures to the actual ones. The root mean squared deviation (RMSD) is a common one. RoseTTAFold uses a **TM-score to assess** the topological similarity of protein structures. Compared to RMSD, the TM-score weights smaller distance errors higher than larger ones, making it sensitive to the global fold, not local structural differences. TM values range from 0-100 (100 is a perfect match). Scores below 17 indicate no topology match, while those above 50 suggest a common fold.

AlphaFold uses a "neural network, meaning it simultaneously considers patterns in protein sequences, how a protein's amino acids interact, and its possible three-dimensional structure. In this architecture, one-, two-, and three-dimensional information flows back and forth, allowing the network to collectively reason about the relationship between a protein's chemical parts and its folded structure". This is essentially a statistical probability engine that predicts a structure based on what it is most like. Programs of this

type might allow the generation of proteins with new therapeutic or commercial potential based on sequences. These include vaccines, sensors, specific immune system suppressors or activators, and antivirals. AlphaFold has now been used to predict the structure of 214 million proteins from more than one million species — essentially all known protein-coding sequences. These AlphaFold iCn3D models are available in the AlphaFold Database - Protein Structure Database.

Figure 10.7.3 shows the backbone tube cartoon of the x-ray pdb structure of the small protein (1xww, cyan) and the structure predicted by both RoseTTAFold program and AlphaFold (magenta) just from its primary sequence. Sulfate, a competitive inhibitor, is shown (spacefill) bound in the active site. The alignment is spectacular, except for the N-terminal 5 amino acids at the bottom of the figure (6 o'clock). This stretch has more disorder even in the x-ray structure as the amino acids have high B-factors, indicating more conformational flexibility.



Figure 10.7.3: Comparison of the x-ray and computationally predicted structures of human low molecule weight protein tyrosine phosphatase

Left panel: X-ray structure (cyan) of low molecular weight protein tyrosine phosphatase with bound SO_4^{2-} (1xww) and corresponding structure predicted by the RoseTTAFold (magenta). Right panel: Same structures using AlphaFold for the structural prediction.

This page titled 10.7: Simulations is shared under a CC BY-NC-SA 4.0 license and was authored, remixed, and/or curated by Jonathan Gutow.

- **4.14: Predicting Structure from Sequence and Sequence from Structure/Function (New 10/24)** by Henry Jakubowski and Patricia Flatt has no license indicated.
- **7.3: Molecular Dynamics Simulations** by Jack Simons is licensed CC BY-NC-SA 4.0.

Index

1: A

activated complex
- 5.1: Reaction Mechanisms
- 6.4: Transition State Theory

Activation controlled
- 6.1: Kinetics of Reactions in Solution

activation energy
- 4.6: Temperature Dependence of Rate Constants
- 6.3: Collision Theory

adiabatic process
- 1.4: The Second Law of Thermodynamics

Albert Einstein
- 8.1: Failures of Classical Physics

anode
- 3.5: Half Cells and Standard Reduction Potentials

aromaticity
- 8.6: Particle on a Ring
- 9.7: Benzene and Aromaticity

Arrhenius equation
- 4.6: Temperature Dependence of Rate Constants
- 6.3: Collision Theory
- 6.4: Transition State Theory

arrhenius prefactor
- 6.3: Collision Theory

atmospheric chemistry
- 7.5: Catalysis (ozone example)

autocatalysis
- 7.6: Oscillating Reactions

2: B

benzene
- 9.7: Benzene and Aromaticity

bimolecular
- 5.1: Reaction Mechanisms

bimolecular reaction
- 5.1: Reaction Mechanisms

bimolecular reactions
- 6.3: Collision Theory

biochemical reactions
- 1.3: Thermochemistry

blackbody radiation
- 8.1: Failures of Classical Physics

Boltzmann
- 1.5: The Boltzmann Distribution and the Statistical Definition of Entropy

Boltzmann distribution
- 1.5: The Boltzmann Distribution and the Statistical Definition of Entropy

BornOppenheimer
- 9.1: The Born-Oppenheimer Approximation Simplifies the Schrödinger Equation for Molecules

Brownian motion
- 6.1: Kinetics of Reactions in Solution
- 7.7: Diffusion

3: C

car batteries
- 3.7: Thermodynamics from Electrochemistry

catalyst
- 7.2: The Michaelis-Menten Mechanism
- 7.5: Catalysis (ozone example)

catalytic decomposition of ozone
- 7.5: Catalysis (ozone example)

cathode
- 3.5: Half Cells and Standard Reduction Potentials

cell potential
- 3.5: Half Cells and Standard Reduction Potentials
- 3.7: Thermodynamics from Electrochemistry

chain reaction
- 7.4: Chain Reactions

chemical equilibrium
- 5.5: The Equilibrium Approximation

chemical kinetics
- 5.4: The Rate Determining Step Approximation
- 5.5: The Equilibrium Approximation
- 5.6: The Steady-State Approximation
- 6.3: Collision Theory

chemical pathway
- 5.1: Reaction Mechanisms

chemical reaction
- 4.1: Reaction Rates and Rate Laws

chemical reaction rates
- 6.4: Transition State Theory

chemical reactions
- 1.3: Thermochemistry
- 3.7: Thermodynamics from Electrochemistry
- 4.6: Temperature Dependence of Rate Constants
- 5.6: The Steady-State Approximation

chemicalbonding
- 9.1: The Born-Oppenheimer Approximation Simplifies the Schrödinger Equation for Molecules

chlorofluorocarbons
- 7.5: Catalysis (ozone example)

collision theory
- 4.6: Temperature Dependence of Rate Constants
- 6.3: Collision Theory

collisional cross section
- 6.3: Collision Theory

computational chemistry
- 9.6: Hückel MO Model of Conjugation

concentration
- 4.1: Reaction Rates and Rate Laws
- 5.6: The Steady-State Approximation

conjugated hydrocarbons
- 9.7: Benzene and Aromaticity

conjugated systems
- 9.6: Hückel MO Model of Conjugation

cyclical conjugated systems
- 9.7: Benzene and Aromaticity

4: D

Daniel cell
- 3.7: Thermodynamics from Electrochemistry

degeneracy
- 1.5: The Boltzmann Distribution and the Statistical Definition of Entropy
- 8.5: Particle in a 2-Dimensional Box

degenerate energy levels
- 1.5: The Boltzmann Distribution and the Statistical Definition of Entropy

delocalization energy
- 9.7: Benzene and Aromaticity

Density Functional Theory
- 9.8: Numerical QM Methods

densityFunctionalTheory
- 9.1: The Born-Oppenheimer Approximation Simplifies the Schrödinger Equation for Molecules

diffusion
- 7.7: Diffusion

diffusion constant
- 7.7: Diffusion

Diffusion Controlled
- 6.1: Kinetics of Reactions in Solution

5: E

effective rate constant
- 7.3: The Lindemann Mechanism

electrochemical cells
- 3.5: Half Cells and Standard Reduction Potentials

electrochemistry
- 3.5: Half Cells and Standard Reduction Potentials
- 3.7: Thermodynamics from Electrochemistry

elementary reaction
- 5.1: Reaction Mechanisms

elementary reactions
- 5.1: Reaction Mechanisms

empirical model
- 4.6: Temperature Dependence of Rate Constants

encounter pair
- 6.1: Kinetics of Reactions in Solution

endothermic reaction
- 1.3: Thermochemistry

energy barrier
- 4.6: Temperature Dependence of Rate Constants

energy configuration
- 1.5: The Boltzmann Distribution and the Statistical Definition of Entropy

energy conservation
- 1.4: The Second Law of Thermodynamics

energy levels
- 1.5: The Boltzmann Distribution and the Statistical Definition of Entropy

energy states
- 1.5: The Boltzmann Distribution and the Statistical Definition of Entropy

enthalpy
- 1.3: Thermochemistry

enthalpy change
- 1.3: Thermochemistry

entropy
- 1.4: The Second Law of Thermodynamics
- 1.5: The Boltzmann Distribution and the Statistical Definition of Entropy

entropy change
- 1.4: The Second Law of Thermodynamics

Entropy of galvanic cell
- 3.7: Thermodynamics from Electrochemistry

entropy of universe
- 1.4: The Second Law of Thermodynamics

enzyme catalysis
- 7.2: The Michaelis-Menten Mechanism

enzyme kinetics
- 7.2: The Michaelis-Menten Mechanism

equilibrium
- 1.5: The Boltzmann Distribution and the Statistical Definition of Entropy

equilibrium approximation
- 5.5: The Equilibrium Approximation
- 7.2: The Michaelis-Menten Mechanism

equilibrium constant
- 2.5: Coupled Equilibria
- 6.4: Transition State Theory

exothermic reaction
- 1.3: Thermochemistry

experimental determination
- 4.1: Reaction Rates and Rate Laws

6: F

Fick’s first law of diffusion
7.7: Diffusion

Fick’s second law of diffusion
7.7: Diffusion

first law
1.4: The Second Law of Thermodynamics

frontier orbitals
9.6: Hückel MO Model of Conjugation

7: G

galvanic cell
3.5: Half Cells and Standard Reduction Potentials

glycolysis
2.7: Coupled Equilibria Driving Nonspontaneous Reactions

8: H

Hückel theory
9.6: Hückel MO Model of Conjugation
9.7: Benzene and Aromaticity

Hamiltonian
9.1: The Born-Oppenheimer Approximation Simplifies the Schrödinger Equation for Molecules

harmonic oscillator
8.9: Harmonic Oscillator

heat capacity
1.3: Thermochemistry

heat of formation
1.3: Thermochemistry

heat transfer
1.3: Thermochemistry
1.4: The Second Law of Thermodynamics

Henry's Law
1.9: Henry's Law

Hess's law
1.3: Thermochemistry

heterogeneous equilibria
2.5: Coupled Equilibria

homogeneous equilibria
2.5: Coupled Equilibria

9: I

ideal gas
1.4: The Second Law of Thermodynamics

ideal mixing
1.4: The Second Law of Thermodynamics

initiation step
7.4: Chain Reactions

intermediate
5.6: The Steady-State Approximation

intermediate species
5.5: The Equilibrium Approximation

intermediate state
6.4: Transition State Theory

irreversible process
1.4: The Second Law of Thermodynamics

10: K

Kc
2.5: Coupled Equilibria

kinetic analysis
7.3: The Lindemann Mechanism

kinetic control
6.2: Kinetic vs. Thermodynamic Control of Reactions

kinetic energy
4.6: Temperature Dependence of Rate Constants

kinetics
5.1: Reaction Mechanisms

Kirchhoff's law
1.3: Thermochemistry

Kp
2.5: Coupled Equilibria

11: L

Lagrange multipliers
1.5: The Boltzmann Distribution and the Statistical Definition of Entropy

Law of Mass Action
2.5: Coupled Equilibria

Le Chatelier's principle
2.6: Equilibrium Dependence on Conditions

Lindemann mechanism
7.3: The Lindemann Mechanism

12: M

macrostates
1.5: The Boltzmann Distribution and the Statistical Definition of Entropy

Marcus cross relation
7.11: Kinetics of Electron Transfer Reactions

Marcus Theory
7.11: Kinetics of Electron Transfer Reactions

Max Planck
8.1: Failures of Classical Physics

Michaelis constant
7.2: The Michaelis-Menten Mechanism

microstates
1.5: The Boltzmann Distribution and the Statistical Definition of Entropy

molar enthalpy
1.3: Thermochemistry

molar heat capacity
1.4: The Second Law of Thermodynamics

molecular collision
6.4: Transition State Theory

molecular collisions
4.6: Temperature Dependence of Rate Constants
6.3: Collision Theory

molecular orbitals
9.6: Hückel MO Model of Conjugation

molecularity
5.1: Reaction Mechanisms
5.4: The Rate Determining Step Approximation

molecules
9.1: The Born-Oppenheimer Approximation Simplifies the Schrödinger Equation for Molecules

Montreal Protocol
7.5: Catalysis (ozone example)

multiElectronSystems
9.1: The Born-Oppenheimer Approximation Simplifies the Schrödinger Equation for Molecules

13: N

negative order
5.5: The Equilibrium Approximation

Nernst equation
3.5: Half Cells and Standard Reduction Potentials
3.6: Cell potentials under non-standard conditions (Nernst equation)

nodal lines
8.5: Particle in a 2-Dimensional Box

Numerical Quantum Computations
9.8: Numerical QM Methods

14: O

oscillating reactions
7.6: Oscillating Reactions

Overton relation
7.8: Membrane Diffusion

oxidation
3.5: Half Cells and Standard Reduction Potentials

ozone
7.5: Catalysis (ozone example)

ozone decomposition
7.5: Catalysis (ozone example)

ozone hole
7.5: Catalysis (ozone example)

ozone layer
7.5: Catalysis (ozone example)

15: P

particle in a 2D box
8.5: Particle in a 2-Dimensional Box

particle in a box
8.3: Particle in a One-Dimensional Box

particles
1.5: The Boltzmann Distribution and the Statistical Definition of Entropy

partition function
1.5: The Boltzmann Distribution and the Statistical Definition of Entropy
6.4: Transition State Theory

partition functions
6.4: Transition State Theory

phase change
1.4: The Second Law of Thermodynamics

photoelectric effect
8.1: Failures of Classical Physics

physics
1.5: The Boltzmann Distribution and the Statistical Definition of Entropy

pi bonding
9.6: Hückel MO Model of Conjugation
9.7: Benzene and Aromaticity

position of equilibrium
2.6: Equilibrium Dependence on Conditions

practice problems
1.4: The Second Law of Thermodynamics

probability distribution
1.5: The Boltzmann Distribution and the Statistical Definition of Entropy

products
4.1: Reaction Rates and Rate Laws

propagation step
7.4: Chain Reactions

16: Q

quantumchemistry
9.1: The Born-Oppenheimer Approximation Simplifies the Schrödinger Equation for Molecules

quantummechanics
9.1: The Born-Oppenheimer Approximation Simplifies the Schrödinger Equation for Molecules

17: R

Rapid Equilibrium Approximation
5.5: The Equilibrium Approximation

rate constant
4.1: Reaction Rates and Rate Laws
rate constants
6.3: Collision Theory
rate determining step
5.4: The Rate Determining Step Approximation
rate determining step approximation
5.4: The Rate Determining Step Approximation
rate law
4.1: Reaction Rates and Rate Laws
5.1: Reaction Mechanisms
5.4: The Rate Determining Step Approximation
5.5: The Equilibrium Approximation
5.6: The Steady-State Approximation
rate of change
5.6: The Steady-State Approximation
reactants
4.1: Reaction Rates and Rate Laws
reaction dynamics
5.5: The Equilibrium Approximation
reaction enthalpy
1.3: Thermochemistry
reaction mechanism
5.1: Reaction Mechanisms
5.4: The Rate Determining Step Approximation
5.5: The Equilibrium Approximation
5.6: The Steady-State Approximation
6.4: Transition State Theory
reaction mechanisms
6.3: Collision Theory
reaction order
4.1: Reaction Rates and Rate Laws
5.6: The Steady-State Approximation
reaction orders
6.3: Collision Theory
reaction profile
4.6: Temperature Dependence of Rate Constants
reaction quotient
2.5: Coupled Equilibria
reaction rate
4.1: Reaction Rates and Rate Laws
5.4: The Rate Determining Step Approximation
5.5: The Equilibrium Approximation
6.3: Collision Theory
reaction rates
4.6: Temperature Dependence of Rate Constants
reduction
3.5: Half Cells and Standard Reduction Potentials
reduction potential
3.5: Half Cells and Standard Reduction Potentials
research
9.1: The Born-Oppenheimer Approximation Simplifies the Schrödinger Equation for Molecules
resonance structures
9.7: Benzene and Aromaticity
reversible heat
1.4: The Second Law of Thermodynamics
Reversible Process
1.4: The Second Law of Thermodynamics
reversible reaction
5.5: The Equilibrium Approximation
Rudolf Clausius
1.4: The Second Law of Thermodynamics

18: S

Scanning Tunneling Microscopy (STM)
8.4: Tunneling
schrodingerequation
9.1: The Born-Oppenheimer Approximation Simplifies the Schrödinger Equation for Molecules
scientific method
5.6: The Steady-State Approximation
second law
1.4: The Second Law of Thermodynamics
side products
5.1: Reaction Mechanisms
sigma bonding
9.6: Hückel MO Model of Conjugation
slowest step
5.4: The Rate Determining Step Approximation
solvent cage
6.1: Kinetics of Reactions in Solution
solvent kinetic effect
6.1: Kinetics of Reactions in Solution
sp2 hybridization
9.6: Hückel MO Model of Conjugation
spectral analysis
9.6: Hückel MO Model of Conjugation
spontaneity
3.5: Half Cells and Standard Reduction Potentials
spontaneous process
1.4: The Second Law of Thermodynamics
standard cell potential
3.7: Thermodynamics from Electrochemistry
standard conditions
3.5: Half Cells and Standard Reduction Potentials
standard hydrogen electrode
3.5: Half Cells and Standard Reduction Potentials
standard reduction potential
3.5: Half Cells and Standard Reduction Potentials
standard state
1.3: Thermochemistry
state function
1.3: Thermochemistry
statistical mechanics
1.5: The Boltzmann Distribution and the Statistical Definition of Entropy
statistical thermodynamics
1.5: The Boltzmann Distribution and the Statistical Definition of Entropy
steady state approximation
5.5: The Equilibrium Approximation
5.6: The Steady-State Approximation
stoichiometry
4.1: Reaction Rates and Rate Laws
stress
2.6: Equilibrium Dependence on Conditions

19: T

tabulated data
1.3: Thermochemistry
temperature dependence
1.3: Thermochemistry
4.6: Temperature Dependence of Rate Constants
Temperature Dependence to Rates
4.6: Temperature Dependence of Rate Constants
temperature effects
3.7: Thermodynamics from Electrochemistry
termination step
7.4: Chain Reactions
termolecular
5.1: Reaction Mechanisms
termolecular reaction
5.1: Reaction Mechanisms
thermal decomposition
6.3: Collision Theory
thermodynamic control
6.2: Kinetic vs. Thermodynamic Control of Reactions
thermodynamic observables
1.5: The Boltzmann Distribution and the Statistical Definition of Entropy
thermodynamic stability
9.7: Benzene and Aromaticity
thermodynamics
1.3: Thermochemistry
1.4: The Second Law of Thermodynamics
1.5: The Boltzmann Distribution and the Statistical Definition of Entropy
transition state
6.4: Transition State Theory
transition state theory
4.6: Temperature Dependence of Rate Constants
6.4: Transition State Theory
tunneling
8.4: Tunneling

20: U

unimolecular
5.1: Reaction Mechanisms
unimolecular reaction
5.1: Reaction Mechanisms
unimolecular reactions
6.3: Collision Theory

21: V

valid mechanism
5.1: Reaction Mechanisms
vibrational frequency
6.4: Transition State Theory
voltage measurement
3.5: Half Cells and Standard Reduction Potentials

22: W

water gas shift reaction
2.5: Coupled Equilibria

Glossary

Sample Word 1 | Sample Definition 1

Detailed Licensing

1: Overview

Title: Chem 370: P-Chem 1 for Biophysical & Traditional Students (Gutow)

Webpages: 103

Applicable Restrictions: Noncommercial

All licenses found:

- CC BY-NC-SA 4.0: 100% (103 pages)

2: By Page

- Chem 370: P-Chem 1 for Biophysical & Traditional Students (Gutow) - *CC BY-NC-SA 4.0*
  - Front Matter - *CC BY-NC-SA 4.0*
    - TitlePage - *CC BY-NC-SA 4.0*
    - InfoPage - *CC BY-NC-SA 4.0*
    - Table of Contents - *CC BY-NC-SA 4.0*
    - Licensing - *CC BY-NC-SA 4.0*
  - 1: Thermodynamics - *CC BY-NC-SA 4.0*
    - 1.1: Thermodynamic Variables and Equations of State - *CC BY-NC-SA 4.0*
    - 1.2: The First Law of Thermodynamics - *CC BY-NC-SA 4.0*
    - 1.3: Thermochemistry - *CC BY-NC-SA 4.0*
    - 1.4: The Second Law of Thermodynamics - *CC BY-NC-SA 4.0*
    - 1.5: The Boltzmann Distribution and the Statistical Definition of Entropy - *CC BY-NC-SA 4.0*
    - 1.6: The Gibbs and Helmholtz Energy - *CC BY-NC-SA 4.0*
    - 1.7: Phase Equilibria and Mixtures - *CC BY-NC-SA 4.0*
    - 1.8: Colligative Properties - *CC BY-NC-SA 4.0*
    - 1.9: Henry's Law - *CC BY-NC-SA 4.0*
  - 2: Chemical Equilibria - *CC BY-NC-SA 4.0*
    - 2.1: Chemical Equilibria - *CC BY-NC-SA 4.0*
    - 2.2: Composition Dependence of Free Energy (G) - *CC BY-NC-SA 4.0*
    - 2.3: Equilibrium Calculations (ICE) Review - *CC BY-NC-SA 4.0*
    - 2.4: Fractional Composition at Equilibrium - *CC BY-NC-SA 4.0*
    - 2.5: Coupled Equilibria - *CC BY-NC-SA 4.0*
    - 2.6: Equilibrium Dependence on Conditions - *CC BY-NC-SA 4.0*
    - 2.7: Coupled Equilibria Driving Nonspontaneous Reactions - *CC BY-NC-SA 4.0*
    - 2.8: Brønsted-Lowry Acids and Bases - *CC BY-NC-SA 4.0*
    - 2.9: pH and pOH - *CC BY-NC-SA 4.0*
    - 2.10: Acid-Base Equilibria - *CC BY-NC-SA 4.0*
    - 2.11: Hydrolysis of Salts - *CC BY-NC-SA 4.0*
    - 2.12: Polyprotic Acids - *CC BY-NC-SA 4.0*
    - 2.13: Buffers - *CC BY-NC-SA 4.0*
  - 3: Ions and Electrochemistry - *CC BY-NC-SA 4.0*
    - 3.1: Mean Ionic Activity Coefficients and the Debye-Hückel Model - *CC BY-NC-SA 4.0*
    - 3.2: Extending Debye-Hückel Theory to Higher Concentrations - *CC BY-NC-SA 4.0*
    - 3.3: Ion Transport - *CC BY-NC-SA 4.0*
    - 3.4: Review of Redox Chemistry - *CC BY-NC-SA 4.0*
    - 3.5: Half Cells and Standard Reduction Potentials - *CC BY-NC-SA 4.0*
    - 3.6: Cell potentials under non-standard conditions (Nernst equation) - *CC BY-NC-SA 4.0*
    - 3.7: Thermodynamics from Electrochemistry - *CC BY-NC-SA 4.0*
    - 3.8: Redox Examples - *CC BY-NC-SA 4.0*
  - 4: Reaction Kinetics - *CC BY-NC-SA 4.0*
    - 4.1: Reaction Rates and Rate Laws - *CC BY-NC-SA 4.0*
    - 4.2: Measuring Reaction Rates - *CC BY-NC-SA 4.0*
    - 4.3: Determining Rate Laws - *CC BY-NC-SA 4.0*
    - 4.4: Integrated Rate Laws - *CC BY-NC-SA 4.0*
    - 4.5: Examples of Using Graphs to Determine Reaction Order - *CC BY-NC-SA 4.0*
    - 4.6: Temperature Dependence of Rate Constants - *CC BY-NC-SA 4.0*
  - 5: Kinetic Mechanisms 1 - *CC BY-NC-SA 4.0*
    - 5.1: Reaction Mechanisms - *CC BY-NC-SA 4.0*
    - 5.2: Relaxation Methods - *CC BY-NC-SA 4.0*
    - 5.3: Representative Reaction Mechanisms - *CC BY-NC-SA 4.0*
    - 5.4: The Rate Determining Step Approximation - *CC BY-NC-SA 4.0*
    - 5.5: The Equilibrium Approximation - *CC BY-NC-SA 4.0*

- 5.6: The Steady-State Approximation - *CC BY-NC-SA 4.0*

- 6: Molecular Level Models of Kinetics - *CC BY-NC-SA 4.0*
  - 6.1: Kinetics of Reactions in Solution - *CC BY-NC-SA 4.0*
  - 6.2: Kinetic vs. Thermodynamic Control of Reactions - *CC BY-NC-SA 4.0*
  - 6.3: Collision Theory - *CC BY-NC-SA 4.0*
  - 6.4: Transition State Theory - *CC BY-NC-SA 4.0*
  - 6.5: Reactions Involving Ions - *CC BY-NC-SA 4.0*
- 7: Kinetic Mechanisms 2 - *CC BY-NC-SA 4.0*
  - 7.1: Numerical Modeling of Mechanisms - *CC BY-NC-SA 4.0*
  - 7.2: The Michaelis-Menten Mechanism - *CC BY-NC-SA 4.0*
  - 7.3: The Lindemann Mechanism - *CC BY-NC-SA 4.0*
  - 7.4: Chain Reactions - *CC BY-NC-SA 4.0*
  - 7.5: Catalysis (ozone example) - *CC BY-NC-SA 4.0*
  - 7.6: Oscillating Reactions - *CC BY-NC-SA 4.0*
  - 7.7: Diffusion - *CC BY-NC-SA 4.0*
  - 7.8: Membrane Diffusion - *CC BY-NC-SA 4.0*
  - 7.9: Ion Mobilities - *CC BY-NC-SA 4.0*
  - 7.10: Transport Across Cell Membranes - *CC BY-NC-SA 4.0*
  - 7.11: Kinetics of Electron Transfer Reactions - *CC BY-NC-SA 4.0*
- 8: Quantum Chemistry Fundamentals - *CC BY-NC-SA 4.0*
  - 8.1: Failures of Classical Physics - *CC BY-NC-SA 4.0*
  - 8.2: The Schrödinger Wave Equation - *CC BY-NC-SA 4.0*
  - 8.3: Particle in a One-Dimensional Box - *CC BY-NC-SA 4.0*
  - 8.4: Tunneling - *CC BY-NC-SA 4.0*
  - 8.5: Particle in a 2-Dimensional Box - *CC BY-NC-SA 4.0*
  - 8.6: Particle on a Ring - *CC BY-NC-SA 4.0*
  - 8.7: The Schrödinger Wave Equation for the Hydrogen Atom - *CC BY-NC-SA 4.0*
  - 8.8: Many-Electron Atoms and the Periodic Table - *CC BY-NC-SA 4.0*
  - 8.9: Harmonic Oscillator - *CC BY-NC-SA 4.0*
- 9: Molecular Quantum Mechanics - *CC BY-NC-SA 4.0*
  - 9.1: The Born-Oppenheimer Approximation Simplifies the Schrödinger Equation for Molecules - *CC BY-NC-SA 4.0*
  - 9.2: Valence Bond Theory - *CC BY-NC-SA 4.0*
  - 9.3: Hybridization of Atomic Orbitals - *CC BY-NC-SA 4.0*
  - 9.4: Molecular Orbital Theory - *CC BY-NC-SA 4.0*
  - 9.5: Diatomic Molecules With More Than s Orbitals - *CC BY-NC-SA 4.0*
  - 9.6: Hückel MO Model of Conjugation - *CC BY-NC-SA 4.0*
  - 9.7: Benzene and Aromaticity - *CC BY-NC-SA 4.0*
  - 9.8: Numerical QM Methods - *CC BY-NC-SA 4.0*
- 10: Aggregates and Macromolecules - *CC BY-NC-SA 4.0*
  - 10.1: Mass Spectrometry - *CC BY-NC-SA 4.0*
  - 10.2: X-Ray Crystallography - *CC BY-NC-SA 4.0*
  - 10.3: Cryo-Electron Microscopy - *CC BY-NC-SA 4.0*
  - 10.4: Intermolecular Forces - *CC BY-NC-SA 4.0*
  - 10.5: Structure of Gases, Liquids and Glasses - *CC BY-NC-SA 4.0*
  - 10.6: Macromolecules - *CC BY-NC-SA 4.0*
  - 10.7: Simulations - *CC BY-NC-SA 4.0*
- Back Matter - *CC BY-NC-SA 4.0*
  - Index - *CC BY-NC-SA 4.0*
  - Glossary - *CC BY-NC-SA 4.0*
  - Detailed Licensing - *CC BY-NC-SA 4.0*
  - Detailed Licensing - *CC BY-NC-SA 4.0*

Detailed Licensing

1: Overview

Title: Chem 370: P-Chem 1 for Biophysical & Traditional Students (Gutow)

Webpages: 103

Applicable Restrictions: Noncommercial

All licenses found:

- CC BY-NC-SA 4.0: 100% (103 pages)

2: By Page

- Chem 370: P-Chem 1 for Biophysical & Traditional Students (Gutow) - *CC BY-NC-SA 4.0*
  - Front Matter - *CC BY-NC-SA 4.0*
    - TitlePage - *CC BY-NC-SA 4.0*
    - InfoPage - *CC BY-NC-SA 4.0*
    - Table of Contents - *CC BY-NC-SA 4.0*
    - Licensing - *CC BY-NC-SA 4.0*
  - 1: Thermodynamics - *CC BY-NC-SA 4.0*
    - 1.1: Thermodynamic Variables and Equations of State - *CC BY-NC-SA 4.0*
    - 1.2: The First Law of Thermodynamics - *CC BY-NC-SA 4.0*
    - 1.3: Thermochemistry - *CC BY-NC-SA 4.0*
    - 1.4: The Second Law of Thermodynamics - *CC BY-NC-SA 4.0*
    - 1.5: The Boltzmann Distribution and the Statistical Definition of Entropy - *CC BY-NC-SA 4.0*
    - 1.6: The Gibbs and Helmholtz Energy - *CC BY-NC-SA 4.0*
    - 1.7: Phase Equilibria and Mixtures - *CC BY-NC-SA 4.0*
    - 1.8: Colligative Properties - *CC BY-NC-SA 4.0*
    - 1.9: Henry's Law - *CC BY-NC-SA 4.0*
  - 2: Chemical Equilibria - *CC BY-NC-SA 4.0*
    - 2.1: Chemical Equilibria - *CC BY-NC-SA 4.0*
    - 2.2: Composition Dependence of Free Energy (G) - *CC BY-NC-SA 4.0*
    - 2.3: Equilibrium Calculations (ICE) Review - *CC BY-NC-SA 4.0*
    - 2.4: Fractional Composition at Equilibrium - *CC BY-NC-SA 4.0*
    - 2.5: Coupled Equilibria - *CC BY-NC-SA 4.0*
    - 2.6: Equilibrium Dependence on Conditions - *CC BY-NC-SA 4.0*
    - 2.7: Coupled Equilibria Driving Nonspontaneous Reactions - *CC BY-NC-SA 4.0*
    - 2.8: Brønsted-Lowry Acids and Bases - *CC BY-NC-SA 4.0*
    - 2.9: pH and pOH - *CC BY-NC-SA 4.0*
    - 2.10: Acid-Base Equilibria - *CC BY-NC-SA 4.0*
    - 2.11: Hydrolysis of Salts - *CC BY-NC-SA 4.0*
    - 2.12: Polyprotic Acids - *CC BY-NC-SA 4.0*
    - 2.13: Buffers - *CC BY-NC-SA 4.0*
  - 3: Ions and Electrochemistry - *CC BY-NC-SA 4.0*
    - 3.1: Mean Ionic Activity Coefficients and the Debye-Hückel Model - *CC BY-NC-SA 4.0*
    - 3.2: Extending Debye-Hückel Theory to Higher Concentrations - *CC BY-NC-SA 4.0*
    - 3.3: Ion Transport - *CC BY-NC-SA 4.0*
    - 3.4: Review of Redox Chemistry - *CC BY-NC-SA 4.0*
    - 3.5: Half Cells and Standard Reduction Potentials - *CC BY-NC-SA 4.0*
    - 3.6: Cell potentials under non-standard conditions (Nernst equation) - *CC BY-NC-SA 4.0*
    - 3.7: Thermodynamics from Electrochemistry - *CC BY-NC-SA 4.0*
    - 3.8: Redox Examples - *CC BY-NC-SA 4.0*
  - 4: Reaction Kinetics - *CC BY-NC-SA 4.0*
    - 4.1: Reaction Rates and Rate Laws - *CC BY-NC-SA 4.0*
    - 4.2: Measuring Reaction Rates - *CC BY-NC-SA 4.0*
    - 4.3: Determining Rate Laws - *CC BY-NC-SA 4.0*
    - 4.4: Integrated Rate Laws - *CC BY-NC-SA 4.0*
    - 4.5: Examples of Using Graphs to Determine Reaction Order - *CC BY-NC-SA 4.0*
    - 4.6: Temperature Dependence of Rate Constants - *CC BY-NC-SA 4.0*
  - 5: Kinetic Mechanisms 1 - *CC BY-NC-SA 4.0*
    - 5.1: Reaction Mechanisms - *CC BY-NC-SA 4.0*
    - 5.2: Relaxation Methods - *CC BY-NC-SA 4.0*
    - 5.3: Representative Reaction Mechanisms - *CC BY-NC-SA 4.0*
    - 5.4: The Rate Determining Step Approximation - *CC BY-NC-SA 4.0*
    - 5.5: The Equilibrium Approximation - *CC BY-NC-SA 4.0*

- 5.6: The Steady-State Approximation - *CC BY-NC-SA 4.0*

- 6: Molecular Level Models of Kinetics - *CC BY-NC-SA 4.0*
  - 6.1: Kinetics of Reactions in Solution - *CC BY-NC-SA 4.0*
  - 6.2: Kinetic vs. Thermodynamic Control of Reactions - *CC BY-NC-SA 4.0*
  - 6.3: Collision Theory - *CC BY-NC-SA 4.0*
  - 6.4: Transition State Theory - *CC BY-NC-SA 4.0*
  - 6.5: Reactions Involving Ions - *CC BY-NC-SA 4.0*
- 7: Kinetic Mechanisms 2 - *CC BY-NC-SA 4.0*
  - 7.1: Numerical Modeling of Mechanisms - *CC BY-NC-SA 4.0*
  - 7.2: The Michaelis-Menten Mechanism - *CC BY-NC-SA 4.0*
  - 7.3: The Lindemann Mechanism - *CC BY-NC-SA 4.0*
  - 7.4: Chain Reactions - *CC BY-NC-SA 4.0*
  - 7.5: Catalysis (ozone example) - *CC BY-NC-SA 4.0*
  - 7.6: Oscillating Reactions - *CC BY-NC-SA 4.0*
  - 7.7: Diffusion - *CC BY-NC-SA 4.0*
  - 7.8: Membrane Diffusion - *CC BY-NC-SA 4.0*
  - 7.9: Ion Mobilities - *CC BY-NC-SA 4.0*
  - 7.10: Transport Across Cell Membranes - *CC BY-NC-SA 4.0*
  - 7.11: Kinetics of Electron Transfer Reactions - *CC BY-NC-SA 4.0*
- 8: Quantum Chemistry Fundamentals - *CC BY-NC-SA 4.0*
  - 8.1: Failures of Classical Physics - *CC BY-NC-SA 4.0*
  - 8.2: The Schrödinger Wave Equation - *CC BY-NC-SA 4.0*
  - 8.3: Particle in a One-Dimensional Box - *CC BY-NC-SA 4.0*
  - 8.4: Tunneling - *CC BY-NC-SA 4.0*
  - 8.5: Particle in a 2-Dimensional Box - *CC BY-NC-SA 4.0*
  - 8.6: Particle on a Ring - *CC BY-NC-SA 4.0*
  - 8.7: The Schrödinger Wave Equation for the Hydrogen Atom - *CC BY-NC-SA 4.0*
  - 8.8: Many-Electron Atoms and the Periodic Table - *CC BY-NC-SA 4.0*
  - 8.9: Harmonic Oscillator - *CC BY-NC-SA 4.0*
- 9: Molecular Quantum Mechanics - *CC BY-NC-SA 4.0*
  - 9.1: The Born-Oppenheimer Approximation Simplifies the Schrödinger Equation for Molecules - *CC BY-NC-SA 4.0*
  - 9.2: Valence Bond Theory - *CC BY-NC-SA 4.0*
  - 9.3: Hybridization of Atomic Orbitals - *CC BY-NC-SA 4.0*
  - 9.4: Molecular Orbital Theory - *CC BY-NC-SA 4.0*
  - 9.5: Diatomic Molecules With More Than s Orbitals - *CC BY-NC-SA 4.0*
  - 9.6: Hückel MO Model of Conjugation - *CC BY-NC-SA 4.0*
  - 9.7: Benzene and Aromaticity - *CC BY-NC-SA 4.0*
  - 9.8: Numerical QM Methods - *CC BY-NC-SA 4.0*
- 10: Aggregates and Macromolecules - *CC BY-NC-SA 4.0*
  - 10.1: Mass Spectrometry - *CC BY-NC-SA 4.0*
  - 10.2: X-Ray Crystallography - *CC BY-NC-SA 4.0*
  - 10.3: Cryo-Electron Microscopy - *CC BY-NC-SA 4.0*
  - 10.4: Intermolecular Forces - *CC BY-NC-SA 4.0*
  - 10.5: Structure of Gases, Liquids and Glasses - *CC BY-NC-SA 4.0*
  - 10.6: Macromolecules - *CC BY-NC-SA 4.0*
  - 10.7: Simulations - *CC BY-NC-SA 4.0*
- Back Matter - *CC BY-NC-SA 4.0*
  - Index - *CC BY-NC-SA 4.0*
  - Glossary - *CC BY-NC-SA 4.0*
  - Detailed Licensing - *CC BY-NC-SA 4.0*
  - Detailed Licensing - *CC BY-NC-SA 4.0*